

Anti-inflammatory and Immuno-metabolic Effects of Pinolenic Acid in Rheumatoid Arthritis



Dr Rabaa Takala

MBCChB (Hons), PGDipFM

A dissertation presented for the degree Doctor of Philosophy

November 2022

School of Medicine and Biosciences

Cardiff University

Table of Contents

| | |
|--|-------------|
| Table of Figures | viii |
| Table of Tables..... | xi |
| Acknowledgement | xiv |
| Publications and Presentations Arising during this PhD | xvi |
| Abbreviations | xvii |
| Declaration of Authorship | xx |
| Abstract..... | xxii |
| Chapter 1: General Introduction | 1 |
| 1.1 Rheumatoid arthritis (RA)..... | 1 |
| 1.2 Clinical features | 1 |
| 1.3 Epidemiology of RA..... | 2 |
| 1.3.1. Cardiovascular diseases (CVDs) as the major cause of increased mortality in RA patients | 2 |
| 1.4 Cardiovascular diseases (CVDs) in RA..... | 3 |
| 1.4.1 Traditional cardiovascular risk factors do not predict CVD events in RA | 3 |
| 1.4.2 Risk factors for CVD events in RA..... | 3 |
| 1.4.3 Inflammation in atherosclerosis and rheumatoid arthritis | 5 |
| 1.5 The pathogenesis of RA..... | 9 |
| 1.5.1 Overview..... | 9 |
| 1.5.1.1 Genetic involvement | 10 |
| 1.5.1.2 Environmental factors..... | 10 |
| 1.5.2 T cells | 11 |
| 1.5.3 B cells | 11 |
| 1.5.4 Monocytes and Macrophages | 12 |
| 1.5.4.1 Characteristics of monocytes..... | 12 |
| 1.5.4.1.1. Phenotypic characteristic of monocytes..... | 12 |
| 1.5.4.1.2. Classification of monocytes..... | 13 |
| 1.5.4.2 Characteristics of monocytes in RA..... | 14 |
| 1.5.4.2.1. Phenotypic characteristics of monocytes in RA | 14 |
| 1.5.4.2.2. Functional characteristics of monocytes in RA..... | 15 |
| 1.5.4.3 Characteristics of macrophages | 16 |
| 1.5.4.3.1. Phenotypic characteristics of macrophages | 16 |
| 1.5.4.3.2. Functional characteristics of macrophages | 17 |
| 1.5.4.4 Characteristics of macrophages in RA | 18 |
| 1.5.4.4.1. Phenotypic characteristics of macrophages in RA | 19 |
| 1.5.4.4.2. Functional characteristics of macrophages in RA | 20 |
| 1.6 Cytokines | 22 |
| 1.6.1. Tumour Necrosis Factor-α (TNF-α)..... | 25 |

| | |
|--|-----------|
| 1.6.1.1 TNF- α signal transduction | 25 |
| 1.6.1.2 The biological effectors of TNF- α | 27 |
| 1.6.1.3 The role of TNF- α in RA | 28 |
| 1.6.1.4 TNF- α inhibition in RA. | 31 |
| 1.6.2 Interleukin-1 (IL-1) | 31 |
| 1.6.2.1 IL-1 signal transduction | 31 |
| 1.6.2.2 Biological effectors of IL-1 | 33 |
| 1.6.2.3 The role of IL-1 in RA | 34 |
| 1.6.2.4. IL-1 inhibition in RA. | 35 |
| 1.6.3 Interleukin-6 (IL-6) | 35 |
| 1.6.3.1 IL-6 signal transduction | 35 |
| 1.6.3.2 Biological effectors of IL-6 | 38 |
| 1.6.3.3 IL-6 role in RA..... | 38 |
| 1.6.3.4 IL-6 inhibition in RA | 39 |
| 1.7 Non-cytokine mediators | 39 |
| 1.7.1 Nitric Oxide (NO) | 39 |
| 1.7.2 Eicosanoids (Prostaglandins) | 42 |
| 1.7.2.1 Prostaglandin E2 (PGE2) in RA..... | 43 |
| 1.7.2.2 PGs inhibitions | 44 |
| 1.8 Management of RA..... | 45 |
| 1.8.1. Diet and lifestyle modifications..... | 45 |
| 1.8.2. Pharmacological treatment..... | 48 |
| 1.8.3. Conclusion | 52 |
| 1.9 Fatty acids in inflammation | 53 |
| 1.9.1 Fatty acid's chemical structure and nomenclature | 53 |
| 1.9.2 Omega-3 and -6 polyunsaturated fatty acids (n-3 and n-6 PUFA)..... | 54 |
| 1.9.3 Pine nuts oil (PNO) and Pinolenic acid (PNLA). | 57 |
| 1.10 Pinolenic acid | 58 |
| 1.10.1 Structure, biosynthesis, and metabolism | 58 |
| 1.10.2 Potential effects of PNLA and PNO in RA | 61 |
| 1.10.3 Beneficial effects of PNLA and general systemic implications | 63 |
| 1.11 Project hypothesis; RA and future prospective therapy | 65 |
| 1.12 Aims and Objectives | 66 |
| Chapter 2: Materials and Methods | 67 |
| 2.1. Materials..... | 67 |
| 2.2. Preparation of reagents, PNLA, and the vehicle..... | 70 |
| 2.3. Patients and healthy controls; the recruitment and selection criteria | 71 |

| | |
|---|------------|
| 2.4. Cell culture techniques | 72 |
| 2.4.1. Human leukemic THP-1 cell line | 72 |
| 2.4.2. Primary culture of human monocyte-derived macrophages (HMDM) | 73 |
| 2.4.3. Peripheral blood mononuclear cells (PBMCs) isolation and preparation | 74 |
| 2.5. Cell counting | 76 |
| 2.6. Treatment of the cells (PNLA and vehicle incubation) | 77 |
| 2.7. LPS stimulation of pre-treated monocytes and macrophages | 78 |
| 2.8. Flow cytometry | 78 |
| 2.8.1. Principle of flow cytometry..... | 78 |
| 2.8.2. CD14 monocytes and optimisation of LPS and Brefeldin A (BFA) incubation time | 79 |
| 2.8.3. Cell surface staining | 79 |
| 2.8.4. Intracellular staining..... | 79 |
| 2.8.5. Flow cytometry analysis..... | 81 |
| 2.8.6. Gating strategy | 81 |
| 2.8.7. Fluorescent sorting of CD14CD16 monocytes using the FACS Aria III cell sorter. | 82 |
| 2.8.8. Purity of Sorted CD14CD16 monocytes. | 84 |
| 2.8.9. CD14CD16 monocytes treatment | 84 |
| 2.8.10. Preparation of cells for bulk RNA extraction..... | 86 |
| 2.9. Cell-based assays | 85 |
| 2.9.1 Cell Viability and Proliferation | 85 |
| 2.9.1.1 LDH assay..... | 87 |
| 2.9.1.2 CV assay | 87 |
| 2.9.1.3 Alarm blue..... | 88 |
| 2.9.1.4 BrdU..... | 88 |
| 2.9.2. Migration assay | 89 |
| 2.9.3. Lipid methods | 89 |
| 2.9.3.1 Macropinocytosis assay | 89 |
| 2.9.3.2 Dil-oxLDL uptake assay | 90 |
| 2.9.4. Phagocytosis | 90 |
| 2.9.5. Measurement of reactive oxygen species (ROS) | 91 |
| 2.9.6. Measurement of protein | 92 |
| 2.9.6.1. Enzyme-linked immunosorbent assay (ELISA) | 92 |
| 2.9.6.2 ELISA measurement of TNF-α, IL-6, and IL-1β | 92 |
| 2.9.6.3 ELISA measurements of PGE2 | 95 |
| 2.9.6.4 Indirect measurements of nitric oxide (NO) via the Griess system | 98 |
| 2.10. Molecular techniques and general workflow of the different stages of gene expression analysis | 99 |
| 2.10.1. RNA extraction and quality control (QC) check | 99 |
| 2.10.2. Library preparation, including ribosomal RNA depletion, using the NEBNext Ultra II RNA Library Prep Kit for Illumina. | 109 |
| 2.10.3 Library and QC check | 112 |
| 2.10.4. Sequencing | 113 |
| 2.10.5. RNA-seq data processing and read mapping strategy | 113 |
| 2.10.6. Evaluation of duplicated reads (ensuring gene expression is not affected by duplication) | 114 |
| 2.10.7. Normalisation and estimation of differential gene expression (DGE) analysis | 115 |
| 2.10.8. Bioinformatic analysis | 115 |
| 2.10.9. Identification of differentially expressed (DEG) genes and further down and upstream pathway analysis | 115 |
| 2.10.9.1. Heatmap | 116 |
| 2.10.9.2. Gene set enrichment analysis | 116 |
| 2.10.9.3. Pathway analysis | 116 |

| | |
|--|------------|
| 2.10.10. Statistical analysis of RNA sequencing read pairs and percentage of a total number of reads and QC check..... | 117 |
| 2.11. Statistical analysis..... | 118 |
| Chapter 3: Effects of PNLA on key inflammatory processes using human THP-1 cell lines and primary cultures of human monocyte-derived macrophages..... | 119 |
| 3.1. Introduction and aims | 119 |
| 3.2. Results..... | 122 |
| 3.2.1. THP-1 cell line..... | 122 |
| 3.2.1.1 The viability and proliferation of THP-1 macrophages were unaffected by PNLA <i>in vitro</i> | 122 |
| 3.2.1.2 The CCL2-driven migration of THP-1 monocytes was inhibited by PNLA. | 123 |
| 3.2.1.3 PNLA attenuates macropinocytosis in THP-1 macrophages..... | 123 |
| 3.2.1.4 PNLA reduces Dil-oxLDL uptake by THP-1 macrophages..... | 124 |
| 3.2.1.5 PNLA does not affect the phagocytic activity of THP-1 macrophages..... | 125 |
| 3.2.1.6 PNLA does not affect ROS production in THP-1 monocytes and macrophages | 125 |
| 3.2.2. Primary cultures of human monocyte-derived macrophages. | 126 |
| 3.2.2.1 The viability and proliferation of human macrophages were unaffected by PNLA <i>ex-vivo</i> | 127 |
| 3.2.2.2 PNLA attenuates macropinocytosis in human macrophages | 127 |
| 3.2.2.3 PNLA reduces Dil-oxLDL uptake in human macrophages | 128 |
| 3.3. Discussion | 130 |
| Chapter 4: Effects of PNLA on the expression of pro-inflammatory cytokines involved in the pathogenesis of RA and atherosclerosis | 136 |
| 4.1. Introduction and aims | 136 |
| 4.2. Results..... | 137 |
| 4.2.1. PNLA does not affect the viability and proliferation of PBMCs from HCs or patients with RA..... | 137 |
| 4.2.1.1 Viability of HCs and RA PBMCs <i>ex-vivo</i> | 137 |
| 4.2.1.2 Proliferation of PBMCs <i>ex-vivo</i> from HCs and patients with RA..... | 139 |
| 4.2.2. TNF- α level was reduced significantly upon PNLA treatment..... | 140 |
| 4.2.2.1 HCs and RA adherent monocytes..... | 140 |
| 4.2.2.2 HCs and RA differentiated macrophages | 140 |
| 4.2.3. IL-6 level was reduced significantly upon PNLA treatment..... | 143 |
| 4.2.3.1 HCs and RA adherent monocytes..... | 143 |
| 4.2.3.2 HCs and RA differentiated macrophages | 145 |
| 4.2.4. IL-1 β level was reduced in HCs adherent monocytes but not in RA patients or macrophages upon PNLA treatment. | 147 |
| 4.2.4.1 HCs and RA adherent monocytes..... | 147 |
| 4.2.4.2 HCs and RA differentiated macrophages | 148 |
| 4.2.5. PGE2 level was reduced significantly upon PNLA treatment. | 150 |
| 4.2.5.1 HCs and RA adherent monocytes..... | 150 |
| 4.2.5.2 HCs and RA differentiated macrophages | 151 |
| 4.2.6. Nitrite (NO ₂) | 153 |
| 4.2.6.1 HCs and RA adherent monocytes..... | 153 |
| 4.2.6.2 HCs and RA differentiated macrophages | 153 |
| 4.3. Discussion | 155 |
| Chapter 5: Effects of PNLA on the inflammatory gene expressions implicated in the pathogenesis of RA and atherosclerosis | 158 |
| 5.1. Introduction and aims | 158 |
| 5.2. Results..... | 159 |
| 5.2.1. Principle component analysis (PCA) | 159 |

| | |
|--|------------|
| 5.2.2. Heatmap | 161 |
| 5.2.3. Volcano plots..... | 163 |
| 5.2.4. DEGs that were statistically significantly regulated by PNLA in PBMCs from RA patients or HCs. | 164 |
| 5.2.5. Canonical Pathways | 167 |
| 5.2.6. Venn diagrams for significant DEGs in HCs and RA patients..... | 168 |
| 5.2.7. Comparison analysis..... | 178 |
| 5.2.8. Upstream regulator effectors..... | 181 |
| 5.3. Discussion | 192 |
| Limitations | 205 |
| Chapter 6: Effect of PNLA on the levels of intracellular cytokines expressed by CD14CD16 monocyte subsets that are implicated in the pathogenesis of RA and Atherosclerosis | 206 |
| 6.1. Introduction and aims | 206 |
| 6.2. Results..... | 207 |
| 6.2.1. Monocyte's phenotyping (granularity) was increased upon PNLA treatment | 207 |
| 6.2.2. CD14CD16 monocyte's microscopic morphology was affected upon LPS stimulation and PNLA treatment..... | 212 |
| 6.2.3. CD14 ⁺ monocytes expressing (TNF- α , IL-6, IL-1 β , CCL2) cytokines..... | 213 |
| 6.2.3.1. Intracellular TNF- α expression was reduced significantly upon PNLA treatment..... | 214 |
| 6.2.3.2. Intracellular IL-6 expression was reduced significantly upon PNLA treatment..... | 214 |
| 6.2.3.3. Intracellular IL-1 β expression was reduced significantly upon PNLA treatment..... | 214 |
| 6.2.3.4. Intracellular CCL2 expression was not reduced significantly upon PNLA treatment | 214 |
| 6.2.3.5. Intracellular IL-8 expression was reduced significantly upon PNLA treatment..... | 214 |
| 6.2.3.6. Intracellular IL-10 expression was unaffected upon PNLA treatment | 215 |
| 6.2.4. Intracellular cytokine expression upon PNLA treatment did not significantly correlate with the patients' characteristics; gender, ACPA, RF, CRP, ESR, DD, age, and DAS28..... | 217 |
| 6.2.4.1. There is no correlation between the reduction in different cytokines expressed by CD14 ⁺ monocytes | 221 |
| 6.2.4.2. Gender and reduction in cytokines expressed by CD14 ⁺ monocytes | 222 |
| 6.2.4.3. Serological status and level of cytokines (TNF- α , IL-6, and IL-1 β); RF and ACPA positivity | 222 |
| 6.3. Discussion | 224 |
| Chapter 7: Effects of PNLA on the inflammatory gene expressions of activated CD14CD16 monocytes implicated in the pathogenesis of RA and atherosclerosis..... | 227 |
| 7.1. Introduction and aims | 227 |
| 7.2. Results..... | 229 |
| 7.2.1. Principle component analysis (PCA)..... | 230 |
| 7.2.2. Heatmap..... | 232 |
| 7.2.3. Volcano plots | 233 |
| 7.2.4. Protein-coding genes of CD14CD16 monocytes whose expression was significantly affected by PNLA treatment. | 234 |
| 7.2.5. Noncoding microRNA (miRNA) analysis of CD14CD16 monocytes | 236 |
| 7.2.6. Impact of combination PNLA supplementation and LPS stimulation versus LPS stimulation | 236 |
| 7.2.7. miRNAs target mRNAs | 237 |
| 7.2.8. Pathway analysis | 241 |
| 7.2.8.1. Graphical summary of pathways analysis | 241 |
| 7.2.8.2. Canonical pathway | 245 |
| 7.2.8.3. Overlapping canonical pathways..... | 248 |

| | |
|---|------------|
| 7.2.9. Comparison analysis..... | 249 |
| 7.2.10. Upstream regulators..... | 251 |
| 7.3. Discussion..... | 256 |
| Chapter 8: General Discussion | 265 |
| 8.1 Introduction..... | 265 |
| 8.2 Dietary intervention in RA..... | 265 |
| 8.3 Key findings from the study..... | 267 |
| 8.4 The role of mitochondrial dysfunction in driving inflammation in RA..... | 269 |
| 8.5 Macrophages immunometabolism during inflammation and diseases..... | 269 |
| 8.6 Biologic effects of PNLA..... | 272 |
| 8.6.1 Regulation of inflammation and immune pathways..... | 272 |
| 8.6.2 Modulation of metabolic genes/pathways..... | 273 |
| 8.6.3 Modulation of cellular miRNA signatures..... | 274 |
| 8.7 Future direction and clinical implications..... | 274 |
| 8.8 Conclusion..... | 276 |
| Supplementary..... | 277 |
| S1. Library Preparation, including ribosomal RNA depletion, using the NEBNext Ultra II RNA Library Prep Kit for Illumina..... | 282 |
| 1. Depletion of ribosomal RNA..... | 282 |
| 2. Probe Hybridisation to RNA..... | 282 |
| 3. RNase H Digestion..... | 283 |
| 4. DNase I Digestion..... | 283 |
| 5. RNA Purification using NEBNext RNA Sample Purification Beads..... | 283 |
| 6. RNA Fragmentation and Priming..... | 284 |
| 7. First Strand cDNA Synthesis..... | 284 |
| 8. Second Strand cDNA Synthesis..... | 285 |
| 9. Purification of double-stranded cDNA using AMPure XP Purification Beads..... | 285 |
| 10. End Prep of cDNA Libraries..... | 286 |
| 11. Adaptor Ligation..... | 286 |
| 12. Purification of the ligation reaction using AMPure XP beads (Beckman Coulter)..... | 287 |
| 13. PCR Library Enrichment..... | 287 |
| 14. Purification of the PCR reaction using AMPure XP beads (Beckman Coulter)..... | 288 |
| 15. Library Quantification..... | 288 |
| S2. Optimisation of RNA-seq of PBMCs..... | 289 |
| S3. Sequencing on HiSeq 4000 flow cells in Chapter 5..... | 290 |
| S4. Sequencing on HiSeq 6000 flow cells in Chapter 7..... | 291 |
| References | 298 |

Table of Figures

| | |
|---|-----|
| Figure 1.1. Important pathological features common to both atherosclerotic plaque and the inflamed rheumatoid synovium..... | 9 |
| Figure 1.2. A general model showing a summary of RA pathogenesis and development..... | 11 |
| Figure 1.3. A schematic view of a normal joint and a joint affected by RA shows increased inflammation and cellular activity..... | 18 |
| Figure 1.4. Overview of the process of monocyte adhesion to the endothelium and migration into the sub-endothelial space during the development of an atherosclerotic plaque..... | 19 |
| Figure 1.5. The TNF signalling pathway that leads to the main cellular responses..... | 27 |
| Figure 1.6. Illustration for the summary of TNF- α action on immune and endothelial cells in RA..... | 29 |
| Figure 1.7. Reverse cholesterol transport..... | 30 |
| Figure 1.8. IL-1 signalling of and activation | 33 |
| Figure 1.9. Classical IL-6 receptor signalling and IL-6 trans-signalling pathways and their role in RA. | 37 |
| Figure 1.10. Prostaglandins synthesis pathway..... | 45 |
| Figure 1.11. Schematic illustration of the gut microbiome, genetic and environmental factors as a leader of the autoimmunity and chronic inflammation..... | 46 |
| Figure 1.12. Simple linear structure of polyunsaturated fatty acids..... | 59 |
| Figure 1.13. Mass spectrometry total ion chromatogram of ETrA..... | 60 |
| | |
| Figure 2.1. Schematic of flow cytometry principle..... | 79 |
| Figure 2.2. Experimental setup for intracellular cytokines assessment. | 80 |
| Figure 2.3. CD14CD16 monocytes, unstained, representative sample..... | 81 |
| Figure 2.4. Gating strategy for sorting CD14 ⁺ monocytes | 82 |
| Figure 2.5. Gating strategy for sorting of CD14 ⁺ CD16 ⁺ monocytes on FACS Sort Aria III..... | 83 |
| Figure 2.6. The experimental set-up of modified Boydon chambers was used to assess monocyte migration..... | 89 |
| Figure 2.7. IL-6 level assessment in optimization experiments with 50 and 100 μ M PNLA..... | 95 |
| Figure 2.8. PGE2 ELISA standard curve | 98 |
| Figure 2.9. Schematic figure of experimental workflow from sample preparation to bioinformatic work. | 100 |
| Figure 2.10. Flow diagram of the spin column RNA isolation method..... | 101 |
| Figure 2.11. RNA integrity assessment. | 102 |
| Figure 2.12. A representative sample of nanodrop spectrophotometry plot of a high-quality RNA. . | 104 |
| Figure 2.13. Screen Tape device architecture used for RNA QC check..... | 105 |
| Figure 2.14. Qubit 2.0 Fluorometer used for RNA and DNA quantification | 105 |
| Figure 2.15. Summary of the workflow of RNA-seq library preparation..... | 110 |
| Figure 2.16. Electropherogram of Agilent TapeStation..... | 111 |
| Figure 2.17. Electropherogram of the QC of generated pool library.. | 112 |

| | |
|--|-----|
| Figure 2.18. Workflow of RNA-seq data mapping..... | 114 |
| Figure 2.19. Gene duplication does not affect gene expression..... | 115 |
| Figure 2.20. Schematic outlines of bioinformatics workflow..... | 116 |
| | |
| Figure 3.1. No adverse effects of PNLA in comparison to the vehicle on the viability and proliferation of THP-1 macrophages. | 122 |
| Figure 3.2. PNLA inhibits the CCL2-induced migration of THP-1 monocytes. | 123 |
| Figure 3.3. LY uptake is attenuated following the incubation of THP-1 macrophages with PNLA. . | 124 |
| Figure 3.4. PNLA reduces the uptake of ox-LDL by THP-1 macrophages..... | 124 |
| Figure 3.5. The phagocytosis in THP-1 macrophages is not affected by PNLA. | 125 |
| Figure 3.6. PNLA has no detrimental effect on the TBHP-induced ROS production in THP-1 monocytes and macrophages..... | 126 |
| Figure 3.7. No adverse effects of PNLA in comparison to the vehicle on the viability and proliferation of HMDMs..... | 127 |
| Figure 3.8. LY uptake was attenuated following the incubation of HMDM with PNLA..... | 128 |
| Figure 3.9. PNLA reduces the uptake of ox-LDL by HMDMs. | 129 |
| | |
| Figure 4.1. PNLA has no detrimental effect on the viability of PBMCs isolated from HCs and RA patients. | 138 |
| Figure 4.2. PNLA does not affect the proliferation of PBMCs from HCs and RA patients. | 139 |
| Figure 4.3. TNF- α level is reduced following incubation of activated enriched monocytes from HCs and RA patients with PNLA. | 141 |
| Figure 4.4. TNF- α level is reduced following incubation of activated enriched macrophages from HCs and RA with PNLA..... | 142 |
| Figure 4.5. IL-6 level is reduced following incubation of activated enriched monocytes from HCs and RA patients with PNLA. | 144 |
| Figure 4.6. IL-6 level is reduced following incubation of activated enriched macrophages from HCs and RA patients with PNLA. | 146 |
| Figure 4.7. IL-1 β level is reduced following incubation of activated monocytes from HCs but not RA patients. | 148 |
| Figure 4.8. PNLA has no effect on IL-1 β level from LPS-activated enriched macrophages of HCs and RA patients..... | 149 |
| Figure 4.9. PGE2 level is reduced following incubation of activated enriched monocytes from HCs and RA patients with PNLA. | 150 |
| Figure 4.10. PGE2 level is reduced following incubation of activated macrophages of HCs and RA patients with RA. | 152 |
| Figure 4.11. NO $_2^-$ level is reduced following incubation of activated enriched macrophages from HCs and RA patients with PNLA. | 154 |
| | |
| Figure 5.1. PNLA affects TNF- α , IL-6, NO, and PGE2 levels in the cell supernatants. | 159 |
| Figure 5.2. Principal component analysis (PCA) from DESeq2 analysis of HCs and RA patients DEGs. | 160 |

| | |
|---|-----|
| Figure 5.3. Heatmap for the whole genomic transcriptome of HCs and RA patients..... | 161 |
| Figure 5.4. Volcano plots of the global gene expression profile of HCs. | 162 |
| Figure 5.5. Volcano plots of the global gene expression profile of RA patients. | 163 |
| Figure 5.6. The network of the top significantly affected genes by PNLA treatment. | 166 |
| Figure 5.7. Canonical pathways of HCs and RA patients with PNLA treatment and LPS stimulation versus vehicle treatment and LPS stimulation of PBMCs | 167 |
| Figure 5.8. Venn diagram of HCs DEGs A and B | 168 |
| Figure 5.9. Venn diagram of HCs DEGs overlap comparisons A, B, and C | 171 |
| Figure 5.10. Venn diagram of RA patients DEGs overlap comparison of A and B | 173 |
| Figure 5.11. Venn diagram of RA patients DEGs overlap comparisons A, B, and C | 177 |
| Figure 5.12. Heatmap of differentially expressed upstream regulators for the comparison analysis of HCs. | 179 |
| Figure 5.13. Heatmap of differentially expressed upstream regulators for the comparison analysis of RA. | 180 |
| Figure 5.14. NF- κ B upstream regulator as an effector of PNLA treatment of LPS stimulated PBMCs from R patients and HCs..... | 181 |
| Figure 5.15. STAT1 upstream regulator as an effector and their pathologic roles in RA. | 183 |
| Figure 5.16. PPARA upstream regulator as an effector following PNLA treatment of LPS stimulated PBMCs from HCs and RA patients. | 185 |
| Figure 5.17. PPARD upstream regulator as an effector following PNLA treatment of LPS stimulated PBMCs from HCs and RA patients. | 186 |
| Figure 5.18. PPARGC1A upstream regulator as an effector following PNLA-treated LPS stimulated PBMCs from RA patients. | 187 |
| Figure 5.19. The upstream regulators for IL-1 α and IL-1 β | 188 |
| Figure 5.20. The upstream regulation networks for CCR2. | 189 |
| Figure 5.21. Transcriptional regulation pathways of PDK4 in different tissues under various nutritional states..... | 195 |
| Figure 5.22. The physiological effects of PDK4 show PDK4 as a checkpoint in NF- κ B/TNF-mediated response. | 197 |
| Figure 5.23. tPA and uPA activate the conversion of plasminogen into plasmin..... | 198 |
| Figure 5.24. The effects of PPAR- γ activation in macrophages and general effects of PPAR- α | 201 |
| | |
| Figure 6.1. Smoothed density plots for the visualisation of unstimulated or LPS-stimulated CD14CD16 monocytes after vehicle or PNLA exposure..... | 209 |
| Figure 6.2. Smoothed density plots and contour plots of unstimulated or LPS-stimulated CD14 ⁺ monocytes after vehicle or PNLA exposure..... | 210 |
| Figure 6.3. The granularity of CD14 ⁺ is increased following PNLA treatment..... | 212 |
| | |
| Figure 6.4. Visualisation of unstimulated or LPS stimulated CD14CD16 monocytes after vehicle or PNLA exposure..... | 213 |
| Figure 6.5. Percentage of CD14 ⁺ monocytes positively expressing cytokines was determined by flow cytometry analysis..... | 214 |

| | |
|---|-----|
| Figure 6.6. CD14 ⁺ expressing cytokines were reduced significantly following PNLA treatment..... | 217 |
| Figure 6.7. There was no correlation between the levels of reduced cytokines and ESR or CRP..... | 219 |
| Figure 6.8. There was no correlation between the levels of reduced cytokines and the age or DD.... | 220 |
| Figure 6.9. There was no correlation between the levels of reduced cytokines and DAS28. | 221 |
| Figure 6.10. There was no correlation between the levels of all reduced cytokines..... | 222 |
| Figure 6.11. There was no correlation between the levels of reduced cytokines and the gender of RA patients..... | 223 |
| Figure 6.12. There was no correlation between the levels of reduced cytokines and RF status..... | 224 |
| | |
| Figure 7.1. Eukaryotic RNA categories. | 229 |
| Figure 7.2. Principal component analysis (PCA) from the DESeq2 analysis of all DEGs. | 230 |
| Figure 7.3. Principal component analysis (PCA) from the DESeq2 analysis of the top 50 DEGs..... | 231 |
| Figure 7.4. Heatmap for the whole genomic transcriptome of significantly expressed genes..... | 232 |
| Figure 7.5. Volcano plots of the global gene expression profile of RA patients. | 233 |
| Figure 7.6. Venn diagrams showing the significantly affected miRNAs..... | 236 |
| Figure 7.7. mRNA PDK4 is a target for miRNAs. | 239 |
| Figure 7.8. SIGIRR is downstream for miRNAs and upstream for canonical pathways..... | 240 |
| Figure 7.9. Graphical summary showing the most significant transcription factors and regulators affected by PNLA.. | 242 |
| Figure 7.10. Immune-specific functions of TFEB and TFE3. | 245 |
| Figure 7.11. Canonical pathways bar chart for PNLA effect on activated CD14CD16 monocytes... | 246 |
| Figure 7.12. Oxidative phosphorylation downstream pathway analysis affected by PNLA. | 247 |
| Figure 7.13. Overlapping canonical pathway | 249 |
| Figure 7.14. Heatmap of differentially expressed upstream regulators from the comparative analysis of RA patients..... | 250 |
| Figure 7.15. Upstream regulators as effectors of PNLA treatment to LPS stimulated CD14CD16 monocytes | 253 |
| Figure 7.16. Upstream regulators as effectors of PNLA treatment to LPS stimulated CD14CD16 monocytes. | 254 |
| Figure 7.17. Let 7 associated networks as supported by the IPA database..... | 255 |
| Figure 7.18. Overview of potential interactions of SIRT6 with the pathophysiological process of atherosclerosis..... | 257 |
| | |
| Figure 8.1. key experimental procedures conducted in Chapter 3..... | 268 |
| Figure 8.2. Summary on the consequences of OXPHOS in inflammatory and PNLA-treated cells..... | 276 |

Table of Tables

| | |
|---|-----|
| Table 1.1. Similarities between atherosclerosis and RA..... | 7 |
| Table 1.2. List of monocyte subsets in humans, their markers, their ligands, and their general functions | 14 |
| Table 1.3. Subsets of human macrophages, stimuli, and general functions..... | 17 |
| Table 1.4. Classifications of cytokines in RA..... | 22 |
| Table 1.5. Cytokines implicated in the pathogenesis of RA and their sources..... | 23 |
| Table 1.6. Some selected natural nutritional elements and their effects on RA. | 47 |
| Table 1.7. EULAR recommendations for the management of RA with DMARDs..... | 50 |
| | |
| Table 2.1. A list of specific materials and their suppliers..... | 68 |
| Table 2.2. Antibodies used in flow cytometry | 70 |
| Table 2.3. Identical isotypes for the antibodies used in flow cytometry..... | 70 |
| Table 2.4. Antibodies used in Sort Aria III are specific for monocyte sorting..... | 69 |
| Table 2.5. Concentrations of PNLA were used throughout the study. | 70 |
| Table 2.6. The vehicle control constitution..... | 70 |
| Table 2.7. Purity checks for CD14CD16 monocytes from RA patients. | 84 |
| Table 2.8. Protocol for ELISAs; human TNF- α , IL-6, and IL-1 β supernatants..... | 93 |
| Table 2.9. Human TNF- α , IL-6, and IL-1 β antibodies and standards used in ELISAs experiments. ... | 94 |
| Table 2.10. The pipetting summary for the wells in the PGE2 ELISA plate..... | 97 |
| Table 2.11. QC of RNA samples from PBMCs as per the Nanodrop spectrophotometer. | 106 |
| Table 2.12. QC of RNA samples from PBMCs used for library preparations as per TapeStaion. | 107 |
| Table 2.13. QC of RNA samples from monocytes that were used for library construction as per the Nanodrop spectrophotometer..... | 108 |
| Table 2.14. QC of RNA samples from monocytes that were used for library construction as per the TapeStaion..... | 109 |
| | |
| Table 5.1. Genes that overlap between 2 comparison groups in HCs..... | 168 |
| Table 5.2. Genes that overlap between 3 comparison groups in HCs..... | 171 |
| Table 5.3. Genes that are upregulated by LPS and downregulated by PNLA in RA..... | 173 |
| Table 5.4. Genes that are downregulated by LPS and upregulated by PNLA | 175 |
| Table 5.5. Genes that overlap between the 3 comparison groups in RA | 177 |
| Table 5.6. NF- κ B measurement prediction is inhibited. | 181 |
| Table 5.7. STAT1 measurement prediction is inhibited. | 183 |
| Table 5.8. PPAR- α measurement prediction is activated..... | 185 |
| Table 5.9. PPAR- δ measurement prediction is activated..... | 186 |

| | |
|--|-----|
| Table 6.1. The granularity of unstimulated or LPS-stimulated CD14 ⁺ monocytes after vehicle or PNLA exposure. | 210 |
| Table 6.2. Correlation analysis of the reduction in CD14 ⁺ cells expressing cytokines against a variety of clinical indices and laboratory biomarkers. | 217 |
| Table 7.1. Down-regulated protein-coding genes. | 234 |
| Table 7.2. Upregulated protein-coding genes | 235 |
| Table 7.3. Down-regulated miRNAs | 236 |
| Table 7.4. Upregulated miRNAs. | 237 |
| Table 7.5. Selected miRNAs target mRNA and the relevant associated pathways as per the IPA database. | 238 |
| Table 7.6. Top predicted upstream regulators based on the IPA dataset. | 252 |

Acknowledgement

I would like to sincerely thank Almighty Allah, the Lord of the universe (God), for His richest grace and mercy for the accomplishment of this thesis.

The completion of this thesis would not have been possible without the help, support, and guidance of numerous people in both the Sir Martin Evan and Tenovus buildings, all of whom I would like to thank.

I would like to take this opportunity to express my thanks to my supervisors, Prof. Ernest Choy, and Prof. Dipak Ramji, for finding me a PhD project and for their professional guidance and encouragement during this research. Your scientific input and valuable feedback during my research have been greatly appreciated while allowing me the room to work on my way. Thanks, both for always making time for my project and for being patient with all my questions. I am very grateful for the multitude of opportunities you have given me, including presenting my research abroad and developing many new skills. I would like to deeply thank my advisor, Dr. Peter Watson for his continuous support and guidance.

Throughout my PhD, many people have helped me in many ways to reach this point, and I am so grateful to have met you all. Thank you during my time at Cardiff and for getting me through the bad science days. I extend my gratitude to Dr. Robert Andrews for the bioinformatic assistance. A special thanks go to Dr. James Burston for the great scientific guidance. Many thanks to Dr. You Zhug for his most welcome assistance with the transcriptome analysis. Thank you to my other colleagues, especially Dr. Jess Williams, Dr. Victoria O'Morian, Yee Chan, Dr. Ismail Taban, and Hyun Sun. I wish to express my appreciation to them for taking the time to teach me various practical skills and techniques during the last 4 years. Finally, I would like to acknowledge our colleagues at Wales Gene Park (WGP) for their insight and expertise that assisted this research, for their technical support in generating the next-generation sequencing data. WGP is an infrastructure support group funded by the Welsh Government through Health and Care Research Wales.

A special thank you must go to all the patients from the rheumatology clinic and volunteers who donated blood samples for my study, and to all the doctors and nurses who helped with obtaining patients' consents and taking the samples.

A big thank you to my wonderful family, and my husband, Moammar, who has believed that I could do this from day one, even when I didn't believe it myself. Thanks for putting up with a grumpy wife. I am very grateful to my lovely daughters Maab, Mareb, and Mtab, who have been asking me every day when I am going to finish my studies so I can spend more time with them, and they are so proud of my achievement. Thanks for their patience, love, and support and for being a source of inspiration during my PhD study. Without you, this end would not have been easily accomplished. A very special thank you to my amazing mum for being so encouraging with her unwavering support throughout my life, I will be eternally grateful. I can never thank you enough, mum, you are my inspiration, and I appreciate your prayers and wishes for me to succeed in my studies. I would like to express my deepest gratitude to my brothers and sisters. I cannot list all the names, but you are all in my mind.

A debt of gratitude is owed to the Libyan government for the financial support. Also, I am greatly beholden to my home country, from which I received this opportunity to complete my postgraduate studies at Cardiff University.

Publications and Presentations Arising during this PhD

Manuscripts

Takala, R., Ramji, D.P and Choy, E. 2023. The beneficial effects of pine nuts and its major fatty acid, pinolenic acid, on inflammation and metabolic perturbations in inflammatory disorders. *Int. J. Mol. Sci.* **2023**, 24(2), 1171; <https://doi.org/10.3390/ijms24021171>

Takala, R., Ramji, D.P., Andrews, R., Zhou, Y., Farhat, M., Elmaji, M., Rundle, S., and Choy, E. 2022. Pinolenic acid exhibits anti-inflammatory and anti-atherogenic effects in peripheral blood-derived monocytes from patients with rheumatoid arthritis. *Sci Rep* **12**, 8807 <https://doi.org/10.1038/s41598-022-12763-8>

Takala, R., Ramji, D.P., Andrews, R., Zhou, Y., Burston, J. and Choy, E. 2021. Anti-inflammatory and immunoregulatory effects of pinolenic acid in rheumatoid arthritis. <https://doi.org/10.1093/rheumatology/keab467>

Conference abstracts/presentations

Anti-inflammatory and immuno-metabolic effects of Pinolenic acid in rheumatoid Arthritis **Oral presentation at the Infection and Immunity Annual Meeting, Cardiff, December 2021.**

R. Takala, D. Ramji, R. Andrews, Y. Zhou, J. Burston, and E. Choy. The therapeutic effects of omega-6 PUFA (Pinolenic acid) on the transcriptomic profile of activated peripheral blood mononuclear cells isolated from healthy controls and rheumatoid arthritis patients. DOI: 10.1136/annrheumdis-2021-eular.747 **e-Poster presentation and poster tour at the EULAR Meeting, Madrid, June 2021.**

Anti-inflammatory and immunoregulatory effects of Pinolenic Acid in rheumatoid arthritis **Oral presentation at the Speaking of Sciences Conference at Cardiff University, May 2021.**

The therapeutic effects of Omega-6 PUFA (Pinolenic acid) on the transcriptomic profile of PBMCs isolated from healthy controls and Rheumatoid patients **e-Poster presentation at the British Society of Immunology, December 2020.**

Transcriptomic Profile of Pinolenic acid treatment of activated PBMCs isolated from Rheumatoid Patients **e-Poster presentation at Infection and Immunity Annual Meeting, Cardiff, November 2020.**

Takala, R., Ramji, D. and Choy, E. P201 Anti-inflammatory and immunologic actions of pinolenic acid in rheumatoid arthritis, *Rheumatology*, Volume 59, Issue Supplement 2, April 2020, keaa111.196 **e-Poster presentation at British Society of Rheumatology, April 2020.**

Takala, R and Choy, E. Anti-inflammatory, and immunologic actions of pinolenic Acid **Poster presentation at British Society of Immunology, Liverpool, December 2019.**

Takala, R and Choy, E. Anti-inflammatory and immunologic actions of pinolenic acid **Poster presentation at the Infection and Immunity Annual Meeting, Cardiff, November 2019**

Takala, R and Ramji, D, P. Pinolenic acid acts as an anti-inflammatory and anti-atherogenic agent **Poster presentation at Cardiff University, Postgraduate Research Day, April 2018.**

Prizes

The Rank Prize for Nutrition Award, September 2020.

Abbreviations

AA- Arachidonic acid
ACR- American college of rheumatology
AGO2- Argonaute RISC catalytic component 2
AKT/PKB- Protein kinase B
ALA -alpha-lipoic acid
AMPK- AMP-activated protein kinase
ANOVA- Analysis of variance
Anti-CCP- Anti-cyclic citrullinated peptide
Arg2- Arginase 2
ATP- Adenosine triphosphate
BAM- binary alignment and map
BFA- Brefeldin A
BP- Base pair
BrdU-5-Bromo-2'-deoxyuridine
BSA- Bovine serum albumin
CCL2- Chemokine ligand type 2
CCR2- C-C chemokine receptor type 2
CD- Cluster of differentiation
cDNA- Complementary DNA
CIA- Collagen-induced arthritis
COX- Cyclooxygenase
CRP- C-reactive protein
CTLA4- Cytotoxic T lymphocyte antigen-4
CV- Crystal violet
CVD- Cardiovascular disease
CYP7A1- Cytochrome p450 family 7 subfamily A member 1
DAMP- Danger-associated molecular pattern
DAP3- Death-associated protein-3
DAS- Disease activity score
DC- Dendritic cell
DCFDA- 2'7'-dichlorofluorescein diacetate2'7'
DD-Disease duration
DEG- Differentially expressed gene
DGLA- Di-homo gamma linolenic acid
DHA- Docosahexaenoic acid
DMARD- Disease-modifying anti-rheumatic Drug
DMSO- Dimethyl sulfoxide
DNA- Deoxyribonucleic acid
DPA- Docosapentaenoic acid
EBV- Epstein Barr Virus
EC- Endothelial cell
ECM- Extracellular matrix
EDTA-Ethylenediaminetetraacetic acid disodium salt dihydrate
ESR- Erythrocyte sedimentation rate
EULAR- European Alliance of Associations for Rheumatology
EPA- Eicosapentaenoic acid
ELISA- Enzyme-linked immunosorbent assay
ELOVL5- Elongase of Very-Long Fatty Acid 5
EPO- Evening primrose oil
ERK- Extracellular signal-related kinase

EtrA- Eicosatrienoic acid
FA- Fatty acid
FAD- Flavin adenine dinucleotide
FADD- Fas-associated death domain
FAME- Fatty acid methyl ester
FAO- Food agricultural organization
FBP-1- Fructose biphosphatse-1
Fc- Fragment crystallisable
FGF- Fibroblast growth factor
FoxP3- Forkhead box P3
FPKM- Fragments per kilobase of transcript per million mapped
FSC- Forward scatter
GC- Glucocorticoid
GLA- Gamma-linolenic acid
GO- Gene-ontology
GPCR-G protein-coupled receptor
GPI- Glycosylphosphatidylinositol
GSEA- Gene set enrichment analysis
GSH-Glutathione
GTF-Gene transfer form
GWAS-Genome-Wide Association Study
HDL- High-density lipoprotein
HIF1-Hypoxia-inducible factor 1
HI-FCS- Heat-inactivated foetal calf serum
HLA- Human leucocyte antigen
HMDM- Human monocytes derived macrophages
HMG- CoA 3-Hydroxy-3-methyl-glutaryl-coenzyme-A
HRP- Horseradish peroxidase
IA- Inflammatory arthritis
ICAM- Intracellular adhesion molecule
IKK- IKappa B kinase
IKK α - Inhibitor of nuclear factor kappa-B kinase subunit alpha
IL- Interleukin
iNOS- Inducible nitric oxide synthetase
IPA- Ingenuity pathway analysis
IRAK4- IL-1 receptor-associated kinase 4
JAK- Janus-activated kinase
JNK- c-Jun N-terminal kinase
KLF15- Kruppel like factor 15
LA- Linolenic acid
LC- Long chain
LDL- Low density lipoprotein
Let-7 -Letal-7
LIF- Leukemic inhibitory factor
lncRNA- Long non-coding RNA
Log2FC- Log2 fold change
LOX- Lipoxygenase
LPS- Lipopolysaccharide
LRP-Low-density lipoprotein receptor-related protein
LXR- Liver X receptor
LY- Lucifer yellow

MACS- Magnetic-activated cell sorting
MAPK- Mitogen activated protein kinase
MCP-1- Monocyte chemoattractant protein-1
MD- Mediterranean diet
MDA- Malondialdehyde
MHC- Major histocompatibility complex
miRNAs- MicroRNA
MMF - Mycophenolate mofetil
MMP- Matrix metalloproteinase
mRNA- Messenger RNA
MTX- Methotrexate
MUFA- Monounsaturated fatty acid
NAD- Nicotinamide adenine dinucleotide
NDRG2- N-myc downregulated gene
NF- κ B- Nuclear factor-kappa B
NGS- Next-generation sequencing
NK- Natural killer
NO- Nitric oxide
NOS- Nitric oxide synthase
NSAID- Nonsteroidal anti-inflammatory drug
O₂⁻-Superoxide
OA- Osteoarthritis
ONOO- Peroxynitrite
OXPHOS- Oxidative phosphorylation
PAMP- Pathogen-associated molecular pattern
PAI-1- Plasminogen activator inhibitor 1
PB- Peripheral blood
PBMC- Peripheral blood mononuclear cell
PBS- Phosphate buffered saline
PCA- Principle component analysis
PDK4- Pyruvate dehydrogenase kinase-4
PCSK9- Proprotein convertase subtilisin/kexin 9
PFH- Paraformaldehyde
PGE2- Prostaglandin E2
PI3K- Phosphoinositide-3-kinase
PKC- Protein kinase C
PLA2- Phospholipase A2
PMA- Phorbol-12-myristate-13-acetate
PNLA- Pinolenic acid
PPAR- Peroxisome proliferator activated receptor
PTPN22-Protein tyrosine phosphatase, non-receptor type 22
PUFA- Polyunsaturated fatty acid
qPCR- Quantitative polymerase chain reaction
RA- Rheumatoid arthritis
RANKL- Receptor activator of nuclear factor-kB ligand
RASf- Rheumatoid arthritis synoviocyte-like fibroblast
RBC-Red blood cell
RCT-Randomized control trial
RF-Rheumatoid factor
RIN- RNA integrity number
RNA-seq- RNA sequencing

ROS- Reactive oxygen species
rRNA- Ribosomal RNA
RUNX2- Runt Related Transcription Factor 2
SC- Scavenger receptor
SEM- Standard error of the mean
SERPINE-1- Serine protease inhibitor-1
SF-Synovial fluid
SHP2- SH2 domain containing tyrosine-protein phosphatase
SIGIRR- Single-immunoglobulin interleukin-1 receptor-related molecule
SIRTS- Sirtuin
SM- Synovial macrophages
SMC-Smooth muscle cell
SOCS- Suppressor of cytokine signalling
SOD- Superoxide dismutase
SREBP2- Sterol regulatory element-binding transcription factor 2
SSC- Side scatter
STAT- Signal transducers and activators of transcription
TBHP- Tert- butyl hydrogen peroxide.
TCA- Tricarboxylic acid/ Krebs cycle
TFE3 - Transcription Factor E3
TGFb-Transforming growth factor-beta
Th-T helper
TLR- Toll-like receptor
TMP- 3,3',5,5'-Tetramethyl benzidine
TNF- α - Tumour necrosis factor- α
TRADD- TNFR1 associated death domain
TRAF2- TNF- α receptor-associated factor-2
TREM1- Triggering receptor expressed on myeloid cells 1
Tyk2- Tyrosine kinase 2
VCAM- Vascular cell adhesion molecule
VEGF- Vascular endothelial growth factor
VSMCs- Vascular smooth muscle cells
WGT- Whole genomic transcriptome

Declaration of Authorship

I, Rabaa Takala, declare that this thesis and the work presented in it are my own and have been generated by me as the result of my original research. I confirm that:

- 1. This work was done wholly or mainly while in candidature for a research degree at this University.*
- 2. Where any part of this thesis has previously been submitted for a degree or any other qualification at this University or any other institution, this has been clearly stated.*
- 3. Where I have consulted the published work of others, this is always clearly attributed.*
- 4. Where I have quoted from the work of others, the source is always given. Except for such quotations, this thesis is entirely my own work.*
- 5. I have acknowledged all the main sources of help.*
- 6. Where the thesis is based on work done by myself jointly with others, I have made clear exactly what was done by others and what I have contributed myself.*
- 7. I was responsible for the experimental work undertaken in this thesis, excluding:*
 - I. The author was not responsible for recruiting eligible patients for the study. This was undertaken by Professor Ernest Choy.*
 - II. Library preparation, QC, and bulk mRNA-seq were performed by members of Wales Gene Park at Cardiff University. This is detailed in the Chapter on Materials and Methods.*
 - III. While the majority of the statistical analysis was performed by the author, initial bioinformatics: gene alignment, mapping to reference genome and differential expression of the raw data were performed by Dr Robert Andrews.*
 - IV. Two figures in Chapter 2: Methods (figure 2.16, 2.17) for QC RNA and the completed library were provided by Wales Gene Park. Chapter 5 (figure 5.2) and Chapter 7 (figure 7.2, 7.3) principal component analysis were provided by Dr. Robert Andrews.*
 - V. The author was not responsible for sorting and purifying of CD14CD16 monocytes for RNA sequencing. In Chapter 2 (figure 2.5), the sorting of CD14CD16 monocytes on FACS Sort Aria III was undertaken by members of CBS at Cardiff University under the authors' supervision of the gating strategy.*
 - VI. The scientific writing of the methodology of RNA-seq was corrected and revised by members of the Wales Gene Park at Cardiff University.*

This statement has been supplied on the understanding that it is copyright material, ownership, and that no quotation from the thesis has been published without proper acknowledgement.

Signed:Rabaa Takala.....

Date:04.11.2022.....

Abstract

Introduction: Rheumatoid arthritis (RA) is an autoimmune inflammatory disease that causes chronic joint inflammation. Cardiovascular disease (CVD) is the leading cause of death in patients with RA due to accelerated atherosclerosis. In addition, patients have a higher susceptibility to plaque instability and atherothrombosis. Monocytes and macrophages cause synovitis and produce pro-inflammatory cytokines. Despite the increasing number of new treatments, complete long-term disease remission is rarely achieved. Moreover, side effects and safety concerns lead to poor adherence. The American College of Rheumatology (ACR) and the European Alliance of Associations for Rheumatology (EULAR) recommend consuming a healthy and balanced diet to reduce the risk of RA. However, there is no specific recommendation for a specific type of food due to limited scientific evidence.

Previous research on omega (n)-3 and -6 polyunsaturated fatty acids (PUFAs) has demonstrated anti-inflammatory and anti-atherogenic properties. Preliminary studies on pinolenic acid (PNLA), which is one of the unusual PUFAs found in pine nuts, showed anti-inflammatory actions in cell lines and animal models, while patients' samples have not been studied. This project aims to explore the therapeutic potential of PNLA in RA and atherosclerosis.

Methods: The THP-1 cell line and primary culture of human macrophages were initially used, followed by peripheral blood (PB) samples from RA patients and healthy individuals (HIs). Release of IL-6, TNF- α and IL-1 β after lipopolysaccharide stimulation (LPS) by monocytes and macrophages was measured intra-cellularly and in cell-free supernatants with or without PNLA treatment. RNA sequencing was used to assess the gene expression level of peripheral blood mononuclear cells (PBMCs) and purified monocytes. Bioinformatic analyses were used to explore the effects of PNLA on biological pathways.

Results: Key pro-atherogenic processes were inhibited by PNLA *in vitro* and *ex vivo*. PNLA does not affect the viability or proliferation of the THP-1 cell line, primary culture of macrophages or PBMCs from RA patients or HCs. PNLA attenuated monocyte chemoattractant protein-1 (MCP-1) or CCL2-induced monocyte migration, reduced micropinocytosis, and oxidised low-density lipoprotein (ox-LDL) uptake by macrophages. Gene expression analysis revealed that PNLA attenuated several key pro-inflammatory genes and regulated metabolic genes and transcription factors. Several mitochondrial pathways, such as mitochondrial phosphorylation and mitochondrial dysfunction, were identified as being regulated by PNLA. PNLA also has protective effects as identified by canonical pathways and differentially expressed genes such as pyruvate dehydrogenase kinase-4 (PDK4), serine protease inhibitor-1 (SERPIN1), fructose biphosphate-1 (FBP1), and single-immunoglobulin interleukin-1 receptor-related molecule (SIGIRR). MicroRNAs (miRNAs) were discovered to be regulated by PNLA, suggesting potential post-transcriptional regulation of the immune response that has not been described previously.

Conclusion: PNLA has anti-inflammatory and metabolic effects in experimental and *ex vivo* studies in patients with RA. Dietary supplements with PNLA may be beneficial for articular and vascular diseases in patients with RA through their immuno-metabolic effects and can potentially augment current treatments. Therefore, PNLA is a promising dietary element for RA and atherosclerosis. These beneficial effects have been illustrated in this thesis, and the necessary functional studies and clinical trials to further complement this work have also been discussed.

Chapter 1: General Introduction

1.1 Rheumatoid arthritis (RA)

Rheumatoid arthritis (RA) is a chronic inflammatory disease characterised by symmetrical polyarthritis. It is more prevalent among women than men (3:1) and has a peak incidence at 50-60 years of age (Cross *et al.* 2014). Systemic manifestations include anaemia, fatigue, depression, osteoporosis, and cardiovascular diseases (CVD) (Choy 2012). CVD is the leading cause of death in patients with RA. Despite the increasing number of new treatments, complete long-term disease remission is not achieved for many patients (Guo *et al.* 2018).

1.1.1. Diagnosis of RA

RA is typically divided into two subtypes designated ‘seropositive’ and ‘seronegative’, with seropositivity being defined as the presence of rheumatoid factor (RF) and/or antibodies to citrullinated protein/peptide antigens (ACPAs) in the serum. Between 70% and 80% of patients with RA have RF, which are autoantibodies directed against the Fc fragment of IgG. ACPAs are specific to RA and are associated with disease severity (Deane *et al.* 2017). RF or ACPA can be found before the diagnosis of RA. The diagnosis criteria developed in 2010 by the European Alliance of Associations for Rheumatology (EULAR) and the American College of Rheumatology (ACR) contain mainly descriptions of joint inflammation and pain as well as immunological criteria, i.e., the presence of ACPAs and/or RFs (Catrina *et al.* 2016).

1.2 Clinical features

1.2.1. Articular manifestations

Patients with RA present with polyarthritis involving the small joints of the hands and feet, although monoarticular presentation can occur initially. Most patients experience morning stiffness that persists for more than an hour. Patients may also present with difficulties performing daily activities and reduced grip strength (Nordenskiöld 1990). Synovitis, with an accumulation of inflammatory cells, predominantly T cells and macrophages, but also B cells, plasma cells, and dendritic cells (DCs), synovial hyperplasia, and angiogenesis, are prominent features in RA. Many pro-inflammatory cytokines, including interleukin-1 (IL-1), interleukin-6 (IL-6), tumour necrosis factor (TNF), and granulocyte–macrophage colony-stimulating factor (GM-CSF), are produced within the inflamed joint (McInnes and Schett 2007). In RA, inflammation of synovial tissue leads to progressive damage, erosion of adjacent cartilage, bone, and chronic disability, as well as radiological abnormalities including periarticular erosions and osteopenia.

Pain is one of the key clinical features and a significant problem in RA. It is caused by the infiltration of immune cells into the synovium of the joints. Activated immune cells secrete pro-inflammatory mediators, which convert n-6 polyunsaturated fatty acids (PUFA) and arachidonic acid (AA) in the cell membrane to prostaglandins (PGs), particularly PGE2, and thromboxans (TXs) through the cyclooxygenase (COX) enzymes (Abdulrazaq *et al.* 2017). PGE2 increases vascular permeability, vasodilation, and the production of destructive matrix metalloproteinases (MMPs) (Abdulrazaq *et al.* 2017).

1.2.2. Extra- articular manifestations

Extra-articular diseases occur in approximately 40% of patients with RA (Moura *et al.* 2011; Turesson *et al.* 2003). These include subcutaneous nodules, serositis, episcleritis, glomerulonephritis, pulmonary granulomas, and small vessel vasculitis (Guo *et al.* 2018).

1.3 Epidemiology of RA

RA is the most common autoimmune inflammatory arthritis (IA) and affects approximately 1 in 100 people worldwide (Gibofsky 2012; Taylor 2020). In Western countries, the incidence of RA is estimated to be 10-50 per 100,000 people annually (Alamanos *et al.* 2006; Eriksson *et al.* 2013), although the prevalence of RA varies with time and country. In the UK, prevalence has decreased over recent years (Abhishek *et al.* 2017). A higher prevalence has been reported in certain Native Americans and a very low frequency of RA in some areas of rural Africa (Aviña-Zubieta *et al.* 2008; Sholter and Armstrong 2000); the adoption of a Western diet and sedentary work habits might be related. RA is a common cause of severe long-term pain and physical disability (Hagen *et al.* 2012), contributing to societal and economic costs, including loss of productivity in the workplace (Connolly *et al.* 2015). RA not only affects the people suffering from it but also their families in terms of emotional and social costs (Brouwer *et al.* 2004; Jacobi *et al.* 2001; Matheson *et al.* 2010).

1.3.1. Cardiovascular diseases (CVDs) as the major cause of increased mortality in RA patients

RA patients have a higher prevalence of preclinical atherosclerosis, such as asymptomatic carotid artery atherosclerotic plaques, than the general population (Roman *et al.* 2006). CVDs are responsible for about 50% of all global deaths in patients with RA (Arora *et al.* 2016; Jagpal and Navarro 2018). A meta-analysis covering 111,758 patients found a 50% increased risk of CVD death, with ischemic heart disease (IHD) and cerebral vascular accidents (CVA) accounting for 59% and 52% increased risks, respectively (Aviña-Zubieta *et al.* 2008). A more recent meta-analysis of 14 observational studies concluded a 48% increase in the incidence of

CVDs in patients with RA, with the risk of myocardial infarction (MI) and CVA being increased by 68% and 41%, respectively, and one study found an 87% increased risk of congestive heart failure (CHF) (Avina-Zubieta *et al.* 2012). Another meta-analysis of 17 studies enrolling 124,894 RA patients reported a significantly increased risk of both MI and ischemic stroke (Carbone *et al.* 2018).

1.4 Cardiovascular diseases (CVDs) in RA

1.4.1 Traditional cardiovascular risk factors do not predict CVD events in RA.

The clinical features and risk factors for CVDs in patients suffering from RA differ significantly from those in the general population. In RA, silent IHD and sudden death are more common (Gabriel 2008). Traditional cardiovascular risk factors such as hypertension (HTN), diabetes mellitus (DM), obesity, and hyperlipidemia are common in RA patients. Some treatments for RA, such as glucocorticoids (GCs) and non-steroidal anti-inflammatory drugs (NSAIDs), have been associated with an increased risk of MI (Choy *et al.* 2014). These features are identified as potential additional cardiovascular risk factors in RA patients. Some authors consider atherosclerosis an extra-articular manifestation of RA since traditional cardiovascular risk factors, do not fully predict future cardiovascular events in RA patients (Choy *et al.* 2014). Instead, systemic inflammation is associated with increased cardiovascular events in RA, which will be discussed in section (1.4.2). Consequently, EULAR recommended multiplying the traditional cardiovascular risk score by 1.5 to compensate for RA-associated increased risk (Agra *et al.* 2017).

1.4.2 Risk factors for CVD events in RA

1.4.2.1 RA-associated genes

Gonzalez-Gay *et al.* investigated the role of human leukocyte antigen-DRB1 (HLA-DRB1) on both cardiovascular mortality and morbidity and first published the association between genetic risk factors for RA and increased risk for CVDs (Gonzalez-Gay *et al.* 2007). Gonzalez-Gay *et al.* found that having a single or double copy of HLA-DRB1*0404 was associated with cardiovascular events and mortality. This was further confirmed in 2008 by Farragher *et al.* who reported an association between HLA-DRB1 alleles and cardiovascular mortality. In their study, they found that carrying two copies of HLA-DRB1*01/04 was associated with a two-fold increased risk of cardiovascular death compared with having one or no (shared epitope) SE allele (Farragher *et al.* 2008). A study by Palomino-Morales *et al.* indicated that patients with RA who have a polymorphism in the MTHFR gene have a significantly increased risk of

suffering cardiovascular events compared with those who do not have this polymorphism (Palomino-Morales *et al.* 2010).

1.4.2.2 RA autoantibodies

Many studies have shown that RF positivity is significantly associated with increased CVDs, with a 3-fold increased risk of mortality after adjusting for age, sex, disease severity, and smoking (Goodson *et al.* 2002). The Hertfordshire Cohort Study (Edwards *et al.* 2007) found a significant association between RF positivity and prevalent IHD. Another study found subjects with ACPA-positive RA have a greater prevalence of CVD independent of traditional risk factors, such as smoking and CRP levels (Cambridge *et al.* 2013). The authors hypothesised that the presence of ACPA might impair the resolution of inflammation within the atherosclerotic plaque, enabling the progression of lesions (Cambridge *et al.* 2013).

1.4.2.3 Lipids

RA is associated with a unique type of dyslipidemia characterised by high levels of triglycerides (TGs) and low levels of low-density lipoproteins (LDL) and high-density lipoproteins (HDL), known as the “lipid paradox” (Frommer *et al.* 2010). Although lipoprotein levels are low, there is a paradoxical increase in CVD risk. Low lipoprotein levels are associated with elevations in ESR and CRP (Urman *et al.* 2018). Furthermore, a clinically significant portion of HDL is altered in structure and function instead of being anti-inflammatory and atheroprotective. RA patients are more likely to have a pro-inflammatory form of HDL, named piHDL, which enhances LDL oxidation and foam cell formation, hence an atherosclerotic plaque. The altered lipid profile in RA is thought to cause an increased instability of atherosclerotic plaques, which is responsible for increased cardiovascular events (Carbone *et al.* 2018). ApoA-1 is the major protein present in HDL that induces cholesterol efflux within cells via ATP Binding Cassette Subfamily A Member 1 (ABCA1) and allows nascent HDL to collect free cholesterol. Shifting HDL and ApoA-1 from the circulation to the site of infection or inflammation is another possibility for the development of atherosclerosis. It has been reported that the joints of RA patients are infiltrated by ApoA-1 (Ananth *et al.* 1993). This could be due to the activation of the reticuloendothelial system (RES), which leads to a reduction in lipid components. Choy *et al.* suggested a cytokine-induced activation of the RES, which would lead to a reduction in HDL and total cholesterol (Choy and Sattar 2009). In contrast, suppression of RA-associated inflammation coincides with some increases in lipid values, but also a reduction in cardiovascular events (Myasoedova *et al.* 2011; Steiner and Urowitz 2009). Furthermore, oxidized LDL (ox-LDL) has been shown to directly induce endothelial dysfunction and reduce vasorelaxation by stimulating endothelial cell (EC) death,

as well as enhance the expression of the cytoplasmic adapter protein TNF receptor-associated factor 3 interacting protein 2 (TRAF3IP2) (Valente *et al.* 2014). TRAF3IP2 is known to regulate the activation of nuclear factor kappa-B (NF- κ B) and Janus kinase (JAK) (Li *et al.* 2000), both of which can modulate the immune response and contribute towards atherosclerosis progression.

1.4.2.4 Chronic inflammatory markers

C-reactive protein (CRP) mediates the uptake of LDL and ox-LDL by macrophages, induces LDL deposition, and increases LDL uptake by hepatocytes (Singh *et al.* 2008; Wang *et al.* 2008). It also decreases eNOS expression by destabilising its mRNA and increases the expression of endothelial adhesion molecules like ICAM, VCAM, E-selectin, and chemokine ligand type 2 (CCL2) (Singh *et al.* 2009; Singh *et al.* 2008). Goodson noted that CRP levels of more than 4 mg/l at baseline were associated with an increased risk of CVD death during the follow-up period (Goodson *et al.* 2005; Kaptoge *et al.* 2010). Indeed, in RA, many studies have demonstrated a significant association between inflammatory measures, particularly ESR, and CVDs (Book *et al.* 2005; Innala *et al.* 2011; Maradit-Kremers *et al.* 2007; Myasoedova *et al.* 2011). Gonzalez-Gay *et al.* also confirmed that high levels of both CRP and ESR were associated with both CV morbidity and mortality (Gonzalez-Gay *et al.* 2007).

1.4.3 Inflammation in atherosclerosis and rheumatoid arthritis

Atherosclerosis is a chronic inflammatory disease of the medium and large arteries and the underlying cause of heart attacks and strokes worldwide. RA and atherosclerosis are both considered inflammatory diseases that share genetic and environmental risk factors, including polymorphisms in genes within the HLA region, smoking, obesity (Skeoch and Bruce 2015), and reduced HDL, which is a common finding during infection or inflammation (Szekanecz *et al.* 2007). In addition, patients with RA have a higher susceptibility to plaque instability and atherothrombosis (Karpouzas *et al.* 2014; Van den Oever *et al.* 2014). Current algorithms for cardiovascular risk scores for the general population underestimate CV events in patients with RA due to accelerated atherosclerosis (Carbone *et al.* 2018). In 2013, a comparison study of coronary computed tomography (CT) findings was conducted between patients with and without RA who had no history of clinical CVDs. They found not only an increased plaque burden but also an increased prevalence of 'high risk' lesions in the RA cohort (Karpouzas *et al.* 2014). The clinical trend of patients with RA having fewer 'warning' symptoms and a higher risk of fatality also suggests the presence of a more rupture-prone plaque phenotype called "subclinical atherosclerosis" (Karpouzas *et al.* 2014). Semb *et al.* (2013) also demonstrated by

ultrasonography that RA patients with active disease had a more vulnerable carotid plaque phenotype relative to those with low disease activity. The similarities in the cell activations and cytokines involved in both atherosclerosis and rheumatoid synovitis are summarised in **Table 1.1**. While **Figure 1.1** shows the similarities in key immune processes in both atherosclerotic lesions and inflamed RA synovium.

1.4.3.1 Cytokines

Cytokines associated with RA such as TNF- α , IL-17, IL-6, and IL-1 β are also central to the development of atherosclerosis (Cesari *et al.* 2003; Moss and Ramji 2017; Wæhre *et al.* 2004), with higher levels being present in RA (Pasceri and Yeh 1999). These pro-inflammatory cytokines have been implicated in EC activation, a crucial step in the initiation of atherosclerosis, and synovial pannus formation (Urman *et al.* 2018). The IL-6 pathway is associated with RA and CVDs in the general population (IL6R Genetics Consortium Emerging Risk Factors Collaboration 2012). Elevated IL-6 is associated with higher levels of markers of endothelial dysfunction (ICAM-1) and vascular cell adhesion molecule-1 (VCAM-1) (Dessein *et al.* 2005). Higher IL-6 levels are reported to be associated with increased mortality in patients with acute coronary syndromes (ACS). Genetic variants of cytokines are common risk factors for RA and CVD (Carbone *et al.* 2018). Within the TNF superfamily, at least two variants of TNF- α (rs1800629 and 1799964) are associated with both RA and related CVD complications. Similarly, the IL-1 family (especially IL-33) mediates CVD risk in RA patients (López-Mejías *et al.* 2015). These inflammatory cytokines will be discussed in detail later in this Chapter.

Table 1.1. Similarities between atherosclerosis and RA.

| | Atherosclerosis | RA |
|--|-----------------|----------------------------------|
| <u>Macrophage activation:</u> | | |
| TNFα | ↑ | ↑ |
| Metalloproteinase expression | | |
| IL-6 | ↑ | ↑ |
| IL-1 | ↑ | ↑ |
| <u>T-cell activation:</u> | | |
| Soluble IL-2 receptor | ↑ (UA) | ↑ |
| CD4⁺CD28⁻ | ↑ (UA) | ↑ |
| CD4⁺IFNγ⁺ | ↑ (UA) | ↑ |
| Th1/Th2 balance | ↑ Th1 | ↑ Th1 |
| <u>B-cell activation:</u> | | |
| Autoantibodies (ox-LDL) | 0 or ↑ | 0 or ↑ |
| Rheumatoid factor | 0 | ↑ |
| C-reactive protein | ↑ (UA) | ↑↑ |
| <u>Endothelial cell activation</u> | | |
| Adhesion molecules (VCAM-1, ICAM-1, E-selectin, and P-selectin) | ↑ | ↑ |
| Endothelin | ↑ | ↑ |
| Neo-angiogenesis | ↑ | ↑ |
| Possible antigens | Ox-LDL | Collagen II, cartilage antigens. |
| NO | ↑↑ | ↑ |

Ox-LDL, oxidised low-density lipoproteins; ↑, increased; ↑↑, markedly increased; UA, unstable angina; NO, nitric oxide; ICAM/VCAM, intracellular adhesion molecules/vascular cell adhesion molecules. Modified from Pasceri and Yeh (1999).

1.4.3.2 T cells, monocytes, and macrophages

Of interest, many pathophysiological features of atherosclerotic plaques mirror those occurring in the inflamed RA synovium (**Figure 1.1**). Indeed, endothelial activation, infiltration by monocytes, macrophages, and type 1 T helper (Th1) cells, neovascularization, the release of matrix-degrading metalloproteinase enzymes, and collagen degradation characterise both diseases (Skeoch and Bruce 2015; Carbone *et al.* 2018). In a cohort study of 72 patients with RA who underwent cardiac CT to assess coronary artery calcification (CAC), 33% had CAC and exhibited significant increases in the levels of circulating CD4 T cell subsets, CD8 T cell subsets, and the CD14⁺CD16⁺ intermediate monocyte subset when compared to those patients without CAC. The levels of CD4⁺CD56⁺CD57⁺ T cells and the CD14⁺CD16⁺ monocytes remained associated with the presence of CAC (Winchester *et al.* 2016) after adjusting for multiple confounders. The CD4 and CD8 T cell subsets increases were highly intercorrelated, while increases in CD14⁺CD16⁺ monocytes were independent of the elevated CD4 subsets (Winchester *et al.* 2016). These findings suggest that PBMC subsets are markers for the presence of CAC and that the mechanisms of atherogenesis in RA may be related to the elevations in these subsets.

In summary, evidence supports that inflammation is the major driver of excess atherosclerosis in RA (Gonzalez-Gay *et al.* 2007; Sattar and McInnes 2005). In RA, synovitis results in the activation and enhanced recruitment of inflammatory cells, and further increases the release of inflammatory cytokines, chemokines, and adhesion molecules. These steps are the same mechanism proposed in atherosclerosis pathogenesis (**Figure 1.1**). From this, it can be concluded that cytokines generated in the inflamed synovium have secondary effects on the vessel wall, or there may be a simultaneous process affecting both the synovium and arteries in RA.

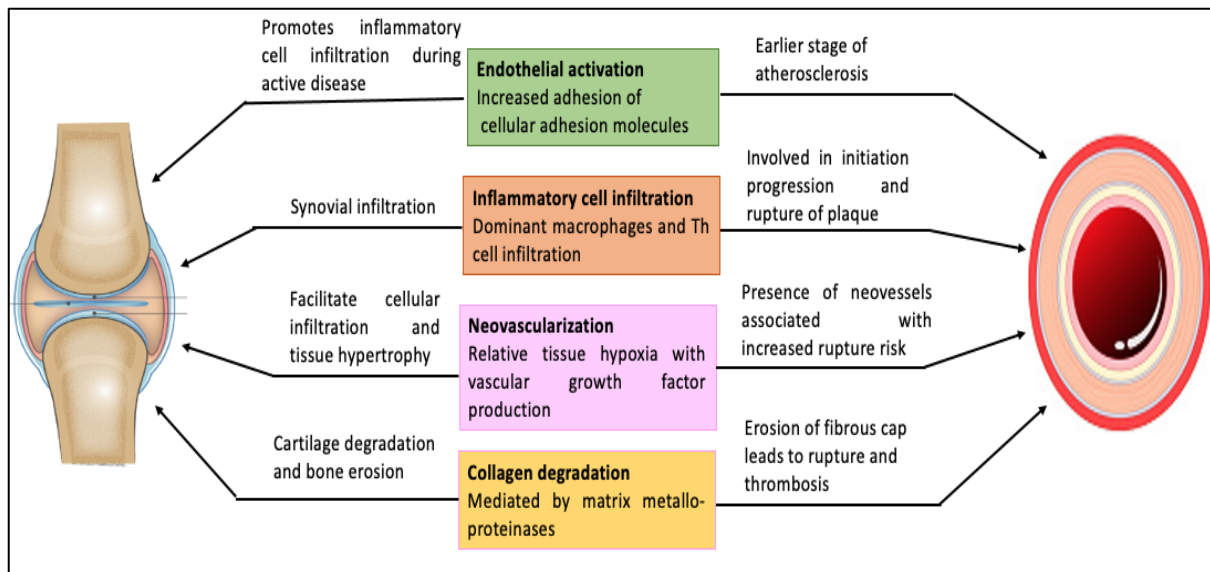


Figure 1.1. Important pathological features are common to both the inflamed rheumatoid synovium and atherosclerotic plaque. Adapted from Skeoch and Bruce (2015).

1.5 The pathogenesis of RA

1.5.1 Overview

The pathogenesis of RA is still not fully understood. However, genetic factors along with environmental factors likely represent the main aetiology of the disease (Gibofsky 2012), as summarised in **Figure 1.2**. Hyperplasia of the synovium is accompanied by inflammatory cell infiltration, angiogenesis, bone and cartilage erosion, and T-cell imbalance, in addition to activated B cells, monocytes, macrophages, and ECs that produce cytokines and chemokines. Both the innate and adaptive immune cells contribute to the amplification and perpetuation of the chronic inflammatory state. Cytokines such as TNF- α , IL-6, and IL-1 β play key roles in the pathogenesis of RA. Cytokine inhibitors have indicated a critical role for TNF- α and IL-6 in disease pathogenesis, which has been extensively studied (Gioxari *et al.* 2018). More recently, clinical trials with JAK inhibitors have shown that cytokine receptors that signal through the JAK-signal transducer and activator of transcription (STAT) signalling pathway are important in disease pathogenesis, further informing the pathogenetic function of additional cytokines. Chemokines such as monocyte chemoattractant protein-1 (MCP-1) or CCL2, and macrophage-colony stimulating factor (M-CSF) (Bobryshev 2006) play a critical role in recruiting monocytes and T cells to the site of the inflammation and also promote the influx and differentiation of the monocytes into osteoclasts.

1.5.1.1 Genetic involvement

A major conclusion from genetic data is that ACPA-positive RA is very dependent on MHC class II-driven adaptive immunity. However, the general heritability and the number of polymorphisms associated with ACPA-negative diseases are much lower than those associated with ACPA-positive diseases (Catrina *et al.* 2016). ACPA-negative RA most probably consists of several different subsets, and adaptive immunity appears to be less important in these subsets. Although the clinical presentation at disease initiation is very similar between patients with ACPA-positive and ACPA-negative RA, the disease course, possibly disease pathogenesis, and genetic susceptibility are different (Viatte *et al.* 2013).

1.5.1.2 Environmental factors

1.5.1.2.1 Smoking

Lahiri *et al.* found that the effect of smoking on susceptibility to RA is dose-related, stronger in males and that upon smoking cessation, there is a 20-year latency in the baseline risk (Lahiri *et al.* 2012). There is a striking association between smoking, HLA-DR, and ACPA-positive RA (Deane *et al.* 2017). Smokers carrying 2 HLA-DR alleles have a 21-fold increased risk of developing ACPA-positive disease. Furthermore, smoking has long been associated with the presence of RF, even in the absence of RA. Aside from smoking, a series of other noxious agents affecting the lung, including silica dust and solvents, have been associated with ACPA-positive RA (Catrina *et al.* 2016). Notably, there are major interactions between exposures to these agents and the presence of HLA variants predisposing to RA. Key observations are that smoking and other stimuli may initiate citrullination of the series of autoantigens by activation of the citrullinating enzymes. Events in the lungs have potential triggers of autoimmunity to the autoantigens that have been post-translationally modified by citrullination.

1.5.1.2.2 Infection

Anti-*P. gingivalis* antibodies are classified as another risk factor for developing RA (Mankia and Emery 2016). *P. gingivalis* infection leads to citrullinated autoantigen and ACPA production in two ways. First, peptidyl-arginine deiminases can cleave proteins at arginine residues and citrullinate proteins, thereby producing more neoantigens that drive the autoimmune response in RA (Wegner *et al.* 2010). Second, through the neutrophil extracellular trap (NET) formation induced by *P. gingivalis* during the process of NETosis. ACPAs induce NETosis, and in turn, NETosis provides citrullinated autoantigens for ACPA generation (Khandpur *et al.* 2013).

Figure 1.2. shows a model in which genetic and environmental factors interact to initiate autoimmunity, propagate autoimmunity, and ultimately lead to RA. The period of disease development during which there are detectable RA-related biomarkers without a clear disease can be termed ‘preclinical RA’. Importantly, the genetic and environmental factors that influence each of these stages of the disease may be different.

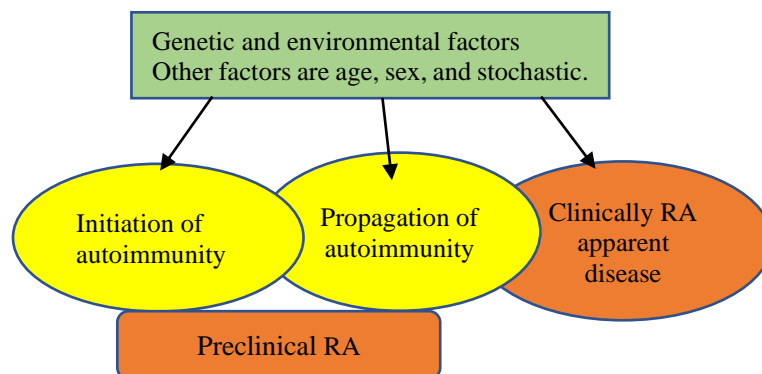


Figure 1.2. A general model showing a summary of RA pathogenesis and development.

1.5.2 T cells

RA is thought to be a T cell-mediated disease based on the presence of CD4⁺ T cells in the inflamed rheumatoid joint. In the inflammatory process of RA, T cells migrate from the bloodstream to the synovial tissue via their interactions with the ECs that line synovial capillary venules. At this stage, selectins, integrins, and chemokines have the main role in blood cell invasion of synovial tissue and therefore in the severity of the inflammatory response (Mellado *et al.* 2015). It is suggested that RA-associated HLA class II molecules present citrullinated peptides that modulate the CD4⁺ T cell response and subsequently activate B cells (Kampstra and Toes 2017). Self-reactive T and B lymphocytes cooperate to promote antibody responses against self-proteins and are major drivers of the disease (Nevius *et al.* 2016). T lymphocytes also promote RA independently of B lymphocytes, mainly through the production of key inflammatory cytokines that promote pathology, such as IL-17.

1.5.3 B cells

B cells are found in the systemic circulation, synovium, BM, and draining lymph nodes (Bugatti *et al.* 2014). B cells and plasma cells are abundantly present in the synovial membrane of patients with RA. The roles of B cells in RA include the production of RF and ACPA (McInnes and Schett 2017; Sweet *et al.* 2011), T-cell activation and cytokine synthesis (Yeo *et al.* 2011), as well as osteoclast activation and immunoregulation through IL-10 (Bugatti *et al.* 2014). It has been discovered that B cells also function as antigen-presenting cells (APC) for T cells. Recently, CD19⁺ B cells produced IL-17 in both RA patients and healthy individuals

(Bugatti *et al.* 2014). B-cells are activated via B-cell receptor (BCR) and toll-like receptor (TLR) signalling. In addition, B-cell tolerance defects have been observed in RA (Bugatti *et al.* 2014), along with the functional impairment of regulatory B-cell circulation and bone homeostasis (Ma *et al.* 2014).

In RA, B cell production of ACPA is strongly predictive of erosive bone disease (Nevius *et al.* 2016). As a therapy for RA, B cell depletion has been successfully implemented over the past decades and works directly through RF and ACPA reduction on B cells or indirectly through B cells (Choy *et al.* 2013).

1.5.4 Monocytes and Macrophages

Although the pathogenesis of RA has not been fully elucidated, monocytes and macrophages have pivotal roles in the initiation and sustaining of synovial inflammation (Rana *et al.* 2018). Bloodstream monocytes migrate into peripheral tissues and differentiate into macrophages and DCs (Auffray *et al.* 2009; Shi and Pamer 2011). Under inflammatory conditions, the differentiation of monocytes into macrophages and DCs is largely regulated by the chemokines M-CSF and GM-CSF (Bobryshev 2006; Hamilton 2008).

1.5.4.1 Characteristics of monocytes

1.5.4.1.1. Phenotypic characteristic of monocytes

In humans and mice, monocytes contribute 4-10% of all circulating leukocytes (Kamei and Carman 2010). Monocytes are heterogeneous populations, and each sub-population mediates host defence and inflammation differently (Hirose *et al.* 2019). Monocytes characteristically express multiple antigens on their cell surface, with some variations among monocyte subsets. Monocytes, along with myeloid series cells, express CD115 (M-CSF) (Ingersoll *et al.* 2010a). They also exhibit specific antigenic expressions and markers; many of these are upregulated in RA (Hirose *et al.* 2019; Rana *et al.* 2018). The most notable are CD14, CD16, TLRs, HLA-DR, and adhesion molecules B1 and B2 integrins, as explained in sections 1.5.4.1.1.1-1.5.4.1.1.5. High expression levels of CD14, a cell surface-localised glycosylphosphatidylinositol (GPI)-anchored monocyte differentiation antigen (Bosshart and Heinzelmann 2016), and a co-receptor with TLR4 to which lipopolysaccharide (LPS) binds are the reason human monocytes are more responsive to LPS than the human leukemic cell line THP-1.

1.5.4.1.1.1. CD14 marker

CD14, expressed on the membrane surface of the monocyte, is the receptor for the LPS-LPS binding protein. The binding of the LPS-LPS binding protein complex to CD14 induces signal transduction through TLR4 on the surface of monocytes, which then triggers the synthesis and release of pro-inflammatory cytokines TNF- α , IL-6, and IL-1 (Zamani *et al.* 2013).

1.5.4.1.1.2. Immunoglobulin Fc- γ receptors (CD16) marker

Fragment crystallisable (Fc) antibodies bind to the cell surface Fc γ receptor (Fc γ R). Fc γ R is essential to many immune system effector functions, such as phagocytosis of opsonized cells, the release of inflammatory mediators, and antibody-dependent cellular cytotoxicity. CD16 on the surface of monocytes is Fc γ RIIIa that stimulates phagocytosis of a microbe (Rana *et al.* 2018), and they are predisposed to become migratory DCs that transiently survey tissues and migrate to lymph nodes (Randolph *et al.* 2002).

1.5.4.1.1.3. Human leukocyte antigen-DR (HLA-DR) marker or MHC II

Monocytes express MHC II or CD68, which present antigenic peptides to CD4⁺ T cells.

1.5.4.1.1.4. TLRs

Innate immune cells such as monocyte, macrophages, neutrophils, and DCs express TLRs on their membrane surfaces. TLR2 triggering occurs via lipoteichoic acid (LTA) and peptidoglycan recognition. TLR4 triggering occurs via LPS recognition, as discussed previously. TLR9 triggering stimulates the production of pro-inflammatory cytokines IL-1 β , TNF- α , IL-6, and chemokine macrophage inflammatory protein-1 (MIP-1) (Rana *et al.* 2018). TLR stimulation with LPS or zymosan significantly downregulated CD16 expression, such that the monocyte subsets could not be identified (Yoon *et al.* 2014).

1.5.4.1.1.5. B1 (VLA-4) and B2 (CD18) integrins

Migration of circulating monocytes is a critical step in the inflow of monocytes and macrophages into the synovium to promote inflammation. The adhesion of activated monocytes to the vascular endothelium initiates the migration of circulating monocytes. B1 integrins (very late antigen 4 (VLA4)) and VLA5, and B2 integrins (CD18), mainly CD11b molecules, facilitate monocyte adhesion to activated endothelium, promoting the migration process.

1.5.4.1.2. Classification of monocytes

Peripheral blood (PB) monocytes are sub-classified into three different populations based on the expression of cell surface molecules, CD14 and CD16 (Ziegler-Heitbrock *et al.* 2010): classical monocytes (CD14⁺⁺CD16⁻) constitute ~ 85-90% of blood monocytes, intermediate

monocytes (CD14⁺CD16⁺) constitutes ~ 10-15% of circulating monocytes, and non-classical monocytes (CD14⁺CD16⁺⁺) are summarised in **Table 1.2**.

Table 1.2. A list of monocyte subsets in humans, their markers, their ligands, and their general functions. Adapted from Rana *et al.* (2018).

| Monocyte subsets | Markers | Chemokine receptors | Differentiation | Function |
|--------------------------------|--------------------------------------|--|---|--|
| Classical monocytes | CD14 ⁺⁺ CD16 ⁻ | CCR2 ^{high} CX3CR1 ^{low} | Intermediate monocytes, inflammatory (M1) macrophages, and osteoclasts. | Osteoclasts inflame synovial joints, causing bony erosions. |
| Intermediate monocytes | CD14 ⁺⁺ CD16 ⁺ | CCR2 ^{low} CX3CR1 ^{high} | Inflammatory-subtypes and inflammatory (M1) macrophages | Sustain synovial inflammation, which is the reason for increased disease activity, and activate Th17 cells. |
| Non-classical monocytes | CD14 ⁺ CD16 ⁺⁺ | CCR2 ^{low} CX3CR1 ^{high} | Patrolling monocytes and tissue resident (M2) macrophages. | Assists in the adhesion of monocytes in the microvessels of joints, resulting in an early inflammatory response. |

1.5.4.2 Characteristics of monocytes in RA

Monocytes are pro-inflammatory in RA through the release of cytokines like IL-6, TNF- α , and IL-1 β . They express “activated” phenotypes in RA. Egress of the monocytes from the BM into the circulation or from the circulation into the tissue requires migration across the monolayer of ECs that line the vascular circulatory system; this process is known as diapedesis. Moreover, monocytes will differentiate into pro-inflammatory macrophages and then subsequently into osteoclasts. In this study, monocytes are the main therapeutic targets, and their role in RA pathogenesis will be discussed.

1.5.4.2.1. Phenotypic characteristics of monocytes in RA

1.5.4.2.1.1. CD14 and CD16

CD14 and CD16 expressions are widely accepted markers for identifying and classifying monocytes. The expression of CD16 on blood monocytes in RA patients is correlated with disease activity (Baeten *et al.* 2000; Hepburn *et al.* 2004; Kawanaka *et al.* 2002). High expression of Fc γ IIIa (CD16⁺) on CD14⁺⁺ monocytes from RA patients produces more TNF- α in response to an IgG-containing immune complex (IC) such as an IC containing ACPA (anti-CCP) than healthy individuals (HIs) (Villar-Vesga *et al.* 2019); this was associated with non-response to MTX therapy (Cooper 2012).

1.5.4.2.1.2. TLRs

The role of TLRs in RA is evident by their increased expression in resident and infiltrating cells in the inflamed joint. CD14⁺⁺CD16⁺ monocyte subsets in comparison to CD14⁺⁺CD16⁻ in PB and SF of RA patients as well as HCs express markedly higher levels of TLR2 (Iwahashi *et al.* 2004). Monocytes in patients with RA also have increased levels of surface TLR2 compared to HCs. High expression of TLR2 on CD16⁺ blood and synovial macrophages (SM) of RA patients induces increased production of TNF- α (Iwahashi *et al.* 2004).

1.5.4.2.2. Functional characteristics of monocytes in RA

Monocytes and macrophages have been found to accumulate in arthritic synovial-joint tissues, abundantly infiltrate synovial membranes, and be central to the pathophysiology of inflammation (Guo *et al.* 2018). ACPA can enhance NF- κ B activity and TNF- α production in monocytes and macrophages via binding to a surface-expressed citrullinated glucose receptor protein 78 (Grp78) (Lu MC *et al.* 2010). As mentioned, monocytes are a potent source and producer of large amounts of pro-inflammatory cytokines and MMPs, which lead to EC activation, acute phase reactions, and cartilage damage. These cells can also produce a wide range of chemokines, which help recruit additional leukocytes through *trans*-endothelial migration to the inflamed joint (Roberts *et al.* 2015). RA monocytes also interconnect with other cells in a positive loop manner for augmentation of the rheumatoid process.

1.5.4.2.2.1. Monocytes in RA

RA patients display an increased number of intermediate and classical monocytes (Rana *et al.* 2018). A study reported on RA patients and HCs shows that the proportion of circulating intermediate monocytes positively correlates with RA disease activity and that their level of PB elevates during increased disease activity (Tsukamoto *et al.* 2017). Kawanaka *et al.* also confirmed that patients with active RA showed higher frequencies of intermediate monocytes, with the frequency of these cells decreasing in patients that respond well to therapy (Kawanaka *et al.* 2002). Another study showed that the increased level of total circulating monocytes (classical and intermediate monocytes) in treatment-naive RA patients predicted a sub-optimal or non-response to the MTX treatment (Chara *et al.* 2015).

1.5.4.2.2.2. Monocyte activation, inflammatory cytokine production, and joint damage.

The presence of IgG autoantibodies directed against ACPA (Sokolove *et al.* 2012; Pruijn 2015) can form immune complexes (ICs). ICs influence monocytes by inducing the production of TNF- α through the binding of CPs by TLR4 and IgG by Fc γ R (Sokolove and Robinson 2011). This response was suggested to be directly related to joint damage and the systemic manifestations in patients with RA (Villar-Vesga *et al.* 2019). TNF- α and IL-1 can induce

haematopoietic shifts that favour the production of inflammatory innate-type cells, such as neutrophils and monocyte-lineage cells. Such shifts in haematopoiesis are most likely dependent on local G-CSF production (Manz and Boettcher Sin 2014).

1.5.4.2.2.3. Monocyte migration into RA synovium

Recruitment of monocytes from the circulation into the synovium depends on the interaction of chemokines (ligands) with chemokine receptors on the monocyte surface. Two widely demonstrated chemokine receptors on the monocyte surface are CCR2 and CX3CR1. CCR2, on binding with its ligand CCL2, and CX3CR1, on binding with its ligand CX3CL1 (fractalkine), a cellular adhesion molecule and a chemotactic chemokine for monocytes and lymphocytes (Bazan *et al.* 1997; Ruth *et al.* 2000; Volin *et al.* 2001), induce the migration of circulating monocytes into the synovium during RA. Studies reported the constitutive expression of chemokine receptors on monocyte and macrophage surfaces in the PB and SF of RA patients and explained the migration and retention of monocytes (Lioté *et al.* 1996). The movement across the vascular endothelium may either be paracellular, where the monocytes move in between two ECs, or transcellular, where the monocytes pass directly through individual ECs through the formation of a transcellular pore (Carman 2009).

1.5.4.3 Characteristics of macrophages

1.5.4.3.1. Phenotypic characteristics of macrophages

Macrophages contribute to defence, innate or acquired immunity, inflammation, and non-infectious disease processes both within and outside the lymphohematopoietic organs. Metchnikoff in 1893 was the first to use the term macrophage to describe a large cell able to take up microorganisms (Karnovsky and Metchnikoff 1981), and Randolph *et al.* 2019 showed that macrophages do not die locally but migrate to the draining lymph nodes, although the macrophages are less migratory than monocytes (Randolph 2019). Macrophages exist in different subsets with different functions within the immune response. Both tissue-resident and BM-derived macrophages exhibit significant functional heterogeneity and can be classified into two main subtypes: classically activated, M1 (pro-inflammatory) linked to glycolysis, and alternatively activated, M2 (anti-inflammatory/resolution phase) linked to mitochondrial activity and oxidative phosphorylation (Johnson and Newby 2009; Lech and Anders 2013; Sica and Mantovani 2012). The latter can be further sub-classified into M2a, M2b, and M2c subsets by their immune function, as shown in **Table 1.3**.

Table 1.3. Subsets of human macrophages, stimuli, and general functions

| Macrophage subset | Name | Stimuli | Function |
|-------------------|-------------------------|--------------------|---|
| M1 | Classically activated | LPS/IFN- γ | Defence/pro-inflammatory/microbicidal |
| M2a | Alternatively activated | IL-4 | Anti-inflammatory/wound healing |
| M2b | Type 2 | Fc γ -R+LPS | Antigen presentation and generation of the Th2 response |
| M2c | Regulatory | IL-10/TGF β | Inhibit the immune response |

1.5.4.3.2. Functional characteristics of macrophages

Macrophages have three major functions: antigen presentation, in which antigens are presented to T or B cells within follicles of the lymph node (Martinez-Pomares and Gordon 2007), phagocytosis, which provides immunity; and releasing cytokines TNF- α , IL-1, and IL-6 that activate other immune cells. These are in addition to their critical roles in the maintenance and resolution of inflammation.

Macrophages express a variety of receptors that participate in the phagocytic uptake of antigens, including those that recognise complement activation products or Ig Fc fragments. They express both MHC class I and II molecules and therefore can present antigen derived from cytosolic or extracellular proteins for recognition by the appropriate CD8⁺ (MHC class I expressing) or CD4⁺ (MHC class II expressing) restricted antigen-specific T cells (Mantegazza *et al.* 2013).

Macrophages, as phagocytes, scavenge foreign particles around the body. To do this, macrophages express many pattern-recognition receptors (PRRs), including scavenger receptors (SRs) and TLRs, to recognise and bind foreign particles (Libby 2012). SRs are a family consisting of 8 structurally unrelated receptors that, along with their role in immunity, possess the ability to bind modified LDL (Moore and Freeman 2006). Oxidation of LDL is a key inducer of atherosclerosis (Ramos *et al.* 1998; Stocker and Keaney 2004), and the contribution of macrophages has long been studied in atherosclerosis. Macrophages can uptake ox-LDL via SR-mediated endocytosis, micropinocytosis, or phagocytosis (Bobryshev 2006; Li and Glass 2002).

1.5.4.4 Characteristics of macrophages in RA

Type A synovial cells (the macrophage) interdigitate with type B cells (the fibroblast) in the synovial membrane (Athanasou 1995). Under normal conditions, the predominant cell type in the synovium is B cells, whereas in RA, type A cell numbers are greatly elevated (Athanasou 1995). In addition, the synovial membrane becomes hypertrophic due to synovial fibroblast proliferation, increased blood and lymphatic vasculature, and an inflammatory influx of immune cells from the circulation (Alivernini *et al.* 2016), which include monocytes that differentiate locally into pro-inflammatory macrophages that produce TNF- α and MMPs (Gibbs *et al.* 1999). Articular destruction is accompanied by pannus formation, which is an intrusion of the bone and cartilage by the proliferating synovial membrane (**Figure 1.3**). In the RA synovial membrane, a surface layer of HLA-DR⁺, CD14⁺, and CD68⁺ macrophages is typically followed by a layer of fibroblasts. By this arrangement, they display a typical morphology, which is believed to be centrally involved in tissue destruction (Kinne *et al.* 2000).

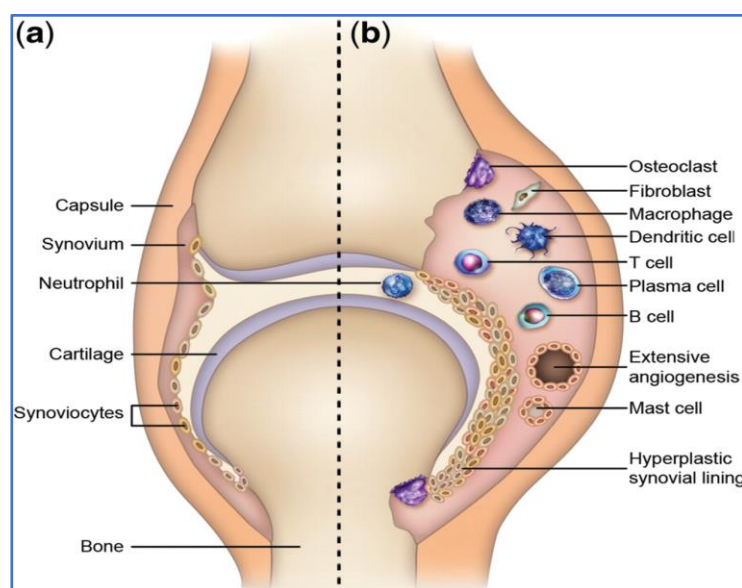


Figure 1.3. A schematic view of a normal joint and a joint affected by RA shows increased inflammation and cellular activity. This illustration demonstrates the presence of various inflammatory cell infiltrates, synovial membrane hyperplasia, cartilage destruction, and bone erosion. Taken from Smolen and Steiner (2003).

Macrophages account for the majority of the cellular component in atherosclerotic plaque, suggesting they may contribute to the raised incidence of accelerated atherosclerosis in RA (Mikołajczyk *et al.* 2016; Winchester *et al.* 2016). Also, macrophages have been shown to promote the migration of smooth muscle cells (SMCs) to growing lesions (Rudijanto 2007) and induce their apoptosis, leading to a thinning of the fibrous cap, which once again increases the risk of plaque rupture (Boyle *et al.* 2001; Ramji and Davis 2015). At the plaque site,

macrophages also produce chemokines and cytokines, which act to recruit further monocytes and promote diapedesis, and inhibit the synthesis of plaque stabilising components of the ECM produced by SMC, shifting the balance towards ECM degradation, and increasing the risk of a plaque rupture (McLaren *et al.* 2011a; Newby 2006). As the monocytes migrate from the lumen into the intima of the artery, their migration is enabled by EC activation in synovial microvessels and lipoprotein (LP) retention in the subendothelial layer of the arteries, which increases expression of adhesion molecules including selectins, ICAM-1, and VCAM-1, together with chemokines. **Figure 1.4** shows the initial stages of atherosclerosis, EC activation, monocyte transmigration, macrophage differentiation, foam cell formation, and SMC migration.

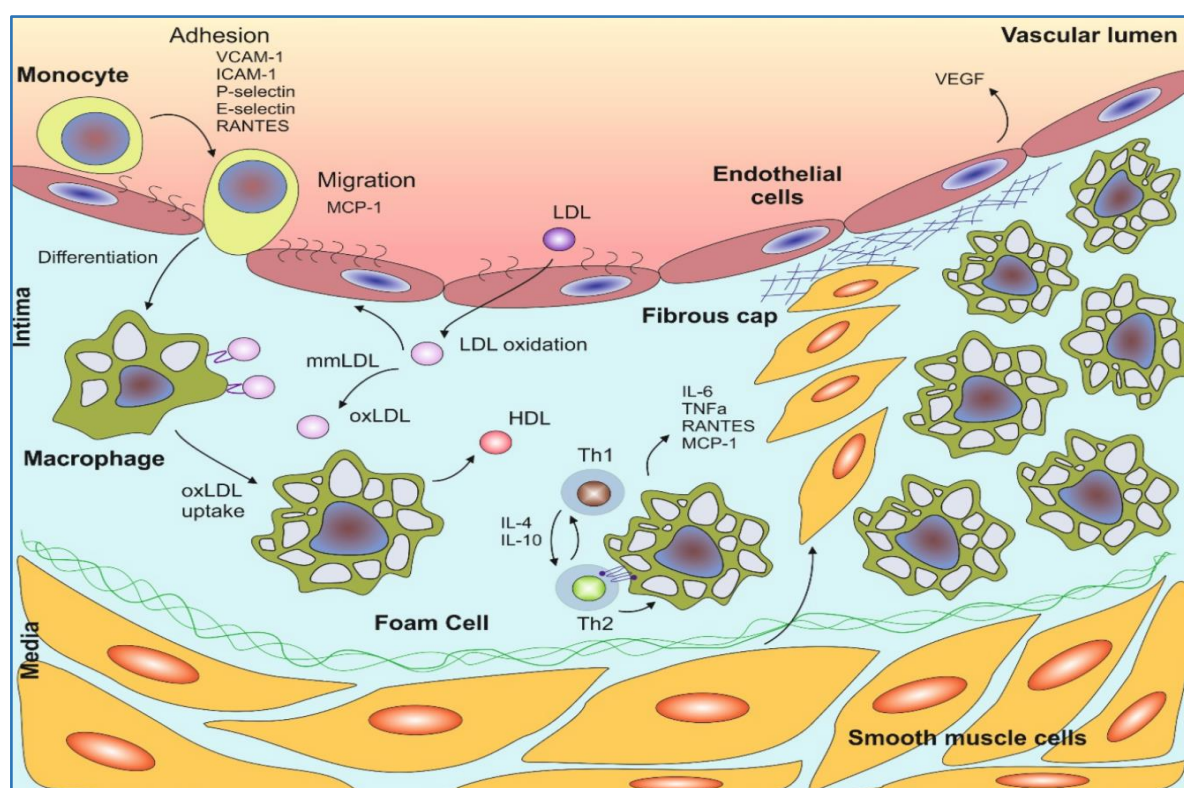


Figure 1.4. Overview of the process of monocyte adhesion to the endothelium and migration into the sub-endothelial space during the development of an atherosclerotic plaque. Inflamed endothelial cells express cell adhesion molecules and inflammatory cytokines, which recruit monocytes to the site of inflammation. Monocytes then begin to roll along the monolayer, forming weak interactions, once firmly attached, they begin to cross into the intima, where they differentiate into macrophages. These then take up oxidised LDL (ox-LDL), becoming lipid-laden foam cells. Macrophages exert both pro- and anti-atherogenic effects, causing the movement of smooth muscle cells from the media to the intima, which begins to secrete extracellular matrix (ECM) proteins, which then form a fibrous plaque. Taken from Baker *et al.* (2018).

1.5.4.4.1. Phenotypic characteristics of macrophages in RA

In collagen-induced arthritis (CIA), a murine model of RA, embryonic synovial macrophages (ESM) are skewed towards M2, while bone marrow-derived synovial macrophages (BMSM) show a more M1 phenotype during arthritis development (Tu *et al.* 2019). In patients with RA,

SMs, which are found within the lining and sublining layers of the synovium, express CD68⁺ and CD163⁺. CD68⁺ is an SR that binds to ox-LDL. CD163⁺ belongs to the group of B-SRs that bind and internalise haemoglobin–haptoglobin complexes, promoting the release of IL-10 and carbon oxide, leading to profound anti-inflammatory effects (Siouti and Andreakos 2019).

1.5.4.4.2. Functional characteristics of macrophages in RA

1.5.4.4.2.1 Macrophages in RA

Macrophages are critically involved in the pathogenesis of RA; they contribute to cartilage and bone destruction through multiple mechanisms (Ma and Pope 2005). They are responsible for inducing inflammation, matrix destruction, cytokine production, and angiogenesis (Maruotti *et al.* 2007). The number of differentiating synovial macrophages (SM) correlates with joint damage (Mulherin *et al.* 1996), clinical response to therapy (Haringman *et al.* 2005), radiological permanent joint damage (Kinne *et al.* 2002; Mulherin *et al.* 1996), and joint pain and inflammation (Tak *et al.* 1997).

1.5.4.4.2.2 Macrophages' activation

Macrophages in inflammatory tissues are activated by TNF- α , IL-1, IFN- γ , T-lymphocytes, ligation of chemokine receptors, pathological collagen deposition, and hypoxia. Macrophages can be activated by cell contact within the joint in the absence of an antigen. Their interaction with SF results in the production of the pro-inflammatory cytokines IL-6, IL-8, and GM-CSF. They also interact with activated T cells, leading to the production of IL-1 β , TNF- α , and MMPs (Burger and Dayer 2002). Macrophages' contact with the ECs results in the upregulation of ICAMs, which are critical for the continuous recruitment of circulating monocytes into the synovial joint and the arterial intima, as shown in **Figure 1.4** above.

In RA, IL-17 in the joint can activate and amplify SM (Lundy *et al.* 2007). Furthermore, ligation of TLRs by pathogen-associated molecular patterns (PAMPs) or endogenous joint-derived particles damage-associated molecular patterns (DAMPs) released due to joint damage (Midwood *et al.* 2009) can also activate SM. Dead cells are phagocytosed by macrophages, resulting in their activation and the production of pro-inflammatory cytokines such as TNF- α , IL-1 β , and IL-12 (Mueller *et al.* 2005).

Several studies have shown that classical macrophage activation depends on the pro-inflammatory cytokines TNF- α , IFN- γ , and LPS as well as microbial products (Gordon 2003). This resulted in a macrophage population, that had enhanced microbicidal activity and secreted high levels of the pro-inflammatory cytokines TNF- α , IL-1, and IL-6. This, therefore, activated the macrophages in an autocrine fashion. Macrophages can alternatively be activated by the

cytokines IL-4, IL-33 (Th2), IL-10, or GCs, and these have a role in tissue repair (Gordon and Martinez 2010), as illustrated in **Table 1.3** above.

1.5.4.4.2.3 Macrophages in joint damage

Bone erosion by osteoclasts is a hallmark of RA (Schett and Teitelbaum 2009). Osteoclasts are highly specialised cells with the ability to remove calcium and degrade bone. In a healthy setting, osteoclasts along with osteoblasts maintain bone homeostasis (Schett *et al.* 2010). During inflammation, the balance between these two cells is disrupted, and an accumulation of osteoclasts in the joint results in a high level of bone resorption, leading to damage and erosion (Schett *et al.* 2006). Osteoclasts are multi-nucleated cells that resorb bone matrix. These cells differentiate from osteoclast precursors, tissue macrophages, which originated primarily from monocytes in the BM and PB fields (Boyle *et al.* 2003; Gordon and Taylor 2005). The processes of osteoclastogenesis and bone erosion are controlled by the interaction of receptor activator of NF- κ B (RANK) (Guo *et al.* 2018) expressed on osteoclast precursors with its ligand RANKL, which is expressed on synovial fibroblasts, osteoblasts, and Th17 cells. RANKL expression on these cells is up-regulated by inflammatory cytokines such as TNF- α , IL-1, IL-6, and IL-17 (Takayanagi 2012).

1.5.4.4.2.4 Macrophages and chemokines in RA

MIP-1, CCL2, and fractalkine have a role in macrophage activity and chemotaxis in RA. MIP-1 has been considered important in favouring the production of IL-1, IL-6, and TNF- α by murine macrophages in SF and sera of RA patients, where it exerts its chemotactic activity on macrophages (Akahoshi *et al.* 1993; Koch *et al.* 1992). In patients with RA, SM produces fractalkine; an ICAM, and a chemotactic chemokine for monocytes and lymphocytes (Ruth *et al.* 2001; Volin *et al.* 2001). *Ex vivo* functional studies demonstrated that macrophages isolated from active RA ST spontaneously release CCL2 (Koch *et al.* 1992; Okamoto *et al.* 1997).

1.5.4.4.2.5 Macrophages and pro-inflammatory cytokines in RA

Macrophages can synthesise a variety of pro-inflammatory cytokines that are present in the joints of patients affected by RA, e.g., TNF- α , IL-1, IL-6, IL-8, IL-15, IL-18, and MIF (Fadok *et al.* 1998; Rückert *et al.* 2009). IL-18 is a pro-inflammatory cytokine expressed in RA synovium, most prominently in CD68⁺ macrophages. In the RA joint, IL-18 acts in conjunction with other cytokines, including IL-12 and IL-15, to stimulate the SM release of TNF- α (Gracie *et al.* 1999).

1.5.4.4.2.6 Macrophages and other pro-inflammatory mediators in RA

Macrophages release PGE₂, proteases, neutrophil chemotactic factors, ROS, NO, and superoxide. According to Martinez and Gordon (2014), the phenotypes M1 and M2 after

activation in the synovial tissue from RA patients were dramatically different from the M1 and M2 phenotypes obtained *in vitro* using LPS/IFN- γ or IL-4, respectively. For example, inducible nitric oxide synthase (iNOS), a hallmark of *in vitro* M1 activation, is not elevated at the peak of STIA, while SMs exposed to NO increase their TNF- α production (McInnes *et al.* 1996), possibly adding to the mechanisms that promote synovitis (Kinne *et al.* 2000).

1.6 Cytokines

The name “cytokine” comes from the Greek cyto meaning “cell” and kinin meaning “movement”. Cytokines are local and small non-antibody protein mediators synthesised during the effector phase of innate and adaptive immunity. They can be subdivided into several categories, which include monokines (produced by monocytes), lymphokines (produced by lymphocytes), chemokines (which mediate chemotaxis between cells), and interleukins (produced by leukocytes). They are secreted by immune cells (autocrine), neighbouring or adjacent cell activation (paracrine), or cell-to-cell contact (juxtacrine) by immune responses and stimulate the movement of these cells towards sites of inflammation, infection, and injury. Cytokines operate through receptors, which are expressed on the surfaces of a variety of cells. The binding of cytokines to their receptors activates diverse intracellular signalling cascades. For example, the binding of TNF- α to its receptor activates the NF- κ B and mitogen-activated protein kinase (MAPK) cascades (Aggarwal 2003), whereas IL-6 binding to its receptor predominantly activates the JAK/STAT pathway (Hunter and Jones 2015). Through the activation of these pathways, cytokines control almost all biological processes, including cellular proliferation, activation, differentiation, and immunity. Cytokines are expressed transiently after an inducing stimulus, unlike hormones that are expressed constitutively (Feldmann and Maini 2001).

In RA, cytokines can be classified into four groups: pro-inflammatory, inflammatory cytokines in joints, anti-inflammatory, and natural cytokine antagonists, as summarised in **Table 1.4**.

Table 1.4. Classifications of cytokines in RA

| | |
|------------------------------------|---|
| Pro-inflammatory cytokines | TNF α , IL-1. |
| Inflammatory cytokines | TNF- α , IL-1, IL-6, IL-12, IL-18, IL-15, IL-23, GM-CSF, IFN- γ , and IL-17. |
| Anti-inflammatory cytokines | IL-4, IL-10, TGF- β , IL-13, IL-33. |
| Natural antagonists | IL-1RA, soluble type 2 IL-1 receptors, soluble TNF- α receptor I, IL-18 binding protein. |

Monocytes, macrophages, and synovial fibroblasts produce higher levels of cytokines in RA synovium compared to T cells (McInnes and Schett 2007). Notably, cytokines secreted by monocytic cells are also an important component of the inflammatory response in RA (Kinne 2000).

In RA joints, an imbalance between pro- and anti-inflammatory cytokine activities contributes to the induction of autoimmunity, chronic inflammation, and thereby joint damage. Inflammatory cytokines (TNF- α , IL-1, and IL-6) released from the synovium in RA patients generate a spectrum of pro-atherogenic changes such as insulin resistance, dyslipidemia, oxidation, upregulation of cellular adhesion molecule expression on ECs, thrombin generation, and platelet activation. These, in turn, contribute to accelerated atherosclerosis (Sattar *et al.* 2003). TNF- α , IL-6, and IL-1 β (which will be discussed in detail) activate macrophages (monocytes), which increase their stickiness, mobility, phagocytosis, lipid uptake, LDL oxidation, and cell migration into the intima. Furthermore, these pro-inflammatory cytokines promote the proliferation of various cell types, including SMCs, and increase ECM production, hence atherosclerotic plaque (Huber 1995; Kunkel *et al.* 1995). ECM is a three-dimensional network of extracellular macromolecules (collagen, enzymes, and glycoproteins) that provide structural and biochemical support to surrounding cells. The balance between ECM deposition and degradation is a key element in the clinical complications of atherosclerosis. Cytokines modulate several steps in the control of plaque stability and rupture. For instance, IFN- γ , TNF- α and IL-1 β promote the apoptosis of macrophages along with foam cells, leading to the enlargement of the lipid core (Andre's *et al.* 2012). **Table 1.5** provides a summary of common cytokines implicated in the pathogenesis of RA and atherosclerosis.

Table 1.5. Cytokines implicated in the pathogenesis of RA, their source and potential biological activity. Adapted from McInnes and Schett (2007).

| Cytokine | Principal Source | Potential Biological Activity |
|-------------------------|---|--|
| TNF- α | Monocytes, macrophages, DCs B, T cells, fibroblasts, and neutrophils | Activates macrophages, ECs, monocytes, increase ICAM-1, VCAM-1, PG, MMP, and cytokine release, and T-cell apoptosis. |
| IL-1 α / β | Monocytes, macrophages, DCs B cells, fibroblasts. | Induces cytokine secretion from monocytes, and fibroblasts; increase endothelial adhesion molecule expression; osteoclast activation. |
| IL-1Ra | Monocytes | Antagonizes effects of IL-1 α and IL-1 β . |
| IL-6 | Monocytes, fibroblasts macrophages, T, and B cells | B cell proliferation and antibody production. thrombopoiesis; Th17 differentiation, cytotoxicity; acute phase response. |
| IL-10 | Monocytes, T-cells, B-cells DCs, and epithelial cells | Decreases DC activation and cytokine, release; decrease fibroblast cytokine and MMP release. Inhibit T cell proliferation. |
| IL-12 | Monocytes, macrophages, DCs | Th1-cell proliferation, maturation; T cell and NK-cell cytotoxicity; B-cell activation. |
| IL-15 | T cells, monocytes macrophages, DC | Increased T cell and NK cell recruitment, B cell differentiation, fibroblast, and macrophage activation. |
| IL-17 | T cells, macrophages DC and T cells | Induces pro-inflammatory cytokine release from macrophages, fibroblasts, and ECs, T-cell expansion. |
| IL-18 | Monocytes, DCs, ECs, and macrophages. | Promotes T-cells differentiation, cytokines release. |
| IL-23 | Monocytes, DC, and macrophages | Th17 cell proliferation. |
| IFNs | Widespread | Antiviral response; \uparrow MHC expression. Macrophage and lymphocyte activation, |
| RANKL | Stromal cells, osteoblast, T-cells | Stimulate osteoblasts-mediated bone resorption. |
| GM-CSF | Lymphocytes, fibroblasts, monocytes and osteoclasts | Stimulates the differentiation and survival of macrophages and neutrophils. |
| M-CSF | Lymphocytes, fibroblasts monocytes and osteoclasts | Regulator of monocyte differentiation, proliferation and macrophage survival. |
| VEGF | Monocytes, ECs, fibroblasts | Angiogenesis |
| MIF | Macrophages, activated T cells | Increases macrophage phagocytosis, cytokine, NO release; T- Cell activation and fibroblast proliferation; COX and PLA ₂ expression. |

1.6.1. Tumour Necrosis Factor- α (TNF- α)

TNF- α was discovered in 1975 as an endotoxin-induced protein leading to necrosis in sarcomas transplanted into mice (Carswell 1975). TNF- α was originally described as a circulating factor that can cause necrosis of tumours but has since been identified as a key regulator of inflammatory responses. TNF- α is not usually detectable in a normal, healthy state, but elevated serum and tissue levels are found in inflammatory and infectious conditions (Bradley 2008), and the serum levels correlate with the severity of infections. TNF- α is mainly produced by activated macrophages and monocytes, but a wide range of cells can also produce TNF- α including neutrophils, ECs, NK-cells, activated CD4⁺ lymphocytes, SMC, cardiac cells, fibroblasts, and osteoclasts (Vasanthi *et al.* 2007).

TNF- α binds to TNF-receptors (TNFRs) and initiates both distinct and overlapping signal transduction pathways. This diversity of signalling cascades leads to various cellular responses, including cell death, survival, differentiation, proliferation, and migration (Bradly 2008). Early findings on a transgenic mouse model carrying a modified human TNF- α gene showed that transgenic mice developed chronic inflammatory polyarthritis. While *in vivo* administration of a monoclonal antibody against human TNF- α effectively reversed the disease progression (Keffer *et al.* 1991).

1.6.1.1 TNF- α signal transduction

TNF- α performs its function by binding to two structurally distinct membrane receptors: TNFR1 (also known as p55) or TNFR2 (also known as p75). TNFR1 is activated by both the membrane-bound and soluble forms of TNF- α , whereas TNFR2 only signals after binding membrane-bound TNF- α (Popa *et al.* 2007). TNFR1 is expressed in a wide variety of cell types, whereas TNFR2 is selectively expressed by immune cells and ECs (Aggarwal 2003; Callard and Gearing 1994). TNF- α responses are initiated by binding to one of its two receptors, and this activates the intracellular signalling pathways leading to gene transcription as shown in **Figure 1.5**. Regulation of the transcription factor NF- κ B is a key component of TNF- α signalling. The extracellular, ligand-binding domains of TNF- α receptors contain cysteine-rich subdomains, which are characteristic of members of the TNF- α receptor gene family. In contrast, the intracellular domains of the two receptors are devoid of intrinsic enzyme activity and activate distinct signal transduction pathways by the recruitment of different proteins from the cytosol through specific protein-protein interaction domains (Bradley 2008). The ability of TNFR1 and TNFR2 to interact with both identical and unrelated molecules may explain their shared and diverse functions. Based on cell culture work and studies with receptor knockout

mice, both the pro-inflammatory and the programmed cell death pathways activated by TNF- α and associated with tissue injury are mainly mediated through TNFR1. The consequences of TNFR2 signalling are less well characterised than those of TNFR1 signalling via recruitment of TRADD (Bradley 2008) (**Figure 1.5**). TNFR1 is a type I transmembrane protein that, in resting cells, is predominantly sequestered in the Golgi apparatus, from where it can be mobilised to the cell surface. Upon stimulation, the intracellular domain of TNFR1 binds to the TRADD, which can further activate either the (apoptotic) pathway via the Fas-associated death domain (FADD) protein or the subsequent recruitment of pro-caspase-8 by the TRADD–FADD complex. Alternatively, the pro-inflammatory (necroptosis) pathway can be activated via TNF- α receptor-associated factor 2 (TRAF2) and receptor-interacting protein (RIP). The TRADD–RIP–TRAF2 complex is released from TNFR1, resulting in the activation of NF- κ B. Inhibitors of this process can interfere with signalling. RIP is thought to activate the β -subunit of the Inhibitor of κ B (I κ B) kinase (IKK) complex, leading to phosphorylation of I κ B that normally masks nuclear localisation signals within NF- κ B. I κ B degradation allows NF- κ B to enter the nucleus and initiate gene transcription, mediating cell survival and pro-inflammatory signals through activating protein-1 (AP-1). The TRADD–RIP–TRAF-2 complex can also recruit mitogen-activated protein kinase kinase kinases (MAP3K) that associate with TRADD (Nishitoh *et al.* 1999) and activate MAP3Ks, which in turn phosphorylate and activate c-Jun N-terminal kinases (JNKs) and p38 MAPKs/ERK. Activated JNKs phosphorylate the amino-terminal region of c-Jun, leading to the initiation of transcription.

In contrast to TNFR1, TNFR2 is unable to activate the TRADD/FADD pathway and signals through the TRAF2-associated pathway by binding the IKK complex (Bradley 2008). TNFR2 can also activate endothelial/epithelial tyrosine kinase (Etk), a cytosolic kinase implicated in cell adhesion, migration, proliferation, and survival. Etk is a regulator of epithelial cell junctions and mediates the TNF-induced phosphatidylinositol 3-kinase (PI3K)/Akt angiogenic pathway in vascular ECs through Etk-mediated crosstalk with vascular endothelial growth factor receptor 2 (VEGR2) (**Figure 1.5**).

Ligation of TNFR1 is both necessary and sufficient to induce cytotoxic and proinflammatory TNF- α responses, whereas TNFR2 may promote cell activation, migration, or proliferation.

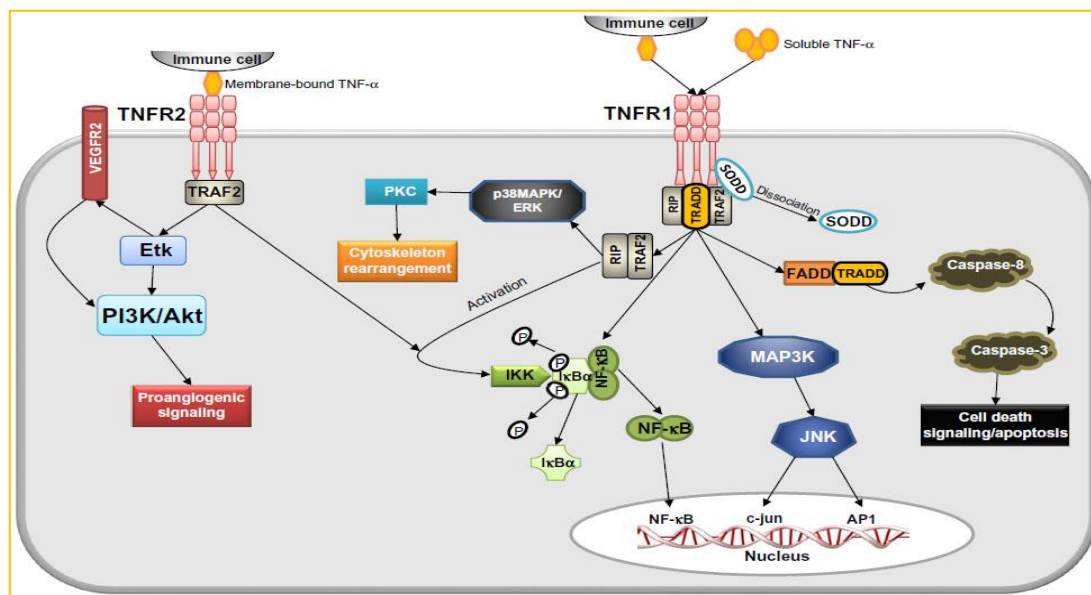


Figure 1.5. The TNF signalling pathway leads to the main cellular responses. Soluble TNF receptors and monoclonal anti-TNF antibodies, prevent TNF from interacting with its receptors and activating these pathways. These were used as targets for therapy in RA (Urschel and Cicha 2015).

Inflammatory mediators are known to induce the shedding of TNFR1 from ECs (Bradley 1993; Madge 1999). NO and H₂O₂ have been implicated in the activation of a metalloproteinase involved in the shedding of TNFR1. Stimuli including TNF- α , IL-1, IL-10, and plasminogen activator-tissue type (tPLA) down-regulate TNFR1 expression while increasing the expression of TNFR2 (Bradley 2008).

1.6.1.2 The biological effectors of TNF- α

TNF- α , being an internal pyrogen, can induce general fever, apoptotic cell death, and cachexia and is involved in systemic inflammation. In addition, it inhibits tumourigenesis and induces pain and fever by promoting PGE₂ synthesis and nociceptor sensitisation (Kinne *et al.* 2007). One of the major biological roles of TNF- α in the host is as a defence against bacterial, viral, and parasitic infections. As a result, inhibition of TNF- α may result in unwanted side effects such as reactivation of tuberculosis in RA patients treated with TNF- α blockers (Mohan *et al.* 2003). TNF-induced expression of COX-2 can increase EC production of the vasodilatory prostaglandin I₂ (PGI₂), resulting in vasodilatation. Additionally, TNF upregulates pro-coagulant proteins such as tissue factors and downregulates anticoagulant proteins, which increases the risk of venous thrombosis.

1.6.1.3 The role of TNF- α in RA

Indirect action of TNF- α by the induction of mediators

An excessive amount of TNF- α is present in the blood and joints of patients with RA (Choy 2016). TNF- α indirectly exerts different functions in the pathogenesis of RA. First, in response to TNF- α , ECs promote inflammation by expressing adhesion molecules for leukocytes, including E-selectin, ICAM, and VCAM-1 (Haraldsen *et al.* 1996). In combination with the chemokines, including IL-8 and CCL2 (Rollins *et al.* 1990), TNF- α leads to the recruitment of different populations of leukocytes independent of antigen recognition, including neutrophils, monocytes, and activated T cells (Koch 2005). ICAM-1 is required for the extravasation of neutrophils from the bloodstream into the inflamed joint tissue. Secondly, TNF- α induces the production and release of chemokines such as CXCL8, CCL2, CCL3, and CCL5, which are also important for leukocyte recruitment and angiogenesis. The attracted inflammatory cells produce additional TNF- α resulting in positive feedback and enhanced inflammation. The third function of TNF- α is the induction of other proinflammatory cytokines like IL-1, IL-6, and GM-CSF, which also stimulate the production of osteoclastogenic cytokines such as M-CSF by ECs and the production of RANKL, which enhance the inflammatory environment and drive tissue destruction (Moelants *et al.* 2013). Furthermore, TNF- α stimulates RA pathogenesis by promoting DC differentiation, leading to autoantigen presentation to T cells in the synovium (Park *et al.* 2017). Finally, TNF- α also stimulates cartilage destruction by accelerating the chondrocyte's ability to synthesise cytokines or respond to local cytokine release, particularly TNF- α , IL-1 β , IL-17, and IL-18, and the production of matrix-degrading enzymes and MMPs (McInnes and Schett 2007).

Direct action of TNF- α

Elevated levels of TNF- α detected in the SF of RA patients can cause osteoclastogenesis directly by binding to TNFR1 on osteoclast precursors. It is hypothesised that the initial binding of ACPAs to osteoclast precursor cells stimulates the release of TNF- α , which then promotes the differentiation of these cells into mature osteoclasts, leading to synovitis and initial bone loss (Schett and Gravalles 2012). TNF- α mobilises CD11b⁺ osteoclast precursors from the BM (Li *et al.* 2004) and induces IL-1 and IL-1R expression by mesenchymal cells and cells of the osteoclast lineage, which subsequently support the RANKL–RANK system (Wei *et al.* 2005). TNF- α and IL-1 β expression boost the activation of synovial fibroblasts and osteoclasts, which disturb the cartilage and lead to damage to the joint (Brzustewicz and Bryl 2015). Moreover, TNF- α inhibits the functions of T-reg cells and induces effector T cells resistance to T-reg-

mediated suppression. TNF- α is a major player in the autoimmune response in RA, as summarised in **Figure 1.6**.

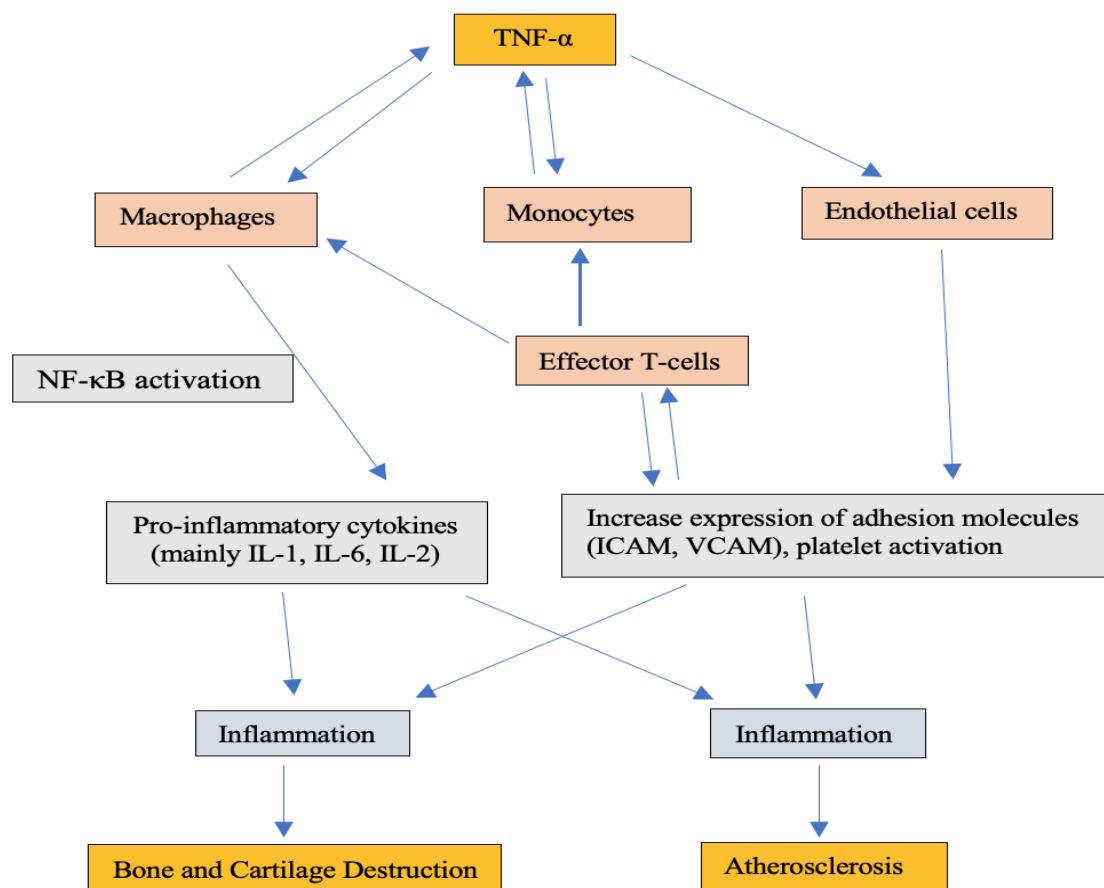


Figure 1.6. Illustration for the summary of TNF- α action on immune and endothelial cells in RA.

DCs, T cells, and B-cells are co-stimulated, and this leads to T-cell activation and functional differentiation. The stimulated macrophages in turn activate nuclear factor kappa-light-chain-enhancer of activated B-cells (NF- κ B)-dependent signalling, which induces pro-inflammatory cytokines that enhance local inflammation of the synovial membrane (synovitis) and result in damage to cartilage and bone. Increasing the expression of ICAM and VCAM by endothelial cells promotes atherosclerosis.

TNF- α and lipid metabolism

HDL protects against atherogenesis through several mechanisms. One of the most extensively studied and accepted theories suggests that HDL plays a role in removing excess cholesterol from peripheral cells and returning it to the liver for excretion. This mechanism, known as reverse cholesterol transport, plays a key role in preventing or reversing the development of atherosclerotic lesions (Linsel-Nitschke and Tall 2005; Ohashi *et al.* 2005) (**Figure 1.7**). Reverse cholesterol transport, is initiated by the efflux of cholesterol from arterial cell walls onto lipid-poor apolipoprotein A-1 (apoA-I) or pre β -HDL particles and is regulated by ABCG1 and ABCA1 (Duffy and Rader 2006). Subsequently, the lecithin-cholesterol acyltransferase (LCAT) esterifies free cholesterol in HDL, a process that is essential for HDL to efficiently remove cholesterol from cells and tissues, thus contributing to the anti-

atherogenic properties of HDL. Cholesteryl ester transfer protein (CETP) transfers cholesteryl esters from HDL to TG-rich lipoproteins, whereas phospholipid transfer protein transfers phospholipids from TG-rich lipoproteins to HDL. Finally, HDL hydrolyzes TG and phospholipids, generating small pre- β -HDL particles that begin a new cycle in the reverse cholesterol process (Linsel-Nitschke and Tall 2005; Ohashi *et al.* 2005). TNF- α has been shown to induce a reduction in reverse cholesterol transport due to multiple changes at each step in this pathway, as illustrated in **Figure 1.7**. Subsequent studies described the proatherogenic changes in lipid metabolism induced by this cytokine (Popa *et al.* 2007). TNF- α is also able to decrease scavenger receptor class B type I (SRB-I) mRNA expression in the liver, resulting in impaired cholesterol uptake and excretion (Khovidhunkit *et al.* 2001). CYP7-A1 plays a role in cholesterol catabolism and bile acid excretion, and impairment of this step by TNF- α can result in hyperlipidemia (Khovidhunkit *et al.* 2001).

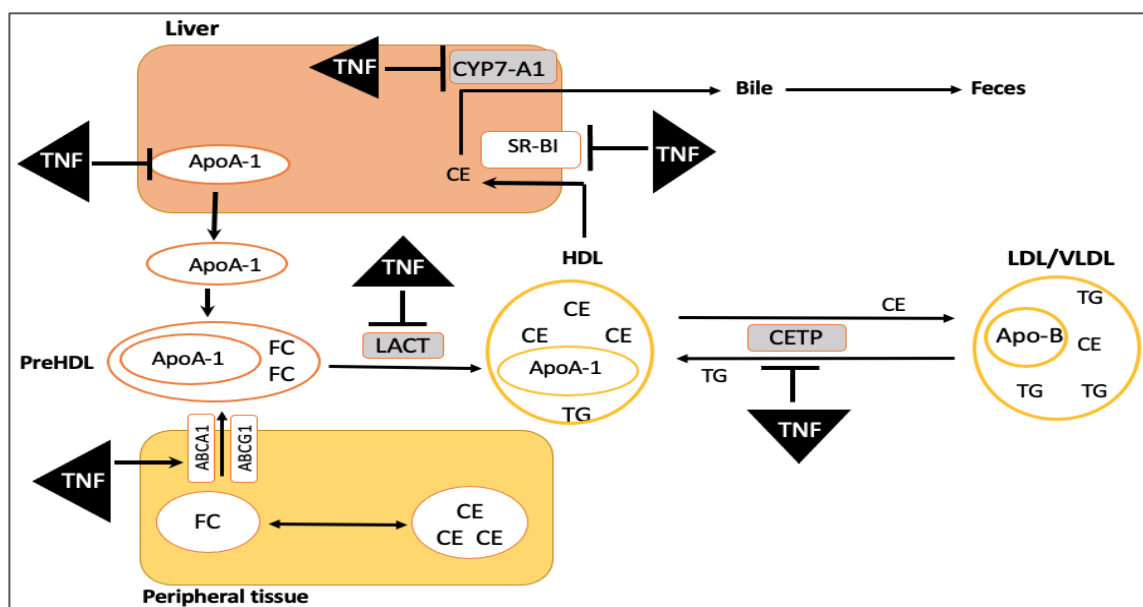


Figure 1.7. Reverse cholesterol transport.

TNF- α can interfere at several levels with the major mechanism responsible for the removal of cholesteryl esters from peripheral tissue. (CE, cholesteryl esters; CETP, cholesteryl ester transfer protein; FC, free cholesterol; SR-B1, scavenger receptor class B type 1, Apo; apolipoproteins, LCAT; lecithin-cholesterol acyltransferase, TG; triglycerides, VLDL; very low-density lipoprotein, CYP7A1; cytochrome p450 family 7 subfamily A member 1. Modified from Popa *et al.* (2007).

Another mechanism through which TNF- α can increase plasma TG concentrations in both humans and rodents is the inhibition of lipoprotein lipase (LPL) activity (Popa *et al.* 2007). The inhibitory effect is seen at both the transcriptional and posttranscriptional levels, leading to a reduction in the clearance of TG-rich lipoproteins, thereby contributing to hypertriglyceridemia. In addition, TNF- α can decrease Apo-E mRNA expression in rat hepatocytes and consequently reduce the receptor-mediated uptake of TG-rich lipoproteins,

which therefore remain longer in the circulation (Popa *et al.* 2007). In rodents, TNF- α may increase hepatic cholesterol synthesis by stimulating the activity of 3-hydroxy-3-methylglutaryl-coenzyme A reductase (HMG-CoA reductase), the rate-limiting enzyme in the cholesterol biosynthetic pathway. TNF- α is likely to induce changes in LDL composition that eventually increase the atherogenicity of this molecule.

1.6.1.4 TNF- α inhibition in RA

The importance of TNF- α in inflammation has been highlighted by the efficacy of anti-TNF- α antibodies or the administration of soluble TNF- α receptors (TNFRs) in controlling disease activity in RA and other inflammatory conditions. In RA management, there are currently many licenced treatments, such as etanercept, infliximab, adalimumab, certolizumab, and golimumab, that can block the effect of TNF α (Edwards 2005; Thalayasingam and Isaacs 2011), and these are nowadays standard treatments for patients (reviewed in some detail in the section on the management of RA). Therapeutic blockade of TNF- α yields clinical responses in approximately 70% of patients with established RA, and it results in a rapid (<24 hour) decrease in plasma levels of IL-6 and CRP, suppression of leukocyte migration, EC deactivation, and recovery of regulatory T-cell function (McInnes and Schett 2007).

1.6.2 Interleukin-1 (IL-1)

The IL-1 family consists of IL-1 α , IL-1 β , IL-18, IL-33, and IL-1 receptor antagonist (IL-1Ra). IL-1Ra is an endogenous inhibitor that blocks the actions of the other two members, IL-1 α and IL-1 β (Fearon and Fearon 2008). The production of IL-1 and IL-1Ra has been investigated in tissue culture using synovial cells isolated from RA patients. In one study, spontaneous IL-1Ra production predominated in one-third of the synovial specimens; however, in the other two-thirds, IL-1 was produced in higher amounts than IL-1Ra (Firestein *et al.* 1994). IL-1 is produced by monocytes, macrophages, neutrophils, lymphocytes, and transformed fibroblasts. Interactions between monocytes/macrophages and T cells were found to play an important role in the production of IL-1 by monocyte/macrophages, giving rise to the first descriptions of the pathways going from lymphocytes to monocytes/macrophages and synovial fibroblast cells (Dayer *et al.* 1979).

1.6.2.1 IL-1 signal transduction

Each member of the IL-1 family binds with high affinity to specific receptors located on the surface of target cells. The binding of IL-1 α or IL-1 β to type I IL-1 receptors (IL-1RI), which is enhanced by an accessory protein (IL-1R-AcP) as shown in **Figure 1.8**, leads to intracellular

signal transduction and regulation of gene expression. As a result, IL-1 β induces cellular responses by binding to the IL-1RI whereas IL-1Ra blocks these IL-1 β -induced responses. Because of type 2 IL-1 receptor (IL-1RII) has a very short intracellular domain, IL-1 binding to IL-1RII does not produce a cellular response. IL-1 α is generally retained within the cell or expressed on the cell surface, in contrast with IL-1 β , which is secreted and acts on other cells. IL-1R-AcP forms a complex with IL-1RI and enhances high-affinity IL-1 β binding with that receptor (Kay and Calabrese 2004).

The biologically active form of IL-1 β results from intracellular processing of a biologically inactive precursor, pro-IL-1 β (Thornberry *et al.* 1992; Wilson *et al.* 1994). Activation of IL-1 β usually occurs as a two-step process. First, transcription of IL-1 β mRNA is induced, and the mRNA is translated as IL-1-precursor protein. This process can occur after the activation of PRRs such as TLRs, in the case of infection, or after the release of alarmins such as IL-1 α which occurs after cell death and necrosis (Chen *et al.* 2007). The second step in IL-1 β activation is based on the action of intracellular enzymes such as inflammasomes, which cleave the pro-IL-1 β into the biologically active molecule. Mature IL-1 β is then secreted, binds to the IL-1 receptor, and exerts its biological effect. IL-1 β binds to IL-1R1 on target cells, which then interacts with the IL-1RAP to induce cell activation via the recruitment of intracellular signalling molecules, including IL-1 receptor-associated kinase 4 (IRAK4) **Figure 1.8**. Signalling through these pathways will result in the activation of NF- κ B, as well as p38, c-JNK, extracellular signal-regulated kinase (ERK), and MAPK.

Inflammasome-mediated IL-1 β activation.

The cleavage of pro-IL-1 β can be achieved by two distinct mechanisms: eliciting a response and releasing active IL-1 β . The first, typically occurring in monocytes and macrophages, is inflammasome-dependent and involves caspase-1, an intracellular protein initially named IL-1-converting enzyme. Once activated, caspase-1 processes pro-IL-1 β and enables the release of the mature cytokine. The inflammasomes involved in the processing of caspase-1 activation and IL-1 β cleavage are also named canonical nodal-like receptors or inflammasomes. These inflammasomes are activated by distinct ligands such as PAMPs or DAMPs (extracellular glucose, amyloid B peptide, uric acid, cholesterol crystals, and ox-LDL) (Liu *et al.* 2014; Schroder and Tschopp 2010). IL-1 β is not released unless additional inflammasome activation takes place (**Figure 1.8**). In general, IL-1 is processed and activated by a caspase-1 dependent mechanism in conjunction with inflammasome assembly, as well as by caspase-1-independent processes (**Figure 1.8**).

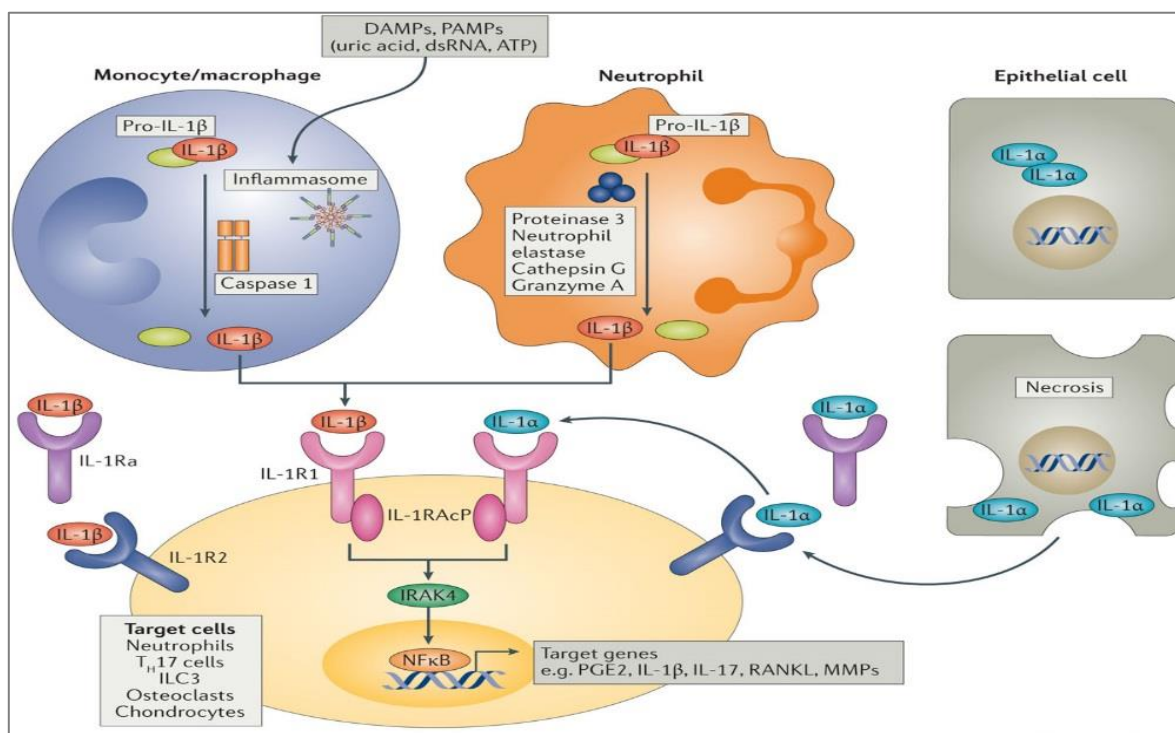


Figure 1.8. IL-1 signalling and activation. The release of IL-1 β from monocytes, macrophages, and neutrophils requires the enzymatic processing of its intracellular precursor protein (pro-IL-1 β). This step can occur via two different pathways. Caspase-1-mediated cleavage of pro-IL-1 β is based on the activation of an intracellular protein complex called the inflammasome (inflammasome-dependent IL-1 β activation). The inflammasome is induced by damage-associated molecular patterns (DAMPs) or pathogen-associated molecular patterns (PAMPs), such as uric acid crystals, dsDNA, or ATP. Alternatively, pro-IL-1 β can be cleaved by neutrophil-derived serine proteases (a cycle independent of inflammasome activation). IL-1 α is produced and confined intracellularly (for example, in epithelial cells). In the event of cell necrosis, IL-1 α is released and acts as an alarmin. IL-1 α and IL-1 β bind to IL-1 receptor type 1 (IL-1R1) on target cells, attracting IL-1 receptor accessory protein (IL-1RAcP) and leading to activation of IL-1 receptor-associated kinase 4 (IRAK4) and NF- κ B, which, in turn, induce the transcription of IL-1 target genes. ILC3; innate lymphoid cells type 3. Taken from Schett *et al.* (2016).

1.6.2.2 Biological effectors of IL-1

IL-1 α and IL-1 β are highly potent proinflammatory mediators in the tissue that lead to vasodilatation, promote the attraction of leukocytes to the inflamed tissue, and induce the expression of PGs. IL-1 β , together with IL-23, influences a specific subset of innate lymphoid cells (ILCs), ILC type 3, which produce IL-17 and IL-22. A strong link exists between IL-1 β release and the activation of Th17, which produces pro-inflammatory cytokines and facilitates the development of chronic inflammation, in addition to bone and cartilage destruction, as shown in **Figure 1.3**. Interestingly, PGE2 amplifies this process (Schett *et al.* 2016). Several genetically determined auto-inflammatory diseases are characterised by the overproduction of IL-1 β (Schett *et al.* 2016). IL-1-driven animal models of arthritis, such as IL-1RA-deficient mice and CIA, show rapid and extensive cartilage damage (van den Berg 2002).

1.6.2.3 The role of IL-1 in RA

Polymorphism has been found in the genes encoding IL-1 α , IL-1 β , and IL-1RA. IL-1 α polymorphisms are associated with increased susceptibility to RA and altered production of IL-1 (Bax *et al.* 2011). IL-1 β gene polymorphisms also influence IL-1 expression and are associated with pro-inflammatory effects and erosive damage in RA patients (Mateen *et al.* 2016).

IL-1 α , 1 β , 18, and 33 are abundantly expressed in RA. They promote the activation and migration of leukocytes, ECs, chondrocytes, and osteoclasts into the joints (McInnes and Schett 2011). Production of IL-1 in the joint further produces or secretes additional cellular messengers, such as proteoglycans and proteases, that can lead to the formation of the pannus, which accumulates in the joints. Destructive enzymes can then go on to degrade cartilage and ultimately destroy and erode bone. Local production of IL-1 in murine arthritis model shows that it is directly responsible for the inhibition of proteoglycan synthesis. At the cellular level, IL-1 induces other cytokines, including IL-6 and TNF- α . In animal studies, TNF- α has been established as a very potent inducer of IL-1. Together, IL-1 and TNF- α act synergistically to cause further damage to the joints in patients with RA (Schiff 2000). At the systemic level, the main effects of IL-1 β are the induction of the fever response and the production of PGE₂ by the hypothalamus (Schett *et al.* 2016).

IL-1 β production by CD14⁺ macrophages induce the production and expression of matrix-degrading enzymes (MMPs), NO, and RANKL (Catterall *et al.* 2001; Eberhardt *et al.* 2000) and is regulated by TNF- α . IL-1 β is a basic component of TNF-mediated osteoclastogenesis and regulates RANK expression. In RA patients, plasma and SF concentrations of IL-1 β are elevated, and these correlate with various parameters of the disease activity (Kay and Calabrese 2004) including the duration of morning stiffness and pain score.

The cytokines IL-1 α , IL- β , IL-6, and IL-17 are pro-inflammatory and play a major role in atherosclerosis disease progression (Dinarello 2011; Ramji and Davies 2015). While IL-1Ra, IL-33, and IL-10 are anti-atherogenic, ApoE^{-/-} mice, which were also deficient for IL-1 α and IL- β showed a 30% decrease in atherosclerotic lesions compared to the control mice (Kamari *et al.* 2011). Likewise, the administration of an anti-IL-1 β antibody to ApoE^{-/-} mice inhibited atherosclerotic lesion formation (Bhaskar *et al.* 2011). In addition, inhibition of IL-1 β increased plasma HDL levels, lowered plaque lipid and macrophage content, and reduced secretion of IL-6, IL-8, CCL2, and TNF- α (Bhaskar *et al.* 2011). IL-1 β expression was found to be increased in the vessel walls of atherosclerotic arteries and plaque macrophages (Galea *et al.* 1996). Anti-IL-1 monoclonal antibodies such as canakinumab reduced the risk of future MI in

patients with established atherosclerotic disease who had already survived a MI (Canakinumab Anti-Inflammatory Thrombosis Outcome Study; CANTOS) (Ridker *et al.* 2011; Ridker *et al.* 2017).

1.6.2.4. IL-1 inhibition in RA

In CIA, treatment with neutralising antibodies against both IL-1 α and IL-1 β is highly effective in preventing established arthritis, reducing both inflammation and the progression of cartilage destruction (Jiang *et al.* 2000; Rau *et al.* 2003). The efficacy of blocking IL-1 in patients with active RA has long been established in clinical trials. Nowadays, anakinra, a recombinant human IL-1Ra, is used for the treatment of RA.

1.6.3 Interleukin-6 (IL-6)

IL-6 is a multifunctional cytokine that has a pleiotropic nature. Serum levels of IL-6 in healthy subjects range between 1 and 5 pg/ml. It can increase rapidly in inflammatory states, such as infection and septic shock, when levels reach the ng/ml range (Jones *et al.* 2018). In RA, serum levels range from around 1.5–234 pg/ml. All stromal cells (fibroblasts, osteoblasts, and ECs) and cells of the immune system (monocytes, macrophages, B cells, and T cells) produce IL-6, which can activate cells through both membrane-bound (mIL-6R) and soluble receptors (sIL-6R), thus widening the number of cell types responding to this cytokine (Choy and Dayer 2009). IL-6, via *classic* signalling has regenerative and anti-inflammatory functions, whereas *trans*-signalling is pro-inflammatory. IL-6R signals through the JAK/STAT pathway by the latent transcription factors STAT1 and STAT3. IL-6 is usually produced because of the effects of IL-1 β , TNF- α , TGF- β , or LPS stimulation. IL-6 is controlled at multiple levels by microRNAs (e.g., let-7a), RNA-binding proteins (for example, Lin28B), circadian control factors, and protein levels (for example, IL-6R shedding, sgp130 antagonism) through mechanisms that either inhibit or promote its action (Hunter and Jones 2015; Jones 2011). GWAS and analyses of single-nucleotide polymorphisms and microarray data have identified links between IL-6 and disease outcomes. For example, a G-to-C mutation proximal to the transcriptional start of the IL-6 *gene* (rs1800795) causes elevated IL-6 expression, and carriers of this mutation have an increased incidence of coronary heart disease and idiopathic juvenile arthritis (Hunter and Jones 2015).

1.6.3.1 IL-6 signal transduction

IL-6 biology is highly complicated. It has been reported that IL-6 uses three forms of signalling: *classical* IL-6 receptor signalling, IL-6 *trans*-signalling, and a third, more recently reported

mechanism described as IL-6 *trans*-presentation. As illustrated in **Figure 1.9**, IL-6 binds to the transmembrane type of mIL-6R (classic signalling), soluble forms of IL-6R (*trans* signalling) or is presented to neighbouring cells via membrane-bound mIL-6R (*trans*-presentation). These three different modes of signalling all require binding to the signal-transducing receptor subunit (gp130). All cells in the body express gp130, thereby acquiring responsiveness to IL-6 via *trans*-signalling. mIL-6R is restricted to hepatocytes, specialised epithelia, and leukocytes (Calabrese and Rose-John 2014; Hunter and Jones 2015; Jones *et al.* 2011). Classical IL-6 signalling via mIL-6R plays a prominent role in the maintenance of immune homeostasis. Studies of human neutrophils have shown that CRP, inflammatory chemokines, bradykinin, complement regulators, and lipid mediators, including platelet-activating factors and leukotrienes (LTs), activate the shedding of IL-6R. Soluble gp130 (sgp130) antagonises IL-6 activities driven by sIL-6R, leading to competitive inhibition of the IL-6/sIL-6R response and selectively inhibiting IL-6 *trans*-signalling (Hunter and Jones 2015; Jones *et al.* 2011). The high concentrations of sgp130 in human serum (200–400 ng/ml) remain largely unaltered during inflammation and may function as a physiological buffer of IL-6 *trans*-signalling (Hunter and Jones 2015).

JAK is bound to the cytoplasmic domain of gp130. Once gp130 signalling is initiated, two main downstream pathways are activated: the JAK-STAT1 and STAT3 pathways. When IL-6 binds to its receptor, JAK activates the phosphorylation (p) of STAT1 and STAT3. pSTAT is then translocated into the nucleus, where it exerts transcriptional activity, influencing the expression of IL-6-responsive genes involved in local and systemic manifestations such as acute phase-proteins (**Figure 1.9**). STAT3-dependent IL-6R signalling induces suppressor of cytokine signalling 1 (SOCS1) and SOCS3 expression (Yoshimura *et al.* 2007). SOCS1 binds immediately to activated JAK, thereby attenuating its catalytic activity. On the other hand, SOCS3 binds to phosphorylated gp130 and terminates the activation of JAK as a negative feedback loop to suppress STAT1 and STAT3 activity, respectively.

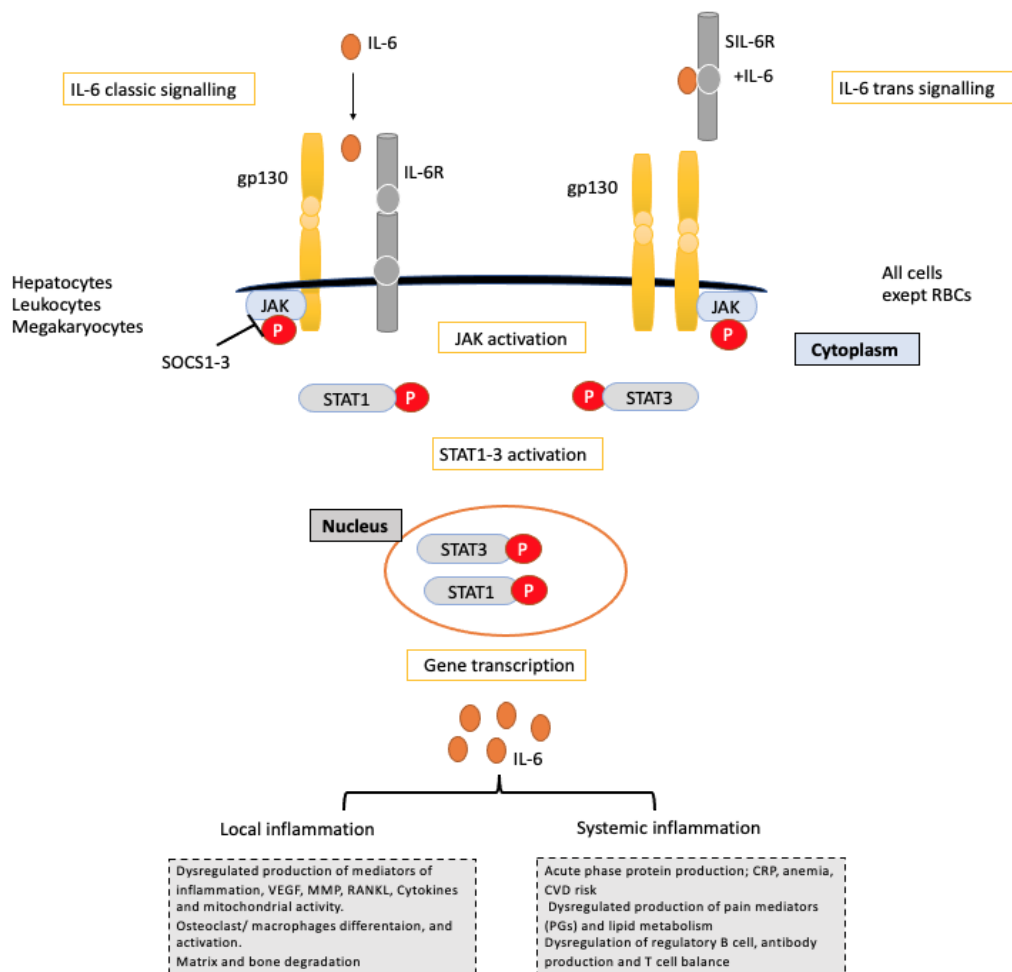


Figure 1.9. Classical IL-6 receptor signalling and IL-6 trans-signalling pathways and their role in RA

IL-6 binds to the IL-6 receptor (IL-6R) and glycoprotein 130 (gp130) to form a classic complex. IL-6 *trans*-signalling requires sIL-6R. Both membrane-bound (mIL-6R) and soluble (sIL-6R) are associated with the classical signalling and *trans*-signalling pathways, respectively, and all end in complexes with the signal-transducing receptor subunit gp130. The cell types expressing the receptors are shown. Intracellular signalling pathways involve the Janus kinase (JAK) and signal transducer and activator of transcription (STAT) pathways. IL-6 participates in a broad spectrum of biological events with both local inflammatory and systemic effects, such as synovial inflammation, acute-phase reactions, immune responses, and haematopoiesis. Adapted from Choy *et al.* (2020).

1.6.3.2 Biological effectors of IL-6

IL-6 is involved in a wide range of biological activities, including immune regulation, haematopoiesis, and inflammation (Hunter and Jones 2015). IL-6 has hormone-like characteristics that affect many systems and processes, such as lipid metabolism (Glund and Krook 2008), vascular system (Hou *et al.* 2008), and bone homeostasis (Jones *et al.* 2018). IL-6 can activate cells to manifest many of the local and systemic effects of inflammatory diseases (Choy and Dayer 2009).

IL-6 differs from IL-1 and TNF- α in its inability to stimulate PGs, and collagenase production in chondrocytes and synovial fibroblasts (Arend and Dayer 1990). Also, IL-6 is a more potent inducer of hepatic synthesis of CRP and Ig (autoantibodies) by B-cells than either IL-1 or TNF- α . Even though IL-1 and TNF- α are the major activators of IL-6 expression, other pathways such as TLRs, PGs, stress responses, and other cytokines can promote the synthesis of IL-6. IL-6 modulates the expression of the adhesion molecules ICAM-1 and VCAM-1 (Hunter and Jones 2015). IL-6 governs the proliferation and survival of T cells and modulates their effector cytokine production, the proliferation and survival of T helper cells, the inhibition of Treg, and the maintenance of immune homeostasis. IL-6 also controls the expression of chemokine receptors as well as the proliferation and differentiation of B cells (Huber *et al.* 1999). IL-6 also alters the effector characteristics of defined T cell populations (Hunter and Jones 2015). IL-6 *trans*-signalling promotes the secretion of the chemokines CCL2, CCL8, and cellular adhesion controlled by the lymph node (Hunter and Jones 2015). IL-6 stimulates IL-17 generation, whereas IL-17 provokes IL-6 production, thereby creating a vicious pro-inflammatory cycle (McInnes *et al.* 2016). IL-6 increases neutrophil adhesion to the EC and migration into the joint (Srirangan and Choy 2010). *In vitro*, IL-6 promotes macrophage differentiation, and STAT1 is activated during monocyte to macrophage differentiation (Bleier 2004; Chomarat *et al.* 2000).

IL-6 transgenic mice exhibit osteopenia with increased osteoclast and decreased osteoblast populations (Kang *et al.* 2019). IL-6 deficiency leads to impaired innate and adaptive immunity to viral, parasitic, and bacterial infections (Hunter and Jones 2015), affecting both mice (Kopf *et al.* 1994) and humans (Puel *et al.* 2008).

1.6.3.3 IL-6 role in RA

According to its physiological and pathological roles, many of the articular and systemic manifestations of RA can be attributed to the biological effects of IL-6. In RA, IL-6 in the joints has been shown to promote pannus formation, osteoclast activation, and chronic synovitis

(Choy *et al.* 2014). High IL-6 levels drive local leukocyte activation and autoantibody production as well as mediate systemic effects that promote acute-phase responses, anaemia, and cognitive dysfunction (González *et al.* 2017). IL-6 was also implicated in damage to the articular cartilage in RA, as IL-6 and sIL-6R markedly inhibited proteoglycan synthesis in cultures of human articular chondrocytes from patients with RA (Guerne *et al.* 1999). In addition, levels of IL-6 and sIL-6R in SF correlated with a histological characteristic of chronic synovitis in patients with RA (Sack *et al.* 1993) and sIL-6R correlated with leucocyte infiltration and correlated with disease activity score (Heinrich *et al.* 1990; Madhok *et al.* 1993). IL-6 can propagate joint destruction through the induction of RANKL production from synovial fibroblasts and the production of MMPs, resulting in increased osteoclastogenesis. In terms of lipid metabolism dysregulation, it was reported that IL-6 affects lipid metabolism by stimulating hepatic fatty acid (FA) synthesis and adipose tissue lipolysis. Moreover, IL-6 increases cholesterol synthesis while decreasing cholesterol excretion (Khovidhunkit *et al.* 2004). Various studies have examined the association between IL-6 and CVDs. In general, there is a significant association between inflammatory measures, particularly ESR, and the risk of CVD (Choy *et al.* 2014) in RA patients. Additionally, there is evidence that reducing inflammation in RA lowers CV risk (Choy and Sattar 2005; Dixon *et al.* 2007; van Halm *et al.* 2006). Notably, Ridker *et al.* mentioned that elevated IL-6 levels in healthy men were associated with increased risk for future MI independently of hs-CRP (Ridker *et al.* 2000). It was also reported that among women with prevalent CVD, those with high IL-6 levels had a > 4-fold risk of death compared to women with normal IL-6 levels (Volpato *et al.* 2001). Moreover, IL-6 levels are linked to increasing mortality in patients with acute coronary syndromes (Biasucci *et al.* 1999).

1.6.3.4 IL-6 inhibition in RA

Over the last three decades, IL-6 blockade has shown good clinical efficacy and good safety profiles. Anti-IL-6R monoclonal antibodies are approved for the treatment of RA. These will be discussed in detail under the section “Management of RA”.

1.7 Non-cytokine mediators

1.7.1 Nitric Oxide (NO)

NO is a crucial physiological messenger and effector molecule in many biological systems, including immunological, neuronal, and CV tissues (Nagy *et al.* 2010). Due to its involvement in these various systems, interest in measuring NO in biological tissues and fluids remains strong. Recent studies have reported that aberrant NO production is responsible for the

pathogenesis of various inflammatory diseases, including HTN, atherosclerosis, and RA (Kats *et al.* 2016).

1.7.1.1 NO production is upregulated in RA patients

Several studies confirmed increased endogenous NO synthesis in RA. Under physiological conditions, NO contributes to the regulatory functions of T cells; however, overproduction of NO may contribute to T lymphocyte dysfunction in autoimmune diseases (Nagy *et al.* 2010). Patients with RA have a dual abnormality in NO-dependent vascular function, characterised by reduced endothelial nitric oxide synthase (eNOS) and enhanced inducible nitric oxide synthase (iNOS) by leukocytes and vascular smooth muscle cells (VSMCs) (Kaur *et al.* 2014). The enzyme iNOS catalyses the production of NO from arginine and hence may further potentiate the production of Peroxynitrite (ONOO⁻) (Panga *et al.* 2019). NO mediates various cellular functions at the site of synovial inflammation, including cytokine production, signal transduction, mitochondrial functions, and apoptosis.

Cytokines such as IL-1, TNF- α and IFN- γ induce NO production by PBMCs, whereas TGF- β and IL-10 suppress it (Yamamoto *et al.* 1998). These cytokines are abundant in rheumatoid synovium, and the amount of NO present in inflamed joints could therefore be a net effect of these pro-inflammatory cytokines. It has been reported that IL-1 alone does not induce NO production by macrophages and hepatocytes, though it potentiates the effects of other inducers (Stefanovic-Racic *et al.* 1993). However, a study by Liew reported that IL-1 β and TNF- α increase iNOS expression in many cells, either alone or in synergistic combination (Liew 1994). TNF- α or IFN- γ induce the synthesis of NO by Kupffer cells and murine macrophages (RAW 264.7) *in vitro*. These cytokines show similar effects on the induction of MMP in rabbit chondrocytes and synovial fibroblasts, a response that is blocked strongly by TGF- β and weakly by IFN- γ . This effect of IFN- γ contrasts with its effects on macrophages and hepatocytes, where it promotes the induction of NO. The principal source of NO production in RA has yet to be fully identified, though Sakurai in 1995 suggested the presence of iNOS in human synovium and implied that macrophages are the major source of synovial NO. McInnes reported that there is a capacity for high output of NO by human synovial tissue, and although human macrophages can express high levels of iNOS, most cells expressing iNOS are fibroblasts (McInnes 1996).

1.7.1.1.1 Serum NO level

A study using a sensitive chemiluminescence assay indicated that serum NO levels are higher in patients with RA than in patients with OA or healthy subjects (McInnes 1996; Ueki *et al.*

1996). Moreover, NO levels correlate with disease activity when assessed by the duration of morning stiffness, the number of tender or swollen joints, and CRP in the same study. These studies suggest that upregulated NO production in the sera of RA patients may reflect exaggerated inflammatory changes in the joint.

1.7.1.1.2 NO concentration in PBMCs

Activation of PBMC with IFN- γ results in increased iNOS expression and nitrite and nitrate production *in vitro*. Increased iNOS production in fresh PBMCs from RA patients has been reported, and it suggests systemic activation for iNOS expression in RA patients (St Clair 1996). In the same study, PBMC iNOS activity was highly correlated with disease activity as measured by tender and swollen joint counts. The temporal sequence of ligand binding appears important since pre-exposure of macrophages to LPS suppresses subsequent IFN- γ induced NO production (Severn *et al.* 1993). Cell-cell contact between T lymphocytes of both the Th1 and Th2 subsets and macrophages led to iNOS expression in inflammatory lesions (McInnes 1996).

1.7.1.1.3 NO concentration in SF

SF nitrate is significantly higher than serum nitrate in patients with RA, indicating local NO synthesis in the rheumatoid synovium (Farrelt *et al.* 1992). Two separate studies found that nitrite concentrations are increased in not only RA patients but also in OA and gouty arthritis patients (Farrelt *et al.* 1992; Sakurai *et al.* 1995). Increased NO production may therefore not be unique to RA and reflect non-specific inflammation.

1.7.1.1.4 NO production in cartilage and synovial tissue

Immunohistochemical studies and *in situ* analysis revealed that both iNOS proteins and mRNA are predominantly expressed in synovial lining cells, ECs, chondrocytes, and, to a lesser extent, mononuclear cells, and synovial fibroblasts. *Ex vivo* cultured rheumatoid synovium produces a significant amount of nitrite (Miyasaka 1997). Most of the synovial lining cells and infiltrating mononuclear cells reacting with anti-iNOS antibodies express CD14 and HLA-DR, which suggests that most iNOS producers are macrophages. Studies have confirmed that upon stimulation of human chondrocytes with IL-1 β , TNF- α or LPS, there is a high expression of iNOS and marked production of NO (Sakurai *et al.* 1995; Stadler *et al.* 1991). Studies also found that both *ex vivo* cultures of cartilage and *in vitro* cultures of chondrocytes obtained from RA patients produce large amounts of NO (Rediske *et al.* 1994).

1.7.1.2 Pathophysiological role of NO in RA

The precise role of NO in RA remains less clear. Possible pro-inflammatory effects of NO include the induction of COX and inflammatory cytokines like TNF- α and IL-1 β . NO can also

be involved in the production of angiogenic chemokines and reactive nitrogen species (RNS) (Leibovich *et al.* 1994). Superoxide reacts with NO to form ONOO⁻, which is a component of the RNS. This reactive species plays a role in the NF- κ B mediated production of inflammatory mediators such as TNF, IL-1 β and iNOS (Panga *et al.* 2019). Also, this can lead to the activation of MMP and the depletion of GSH, the augmentation of vascular permeability in inflamed tissues, and the generation of destructive free radicals such as the hydroxyl radical. As reported, NO may also exert an anti-inflammatory effect; it may therefore have biphasic or opposite biological effects in the joints, depending on its local concentration.

A reciprocal pathway may exist whereby NO from synovial fibroblasts enhances pro-inflammatory cytokine production by macrophages, which in turn may upregulate iNOS expression, thereby generating a positive feedback loop. NO is implicated in IL-1 β mediated inhibition of proteoglycan synthesis, suggesting a pro-inflammatory role for NO (McInnes *et al.* 1996).

1.7.2 Eicosanoids (Prostaglandins)

Eicosanoids are a family of bioactive lipid mediators, 20 carbons in length, with a wide variety of actions having hormone-like effects. The eicosanoid family includes PG, leukotrienes (LT), thromboxanes (TX), and numerous hydroxyl FAs (McDaniel *et al.* 2011).

PGs are derived from the membrane phospholipids by phospholipase A2 (PLA2) and then brought to either the COX pathway or the lipoxygenase (LOX) pathway. The COX pathway produces TX, prostacyclin (PGI₂), PGD₂, E₂, and F₂ α (**Figure 1.10**). Alternatively, the LOX enzyme pathway is active in monocytes and macrophages and synthesises LTs. Studies have focused on the role of individual PGs as anti-inflammatory eicosanoids (PGD₂, PGJ₂) and pro-inflammatory eicosanoids (PGE₂, LTB₄, PGI₂). In this thesis, I focused on PGE₂, as in next section 1.7.2.1.

PGs are small, potent inflammatory mediators that have a short half-life before being inactivated and excreted from the circulation. PGs are powerful vasodilators and inhibit the aggregation of blood platelets, as well as regulating the contraction of smooth muscle tissue. Conversely, TXs produced by platelets are vasoconstrictors and facilitate platelet aggregation. Their terminology comes from their role in clot formation (thrombosis) (Ricciotti and FitzGerald 2011). COX-1 is responsible for the baseline levels of PGs, whereas COX-2 produces PGs after stimulation (**Figure 1.10**). COX-1 and COX-2 are both located in blood vessels, the kidney, and the stomach. AA metabolites can stimulate the activity of different

cytokines TNF- α , IL-1, IL-6, CCL2, RANTES, and IL-8, or integrins (Adam 2003; Yao and Narumiya 2019).

Macrophages are one of the main cell sources of PGs in inflammation, and the autocrine feedback of PGs on macrophages amplifies their function. Cytokines and PGs synergistically activate NF- κ B to induce the expression of inflammation-related genes, one of which is COX-2 itself, which makes a PG-mediated positive feedback loop (Yao and Narumiya 2019). Earlier studies identified the PGE2-EP2 (receptor) NF- κ B signalling cascade in macrophages infiltrating the arterial wall as a factor sustaining the pathogenesis of IA (Yao and Narumiya 2019). It has been reported that PGE2 activates NF- κ B synergistically with TNF- α via EP2 in macrophages *in vitro* to induce proinflammatory genes, including COX-2 and CCL2, and that CCL2 mRNA is also stabilised by this pathway. This enables sustained infiltration of these cells and further amplifies chronic inflammation. PGs are also involved in angiogenesis (Yao and Narumiya 2019).

1.7.2.1 Prostaglandin E2 (PGE2) in RA

PGE2 is a well-known lipid mediator that contributes to inflammatory pain and has a great impact on pain signals. PGE2 is involved in every single process leading to the classic signs of inflammation: redness, swelling, and pain. Redness and oedema result from increased blood flow into the inflamed tissues through PGE2-mediated augmentation of arterial dilatation and increased microvascular permeability. Pain results from the action of PGE2 on peripheral sensory neurons and on central sites within the spinal cord and the brain (Funk 2001).

Elevated levels of PGs have been found in the SF and synovial membranes of RA patients (Stańczyk and Kowalski 2001). PGE2 is generated by chondrocytes and synovial fibroblasts and is involved in synovial inflammation in RA. (Hoxha 2018). Microparticles (Schaiff *et al.* 2000), which are small vesicles that are released from activated or dying cells and express DAMP and are found in the SF of RA patients, up-regulate the production of PGE2 in synovial fibroblasts by inducing COX-2. Chondrocytes and synoviocytes from patients with RA or OA have increased levels of COX-2 and PGE2 (Li *et al.* 2005; Martel-Pelletier *et al.* 2003; Masuda *et al.* 2005).

Sheibanie *et al.* and others showed that in addition to upregulating IL-23 (Sheibanie *et al.* 2007), PGE2 produced by rheumatoid synovium is thought to be implicated in IL-6 production and joint destruction and regulates VEGF (Portanova *et al.* 1996; Sheibanie *et al.* 2004). In CIA, administration of the PGE2 analogue misoprostol exacerbated joint inflammation, which was associated with increased mRNA levels of IL-23p19 (Sheibanie *et al.* 2007) and increased

levels of IL-6, IL-1 β , IL-17 and TNF- α in the affected joints (Sheibanie *et al.* 2004). Studies indicate that IL-6 is directly involved in Th17 cell differentiation (Sutton *et al.* 2006; Mangan *et al.* 2006) suggesting that PGE2 also contributes to the differentiation and maintenance of Th17 effectors through multiple molecular mechanisms involving a plethora of cytokines relevant to Th17 cell differentiation and survival).

PGs bind to their G protein-coupled receptors (GPCRs). PGE2 exerts its diverse roles by acting on these transmembrane receptors: EP1, EP2, EP3, and EP4 (**Figure 1.10**). PGE2, through binding to different EP receptors, can regulate the function of many cell types, including macrophages, DCs, T, and B cells, leading mainly to pro-inflammatory effects. Osteoclast precursors express PG receptors (EP1, EP2, and EP4) because osteoclasts were differentiated from a monocyte/macrophage lineage that expresses EP receptors (Kobayashi *et al.* 2005; Tsuboi *et al.* 2002). cAMP signalling is mediated by EP2 and EP4-enhanced osteoclastogenesis (Kobayashi *et al.* 2005).

1.7.2.2 PGs inhibitions

NSAIDs. Inhibit PG production through the inhibition of COX-1 and COX-2. However, NSAIDs can cause gastrointestinal side effects such as gastric ulceration and bleeding, and they are also associated with increased cardiovascular risk (Hoxha 2018).

COX-2 selective inhibitors, or coxibs. COX-2 selective inhibitors are approved for the treatment of RA demonstrating the importance of PGs and specifically PGE2 in mediating pain and/or inflammation. There is supporting evidence for the role of the EP1 receptor in mediating pain and inflammation.

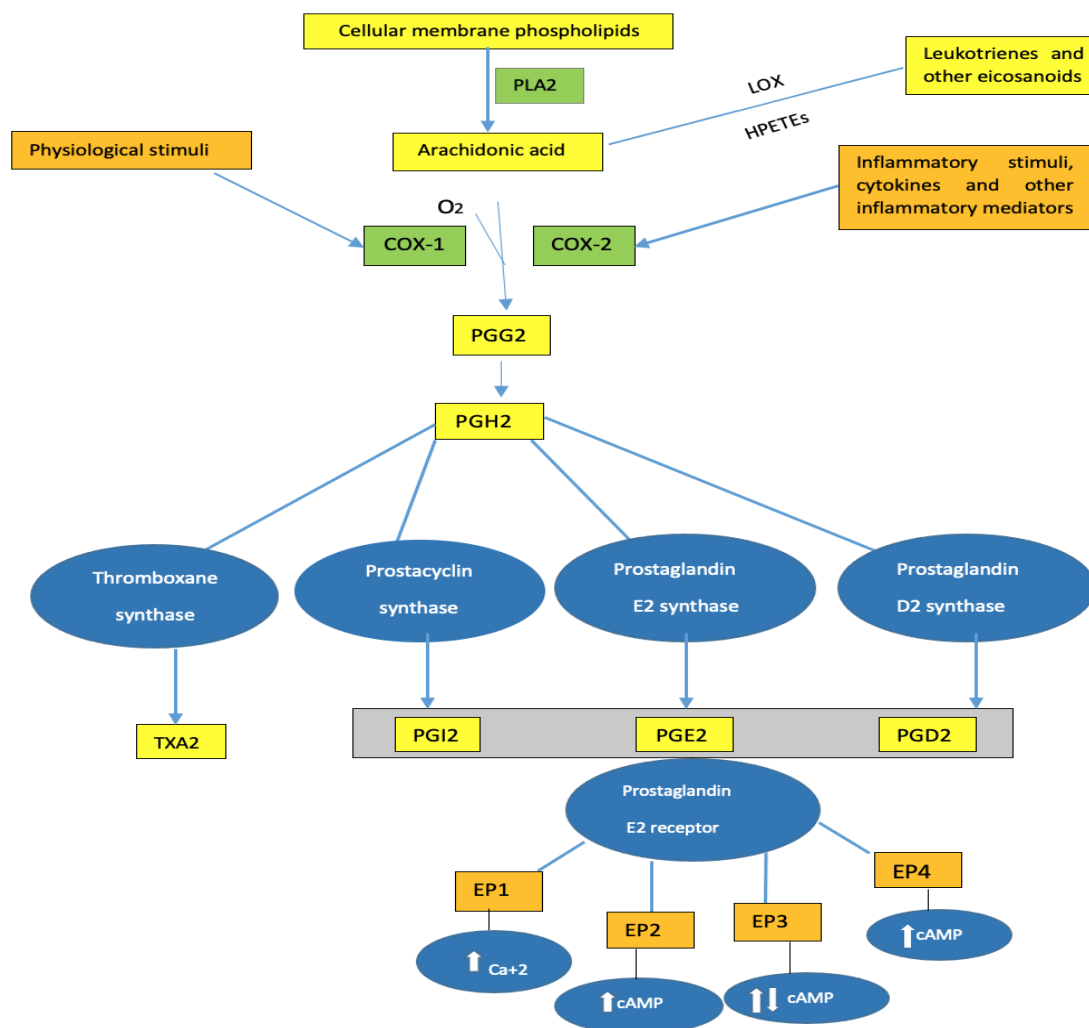


Figure 1.10. Prostaglandin's synthesis pathway. Arachidonic acid (AA), liberated from cellular membrane phospholipids by the action of phospholipases A2 (PLA2), and cyclooxygenases (COX) are the rate-limiting step in the biosynthesis of prostaglandin (PG). COX1 and COX2, which convert AA to prostaglandin H2 (PGH2), are the main targets of COX2-specific inhibitors and NSAIDs. PGH2 becomes a substrate for thromboxane, prostacyclin, and prostaglandin synthases, which are converted into thromboxane A2 (TXA2), PGI2, PGE2, and PGD2. Arachidonic lipoxygenases and hydroperoxides (HPETEs) convert AA into leukotrienes (LTs), and another inflammation-mediating eicosanoid. There are four receptor subtypes for PGE2 (EP1-4). Their actions are mediated via increases in intracellular calcium level (EP1), increases in cAMP levels (EP2, EP4), and increases or decreases in intracellular cAMP levels (EP3). Modified from Khan *et al.* (2008) and Ressler *et al.* (2014).

1.8 Management of RA

1.8.1. Diet and lifestyle modifications

Non-pharmacological treatment includes patient education and lifestyle changes, which are important considerations in RA management. EULAR recommendations for management of RA stated that lifestyle recommendations should emphasise the benefits of a healthy diet, regular exercise, and smoking cessation for all patients (Agca *et al.* 2017; Chehade *et al.* 2019). Abstaining from smoking is universal advice to all RA patients given its impact on RF and ACPA formations. Exercise is vital to support joint flexibility and function. There is accumulating evidence that structured exercise therapy has beneficial effects on CVDs in

patients with RA. However, there is no specific recommendation on specific food types (Gwinnutt *et al.* 2022).

Patients with RA frequently ask their doctors about the foods or diet that will help their arthritis. Even if their physicians could not provide definitive advice, many patients try various dietary interventions, including complementary medicines. This is not unique to patients with RA but applies to all patients with inflammatory rheumatic diseases. The key question for physicians is: Can we reduce inflammation with a diet? Whilst it may seem unlikely that diet could be as effective as disease-modifying anti-rheumatic drugs (DMARDs), it is safe, can be complementary to DMARDs and may reduce the dose, number, and frequency of medications, including NSAIDs and GCs, which are associated with side effects.

Although the origins of our understanding of diet and disease stem back to paleontological times (David *et al.* 2010), the precise mechanisms whereby diet improves symptoms such as pain, stiffness, and fatigue remain largely unknown. In RA, the Mediterranean diet (MD) has been suggested to be beneficial for disease activity (Masuko 2018). This has been hypothesised as one of the reasons why RA is milder in Southern Europeans compared with Northern Europeans (Drosos *et al.* 1992). Various dietary components of the MD, including polyphenols and n-3 PUFA, have been demonstrated to have key anti-inflammatory properties. Along with improving metabolic imbalance and modulating gut microbiota, diet may gradually adjust the physiological condition as well as the immunological response in RA patients (Masuko 2018). A balanced intake of a variety of natural and healthy foods, including dietary fibre and low carbohydrate, is important for maintaining diverse intestinal flora and reducing metabolic and inflammatory risks (Masuko 2018). The human gut microbiome regulates local and systemic immune responses, and its bacterial composition can be modulated by diet and other environmental factors (Masuko 2018), as shown in **Figure 1.11**.

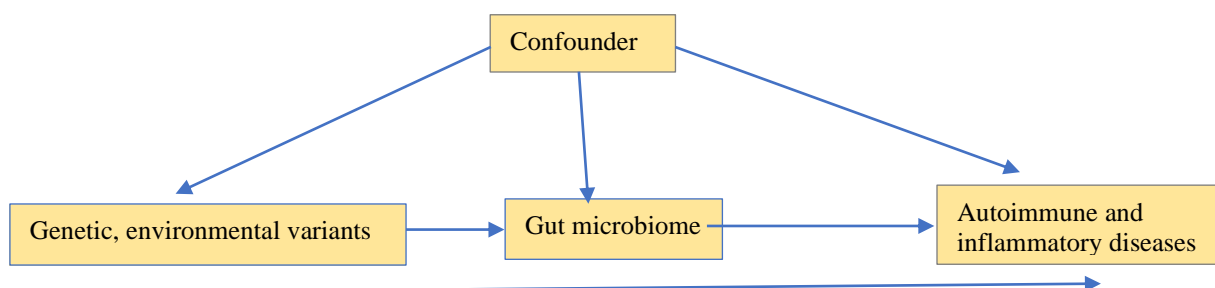


Figure 1.11. Schematic illustration of gut microbiome, genetic, and environmental factors as a leader of autoimmunity and chronic inflammation.

Lourdudoss *et al.* indicated that higher intake of dietary vitamin D and n-3 FA during the year preceding DMARD initiation is associated with better treatment results in patients with early RA (Lourdudoss *et al.* 2017). In 2018, Cutolo and Nikiphorou and Calder *et al.* reviewed some nutrients that have a regulatory effect on the immune-inflammatory system response in RA, such as n-3 FA, vitamin D, red peppers, cocoa, gluten-free diets, and strawberries. While salt and coffee may aggravate RA. These nutrients and their effects on RA are presented in **Table 1.6**.

Table 1.6. Some selected natural nutritional elements and their effects in RA.

| | |
|--|--|
| Omega-3 | Decreases autoantibody and pro-inflammatory cytokine production, reduces T-cell proliferation, decreases LTb4, decreases pain associated with RA, and lowers the risk of transition from anti-CCP positivity to IA (Gan <i>et al.</i> 2017). |
| Vitamin D | Increases the innate immunity response against infections, decreases adaptive immunity, and decreases pro-inflammatory cytokines and angiogenesis (Vojinovic <i>et al.</i> 2017) |
| Genistein (Soya beans) | Inhibits IL-1 β , TNF- α and MMP-9 expression in RAFS and improves lipid profiles in rats (Rossillo <i>et al.</i> 2016) |
| Curcumin (turmeric) | Blocks the TRAF1 receptor, decreases pro-inflammatory cytokines and chemokines, and leads to polarisation into anti-inflammatory (M2) macrophages in a murine model (Gao <i>et al.</i> 2015). |
| Red hot chilli peppers (capsaicin) | Increases anti-inflammatory (M2) macrophages, modulates the neuro-immune response, and decreases neurogenic pain (Deng <i>et al.</i> 2016). |
| Cocoa | Antioxidant (flavonoids), decreases autoantibody and pro-inflammatory cytokine production, and increases anti-inflammatory cytokines (Ramiro-Puig and Castell 2009). |
| Gluten-free diet | Decreases LDL and ox-LDL levels, raises atheroprotective natural antibodies, and reduces activity in patients with RA (Elkan <i>et al.</i> 2008). |
| Blueberries, strawberries, and pomegranates | Anti-oxidant, anti-inflammatory, and analgesic (reduce joint stiffness and swelling) (Basu <i>et al.</i> 2018). |
| Nano-powdered red ginseng | Decreases pro-inflammatory cytokine production (Lee <i>et al.</i> 2018). |
| Sodium-chloride salt | Activates pro-inflammatory (M1) macrophages, and Th17 cells and decreases T reg cells (Sharif <i>et al.</i> 2018) |
| Coffee | Exacerbates disease due to the blocking of methotrexate receptors (Sharif <i>et al.</i> 2017) |

However, none of these diets or nutrients have been established so far as bringing substantial benefit with a clinically proven disease-modifying effect (Hagen *et al.* 2009). This may be due to the lack of research to prove the dietary component should be used as an additional remedy in RA. Studies that link diet with RA and specific pathways of inflammation and immune regulation afford the possibility of identifying new therapeutic approaches for select patients.

A better understanding of dietary factors and how they relate to the immuno-inflammatory response can contribute to new insights in disease pathogenesis and RA-specific recommendations. In this thesis, I worked on PNLA derived from pine nuts to investigate its immunologic and anti-inflammatory actions in RA.

1.8.2. Pharmacological treatment

Currently, DMARDs are the cornerstone of treatment for RA. Prior to this, before 1970, GCs, and NSAIDs were widely used for treating rheumatic symptoms (Burmester *et al.* 2017). While these agents improved joint symptoms, disability, and related morbidity, they were associated with significant toxicity and cost (Rau 2014; Ramiro *et al.* 2014).

1.8.2.1. NSAIDS

NSAIDs are medications commonly used to reduce inflammation and relieve pain in many conditions, including RA. NSAIDs act as nonselective inhibitors of the COX enzymes, as they inhibit both COX-1 and COX-2. However, NSAIDs are associated with gastropathy and hence have been a major cause of drug-related mortality globally, which led to the development of COX-2 selective agents such as rofecoxib and celecoxib. Although these have less gastrointestinal toxicity than non-selective NSAIDs, cardiovascular safety emerged as a concern from trials and real-world data (Al-Saeed 2011). Rofecoxib was withdrawn from the market in 2004 because of the cardiovascular side effects reported in a randomised control trial (RCT) (Jüni *et al.* 2004). Recent data suggests that all NSAIDs are associated with an increase in cardiovascular risk. Hence, the current guidelines recommend using low doses intermittently (NICE guidelines, non-steroidal anti-inflammatory drugs).

1.8.2.2. GCs

In 1959, the first RCT of GCs in RA showed that 20 mg/day of prednisolone was significantly superior to 6 grams of aspirin daily (Duthie *et al.* 1960; M. R. C. Report. 1959). However, the authors concluded that the highest acceptable dose for long-term treatment was probably in the region of 10 mg daily due to the high toxicity of the 20 mg daily dose. Since the early 1980s, Harris suggested that low-dose, long-term GCs may decrease the progression of radiological damage and reduce inflammation in RA (Harris *et al.* 1983). The effect of GC on both clinical and radiographic parameters in early RA has been the subject of considerable research effort and much debate (Boers *et al.* 1997; Bores 2007). Further RCTs using intensive GC therapy in early RA have been published since then (Goekoop-Ruiterman 2005; van Everdingen 2002) and have consistently supported the concept that GCs have a disease-modifying effect and renewing the debate over the risk/benefit ratio of this treatment (Bores 2007; Carette 2007).

GCs have many beneficial effects but also have detrimental aspects. The safety of GCs has often been debated; current consensus is that long-term use of prednisone at a dose of ≤ 5 mg/day is safe (Ajeganova *et al.* 2014), whereas long-term use of prednisone ≥ 10 mg /day is generally not advised (Strehl *et al.* 2016). GC is regulated by the hypothalamic-pituitary-adrenal axis; a defect of the hypothalamic pituitary-adrenal axis has been reported in RA (Chikanza *et al.* 1992). Furthermore, data from RA cohorts showed that disease activity unfavourably alters the blood lipid profile and that reduction of disease activity with treatment (including GC) can reverse these changes (Boers *et al.* 2003). In a study using an animal model of atherosclerosis, the administration of dexamethasone-induced hyperlipidemia also reduced aortic plaque formation, an effect attributed to the inhibition of infiltration of inflammatory and foam cells in plaques (Munford 2001). On the other hand, treatment with GC is controversial, and long-term use should be avoided with respect to the increased risk of adverse effects such as infections, osteoporosis, DM, and HTN (Hoes *et al.* 2007, Morrison *et al.* 2006). Treatment is still considered a risk factor for dyslipidemia and atherosclerosis. In RA patients, longer GC use has been significantly associated with hypercholesterolemia and increased risk of coronary artery disease (MacGregor *et al.* 1992; Petri *et al.* 1992; del Rincon *et al.* 2005). In 2006, Davis *et al.*, in a population-based inception cohort of 603 patients with RA that GC exposure was associated with an increased risk for CVD only in patients with positive RF (Davis *et al.* 2006). Subsequently, most observational studies concluded there is an association between GC use and the risk of CVD (Huscher *et al.* 2009; Wei *et al.* 2014).

1.8.2.3. DMARDs

High-grade inflammation is perpetuated by pro-inflammatory cytokines (McInnes *et al.* 2016; Schett *et al.* 2013). Conventional synthetic DMARDs (csDMARDs) are non-specific immune-suppressants; in contrast, target synthetic DMARDs (tsDMARDs) and biologic DMARDs (bDMARDs) target specific immune pathways (Burmester *et al.* 2017; Firestein and McInnes 2017). **Table 1.7** displays a summary of the most widely used DMARDs in RA, their mode of action, and some of their reported adverse effects (Smolen *et al.* 2020). Observational studies suggest that CVDs are reduced following treatment with cs/bDMARDs (Roubille *et al.* 2015).

Table 1.7. EULAR recommendations for the management of RA with DMARDs.

| Classification | Name | Mode of action | Side effects |
|---|---|---|---|
| Conventional synthetic (cs) DMARDs | Methotrexate | An analogue of folic acid | Hepatotoxicity, pulmonary damage, and BM suppression. |
| | Sulfasalazine | Anti-inflammatory and immunosuppression | Gastrointestinal, central nervous system, haematological adverse effect, and cardiotoxicity. |
| | Leflunomide/ Teriflunomide | Pyrimidine synthesis inhibitor | HTN, BM suppression, diarrhoea, and hepatotoxicity. |
| | Chloroquine /Hydroxychloroquine | Immunoregulation | Gastrointestinal tract, skin, central nervous system adverse effects and retinal damage. |
| Targeted synthetic (ts) DMARDs Janus Kinase Inhibitors | Tofacitinib, baricitinib, filgotinib, and upadacitinib. | Inhibit intra cellular signalling pathway (JAK/STAT and Tyk2) | LFT elevation, dyslipidaemia Lymphopenia, anaemia, and infection. |
| Biological (b) DMARDs (monoclonal antibody) TNF-α targeted therapy | Infliximab | Anti-TNF- α monoclonal antibody | Infection (pneumonia and a typical tuberculosis), injection site reaction (Lau <i>et al.</i> 2019). |
| | Adalimumab | Anti-TNF- α monoclonal antibody | HTN, drug induced lupus. |
| | Golimumab | Anti-TNF- α monoclonal antibody | Lymphoma risk, drug induced lupus, and neurologic deficit. |
| | Certolizumab pegol | Pegylated anti-TNF- α monoclonal antibody | As above. |
| | Etanercept | TNF- α receptor-Fc immunoconstruct | Sever anaphylactic, transfusion reaction. |
| IL-6 targeted therapy | Tocilizumab, sarilumab | Anti-IL-6R antibody | Increase lipid profile. |
| IL-1 targeted therapy | Anakinra | Recombinant IL-1 receptor antagonist | Immune system suppression, headache, pneumonia, and diarrhoea. |
| Co-stimulation pathway inhibitor | Abatacept | CTLA4-Fc immune-construct | |
| B cell depletion | Rituximab | Anti-CD20 monoclonal antibody | Increase risk of cancer, immune suppression, and hepatitis B reactivation. |

I. Conventional synthetic DMARDs (csDMARDs)

Methotrexate (MTX) is a potent immunosuppressive drug and commonly considered one of the 'anchor drugs' in the treatment of RA (Smolen *et al.* 2017). Chloroquine and hydroxychloroquine are anti-malarial agents commonly used in combination with MTX in RA. MTX has a favourable effect on lipid profiles and insulin sensitivity (Morris *et al.* 2011). Sulfasalazine is currently used in RA, particularly as a component of 'triple therapy' (in combination with MTX and hydroxychloroquine) or as monotherapy in MTX-intolerant patients. Leflunomide, a T cell immunosuppressant, offers an alternative treatment for RA in cases where MTX is ineffective or contraindicated. A variety of other csDMARDs, such as gold, d-Penicillamine, and auranofin, were used for many years before the introduction of MTX but are rarely used in the era of targeted therapies. csDMARDs are associated with serious adverse effects such as neutropenia and hepatotoxicity (**Table 1.7**). Monitoring of these potential serious side effects requires regular blood monitoring (British Society for Rheumatology guidelines).

II. Targeted synthetic DMARDs (tsDMARDs)

In the past few years, medications inhibiting the JAK pathways have supplemented the therapeutic armamentarium against RA. JAKs are intracellular tyrosine kinases (tyk) linked to many cytokine receptors (Choy 2019). Tofacitinib became the first JAK inhibitor to be approved in many countries for the treatment of RA. Since then, baricitinib, upadacitinib and filgotinib have been approved by the European Medicines Agency for treating patients with RA after the failure of MTX (European Medicines Agency 2017; Yamaoka 2016). JAK inhibitors are associated with infection, anaemia and lymphopenia so regular blood monitoring is required (Choy 2019).

III. Biologics DMARDs (bDMARDs)

bDMARDs are so named because they are biologic proteins often manufactured by cell lines for the treatment of RA. Most bDMARDs are monoclonal antibodies and less often immunoglobulin constructs, which are conjugates of cell surface molecules and human immunoglobulin Fc. bDMARDs have transformed the outcome of RA, though they are expensive and associated with an increased risk of serious infections, including reactivation of latent tuberculosis (Lau *et al.* 2019)

1-Anti- cytokines therapy

A. Anti-TNF- α

TNF- α was identified as a therapeutic target by elegant research that led to the discovery of its role in the pathogenesis of RA and the use of anti-TNF- α therapy in patients with RA. The first

biological therapy licenced for the treatment of RA was infliximab (a monoclonal antibody directed against TNF- α). TNF- α inhibitors reduce radiological progression even in the absence of clinical response via direct inhibitory effects on osteoclast differentiation and activity (Smolen *et al.* 2005).

B. Anti-IL-6

Anti-IL-6R monoclonal antibodies (tocilizumab and sarilumab) inhibit the IL-6 pathway by binding and blocking IL-6R. Among their beneficial aspects is the reduction of CRP (Xu *et al.* 2019), which leads to an increase in serum lipid levels as mentioned earlier (CRP increases LDL uptake) and excretion by hepatocytes.

C. IL-1 inhibitor

Anakinra is a recombinant and slightly modified version of the human IL-1Ra protein (**Table 1.7**). It is used as a second-line treatment to manage symptoms of RA after treatment with a csDMARD has failed and can be used in combination with some csDMARDs.

2-Anti-lymphocytes therapy

A. T cell co-stimulation inhibitor

Abatacept is an immunoconjugate of cytotoxic T-lymphocyte antigen-4 and human IgG Fc (CTLA4-IgG). It binds to CD80/86 co-stimulation molecules on antigen-presenting cells to inhibit T cell activation. This, in turn, reduces downstream cytokine release and inhibits osteoclastogenesis.

B. B cell depletion

Rituximab is an anti-CD20 monoclonal antibody targeting B-lymphocytes and causes B cell depletion. It was initially licenced as a treatment for lymphoma. However, a case report published in 1999 described the sustained improvement of RA in a patient undergoing rituximab treatment for lymphoma (Protheroe *et al.* 1999). A subsequent RCT confirmed the efficacy of Rituximab in treating refractory RA (Cohen *et al.* 2006).

1.8.3. Conclusion

Pharmaceutical therapy for RA is effective but expensive and associated with side effects. Non-pharmaceutical treatments, including lifestyle changes and diet, are recommended by international guidelines and have an important supplementary role in the management of RA. Nutrition and its impact on chronic musculoskeletal diseases, including RA, remain poorly taught subjects, both in medical schools and in postgraduate rheumatology training. Some argue that addressing nutrition in our patients is not the 'job' of a rheumatologist, but instead it is for dieticians. While this may be partly true, rheumatologists are the ones who come face

to face with patients and their families, and access to a dietician may not always be easily and readily available or at all possible. Similarly, working in a multidisciplinary team setting with dieticians is certainly optimal, but not always possible. Research on the effects of diet on mediators of inflammation is needed. In this thesis, I examined PNLA, a PUFA found in pine nuts, investigating its effects on the levels of proinflammatory cytokine production implicated in RA and atherosclerosis, the genes and transcription factors annotated in those cytokines, and their pathways.

1.9 Fatty acids in inflammation

Fatty acids (FAs) are widely dispersed in nature and are major components of triacylglycerols (TAGs), phospholipids (PL) and other complex lipids (Calder 2015). They are organic components of living cells and have biological activities that influence cell and tissue metabolism and function. The FA composition of the cell membrane varies depending on cell type and is influenced by diet, metabolism, genetics, and hormone fluctuations (Calder 2015). The relative quantity of FAs within a membrane can then affect its physical nature, which in turn can influence membrane protein functions and protein movement within the membrane. Furthermore, membrane PLs are precursors of molecules involved in cell signalling processes. Previously, it was demonstrated that several of the plant-derived FAs possess some anti-inflammatory actions and therefore may have the potential to serve as alternatives to marine source FAs (Baker *et al.* 2020).

1.9.1 Fatty acid's chemical structure and nomenclature

FA consists of a long hydrocarbon chain ($-\text{CH}_2-\text{CH}_2-$) with a carboxylic acid group ($-\text{COOH}$) at one end of the chain and a methyl group ($-\text{CH}_3$) at the other end. FAs can be divided into saturated (SFAs) and unsaturated (USFAs). SFAs are referred to as saturated because the hydrocarbon chain is saturated with hydrogen atoms due to the absence of double bonds. Saturated hydrocarbon chains are straight with, usually, an even number of carbons (between 12 and 22) (Ruston and Drevon 2001). An example of SFAs is octadecanoic acid, which is denoted as (C18: n-0). USFAs can be either monounsaturated (MUFAs) containing one double bond or alternatively, PUFAs where two or more methylene-interrupted double bonds are present (Schmitz *et al.* 2008). PUFAs consist of long chains of 18 or more carbon atoms; the location of the last double bond of a carbon atom allows the classification either from the carboxyl-terminal end, using the delta (Δ) numbering system, or from the methyl end of the molecule, using the omega (n or ω). They are named after the length of the hydrocarbon chain

and the position of the double bond (numbered from the methyl end) (Vasudevan 2013). Examples of common PUFAs are eicosapentaenoic acid (EPA), docosahexaenoic acid (DHA) (both n-3 FAs), gamma-linolenic acid (GLA), pinolenic acid (PNLA), alpha-linolenic acid (ALA), and stearidonic acid (SDA) (all n-6 FAs).

Omega-3 (essential) FAs have a carbon-carbon double bond located three carbons from the methyl end of the chain n-3 or (ω -3). There are different n-3s that exist, but most of the scientific research focuses on three FAs: ALA (C18:3n-3), EPA (C20:5n-3), and DHA (C22:6n-3). ALA contains 18 carbon atoms, whereas EPA and DHA are considered “long-chain” (LC) n-3s because EPA consists of 20 carbons and DHA contains 22. n-6 FA has a carbon-carbon double bond that is six carbons away from the methyl end of the FA chain, n-6 or ω -6 (Wall *et al.* 2010), LA (C18:2n-6) and AA (C20:4n-6).

The human metabolic biochemistry cannot generate n-3 or n-6 FA, so these are therefore essential FAs of dietary components that humans must ingest because the body requires them for good health but cannot synthesise them. Once obtained from the diet, they can be metabolised by enzymes by the removal of hydrogen and the addition of carbon (desaturation) (Ruston and Drevon 2001) to produce several different products. Nuts, flax seeds, and, especially, oily fish are key sources of n-3 PUFAs, whereas animal fats and vegetable oils can provide n-6 PUFAs (Marszalek *et al.* 2005; Wall *et al.* 2010). The conversion of ALA into EPA and DHA is not sufficient in humans. Thus, increasing evidence shows that an adequate dietary intake of a variety of PUFAs is important for many physiological processes.

PUFAs are produced during the metabolism of dietary lipids and also serve as precursors for several biologically active molecules, such as eicosanoids, growth regulators, and hormones (Huang *et al.* 2004). Thus, PUFAs have profound effects on human health. The role of AA as a precursor for the synthesis of eicosanoids indicates the potential for dietary n-6 PUFAs (LA or AA) to influence inflammatory processes (Lourdudoss *et al.* 2017). Eicosanoids synthesised from AA and cytokines cause progressive destruction of cartilage and bone (Zurier and Calder 2001). Thus, increased AA synthesis in the cell membrane may result in changes indicative of selectively increased inflammation or inflammatory responses in humans (Calder 2019). Importantly, from a nutritional point of view, excess consumption of any oil or fat will also increase total energy intake, and the relative proportions of protein, fat, and carbohydrate intake may disturb that individual's overall health outcome, including the immunological responses.

1.9.2 Omega-3 and -6 polyunsaturated fatty acids (n-3 and n-6 PUFA)

The relationship between PUFAs and RA has been evaluated in many studies, but many questions remain unanswered. n-6 PUFAs exert mostly pro-inflammatory features with some anti-inflammatory actions, as for DGLA (Gallagher *et al.* 2019). While n-3 PUFAs have anti-inflammatory and pro-resolving effects by reducing the production of n-6 PUFA-derived lipid mediators, AA, and inflammatory eicosanoids (Calder *et al.* 2015; Galli and Calder 2009). Calder and Zurier mentioned that PUFAs should be included as part of the normal therapeutic approach to RA. However, it is unclear what the optimal dosage of FA is, or whether there would be extra benefits from using them in combination. The metabolism of EPA leads to the formation of the Resolvin E (RvE) series, and the metabolism of DHA can lead to the formation of the Resolvin D (RvD) series, maresins, and protectins, which are able to resolve inflammation (Calder *et al.* 2015). Protectins can inhibit IL-1 β and TNF- α production (Calder *et al.* 2015). PNLA metabolites will be discussed in section 1.10.1.

The recommendations by EULAR in 2022 regarding lifestyle management did not recommend specific types of food for RA patients (Gwinnutt *et al.* 2022). It highlighted the lack of high-quality trials in various musculoskeletal diseases (Gwinnutt *et al.* 2022). Also, greater understanding and research focus on single food is still needed. In this thesis, the focus was on one of PUFAs, PNLA.

1.9.2.1 n-3 PUFAs in RA

In 1985, the first clinical trial on n-3 PUFA dietary supplementation in RA was reported by Kremer and co-authors (Kremer *et al.* 1985). The experimental group of RA patients was treated with an experimental diet high in EPA (1.8 g/day). After 12 weeks, the authors reported an improvement in tender joint count (TJC) and morning stiffness (Kremer *et al.* 1985). In a separate study, 20 RA patients consumed daily low-dose dietary supplements of n-3 FAs, 17 patients ingested daily high-dose dietary supplements of n-3 FAs, and 12 patients ingested placebo capsules. At week 24, significant improvement in TJC and swollen joint count (SJC) was observed in high and low-dose groups taking n-3 FAs. The added value of this study was the long-term observation and the evidence that only high-dose n-3 PUFA supplementation can lead to RA clinical improvement as well as reduce NSAID and DMARDs use (Navarini *et al.* 2017). Furthermore, after treatment with n-3 PUFAs, the patients were found to need less NSAID treatment in 3 RCTs. These studies showed that patients who received n-3 PUFA treatment for 3 to 4 months reported less joint pain, reduced joint swelling, and improved grip strength (Boe and Vangsnæs 2015; Calder 2015; Fattori *et al.* 2016). These clinical benefits

are thought to be due to a reduction in the levels of pro-inflammatory cytokines (Boe and Vangsness 2015).

Lau *et al.* (1993) and Geusens *et al.* (1994) performed a double-blind placebo-controlled study for 1 year. The patients were treated with n-3 FAs and were able to decrease the long-term requirements of NSAIDs, 41% in the group of n-3 FAs versus 84% in the placebo group at the end of the trial. There were no significant changes in other measured outcomes. In a second study by Geusens *et al.* supplementation with n-3 FAs was associated with a decrease in the requirements for NSAIDs and DMARDs (47% versus 15% compared with placebo). In addition, data from large observational studies support the efficacy of n-3 PUFAs (EPA and DHA) to prevent inflammation by lowering the blood levels of inflammatory biomarkers such as IL-6, TNF- α , CRP, serum amyloid A, and leukocyte count (de Roos *et al.* 2009).

Although WHO recommended people eat less high-calorie food, especially, high in saturated or trans fats and sugars; eat more fruits, vegetables, and select foods of plant and marine origin (e.g, PUFA) (Gwinnutt *et al.* 2022), the beneficial effects of specific diet foods in RA remained controversial. A systematic review and meta-analysis of randomised trials that were conducted in 2017 by Senftleber *et al.* concluded that there is a significant reduction in arthritic pain in patients with RA following supplementations with marine oils (EPA and DHA) (Senftleber *et al.* 2017). While Gioxari *et al.* reviewed studies from a large meta-analysis regarding n-3 PUFA supplements in RA, which resulted in significant amelioration of disease severity markers, namely morning stiffness, TJC, ESR, pain scale, and LTB₄ in addition to TGs, no reduction in IL-1, IL-6, or TNF was reported (Gioxari *et al.* 2018). However, Gioxari *et al.* reported in their conclusions that the overall quality of these trials was poor.

Many studies demonstrated the beneficial effect of n-3 supplementation in primary and secondary CV prevention (Bowen *et al.* 2016; Shah *et al.* 2007). Caterina *et al.* showed that ECs treated with DHA had decreased both cytokine-induced expressions of adhesion molecules (VCAM-1 and ICAM-1) and secretion of inflammatory mediators (IL-6 and IL-8) (Catrina *et al.* 1994). A study by Alfaddagh *et al.* found that an n-3 FAs (EPA and DHA) plasma index \geq 4% prevents progression of coronary artery plaque in non-diabetic patients with coronary artery disease on statin treatment (Alfaddagh *et al.* 2019).

1.9.2.2 n- 6 PUFAs in RA

Calder and Zurier reported that dietary GLA and DGLA (n-6) suppressed acute and chronic inflammation, including joint damage, in several experimental animal models; this was accompanied by changes in inflammatory cell FA composition, decreased production of AA-derived eicosanoids, decreased function of leucocytes, and decreased production of ROS

(Calder and Zurier 2001). In a southern European multicentre nested case-control study by de Pablo *et al.*, higher levels of LA, an n-6 PUFA, were associated with a reduced occurrence or lower risk of RA (de Pablo *et al.* 2018). Preliminary evidence suggests evening primrose oil (EPO) may reduce pain, swelling, and morning stiffness, but other studies have found no effect (de Pablo *et al.* 2018). In general, there are limited pre-clinical or clinical studies regarding n-6 PUFA in RA. However, there were some studies regarding n-6 supplementation in HCs. Supplementation studies using GLA-rich oils to provide 2.4 g/day in healthy human volunteers reported a range of effects, including decreased production of pro-inflammatory cytokines (TNF- α , IL-1, and IL-6) by monocytes, decreased lymphocyte reactivity, and decreased chemotaxis of neutrophils (DeLuca *et al.* 1999). TNF- α and IL-1 β production by LPS-stimulated human PBMCs is reduced by n-6 PUFA dietary supplementation (DeLuca *et al.* 1999). Studies using 1g/day GLA or less reported no effect on lymphocyte proliferation (Yaqoob *et al.* 2000) or production of TNF- α , IL-1 β , IL-2 or IFN- γ (Wu *et al.* 1999; Yaqoob *et al.* 2000). These observations suggest that a GLA intake of somewhere between 1 and 2.4 g/day is required to exert immunological effects in healthy humans. N-6 PUFAs inhibit activation of NF- κ B in ECs by yet another mechanism that involves anti-inflammatory epoxyeicosatrienoic acids (EETs) (Node *et al.* 1999). EETs are produced from n-6 PUFAs by a cytochrome P450 epoxygenase. EETs also have important vasodilator properties via hyperpolarization and relaxation of VSMCs (Spiecker *et al.* 2014).

1.9.2.3 Conclusion

The cost of production for the above-mentioned oils is very high. The increasing cost involved in the development, refining, and stabilising of fish oils, and the decreased yields due to over-fishing, have continuously driven up the cost of fish oils. In addition to the increasing number of vegans and vegetarians in the world, the need for finding a plant source of PUFA is on the rise. This increase in demand has raised the desire to obtain these PUFAs from alternate sources that are more economical and sustainable. One attractive option is to use plant derived nutraceuticals. Plant derived n-6 FAs such as GLA have potential anti-inflammatory and anti-atherogenic effects (Gallagher 2016). All this data gives a strong scientific rationale to assess if PNLA has anti-inflammatory effects in monocytes and macrophages in rheumatoid arthritis.

1.9.3 Pine nuts oil (PNO) and pinolenic acid (PNLA)

Pine nuts are a traditional Korean food that has been used as a direct source of energy and to treat neuralgia (Kang *et al.* 2015). Pine nuts have a unique flavour and are highly caloric due to their high lipid content. The nutritional content of pine nuts is: 64.2% fat, 18% protein, and

4.3% carbohydrate (Kang *et al.* 2015). Approximately 90% of the lipids contained in pine nuts are USFAs, and 10% are SFAs (Ryan *et al.* 2006). Pine nuts contain high amounts of LA 48.4%, oleic acid (OLA) 24%, PNLA 14.9%, and taxoleic acid 1.8%, which are not found in other nuts (Xie *et al.* 2016). Indeed, phytosterols, tocopherols, and squalene proanthocyanidins, and flavonoids including, catechin, epicatechin, quercetin, dihydroquercetin, taxifolin, and phenolic acids, are all found in pine nuts and PNOs (Amr and Abeer 2011; Ryan *et al.* 2006). The high demand for pine nuts has led to an increase in their worldwide production (FAO 2015). China, Korea, Russia (Siberia), and Pakistan are the main exporting countries of pine nuts (FAO 2015). Park *et al.* (2002) reported that consumption of a high-fat diet (HFD) containing Korean pine nuts by mice resulted in significantly less weight gain compared with an HFD containing soybean oil. Yoon and Lee (1994) reported that dietary supplementation with Korean pine nuts in New Zealand white rabbits decreased liver TGs and PLs. Pine nut oil (PNO) possesses a wide range of therapeutic effects, such as being antibacterial, antifungal, antiviral, antiseptic, anti-neuralgic, anti-rheumatic, cholagogue, cholaretic, diuretic, expectorant, and antihypertensive (Amr and Abeer 2011).

1.10 Pinolenic acid

1.10.1 Structure, biosynthesis, and metabolism

PNLA is an n-6 PUFA found exclusively in PNO (*Pinus orientalis*) and maritime pine (*Pinus pinaster*) seed oils, and pine nuts are a rich source of PNLA (Change *et al.* 2009; Chen *et al.* 2011; Lee and Han 2016). According to nutritional science, the richest source of PNLA is the oil pressed from Siberian pine nuts, which contains up to 27% of this PUFA. Korean pine nuts are another good source of PNLA, making up to 20% of its content. PNLA is a $\Delta 5$ -unsaturated polymethylene-interrupted FA, and its chemical structure is similar to that of; LA (n-6 and GLA precursor); GLA (n-6 and DGLA precursor) and ALA (n-3 and the precursor of both EPA and DHA) **Figure 1.12**. GLA was reported to suppress chronic inflammation by increasing the cellular levels of DGLA. DGLA can compete with AA as a substrate for COX-2 and is metabolised to PGE1, which has been shown to suppress inflammation. DGLA is also a substrate for lipoxygenase (LOX). It is possible that both the precursor FAs (i.e., GLA and PNLA) and their elongation products (i.e., DGLA and ETrA, respectively) act simultaneously to decrease or resolve inflammation. (Eicosatrienoic acid) or ETrA (a PNLA metabolite) may also act via COX and LOX metabolism.

PNLA is not considered an essential FA, but it is biologically active and can relieve the deficiency symptoms of essential FAs (Change *et al.* 2009; Chen *et al.* 2011; Lee and Han

2016). PNLA has become popular in recent years due to its ability to suppress appetite and reduce weight (Pasman *et al.* 2008). There are also antioxidant compounds in the oil pressed from Siberian nuts (Xie *et al.* 2016).

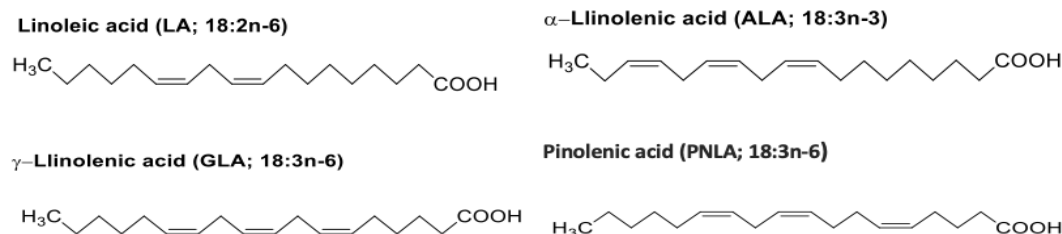


Figure 1.12. Simple linear structures of polyunsaturated fatty acids.

Linolenic (LA), α -linolenic (ALA), γ -linolenic (GLA), and pinolenic acid (PNLA) demonstrate the positions of double bonds and the similarities between these FAs.

PNLA is not converted to AA metabolically and can reduce AA levels in the phosphatidylinositol fraction of HepG2 cells from 15.9% to 7.0%. (Chen *et al.* 2011; Tamotsu *et al.* 1999). Structured pine nut oil (SPNO) was previously developed with PNLA evenly distributed at all sn-positions on the glycerol backbone, whereas natural pine nut oil (NPNO) has PNLA positioned mostly at the sn-3 position. This SPNO has been reported to exhibit greater lymphatic PNLA absorption than NPNO (Chung *et al.* 2019).

The pathway of PNLA synthesis has not been fully established yet. In mammals, GLA is synthesised from LA by Δ 6-desaturase (Kapoor and Huang 2006). Thereafter, GLA is elongated to DGLA by an elongase enzyme (Kapoor and Huang 2006). Accordingly, the similarity of GLA and PNLA suggests that PNLA can be synthesised from LA by Δ 5-desaturase because of the different positions of the double bond in GLA and PNLA as Δ -6 and Δ -5 respectively (Kajikawa *et al.* 2006). Kajikawa *et al.* who have investigated the presence of Δ 5-desaturase genes in a microalga that could be involved in the synthesis of PNLA from LA. Baker in 2020 confirmed that silencing of the elongase 5 gene significantly inhibited the production of DGLA and ETrA in EC line (EA.hy 926) pre-treated with GLA and PNLA respectively. Chapkin *et al.* also described that, macrophages incubated with GLA had no changes in AA content but an increase in DGLA. This can support the results mentioned earlier by Tamostu *et al.* in (1999) who stated that PNLA is not converted to AA but reduces it. This may be a metabolic attempt to restrict the endogenous biosynthesis of pro-inflammatory and prothrombotic AA within the cell. Knowing that FAs are metabolised through a series of elongation and desaturation steps. Elongase 5, enzyme encoded by the elongase of very-long fatty acid 5 (ELOVL5) gene, participates in the elongation of mono- and polyunsaturated FAs of 18-20 carbons in length. Elongase 5 catalyses the first and rate-limiting reaction of the long-

chain FA elongation cycle, it is the enzyme responsible for the elongation of PNLA, as demonstrated and reviewed recently (Baker *et al.* 2020).

The metabolism of PNLA in mammalian systems of rat liver microsomes, human hepatoma HepG2 cells, and murine macrophages (RAW264.7), which were incubated with medium containing 50 μ M of PNLA for 24 hours; form Δ 7,11,14–20:3 elongated metabolites (ETrA), an elongation product of PNLA and an isomer of DGLA. This is in line with the literature (Chuang *et al.* 2009; Chen *et al.* 2015; Tanaka *et al.* 1999). A small portion of this elongated metabolite was further elongated to form Δ 9,13,16–22:3. Incorporation of PNLA in the ECs (EA. hy926) for 48 hours gives an elongation product, ETrA (**Figure 1.13**). Most of the anti-inflammatory effects of PNLA were abolished by silencing elongase 5, suggesting that PNLA acts via its elongation product (Baker *et al.* 2018).

The degree of incorporation of PNLA and its metabolites into cellular PLs varied with the length of incubation time and the concentration of PNLA in the medium. Incubation of PNLA also modified the FA profile of phospholipids: the levels of 18- and 20-carbon PUFA were significantly decreased, whereas those of 22-carbon FAs were increased (this means that the levels of SFA decreased while UFA increased in the PL fraction). This might be one reason for the anti-inflammatory actions of PNLA.

The syntheses of PGE1 from DGLA and PGE2 from AA were also suppressed by the presence of PNLA and its metabolite. As the expression of COX-2 was not suppressed, the inhibitory effect of PNLA on PG activity was attributed in part to substrate competition between the PNLA metabolite (i.e. 7,11,14–20:3) and DGLA or AA (Chuang *et al.* 2009).

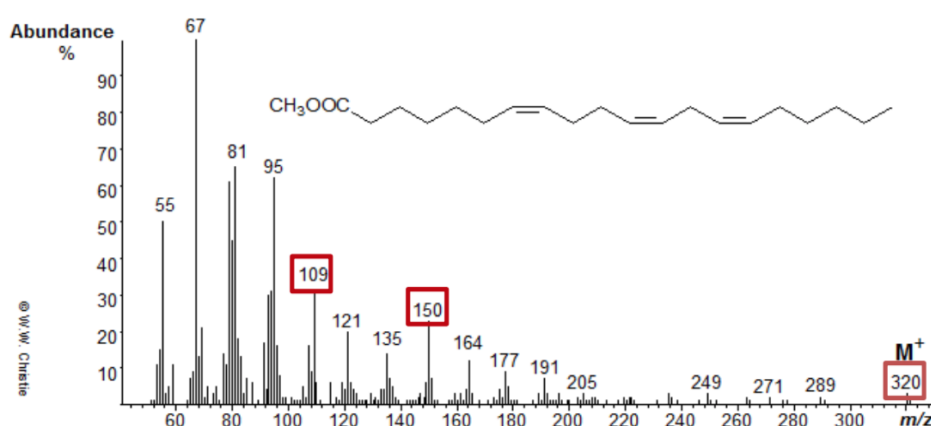


Figure 1.13. Mass spectrometry total ion chromatogram of ETrA.

Unique fragments are 109, 150, and 320. Mass spectrometry (MS) depicts the ion fragments of ETrA. PNLA converted to ETrA in murine microglial BV-2 cells (Szu-Jung *et al.* 2015), in murine macrophages (RAW264.7) (Chuang *et al.* 2009), and in ECs (EA. hy926) (Baker *et al.* 2020) after treatment with 50 μ M PNLA. Taken from the lipid-home database.

1.10.2 Potential effects of PNLA and PNO in RA

1-Anti-inflammatory and immunologic actions

PNLA has been found to decrease the production of pro-inflammatory mediators. In murine microglial BV-2 cells stimulated with *E. coli*-LPS, the production of a range of pro-inflammatory mediators was decreased by PNLA (Chen *et al.* 2015). Incubation of the cells with PNLA at a concentration of 50 μ M decreased the production of NO, IL-6, and TNF- α by 41, 74, and 27%, respectively (Chen *et al.* 2015). A significant decrease in PGE2 production was also observed (Chen *et al.* 2015). The same findings were observed when rat primary peritoneal macrophages were used; PNLA decreased the production of NO and PGE2 (by 35% following LPS-stimulation) (Chen *et al.* 2015). Similarly, PNLA decreased PGE1 and PGE2 production by LPS-stimulated murine macrophage RAW264.7 cells (Chuang *et al.* 2009), and the effect of PNLA was dose-dependent. However, Chuang *et al.* reported that PNLA decreased PGE2 production, although they found an increase in COX-2 protein expression (12%). LPS stimulation of macrophage-type cells induces the expression of iNOS and COX-2. The up-regulation of iNOS and COX-2 gene expression in response to LPS often involves activation of the NF- κ B pathway. Chen *et al.* (2015) confirmed there is a downregulation of LPS-induced iNOS protein expression (54%). This suggests that PNLA can inhibit the activation of NF- κ B, which has been shown with n-3 PUFAs (Calder 2012; Calder 2015a). In male Wistar rats, PNLA topical ointment reduced oedema after carrageenan injection into the right hind paw (Shikov *et al.* 2008). Baker reported that EA.hy926 cells pre-treated with PNLA and DHA for 48 hours and activated with TNF- α for 6 hours, PNLA appeared to increase the relative gene expression of I κ B at 50 μ M compared to control but significantly low compared to DHA both at 25 μ M, and lead to lower PPAR α relative gene expression compared to DHA at 25 μ M. PNLA treatment led to significantly lower relative gene expression of COX-2 and IL-6 when compared to DHA both at 25 μ M but not reduced when compared to control cells. CCL2 and NF- κ B gene expressions were not reduced after PNLA and DHA treatment, both at 25 and 50 μ M in comparison to stimulated control cells. In summary, none of these inflammatory genes examined were downregulated by PNLA or DHA treatment in comparison to stimulated control cells (Baker *et al.* 2020). These gene expression studies were further validated using Western blotting analysis to determine the protein levels. FAs may modulate the levels and activities of these intracellular proteins and signalling proteins. PNLA and DHA decreased COX-2 protein expression on the ECs model, and PNLA tended to decrease NF- κ B activity while DHA significantly reduced NF- κ B activity when compared to control stimulated

cells. PNLA reduced the adhesion of calcein-labelled THP-1 cells to EC monolayers (exposed to TNF- α) by ~23%. This may further inform on the anti-atherogenic properties of PNLA, and IL-8 production by activated ECs was significantly decreased after exposure to PNLA.

These results indicate the complex nature of the activity of PNLA. Changes in gene expression do not necessarily result in changes in cellular protein abundance. This is clearly seen in the EC inflammatory model, whereby FAs decrease IL-6 secretion by stimulated cells yet increase IL-6 relative gene expression. Decreased expression of the NF- κ B gene would be anti-inflammatory in nature and could lead to decreased NF- κ B protein, which is a key transcription factor involved in the up-regulation of the expression of genes encoding many proteins involved in inflammatory RA and atherosclerosis.

2-Effects on hyperlipidemia and hypercholesterolemia

Pine nuts are cholesterol-free and a good source of nutrients. PNO diminished lipid accumulation in the rat liver (Lee and Han 2016). It was reported that pine nuts produced a reduction in lipid profile, lipoprotein cholesterol, and liver weight; this was concentration-dependent, and it has no significant alterations on serum alanine transferase (ALT), aspartate transferase (AST), and alkaline phosphatase (ALP) levels in rabbits (Amr and Abeer 2011). A study by Asset *et al.* (1999) in rats showed that dietary maritime pine seed oil (MPSO) lowers TG, VLDL-TG, and VLDL-cholesterol, and diminishes cholesterol efflux *in vitro* (Asset *et al.* 2001). Moreover, a diet containing MPSO lowered HDL and ApoA-I levels in transgenic mice expressing human ApoA-I and ApoB genes. There are several hypotheses that have been suggested for hypolipidaemic properties, one of them is that PNLA is altering the expression of various Apo genes. ApoA-I and ApoA-II are key proteins in HDL metabolism. ApoE is necessary for lipoprotein remnant clearance. ApoC-III is a major component of TAG-rich bioparticles and interferes with VLDL lipolysis and uptake by a cellular receptor (No and Kim 2013). Another mechanism that has been suggested is that PNLA contributes to TAG-lowering properties such as (I) decreased *de novo* lipid synthesis, (II) reduced substrate availability for lipoprotein formation, or (III) changes in VLDL physicochemical properties (No and Kim 2013). PNLA downregulated the lipid anabolic pathway *in vitro* in hepatoma HepG2 by reducing the expression of genes related to lipid synthesis and lipoprotein uptake. However, PNLA produced no significant differences in the protein expression of LDL receptors compared to the control in the same HepG2 cell line model. However, *in vivo*, the hypocholesterolemic activity of PNLA is attributed to a greater hepatic accumulation of PNLA,

suggesting that PNLA has LDL-lowering properties by enhancing hepatic LDL uptake via increased SREBP2 levels and upregulation of LDLr gene expression in the livers of obese mice (Chung *et al.* 2019).

1.10.3 Beneficial effects of PNLA and general systemic implications

1- Effects on satiety and metabolism

PNLA has been found to reduce body weight due to a reduced desire to eat, as people taking PNO had an increase in the satiety hormones cholecystinin-8 (CCK)-8, a hormone that is synthesised in the duodenum and promotes digestion of protein and lipid, and glucagon-like peptide-1 (GLP)-1, which is produced in the ileum in response to carbohydrates and fat in the diet. Both hormones are responsible for inducing satiety and suppressing appetite (Degen *et al.* 2001; Gutzwiller *et al.* 2004). In a study by Pasma *et al.* (2008), in an RCT of 18 overweight post-menopausal women, circulating CCK-8 and GLP-1 concentrations were measured after *P. koraiensis* free fatty acid (FFA) and TAG, or olive oil (as a placebo) consumption. After 4 hours, the circulating concentration of CCK-8 was higher by 60% and 22% with PNO FFA and PNO TAG relative to placebo, respectively. For GLP-1, the increase was 25% higher with PNO FFA compared to placebo (Pasma *et al.* 2008). Genes related to FA oxidation, skeletal muscle oxidative metabolism, and mitochondrial oxidation were upregulated by feeding PNO compared with soybean oil (Le *et al.* 2012). Taken together, these observations suggest that PNO has a range of effects that result in reduced food and energy intake through enhanced production of appetite-controlling hormones (Le *et al.* 2012; Park *et al.* 2013; Pasma *et al.* 2008) and enhanced energy expenditure (through increased oxidative metabolism in key organs and an increase in brown adipose tissue thermogenesis). PNLA reduced adipose tissue mass and prevented liver steatosis and hyperinsulinemia seen with the other diets (Ferramosca *et al.* 2008). These effects would result in less adipose tissue deposition, less weight gain, less ectopic fat deposition, and a healthier metabolic state.

2- Effects on hyperglycaemia and insulin sensitivity

PNO, together with pure PNLA free and esterified (PNLA ethyl ester), were tested in an acute glucose tolerance test in mice (Christiansen *et al.* 2015). It was found that PNO significantly improved glucose tolerance compared with maize oil. Pure PNLA or its ethyl ester gave robust and highly significant improvements in glucose tolerance (Christiansen *et al.* 2015). The results indicated that PNLA is a comparatively potent and efficacious dual free fatty acid receptor-1 and free fatty acid receptor-4 (FFA1/FFA4) agonist (Calder 2015b; Christiansen *et al.* 2015)

that exerts antidiabetic effects in an acute mouse model. The FA receptors FFA1 and FFA4 are G protein-transmembrane receptors activated by different groups of medium- to long-chain non-esterified fatty acids (NEFA), and all have been associated in various ways with type-2 diabetes and other metabolic and inflammatory disorders. FFA1 is highly expressed in pancreatic B-cells, while FFA4 is expressed in intestinal entero-endocrine cells, the pancreas, adipose tissue, macrophages, and the brain. It seems that the co-activation of FFA1 enhances glucose-dependent insulin secretion, and FFA4 promotes insulin sensitivity and has anti-inflammatory effects, as reviewed by Christiansen *et al.* (2015). The ethylene-interrupted PNLA was one of the most potent NEFAs on both FFA1 and FFA4 and displayed high efficacy on both receptors, where the study included ALA, AA, DGLA, and GLA. In those studies, PNLA was superior to all other FAs studied, including marine n-3 PUFAs (Christiansen *et al.* 2015). FA thus deserves attention as a potential active dietary ingredient to counteract or prevent metabolic diseases.

3- Effects on blood pressure

In rats, *Pinus koraiensis* oil had the potential to lower age-related elevation of blood pressure and enable better blood cholesterol concentration management compared to safflower oil (SAO), although PNO was less effective than flaxseed oil (FSO) (Sugano *et al.* 1994). PNO and EPO stimulated the aortic production of PGI more than SAO, and the difference between the PNO and SAO groups was significant. In rats given PNO, the age-related elevation of blood pressure was attenuated after 5 weeks of feeding and remained apparently constant until 8 weeks, in contrast to a gradual increase in rats given either EPO or SAO. The difference between PNO and EPO at 8 weeks was significant (Sugano *et al.* 1994). The authors concluded that pine extracts not only reduce blood pressure but also decrease kidney damage caused by HTN. Other studies have shown that the potential effect of pine nuts on cardiovascular benefits includes improvements in endothelial function, a reduction in plasma fibrinogen concentrations (Young *et al.* 2006), and reduced plasma viscosity and systolic blood pressure (Shand *et al.* 2003). These results were noteworthy and attributed to the type of FA composition in pine nuts, especially PNLA, which is the main FA in pine seed oil, or some of its metabolites (Amr and Abeer 2011).

4- Effects on cancer metastasis and invasiveness

While AA seems to promote cancer development (Rose *et al.* 1995; Chen *et al.* 2011), some PUFAs, like EPA, seem to have inhibiting effects. Chuang *et al.* (2011) investigated the effect

of PNLA on cell proliferation and metastasis in human breast cancer cells, MDA-MB-231 *in vitro*. Cells supplemented with PNLA had a 25% decrease in motility and invasiveness. However, no effect on cell proliferation or cell-matrix adhesion was observed. Incubation of the cells with PNLA also changed the cellular PUFA composition. The percentage of AA decreased from 12.6% to 4.9% because of the reduction in PGE₂, since AA is a precursor to PGE₂ (Chen *et al.* 2011). Thus, PNLA is a potential anti-cancer agent. Oil of *Pinus koraiensis* inhibits cell proliferation and migration in human colorectal cancer cells HCT116 *in vitro* through inhibition of the p21-activated kinase 1 (PAK-1) pathway (Cho *et al.* 2014).

5- Effects on antioxidants' protective mechanisms

Antioxidant enzymes play a major role in cell defence against free radical-induced damage to macromolecules and cells. These enzymes include superoxide dismutase (SOD) and phospholipid hydroperoxide glutathione peroxidase (GSH-Px). In a study by Chen *et al.* rats fed on a diet containing *P. koraiensis* oil showed elevated activity of SOD and GSH-Px in the serum. Malondialdehyde (MDA) is an indicator of free radical-induced lipid damage. There was a reduction in serum MDA levels in the PNO group (Chen *et al.* 2011). A deeper understanding of the determinants of PNLA actions in patients with chronic inflammatory diseases such as RA and atherosclerosis may provide insights into the relationship between inflammation, immunity, and some antioxidant protective effects of PNLA.

1.11 Project hypothesis; RA and future prospective therapy

New treatment strategies have substantially changed the course of RA. If the disease is recognised early and treated promptly and continuously, many patients can achieve remission; however, some individuals do not respond adequately to treatment or experience side effects. The treatment of RA aims at providing remission from the symptoms associated with inflammation, pain, and stiffness and preventing long-term disability. Current drug therapies allow for significantly improving the quality of life of RA patients; however, they are still insufficient to reverse tissue injury, often generate side effects (Jung *et al.* 2019), and are highly expensive. Given the high rates of serious infections following bDMARDs treatment in RA (Christensen *et al.* 2022), clinicians should carefully consider this when assessing the risk of future serious infections in patients starting a new pharmacologic treatment such as anti-TNF. Furthermore, it is worth noting that nearly half of the mortality rates in RA patients are due to CVD events. As mentioned earlier, findings in previous studies and the published literature highlight the prominent role inflammation plays in CVD risk in RA. Thus, assessing the effect

of PNLA on biological processes important in atherosclerosis or synovitis, such as lipid uptake and migration by monocytes and macrophages, as well as cytokine production, were the initial objectives of this project.

Accordingly, based on pre-clinical studies on the effect of PNLA on cell lines and animal work, I hypothesise that PNLA has the following effects:

- I. PNLA can reduce the processes implicated in early atherosclerosis and synovitis, such as monocyte migrations, lipid uptake, macropinocytosis, and ROS production.
- II. PNLA can reduce the release of pro-inflammatory cytokines by activating monocytes and macrophages.

1.12 Aims and Objectives

1. Chapter 3 aims to broadly investigate the effects of PNLA on key processes implicated in atherosclerosis and inflammation (*in-vitro*) using the THP-1 human cell line. Key findings were confirmed on primary cultures of human macrophages (HMDMs) isolated from human buffy coats.
2. Chapter 4 determines the effect of PNLA on the levels of pro-inflammatory cytokines and non-cytokine mediators associated with chronic inflammation in the supernatants of activated monocytes and macrophages isolated from blood samples of RA patients and healthy controls (HCs) (*ex vivo*).
3. Chapter 5 uses the analysis of the transcriptomic profile of the PNLA effect on activated PBMCs isolated from RA patients and HCs, using RNA sequencing of the whole genomic transcriptome, to explore possible underlying mechanisms of the overall observed anti-inflammatory effects.
4. Chapter 6 aims to confirm the effects of PNLA on the intracellular pro-inflammatory cytokines produced by LPS-stimulated CD14 monocytes from RA patients using flow cytometry; to find out the percentage of these cells expressing cytokines upon PNLA treatment.
5. Chapter 7 aims to confirm, extend, and compare findings of the anti-inflammatory effect of PNLA on the transcriptomic profile of activated pure monocytes isolated from active RA patients to those of PBMCs in Chapter 5, using RNA sequencing of the whole genomic transcriptome.

Chapter 2: Materials and Methods

2.1. Materials

Reagents, buffers, the antibodies together with isotype controls for flow cytometry that were used in this study are listed in **Tables 2.1, 2.2, 2.3** and **2.4** below.

Table 2.1. A list of specific materials and their suppliers

| Item(s) | Supplier |
|--|-----------------------------|
| Vybrant™ Phagocytosis Assay Kit; Macrophage-colony stimulating factor (CSF); Absolute ethanol; RPMI 1640/stable glutamine; Pierce lactate dehydrogenase (LDH) cytotoxicity assay kit; Hydrochloric acid. Alarm Blue® Cell Viability Reagent; TMB substrate; H ₂ O ₂ ; concentrated hydrochloric acid (HCl); Negative control (rabbit immunoglobulin (Ig) fraction); Saponin 0.5% in PBS; ArC™ Amine Reactive live/dead compensation beads; Zombie Aqua (Live dead) fixable viability stain | Fisher Scientific, UK |
| DCDFA cellular detection assay kit | Abcam, UK |
| Dil-oxLDL kit | Alfa-Aesar, UK |
| Pinolenic acid 10 mg; 40/70 µm sterile cell strainer Human PGE2 (ELISA Kit) kit, catalogue number 514010 | Cayman Chemical, USA |
| Trypsin (0.05%); Dulbecco's Phosphate Buffered Saline (without Ca ²⁺ or Mg ²⁺); Methylated Spirit Industrial (MSI); RPMI media; 2-Mercaptoethanol | Gibco Life Science, UK |
| Tissue culture flasks | Corning Costar, Netherlands |
| Cell scrapers; Pasteur pipettes, 5, 10 and 35 glass pipettes | Helena Biosciences, UK |
| Penicillin; Streptomycin (Pen; Strep); Fetal calf serum (FCS) Trypsin EDTA (0.1%) | Life Technologies, UK |
| RPMI 1640 with L-glutamine media; HI-FCS; RPMI media; 96-well plates; 0.2, 0.5 and 1.5-ml Eppendorf tubes | Lonza, UK |
| Lymphoprep™ | Norge As, Norway |
| 6, 12, 24 and 96-well plates (for seeding cells); 15/50 ml Falcon tubes | Starlab, UK |
| Falcon® cell culture inserts (8 µm pore size); Falcon®12-well companion plates (modified Boyden chamber) | VWR Jencons, UK |
| Chemokine (C-C motif) ligand 2 (CCL2) or monocyte chemoattractant protein-1 (MCP-1) | Peprtech, UK |

| | |
|--|--|
| Phorbol 12-myristate 13-acetate (PMA); Lucifer yellow CH dipotassium salt (LY); Paraformaldehyde (PFH 3%); Bovine serum albumin (BSA); Phosphate buffered saline (PBS) tablets; Tris-borate EDTA (TBE), Crystal violet (CV); Sodium chloride; Formaldehyde 2% (v/v); Trypsin EDTA (0.1-0.5%); THP-1 leukemic cell line catalogue number 88081201; Sodium hydroxide; Histopaque®-1077; Dimethyl sulphoxide (DMSO); RNaseZap; Lipopolysaccharides (L2630-10mg); Accuatase® solution; 70 and 100% Ethanol; RNase/Nuclease free water; Tween-20; Lipopolysaccharides (L2630-10MG); 0.4% Trypan blue solution; Bovine serum albumin (BSA); phosphate buffered saline (PBS); 2.5 mM EDTA in PBS; Brefeldin A (BFA); Sodium hydroxide (1M NaOH); Ethylenediaminetetraacetic acid disodium salt dihydrate (EDTA) | Sigma-Aldrich, UK |
| Human IL-6 (ELISA Kit) catalogue number DY206 Human TNF- α (ELISA Kit) catalogue number DY210 Human IL-1 β /IL-1F2 (ELISA Kit) catalogue number DLB50 Human CCL2/MCP-1 (ELISA Kit) catalogue number DCP00 Substrate reagent DY999 | R and D Systems Life Technology, UK |
| BrdU Cell Proliferation Assay Kit | Life Science (Biovision), USA |
| ELISA microplate Flat bottomed 96 well culture plates | Greinerbio-One, UK |
| Fetal bovine serum (FBS) | HyClone, Logan, USA |
| Griess Reagent System catalogue number G2930 | Promega, USA |
| RBCs lysis buffer (10X); Red blood cells lysis buffer (10X); Cell staining buffer; 10X RBCs lysis buffer. | Biologend, USA |
| RNeasy Mini kit; RNase free DNase set | Qiagen, USA |
| RNA ScreenTape kit; cBot 2 System - Illumina | Agilent Technologies, UK |
| Ultra II ligation master mix NEBNext® rRNA Depletion Kit rRNA Depletion Kit (Human/Mouse/Rat) catalogue number NEB #E6310X | New England BioLabs (NEB), Germany |
| NEB® Ultra™ II Directional RNA Library Prep Kit NEBNext® Ultra II Directional RNA Library Prep Kit for Illumina catalogue number NEB #E7760L; TG MiSeq® Reagent Kit v3 (150 cycle) catalogue number TG-142-3001; Xp-2 Lane Kit; NovaSeq 6000 S1 Reagent Kit (200 cycles) catalogue number 20012864 | Illumina® (NEB), USA |
| MACS BSA separation buffer (autoMACS Buffer) Pan-monocytes isolation kit; MACS BSA Stock Solution; MACS separation buffer (autoMACS Running Buffer); Negative selection isolation columns; FcR human blocking reagent | Miltenyi Biotec, UK |
| Anti-Mouse Ig/negative control compensation beads Anti-Rat/Anti-Hamster Ig/negative control compensation beads EDTA Vacutainer® tubes | BD Biosciences, UK BD Bioscience, Becton Dickinson, USA |
| FACS tubes | Stem cell, UK |

Table 2.2. Antibodies used in flow cytometry

| Target | Conjugate | Clone | species | Isotype | Company |
|--------------------------------|-----------------------|----------|------------------------------|---------|----------------|
| CD14 | BV 711 | M5E2 | Mouse anti human | IgG2a | Biolegend |
| CD16 | APC/Cyanine7 | 3G8 | Mouse anti human | IgG1 | Biolegend |
| CD33 | PerCP/Cy5.5 | P67.6 | Mouse anti human | IgG1 | Biolegend |
| IL-6 | FITC | MQ2-13A5 | Rat anti human | IgG1 | Biolegend |
| TNF-α | BV 421 | MAB11 | Mouse anti human/cat | IgG1 | Biolegend |
| CCL2 | PE | 2H5 | Hamster anti human/rate/mice | IgG | Biolegend |
| IL-1β | AF 647 | JK1B-1 | Mouse anti-human | IgG1 | Biolegend |
| IL-10 | Per CP/Cyanine 5.5/ 7 | JES3-9D7 | Rate anti human | IgG1 | Biolegend |
| IL-6 | AF700 | MQ2-13A5 | Rat anti human | IgG1, k | BD Biosciences |
| IL-8 | PE-CY7 | E8N1 | Mouse anti-human | IgG1, k | BD Biosciences |
| CD14 | FITC | HCD14 | Mouse anti-human | IgG1, k | Biolegend |

Table 2.3. Identical isotypes for the antibodies used in flow cytometry

| Target | Conjugate | species | Clone | Company |
|--------------------------------|-----------------------|---------------------------------|----------|----------------|
| CD14 | BV 711 | Mouse anti human IgG2a | MOPC-173 | Biolegend |
| CD16 | APC/Cyanine7 | Mouse anti human IgG1 | MOPC-21 | Biolegend |
| IL-6 | FITC | Rat anti human IgG1 | RTK-2071 | Biolegend |
| TNF-α | BV 421 | Mouse anti human/cat IgG1 | MOPC-21 | Biolegend |
| IL-1β | AF 647 | Mouse anti-human IgG1. | MOPC-21 | Biolegend |
| CCL2 | PE | Hamster/anti human/rate/mic IgG | HTK888 | Biolegend |
| IL-6 | AF700 | Rat/anti human IgG1, k | eBGR1 | BD Biosciences |
| IL-8 | PE-CY7 | Mouse anti-human IgG1, k | MOPC-21 | Biolegend |
| IL-10 | Per CP/Cyanine 5.5/ 7 | Rate anti human IgG1, k | RTK-2071 | Biolegend |

Table 2.4. Antibodies used in Sort Aria III are specific for monocyte sorting.

| Target | Conjugate | Clone | species | Isotype | Company |
|--------|--------------|-------|------------------|---------|-----------|
| CD14 | FITC | M5E2 | Mouse anti human | IgG2a | Biolegend |
| CD16 | APC/Cyanine7 | 3G8 | Mouse anti human | IgG1 | Biolegend |

2.2. Preparation of reagents, PNLA, and the vehicle

2.2.1 Preparation of glassware and solutions

All glassware and solutions were autoclaved (if necessary) for 20-30 minutes (min) at 121°C (975kPa).

2.2.2 Preparation of PNLA and vehicle control (DMSO)

10 mg of PNLA was purchased from Cayman Chemical, USA, with an overall purity of 98% in 200 µl ethanol as a solvent. The ethanol was evaporated under a stream of nitrogen in a fume hood to prevent oxidation. A 100 mM stock solution was prepared by adding 359.1 µl of DMSO to the 10 mg of PNLA in the bottle and storing it in aliquots at -20°C. For use in experiments, a small aliquot was taken and diluted in RPMI 1640 media supplemented with 10% (v/v) heat-inactivated foetal calf serum (HI-FCS), pen/strep (100 U/mL) and DMSO to produce working concentrations of 25, 50, 75, and 100 µM fresh each time to prevent oxidation and degradation of PNLA that could potentially occur by repeated freeze-thaw cycles of the stock solution. As shown in **Table 2.5**, all the concentrations were performed based on the formula $C_1V_1 = C_2V_2$, where C is the concentration, and V is the volume.

Vehicle control was used in each experiment that contained a final DMSO concentration of 0.1% (**Table 2.6**).

Table 2.5. Concentrations of PNLA were used throughout the study.

| Concentration (µM) | Amount of PNLA stock (µl) | Amount of Media (µl) | Amount of DMSO (µl) | Final volume (µl) |
|--------------------|---------------------------|----------------------|---------------------|-------------------|
| 100 | 10.00 | 990.00 | 0.00 | 1000 |
| 75 | 7.5 | 992.25 | 0.25 | 1000 |
| 50 | 5.00 | 994.50 | 0.50 | 1000 |
| 25 | 2.5 | 996.75 | 0.75 | 1000 |

Table 2.6. The vehicle control constitution.

| Amount of Media (µl) | Amount of DMSO (µl) | Final volume (µl) |
|----------------------|---------------------|-------------------|
| 999 | 1 | 1000 |

2.3. Patients and healthy controls; the recruitment selection criteria

RA patients were recruited from the Rheumatology Department of the University Hospital of Wales (UHW). Written consent was obtained from all the participants. The study was approved by Welsh Research Ethics Committee 3 (ethics reference 12/WA/0045).

Inclusion criteria

1. Age 18 or over.
2. Patients with RA as defined by the 2010 American College of Rheumatology/European League Against Rheumatism classification criteria (Aletaha *et al.* 2010).
3. Able and willing to give written consent and comply with the requirements of the study protocol.

Exclusion criteria

1. Known pregnancy.
2. Active infection.
3. Current malignancy.
4. Patients with untreated anaemia or haemoglobin level <10.5g/dl.

Demographic data as evaluated at the time of PB collection from RA patients from the Outpatient Rheumatology Clinic, UHW (Cardiff, UK) are listed in the Appendix. Available data included age, gender, disease duration (DD), treatment, as well as laboratory parameters such as ESR, CRP, RF, and ACPA seropositivity. The disease activity of RA patients recruited for this project was calculated using the DAS28ESR (DAS28). DAS28 is a combined index that assesses the number of swollen and tender joints and measures the ESR. DAS28 scores < 2.6 indicate remission, ≥ 2.6 and < 3.2 is low disease activity, ≥ 3.2 and < 5.1 indicate moderate disease activity, and ≥ 5.1 indicates high disease activity. The candidate “Rabaa Takala” was not involved in either the patients’ recruitment or clinical data collection.

For the recruitment of the HCs, the selection was as the following:

Inclusion criteria

1. Age 18 or over.
2. Able and willing to give written consent and comply with the requirements of the study protocols.

Exclusion criteria

1. Any significant medical illness through clinical history.
2. Synovitis on clinical examination.
3. Known pregnancy.

The use of human material throughout this PhD study was as follows:

- In Chapter 4, for the assessment of cytokines using ELISA with monocytes and macrophages, a study was conducted between September 2018 to January 2019 with 10 HCs and 20 patients with RA. As this was the first study to test PNLA on clinical samples from RA patients, it was considered a pilot study, and no additional selection criteria were added to those specified above. Patients' characteristics were shown in **Table 1** in the Appendix.
- In Chapter 5, for the assessment of gene expressions using PBMCs, 6 HCs, and 6 RA patients were recruited between April 2019 and June 2019; their demographic details are shown in **Table 2** in the Appendix.
- In Chapter 6, we assessed intracellular cytokines using flow cytometry with purified monocytes. Twenty patients with RA (n=20) were recruited between October 2020 and March 2021. Their demographic and disease characteristics are shown in **Table 3** in the Appendix.
- In Chapter 7, for assessment of gene expressions using purified CD14CD16 monocytes, 8 patients with seropositive RA were recruited between October 2020 and Jan 2021, as shown in **Table 4** in the Appendix. RA is a heterogeneous disease. In order to minimize heterogeneity, we recruited patients aged 55-70 years old (mean age = 61.5 years old), with a DAS28 score range of 4.8-5.7, and receiving intravenous biologic treatments. Blood samples were drawn before intravenous treatment as part of clinical care. Therefore, serum monoclonal antibodies were at low levels. Rituximab has a half-life of 3 weeks, and it is given for 6 months for the treatment of RA. So, before each cycle of treatment, it is unlikely for rituximab to be present in the blood sample. Furthermore, rituximab is an anti-CD20 monoclonal antibody that acts by depleting B cells, so it will not have any direct effects on monocytes.

2.4. Cell culture techniques

2.4.1. Human leukemic THP-1 cell line

Human THP-1 monocytic leukaemia cell line was initially used in this study as a model for normal human monocytes and macrophages to make the results of studies in Chapter 3 more applicable to humans. THP-1 designates a spontaneously immortalised monocyte-like cell line derived from the PB of a childhood case of acute monocytic leukaemia. THP-1 cells, including their genetically engineered derivatives, represent valuable tools for investigating monocyte and macrophage properties and functions in both health and disease. THP-1 monocytes grow

in suspension and require treatment with PMA for at least 24 hours for them to adhere to plastic and differentiate into macrophages. PMA-differentiated THP-1 macrophages make them popular cell models for studies on macrophage function, cell signalling, and inflammatory gene expression as they exhibit similar traits to HMDMs both *in vitro* and *ex vivo* (Auwerx 1991; Chanput *et al.* 2014; Qin 2012). In addition, responses observed in THP-1 cells are highly conserved in HMDM and in *in vivo* studies (McLaren *et al.* 2010; Michael *et al.* 2012b).

2.4.1.1. Thawing frozen cells

For long-term storage of the cell lines, they were stored either in liquid nitrogen or at -80°C. The cells were warmed to 37°C using a water bath and once thawed, the cells were immediately added to 10 ml of pre-incubated culture media and centrifuged at 250 x g for 5 min at room temperature (RT). The supernatant was then discarded, and a further 5 ml of culture media pre-incubated at 37°C was used to re-suspend the cells. This was then added to tissue culture flasks.

2.4.1.2. Maintenance and subculturing of cells.

THP-1 cells were maintained in suspension in complete RPMI media at 37°C in 5% (v/v) CO₂ in 25 cm² tissue culture flasks. When they reached 80% confluency, they were sub-cultured by transferring to a 15 ml Falcon tube and centrifuged at RT at 250 x g for 5 min. The supernatant was then removed, and the cell pellet was re-suspended in 4-5 ml of fresh, pre-warmed culture media and split in a ratio of approximately 1:30 using 75 cm² tissue culture flasks (kept in a standing position). The cells were maintained at 37°C in 5% (v/v) CO₂ until required. Cells between passages 4 and 14 were used in experiments. No difference in responses between passages was seen when such assays were used on different nutraceuticals and PUFAs in the laboratory of Professor Dipak Ramji, and this was also found to be the case with studies on PNLA carried out in this thesis.

2.4.2. Primary culture of human monocyte-derived macrophages (HMDM)

2.4.2.1. Maintenance, and culturing of the cells

HMDMs were isolated from human buffy coats provided by the National Blood Service Wales, using the protocol detailed below. Ethical approval was granted by the National Blood Service Wales for use in research. Peripheral blood mononuclear cells (PBMCs) were separated using Lymphoprep. In order to place the Lymphoprep in the bottom of a 50 ml Accuspin tube, 15 ml of Lymphoprep was centrifuged at 1000 x g for 60 sec at RT. Subsequently, 30 ml of blood was carefully added on top of the Lymphoprep and centrifuged at RT at 800 x g for 10 min. No brake was used to slow the centrifuge at this step. The mononuclear layer of cells was

aspirated and placed in a fresh Falcon tube, where an equal volume of ice-cold 0.4% (w/v) tri-sodium citrate phosphate-buffered saline (tris-PBS) was added to remove platelet contamination. The mixture was centrifuged at 1000 x g for 5 min at RT. Red blood cells (RBCs) were lysed by re-suspending the cell pellet in 10 ml of 0.2% (w/v) saline and placing it on ice for 30 sec before the addition of an extra 10 ml of 1.6% (w/v) saline to the mixture. Following centrifugation at 1000 x g for 5 min at RT, the resulting pellet was resuspended in ice-cold 0.4% (w/v) tri-sodium citrate PBS and centrifuged at 800 x g for 5 min at RT (6-10) times to remove platelets. The final cell pellet was re-suspended in culture media and, seeded into 12 well plates at 500,000 cells/ml and incubated at 37°C in 5%(v/v) CO₂. 20 ng/ml of M-CSF was then added. The monocytes required 5 days to differentiate by adherence to the plate before they could be used in the experiments. They were known as fully differentiated macrophages based on the morphological changes under the microscope. HMDMs were washed before use to remove non-adhering leukocytes and cell debris. The primary human macrophages were utilised and treated in the same way and under the same conditions as THP-1 macrophages as discussed in section (2.6).

2.4.3. Peripheral blood mononuclear cells (PBMCs) isolation and preparation

Peripheral blood (PB) was collected in a BD Vacutainer™ blood collection tubes with 158 USP units/mL Sodium Heparin. At least 10 ml of PB was taken per participant, each leucocyte concentrate was prepared and processed from the blood of a single donor individually. PBMCs were prepared from the leucocyte to concentrate by Ficoll–hypaque density gradient centrifugation of fresh blood layered over Histopaque®-1077 (Sigma-Aldrich; UK) at volume (1:1) from RA patients and HCs, was centrifuged at 400 x g for 30 min at 22°C no brakes allowed. The top plasma layer was discarded and the PBMCs layer was carefully harvested using a pasture pipette, washed repeatedly with Dulbecco's PBS without Ca²⁺ or Mg²⁺ at RT to remove platelet contamination, and centrifuged at 350 x g for 10 min at 10°C until the supernatants became clear. The cells were re-suspended in 3-5 ml PBS without Ca²⁺ or Mg²⁺ after lysing erythrocytes with 10 ml RBCs lysis buffer (10X) from (Biolegend, USA) reconstituted previously in distilled water (dH₂O) and incubated on ice for 3-5 min according to manufacturer's instruction. Cell viability was assessed using a trypan blue exclusion test, where 10 µl of cell suspension was added to 40 µl of a diluted 0.4% (w/v) trypan blue, which was previously prepared in PBS at dilution (1:1) to count only viable cells. For cell counting, a light microscope and a haemocytometer were used. The surface of the haemocytometer was covered in a 5 x 5 grid, which can be used to count the number of cells by adding 10 µl of cell

suspension. The required cell count then was cultured in RPMI 1640 medium supplemented with 10% v/v (HI-FCS) along with penicillin (100 U/ml) and streptomycin (100 µg/ml) (called RPMI complete medium hereafter).

2.4.3.1. Enrichment of monocytes

Human monocytes were isolated from PBMCs, by adherence to plastic plates in RPMI complete culture medium at 37°C incubator in a humidified 5% (v/v) CO₂. After 2 hours, the cells were washed gently to remove any debris or dead leukocytes, only PBMCs that were adherent to the plastic were considered monocytes. Adherent monocytes at 5×10^5 were cultured in 24 well plates supplemented in complete RPMI media and incubated at 37°C with humidified 5% CO₂ incubator to the section (2.6). Adherent monocytes were used in ELISA experiments in Chapter 4 to assess the cytokine levels in a cell-free supernatants by PNLA treatment.

2.4.3.2. Growing and differentiation of macrophages

Adherent monocytes at a density of 5×10^5 /0.5 ml in 24 well plate/participants as mentioned in section (2.4.3.1) were left in the well plate and allowed to differentiate into macrophages by culturing at 37°C with 5% CO₂ (v/v) in an incubator in complete RPMI media for 8 days. The culture medium was changed to a fresh one periodically every 2-3 days to allow the cells to differentiate into macrophages and take out unviable cells. During optimisation of the experiment, 20 or 25 ng/ml M-CSF were used to promote differentiation and maintain viability but found very high cytokines levels (TNF, IL-6, IL-1), which needed further steps of dilution of the supernatants that were assessed for these cytokines. LPS contamination was a possible explanation for the exaggerated cytokine response. I did not assess this possibility but decided not to use M-CSF. Accordingly, in all subsequent experiments, the cells were left to differentiate without adding M-CSF. Perhaps this was due to increase cytokine release as M-CSF is also known to boost antibody-dependent, cell-mediated cytotoxicity by monocytes and macrophages (Tojo *et al.* 1999). Differentiated macrophages were used in ELISA experiments in Chapter 4 to assess the cytokine levels in cell-free supernatant following PNLA treatment.

2.4.3.3. Negative selection and purification of CD14 monocytes

Purified CD14 monocytes were obtained by negative selection in cascades using magnetic-activated cell sorting (MACS) pan monocyte isolation kit (Miltenyi Biotec) following the manufacturer's protocol. Highly pure unlabelled (untouched) monocytes were obtained by depletion of the magnetically labelled cells. The kit uses a cocktail of biotinylated antibodies

to select non-CD14⁺ cells, these cells are magnetically labelled using anti-biotin microbeads and separated from target CD14⁺ monocytes cells using a magnetic column. Briefly, 1x10⁷ PBMCs were suspended in 100 µl MACS (0.5% BSA, 5 mM EDTA, and 0.09% azide in PBS), 10 µl of FcR blocking reagent and 10 µl of biotin-antibody cocktail (provided in the kit were added). The suspension was then mixed and incubated for 10 min at 2-8°C. A 20 µl MACS buffer and 20 µl of anti-biotin microbeads/10,000,000 were added to PBMCs. This suspension was mixed gently and incubated for another 10 min at 2-8°C before passing through a sterile magnetic column. The column was then washed with MACS buffer to ensure all CD14CD16 monocytes were collected in a sterile 15 ml Falcon tube. The flow through CD14D16 enriched monocytes was centrifugated at 350 x g for 5 min at RT. The number of viable CD14CD16 cells was determined via trypan blue exclusion staining and counted using a haemocytometer and light microscope. Cells at a density of a minimum 10⁶ cells /ml were cultured in a complete RPMI medium at 37C° in a 5% CO₂-controlled environment and treated as described in section (2.6). Purified CD14CD16 monocytes were used in flow cytometry experiments in Chapter 6 to assess the intra-cellular cytokine levels following PNLA treatment.

2.4.3.4. Visualization of CD14 monocytes

As described in the previous section (2.4.3.3), confluent purified CD14⁺ cells were seeded at a density of 1 x 10⁶ cells per ml per well in 12-well flat bottom plates and incubated with or without PNLA at a concentration of 25 and 50 µM for 24 hours at 37°C followed by a 9-hours incubation with or without (100 ng/ml LPS and 10 µg/ml PFA). CD14⁺ cells were then observed and imaged using the brightfield compound microscope with Motic image plus 3 (MIP-3) elements software (version 3.0). Images were taken at a magnification of 20X.

2.5. Cell counting

A hemocytometer was used for counting cells. The surface of the hemacytometer was covered in a 5 x 5 grid, which can be used to count the number of cells by adding 10 µl of either the THP-1/HMDMs or PBMCs cell suspension. A glass coverslip was placed over the surface of the hemocytometer to spread the suspension. The average number of cells in the four corners and centre of the grid was counted and multiplied by 10⁴ to calculate the actual number of unstained cells/ml.

2.6. Treatment of the cells (PNLA and vehicle incubation)

THP-1 cells at 1 x 10⁶/ml were seeded in complete RPMI media in a 12-well plate, and differentiation into macrophage was initiated by the addition of 0.16 µM PMA. Cells were left

to differentiate for at least 24 hours at 37 °C in a humidified 5% CO₂ (v/v) incubator. The media was then removed, and the cells were washed in PBS followed by treatment with the required concentrations of PNLA (0, 25, 50, 75, and 100 µM) or DMSO vehicle for another 24 hours in 1 ml of fresh RPMI complete RPMI media per well.

PBMCs, enriched, purified monocytes or macrophages, were cultured at a density of 1-2x10⁶/1-2 ml in complete RPMI 1640 culture media with 25, 50 µM PNLA, or DMSO vehicle control in 6 well plates and incubated for 24 hours at 37°C in a humidified 5% CO₂ incubator before proceeding to the next section (2.7).

2.7. LPS stimulation of pre-treated monocytes and macrophages

Adherent, purified monocytes or differentiated macrophages were stimulated with 0, 10, 50, and 100 ng/ml *E. Coli* LPS, or left unstimulated as a reference control at 37 °C with humidified 5% CO₂ for 16-18 hours. Each experimental condition was reproduced in triplicate wells.

For adherent monocytes and differentiated macrophages, after LPS stimulation for 16-18 hours, the media was removed into Eppendorf tubes and subjected to centrifugation at 9,000 x g for 5 min to remove cells. The clear supernatants were frozen in sterile Eppendorf tubes at 80°C until assessed as a cohort for TNF-α, IL-6, IL-1β, and PGE2 using ELISAs (Chapter 4).

2.8. Flow cytometry

2.8.1. Principle of flow cytometry

Flow cytometry technique allows researchers to visualise and explore lots of pathobiological functions at the cell level. Flow cytometry measures and analyses cells as they flow in a stream through the beam of a laser. The flow cytometer is composed of:

- A flow chamber, which is designed to deliver the cells in a single file at the point of measurement.
- An optic system whereby lasers create light signals (through which cells/particles are passed) which are then collected/directed by optical filters to specific detectors.
- An electronic system which converts detected light signals into electrical signals. This electronic signal is processed and analysed using computer software.

The sample is injected into the centre of a stream of liquid (water or buffer). **Figure 2.1** is a depiction of the main principle of flow cytometry.

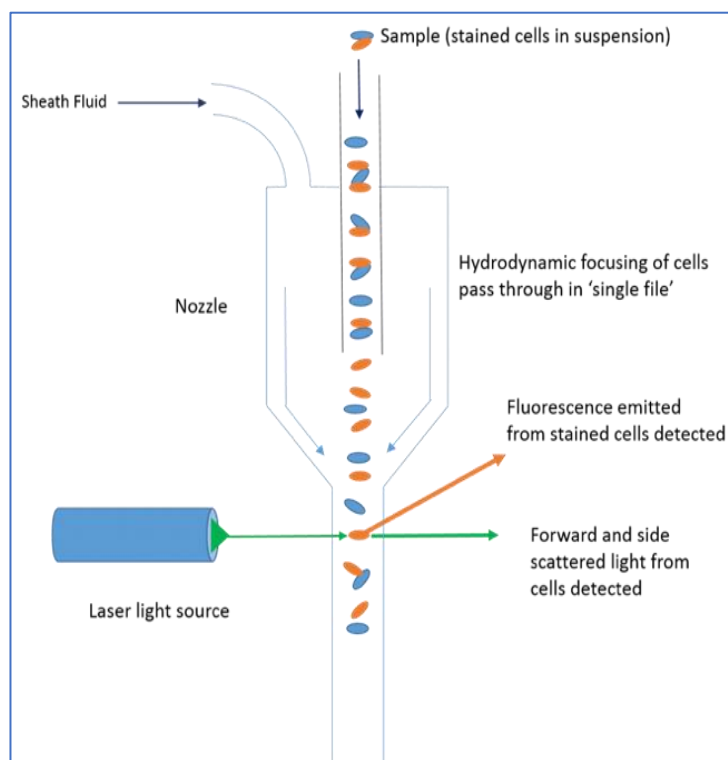


Figure 2.1. Schematic of flow cytometry principle.

Sheath fluid focuses the cell suspension and causing cells to pass through a laser beam one cell at a time. Forward and side scattered light is detected, as well as fluorescence emitted from stained cells.

2.8.2. CD14 monocytes and optimisation of LPS and brefeldin A (BFA) incubation times

In Chapter 6, enriched PB CD14CD16 monocytes were seeded in 12-well plates at a minimum density of 10^6 cells/well in 1 ml of complete RPMI 1640 medium along with 25 and 50 PNLAs or DMSO controls for 24 hours, and after 24 hours some wells were stimulated with LPS (100 ng/ml) and brefeldin (PFA; 10 μ g/ml) for 8-9 hours or left un-stimulated as a control and cultured.

An optimisation step was done regarding the suitable timing of adding BFA to block transport at the endoplasmic reticulum, which prevents the trafficking of proteins outside the cells and keeps them within the cell for intracellular assessment by flow cytometry. A BFA 10 μ g/ml media was added simultaneously with LPS, and the incubation continued for 8, 12, 16 hours, or added in the last 4 hours of LPS incubation. Preliminary results indicated that BFA needed to be added simultaneously with LPS and incubated for 8-9 hours was optimum to detect and measure intracellular cytokines in all treatment conditions (data not shown). Hence, the addition of BFA was revised and adjusted for this time of incubation. As a result, a good percentage of viable cells and the optimal quantity of the cytokine panel (IL-6, TNF- α , IL-1 β ,

CCL2, IL-10, and IL-8) were detected. This kinetic for cytokines produced by CD14⁺ monocytes was also consistent with previous literature (Schuerwegh *et al.* 2001).

2.8.3. Cell surface staining

After LPS stimulation with or without pre-treatment with PNLA, CD14CD16 enriched monocytes were collected by the detachment of the plastic wells using cold PBS containing 2.5 mM EDTA. The plate was left on ice for 15 min, and clumps of monocytes were detached under the microscope. Ca²⁺ ions in EDTA help in detaching the monocytes and dislodging them in the PBS. The monocytes were then washed using PBS supplemented with 2% HI-FCS, centrifuged at 500 x g for 5 min and non-specific binding to FcR was prevented by incubating 10⁶ cells with 2 µl human serum immunoglobulin in 200 µl PBS buffer for 30 min at 4°C. This blocks the non-specific binding of the Fc portion of fluorescently conjugated antibodies during staining steps to FcR. Then, 2 µl of Zombie Aqua live/dead (L/D) stain was added to the samples of 10⁶ cells/200 µl buffer and incubated in the dark for 30 min at RT. Cells were then washed once in FACS staining buffer (0.5% BSA, 5 mM EDTA and 7.5 mM Sodium Azide in PBS). 2 µl of fluorochrome-conjugated antibodies specific to monocyte surface receptors CD14 and CD16 were added to some of the wells, while an identical IgG isotype was added to the other wells as a control (**Table 2.2-2.3**) (optimised working dilution based on initial experiments) and incubated for 30-45 min at 4°C avoiding direct light (tubes wrapped in foil). 2-4 ml FACS staining buffer was then added, washed twice to remove excess antibody, and centrifuged at 350 x g for 5 min at RT. Supernatants were then discarded, and the pelleted cells were resuspended by flicking tubes in 200 µl of 3% paraformaldehyde (PFH) previously prepared in the laboratory. Finally, the cells were vortexed and incubated for 15 min in the dark (in tubes wrapped in foil) at RT before the next step (section 2.8.4).

2.8.4. Intracellular staining

2-4 ml of FACS staining buffer was then added to each tube, mixed well, centrifugated at 350 x g for 5 min at RT, and the supernatants were discarded. 200 µl solution of 0.5% saponin diluted in PBS was added and incubated for 5 min in the dark at RT to allow permeabilization on the monocyte's surface. At this step, anti-cytokine panel antibodies or corresponding IgG isotype controls (**Table 2.3**) were added and incubated at 4°C for 30-45 min. All intra-cellular cytokine panel and surface staining antibodies were titrated and diluted in preliminary optimisation experiments before being used in actual experiments (data not shown). After 30-45 min incubation, the suspension was washed once with 2-4 ml FACS buffer, the supernatants

discarded, and the pellet was resuspended in 200 μ l of 3% PFH. PFH works by creating cross-linking of membrane bound proteins with human PBMCs; this cross-linking preserves the cells without significant alteration of the monocyte subsets. Finally, the cells were acquired on a flow cytometer (BD LSR-FORTESSA).

Compensation for fluorochrome settings was generated using compensation beads. Compensation beads were prepared on the day of acquisition by adding 1 drop positive and 1 drop negative beads mentioned in **Table 2.1** (as per manufacturer protocol) to each surface or intracellular cytokine antibody in an independent FACS tube and suspended in 200 μ l of FACS staining buffer ready for acquisition. The summary of the workflow for intracellular cytokine assessment, starting from blood sample collection until the flow analysis, is summarized in **Figure 2.2**.

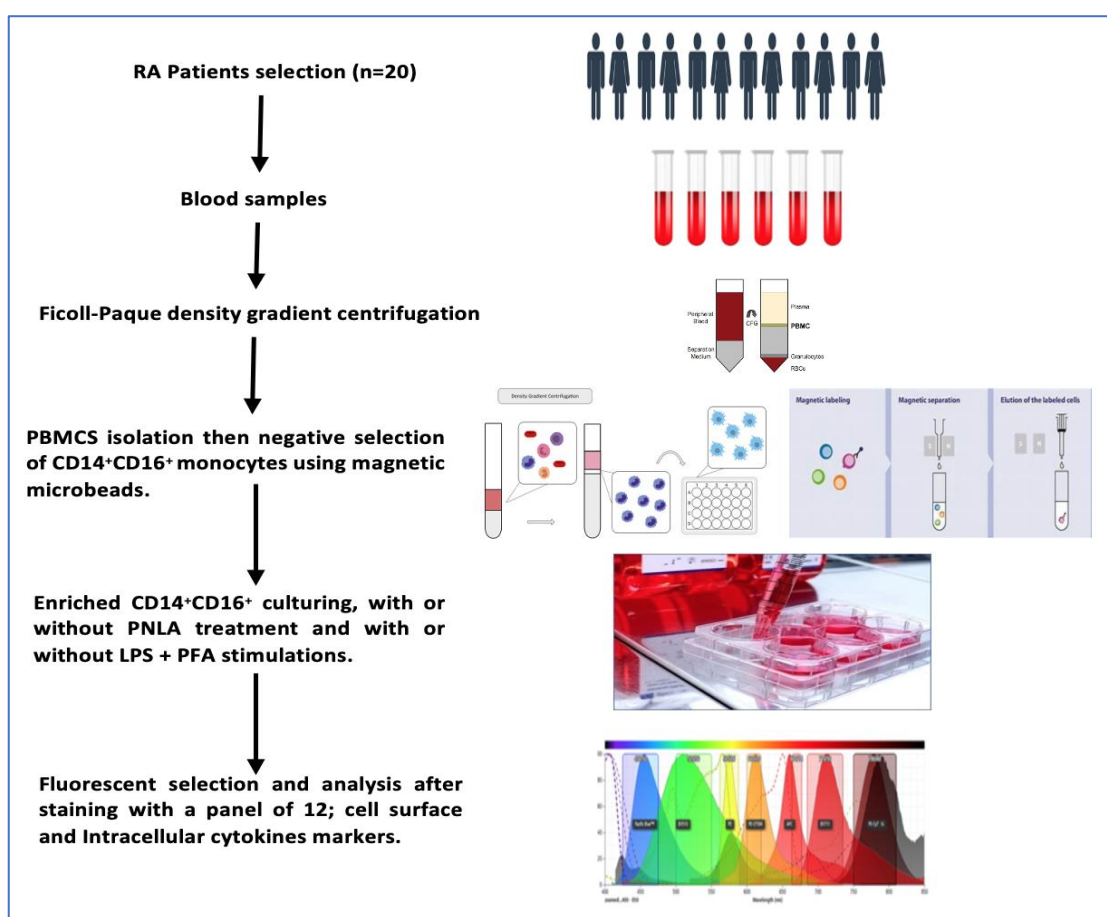


Figure 2.2. Experimental setup for intracellular cytokines assessment.

Enriched CD14⁺CD16⁺ monocytes are seeded at a density of 1×10^6 /mL in 12 well plates in RPMI supplemented media. On day 1, cells are pre-treated with either PNLA (25 or 50 μ M) or DMSO (1:1000) as a vehicle control. Cells are left to incubate for 24 hours. On day 2, cells were stimulated with or without 100 ng/ml LPS and 10 μ g/ml brefeldin-A (PFA) for 8-9 hours. On day 3, the media are gently removed and discarded, and cultures are replenished with warm PBS. Then cells are stained for surface and intracellular antibodies and acquired on a flow cytometry (BD LSR Fortessa) for cytokine expression assessment. IgG isotype controls are included in independent wells, and compensation is performed with each single experiment.

2.8.5. Flow cytometry analysis

For the experiments conducted in Chapter 6, a minimum of 1,000,000 live cells/samples were collected using forward and side scatter gating to avoid dead cells and debris and at least 50,000 events were acquired using a flow cytometer (BD LSR-FORTESSA) in the 2-3-6-5 configuration (16 colours). All acquisition and analysis were performed using the BD FACSDiva software version 8. Every patient sample had a negative control with no staining in the well (unstained cells). This unlabelled sample was run before any sample acquisition, and flow rate voltages were adjusted on FSC and SSC to ensure the cells were visible on the graphs and ensure that the fluorochromes were not signalling in error (**Figure 2.3**) for unstained samples.

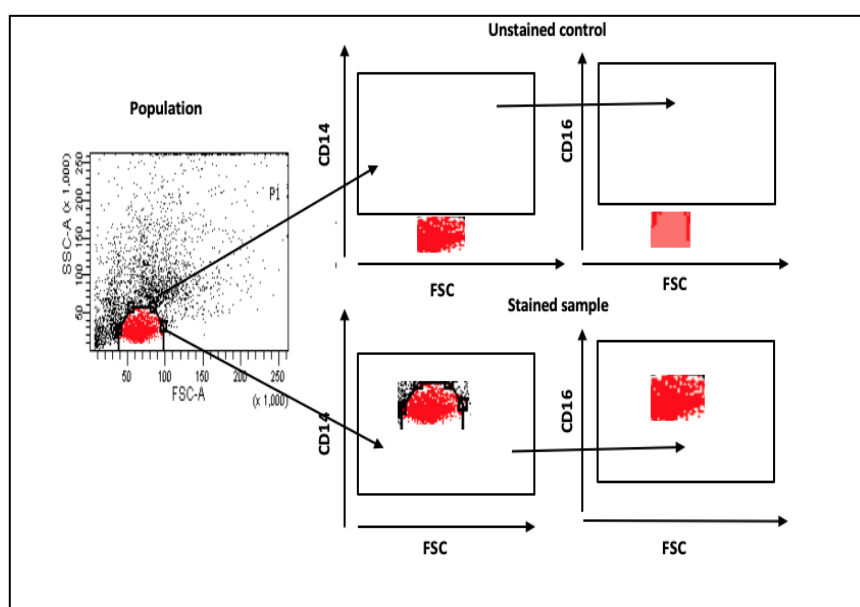


Figure 2.3. CD14CD16 monocytes, unstained, representative sample

Compensation was set before the sample acquisition, needed for final analysis, was completed for each participant in every independent experiment. Single colour compensation made it possible to omit the relative amount of fluorescence that overlaps another detector from the analysis. All the samples were kept as well compensated as possible to avoid under and overcompensations.

2.8.6. Gating strategy

Due to the characteristics of the different leukocytes, the particle size and granularity are used to differentiate cell types and exclude any dead cells or debris. The purity of isolated cells was determined by two-colour flow cytometry for CD14⁺ Brilliant Violet-711 and CD16⁺ APC-cy7

fluorescence-labelled antibodies and the number of cells in each quadrant (%) was determined on forward scatter (FSC) and side scatter (SSC) as described in **Figure 2.4**. The forward scatter area (FSC-A) is a measurement of cell size by determining the amount of light that passes around it. The side scatter area (SSC-A) is a measurement of the amount of light that is reflected by particles within the cells and therefore can be used to determine the granularity of cells allowing discrimination of leukocyte populations such as monocytes. Monocytes are large and less granular cells in comparison to neutrophils, which are relatively small but demonstrate granular morphology, and lymphocytes, which are smaller and less granular than both. FSC-A against forward scatter height (FSC-H) (reflecting particle size), these two parameters should be directly proportional when a single cell is detected. If multiple cells get recorded as a single event, the FSC-A is disproportionately high with FSC-H, when de-selected multiple cells are recorded as a single event, so these were not included in the further analysis. The discrimination of doublets, where multiple cells pass through the flow cytometer in proximity, was excluded as falsely identifying single events (**Figure 2.4**). This gating strategy would eliminate these cells from further analysis and was applied to all flow cytometry analyses as a standard. This protocol yielded CD14⁺ monocytes purity between 80-90%.

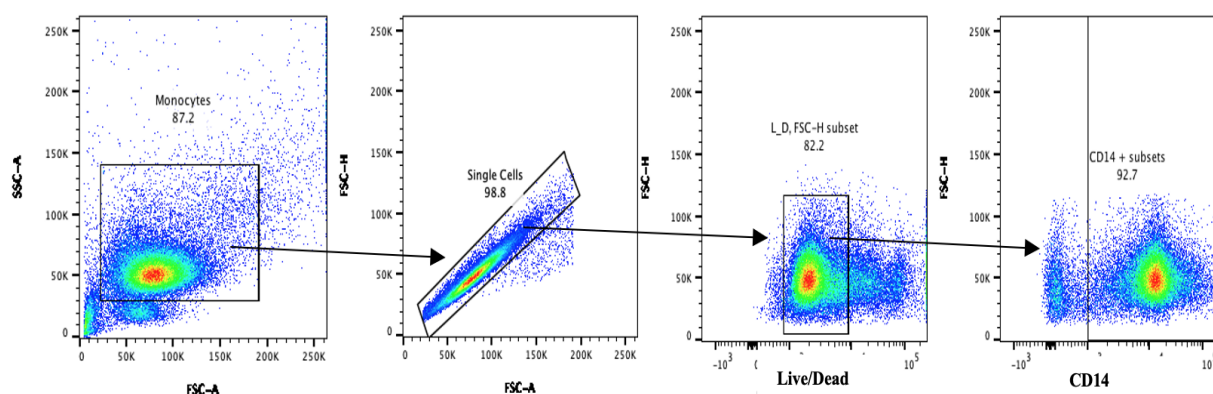


Figure 2.4. Gating strategy for sorting CD14⁺ monocytes

Monocytes were first identified based on their forward scatter and side scatter profiles. Single events were then selected based on the forward scatter area and height profiles, FS-Area and FS-Hight (reflecting particle size) are directly proportional when a single cell is captured as an event. A disproportionate ratio between the area and height indicates multiple cells being acquired at the same time, so these were not included in the further analysis. Live/dead (L/D) stain was used next to the gate only on live populations; monocytes were then identified as CD14⁺ or CD14⁻, where CD14⁺ were used for future assessment of cytokine expressions.

2.8.7. Fluorescent sorting of CD14CD16 monocytes using the FACS Aria III cell sorter.

For studies in Chapter 7, CD14CD16 magnetically labelled cell suspensions were prepared. FACS Aria III-based sorting was used to further purify the isolated monocytes and verify their purity and quantity (purity check), which was conducted under sterile conditions at 0-4°C. To reduce non-specific binding by Fc receptors, enriched CD14CD16 cell suspensions were

incubated with Fc human block (2 $\mu\text{g/ml}$; BD Biosciences) at 4°C for 10 min, and then a small volume was aliquoted into a 15 ml Falcon tube and labelled as unstained that was used for the compensation. After that, cells were stained with L/D (Zombie Aqua) fixable viability stain with fluorochrome-conjugated antibodies to CD16 and CD14 at a final dilution of 1/100 (**Table 2.1**). All experiments were controlled with appropriate isotype antibodies, compensation beads, and unstained cells. Cell sorting was performed using a BD FACS Aria III (BD Biosciences) using the gating strategy presented in **Figure 2.5**. Firstly, after determining the monocytes based on FSC-A and SSC-A, lymphocytes and granulocytes were excluded, and subsequently, monocytes were analysed for height and area to exclude doublets. Specific markers FSC-H and FSC-W were performed further to localise the monocyte populations. Secondly, the dead cells were excluded from analysis by adding L/D to the sample before acquisition, and cells were then sorted based on CD14 and CD16 expression on live-gated cells. Post sorting purity of PB CD14^{hi}CD16^{hi} monocytes was assessed in all experiments, and data generated were confirmed using FlowJo software V10 (USA). The purity of sorted cells was reassessed by repassing through the cell sorter again. The recovered cells were cultured at a density of 10^6 cells/ml at 37°C in a 5% CO₂-controlled environment and treated as described in sections (2.6-2.7).

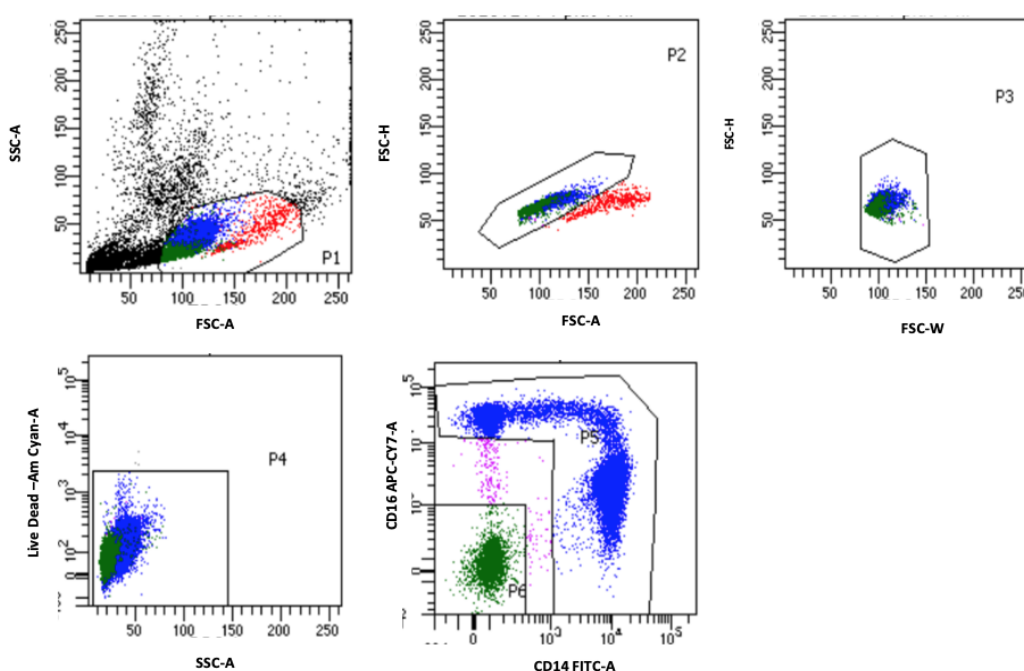


Figure 2.5. Gating strategy for sorting of CD14⁺CD16⁺ monocytes on FACS Sort Aria III.

Monocytes were first identified based on their forward scatter (FSC-A) and side scatter (SSC-A) profiles. Single events were then selected based on the forward scatter area (FSC-A) and height profiles (FSC-H). A disproportionate ratio between the area and height indicates multiple cells are being acquired at the same time; following this, the cells are determined by FSC-H and FSC-W. Monocytes were then identified as CD14^{hi}CD16^{hi} after the exclusion of dead events using L/D dye. A representative sample of n=8 RA patients.

2.8.8. Purity of Sorted CD14CD16 monocytes.

To confirm that sorted PB CD14CD16 monocytes from RA patients were pure monocytes, cell purity was checked using FACS to identify CD14CD16 positive cells, and the number of cells in each quadrant (%) was determined as described in Materials and Methods. In the average of all experiments from RA PB, the purity of CD14CD16 monocyte populations was 80-90 % as shown in **Table 2.7**. The cell yield from isolated samples ranged from $2-4 \times 10^6$ cells/donor (n=8). An approximately 10-15% of purified CD14CD16 monocytes per participant were ultimately obtained from total PBMCs, and this proportion is accurate for what is generally described in the literature with regards to overall proportions of monocytes in total PBMCs.

Table 2.7. Purity checks for CD14CD16 monocytes from RA patients.

| Subject | % CD14 ⁺ CD16 ⁺ Purity |
|---------|--|
| RA1 | 83.8 |
| RA2 | 80 |
| RA3 | 92.3 |
| RA4 | 85.2 |
| RA5 | 89.2 |
| RA6 | 87 |
| RA7 | 90.7 |
| RA8 | 96 |

2.8.9. CD14CD16 monocytes treatment

Monocytes post-sorting were counted and seeded in 6-well plates at a concentration of approximately 1×10^6 cells/ml in a complete RPMI 1640 medium along with either 25 μ M PNLA or DMSO control for 24 hours before being stimulated with LPS (100 ng/ml) or vehicle for 4 hours. Following all incubation, the cell suspension was collected in 15 ml Falcon tubes and centrifuged at 400 x g at RT for 5 min. The adherent cells in the wells were washed with (Ca²⁺ or Mg²⁺) free Dulbecco's PBS medium, detached from the plastic by addition of 1 ml accutase solution (pH 6.8)/well, incubated for 5-8 min at 37°C with 5% CO₂ cells, washed and kept at -80°C in 350 μ l buffer RLT (provided in the RNeasy Mini kit) supplemented with 10% of 2-mercaptoethanol as a lysate until RNA extraction.

2.8.10. Cell preparation for bulk RNA extraction.

The adherent cells in the wells were washed with sodium and magnesium-free Dulbecco's PBS medium to remove any unviable cells, then they were detached from the plastic by addition of 1 ml accuatase solution (pH 6.8)/well, and the incubation continued for further 5-8 min at 37 °C with 5% CO₂. Cells were then recovered by suspension in RPMI 1640 medium with stable glutamine containing (10% FCS and Pen/strep/amp) and centrifuged at 7500 x g at RT for 5 min, the supernatants were discarded, and the cells were suspended in 600 µl buffer RLT (provided by RNeasy Mini kit) supplemented with 10% of 2-mercaptoethanol. Then cells were lysed and homogenised by applying the tip of the pipette several times to the suspension up and down to dislodge the pellet and complete the lysing of cells. Finally, the lysates were kept in sterile, labelled Eppendorf tubes. They were either stored at -80 °C or used immediately in RNA extraction, as in section 2.10.1 (Chapters 5, 7).

2.9. Cell-based assays.

2.9.1 Cell Viability and Proliferation

Lactate dehydrogenase (LDH) cytotoxicity and crystal violet (CV) assays were used to assess the viability and proliferation of THP-1 and HMDMs, respectively, in presence of PNLA, as these assays were routinely used in the laboratory of Professor Dipak Ramji, where the studies presented in Chapter 3 were carried out. For assessing the viability and proliferation of PBMCs from patients with RA and HCs, Alarm blue and BrdU proliferation assays, respectively, were used, as these techniques were routinely used in the Rheumatology laboratory to assess freshly isolated PBMCs, and the kits were accessible in the Rheumatology laboratory where these experiments were carried out.

THP-1 monocytes were first differentiated into macrophages using PMA. A concentration of 200,000 monocytes in 96-well plates was differentiated into macrophages by incubation for 24 hours in the presence of 0.16 µM PMA in 0.2 ml of complete RPMI-media at 37°C with 5% (v/v) CO₂. The differentiated THP-1 macrophages or an identical count of HMDM were incubated for another 24 hours with PNLA (25, 50, 75 or 100 µM) or vehicle control in a complete RPMI medium (a positive control was included representing maximum cell death by addition of 10% of lysis buffer (provided by the kit) together with a negative control to confirm that the effects were not due to the vehicle used to dissolve PNLA). The incubation period of 24 hours corresponds to the maximum length of time the cells were treated with PNLA in this thesis and is based on previous studies in the laboratory on other therapeutic agents. After 23

hours and 15 min, 10% of lysis buffer was added to the positive control wells and the plate was re-incubated for the remaining 45 min to allow cell death to occur in these wells in order to compare with treated wells. Cells were then washed in 1 x PBS before continuing with the CV or LDH assay. For testing the effect of PNLA on the viability and proliferation of PBMCs (Chapter 4) using Alarm blue and BrdU assays, identical experimental conditions (cell count, incubation period, culturing, and treatment) were used for THP-1 macrophages and HMDM.

2.9.1.1 LDH assay.

Cell viability was determined using an LDH assay. LDH is normally localised within the cytoplasm of the cell. However, when cells undergo apoptosis or necrosis, their membranes can become leaky or lysed, causing the secretion of LDH into the surrounding media (Chan *et al.* 2013). Accordingly, dead and dying cells have lost membrane integrity and do not retain the enzyme. Therefore, the amount of LDH present in the media surrounding the cells correlates to the amount of cell death that has occurred. The cell supernatants from THP-1 and HMDMs were removed and assayed for LDH content using the Pierce LDH cytotoxicity kit following the manufacturer's instructions (Abcam, UK). A positive control was also included to achieve 100% cellular lysis, as well as a negative control containing only media for a background reading. For all samples, 50 µl of the supernatant was transferred into a separate well of a 96-well plate and mixed with an equal volume of LDH assay buffer (supplied with the kit), left for a further 30 min at 37°C and the absorbance read immediately at 490 nm on a colourimetric spectrophotometer (microplate reader). Values obtained with the negative control using media alone were subtracted from all others. Viability was expressed as a percentage of the vehicle control that was arbitrarily assigned as 100%.

2.9.1.2 CV assay

When applied to a cell population, the CV stain binds to proteins and nucleic acids such as DNA (Feoktistova *et al.* 2016), and consequently, the amount of CV stain present is proportional to the amount of nucleic acids and proteins present (i.e., depends on the cell number). This approach, therefore, can be used to indirectly assess cell proliferation. Thereby providing a reliable end-point inclusion method to measure cell proliferation. THP-1 and HMDMs were stained with 0.2% (w/v) CV solution in 10% (v/v) ethanol for 5 min at RT and then washed with PBS three times to remove the extracellular stain. Intracellular CV was solubilised using a solubilisation buffer [0.1 M sodium phosphate in 50% (v/v) ethanol] and the absorbance was read at 570 nm using a colorimetric spectrophotometer. As with the LDH

assay, negative control was also included, containing media alone for a background reading. Proliferation was expressed as a percentage of the vehicle control that was arbitrarily assigned as 100%.

2.9.1.3 Alarm blue

Resazurin is a nontoxic, non-fluorescent, and permeable blue compound used in the Alarm blue assay. On entering live cells, the cellular reducing environment reduces resazurin to resorufin, a compound that is red and highly fluorescent. Viable cells continuously convert resazurin to resorufin, increasing the overall fluorescence and colour of the media surrounding the cells. The conversion of resazurin to resorufin results in a pronounced colour change, which, when measured on a fluorescence plate reader, detects any reduction in viability as judged by the resazurin colour and the amount of fluorescence. After PBMCs have been isolated from the PB of HCs and RA patients as mentioned in section (2.4.3), the viability assay was carried out using the Alarm blue kit as per the manufacturer's instructions. Following vehicle or PNLA treatment to 200,000 cells/0.2 ml complete media in a 96-well plate for 24 hours, and vehicle or LPS stimulation for 16-18 hours as discussed in sections (2.6) and (2.7). The cell viability reagent was then brought to RT before use and added at 1/10th volume of medium directly to cells in culture medium according to the manufacturer's instructions. After incubation for 1-4 hours at 37°C in a cell culture incubator, protected from direct light, cell viability was assessed by a fluorescence-based plate reader at 595 nm at RT.

2.9.1.4 BrdU

The proliferation of PBMCs was assessed using 5-bromo-2-deoxyuridine (BrdU), which is a pyrimidine analogue. It gets incorporated into the newly synthesised DNA of proliferating cells. The BrdU cell proliferation assay kit detects incorporated BrdU using a mouse anti-BrdU antibody, which is the same as the ELISA technique. An anti-mouse HRP-linked secondary antibody was used to detect the anti-BrdU antibody bound to BrdU in the nucleus of the cell, which is followed by the addition of TMB (HRP substrate), responsible for colour change. The extent of colour development is proportional to the quantity of BrdU incorporated into the cells and used indirectly as an indicator of cell number and proliferation, this assay detects only the proliferating cells and not the seeded cells. PBMCs (200,000 cells/0.2 mL complete media) were seeded in a 96-well plate (treated and incubated in identical conditions to the viability assay) and then BrdU (1000X) solution was added into these wells at a concentration of 0.1% and the plate was incubated at 37°C for 1-4 hours. Following incubation, the medium was

removed carefully, and 100 µl of fixing/denaturing solution (provided in the kit) was added into each well at RT for 30 min. The solution was then removed carefully, and 100 µl of BrdU (300X) detection antibody (provided in the kit) was added into each well. The incubation was continued at RT for 1 hour with gentle shaking on a plate shaker; the solution was then removed, and the wells were washed with 300 µl wash buffer twice. After washing, 100 µl of anti-mouse HRP-linked antibody at concentrations of 0.2% was added into each well (provided in the kit), and the plate was incubated at RT for 1 hour. The solution was then removed, and wells were washed with 300 µl of wash buffer. Next, a 100 µl of 3,3',5,5'-Tetramethylbenzidine (TMB) substrate (provided in the kit) was added into each well for colour development. The absorbance was measured for 5-30 min at 650 nm at RT.

2.9.2. Migration assay

This assay aimed to investigate the effect of PNLA on monocyte migration by comparing the migration of THP-1 monocyte cells in response to CCL2 in cells incubated with the DMSO vehicle or PNLA. The assay was set up using a modified Boyden chamber, which involves monocytes crossing a porous membrane (mimicking the EC layer of vessels) in which cell culture inserts separated the apical and basolateral compartments, with monocytes in the apical compartment and CCL2 (20 ng/ml; concentrations based on previous optimisation in the laboratory) in the basolateral compartment. Migrating cells that move through the pores (8 µm) of the insert towards the chemoattractant in the basolateral layer are counted to assess migration (in relation to total input cells). THP-1 monocytes (1×10^6 cells/mL) suspended in either vehicle control or different concentrations of PNLA (25, 50, 75, or 100 µM) were added to the apical compartment, whereas complete RPMI supplemented with CCL2 (20 ng/mL) was in the basolateral compartment (**Figure 2.6**). Following 3 hours of incubation at 37°C with 5% (v/v) CO₂, the underside of the cell culture inserts was washed into the wells using PBS to “capture” all the migrating cells. The monocytes present in the wells were centrifuged, and the cell pellet was suspended and counted using a haemocytometer. The migration was expressed as a percentage to the vehicle control, which was assigned 100% as shown in Chapter 3.

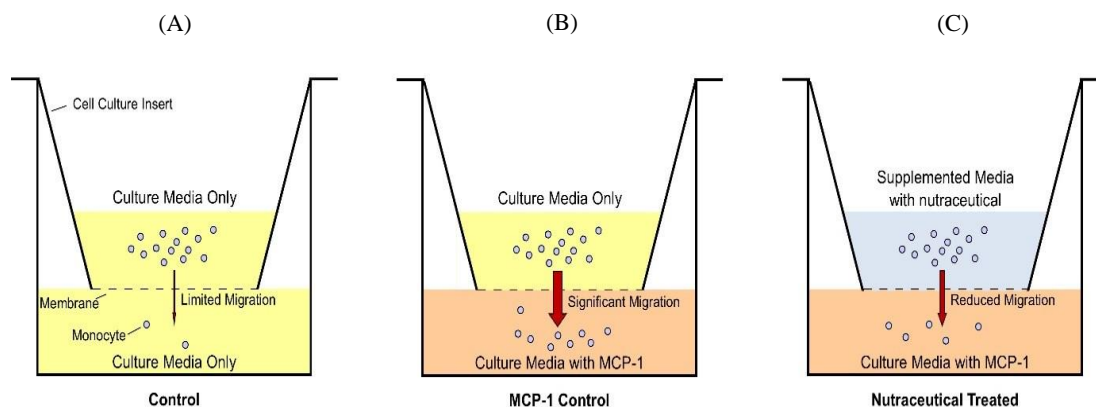


Figure 2.6. The experimental set-up of modified Boyden chambers used to assess monocyte migration.

Monocytes within the control group (A) don't contain the chemoattractant CCL2 (MCP-1) in the bottom half of the chamber, and therefore basal or limited migration should occur. Migration was induced within the CCL2 control group (B) by using culture media supplemented with CCL-2 in the bottom half of the chamber. As the THP-1 monocytes in the top half of the chamber were treated with vehicle control, a significant level of migration across the membrane should occur. The final group (C) also contained CCL2 in the bottom half of the chamber, however, the cells are suspended in culture media containing the fatty acid. A successful nutraceutical treatment would result in a reduction in the percentage of monocytes migrating from the top to the bottom half of the chamber.

2.9.3. Lipid methods

2.9.3.1 Macropinocytosis assay

Macrophages have been known to take up large amounts of native and modified LDL by fluid phase macropinocytosis (Kruth *et al.* 2005; Michael *et al.* 2013). Macropinocytosis is a form of endocytosis that allows nonselective uptake of solute macromolecules. In addition, some studies have reported a contribution of macropinocytosis to the uptake of ox-LDL and acetylated (ac-LDL) (Jones and Willingham 1999; Yao *et al.* 2009). To measure the effect of PNLA on macropinocytosis, Lucifer yellow (LY) was used. LY is a fluorescent dye commonly used in the literature as a marker to measure uptake by micropinocytosis (Michael *et al.* 2013; Al-Ahmadi and Ramji 2022). The uptake of LY was measured by FACS, which can determine the cell population's uptake of LY in cells pre-incubated with PNLA relative to a vehicle.

THP-1 and HMDMs were pre-incubated with PNLA (25, 50, 75, or 100 μ M) or DMSO vehicle control for 24 hours, followed by 100 μ g/mL of LY in RPMI medium supplemented with 0.2% (v/v) FA free bovine serum albumin (BSA). FCS stimulates cholesterol efflux, thereby affecting lipid homeostasis, and based on previous optimisation in the laboratory, BSA was used. The concentrations of LY dye and the number of cells in the wells were based on previous work in the laboratory on similar nutraceutical agents (Alahmadi and Ramji 2022). The overlying medium was then discarded, and the cells were removed by treatment with 0.05% (v/v) trypsin by incubation at 37°C for 1 hour. The cells were then collected in Eppendorf tubes

and subjected to centrifugation at 9,000 x g for 5 min to pellet the cells. The supernatant was discarded, and the pellet was resuspended and fixed in 2% (w/v) paraformaldehyde (PFA) that had been previously prepared and kept at 4°C. The cells were preserved for a maximum of a week before analysis by flow cytometry. LY incorporation was analysed on a BD FACS Canto flow cytometer, and at least 10,000 events were counted for each sample. The sample acquisitions and procedures were carried out as published by Alahmadi and Ramji (2022).

2.9.3.2 Dil-oxLDL uptake assay

Ox-LDL is commonly used in cholesterol uptake as the major form of modified LDL found in atherosclerosis *in vivo* (Lusis 2000; Shashkin *et al.* 2005) and therefore is more clinically relevant than other modified lipoproteins. Ox-LDL labelled with a fluorescent marker (Dil-oxLDL) was used and measured by FACS. Because of the high cost of Dil-oxLDL kit in comparison with LY dye, only one concentration of PNLA was used.

THP-1 and HMDMs were pre-incubated with 25 µM PNLA or vehicle control for 24 hours, followed by 5 µg/ml Dil-oxLDL in RPMI medium supplemented with 0.2% (v/v) FA free BSA. Overlying media was discarded, and the cells were removed by treatment with 0.05% (v/v) trypsin. Cells were collected in Eppendorf tubes and subjected to centrifugation at 9,000 x g for 5 min to pellet the cells. The supernatant was discarded, and the pellet was resuspended in 2% (w/v) PFA. The cells can be preserved for a maximum of a week before the analysis by flow cytometry. Dil-oxLDL uptake was analysed by flow cytometry on a BD FACS Canto flow cytometer, which counts the whole uptake by cell populations. 10,000 events were counted for each sample. The detailed methodology and sample acquisitions were carried out as published by Alahmadi and Ramji (2022).

2.9.4. Phagocytosis

The process of phagocytosis was quantitated in human macrophages by following the internalisation of a foreign particle, such as fluorescently labelled bacterial particles (Rosales and Uribe-Querol 2017). This technique takes advantage of the detectability of the intracellular fluorescence emitted by the engulfed particles as well as the effective fluorescence quenching of the extracellular probe by trypan blue. Vybrant Phagocytosis Assay Kit contains fluorescein-labelled *E. coli* (K-12 strain) bioparticles® and a trypan blue solution, the methodology used was adapted for adherent cell lines. Phagocytosis was assayed according to the manufacturer's instructions (Thermo Fisher Scientific).

THP-1 monocytes (150,000 cells/0.2 mL of supplemented complete RPMI media) were first differentiated into macrophages in a 96 well plate for 24 hours using 0.16 μM PMA. On the second day, the cells were washed using PBS, resuspended in the DMSO vehicle or different concentrations of PNLA, and incubated for 24 hours in a cell culture incubator at 37°C containing 5% (v/v) CO₂. The media was then removed and replaced with that containing 100 μl of *E. coli* bioparticles (provided in the kit) and the incubation continued for an additional 2 hours. The particles were then removed, and 100 μl of trypan blue solution (w/v) (provided in the kit), was added to all wells for 1 min. The trypan blue was then removed by washing three times with PBS, and the plate was read at 480/520 nm in a plate reader fluorescent spectrophotometer. The negative reading (wells with no cells) was subtracted from all the other positive wells with cells and *E. coli* bioparticles (to get a positive reading) and wells with treated cells and *E. coli* bioparticles (to get an experimental reading). Phagocytosis was described and analysed as a percentage.

% phagocytosis = average experimental reading/ average positive reading x 100.

2.9.5. Measurement of reactive oxygen species (ROS)

Measurement of ROS production was performed as per the manufacturer's instructions (Abcam) including concentrations and incubation times. Monocytes and macrophages at 200,000 cells /well were added to a 96-well plate in 0.2 mL of complete RPMI media. The cells were then treated with 25, 50, 75, 100 μM PNLA or vehicle control for 24 hours and then incubated with 35 μM DCFDA. The cells were washed using buffer (provided in the kit) before being stained with DCFDA in buffer for 30 or 45 min for monocytes or macrophages, respectively, in the dark at 37°C in 5% (v/v) CO₂. The fluorogenic dye DCFDA was utilised to measure ROS activity within the cells, it diffuses into cells and is deacetylated by cellular esterases to a non-fluorescent compound, which is later oxidised by cellular ROS to a highly fluorescent compound, 2',7-dichlorofluorescein (DCF). A positive control supplied by the kit, tertbutyl hydroperoxide (TBHP), was used to induce ROS production by monocytes and macrophages. DCF was measured by fluorescence spectroscopy (microplate reader) with excitation/emission spectra of 495/529 nm. Therefore, a reduction in the cumulative fluorescent signal following PNLA treatment would mean it is capable of attenuating ROS generation. The detailed method and set up of the assay have been published by Moss *et al.* (2021) and O'Morain *et al.* (2021). ROS, phagocytosis, and lipid assays were presented in Chapter 3.

2.9.6. Measurement of protein

2.9.6.1. Enzyme-linked immunosorbent assay (ELISA)

ELISA is a biochemical technique used to determine the presence of an antigen or antibody in the examined sample. The principle of the technique is based on an antibody sandwich procedure. All the reagents used were provided in the kit. The first step in this assay involves the addition of a capture antibody provided against the substance of interest to the microtiter plate, this will create a solid phase. After, the addition of the blocking agent (0.2% BSA), the plate was incubated for at least one hour. After washing the plate with wash buffer (0.05% (v/v) Tween 20 in PBS) previously prepared in the laboratory, the standard recombinant proteins, and samples of interest for protein measurement, were added to the plate, and incubated with the solid phase continued for 2 hours. The next step was the plate evacuation and the addition of the detection antibody (provided), and incubation at RT for a further 2 hours. The final step involves the addition of a substrate that will generate color change at a rate proportional to the amount of the protein of interest. In this chapter, the ELISA technique was used to measure TNF- α , IL-6, IL-1 β , and PGE2 using commercial kits in accordance with the manufacturer's instructions, in culture supernatants from 5×10^5 monocytes or macrophages pre-incubated with PNLA or DMSO control for 24 hours and stimulated with LPS or vehicle control for another 18 hours. Detailed methods (reagents and steps) for each assay are demonstrated in sections (2.9.6.2-2.9.6.3). ELISA experiments were presented in Chapter 4.

2.9.6.2 ELISA measurement of TNF- α , IL-6, and IL-1 β

2.9.6.2.1. Principle of the assay

The competitive ELISA was used to measure; TNF- α , IL-6, and IL-1 β in the supernatants of LPS stimulated adherent monocytes and macrophages from rheumatoid patients and HCs. Mouse and rat monoclonal antibodies for ELISA of human TNF- α , IL-6, and IL-1 β and recombinant human TNF- α , IL-1 β , and IL-6 were obtained from R&D systems. Duo-set ELISA development kits from (R&D) Systems were used following the manufacturer's instructions to measure recombinant and human natural TNF- α , IL-6, and IL-1 β .

2.9.6.2.2. Assay procedure

Table 2.8 demonstrates the protocol used for measurement of human TNF- α , IL-6, and IL-1 β in supernatants.

Table 2.8. Protocol for ELISAs; human TNF- α , IL-6, and IL-1 β supernatants.

| Step | Process | Time |
|------|--|----------------------------|
| 1 | 96-well ELISA plate coated with 100 μ l of capture antibody. | Overnight |
| 2 | Any liquid was removed from the wells by inverting and blotting against paper towels. Plate washed three times with 300 μ l per well of 0.05% (v/v) Tween 20 in PBS. | - |
| 3 | 300 μ l blocking buffer to each well was added. | 1 hour. |
| 4 | Step 2 repeated. | - |
| 5 | Addition of 100 μ l of standard and samples. Plate covered and incubated at RT. | 2 hours |
| 6 | Step 2 repeated. | - |
| 7 | 100 μ l detection antibody per well was added. Plate covered and incubated at RT. | 2 hours |
| 8 | Step 2 repeated. | - |
| 9 | 100 μ l of streptavidin-HRP was added, plate was covered and placed in the dark. | 20 min |
| 10 | Addition of 100 μ l of substrate solution to each well, cover and place the plate in the dark. <ul style="list-style-type: none"> The substrate solution is 3,3',5,5'-Tetramethylbenzidine (TMB). | 20 min, note colour change |
| 11 | Addition of 50 μ l stop solution to each well. | |
| 12 | Immediately determine optical density of each well at (450-540) nm. | In < 1 hour |

Briefly, ELISA plates were coated with a working concentration of human capture antibody as detailed in the **Table 2.9**, sealed, and incubated overnight at RT. The day after, plates were washed 3 times with wash buffer (0.05% Tween in PBS), and any liquid was removed from the wells by inverting and blotting against paper towels. The plate was then blocked with reagent diluent (0.5% BSA previously prepared and kept at 4°C) for an hour. The washing and drying of plates were repeated. Samples were diluted in reagent diluent (optimised to fit within the standard curve for the assay before the actual experiment), and standards were made up in serial dilutions of BSA in concentration ranges based on **Table 2.9**. Samples and standards were added to 96 well plates in duplicates and incubated for 2 hours at RT. The washing of plates was repeated. Biotinylated detection antibody (as per assay) was then added to plates

and sealed for two hours at RT, followed by another wash as above. Diluted streptavidin-HRP was incubated on plates for 20 min, washed, and substrate solution (provided in the kit) was added for a further 20 min. Finally, stop solution (1M of concentrated HCl) was added, and optical density (OD) of plates was measured on a microplate reader of a spectrophotometer at 450 nm with a correction at 540 nm. The concentrations of the monoclonal antibodies used in each ELISA kit are detailed in **Table 2.9**.

Table 2.9. Human TNF- α , IL-6 and IL-1 β antibodies and standards used in ELISAs experiments.

| Protein | Capture antibody working concentration | Detection antibody working concentration | High concentration standard |
|--------------------------------|--|--|-----------------------------|
| TNF-α | 4 μ g/ml | 50 ng/ml | 1000 pg/ml |
| IL-6 | 2 μ g/ml | 50 ng/mL | 600 pg/ml |
| IL-1β | 4 μ g/ml | 150 ng/mL | 150 pg/ml |

2.9.6.2.2.3. Calculation and analysis of the results

The OD of the microplates was then immediately measured at 450 nm on a plate reader. The interpolated standard curve was plotted and compiled, and unknown (TNF- α , IL-6, and IL-1 β) protein concentrations were determined and calculated from this. The average of 2 readings was taken from standards and samples that were assayed in duplicate, and the data shown are (mean +/- SEM) from each participant in all experiments. Statistical analysis was performed using a one-way ANOVA followed by Tukey's post hoc analysis. Any data transformations were carried out when needed. A P-value of ≤ 0.05 was considered significant. **Figure 2.7** shows optimisation of PNLA concentrations when assessing IL-6 levels. In the preliminary results, 50 μ M PNLA was optimal; therefore, we used 25 and 50 μ M PNLA in future experiments.

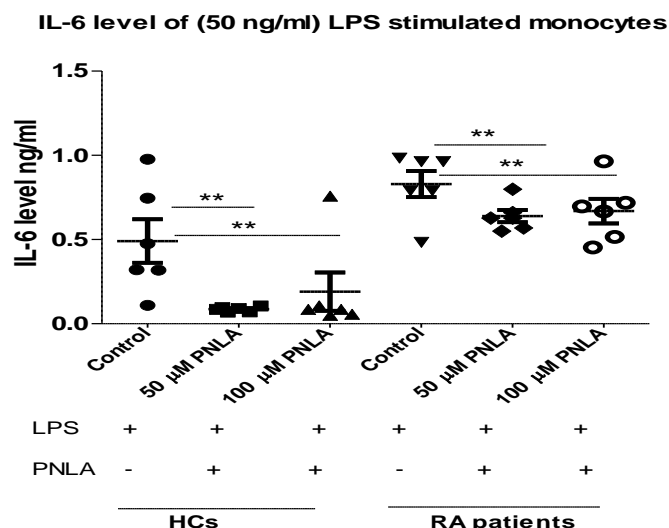


Figure 2.7. IL-6 level assessment in optimization experiments with 50 and 100 μM PNLA.

In the initial experiments, enriched monocytes obtained from HCs (n=6) and RA patients (n=5) were incubated with 50, 100 μM PNLA or DMSO for 24 hours, followed by LPS stimulations at 50 ng/ml for another 16-18 hours. Then, the supernatants were collected and assayed for levels of IL-6 using ELISA; all samples and standards were run in duplicate. The data are presented as mean \pm SEM, each dot (\bullet) represents the average of one participant. Any data transformations were carried out when needed. Statistical analysis was performed using a one-way ANOVA and a Tukey's post hoc test, where (**p \leq 0.01).

2.9.6.3 ELISA measurements of PGE2

2.9.6.3.1. Principle of the assay

PGE2 is rapidly metabolised *in-vivo* and *in-vitro*; hence, PGE2 was assayed by measurement of PGE2 metabolites (Matsuno *et al.* 2019) using ELISA kits purchased from Cayman Chemical. A goat anti-mouse PGE2 monoclonal antibody (provided) was pre-coated onto a microplate. The basis of this assay was a competition between PGE2 and acetylcholinesterase (AChE) conjugate (a PGE2 tracer) for a limited amount of PGE2 antibody. Because the concentration of the PGE2 tracer is held constant while the concentration of PGE2 varies, the amount of PGE2 tracer that can bind to the PGE2 monoclonal antibody will be inversely proportional to the concentration of PGE2 in the well. The plate was washed with wash buffer (provided in the kit) to remove any unbound reagents, and then Ellman's Reagent (which contains the substrate for AChE) was added to the well. The intensity of colour determined is proportional to the amount of PGE2 tracer bound to the well, which is inversely proportional to the amount of free PGE2 present in the well, where: **Absorbance \propto [bound PGE2 tracer] \propto 1/[PGE2].**

2.9.6.3.2. Assay procedure

The addition of the reagents to the wells was done according to the following steps and demonstrated in **Table 2.10.** below:

A total of 100 μl of ELISA buffer (provided in the kit) was added to non-specific binding (NSB) wells, and 50 μl was added to maximum binding (B0) wells. After, 50 μl of culture medium was added to NSB and B0 wells or 50 μl of ELISA buffer to NSB and B0 wells if the culture medium was used to dilute the standard. Then a serial dilution was performed, PGE2 standard (50 μl of highest standard) was added to (A) rows of the wells in the plate (S1) and 50 μl of S1 in (A) wells were added to (B) rows (S2) and so on in a 96-well plate. 50 μl of experimental samples were added/well. All samples and standards were assayed in triplicates. PGE2 Ach E tracer 50 μl was added to each well except the total activity (TA) and the blank (Blk) wells. Finally, 50 μl of PGE2 monoclonal antibody was added to each well except the TA, NSB, and Blk wells.

Table 2.10. The pipetting summary for the wells in the PGE2 ELISA plate.

| Well | ELISA buffer | Standard/sample | Tracer | Antibody |
|-----------------------------------|-------------------|------------------|------------------|------------------|
| Blank (Blk) | - | - | - | - |
| Total activity (A) | - | - | 5 μl | - |
| Non-specific binding (NSB) | 100 μl | - | 50 μl | - |
| B0 | 50 μl | - | 50 μl | 50 μl |
| Standard/ sample | - | 50 μl | 50 μl | 50 μl |

Development of the plate: the plate was covered with plastic film and incubated at 4°C (refrigerator) for a period of 18 hours. Ellman's reagent was prepared immediately the next day before being added to the wells (unstable and should be used on the same day). The following steps were performed: The wells were evacuated and rinsed 5 times with the wash buffer previously prepared. After 200 μl of prepared Ellman's reagent was added to each well. Then 5 μl of tracer was added to the TA wells. Finally, the plate was covered with a plastic film, incubated on an orbital shaker, and covered again with a dark sheet to allow the plate to develop in the dark for a period of 60-90 mins.

Reading the plate: the plate cover was removed carefully to keep the Ellman's reagent from splashing on the cover. The plate was read between 405 and 420 nm, and the absorbance was checked periodically. When the absorbance of the wells exceeded 1.5, the plate was washed, and fresh Ellman's reagent was added to let the plate develop.

2.9.6.3.3. Calculation and analysis of the results

The absorbance readings from the NSB and B0 wells were averaged. The NSB average was then subtracted from the B0 average. This is the corrected B0 or corrected maximum binding. The B/B0 (sample or standard bound/maximum bound) for the remaining wells was calculated. This was done by subtracting the average NSB absorbance from the S1 absorbance and dividing by the corrected B0 (from Step 1). This is done for S2-S8 and all sample wells. (To obtain % B/B0, multiply these values by 100).

%B/B0 plotted for standards S1-S8 versus PGE2 concentration using linear (y) and log (x) axes and performed a 4-parameter logistic fit. (%B/B0) value for each sample was calculated. The concentration of each sample was determined using the equation obtained from the standard curve plot (**Figure 2.8**). Samples with %B/B0 values greater than 80% or less than 20% were re-assayed as they generally fall outside of the linear range of the standard curve. Any dilution or concentration of the sample before addition to wells was transformed later in the analysis in GraphPad Prism.

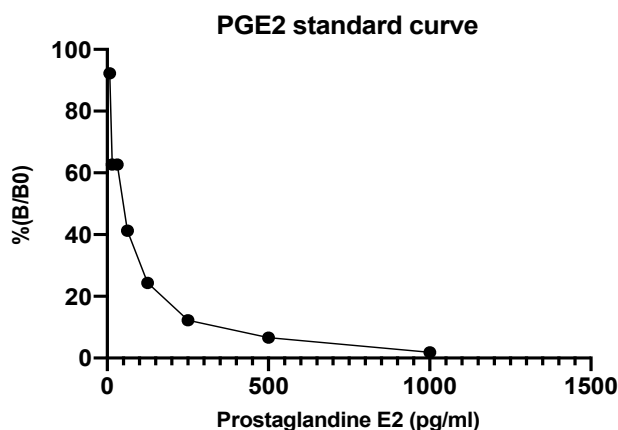


Figure 2.8. PGE2 ELISA standard curve. A percentage of B/B0, from 20-80%, was taken for determining the PGE2 level.

2.9.6.4 Indirect measurements of nitric oxide (NO) via the Griess system

2.9.6.4.1 Principle of the assay

Direct measurement of NO in biological fluids is difficult as it has a very short half-life due to its rapid reaction with many molecules. A commonly used indirect method of estimating NO in biological fluids is measuring nitrite (NO₂), which is a metabolite of NO, and nitrate (NO₃). In this study, NO₂ was determined using the Griess reagent system from Promega as an indicator of NO levels. The Griess system uses sulfonamide and N-1-naphthylethylenediamine di-hydrochloride (NED) under acidic conditions. This system detects NO₂ in a tissue culture medium such as RPMI media.

2.9.6.4.2 Assay procedure

Firstly, a sulfonamide solution was added to the samples, and incubated for 5-10 min, and then another volume of NED solution was added and incubated again for another 5-10 min at RT. To ensure accurate NO₂ quantification, a reference curve was prepared with the nitrite standard of each assay, using the same media or buffer that were used for the experimental samples. All steps were performed according to the kit manufacturer's instructions.

Preparation of a Nitrite Standard Curve

To generate the Nitrite Standard Curve, 1 ml of 100 µM nitrite solution (provided in the kit) was prepared by diluting the provided 0.1 ml of nitrite standard at 1:1000 in the RPMI media used for experimental samples. Then 2 columns (16 wells) of a 96-well plate were designed for the nitrite standard, done in duplicates. 100 µl of nitrite solution was added to the first couple of columns. 50 µl of the appropriate matrix was added to the rest of the wells, and immediately 6 serial twofold dilutions (50 µl/ well) were done in duplicate. The final volume in each well was 50 µl, the nitrite concentration range was 0-100 µM, and the lower limit of detection was 2.56 µM nitrite.

Nitrite measurement (Griess reaction)

The sulfonamide solution and NED (provided in the kit) were allowed to equilibrate to RT (15-30 min). Then, 50 µl of each experimental sample was added to the wells in duplicate. Using a multichannel pipette, 50 µl of sulfonamide solution was dispensed to all the experimental samples and the wells containing the nitrite standard. The plate was then incubated for 5-10 min at RT, protected from light. Using a multichannel pipettor, 50 µl of NED solution was then dispensed to all the wells. The plate was incubated again at RT for another 5-10 min, protected from light. A purple or magenta colour developed immediately. Finally, the absorbance was measured within 30 min in a plate reader between 520-550 nm.

2.9.6.4.3 Calculation and analysis of the results

The standard curve was drawn by plotting the standard nitrite concentrations as a function of (X) with the average absorbance value of each concentration of standard as a function of (Y). The average absorbance value of each experimental sample was determined from this. The average of 2 readings was taken from standards and samples that were assayed in duplicate, and the data shown are the mean +/- SEM from each participant in all experiments. The statistical analysis performed was the same as that used to assess TNF- α , IL-1 β , and IL-6.

2.10. Molecular techniques and general workflow of the different stages of gene expression analysis

Transcriptome analysis is made feasible by deep sequencing technology (Balakrishnan *et al.* 2012). The development of next-generation sequencing (NGS) technologies such as RNA-seq is now replacing ‘first-generation’ Sanger sequencing and hybridisation approaches, such as microarray methods, for genome analysis (Metzker 2010). RNA-seq provides cheaper, faster, and more accurate transcript quantification than previous approaches to identify which genomic loci are expressed in a cell (population) at a given time over the entire expression range. Indeed, RNA-seq was shown to detect lowly expressed transcripts while strongly reducing false positive rates in comparison to microarray-based expression quantification (Illumina 2011; Nookaew *et al.* 2012; Zhao *et al.* 2014). The detection of gene expression changes (mRNA levels) between different cell populations and/or experimental conditions remains the most common application of RNA-seq, as it is more sensitive in detecting low-abundant transcripts and small changes in gene expression (t’Hoen *et al.* 2008; Wilhelm *et al.* 2008). These advantages of RNA-seq make it an ideal tool for the interpretation of gene regulation in a disease and therapy setting. Compared to microarrays, RNA-seq has more specificity and sensitivity, allowing the detection of rare and low-abundance transcripts. Furthermore, RNA-seq does not require species- or transcript-specific probes; it can detect novel transcripts, gene fusions, single nucleotide variants, small insertions and deletions, and other previously unknown changes that arrays cannot detect, thereby allowing simultaneous measurement of thousands of transcripts in a hypothesis-free manner.

Previously, analysis of RNA-seq required specific bioinformatic expertise. Recently, cloud-based technology platforms such as BaseSpace Sequence Hub, DRAGEN Bio-IT Platform, and RNA-seq software tools have allowed researchers, regardless of bioinformatics experience, to evaluate RNA-seq data. Cloud-based platforms store data and computational resources centrally and allow global access, thereby offering the computational power and storage needed to analyse bioinformatic data without the need for computing infrastructure. With advances in technology, biomarker testing strategies have also evolved, with a trend towards higher-order multiplexed technologies as well as cross-modality testing from a single sample to understand correlations between DNA, RNA, and protein markers. More data may be burdensome to analyse, while a focused assay may miss an opportunity for collecting potentially valuable data. In this project, the steps from sample preparation to bioinformatic work performed are demonstrated in the following steps and summarised in **Figure 2.9**.



Figure 2.9. Schematic figure of experimental workflow from sample preparation to bioinformatic work.

2.10.1. RNA extraction and quality control (QC) check

Total RNA was isolated from PBMC using the RNeasy Mini Kit (Qiagen) according to the manufacturer's instructions and purified using RNeasy on-column DNase I digestion (Qiagen) according to the manufacturer's instructions. The cell lysates were passed through a series of spin columns provided in the kit to first bind genomic DNA, then RNA, and finally elute high quality RNA. The experimental procedure is summarised and outlined in brief in **Flow Diagram 2.10**. PBMC lysates in the buffer RLT (600 μ l) in Eppendorf tubes were brought to RT and added to 600 μ l of 70% ethanol (v/v) (prepared previously and kept at RT) at a volume of 1:1 and mixed well by pipetting up and down with no vortexing. Next, 600 μ l of the sample mixture, including any precipitate, was transferred to a RNeasy mini spin column placed in a 2 ml collection tube, the lid closed, centrifuged at 9000 x g for 15 sec, and the flow through was poured off (RNA on the column). The rest of the suspension (cell lysate in the RLT and ethanol mixture) was added to the column, centrifugation was repeated, and the flow through was poured off leaving RNA and DNA on the column. Then, 700 μ l of wash buffer (RW1) (provided in the kit) was added to each sample and centrifuged at 9000 x g for 15 sec, and the flow through was poured off.

Next, 80 μ l of combined 10 μ l of DNase I (previously prepared and kept at -20°C) and 70 μ l of RDD buffer (kept at 4°C) were added to the centre of the column and incubated for 15 min at RT. Then, 700 μ l of RWI buffer was added, centrifuged at 9000 x g for 15 sec, and the flow was discarded. 500 μ l of wash buffer (RPE) (provided in the kit) was added, centrifuged at 9000 x g for 15 sec, and the flow was discarded. Finally, 500 μ l of RPE was added, centrifuged at 1300 x g for 2 min, and the flow was discarded. The RNeasy spin column was then placed into a new 1.5 ml collection tube (supplied), 40 μ l RNase free water was added directly to the column membrane, the lid was closed, and the column was centrifuged at 9000 x g for 1 min to elute the RNA. The spin column was discarded, and the collection tubes, which contain total RNA, were kept at -80°C ready for a QC check and future library construction. The same protocol was conducted when extracting RNA from sorted and purified CD14CD16 monocytes in Chapter 7. Since the lysate obtained by purified monocytes is low in the amount in

comparison with the lysate obtained by PBMCs, I used 350 μ l of buffer RLT and halved the amounts and concentrations of the buffers used as per the manufacturer's recommendation (Qiagen).

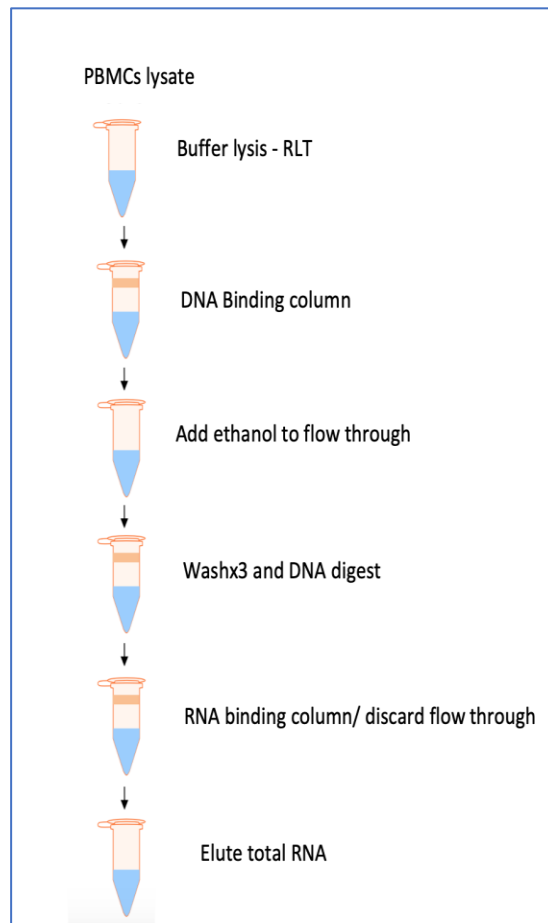


Figure 2.10. Flow diagram of the spin column RNA isolation method. Illustrating the steps involved in the extraction of total RNA using a spin column mini kit (Qiagen), including the DNA digestion step.

Quality control (QC) check of RNA

Traditionally, RNA integrity was assessed via gel electrophoresis and visual inspection of the ribosomal RNA bands. Intact eukaryotic total RNA should yield clear 28S and 18S rRNA bands. The 28S rRNA band is approximately twice as intense as the 18S rRNA band (2:1 ratio). As RNA degrades, the 2:1 ratio of high-quality RNA decreases, and low molecular weight RNA begins to accumulate (**Figure 2.11A**). Since the human interpretation of gel images is subjective and has been shown to be inconsistent, bioanalyzer systems are widely used and allow the calculation of an RNA Integrity Number (RIN) from a digital representation of the size distribution of RNA molecules. The RIN number is based on a numbering system from 1 to 10, with 1 being the most degraded and 10 being the most intact (**Figure 2.11B**). This approach facilitates the interpretation and reproducibility of RNA quality assessments and provides a means by which samples can be compared in a standard manner. Here in this Chapter, we investigated RNA for purity using Nanodrop spectrometry; RNA should be free from protein (e.g., nucleases), salt, or other cellular components; OD260/280 ratio > 1.8 as recommended in the manufacturer's protocol, and there should be no genomic DNA contamination as detailed in the following section 1. While QC was checked using an Agilent developed software algorithm that automatically determines size, quantity, purity, and RIN (which was obtained from an Agilent tape station in a similar principle of a bioanalyzer), details are provided in section 2. The Qubit® 2.0 Fluorometer was used to confirm RNA concentrations as an additional step through fluorometric quantitation of the samples described in section 3.

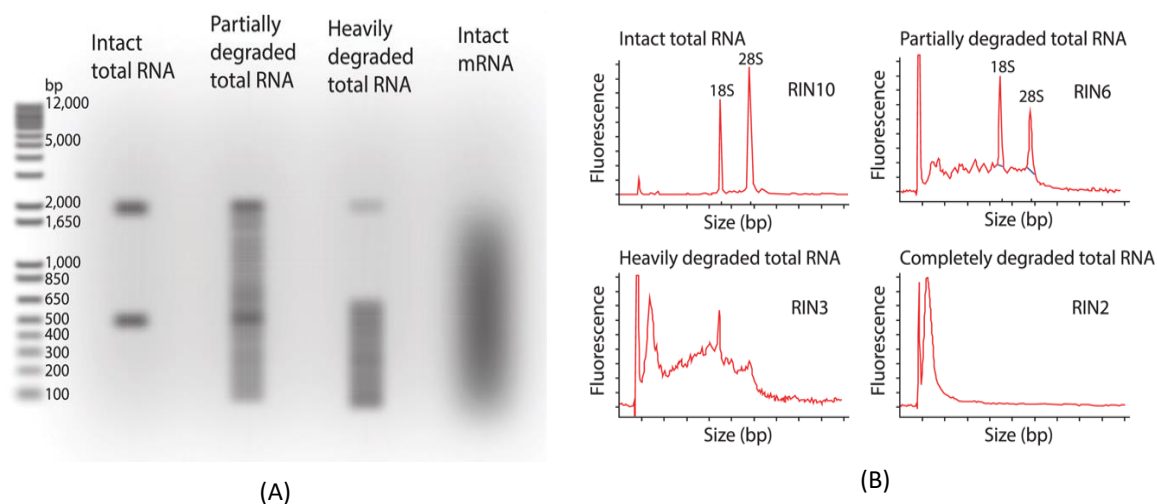


Figure 2.11. RNA integrity assessment.

Based on the ratio of 28S:18S rRNA estimated from the band intensity (A) or digital densitometry plot (B), RNA used for RNA-seq experiments should be as intact as possible.

2.10.1.1. Nanodrop Spectrometry

Following extraction, defrosted RNA samples were quantified, and quality assessed using the Nanodrop ND-2000 spectrophotometer VX (Thermo Scientific). Nanodrop permits RNA quantification with high accuracy, reproducibility, and low sample consumption (1µl of total RNA). The instrument passes ultraviolet light through the RNA sample suspended in a column by surface tension on a pedestal and measures the absorbance at the wavelengths of 230, 260, and 280 nm. The pedestal moves automatically to adjust the path length to the optimal range of (0.05mm-1mm). The values of the absorbance measurements reflect the concentration and purity of the RNA samples. Since RNA absorbs strongly at 260 nm due to its aromatic base moieties, absorbance at this wavelength is used to quantify RNA sample concentrations. Concentration estimates are calculated by the Beer-Lambert law, which relates the amount of absorbed light with the concentration of the absorbing molecules ($A=\epsilon cl$; where A =absorbance, ϵ =extinction coefficient, c =concentration, and l =path length). However, both single- and dsDNA also absorb at 260 nm and can affect perceived concentrations. Thus, potential DNA contamination requires consideration in the interpretation of the results. The ratio of absorbance at 260 nm and 280 nm (260/280) is used to assess RNA purity, with a ratio of 2 generally accepted as pure for RNA. This, however, will fluctuate with the composition of the RNA since each individual nucleotide exhibits widely variable 260/280 ratios. This is particularly prominent with a high uracil content, which also accounts for the typically higher ratios observed for RNA over DNA. While values between 1.8 and 2.2 are considered normal, major divergence from expected 260/280 ratios may indicate contamination with phenol-group containing organic compounds or proteins since aromatic amino acid side chains often absorb at 280 nm. The ratio of absorbance at 260 nm and 230 nm (260/230) is also frequently considered when assessing nucleic acid purity, often higher than 260/280 ratios, typical 260/230 ratios are in the range of 2.0-2.2 (**Figure 2.12**). While there appears to be no consensus on absolute cut-off values for purity, considerably lower values may indicate the presence of contaminants that absorb at 230 nm. These often include chaotropic agents such as guanidinium thiocyanate, frequently present in wash buffers of RNA extraction kits, but also ethylenediaminetetraacetic acid (EDTA), carbohydrates, phenol, and Trizol[®] reagent, which all show absorbance near 230 nm and could contaminate RNA samples. A low 260/230 ratio below 1.8 is indicative of significant contamination, which could impede downstream applications such as reverse transcription, which is commonly performed for RNA-seq. RNA extraction and QC Nanodrop assessment were carried out in the rheumatology laboratory by Rabaa Takala. In collaboration with our colleagues at Wales Gene Park (WGP) at Cardiff

University, the samples were sent in person for further QC checks (as in the subsequent sections (2.10.1.2-2.10.1.3)). Once RNA passed the QC, Dr. Shelley Rundle and Robert Maddison carried out the library construction and the sequencing (2.10.2-2.10.4). The data files were then sent to Dr. Robert Andrews, who kindly performed the basic bioinformatic work (2.10.5-2.10.7) and transferred the data to Rabaa Takala. Dr. You Zhou kindly suggested some analysis plans, and Rabaa Takala performed the detailed bioinformatic upstream and downstream pathway analysis as in sections 2.10.9.

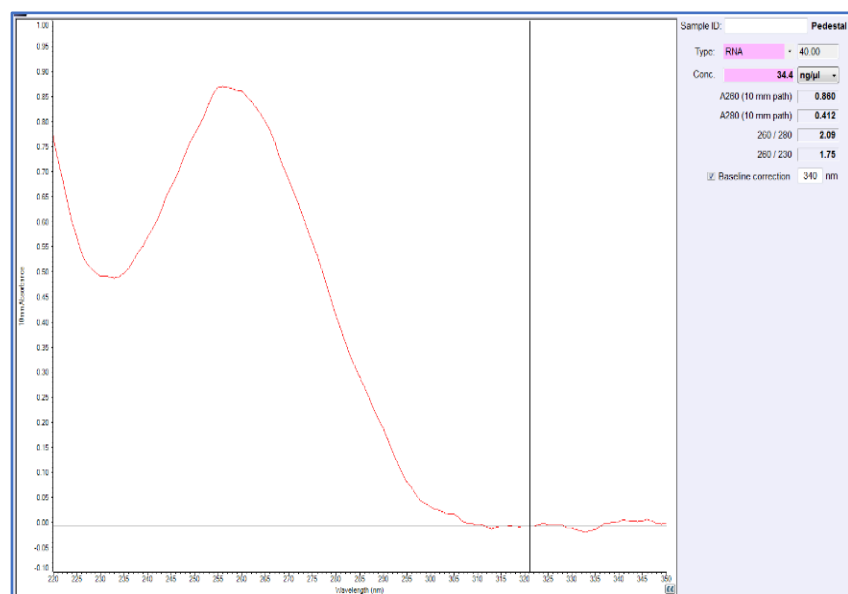


Figure 2.12. A representative sample of nanodrop spectrophotometry plot of a high-quality RNA. In the Nanodrop plot, absorbance (y-axis) is plotted against wavelength (x-axis).

2.10.1.2. Agilent 4200 TapeStation

RNA is much more susceptible to degradation than DNA, and the quality of the extracted RNA molecules can strongly impact the results of the RNA-seq experiment since RNA-seq requires high-quality RNA. Total RNA quality and quantity were further assessed using the Agilent 4200 TapeStation System and RNA ScreenTape Kit (Agilent Technologies, UK). The credit-card-sized disposable (hsRNA ScreenTapes) carries multiple separation lanes for analysing RNA samples (**Figure 2.13**). The ScreenTape device has 16 lanes, so each sample was analysed in an individual lane, eliminating contamination. The integrated electrodes apply a current across the screen tape device, and the gel through which the samples are analysed is contained within individual columns on the tape. The TapeStation software automatically determines size, quantity, purity, and RIN and reduces errors. The data are presented in electropherogram images for the samples, as demonstrated in **Figure 2.16(A)**.

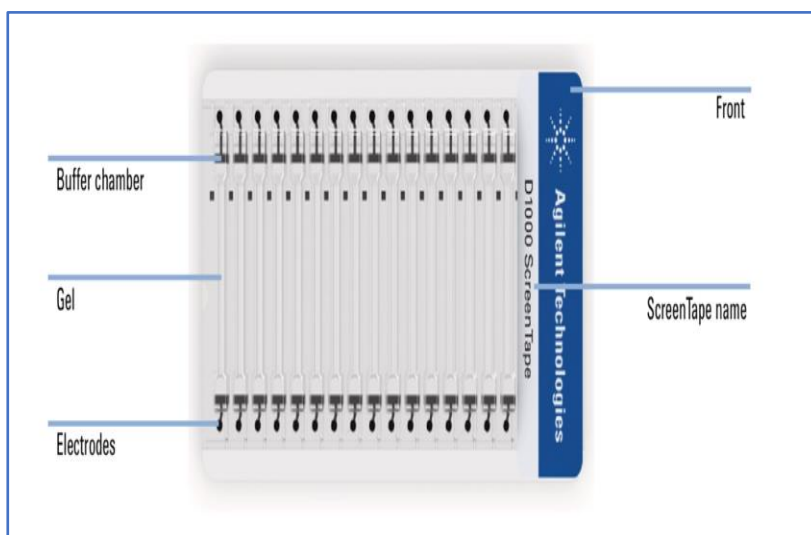


Figure 2.13. Screen Tape device architecture used for RNA QC check.

2.10.1.3. Qubit® 2.0 Fluorometer assay

Qubit® 2.0 Fluorometer Assay Kit (Life Technologies, UK) was used to perform the fluorometric quantitation of the studied samples, according to the manufacturer's instructions. The reagent mix was prepared by diluting Qubit® reagent 1:200 in Qubit® buffer and briefly vortexing. 1-10 µl RNA sample was combined with 190-199 µl of the reagent mix, vortexed briefly, and incubated for 2 min before using the Qubit® Fluorometer (**Figure 2.14**). The RNA high sensitivity (hs) (quantitative range; 5-1,00 ng/µl) assay kit was used to quantify all RNA samples. The dsDNA hs (0.01-100 ng/µl) assay kit was used to measure concentrations of DNA libraries later in sequencing experiments. DNA range (0.1-1,000 ng/µl) kit was used for all other DNA measurements. The fluorometer was calibrated using assay-specific nucleic acid standards.



Figure 2.14. Qubit 2.0 Fluorometer used for RNA and DNA quantification

The quality of the total RNA isolated from PBMCs was thoroughly checked using these methods. High-quality Nanodrop spectrophotometry plots were achieved for almost all

samples with concentrations >16 ng/ μ l (a 260/280 ratio between 1.8 and 2.2 and a 260/230 ratio above 1.15 were considered for the analysis) **Table 2.11**. Similar QC data was obtained from TapeStation with RIN > 8.9 in **Table 2.12**.

Table 2.11. QC of RNA samples from PBMCs as per the Nanodrop spectrophotometer.

| Sample (numb) | Sample name | Concentration ng/ μ l | 260/280 | 260/230 |
|---------------|---------------------|---------------------------|---------|---------|
| 1 | control RA (1) | 26.3 | 2.05 | 1.15 |
| 2 | LPS RA (1) | 21.1 | 1.97 | 1.60 |
| 3 | LPS + PNLA RA (1) | 28.4 | 2.02 | 1.38 |
| 4 | control RA (2) | 96.2 | 2.03 | 0.82 |
| 5 | LPS RA (2) | 142.4 | 2.05 | 0.92 |
| 6 | LPS + PNLA (RA) (2) | 145.7 | 2.04 | 0.93 |
| 7 | control RA (3) | 66.7 | 2.04 | 1.40 |
| 8 | LPS RA (3) | 44.3 | 2.03 | 1.51 |
| 9 | LPS + PNLA RA (3) | 28.4 | 1.98 | 1.60 |
| 10 | control RA (4) | 54.1 | 2.03 | 1.19 |
| 11 | LPS RA (4) | 51.1 | 2.04 | 1.18 |
| 12 | LPS + PNLA RA (4) | 40.5 | 2.06 | 1.13 |
| 13 | control RA (5) | 103.5 | 2.07 | 1.23 |
| 14 | LPS RA (5) | 100.9 | 2.05 | 1.38 |
| 15 | LPS+ PNLA RA (5) | 94 | 2.05 | 1.42 |
| 16 | control RA (6) | 163.4 | 2.03 | 0.95 |
| 17 | LPS RA (6) | 217.3 | 2.04 | 1.54 |
| 18 | LPS+ PNLA RA (6) | 213.4 | 2.05 | 1.52 |
| 19 | control HC (1) | 164.4 | 2.06 | 1.8 |
| 20 | LPS HC (1) | 74.3 | 2 | 1.88 |
| 21 | LPS+ PNLA HC (1) | 25.9 | 1.95 | 1.37 |
| 22 | control HC (2) | 18.4 | 1.94 | 1.52 |
| 23 | LPS HC (2) | 50.1 | 2.01 | 1.62 |
| 24 | LPS+ PNLA HC (2) | 59.2 | 2.03 | 1.47 |
| 25 | control HC (3) | 49.6 | 2.02 | 1.11 |
| 26 | LPS HC (3) | 24.9 | 2.01 | 1.27 |
| 27 | LPS+ PNLA HC (3) | 24.4 | 2.13 | 1.06 |
| 28 | control HC (4) | 32.6 | 2 | 1.79 |
| 29 | LPS HC (4) | 100.6 | 2.08 | 1.69 |
| 30 | LPS+ PNLA HC (4) | 43.4 | 2.07 | 1.2 |
| 31 | control HC (5) | 80 | 2.03 | 1.16 |
| 32 | LPS HC (5) | 36.5 | 2.02 | 1.2 |
| 33 | LPS+ PNLA HC (5) | 44.1 | 2.04 | 1.14 |
| 34 | control HC (6) | 42.6 | 2 | 0.96 |
| 35 | LPS HC (6) | 105.7 | 2.03 | 1.15 |
| 36 | LPS+ PNLA HC (6) | 115.4 | 2.03 | 1.62 |

Table 2.12. QC of RNA samples from PBMCs used for library preparations as per the TapeStation.

| Sample (numb) | Sample name | RIN | Concentration ng/ μ L |
|---------------|--------------------|-----|---------------------------|
| 1 | control RA (1) | 9.9 | 27.6 |
| 2 | LPS RA (1) | 9.7 | 20.0 |
| 3 | LPS+ PNLA RA (1) | 9.3 | 26 |
| 4 | control RA (2) | 9.3 | 22.2 |
| 5 | LPS RA (2) | 9.5 | 26.4 |
| 6 | LPS+ PNLA (RA) (2) | 9.5 | 16.5 |
| 7 | control RA (3) | 9.5 | 98.8 |
| 8 | LPS RA (3) | 9.4 | 88.0 |
| 9 | LPS+ PNLA RA (3) | 9.6 | 80.0 |
| 10 | control RA (4) | 9.9 | 81.2 |
| 11 | LPS RA (4) | 9.7 | 25.6 |
| 12 | LPS+ PNLA RA (4) | 9.5 | 19.3 |
| 13 | control RA (5) | 9.8 | 22.6 |
| 14 | LPS RA (5) | 9.8 | 22.4 |
| 15 | LPS+ PNLA RA (5) | 9.8 | 30.8 |
| 16 | control RA (6) | 8.7 | 42.0 |
| 17 | LPS RA (6) | 9.3 | 45.6 |
| 18 | LPS+ PNLA RA (6) | 9.5 | 46.8 |
| 19 | control HC (1) | 9.6 | 101.2 |
| 20 | LPS HC (1) | 9.5 | 129.6 |
| 21 | LPS+ PNLA HC (1) | 9.5 | 124.8 |
| 22 | control HC (2) | 9.3 | 56.4 |
| 23 | LPS HC (2) | 9 | 32.2 |
| 24 | LPS+ PNLA HC (2) | 8.9 | 29.2 |
| 25 | control HC (3) | 9.2 | 157.8 |
| 26 | LPS HC (3) | 9.5 | 205.2 |
| 27 | LPS+ PNLA HC (3) | 9.7 | 162.0 |
| 28 | control HC (4) | 9.6 | 47.8 |
| 29 | LPS HC (4) | 9.7 | 59.4 |
| 30 | LPS+ PNLA HC (4) | 9.6 | 52.4 |
| 31 | control HC (5) | 9.6 | 104.0 |
| 32 | LPS HC (5) | 9.6 | 13.7 |
| 33 | LPS+ PNLA HC (5) | 9.8 | 75.6 |
| 34 | control HC (6) | 9.6 | 104.0 |
| 35 | LPS HC (6) | 9.7 | 101.2 |
| 36 | LPS+ PNLA HC (6) | 9.9 | 100.4 |

36 RNA sample per 12 participants with 3 conditions each control (unstimulated), LPS (LPS stimulated), and LPS + PNLA are (LPS stimulated and PNLA treated). RIN; RNA integrity number.

The quality of total RNA isolated from purified and sorted monocytes was checked thoroughly, as discussed, using Nanodrop and Agilent 4200. For Qubit® Fluorometer, quantifications were not because the concentrations of RNA were at a minimum range. RNA assessment by Qubit

may require a large volume of each sample, depleting the volume of sample required for library construction. In this scenario, quantity is taken from the TapeStation traces. As some of the samples fell into this group, to keep consistency across the set.

Nanodrop measurement values are shown in **Table 2.13**; most of the concentrations were above 5 ng/ μ l as recommended by the manufacturer, except those shown in red, and a 260/280 ratio between 1.8 and 2.2 was considered high quality for subsequent analysis.

Table 2.13. QC of RNA samples from monocytes that were used for library construction as per the Nanodrop spectrophotometer.

| Sample (numb) | Sample name | Concentration ng/ml | 260/280 | 260/230 |
|---------------|-------------|---------------------|---------|---------|
| 1 | RA -ve.1 | 7.7 | 2.11 | 0.51 |
| 2 | RA -ve.2 | 4.3 | 2.53 | 0.53 |
| 3 | RA -ve.3 | 8.0 | 2.20 | 0.76 |
| 4 | RA -ve.4 | 6.1 | 3.29 | 0.31 |
| 5 | RA -ve.5 | 11.3 | 2.13 | 0.68 |
| 6 | RA -ve.6 | 10.2 | 2.24 | 1.18 |
| 7 | RA -ve.7 | 38.0 | 2.07 | 1.39 |
| 8 | RA -ve.8 | 9.9 | 2.13 | 0.97 |
| 9 | RA +ve.1 | 6.0 | 2.40 | 0.32 |
| 10 | RA +ve.2 | 1.4 | 3.31 | 0.51 |
| 11 | RA+ve.3 | 10.6 | 2.16 | 0.80 |
| 12 | RA +ve.4 | 2.8 | 1.96 | 0.80 |
| 13 | RA +ve.5 | 12.5 | 2.14 | 0.31 |
| 14 | RA +ve.6 | 10.11 | 2.01 | 0.99 |
| 15 | RA +ve.7 | 38 | 2.02 | 1.79 |
| 16 | RA +ve.8 | 7.1 | 1.90 | 0.54 |
| 17 | RA ttt.1 | 6.2 | 2.38 | 0.20 |
| 18 | RA ttt.2 | 3.6 | 2.28 | 0.43 |
| 19 | RA ttt.3 | 12.0 | 2.20 | 0.32 |
| 20 | RA ttt.4 | 1.9 | 2.06 | 0.16 |
| 21 | RA ttt.5 | 16.1 | 2.07 | 1.09 |
| 22 | RA ttt.6 | 6.5 | 2.19 | 0.71 |
| 23 | RA ttt.7 | 33.9 | 2.09 | 0.90 |
| 24 | RA ttt.8 | 6.3 | 2.07 | 0.32 |

24 RNA samples per 8 participants, with 3 conditions each: -ve control (unstimulated untreated), +ve control (LPS stimulated), and treated (ttt) (LPS stimulated and PNLA treated). RIN is the RNA integrity number.

RNA RIN and concentrations as per the RNA ScreenTape assay that were used for future library constructions are illustrated in **Table 2.14** using Agilent 4200 TapeStation. The red-marked RIN samples underwent an amended fragmentation procedure.

Table 2.14. QC of RNA samples from monocytes that were used for library construction as per the TapeStation.

| Sample (numb) | Sample name | RIN | Concentration ng/ μ L |
|---------------|-------------|-----|---------------------------|
| 1 | RA -ve.1 | 7.9 | 13.5 |
| 2 | RA -ve.2 | 7.4 | 10.9 |
| 3 | RA -ve.3 | 8.5 | 14.3 |
| 4 | RA -ve.4 | 9 | 6.1 |
| 5 | RA -ve.5 | 8.6 | 1.6 |
| 6 | RA -ve.6 | 8.8 | 17.2 |
| 7 | RA -ve.7 | 9.5 | 35.4 |
| 8 | RA -ve.8 | 7.4 | 14.9 |
| 9 | RA. +ve.1 | 7.3 | 10.4 |
| 10 | RA. +ve.2 | 5.2 | 0.7 |
| 11 | RA. +ve.3 | 8.8 | 19.1 |
| 12 | RA. +ve.4 | 7.2 | 4.1 |
| 13 | RA. +ve.5 | 9 | 16 |
| 14 | RA. +ve.6 | 9.2 | 18.3 |
| 15 | RA. +ve.7 | 9.4 | 33.3 |
| 16 | RA. +ve.8 | 7 | 11.5 |
| 17 | RA. ttt.1 | 6.3 | 2.9 |
| 18 | RA. ttt.2 | 5.3 | 10.8 |
| 19 | RA. ttt.3 | 9.1 | 14.6 |
| 20 | RA. ttt.4 | 5.4 | 1.06 |
| 21 | RA. ttt.5 | 9.2 | 14.6 |
| 22 | RA. ttt.6 | 8.3 | 12.9 |
| 23 | RA. ttt.7 | 9.5 | 27.5 |
| 24 | RA. ttt.8 | 6.8 | 2.7 |

2.10.2. Library preparation, including ribosomal RNA depletion, using the NEBNext Ultra II RNA Library Prep Kit for Illumina

The NEBNext[®] Ultra II Directional RNA Library Prep Kit for Illumina[®], in conjunction with the NEBNext[®] rRNA Depletion Kit (human, mouse, or rat), is designed to generate cDNA libraries from total RNA suitable for next generation sequencing on Illumina[®] sequencing platforms as in the Appendix (**Figure 3**). Steps of library construction were performed as outlined in **Figure 2.15** and detailed in the Appendix using the polyadenylated (A) capture method to purify mRNA, followed by a Total RNA Library Prep Kit. The kit generates libraries with a high degree of directionality and strand specificity. The kit also provides even coverage across transcripts; retains library complexity when using low RNA input and boasts equivalent transcript concordance across technical replicates in combination with the cBot-2- library. The cBot-2 clusters the libraries onto the flow cell, ready for sequencing, and concentration normalisation was conducted manually to pool libraries.

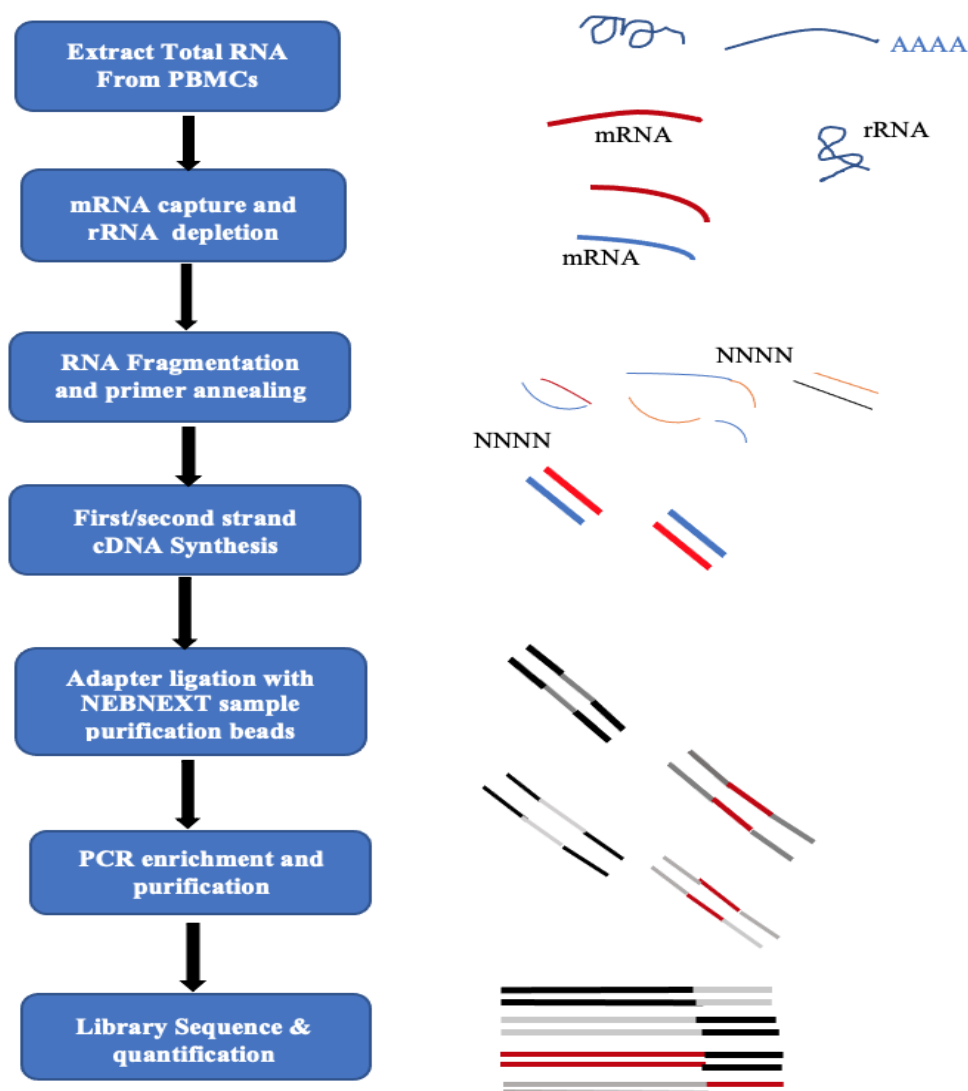


Figure 2.15. Summary of the workflow of RNA-seq library preparation.

Total RNA is extracted from PBMCs. A poly(A) capture method isolates mRNA from rRNA. RNA is fragmented into suitable sizes before the reverse transcription reaction is used to form cDNA. Unique adapters are then added, which serve as barcodes to enable multiplexing of samples as well as primers for amplification on the flow cell. Finally, cDNA libraries are amplified before being quantified and sequenced. cDNA; complementary DNA, NN; random primer, DNA — ; RNA —

Whilst both rRNA depletion kits left peaks that correlated with 18S and 28S peaks in the resulting total RNA (**Figure 2.16(A)**), the poly(A) capture kit was efficient in removing these peaks with significantly reduced (4%) contaminating rRNA (**Figure 2.16(B)**). The QC was obtained from 36 RNA samples, and samples with a RIN > 8 were selected for library preparation as shown in the representative (**Figure 2.16(C)**).

Regarding RNA isolation from purified monocytes, 5 ng of total RNA was depleted of ribosomal RNA using the NEB Next Ultra II RNA Library Prep Kit for Illumina (Human/Mouse/Rat New England BioLabs, NEB) as discussed in the Appendix. Amended

fragmentation procedure was performed to account for partially degraded samples (15 min at 94°C) with RIN values 5-7 (highlighted in red) as shown in **Table 2.14**. Partially degraded RNA samples with RIN values between 2-6 underwent reduced fragmentation time (8 min at 94°C). The steps included RNA fragmentation and priming, 1st strand cDNA synthesis, 2nd strand cDNA synthesis, adenylation of 3'ends, adapter ligation (adapter diluted 1:199), and PCR amplification (16-cycles). The manufacturer's instructions were followed using AMPure XP beads (Beckman Coulter®). The libraries were validated using the Agilent 4200 TapeStation and hs DNA ScreenTapes (Agilent Technologies, Inc) to ascertain the insert size as described in the Appendix. Qubit® (Life Technologies) was used to quantify and assess the concentrations according to the manufacturer's instructions. The validated libraries were then normalised manually to 4 nM with 10 mM Tris-Cl and 0.1% Tween, pooled together, and clustered on the flow cell using XP workflow, following the manufacturer's instructions. Before the final sequencing was performed, a test sequencing run of the complete library was done on the MiSeq Nano Reagent Kit v3 (150-cycles) according to the manufacturer's instructions to ensure a successful sequencing on the XP flow cell later.

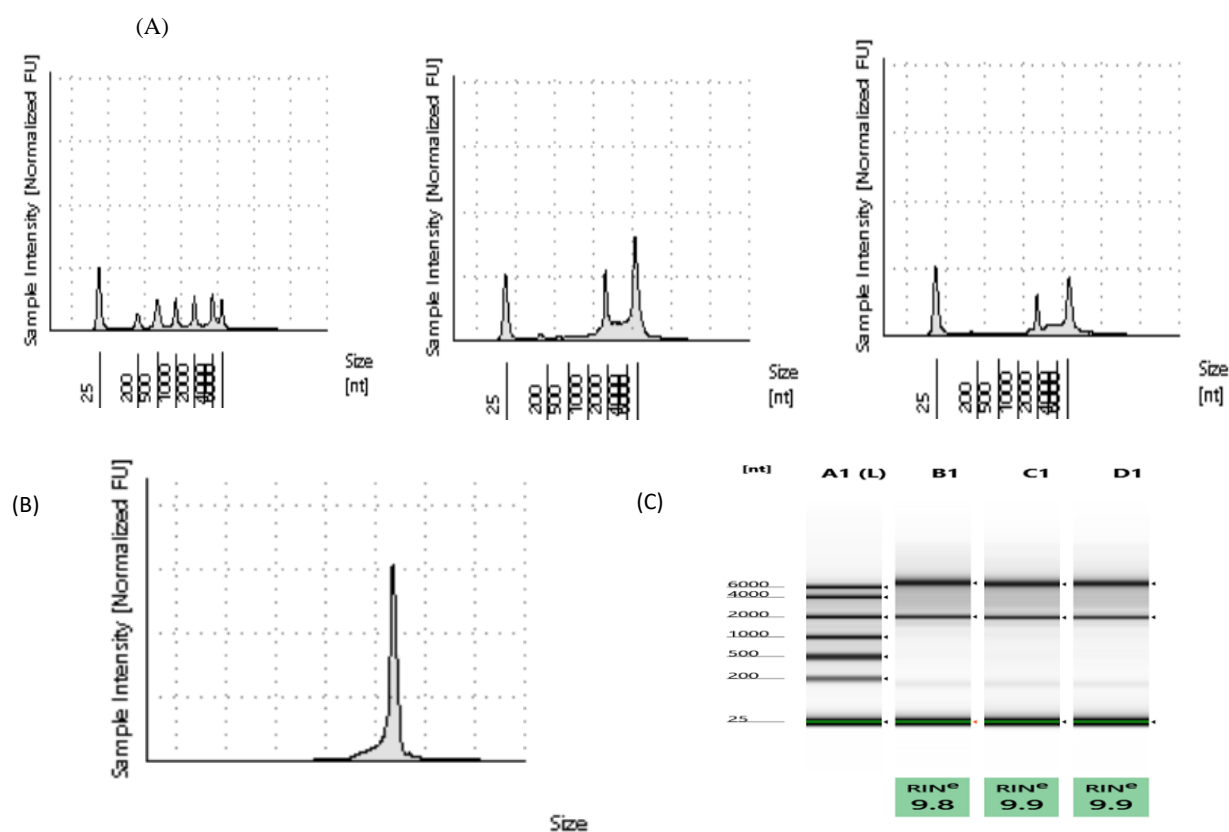


Figure 2.16. Electropherogram of Agilent TapeStation.

(A) RNA ScreenTape of high-quality RNA samples (B) A high sensitivity RNA sample of depleted rRNA, and (C) representative examples of RIN values for the RNA used in the library construction. A1 (L), ladder, B1, C1, and D1 are the experimental samples. (These images were kindly supplied by WGP from the data QC.)

2.10.3 Library and QC check

The resulting libraries were visualised on Agilent TapeStation and had an optimal peak size of 300 bp. **Figure 2.17** shows the average peak sizes of complete libraries for each peak e.g., 305 bp. Each completed library consists of the original ~200 bp fragmented RNA insert, adapters for binding the library to the sequencing flow cell, and the unique i7 and i5 barcode/index pair. Approximately 100 additional bases were added to the 200 bp fragmented RNA. After efficient removal of rRNA, approximately 80-90% of reads map to protein-coding genes and less than 5% are mapped to rRNA. The decrease in rRNA content was further highlighted by a reduction in the duplication of reads. Reads were mapped to the reference genome as outlined in **Figure 2.18**. A high percentage (98%) of reads were mapped to the reference genome, indicating the high quality of the input RNA. Samples 10 and 20 in **Table 2.14** have additional peaks at ~145 bp. This represents adapter-dimers, which are normally removed or cleaned up before sequencing, by using an AMPure bead purification procedure (see Appendix).

The library successfully passed the QC based on the data obtained from Tapestations and Qubit. Quality controls performed during the analysis pipeline also showed a high quality of sequencing with a high accuracy of base calling. For high-complexity random libraries, an equal proportion of each base is expected.

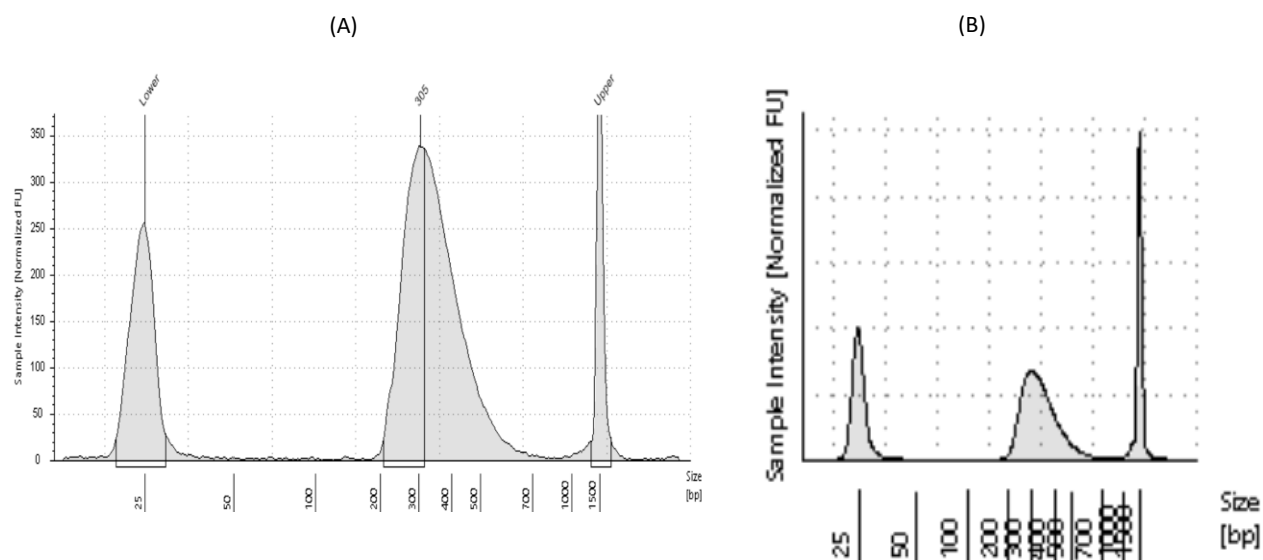


Figure 2.17. Electropherogram of the QC of the generated pool library.

(A) A representative sample of High sensitivity (hs) D1000 ScreenTape showing the peak fragmentation size of 305 bp which is made just before sequencing (B) Thumbnail image showing summary or confirmation to the library product (The images were kindly supplied by WGP from the data QC).

2.10.4. Sequencing

For the sequencing of the completed libraries of total RNA from PBMCs and purified monocytes on HiSeq 4000 and 6000 flow cells, respectively, see the Appendix.

2.10.5. RNA-seq data processing and read mapping strategy

A workflow for the mapping strategy of RNA-seq data is outlined in **Figure 2.18**. Firstly, raw sequencing files (fastq files) were trimmed to take out adapter sequences and low-quality reads, since these would affect mapping to the genome. A quality control was then performed using the fastQC software (Babraham Institute) to ascertain the quality of the sequencing. Paired-end reads from Illumina sequencing were trimmed with Trim Galore (https://.bioinformatics.babraham.ac.uk/projects/trim_galore/) and assessed for quality using FastQC (<https://.bioinformatics.babraham.ac.uk/projects/fastqc/>), using default parameters. The sequencing files were then mapped to the human GRCh38 reference genome using STAR software (Alexander *et al.* 2013). STAR is a splice-aware software, so it can map over splice junctions. Duplicate reads were identified and marked using MarkDuplicates in Picard (Broad Institute), and further analysis was carried out to determine the quality of the libraries (e.g., number of reads, percentage duplication). Count reads per gene was confirmed using the featureCounts software (Liao *et al.* 2014) with the GRCh38.96 Ensembl gene build gene transfer form (GTF). Both the reference genome and GTF were downloaded from the Ensembl FTP site (<http://.ensembl.org/info/data/ftp/index.html/>).

An advantage of RNA-seq over hybridisation techniques is that the depth of sequencing can be varied. As samples are sequenced to a greater depth, more transcripts are identified, and quantification becomes more precise (Conesa *et al.* 2016). To identify genes that have low expression levels as well as highly expressed genes, samples were sequenced to a high depth (>40 million paired end reads). However, increasing the depth of sequencing can also result in increased background and duplication levels (Tarazona *et al.* 2011). The question remains whether removing duplicates results in improved accuracy by reducing background noise from PCR duplicates or whether it reduces accuracy by removing biologically relevant replicates. This was highlighted in the next section (2.10.6).

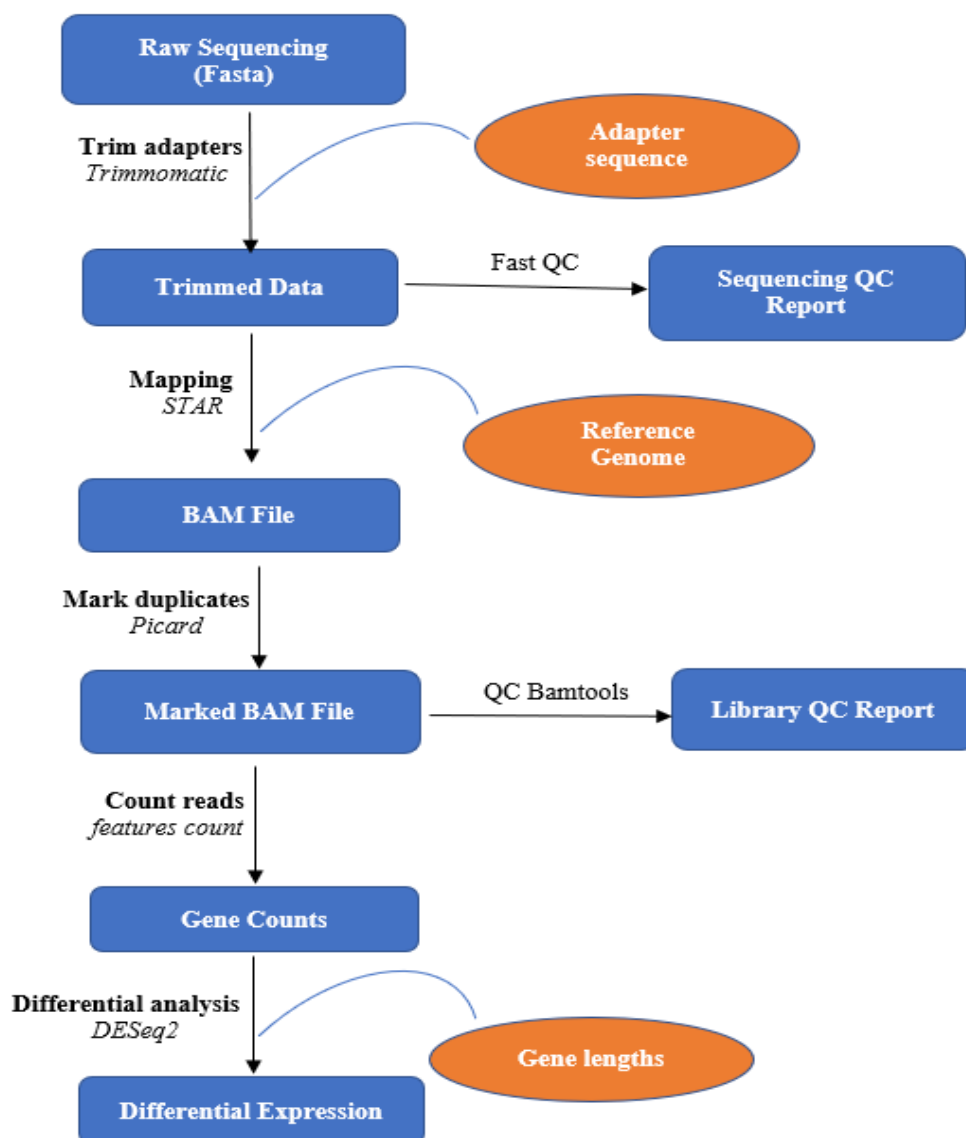


Figure 2.18. Workflow of RNA-seq data mapping.

The process begins with raw sequencing files from Illumina sequencing. The resulting file format from each process is shown in a blue box. Reference files used to trim, map, and assign gene lengths are shown as orange circles. The processes carried out are shown at each stage in bold, and the software used is shown underneath in italics. BAM (binary and alignment map).

2.10.6. Evaluation of duplicated reads (ensuring gene expression is not affected by duplication)

The convention in RNA-seq is to include duplicate reads in the analysis as it does not typically skew data (Parekh *et al.* 2016). Consistent with this, dupRadar analysis within the Bioconductor package confirmed that duplicated reads within the data set did not bias differential gene expression. Here, the number of duplicates per gene showed no correlation with the fold change of the gene (**Figure 2.19**). Duplicated reads were consequently included in the bioinformatic analysis.

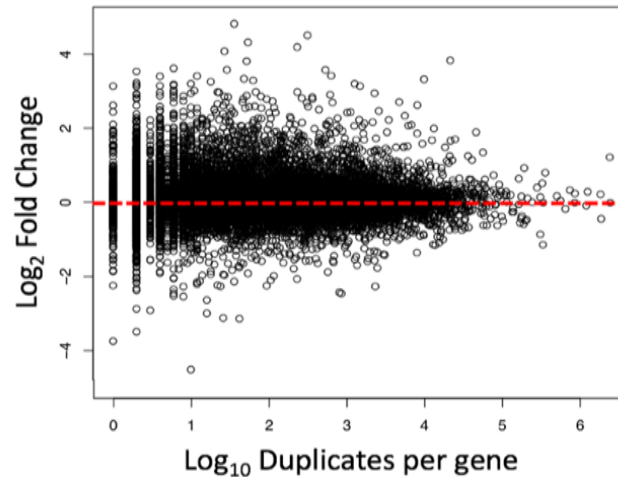


Figure 2.19. Gene duplication does not affect gene expression.

Representative plot showing how duplication of a gene effects the fold change of the gene. Plots were generated using the dupRadar analysis, within the Bioconductor package. The red dotted line indicates a log₂ fold change of 0.

2.10.7. Normalisation and estimation of differential gene expression (DGE) analysis

To identify DEGs between two samples, a differential expression analysis was performed using the DESeq2 package (Bioconductor) (Love *et al.* 2014). Firstly, normalised read counts were calculated, which account for the different sequencing depths of individual samples. The fragments per kilobase of transcript per million mapped reads (FPKM) were then calculated from the normalised counts, which consider the length of the gene. Since the analysis was focused on identifying changes in the same gene in different conditions, the normalised counts were used to calculate fold expression changes and perform statistical analysis. Genes were discarded from the analysis when differential expression failed to be significant ($p > 0.05$) after Benjamini-Hochberg correction for multiple testing.

2.10.8. Bioinformatic analysis

Basic bioinformatic analysis was kindly performed by Dr. Robert Andrews (blue boxes); the principal steps are summarised in the schematic flow chart (**Figure 2.20**). Rabaa Takala conducted the analysis (green boxes), as discussed in section (2.10.9), in addition to microRNA (miRNA) target prediction, which will be discussed in Chapter 7.

2.10.9. Identification of differentially expressed (DEG) genes and further downstream and upstream pathway analysis.

Following the sorting of the DEGs in Excel, a variety of analyses were conducted to identify the clustering, biological processes, and specific pathways of interest.

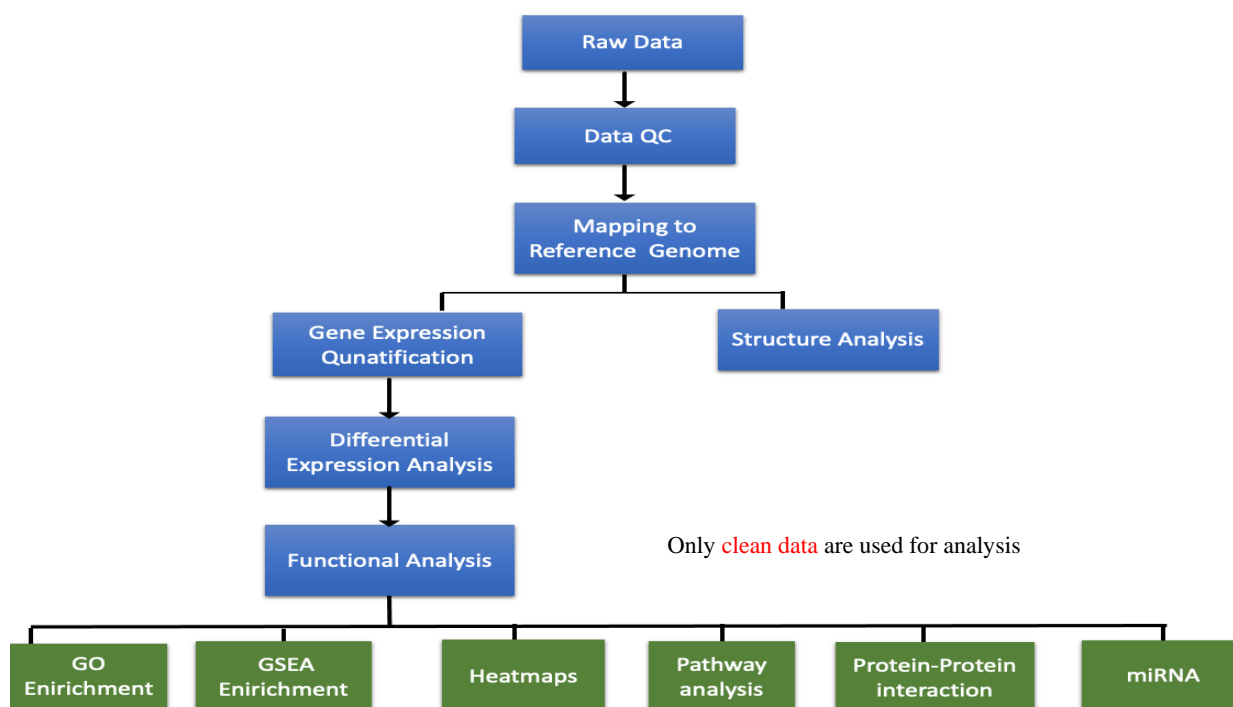


Figure 2.20. Schematic outlines of bioinformatics workflow. Blue boxes: analyses were conducted by Dr. Robert Andrews. Green boxes: analyses were conducted by Rabala Takala.

2.10.9.1. Heatmap

Heatmaps were generated using the Morpheus software available from the Broad Institute (<https://software.broadinstitute.org/morpheus/>). The heatmap visualisations used log₂ fold change (log₂FC) compared to controls from HC or RA at an equivalent time point, as indicated in the text and figure legend. Data sets were hierarchically clustered using the one minus-Pearson correlation coefficient.

2.10.9.2. Gene set enrichment analysis

Gene Set Enrichment Analysis (GSEA) was performed using software from the Broad Institute (<http://www.broad.mit.edu/gsea>). Data sets were pre-ranked using log₂FC before GSEA. The annotation of cellular components (CCs), biological processes (BPs), and molecular functions (MFs) of DEGs were determined using Gene Ontology (GO) enrichment analysis.

2.10.9.3. Pathway analysis

2.10.9.3.1. Database for Annotation, Visualisation, and Integrated Discovery.

Once a list of the most DEGs was generated, the next step was to assess the biological significance of each gene and examine how the genes might interact through an active or passive role in the pathogenesis and the treatment response in RA. Transcripts with an adjusted or false discovery rate (FDR), a p-value ≤ 0.05 and a fold-change (FC) ≥ 1.2 were considered

significantly differentially expressed and submitted as a list for functional annotation on the Amigo gene ontology. It can utilise a list of variable gene IDs and official gene symbols and integrate a variety of analytic tools to perform gene-annotation enrichment analysis, functional annotation clustering, BioCarta and Kyoto Encyclopaedia of Genes and Genomes (KEGG) pathway map visualisation, and disease enrichment analysis.

2.10.9.3.2. Ingenuity Pathway Analysis

Ingenuity Pathway Analysis; IPA (QIAGEN Inc., <https://www.qiagenbioinformatics.com/products/ingenuity-pathway-analysis>) (IPA; Qiagen; version: 33559992) was used to identify differentially regulated genes, permitting more in-depth analysis of canonical pathway analysis and identification of overlapping pathways and global themes within the entire list of differentially expressed transcripts. The software allows for the input of p-values, FDR values, and FC values for a more accurate method of establishing the relevance of characterised pathways, including those involved in disease. In addition, IPA was used to identify key regulators and highlight mechanistic networks of action and downstream effects associated with the up-or down-regulation of key transcripts within the transcriptome data. The software contains a built-in path designer to generate visuals of networks and pathways enriched in the DEGs list. Genes from the identified list that were associated with a canonical pathway in Ingenuity's knowledge base were considered but not taken into detail in the analysis. Fisher's exact test was used to calculate a p-value determining the probability that the association between the genes in the dataset and the canonical pathway is explained by chance alone. Transcripts associated with RA, anti-rheumatic or hyperlipidaemic treatment, and associated immune or inflammatory pathways were highlighted as potential biomarker targets.

2.10.10. Statistical analysis of RNA sequencing read pairs and percentage of a total number of reads and QC check.

For RNA-seq, extracting high-quality RNA is paramount as it influences the ability to map reads to the genome; low-quality RNA leads to poor mapping (Romero 2014). Therefore, RIN values ranging from 7-10 are required, as demonstrated in **Tables 2.12-2.14**. The average total number of read pairs obtained for this project is 44×10^6 . Mapped read pairs are 42×10^6 , while the percentage of total mapped read pairs is 97%. Duplicate read pairs are 22×10^6 , while the percentage of total duplicate read pairs was 51%.

A high proportion of reads mapped to rRNA genes may suggest ineffective removal of rRNA during depletion steps. Consequently, this resulted in a high number of duplicate reads as there were highly abundant and repetitive sequences.

2.11. Statistical analysis

The normality of the data was tested using the Shapiro-Wilk test, histograms, and Q-Q plots conducted using SPSS (version 23). The data were analysed by GraphPad Prism version 5 and 8.0 software, and all values are presented as mean \pm standard error mean (SEM). To compare the means of the two groups, either a t-test (normal data distribution) or a Mann-Whitney test (non-normal distribution) was used. To compare the means of multiple groups, a one-way analysis of variance (ANOVA) was used with a variety of post-hoc tests that were determined by the variation within the data. If there was equal variation between the different test groups, either a Tukey's or Dunnett post-hoc analysis was performed, whereas Dunnett T3 post-hoc tests were used in cases of unequal variation. A p-value ≤ 0.05 has been used as a cut-off value to assign statistical significance. At least 3 independent experiments were carried out in triplicate wells for each assay before conducting the statistical analysis.

FCS data files were analysed using FlowJo v.10 and NoVo Express software. Flow cytometry data analysis was performed in Excel as % gated CD14⁺ positive-expressing cells. Graphs and statistical analysis were performed using GraphPad Prism V8. Spearman correlation was used to analyse the linear association using SPSS version 26. A line of linear regression was added to the graphs to best predict the relationship between variables, and 2 tailed non-parametric t tests were applied to find the comparison between the 2 groups. Scatter diagrams using the mean as well as column graphs were used to illustrate the results.

Chapter 3: Effects of PNLA on key inflammatory processes using human THP-1 cell lines and primary cultures of human monocyte-derived macrophages

3.1. Introduction and aims

Due to the critical role that monocytes and macrophages play during the initiation and progression of chronic inflammatory diseases such as RA and atherosclerosis (Kennedy *et al.* 2011; Moore and Tabas 2011), targeting monocytes and macrophages may represent a promising therapeutic strategy. The health benefits of PUFAs in the prevention and treatment of RA and atherosclerosis have long been known (Calder 2006; Calder and Zurier 2001). PNLA is an interesting plant-based FA, and it is rapidly emerging as a potential anti-inflammatory and lipid-lowering agent (Asset *et al.* 200; Chen *et al.* 2019; Chung *et al.* 2019) in obesity and diabetes (Christiansen *et al.* 2015). The effect of PNLA on key cellular processes in monocytes and macrophages that are associated with atherosclerosis and RA is not known, which formed the focus of the studies presented in this Chapter.

The overall aim of the experiments presented in this Chapter was to investigate the effects of PNLA treatment on a range of key processes in atherosclerosis/synovitis development. These studies used the human THP-1 cell line and primary human monocyte-derived macrophage (HMDM) cultures, thereby providing an initial assessment of the potential anti-inflammatory effects of this n-6 PUFA. Initial experimental investigations were carried out *in vitro* following the incubation of THP-1 monocytes, macrophages, or HMDM with different PNLA concentrations (25-100 μ M) or vehicle control. The time point that was chosen for PNLA incubation in this study, which is 24 hours, was based on literature analysis and previous laboratory studies on a range of nutraceuticals, including PUFAs and PNLA (Baker *et al.* 2020; Chaung *et al.* 2019; Gallagher *et al.* 2019). Primarily, the PNLA effect was investigated on monocyte migration, ROS production, lipoprotein uptake via macropinocytosis, receptor-mediated lipid uptake of ox-LDL, and phagocytosis. The viability and proliferation of both cell types were first assessed. Details of each experimental aim and the objectives are outlined in the next section.

3.1.1 Assessment of PNLA effects on specific monocyte and macrophage functions using THP-1 and HMDMs

To rule out the possibility that the results observed in THP-1 macrophages were due to the cell line used, key assays were further validated in primary cultures of HMDMs.

3.1.1.1 Viability and proliferation assays

As PNLA is a relatively recently identified nutraceutical (Xie *et al.* 2016), it is important to determine whether it exerts any adverse effects at the cellular level. Cell viability and proliferation were determined using two independent assays, as described in Chapter 2.

3.1.1.2 Monocyte recruitment and migration

After determining that PNLA did not exert any adverse effects on cell viability and integrity, its effect on monocyte migration as an initial and important step in inflammation formation was investigated. Once monocytes migrate into tissues (synovial joint or arterial intima), they adhere to the matrix through surface receptors, and their survival and proliferation are stimulated by the cytokine milieu, where they then differentiate into inflammatory macrophages under the control of M-CSF (Bobryshev 2006; Kurowska-Stolarska and Alivernini 2017). The flow of monocytes from the BM into the bloodstream requires the interaction of CCR2/CCL2 on monocytes, which also helps in recruiting them to the site of the lesion. CCL2 is a potent chemotactic inflammatory chemokine. It is a small heparin-binding protein 13 kDa whose main function is to regulate the trafficking of circulating monocytes (Deshmane *et al.* 2009). CCL2 is expressed by the various cells involved in inflammatory synovitis and atherosclerosis, including the inflamed synovium and activated endothelium (Deshmane *et al.* 2009).

The importance of CCL2 has been demonstrated in atherosclerotic mouse models where smaller atherosclerotic lesions are formed in animals that are either deficient in this chemokine or its receptor (Öhman *et al.* 2010). Also, increased expression of CCL2 by leukocytes significantly increases the size of atherosclerotic lesions in Apo-E knockout mice (Aiello *et al.* 1999). Furthermore, previous findings indicated that CCL2 inhibition is a potentially promising therapeutic target and robust marker of atherosclerosis (Yadav *et al.* 2010) and synovitis (Taylor *et al.* 2000). Accordingly, decreasing monocyte recruitment using PNLA would represent a potential preventative therapy.

3.1.1.3 Oxidised LDL (ox-LDL) uptake, oxidative stress, and reactive oxygen species (ROS) production

The purpose of using this assay was to determine the role of PNLA on cholesterol ester accumulation. After the migration of monocytes from the artery lumen into the wall of the artery and their differentiation into macrophages at the site of ox-LDL accumulation, they uptake this lipid to form lipid-laden cells.

Increased levels of ROS are associated with an increase in ox-LDL levels (Buckley and Ramji 2015; Lusis 2000; McLaren *et al.* 2011a). ROS induces signals that can activate ECs, through which monocytes can migrate into the arterial intima. In RA, repetitive cycles of hypoxia and reoxygenation, together with oxidants produced by phagocytic cells, promote chronic oxidative stress within the microenvironment of the affected joint, leading to the generation of ROS with the potential to contribute to joint damage (Taylor and Sivakumar 2005). By normalising ROS in lipoproteins and cellular membranes, PNLA may exert antioxidant effects that can lead to less oxidation of LDL particles, while non-oxidised LDL particles are more efficiently cleared by the LDL receptor and thus less atherogenic (Mason 2019).

3.1.1.4 Macropinocytosis

Previous work indicated that inhibiting macropinocytosis in macrophages decreases foam cell formation and hence inflammation (Yao *et al.* 2009), making it a potential target in atherosclerosis. Measuring LY uptake using FACS can inform us of the potential benefits of PNLA in terms of macropinocytosis.

3.1.1.5 Phagocytosis

Phagocytosis is an important physiological activity of specialised immune cells, often phagocytes. The phagocytic cells of the immune system include macrophages, neutrophils, and DCs. All three types of cells have phagocytic functions. Phagocytosis is the first and immediate line of defence against foreign pathogens. Resolution of inflammation and return to homeostasis involve phagocytosis of apoptotic cells to prevent the persistence of necrosis and leakage of cellular contents, which may itself initiate an inflammatory reaction (Kennedy *et al.* 2011). Some phagocytes, including M1 macrophages, also participate in adaptive immunity, playing a role in the early and advanced stages of the disease. Among their diverse functions, macrophages engulf bacteria and kill them by producing a variety of microbicidal agents that include ROS, NO, and hydrolytic enzymes (Ramji and Davies 2015; Moore *et al.* 2013). By quantifying the engulfment of one of these substrates by macrophages, we may investigate the phagocytic or bactericidal capability and, accordingly, evaluate the effect of PNLA on these phagocytic activities (i.e., to determine if PNLA has effects on this functional process of macrophages).

In inflammatory synovitis, despite the lack of apoptosis occurring in all cell types at early time points after arthritis induction, resident SM retains the capacity to phagocytose apoptotic cells (Kennedy *et al.* 2011). If natural phagocytosis could be maintained in the inflamed synovium, possibly by the effect of PNLA or its stable metabolites, this may lead to homeostasis, the resolution of inflammation, and the maintenance of healthy tissues.

3.2. Results

3.2.1. THP-1 cell line

3.2.1.1 The viability and proliferation of THP-1 macrophages were unaffected by PNLA *in vitro*.

Measuring LDH release from THP-1 macrophages into the overlying media in comparison to a positive and negative control (total lysis and vehicle, respectively), was used as an indication of cellular damage and cell death. As shown in **Figure 3.1A**, no effect on LDH release was observed following incubation of the cells with PNLA when compared to the negative control (i.e., vehicle-treated cells) from three independent experiments.

In addition to the LDH release assay, **Figure 3.1B** shows the results when the CV staining was utilised and PNLA was found not to have any effect on cell numbers, i.e., proliferation. Cells that have detached from the plastic surface of the tissue culture plates are assumed to be non-viable, remain in the supernatant, and are washed away before the addition of CV and subsequent quantification.

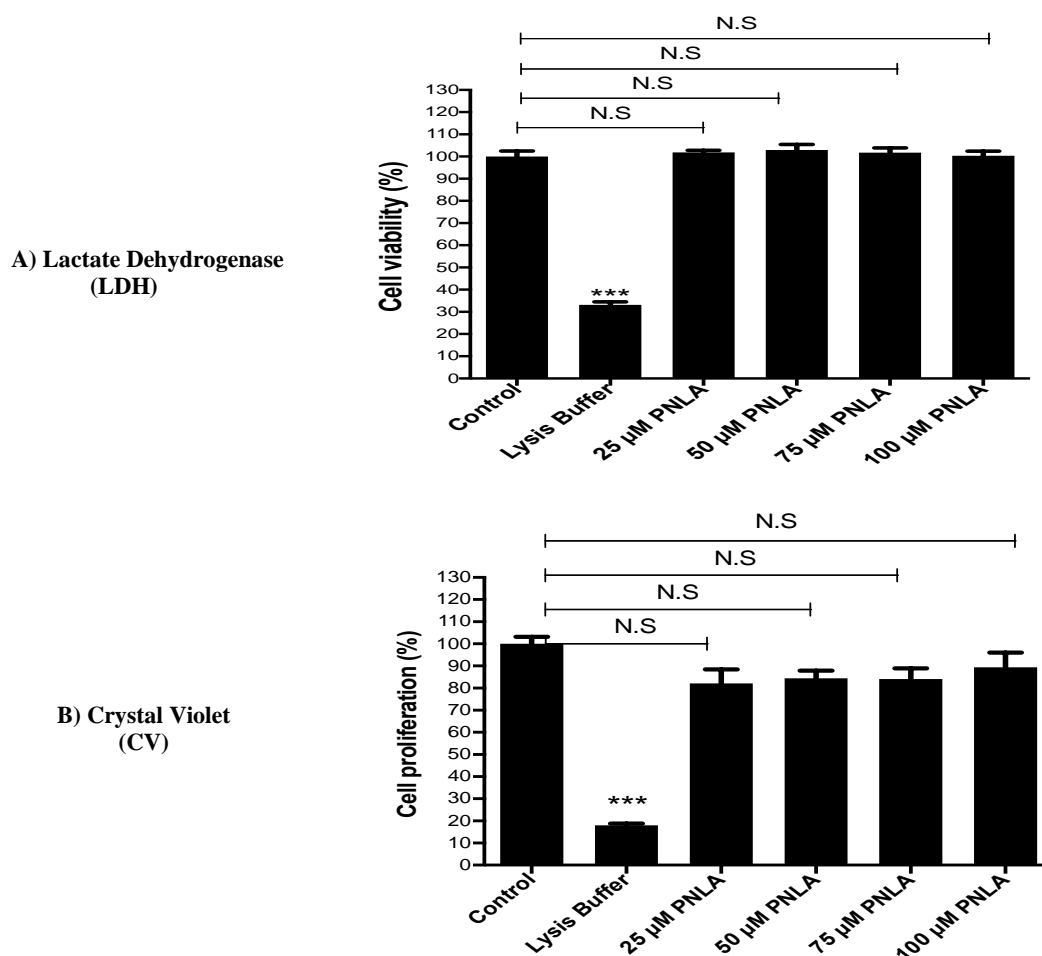


Figure 3.1. No adverse effects of PNLA in comparison to the vehicle on the viability and proliferation of THP-1 macrophages. THP-1 macrophages were incubated with 25, 50, 75, or 100 µM PNLA as indicated, or the DMSO vehicle control, for 24 hours. LDH (A) and CV (B) assays were

carried out as described in Materials and Methods. Both histograms display the percentage of cell viability from absorbance values (mean \pm SEM) in comparison to the control (arbitrarily assigned as 100) from three independent experiments. Statistical analysis was performed using one-way ANOVA and Tukey's post hoc test, comparing each treatment to the control. (N.S – not significant).

3.2.1.2 The CCL2-driven migration of THP-1 monocytes was inhibited by PNLA.

The CCL2-driven monocyte migration observed in vehicle-treated cells was significantly decreased ($P < 0.001$) by 60%, 55%, 55%, and 60%, respectively, with 25, 50, 75, and 100 μ M PNLA from three independent experiments (**Figure 3.2**).

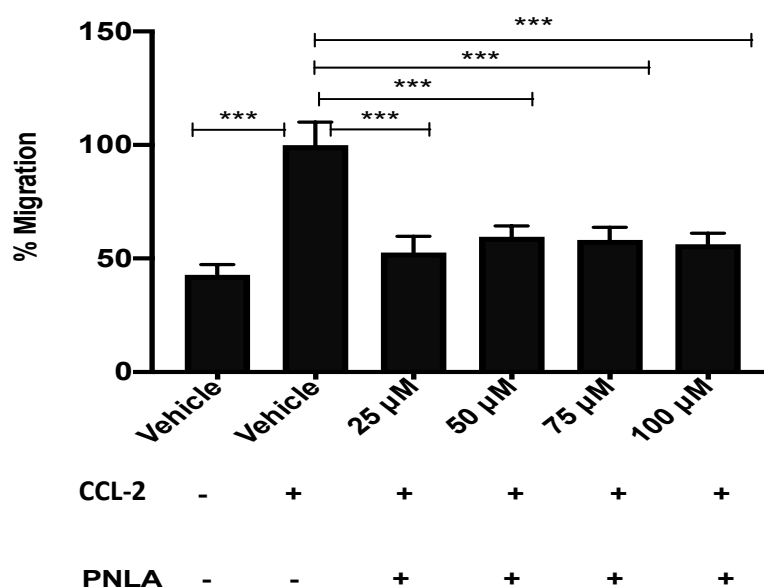


Figure 3. 2. PNLA inhibits CCL2 induced migration of THP-1 monocytes. Migration of THP-1 monocytes in response to CCL2 stimulation (20 ng/ml) was assessed in the presence of indicated concentrations of PNLA or DMSO. Migration in the presence of CCL2 and vehicle has been arbitrarily assigned as 100, with the others represented to this. The data shown are the mean \pm SEM from three independent experiments. Statistical analysis was performed using a one-way ANOVA followed by Tukey's post hoc analysis. (***, $P \leq 0.001$).

3.2.1.3 PNLA attenuates macropinocytosis in THP-1 macrophages.

LY uptake from vehicle-treated cells was arbitrarily assigned as 100%. On treatment with PNLA, LY uptake by THP-1 macrophages was significantly attenuated ($P = 0.0006$, 0.0002) with 25 and 100 μ M PNLA by 55% in both cases and ($P = 0.009$ and 0.0012) at 50 and 75 μ M PNLA by 45% and 50%, respectively (**Figure 3.3**).

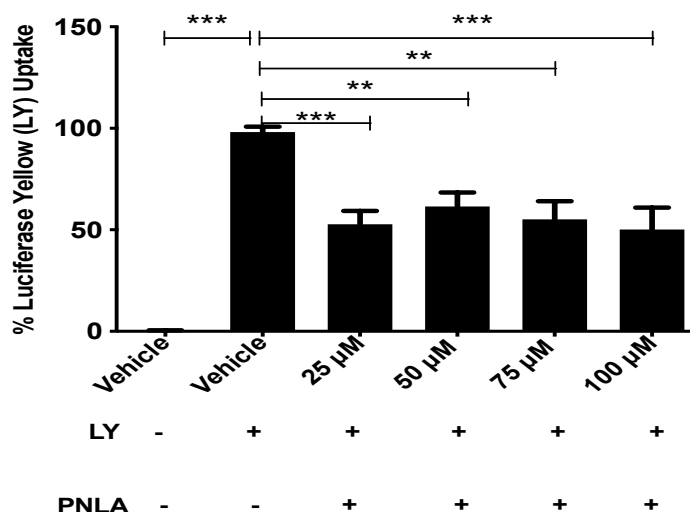


Figure 3.3. LY uptake is attenuated following incubation of THP-1 macrophages with PNLA. THP-1 macrophages were incubated with different concentrations of PNLA for 24 hours, followed by 100 µg/ml LY for another 24 hours in RPMI medium supplemented with 0.2% fatty acid-free BSA. The overlying media was removed, and the cells detached, from the plastic by treatment with 0.05% trypsin. Cells were collected and subjected to centrifugation at 9,000 x g for 5 min. The supernatant was discarded, and the pellet was resuspended in 2% PFA. LY incorporation was analysed as in the Materials and Methods section. 10,000 events were counted for each sample. Data are presented as the mean \pm SEM from four independent experiments, with the value in vehicle treated cells arbitrarily assigned as 100%. Statistical analysis was performed using a one-way ANOVA followed by Tukey's post hoc analysis. (**, $P \leq 0.01$; ***, $P \leq 0.001$).

3.2.1.4 PNLA reduces Dil-oxLDL uptake by THP-1 macrophages.

The effect of PNLA treatment on cholesterol uptake was assessed. Human PMA differentiated THP-1 macrophages were treated with Dil-oxLDL in the presence of vehicle control or PNLA (25 µM) for 24 hours. Following Dil-labelled-oxLDL only treatment, the THP-1 macrophages were able to increase their uptake by 95%, and PNLA significantly reduced this uptake by almost 55% ($P=0.003$) (Figure 3.4).

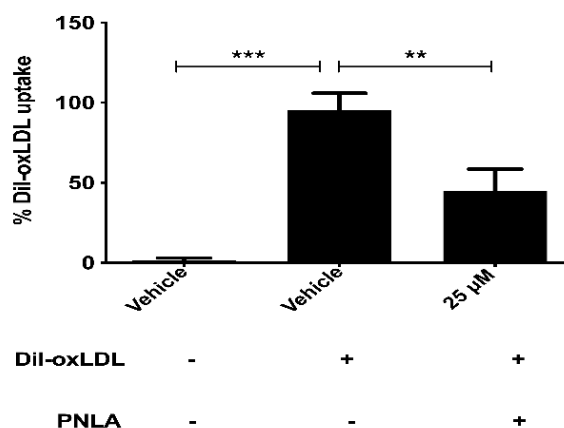


Figure 3.4. PNLA reduces the uptake of ox-LDL by THP-1 macrophages. THP-1 macrophages were incubated with Dil-oxLDL for 24 hours in the presence of vehicle or 25 µM PNLA. The vehicle control was arbitrarily assigned as 100%, and the remaining data was normalised to this. The data are presented as the mean \pm SEM from three independent experiments. Statistical analysis was performed using a one-way ANOVA with a Games-Howell pos-thoc analysis (***, $P \leq 0.001$; **, $P \leq 0.01$).

3.2.1.5 PNLA does not affect the phagocytic activity of THP-1 macrophages.

As shown in **Figure 3.5**, PNLA had no significant effect on phagocytosis compared to vehicle-treated cells from four independent experiments.

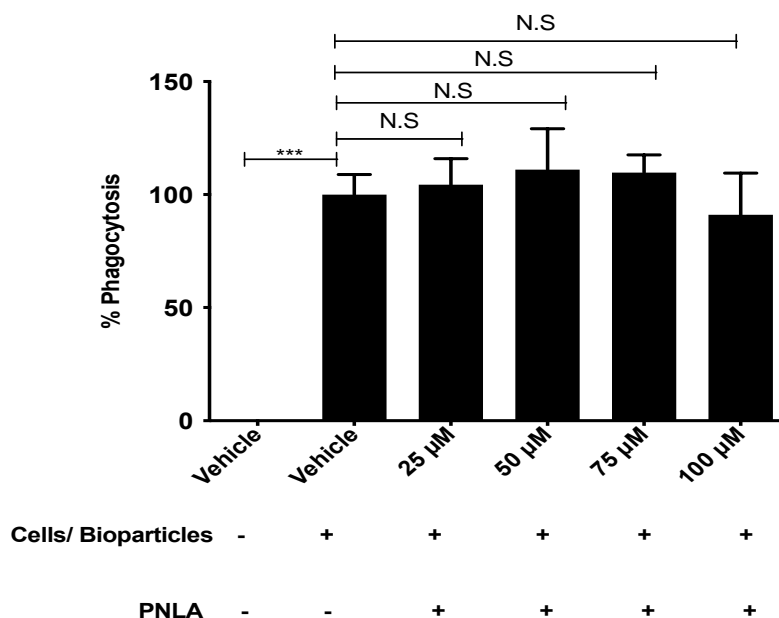


Figure 3.5. The phagocytosis in THP-1 macrophages is not affected by PNLA. THP-1 macrophages were treated with a vehicle or the indicated concentrations of PNLA for 24 hours and phagocytosis was performed as described in Materials and Methods. Data are presented as the mean \pm SEM from three independent experiments, with the value in vehicle-treated cells arbitrarily assigned as 100%. Statistical analysis was performed using one-way ANOVA followed by Tukey's post hoc analysis. (N.S, not significant; ***, $P \leq 0.001$).

3.2.1.6 PNLA does not affect ROS production in THP-1 monocytes and macrophages.

The effect of PNLA on ROS production from THP-1 monocytes and macrophages was measured to determine if the FA possessed any antioxidant capacity. Monocytes and macrophages produce and release ROS in response to stimulation with pro-inflammatory agents and oxidants such as hydrogen peroxide (Forman and Torres 2001). TBHP was used to induce ROS production. PNLA was co-incubated with monocytes and TBHP, whereas macrophages were pre-incubated with PNLA for 24 hours before the addition of TBHP to determine the effect on ROS production. As shown in **Figure 3.6(A, B)**, TBHP significantly induced ROS production in both THP-1 monocytes (A) and macrophages (B) ($p=0.001$) following incubation with the vehicle. However, co-incubation with PNLA in monocytes or pre-incubation in macrophages had no significant effect on this TBHP-induced ROS production.

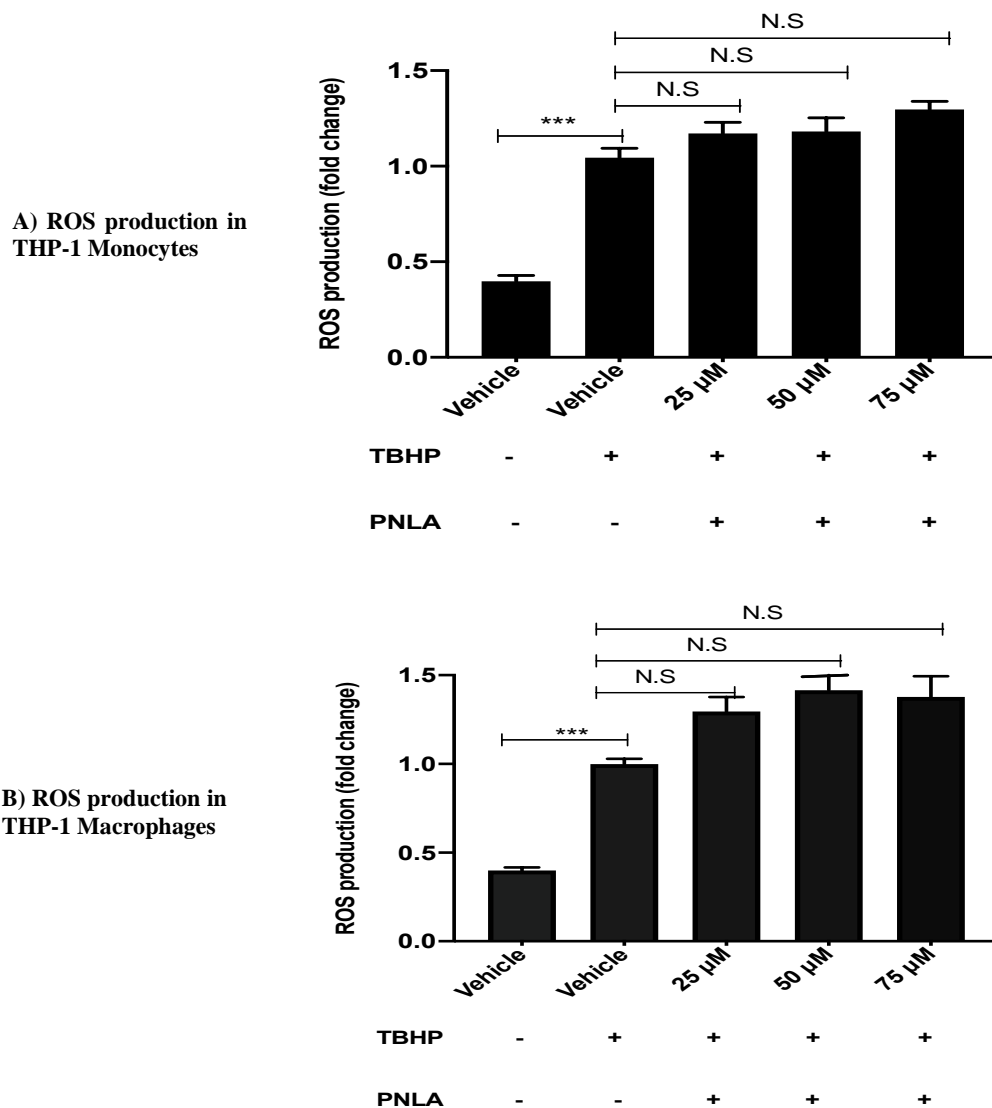


Figure 3.6. PNLA does not affect the TBHP-induced ROS production in THP-1 monocytes and macrophages. (A) THP-1 monocytes were incubated with 35 μM DCFDA for 30 min, followed by 100 μM TBHP in the presence of the indicated concentrations of PNLA or the vehicle control for 3 hours. (B) THP-1 macrophages were pre-incubated with PNLA or the vehicle control for 24 hours prior to incubation with 35 μM DCFDA for 45 min and 100 μM TBHP for 3 hours. Cells incubated with the vehicle in the absence of TBHP were included for comparison. Fluorescence was measured at 495 nm and 520 nm for the excitation and emission spectra, respectively. The graph displays the average mean \pm SEM from three independent experiments. The value in the TBHP positive control fold change has been arbitrarily assigned as 1. Statistical analysis was performed using a one-way ANOVA followed by Tukey's post-hoc test (N.S, not significant; ***, $P \leq 0.001$).

3.2.2. Primary cultures of human monocyte-derived macrophages.

Key experiments were repeated in primary cultures of HMDMs. These experiments were carried out to rule out the possibility that the observed results are specific to the cell line. HMDM were pre-treated with 25, 50, 75, or 100 μM PNLA or vehicle for 24 hours (identical conditions to those used for THP-1 macrophages) unless otherwise stated.

3.2.2.1 The viability and proliferation of human macrophages were unaffected by PNLA *ex-vivo*.

The viability and proliferation of HMDMs were determined by LDH assays and CV assays respectively. As shown in **Figure 3.7**, there was no significant effect on cell viability (**A**; LDH assay) or cell proliferation (**B**; CV assay) following treatment of the cells with different concentrations of PNLA for 24 hours as compared to the vehicle control.

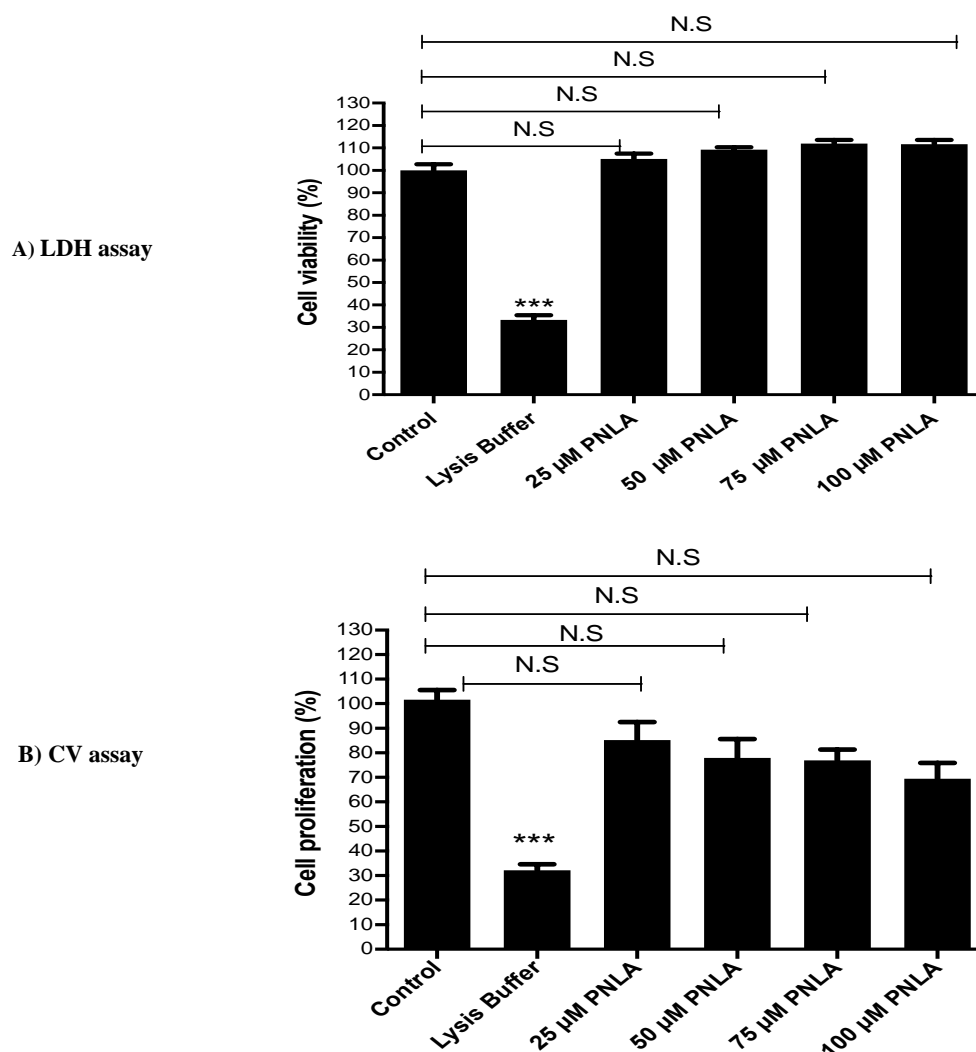


Figure 3.7. No adverse effects of PNLA in comparison to the vehicle on the viability and proliferation of HMDMs. HMDM were incubated with 25, 50, 75, or 100 μ M PNLA as indicated, or the DMSO vehicle control, for 24 hours. LDH (A) and CV (B) assays were carried out as described in Materials and Methods. Both histograms display the percentage of viability or proliferation values (mean \pm SEM) in comparison to the control (arbitrarily assigned as 100%) from three independent experiments. Statistical analysis was performed using one-way ANOVA and Tukey's post hoc test, comparing each individual treatment to the control. (N.S, not significant; ***, $P \leq 0.001$).

3.2.2.2 PNLA attenuates macropinocytosis in human macrophages.

Macropinocytosis in PNLA-treated HMDMs was significantly reduced when compared to

HMDM treated with vehicle control (**Figure 3.8**). LY uptake in PNLA-treated HMDMs was also significantly reduced ($P=0.0039$, 0.0087 and 0.0025) when compared with cells treated with the vehicle control by 50%, 45%, and 50% with 50, 75, and 100 μM PNLA, respectively, and ($P=0.031$) by 40% with 25 μM PNLA.

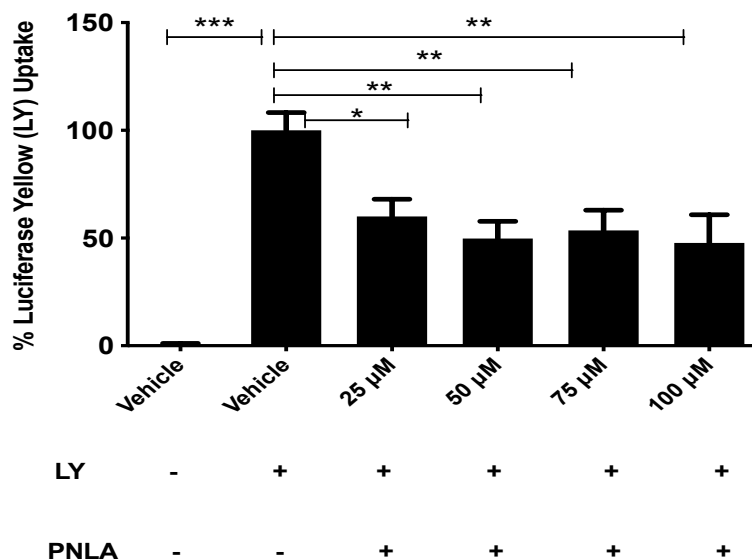


Figure 3.8. LY uptake was attenuated following incubation of HMDMs with PNLA. HMDMs obtained from buffy coats were incubated with different concentrations of PNLA for 24 hours, followed by 100 $\mu\text{g}/\text{ml}$ LY for another 24 hours in RPMI medium supplemented with 0.2% (v/v) fatty acid-free BSA. The overlying media was discarded, and the cells were detached from the plastic by treatment with 0.05% (v/v) trypsin. Cells were collected in Eppendorf tubes and subjected to centrifugation at $9,000 \times g$ for 5 min. The supernatant was discarded, and the pellet was re-suspended and fixed in 2% (w/v) PFA. LY incorporation was analysed by flow cytometry on a BD FACS Canto flow cytometer. At least 10,000 events were counted for each sample. Data are presented as the mean \pm SEM from four independent experiments, with the value in vehicle-treated cells arbitrarily assigned as 100%. Statistical analysis was performed using a one-way ANOVA followed by Tukey's post hoc analysis. (*, $P \leq 0.05$; **, $P \leq 0.01$; ***, $P \leq 0.001$).

3.2.2.3 PNLA reduces Dil-oxLDL uptake in human macrophages

The effect of PNLA treatment on cholesterol uptake was assessed. HMDMs were treated with Dil labelled-ox-LDL in the presence of DMSO vehicle control or 25 μM PNLA for 24 hours. Dil-oxLDL was increased by 95% in the presence of a vehicle compared to a vehicle alone without any Dil-oxLDL. PNLA significantly reduced this uptake by almost 40% ($P=0.047$) (**Figure 2.9**).

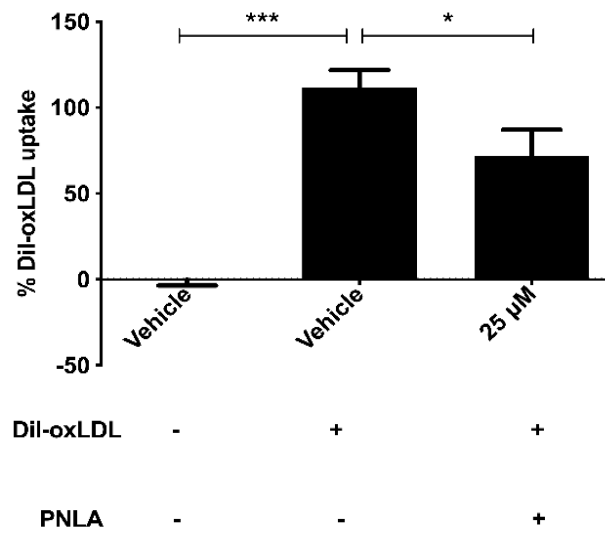


Figure 3.9. PNLA reduces uptake of ox-LDL by HMDMs. HMDMs isolated from buffy coats were incubated with Dil-oxLDL for 24 hours in the presence of vehicle or 25 μ M PNLA. The vehicle control was arbitrarily assigned as 100 and the remaining data normalised to this. The data are presented as the mean \pm SEM from three independent experiments. Statistical analysis was performed using a one-way ANOVA with a Games-Howell post-hoc analysis (***, $P \leq 0.001$; *, $P \leq 0.05$).

3.3. Discussion

The various inflammatory-associated functional assays used for the different experiments in this Chapter demonstrate the ability of PNLA to reduce monocyte recruitment, micropinocytosis, and ox-LDL uptake. However, PNLA had no significant effect on TBHP-induced ROS generation or phagocytosis. This n-6 PUFA is unique to pine nuts, and these studies show beneficial actions against pro-inflammatory processes associated with atherosclerosis and other diseases *in vitro*.

As PNLA is a novel n-6 PUFA, it was essential to initially confirm that it did not exert any detrimental effects on either cell proliferation or viability in THP-1 or human macrophages *in vitro* (**Figures 3.1** and **3.7**). These results also confirm that the changes in macrophage processes observed in other assays were due to PNLA rather than a consequence of altered cell viability.

Expression of CCL2 in inflammation (inflammatory synovitis and atherogenesis) recruits circulating monocytes into the synovium and arterial intima (Bobryshev 2006). It was of interest to determine whether PNLA could inhibit the key role of CCL2 in inducing the migration of monocytes across a barrier that mimics arterial ECs. As shown in **Figure 3.2**, monocyte migration was significantly induced by the treatment of THP-1 monocytes with CCL2. On co-incubation with PNLA, the monocyte migration was attenuated, on average, by 60% in comparison to the CCL2 positive control. *In vivo* inhibition of monocyte migration in ApoE^{-/-} mouse models of atherosclerosis has been shown to be atheroprotective (Mueller *et al.* 2013). For example, gremlin-1 inhibited monocyte migration *in vivo*, resulting in a decreased content of monocytes and macrophages in plaques and reduced atheroprotection (Mueller *et al.* 2013). In addition, a compound, an oxidised PL small molecule (VB-201), selectively inhibited monocyte chemotaxis by 90% *in vitro*. Administration of this compound to ApoE^{-/-} mice *in vivo* inhibited atheroma development (Feige *et al.* 2013). Given the attenuation of CCL2-driven monocyte migration *in vitro*, this may imply that PNLA has the potential to reduce inflammation *in vivo* by reducing the cellular monocyte and macrophage content within the lesion. In human breast cancer cells MDA-MB-231 cultured *in vitro*, cells supplemented with PNLA also had 25% decreased motility and invasiveness (Chuang *et al.* 2011). Although RCTs of an anti-CCL2 monoclonal antibody in RA showed negative results (Haringman *et al.* 2006), CCL2 may be biologically significant as anti-TNF drugs indirectly repress CCL2 and thereby suppress immune cell recruitment and consequently synovial inflammation (Taylor *et al.* 2000).

In this study, we demonstrated that PNLA significantly reduced macropinocytosis and ox-LDL uptake by THP-1 and human macrophages. THP-1 cell line cannot transform directly into foam cells unless incubated with lipoproteins/modified lipoproteins. Following stimulation with M-CSF or phorbol esters (PMA), ruffling at the cell surface of macrophages can be observed, which gives rise to macropinosomes (Swanson and Watts 1995). Macropinocytosis has been linked to LDL and modified LDL uptake by macrophages and contributes to foam cell formation (Michael *et al.* 2013). Macrophages incubated with ox-LDL increased membrane ruffling and formed macropinosomes, resulting in a 1.5-fold increase in fluid phase uptake (Jones and Willingham 1999), suggesting a role for the pathway in modified LDL uptake. Ox-LDL induced foam cell formation was also reduced by an inhibitor of macropinocytosis in RAW264.7 macrophages (Yao *et al.* 2009). In addition to the uptake of modified forms of LDL, macropinocytosis has also been shown to take up native LDL. M-CSF-differentiated macrophages showed increased uptake of native LDL in the fluid phase, which increased cholesterol accumulation (Zhao *et al.* 2006). Similarly, M-CSF stimulated HMDMs treated with a macropinocytosis inhibitor showed a 40% decrease in LDL uptake (Anzinger *et al.* 2010).

As with PNLA, previous work indicated a role for PUFAs in macropinocytosis. Treatment of THP-1 macrophages with EPA and DHA reduced acLDL uptake. This was accompanied by a reduction in the uptake of a marker of macropinocytosis on treatment with the PUFAs (McLaren *et al.* 2011b). The effect of PNLA on macropinocytosis was measured in PMA differentiated macrophages and in HMDM. PMA has been used frequently in the literature to induce macropinocytosis in differentiated macrophages. PMA increased macropinosomes in BMDMs (Swanson 1989), induced LDL and modified LDL uptake in HMDMs (Kruth *et al.* 2002; Kruth *et al.* 2005), and THP-1 macrophages (McLaren *et al.* 2011b; Michael *et al.* 2013). To measure macropinocytosis, LY was used as a marker that can be measured by FACS analysis. LY has been commonly used in measuring macropinocytosis (McLaren *et al.* 2011b; Michael *et al.* 2013). As shown in **Figures 3.3** and **3.8**, pre-incubation with PNLA inhibited LY uptake by approximately 55% in PMA differentiated macrophages and by 50% in HMDMs, respectively. Given the role of macropinocytosis in the uptake of modified forms of LDL, including ox-LDL, this may indicate another mechanism, independent of receptor-mediated uptake, in which PNLA inhibits the uptake and accumulation of lipoproteins and cholesterol, as seen previously in the human hepatoma HepG2 cell line (Lee and Han 2016). In addition, PNLA may also attenuate the uptake of native forms of LDL through inhibiting macropinocytosis. The results presented herein imply that PNLA may reduce the size of foamy

macrophages, which accumulate at the site of ox-LDL buildup in atherosclerotic lesions, and therefore result in a smaller lesion.

Cholesterol crystals are also taken up by macrophages via macropinocytosis (Bobryshev 2006). Cholesterol crystals can activate inflammasomes. The inflammasome is an intracellular multi-protein complex in the innate immune response that can convert the pro-inflammatory cytokines IL-1 β and IL-18 into their mature forms (Hoseini *et al.* 2017). PNLA could affect the activation of the inflammasome through the inhibition of macropinocytosis.

Receptor-mediated uptake of ox-LDL was measured using a fluorescently labelled modified form of LDL, Dil-oxLDL. As shown in **Figures 3.4** and **3.9**, PNLA inhibited the uptake of Dil-oxLDL by 50% and 35% on average with THP-1 and HMDM, respectively. Previous studies reported comparable results using n-6 PUFA the DGLA (Gallagher *et al.* 2019). DGLA inhibited Dil-acLDL and Dil-oxLDL uptake in THP-1 macrophages. This process was found to be dependent on both scavenger receptors and macropinocytosis (Gallagher *et al.* 2019). PNLA may act in a similar way to DGLA, both of which are n-6 PUFA.

The main action of pine nuts has been reported to reduce dietary cholesterol and TG levels and diminish cholesterol uptake *in-vitro* (Asset *et al.* 2001). Indeed, pine nuts produced a reduction in lipid profile and lipoprotein cholesterol in rats fed HFD (Amr and Abeer 2011). For example, long-chain acyl-CoA synthetases (ACSLs) catalyse the formation of fatty acyl-CoA from FAs (lipid biosynthesis), and PNLA downregulated the mRNA levels of ACSL3 and ACSL4 by (30% and 20%, respectively, relative to the BSA control group (Lee and Han 2016). The mRNA levels of the genes related to FA biosynthesis (e.g., sterol regulatory element-binding protein-1c (SREBP1c), fatty acid synthase (FAS), and acyl CO-A desaturase 1(SCD1)) were significantly downregulated in the human hepatoma HepG2 cell line by PNLA treatment compared to control by 53, 54, and 38%, respectively). In addition, the mRNA levels of genes related to cholesterol synthesis and lipoprotein uptake, 3-hydroxy-3-methylglutaryl-CoA reductase (HMGCR) and LDLr, respectively, were significantly lowered by 30%, and 43%, respectively, by PNLA (Lee and Han 2016). The imbalance of cholesterol homeostasis towards increased cholesterol uptake and reduced efflux within macrophages leads to the formation of foam cells. In atherosclerosis, macrophages recognise and internalise excess amounts of modified forms of LDL in an unregulated manner. As a result, excess cholesterol is stored as cholesteryl esters in lipid droplets, which are deposited in the cytoplasm, a hallmark of foam cell formation (Shashkin *et al.* 2005; Lusis 2012). Inhibiting the uptake of modified forms of LDL would therefore prevent the accumulation of excess cholesterol in macrophages and their transformation into foam cells. Future studies would benefit from confirming the regulatory

effect of PNLA on these inflammatory and metabolic genes detailed above in human macrophages.

In atherosclerosis, pathways for foam cell formation involve oxidative modifications of LDL. Native LDL is internalised by macrophages through the LDL receptor, which is subject to negative feedback inhibition as the intracellular concentration of cholesterol increases (Moore *et al.* 2013). Oxidative modifications to LDL allow recognition by scavenger receptors, which are also expressed on macrophages, which take up excess amounts of modified LDL in an unregulated manner. This causes the transformation of macrophages into lipid-loaded foam cells (Singh and Jialal 2006). Given that scavenger receptors only recognise modified forms of LDL, including oxidised LDL, reducing LDL oxidation by decreasing ROS levels would have a beneficial effect on inhibiting foam cell formation. ROS production was stimulated with TBHP (i.e., hydrogen peroxide mimic) in THP-1 monocytes and macrophages, and the effect of PNLA was determined. As shown in **Figure 3.6**, PNLA did not inhibit ROS production from either monocytes (A) or macrophages (B). This initial study suggests that acting as an antioxidant is not the likely mechanism of action of PNLA in THP-1 cells. However, numerous other experiments will be required to conclusively delineate the relationship between PNLA, oxidative stress, and free radical formation. This may include the effect of PNLA on the modification of LDL and other sources capable of oxidative stress, such as NO production, and the investigation of mitochondrial function. To date, little has been published on the effect of PUFAs on ROS production. One such study indicated that prior oral supplementation of n-3 FA in rats had no effect on ROS production but did enhance the activity of antioxidant enzymes (Suresh and Das 2003b). However, studies on PNLA demonstrated its ability to reduce NO production (Chen *et al.* 2015). *In vivo* studies have demonstrated that total antioxidant capacity (TAOC) in the serum was higher with PNO than in the HFD control group, and *P. koraiensis* oil can increase the activity of the antioxidant enzyme SOD (Chen *et al.* 2011). These studies suggest that the impact of PNLA and pine nuts on oxidative stress *in vivo* may differ from that of cultured cells. ROS are produced in many normal and abnormal processes in humans, including atheroma, joint diseases, and ageing (Mirshafiey and Mohsenzadegan 2008). The healthy physiological functions of vascular cells, including VSMC contraction and endothelial homeostasis, is dependent on ROS for cell signalling (Chen *et al.* 2017c). Failure to maintain a balance in ROS formation can have detrimental effects, and increased ROS production has been strongly linked with increased cell damage, lipid peroxidation, immune cell recruitment, and MMP activation (Chen *et al.* 2017c). TNF- α overproduction is believed to be the main reason for increased ROS release in patients with RA. Increased ROS production leads to tissue

damage associated with overall inflammation. Therefore, reducing ROS formation represents a potential therapeutic avenue for attenuating atherosclerosis disease progression as well as joint inflammation and damage in RA. However, a potential future avenue of research should be the effect of PNLA on antioxidant levels and levels of other oxidising species, such as NO, in human macrophages. Antioxidants have been suggested as a potential therapeutic avenue in atherosclerosis and RA. However, results from clinical trials largely contradict one another and have revealed a controversial role for antioxidants (Stephens *et al.* 1996; Yusuf *et al.* 2000).

Dose response experiments suggested a lack of concentration-dependent effects of PNLA when used at 25, 50, 75, and 100 μM on the responses studied, with effects seen at the lowest concentration of 25 μM . Most studies on other PUFAs have used these concentrations (Baker *et al.* 2020; Gallagher *et al.* 2019). So, this allowed direct comparisons and suggested that PNLA is potentially more potent than other studied PUFAs such as DGLA, GLA, and ALA. Future studies should do dose-response experiments between 0 μM and 25 μM PNLA.

PNLA is well known for possessing antibacterial, antifungal, antiviral, and antiseptic properties (Amr and Abeer 2011). Here, we explored the effect of PNLA on the enhancing ability of THP-1 macrophages on microbial phagocytosis using *E. coli* (K-12 strain) bioparticles, which are foreign particles that are fluorescently labelled. The results suggest that PNLA may exert no microbicidal effects on *E. coli* bioparticles (**Figure 3.7**). In comparison, n-3 PUFA (EPA and DHA) have modulatory effects on phagocytosis activity *in vitro* with goat neutrophils using *E. coli* (K-12 strain) bioparticles (Pisani *et al.* 2009) or microglial phagocytosis of the AD pathogen amyloid- β (A β) (Hjorth *et al.* 2013). n-3 PUFA has an inhibitory effect on NK-cell activity, triggering cell death (Pompeia *et al.* 2000), while n-6 PUFAs have both inhibitory and stimulatory effects on leukocytes. N-3 FA-fed animals show decreased cell activation, production of ROS, phagocytosis, and antigen presentation by macrophages (Bellinati-Pires *et al.* 1993; Hughes and Pinder 1997; Lopes *et al.* 1999). While the addition of n-3 and n-6 (AA) FAs to the cell medium increases ROS formation and phagocytosis (Bellinati-Pires *et al.* 1993; Kumaratilake *et al.* 1997), higher doses of FAs can cause necrosis with a rapid loss of membrane integrity, lysosomal enzyme leakage, and cell swelling. Both apoptosis and necrosis seem to be associated with oxidative stress. Interestingly, COX inhibitors and sometimes LOX inhibitors have been found to protect cells from PUFA-induced cytotoxicity (Koller *et al.* 1997; Pompeia *et al.* 1999).

Several mechanisms have been proposed to explain FA modulation of the immune response, such as changes in membrane fluidity and signal transduction pathways such as protein kinase C (PKC), regulation of gene transcription, protein acylation, and calcium release. Evidence has also been identified to support the proposition that changes in cell metabolism also play an important role in the effect of FAs on leukocyte functioning (Pompeia *et al.* 2000). n-6 and n-3 PUFA-rich diets cause marked changes in the activities of key enzymes regulating glucose and glutamine metabolism, together with mitochondrial depolarization, which is associated with impaired lymphocyte proliferation, hydrogen peroxide production, and the phagocytic capacity of macrophages. This effect can be due to the regulation of gene expression. For example, FAs can directly regulate gene transcription via binding to peroxisomal proliferator-activated receptors (PPARs) (Costa-Rosa *et al.* 1995; Miyasaka *et al.* 1996; Schoonjans *et al.* 1995). These metabolites are essential components of the diet and act as both intracellular and extracellular mediators, positively or negatively regulating physiological and pathological conditions.

Chapter 4: Effects of PNLA on the expression of pro-inflammatory cytokines involved in the pathogenesis of RA and atherosclerosis

4.1. Introduction and aims

Cytokines are involved in the effector phase of all inflammatory diseases and thus are targets for therapy. They include more than 50 secreted factors that have numerous roles in cellular communication and networking (Ramji and Davis 2015; Tedgui and Mallat 2006). In RA, cytokines play an important role in initiating symptoms and aggravating manifestations by orchestrating an inflammatory response; inhibition of pro-inflammatory cytokine signalling is therefore a key therapeutic strategy. Anti-cytokine therapy was first introduced in the early nineties of the last century, with the first successful anti-cytokine therapy trial involving anti-TNF- α antibodies in patients with RA (Elliott *et al.* 1993). Since then, several monoclonal antibodies against other cytokines or cytokine receptors, as well as other immune-modulating drugs, have been licenced for the treatment of RA. These treatments include selectively inhibiting IL-6 (Kang *et al.* 2019) or IL-1 (Lubberts and van den Berg 2013). Both IL-6 and IL-1 inhibitors reduced inflammation and cartilage destruction. Furthermore, the reduction of pro-inflammatory oxidative stress in RA monocytes and macrophages significantly correlated with the improvement of joint damage and endothelial function (Nagy *et al.* 2007; Negi *et al.* 2017; Taylor and Sivakumar 2005). In general, suppression of inflammation seems to offer a similar therapeutic benefit as TNF- α blockade (Goekoop-Ruiterman *et al.* 2005).

Based on published literature and results from the previous Chapter, we hypothesised that PNLA may have anti-inflammatory effects in patients with RA. However, it may be argued that in RA, the presence of chronic inflammation and an active immune response may render monocytes more refractory to the anti-inflammatory effects of PNLA. So, it is important to demonstrate the anti-inflammatory effect in HCs, as positive controls, and in patients with RA.

Specifically, I hypothesised that PNLA is able to reduce TNF- α , IL-6, and IL-1 β release by LPS-activated and enriched monocytes and macrophages from HCs and in patients with RA. These inflammatory cytokines are known to be important in driving inflammatory synovitis, and accelerated atherosclerosis (Bobryshev 2006; Lusis 2000; McInnes and Schett 2007). In addition, PNLA may reduce the free radical NO that is involved in inflammatory stress, and PGE₂, the main eicosanoid responsible for pain generation.

I conducted experiments on adherent PBMCs from HCs and patients with RA cells as enriched monocytes to avoid unnecessary costs if the results were negative. If PNLA reduces pro-inflammatory cytokine release by adherent monocytes, I will confirm this using purified CD14⁺ cells. More RA patients were studied than HCs to mitigate against the risk that the magnitude of the anti-inflammatory effect of PNLA may be less in RA.

LPS stimulation of mononuclear cells is commonly used in RA research. Amounts of TNF- α , IL-6, IL-1 β , and PGE2 were measured by ELISA, and nitrite was used as a surrogate for NO using the Griess system. Details of the protocols are provided in Materials and Methods. I assessed the effect of 25 and 50 μ M PNLA in all the experiments except for PGE2, as the assay is very expensive (costs more than £5,000 to assay all the samples for one of the PNLA concentrations), so only 50 μ M PNLA was used. Before assessing the cytokines level, PBMCs viability, and proliferation were assessed in response to LPS and PNLA treatment using Alarm blue, and BrdU, respectively.

4.2. Results

4.2.1. PNLA does not affect the viability and proliferation of PBMCs from HCs or patients with RA.

4.2.1.1 Viability of HCs and RA PBMCs *ex-vivo*

The cell viability was monitored and calculated relative to the control (DMSO), which was assigned 100%. The viability of PBMCs isolated from HCs (n=4) or RA patients (n=4) after treatment with 25, 50, 75, and 100 μ M PNLA or vehicle and stimulated with LPS at 0, 50, and 100 ng/ml, respectively, is shown in **Figure 4.1**. More than 90% of cells were viable, showing that the PNLA treatment has no cytotoxic effect. Since PNLA had no cytotoxic effect on 8 participants, I did not recruit more participants to replicate the results.

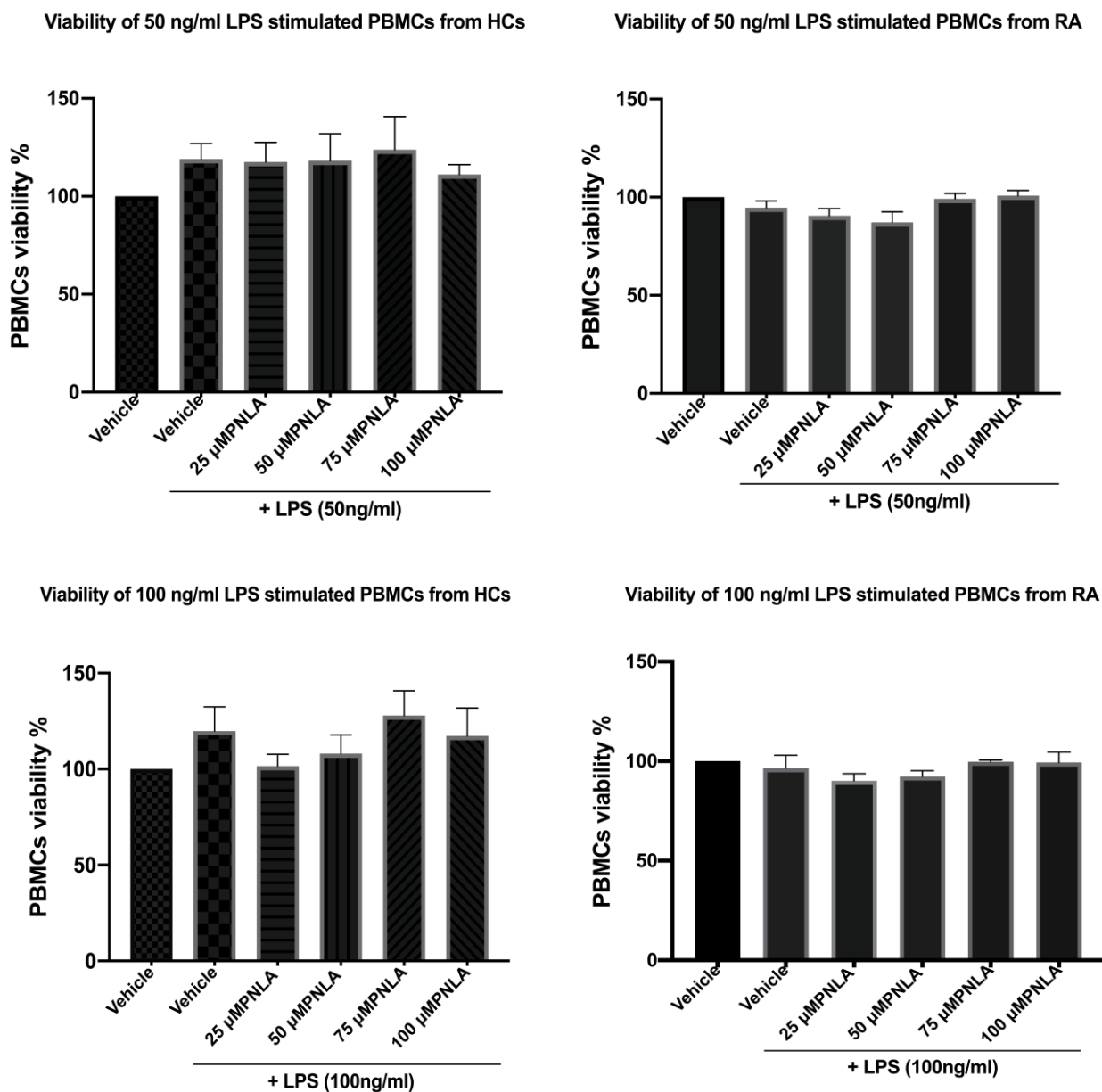


Figure 4.1. PNLA has no detrimental effect on the viability of PBMCs isolated from HCs and RA.

PBMCs from HCs (n=4) and RA patients (n=4) were incubated with 25, 50, 75, or 100 μM PNLA as indicated or the DMSO vehicle control for 24 hours, followed by LPS stimulation for 18 hours. Alarm-blue assays were carried out as described in Materials and Methods. Both histograms display the percentage of cell viability from absorbance values (the mean \pm SEM) in comparison to the control (assigned as 100) from three independent replicates. Statistical analysis was performed using one-way ANOVA and Tukey's post hoc test, comparing each treatment to the control and each other.

4.2.1.2 Proliferation of PBMCs *ex-vivo* from HCs and patients with RA

Intracellular DNA activity was measured by the BrdU assay to indirectly assess the proliferation of PBMCs from HCs (n=3) or RA patients (n=4). The proliferation rate was determined as a percentage of the vehicle control, which was set to 100%. The results showed that proliferation was not affected by PNLA following LPS stimulation at either 50 or 100 ng/ml (**Figure 4.2**). Similar to the assessment of viability, once I found PNLA had no significant effect on 6 participants, I did not recruit more participants to replicate the results.

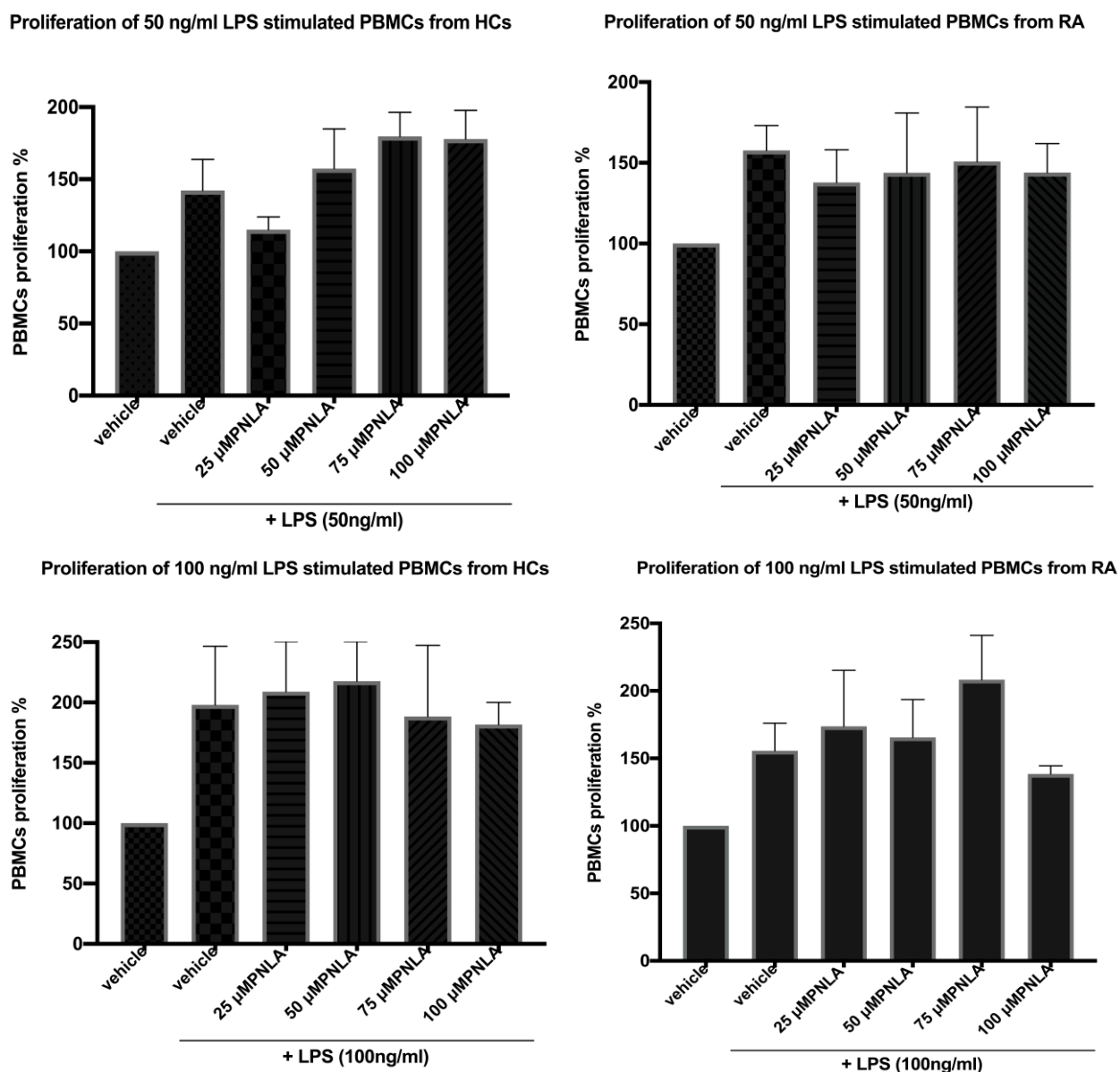


Figure 4.2. PNLA has no effect on proliferation of PBMCs from HCs and RA patients.

PBMCs from HCs (n=3) and RA patients (n=3) were incubated with 25, 50, 75, or 100 μ M PNLA as indicated or the DMSO vehicle control for 24 hours, followed by LPS stimulation for 18 hours. The BrdU assays were carried out as described in Materials and Methods. The proliferation rate was determined as a percentage of the vehicle control, which was set to 100%. Data from three independent replicates are presented as the mean \pm SEM. Statistical analysis was performed using a one-way ANOVA and Dunnett post hoc test to compare the results of each treatment with the LPS-stimulated vehicle control.

4.2.2. TNF- α level was reduced significantly upon PNLA treatment.

4.2.2.1 HCs and RA adherent monocytes

HCs

LPS stimulated monocytes at 50 or 100 ng/ml from HCs (n=10) produced TNF- α (485.6 ± 56.10 pg/ml and 608 ± 120 pg/ml respectively, $p \leq 0.001$) after 18 hours in comparison with non-stimulated enriched monocytes. Pre-incubating enriched monocytes with 25 or 50 μ M PNLA and subsequent stimulation with 50 ng/ml LPS did not change the TNF- α level significantly (**Figure 4.3(A)**). TNF- α levels were (365.7 ± 61.63 pg/ml; $p=0.12$) and (318.7 ± 65.06 pg/ml; $p=0.91$) ($p=N.S$) after pre-treatment with 25 and 50 μ M PNLA, respectively, in comparison with the controls (485.6 ± 56.10 pg/ml). In contrast, the release of TNF- α by 100 ng/ml LPS stimulated monocytes from HCs (608 ± 120 pg/ml) was reduced by 25 and 50 μ M PNLA to 298.03 ± 50.34 pg/ml ($p=0.035$) and 374.43 ± 98.88 pg/ml ($p=0.15$; $N.S$) respectively (**Figure 4.3(C)**).

RA

In patients with RA (n=20), there was a statistically significant reduction in TNF- α level (346.8 ± 43.80 pg/ml) pre-treated with 25 μ M (190.9 ± 22.34 pg/ml; $p \leq 0.01$) or 50 μ M PNLA (221.1 ± 27.09 pg/ml; $p \leq 0.05$) stimulated with 50 ng/ml LPS (**Figure 4.3(B)**). TNF- α levels from 100 ng/ml LPS stimulated enriched monocytes of RA patients were reduced from (443.7 ± 62.7) pg/ml to (270.03 ± 40.34) pg/ml ($p \leq 0.01$) and (250.43 ± 38.88 pg/ml ($p \leq 0.01$)) by 25 and 50 μ M PNLA, respectively (**Figure 4.3(D)**).

4.2.2.2 HCs and RA differentiated macrophages

HCs

There was a statistically significant increase in the production of TNF- α level following 50 or 100 ng/ml LPS stimulation of enriched macrophages from HCs (n=10); (233.9 ± 30.20 pg/ml and 307.7 ± 51.17 pg/ml), respectively ($p \leq 0.001$). Upon 25 or 50 μ M PNLA treatment, there was no statistically significant reduction of TNF- α (**Figure 4.4(A)**) in 50 ng/ml LPS stimulations (226.2 ± 24.32 pg/ml and 360 ± 57.58 pg/ml) ($p=NS$) in comparison with (233.9 ± 30.20) pg/ml level in the control group. In 100 ng/ml LPS activated macrophages, TNF- α was reduced from (307.7 ± 51.17) pg/ml to (277 ± 65.44) pg/ml ($p < 0.05$) and (232 ± 42.61) pg/ml ($p=NS$) by 25 and 50 μ M PNLA, respectively (**Figure 4.4(C)**).

RA

For enriched macrophages from RA patients (n=20), there was a statistically significant increase in TNF- α level after 50 and 100 ng/ml LPS stimulation to (402.0 ± 43.62 pg/ml, and 627.11 ± 71.50 pg/ml) ($p \leq 0.001$), respectively (**Figure 4.4(D)**). There was a statistically

significant difference in TNF- α level between 50 (402.0 ± 43.62 pg/ml) and 100 ng/ml (627.11 ± 71.50 pg/ml) of LPS ($p= 0.0096$). Hence, the graphs and statistics for both 50 and 100 ng/ml are shown in separate figures. In 100 ng/ml LPS-activated enriched macrophages from RA patients, TNF- α was reduced to (439.58 ± 40.44) pg/ml ($p \leq 0.05$) and (441.90 ± 37.31 pg/ml ($p \leq 0.05$) with 25 and 50 μ M PNLA respectively both in comparison with the control (627.11 ± 71.50 pg/ml). However, in 50 ng/ml LPS stimulated enriched macrophages, PNLA was able to reduce TNF- α levels from (402.0 ± 43.62) pg/ml to levels of (358.93 ± 47.60 pg/ml and 273.7 ± 37.61), respectively, with 25 and 50 μ M pre-treatment ($p=N.S$), (**Figure 4.4(B)**).

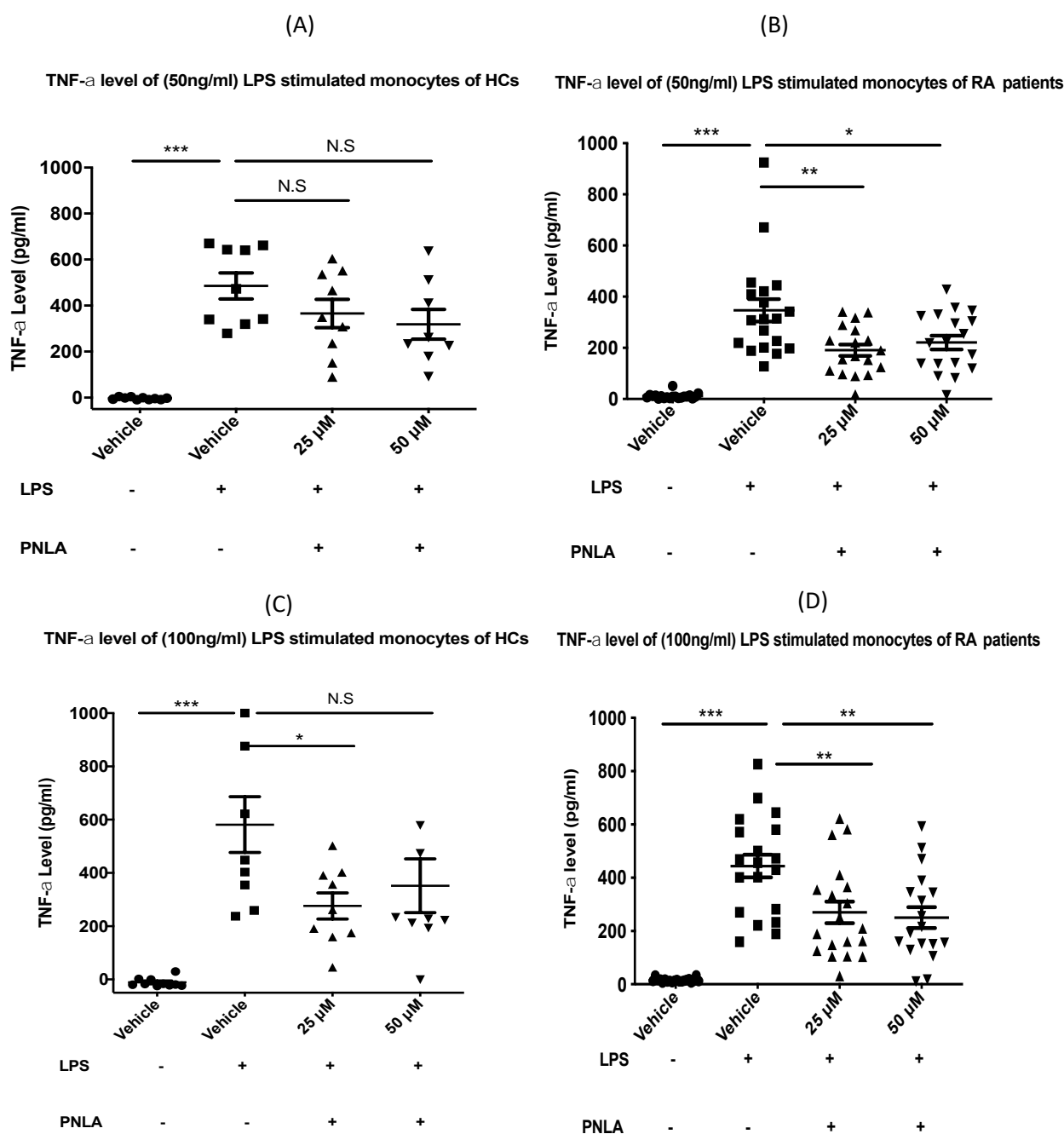


Figure 4.3. TNF- α level is reduced following incubation of activated monocytes from HCs and RA patients with PNLA.

Purified monocytes obtained from RA patients (n=20) and HCs (n=10) were incubated with 25, 50 μ M PNLA or DMSO for 24 hours, followed by LPS stimulations at 50 ng/ml (A, B) or 100ng/ml (C, D) for another 16-18 hour. Then the supernatants were collected and assayed for levels of TNF- α using ELISA, all samples and standard run-in duplicate. The data are presented as the mean \pm SEM, each dot (\bullet) represents the average of one participant; any data transformations were carried out when needed. Statistical analysis was performed using one-way ANOVA and a Tukey's post-hoc-test, where (***) $p \leq 0.001$, ** $p \leq 0.01$, * $p \leq 0.05$, and N.S not significant).

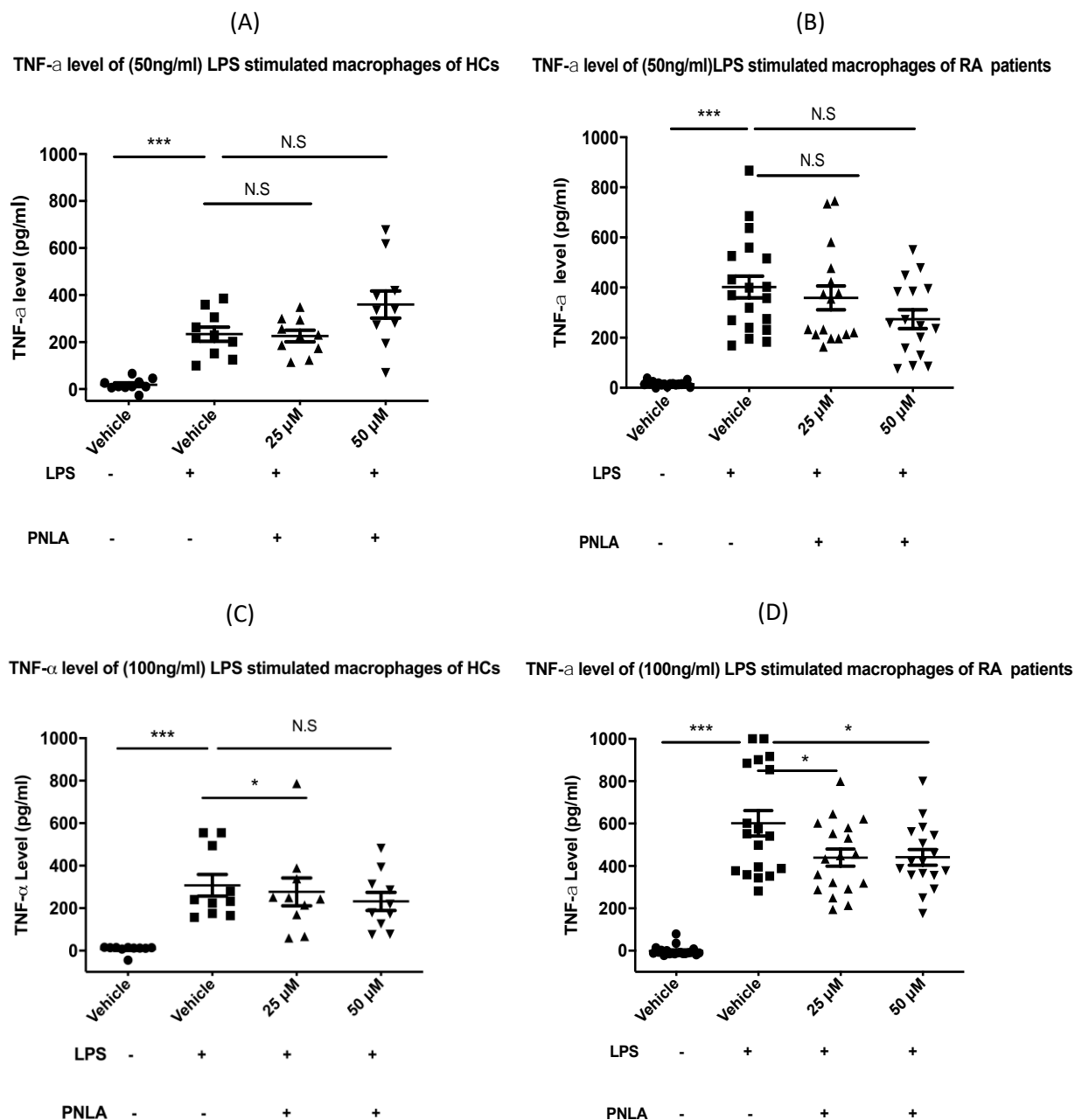


Figure 4.4. TNF- α level is reduced following incubation of activated enriched macrophages from HCs and RA with PNLA.

Differentiated macrophages obtained from HCs (n=10) and RA patients (n=20) were incubated with 25, 50 μ M PNLA or DMSO for 24 hours, followed by LPS stimulations at 50 ng/ml (A, B) or 100 ng/ml (C, D) for another 16-18 hours. Then, the supernatants were collected and assayed for levels of TNF- α using ELISA; all samples and standards were run in duplicates. The data are presented as mean \pm SEM, each dot (\bullet) represents the average of one participant. Any data transformations were carried out when needed. Statistical analysis was performed using a one-way ANOVA and a Tukey's post-hoc-test, where (***) $p \leq 0.001$, * $p \leq 0.05$, N.S=not significant).

4.2.3. IL-6 level was reduced significantly upon PNLA treatment.

4.2.3.1 HCs and RA adherent monocytes

HCs

Under the same experimental conditions (incubation period, PNLA treatment concentrations, and LPS dosing stimulation) as TNF- α ELISA experiments, IL-6 levels produced from 50 ng/ml LPS stimulated enriched monocytes of HCs (n=10) were measured (positive control group) and were (91.60 ± 12.10 pg/ml) ($p \leq 0.001$) (**Figure 4.5(A)**) after 18 hours in comparison with non-stimulated monocytes. Pre-incubating enriched monocytes with 25 or 50 μ M PNLA and subsequent stimulation with 50 ng/ml LPS reduced IL-6 levels to (55.25 ± 9.22 pg/ml) ($p \leq 0.05$) and (50 ± 8.060 pg/ml) ($p = \text{N.S.}$), respectively, in comparison with the positive control. In contrast, the release of IL-6 by 100 ng/ml LPS stimulated enriched monocytes from HCs (206.5 ± 37.78 pg/ml) ($p \leq 0.001$) (**Figure 4.5(C)**) was reduced by 25 and 50 μ M PNLA to (122.33 ± 31.65 pg/ml) and (135.68 ± 38.84 pg/ml) ($p \leq 0.01$), respectively.

RA

In patients with RA (n=20), there was a statistically significant reduction in IL-6 level upon either 25 or 50 μ M PNLA treatment and 50 or 100 ng/ml LPS stimulation (**Figure 4.5(B, D)**). In 50 ng/ml LPS activated enriched monocytes, IL-6 levels (105.3 ± 11.48 pg/ml) ($p \leq 0.001$) were reduced by pre-treatment with 25 μ M PNLA to (59.94 ± 9.538 pg/ml) ($p \leq 0.01$) or 50 μ M PNLA (71.29 ± 9.635) ($p \leq 0.05$). IL-6 levels from 100 ng/ml LPS stimulated enriched monocytes of RA patients were reduced from (206.3 ± 35.87 pg/ml) ($p \leq 0.001$) to (103.94 ± 23.18 pg/ml) and (93.84 ± 14.66 pg/ml) (both at $p \leq 0.01$) with 25 μ M, and 50 μ M PNLA, respectively, (**Figure 4.5(D)**).

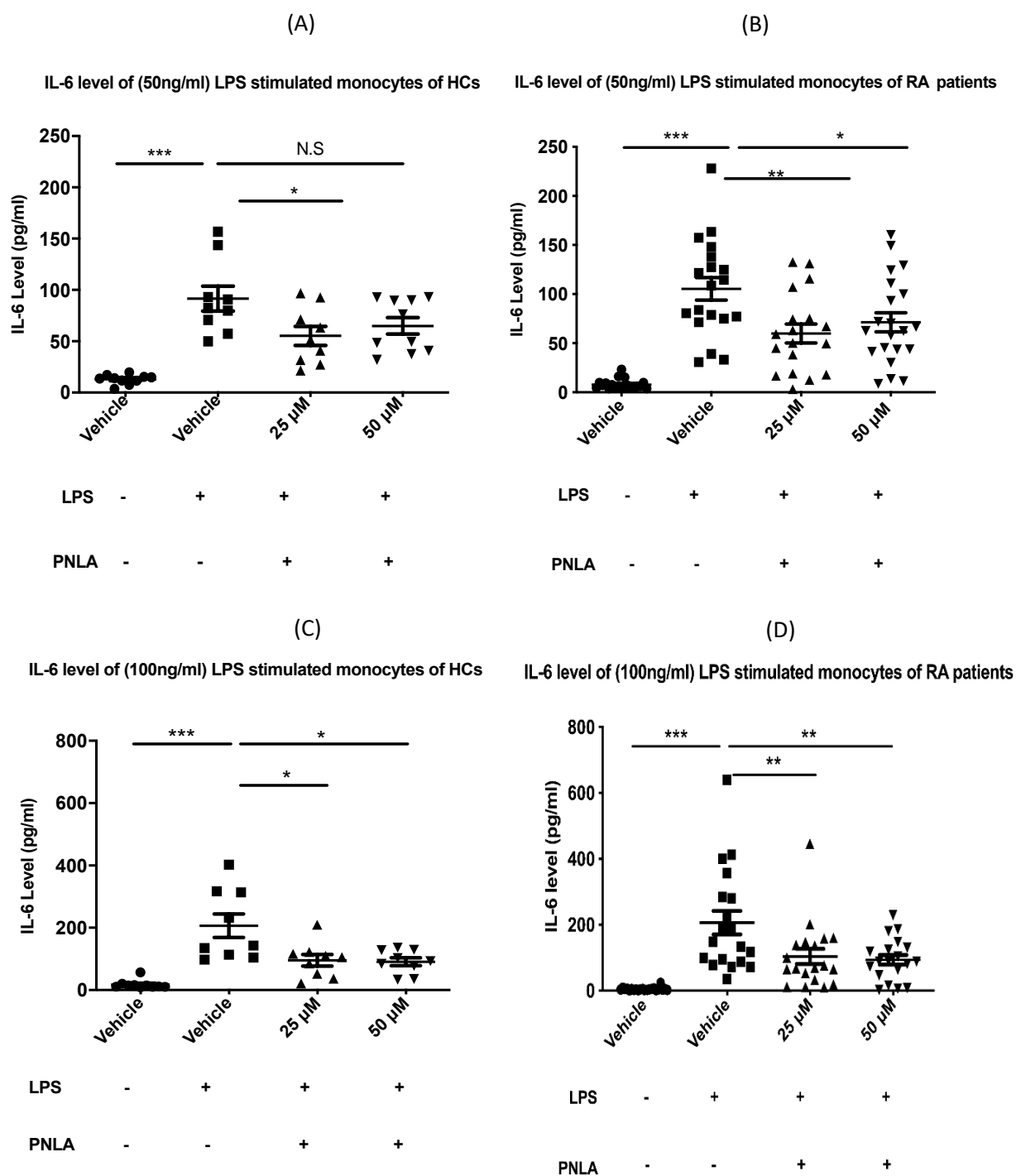


Figure 4.5. IL-6 level is reduced following incubation of activated enriched monocytes from HCs and RA patients with PNLA.

Purified monocytes obtained from RA patients (n=20), and HCs (n=10) were incubated with 25, 50 μ M PNLA or DMSO for 24 hours, followed by LPS stimulations at 50 ng/ml (A, B) or 100 ng/ml (C, D) for another 16-18 hours. Then, the supernatants were collected and assayed for levels of IL-6 using ELISA, all samples and standards were run in duplicates. The data are presented as the mean \pm SEM, each dot (\bullet) represents the average of one participant. Any data transformations were carried out when needed. Statistical analysis was performed using a one-way ANOVA and a Tukey's post hoc test, where (***) $p \leq 0.001$, (**) $p \leq 0.01$, (* $p \leq 0.05$, and N. S.=not significant).

4.2.3.2 HCs and RA differentiated macrophages

HCs

There was a statistically significant increase in the production of IL-6 following 50, 100 ng/ml LPS stimulation of enriched macrophages from HCs (n=10) (83.61 ± 12.88 pg/ml) and (271.6 ± 44.88 pg/ml), respectively; ($p \leq 0.001$) (**Figures 4.6(A, C)**). Upon treatment with 25 μ M and 50 μ M PNLA, IL-6 levels were reduced to (37.60 ± 7.642) ($p \leq 0.01$) and (42.32 ± 10.19) ($p < 0.05$) (**Figure 4.6(A)**) in 50 ng/ml LPS in comparison with the control group (83.61 ± 12.88 pg/ml). In 100 ng/ml LPS activated enriched macrophages, PNLA pre-treatment reduced IL-6 levels from 271.6 ± 44.88 pg/ml to 132.99 ± 30.71 pg/ml and 108.94 ± 19.70 pg/ml with 25 and 50 μ M, respectively (both at $p \leq 0.01$) (**Figure 4.6(C)**).

RA

In enriched macrophages from RA patients (n=20), there was a statistically significant increase in IL-6 level in the positive control group after 50 and 100 ng/ml LPS (**Figures 4.6(B, D)**) to 105.9 ± 23.14 pg/ml and 371 ± 64.82 pg/ml, respectively ($p \leq 0.001$).

In 50 ng/ml LPS stimulated macrophages, IL-6 levels were reduced to (83.49 ± 13.60 pg/ml) and (82.90 ± 15.00 pg/ml) with 25 μ M PNLA and 50 μ M PNLA (both at $p \leq 0.05$) in comparison with the control (105.9 ± 23.14 pg/ml). In 100 ng/ml LPS stimulated macrophages, 25 and 50 μ M PNLA reduced IL-6 levels to (105 ± 21.32 pg/ml) and (104.7 ± 16.95 pg/ml), respectively (both at $p \leq 0.001$) in comparison with the vehicle control group (371 ± 64.82 pg/ml).

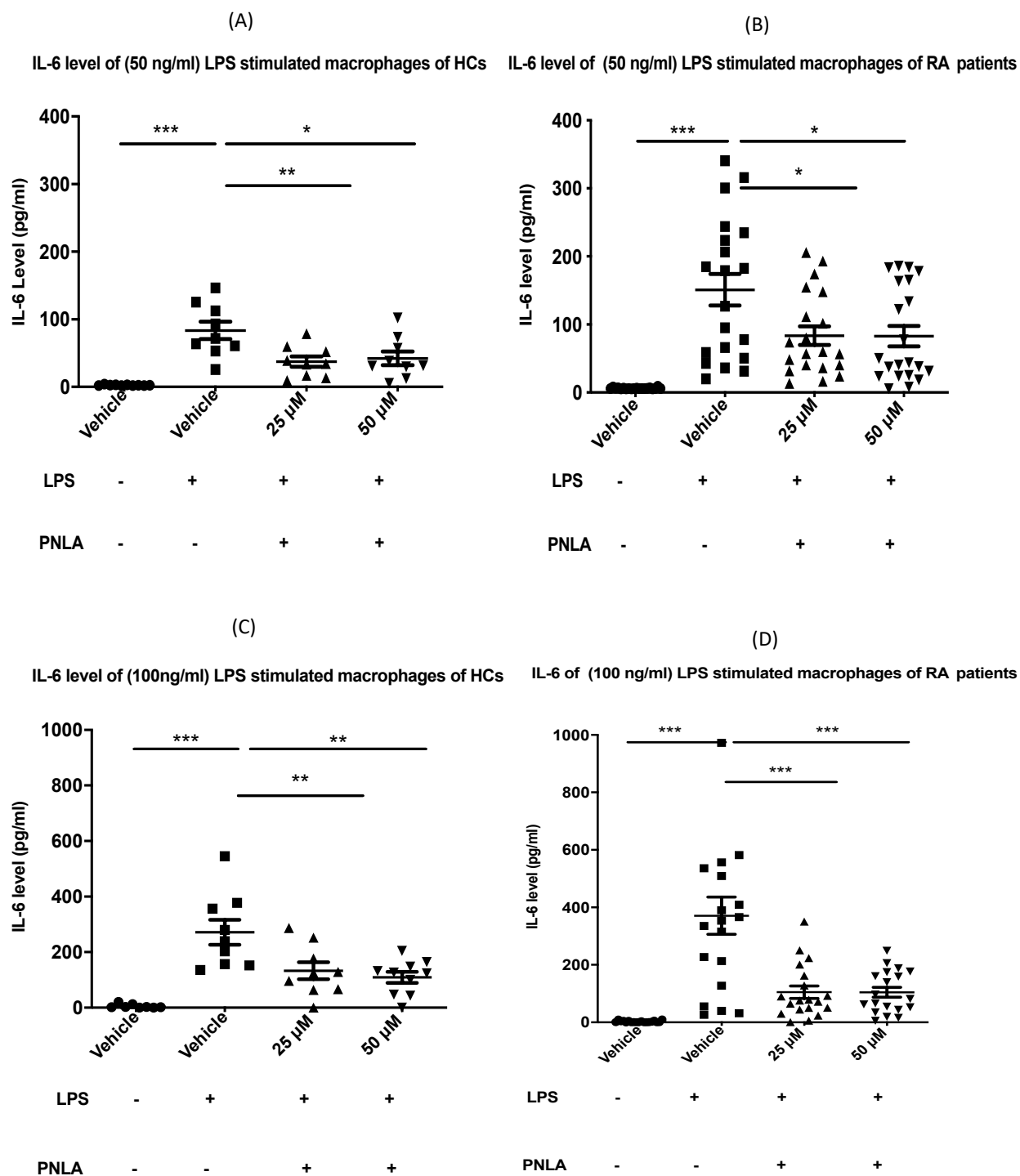


Figure 4.6. IL-6 level is reduced following incubation of activated enriched macrophages from HCs and RA patients with PNLA.

Differentiated macrophages obtained from RA patients (n=20) and HCs (n=10) were incubated with 25, 50 μM PNLA or DMSO for 24 hours, followed by LPS stimulations at 50 ng/ml (A, B) or 100 ng/ml (C, D) for another 16-18 hours. Then, the supernatants were collected and assayed for levels of IL-6 using ELISA; all samples and standards were run in duplicate. The data are presented as the mean \pm SEM, each dot (\bullet) represents the average of one participant. Any data transformations were carried out when needed. Statistical analysis was performed using a one-way ANOVA and a Tukey's post hoc test, where (***) $p \leq 0.001$, (**) $p \leq 0.01$ and (*) $p \leq 0.05$.

4.2.4. IL-1 β level was reduced in HCs adherent monocytes but not in RA patients or macrophages upon PNLA treatment.

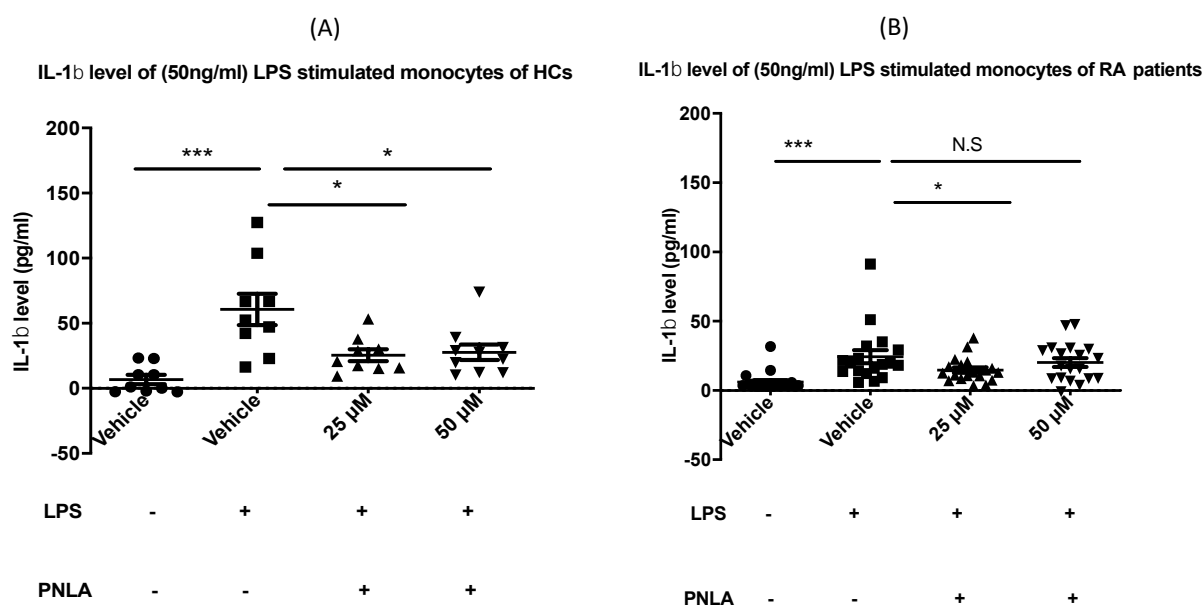
4.2.4.1 HCs and RA adherent monocytes

HCs

LPS-stimulated enriched monocytes at 50 or 100 ng/ml from HCs (n=10) produced IL-1 β (60.66 ± 11.98 pg/ml and 59.80 ± 16.51 pg/ml; $p \leq 0.001$) after 18 hours of stimulation in comparison with non-stimulated monocytes (the negative control). Pre-incubating monocytes with 25 or 50 μ M PNLA and subsequent stimulation with 50 ng/ml LPS significantly reduced IL-1 β levels (**Figure 4.7(A)**) to (25.44 ± 4.566 pg/ml), and (27.74 ± 5.936 pg/ml) respectively (both at $p \leq 0.05$) in comparison with the control (60.66 ± 11.98 pg/ml). In contrast, the release of IL-1 β by 100 ng/ml LPS stimulated monocytes from HCs (59.80 ± 16.51 pg/ml) was reduced to (23.10 ± 8.351 pg/ml, $p \leq 0.05$) and (20.16 ± 3.4 pg/ml, $p \leq 0.05$) by 25 and 50 μ M PNLA treatment (**Figure 4.7(C)**).

RA

There was a statistically significant reduction of IL-1 β level (24.32 ± 4.727 ; $p \leq 0.001$) in cells pre-treated with 25 μ M PNLA (14.75 ± 2.010 pg/ml; $p \leq 0.05$) and then stimulated with 50 ng/ml LPS. There was a trend towards of IL-1 β reduction in cells pretreated with 50 μ M PNLA (20.15 ± 3.146 pg/ml), but this did not reach statistical significance ($p=0.35$) (**Figure 4.7(B)**). IL-1 β levels from 100 ng/ml LPS stimulated enriched monocytes of RA patients were reduced from 34.32 ± 8.419 pg/ml; $p \leq 0.001$) to 21.04 ± 3.807 pg/ml and 25.55 ± 3.587 pg/ml ($p=0.230$ and 0.514) by 25 and 50 μ M PNLA, respectively (**Figure 4.7(D)**). Interestingly, IL-1 β released by 50 and 100 ng/ml LPS-stimulated enriched monocytes from patients with RA was numerically lower than HCs.



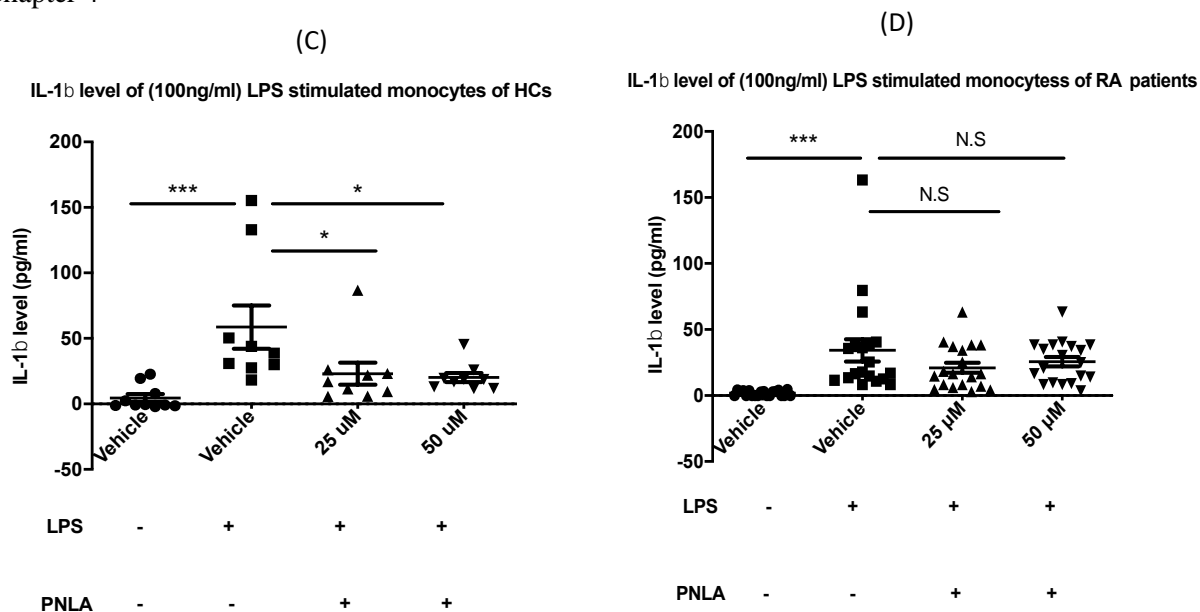


Figure 4.7. IL-1 β level is reduced following incubation of activated monocytes from HCs but not RA patients.

Purified monocytes obtained from RA patients (n=20) and HCs (n=10) were incubated with 25, 50 μ M PNLA or DMSO for 24 hours, followed by LPS stimulations at 50 ng/ml (A, B) or 100 ng/ml (C, D) for another 16-18 hours. Then, the supernatants were collected and assayed for levels of IL-1 β using ELISA; all samples and standards were run in duplicate. The data are presented as the mean \pm SEM, each dot (\bullet) represents the average of one participant. Statistical analysis was performed using a one-way ANOVA and a Tukey's post-hoc-test, where (***) $p \leq 0.001$, ($*$) $p \leq 0.05$, and N.S=not significant).

4.2.4.2 HCs and RA differentiated macrophages

HCs

IL-1 β level in 50 ng/ml LPS stimulated macrophages from HCs was (7.966 ± 0.790 pg/ml; $p \leq 0.025$). PNLA treatment at 25 (6.77 ± 0.311 pg/ml) and 50 μ M (6.821 ± 0.190 pg/ml) did not statistically significantly reduce IL-1 β levels (**Figure 4.8(A)**). This may be due to the low level of IL-1 β produced by LPS stimulation.

RA

For RA patients, IL-1 β level in 50 ng/ml LPS stimulated macrophages was (13.49 ± 0.94 pg/ml, $p \leq 0.028$) and pre-treatment with 25 and 50 μ M PNLA reduced this level to (12.88 ± 0.65 pg/ml) $p=0.139$ and (12 ± 0.687 pg/ml) $p=0.165$, respectively (**Figure 4.8(B)**).

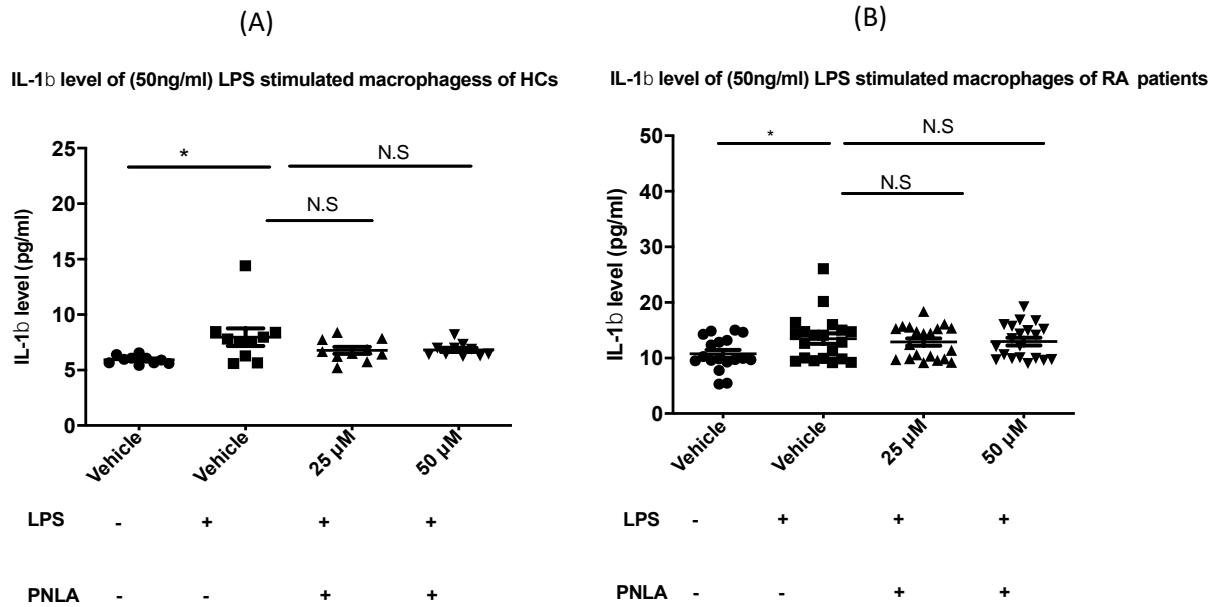


Figure 4.8. PNLA has no effect on IL-1 β level from LPS activated enriched macrophages of HCs and RA patients.

Differentiated macrophages obtained from RA patients (n=20) and HCs (n=10) were incubated with 25, 50 μ M PNLA or DMSO for 24 hours, followed by LPS stimulations at 50 ng/ml (A, B) for another 16-18 hours. Then, the supernatants were collected and assayed for levels of IL-1 β using ELISA, all samples and standards were run in duplicates. The data are presented as the mean \pm SEM, each dot (\bullet) represents the average of one participant. Any data transformations were carried out when needed. Statistical analysis was performed using a One-way ANOVA and Tukey's post hoc test, where (* $p \leq 0.05$ and N.S.=non-significant).

4.2.5. PGE2 level was reduced significantly upon PNLA treatment.

4.2.5.1 HCs and RA adherent monocytes

HCs

LPS at 50 ng/ml stimulated enriched monocytes from HCs (n=10) to increase the release of PGE2 (650.95 ± 85.4 pg/ml) ($p \leq 0.001$) significantly in comparison to unstimulated cells (negative control). When pre-treating these stimulated monocytes with 50 μ M PNLA, there was a significant reduction of PGE2 level to 295.35 ± 26.3 pg/ml ($p \leq 0.001$) (**Figure 4.9(A)**).

RA

Similar to HCs, in patients with RA (**Figure 4.9(B)**), LPS stimulation led to a statistically significant increase in the production of PGE2 at 503.71 ± 48.6 pg/ml ($p \leq 0.001$) in comparison to unstimulated cells (negative control). PNLA treatment at 50 μ M reduced PGE2 levels by a similar proportion to that observed in HCs (288 ± 26.10 pg/ml; $p \leq 0.001$).

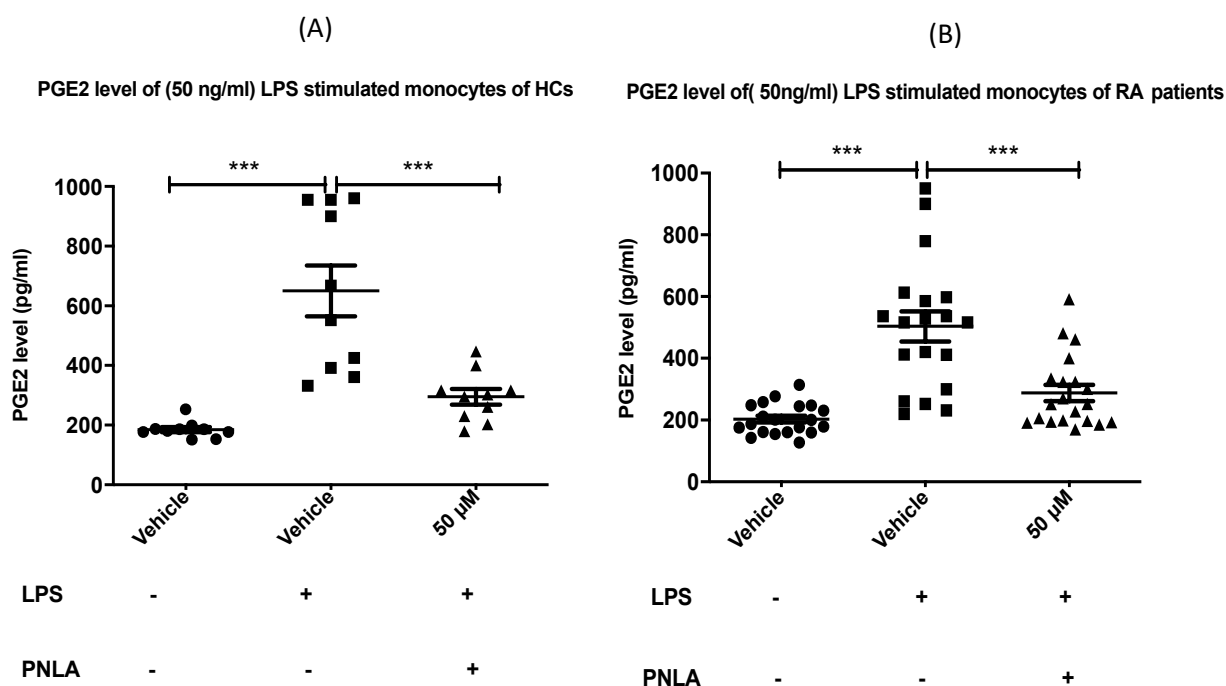


Figure 4.9. PGE2 level is reduced following incubation of activated enriched monocytes from HCs and RA patients with PNLA.

Purified monocytes obtained from RA patients (n=20) and HCs (n=10) were incubated with 50 μ M PNLA or DMSO for 24 hours, followed by LPS stimulations at 50 ng/ml (A, B) for another 16-18 hours. Then, the supernatants were collected and assayed for levels of PGE2 using ELISA; all samples and standard were run in duplicate. The data are presented as the mean \pm SEM, each dot (\bullet) represents the average of one participant. Any data transformations were carried out when needed. Statistical analysis was performed using a one-way ANOVA and a Tukey's post hoc test, where (***) $p \leq 0.001$.

4.2.5.2 HCs and RA differentiated macrophages

HCs

Upon stimulation by 50 ng/ml LPS, enriched macrophages from HCs (n=10) statistically significantly increased the release of PGE2 (279.9 ± 8.95 pg/ml; $p \leq 0.001$) in comparison to the unstimulated cells (**Figure 4.10(A)**). A statistically significant reduction in PGE2 level was observed following pre-treatment with 50 μ M PNLA (254 ± 5.5 pg/ml) ($p \leq 0.05$). However, after 100 ng/ml LPS stimulation, 50 μ M PNLA pre-treated enriched macrophages released 294.9 ± 5.7 pg/ml of PGE2, which was similar to LPS stimulated cells (280.7 ± 10.07 pg/ml; $p = \text{N.S}$) (**Figures 4.10(C)**).

RA

For macrophages from RA patients (n=20), there was a statistically significant increase in the production of PGE2 levels after 50 and 100 ng/ml LPS stimulation, to 321.3 ± 11.4 pg/ml and 354.4 ± 26.2 pg/ml, respectively, (both $p \leq 0.001$). Pre-treating cells with 50 μ M PNLA reduced the levels of PGE2 to 274 ± 9.07 pg/ml ($p \leq 0.001$) and 294.2 ± 8.32 pg/ml ($p \leq 0.01$) respectively (**Figure 4.10(B and D)**).

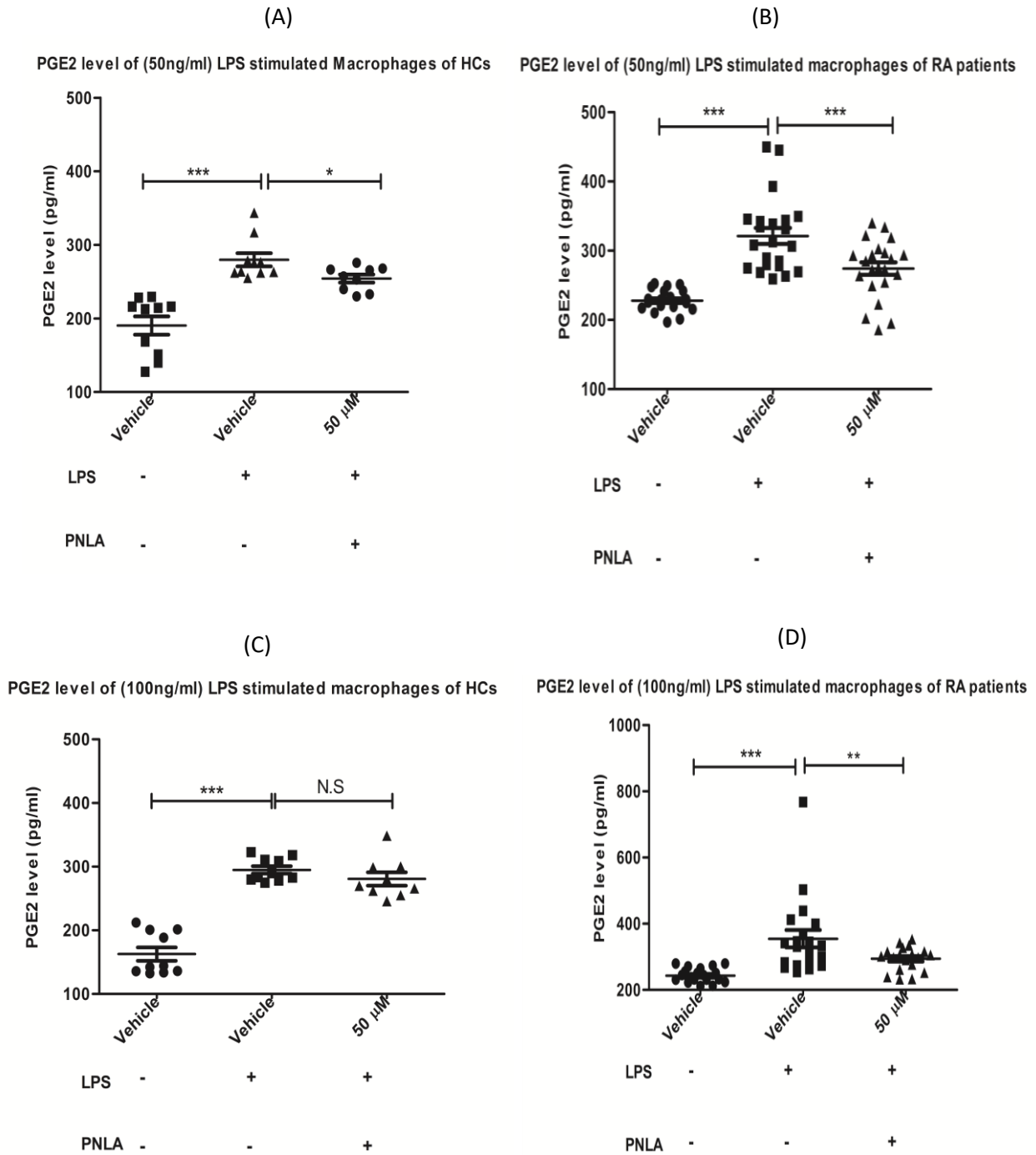


Figure 4.10. PGE2 level is reduced following incubation of activated macrophages of HCs and RA patients with RA.

Differentiated macrophages obtained from RA patients (n=20) and HCs (n=10) were incubated with 50 μ M PNLA or DMSO for 24 hours, followed by LPS stimulations at 50 ng/ml (A, B) or 100 ng/ml (C, D) for another 16-18 hours. Then, the supernatants were collected and assayed for levels of PGE2 using ELISA, all samples and standard were run in duplicate. The data are presented as mean \pm SEM, each dot (\bullet) represents an average of one participant. Any data transformations were carried out when needed. Statistical analysis was performed using a one-way ANOVA and a Tukey's post hoc test, where (***) $p \leq 0.001$, (*) $p \leq 0.05$, and N.S.=non-significant).

4.2.6. Nitrite (NO₂)

4.2.6.1 HCs and RA adherent monocytes

In unstimulated enriched monocytes from RA patients (n=20), nitrite levels were below the detection range of the kit except in 1 patient (data not shown), for the statistical analysis, levels below the detection range (2.5-100 μ M) were imputed as zero. Based on this, there was a statistically significant increase in the production of nitrite upon 50 ng/ml of LPS stimulation (3.56 ± 0.23 pg/ml, $p < 0.0001$) in comparison with unstimulated cells (0 pg/ml). Pre-incubation with 25 μ M PNLA led to a reduction of nitrite levels from enriched monocytes from patients with RA to 1.56 ± 0.18 pg/ml ($p = 0.03$) after imputed levels lower than the detection range to zero. After pre-treating enriched monocytes with 50 μ M PNLA, the nitrite level was below the detection limit in 6 patients. Imputing the results as zero, the mean level of nitrite was 1.37 ± 0.26 pg/ml ($p = 0.62$). The reduction was not statistically significant. Nitrite released by enriched monocytes (LPS stimulated with or without PNLA treatment) from HCs was below the detection limit, and as a result, statistical analysis was not feasible.

4.2.6.2 HCs and RA differentiated macrophages

In activated macrophages from HCs (**Figure 4.11(A)**), there was a statistically significant increase in the production of nitrite upon 50 ng/ml LPS stimulation in comparison with unstimulated cells (10.4 ± 1.29 pg/ml, $p = 0.001$). Pre-treating the cells with 25 μ M PNLA produced a marked reduction of the nitrite level (4.55 ± 0.89 pg/ml, $p = 0.002$). However, this was not the case upon pre-treating with 50 μ M PNLA (9.29 ± 1.37 pg/ml, $p = 0.83$).

In RA patients (**Figure 4.11(B)**), when macrophages were stimulated with 50 ng/ml LPS, there was a significant increase in the production of nitrite (17.4 ± 2.28 pg/ml, $p \leq 0.0001$). Similar to monocytes, many samples were below the detection range. Results from these were imputed as zero. PNLA at 25 μ M reduced nitrite production (9.66 ± 1.8 pg/ml, $p = 0.019$). However, the effect of 50 μ M PNLA (13.7 ± 2.65 , $p = 0.40$) was not statistically significant. These results were similar even when the experiments were replicated by varying the LPS stimulation incubation period to 24, 48, and 72 hours (data not shown).

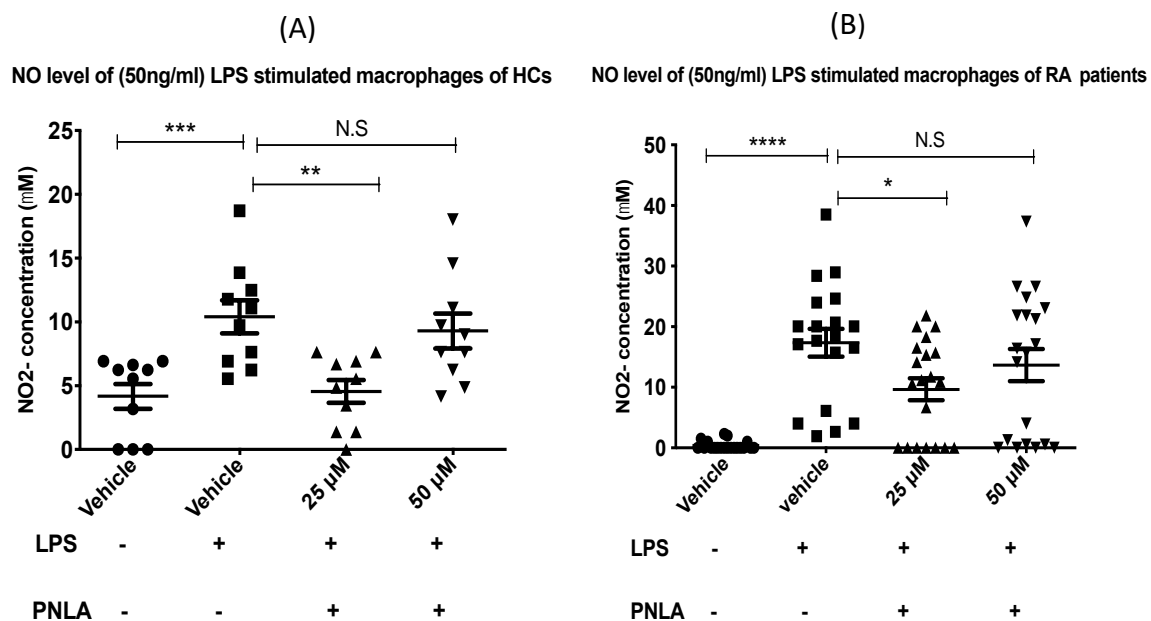


Figure 4.11. NO₂⁻ level is reduced following incubation of activated enriched macrophages from HCs and RA patients with PNLA.

Differentiated macrophages obtained from HCs (n=10) and RA patients (n=20) were incubated with 25, 50 μ M PNLA or DMSO for 24 hours, followed by LPS stimulations at 50 ng/ml (A, B) for another 16-18 hours. Then, the supernatants were collected and assayed for levels of NO₂⁻ using Griess reagent, all samples and standard were run in duplicate. The data are presented as the mean \pm SEM, each dot (\bullet) represents an average of one participant. Any data transformations were carried out when needed.

4.3. Discussion

In this Chapter, we extend previous observations in cell lines and primary culture by demonstrating the anti-inflammatory potential of PNLA using enriched monocytes and macrophages isolated from patients with RA and HCs. Cytokines are currently at the forefront of medicine, both as culprits in the pathogenesis of many diseases associated with inflammation and as increasingly popular targets for therapeutic antibodies. In recent years, cytokine inhibitors have been developed, which are promising new drug treatments focusing on the inhibition of the cytokine pathway with the result of decreasing cytokine production and inflammation in RA. However, side effects of these biologics and conventional treatments, that patients take (for example, JAKi) cause neutropenia in some patients, leading to increased infection rates.

We showed that PNLA significantly reduced TNF- α (**Figures 4.3 and 4.4**), IL-6 (**Figures 4.5 and 4.6**), and PGE2 (**Figures 4.9 and 4.11**) in the supernatants of LPS stimulated enriched monocytes and macrophages from patients with RA and HCs. Given that TNF- α and IL-6 are the main therapeutic targets in RA and that PGE2 has a key role in the induction of inflammatory pain, PNLA may have therapeutic benefits in RA. Results from this Chapter confirm the previous results using murine microglial BV-2 cell lines and murine cell lines (RAW264.7). Chen *et al.* showed that PNLA incorporation into phospholipids suppressed the production and expression of pro-inflammatory mediators; NO, IL-6, TNF- α by 41, 74 and 27%, respectively, and reduced PGE2 significantly (Chen *et al.* 2015). These effects were mediated partially through the alleviation of LPS-activated JNK-MAPK signaling. Furthermore, in 2019, Chen *et al.* confirmed these results in THP-1 macrophages, as they demonstrated that pre-incubation with PNLA reduced the production of TNF- α , IL-6, and PGE2 by 18, 46, and 87%, respectively, in LPS stimulated cells. The expression of the COX-2 protein was significantly suppressed (Chen *et al.* 2019). In 2015, Chen *et al.* reported that there is a downregulation of LPS-induced *iNOS* (54%) protein expression in murine microglial BV-2 cells by PNLA, although *iNOS*, and COX-2 gene expressions were not downregulated. Others reported no suppression in COX-2 protein in LPS stimulated RAW264.7 macrophages after PNLA treatment (Chuang *et al.* 2009), while they reported PGE2 level inhibition in the same cell model by PNLA treatment. Thus, the inhibitory effect of PNLA on PGE2 production may not be exerted through suppression of COX-2 gene expression but through a modified FA composition of cellular phospholipids. One way of testing this hypothesis is to assess cell membrane FA composition using high-performance liquid or gas chromatography.

In support of the murine model and THP-1 human cells; Baker *et al* in 2020 showed a similar observation in an EC line in which NF- κ B and COX2 gene expressions were not down-regulated after PNLA and DHA treatment in comparison with TNF- α stimulated control cells. However, Western blotting showed that PNLA and DHA reduced COX2 and NF- κ B protein expression in stimulated ECs. This data suggests FAs, including PNLA, may modulate some protein expression through post-translational modifications. This hypothesis will require future experiments using techniques such as Western blotting, immunoprecipitation, mass spectrometry, and miRNA experiments.

The effect of a dietary pine nut supplement on inflammation and immunity has not been studied in humans. In this study, we showed that while LPS-stimulated rheumatoid monocytes significantly induced the production of IL-1 β , PNLA was able to reduce this level in the healthy state, but this did not reach statistical significance in monocytes from RA patients (**Figure 4.7**). Similarly, in HCs and RA macrophages, there was no significant reduction in IL-1 β levels by PNLA treatment relative to the stimulated control (**Figure 4.8**). On the other hand, Chen *et al* in 2019 showed a significant reduction in IL-1 β using the THP-1 cell line treated with PNLA, as mentioned earlier. It is worth noting that there are differences between PNLA and dietary pine nuts. Two animal studies have investigated the effect of including PNO in the diet on the immune system. In a study by Matsuo *et al.* in 1996, rats were fed *Pinus koraiensis* oil and immunised with intraperitoneal ovalbumin. The proportion of CD4 T-cells in the spleen, together with the production of LTB4 and immunoglobulins (Ig)-E and -G by spleen cells, were higher in rats that received PNO compared to those that received safflower oil (a source of LA; n-6) or evening primrose oil (a source of GLA; n-6) (Matsuo *et al.* 1996). Therefore, it is concluded that PNLA has the potential to modulate the immune response. However, information regarding the effect of PNO on immune function is still limited. Whether PNLA has a similar effect to a dietary supplement made with pine nuts remains controversial. Some studies suggest that dietary pine nut supplements may exacerbate the immune response. Lin *et al.* (2017) reported that a low dose diet of *Pinus koraiensis* 0.1g/kg/day in immunocompromised (cyclophosphamide injected) mice, increased IL-2, IL-4, IL-6, and IFN- γ in the supernatants of cultured splenocytes activated by concanavalin A (Lin *et al.* 2017). Park *et al.* also suggested there is a probability that PNO has the effect of activating the immune response (Park *et al.* 2013). They suggested the production of IL-1 β by splenocytes was higher in HFD-induced mice fed with PNO in comparison with the control this effect might contradict the anti-inflammatory actions of PNLA reported by others. This difference may be accounted for by the fact that studies by Chen *et al.* (2015) and Chuang *et al.* (2009) used PNLA, whereas

Park *et al.* and Lin *et al.* used PNO. This needs to be studied in some depth in future studies to confirm these findings and may need to be carefully considered when designing future studies.

With regards to NO, although I was able to detect some reduction in nitrite by 25 μ M PNLA in HC and RA macrophages (**Figure 4.11(A, B)**), I could not fully replicate and extend the observation by Chen *et al.* There are several potential explanations. First, Chen *et al.* were able to detect nitrite levels in the supernatants of activated cells using the same reagent as this study (the Griess reagent). Chen *et al.* used DMEM media (which contain an undetectable level of nitrite) rather than the RPMI media that were used in all the experiments in this thesis, although the manufacturer of this assay recommends using RPMI media for both the experimental samples and the standard reference. The second possible explanation is the inability of human monocytes and macrophages to produce NO *in vitro*, unlike murine macrophages (McInnes 1996). The third possibility is that previous studies used a combined stimulus with LPS and IFN- γ rather than only using LPS, which was the case in this thesis. Finally, as NO is metabolised to nitrite and nitrate, assessing nitrite alone may not fully detect NO degradation. Assessing nitrate levels will test this hypothesis.

TNF and IL-6 production by 2 doses of LPS (50, 100 ng/ml) were not similar, while the effects of PNLA were similar, suggesting that the cytokine reduction has reached a plateau. The effects of PNLA in HCs and RA patients were similar, but we did not hypothesize there would be a difference between the 2 groups. I anticipated that patients with RA, due to chronic inflammation, may be more resistant to a reduction in cytokines, but this was not the case. As we did not quantify the monocyte population, we did not attempt to adjust this for monocyte number. To confirm that TNF and IL-6 production were reduced in purified monocyte subsets, we conducted experiments using flow cytometry in Chapter 6.

In summary, the findings in this Chapter can emphasise the potentially beneficial aspects of PNLA in patients with RA, suggesting that PNLA may reduce inflammatory cytokines and pain; a low remission rate and persistent pain are major unmet needs in RA. This provides the scientific rationale to conduct clinical trials to investigate the effect of PNLA given either by diet, as in pine nuts, or as a supplement that may complement current treatment for patients with RA who are taking standard therapy but have failed to achieve remission.

Chapter 5: Effects of PNLA on the inflammatory gene expressions implicated in the pathogenesis of RA and atherosclerosis

5.1. Introduction and aims

In the previous Chapter, we showed that PNLA reduced TNF- α , IL-6, and PGE2 release by LPS-stimulated enriched monocytes and macrophages from HCs and patients with RA. The molecular mechanisms by which PNLA reduced TNF- α , IL-6, and PGE2 are unknown. The aim of this Chapter is to examine the gene expressions and transcript changes annotated for these mediators using RNA-seq. RNA-seq is a readout of the entire set of RNA transcripts found within a cell or population of cells. It also has the potential to discover previously unknown mechanisms and pathways.

The production of IL-1, TNF- α and IL-6 is mediated by different biologic pathways. A pathway is a chain of interactions between proteins in cells and is involved in processes such as cell activation, proliferation, and cell death. The pathway communicates information from chemical signals outside of a cell to the cell nucleus, resulting in the activation of genes through a process called transcription. In this context, it is not feasible to examine multiple potential mechanisms in a time-efficient manner using traditional assays such as qPCR. Thus, the primary objective of this Chapter is to explore the potential pathways whereby PNLA-mediated TNF- α , IL-6, and PGE2 production suppression occurs. Secondary analyses included investigating the transcriptomic profile of PNLA-treated LPS-stimulated PBMCs in comparison with unstimulated and LPS-stimulated PBMCs among both HCs and RA patients.

Transcriptome analysis has been used in the study of rheumatic diseases, including RA. The pathobiology of Early Arthritis Cohort (PEAC) was a multi-centre study of patients with RA at the time of diagnosis before any treatment. Transcriptome analyses were conducted and compared synovial tissues obtained by biopsies with matched PB samples, with synovial transcriptional gene signatures showing three distinct pathotypes: a fibroblastic pauci-immune pathotype, a macrophage-rich diffuse-myeloid pathotype, and a lympho-myeloid pathotype suggestive of divergent pathogenic pathways or activation disease states. Different pathotypes were associated with prognosis and clinical response to initial drug therapy (Lewis *et al.* 2019). However, the transcriptomic profile of CVD associated with RA has not been reported.

Understanding how the expression of transcripts changes during LPS stimulation and after PNLA treatment can provide insight into the mechanisms whereby PNLA reduces TNF, IL-6, and PGE2. Thus, I hypothesised that the potential biological pathways could involve NF- κ B and JAK-STATs as the main downstream intracellular effectors involved in the transcription of these cytokines and the eicosanoid PGE2, as illustrated in **Figure 5.1**. These signalling pathways have been discussed in the introduction in sections 1.6.1.1, 1.6.2.1, and 1.6.3.1.

This Chapter describes the RNA-seq data comparing unstimulated, LPS-stimulated, and PNLA-treated LPS-stimulated PBMCs from patients with RA and HCs for the genes, pathways, and transcription factors of interest. PBMCs were pre-treated with 25 μ M PNLA or vehicle for 24 hours, with or without LPS incubation for a further 16 hours. The chosen concentration of PNLA herein is based on its optimal response that was obtained in Chapters 3 and 4.

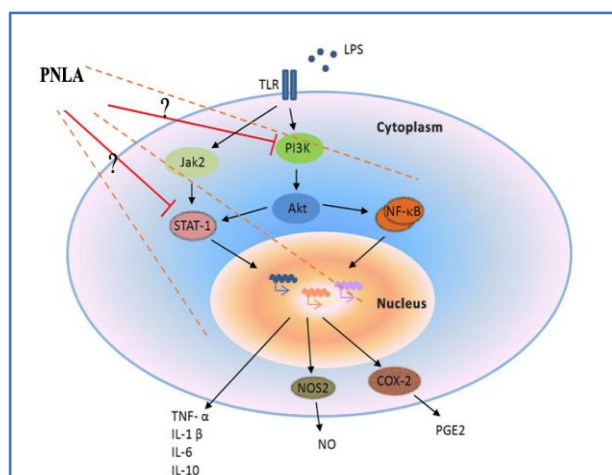


Figure 5.1. PNLA affects TNF- α , IL-6, NO, and PGE2 levels in the cell supernatants. Highlighting the possibility of NF- κ B inhibition and giving implications for intracellular signalling molecules such as STAT1, Jak2, and PI3K inhibition. This hypothesis was explored in this Chapter.

5.2. Results

5.2.1. Principle component analysis (PCA)

PCA was performed in R using normalised data from the DESeq2 analysis. The data were clustered using the top 50 DEGs overall comparisons combined. The plot shows the results of the first 2 principal components. The results show samples clustering within groups, demonstrating that inter-sample variation in gene expression is not greater than the biology we hope to observe. Samples in HC samples are less variable in terms of gene expression compared to the separation within clusters shown by the RA samples (**Figure 5.2**).

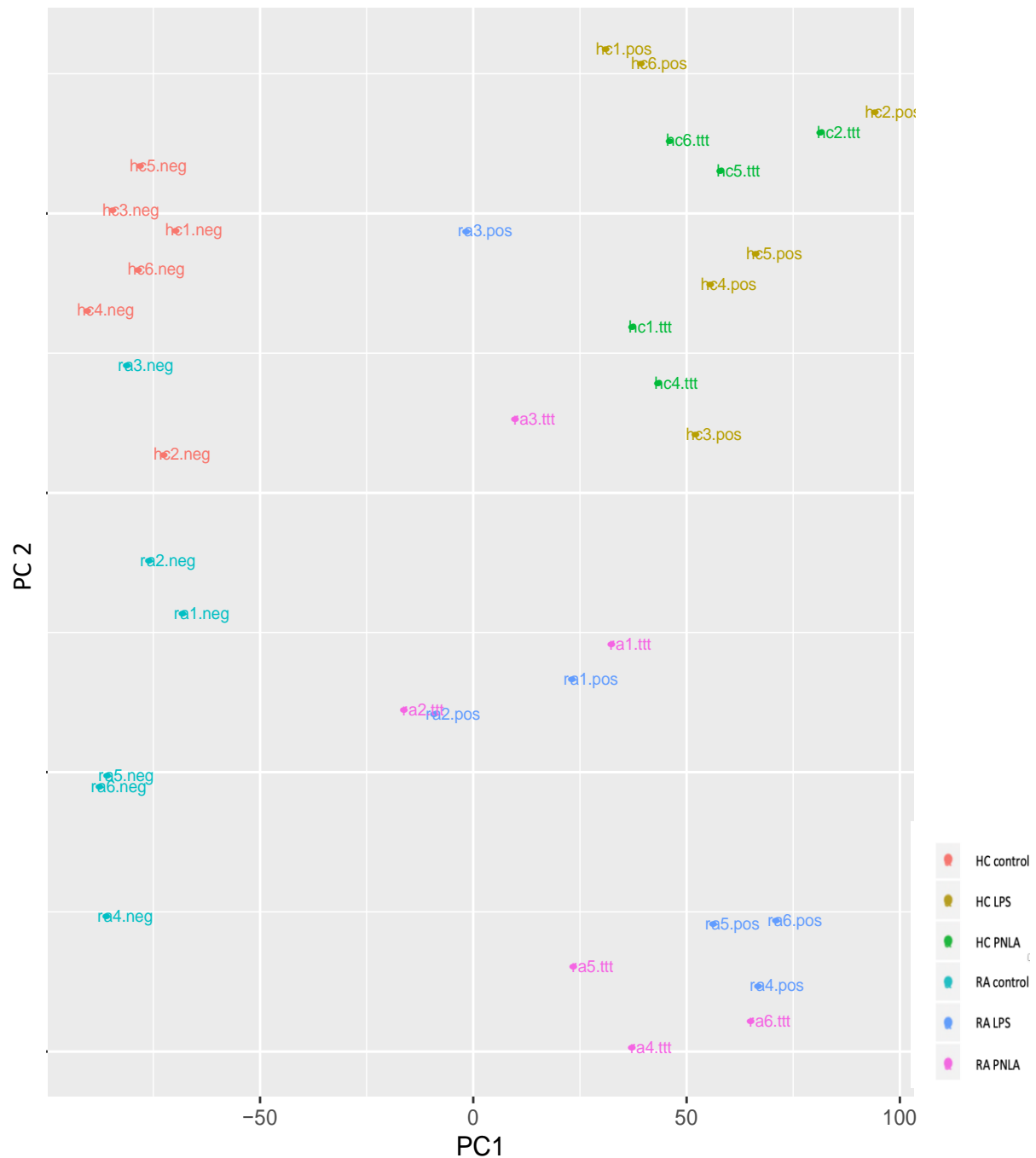


Figure 5.2. Principal component analysis (PCA) from DESeq2 analysis of HCs and RA patients DEGs. Each principal component (PC) on the y-axis is plotted against the variance it contributes within the dataset on the x-axis. The horizontal line indicates an arbitrary threshold for PCs that contribute a significant proportion of the variance. PCA analysis was performed on the 36 samples to try and discover trends in the data, as samples in the same area of the graph are genetically similar. Each dot represents an individual sample representative of 50 genes, and all samples are colour coded per condition.

5.2.2. Heatmap

The heatmap (**Figure 5.3**) shows the main clusters of DEGs for all treatment conditions mentioned. The expression of genes in vehicle treated PBMCs was upregulated, while PNLA and LPS treatment downregulated those genes. The HCs clusters on the left side were more consistent than the RA clusters on the right side, which show some variability.

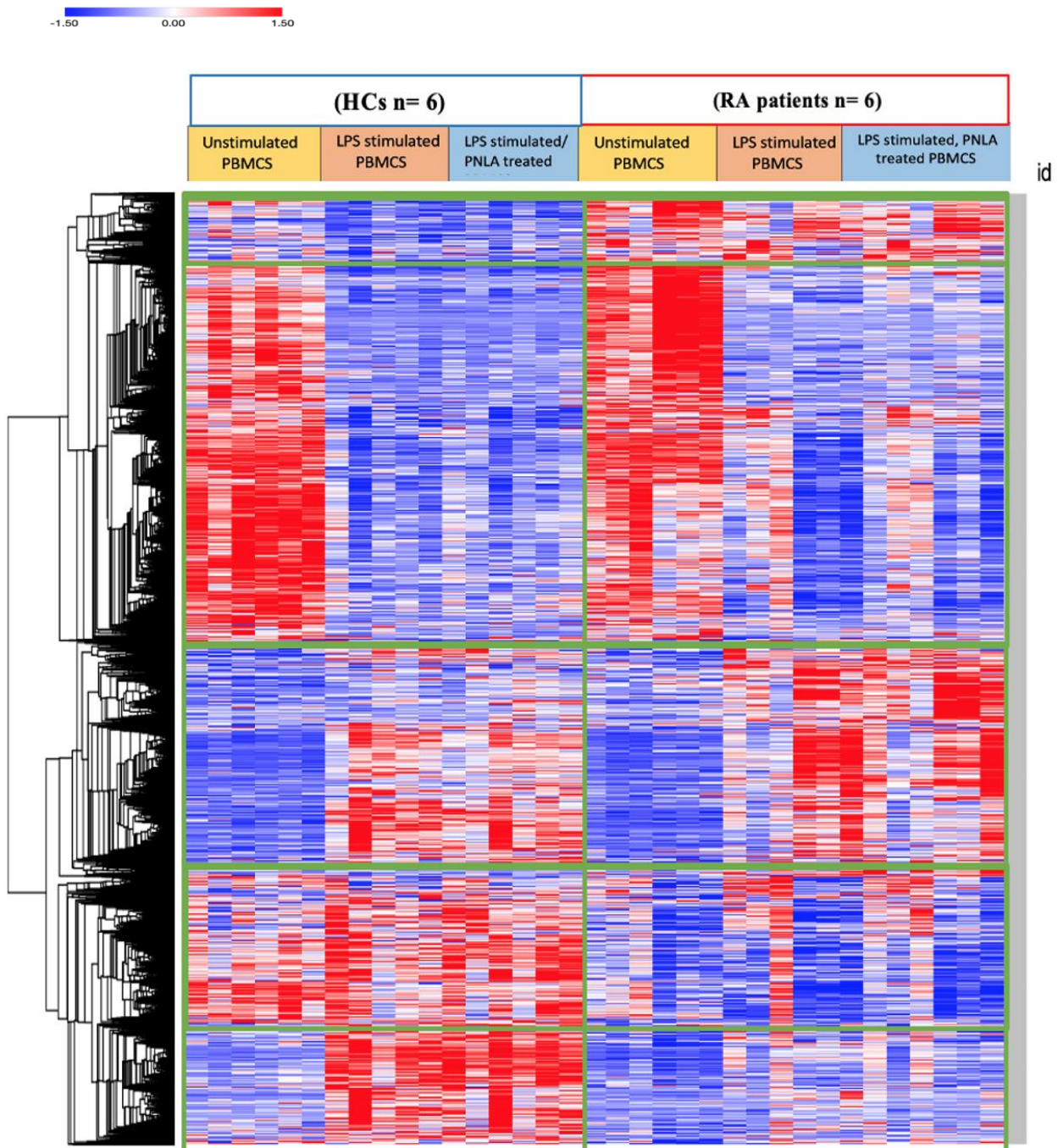


Figure 5.3. Heatmap for whole genomic transcriptome of HCs and RA patients.

Healthy controls` (HCs) and rheumatoid patients` (RA) main clusters. 36 samples from 6 HCs and 6 RA patients with 3 conditions/participant: condition 1 unstimulated PBMCs, condition 2 LPS stimulated plus vehicle treated and condition 3 PNLA treated and LPS stimulated PBMCs. The map was generated using the broad Morpheus software. Heatmap visualisations used log₂ fold change (log₂FC). Data sets were hierarchically clustered using one-minus Pearson correlation coefficient.

5.2.3. Volcano plots

Using GraphPad Prism version 8, HCs and RA patients' global significant and non-significant genes were plotted as volcano plots, and comparisons between groups were performed as shown in **Figure 5.4** for HCs and **Figure 5.5** for RA patients. The significantly regulated genes are shown outside the dotted lines, with $\log_2 \text{FC} < -1.5$ and > 1.5 ; p value < 0.05 .

A. HCs

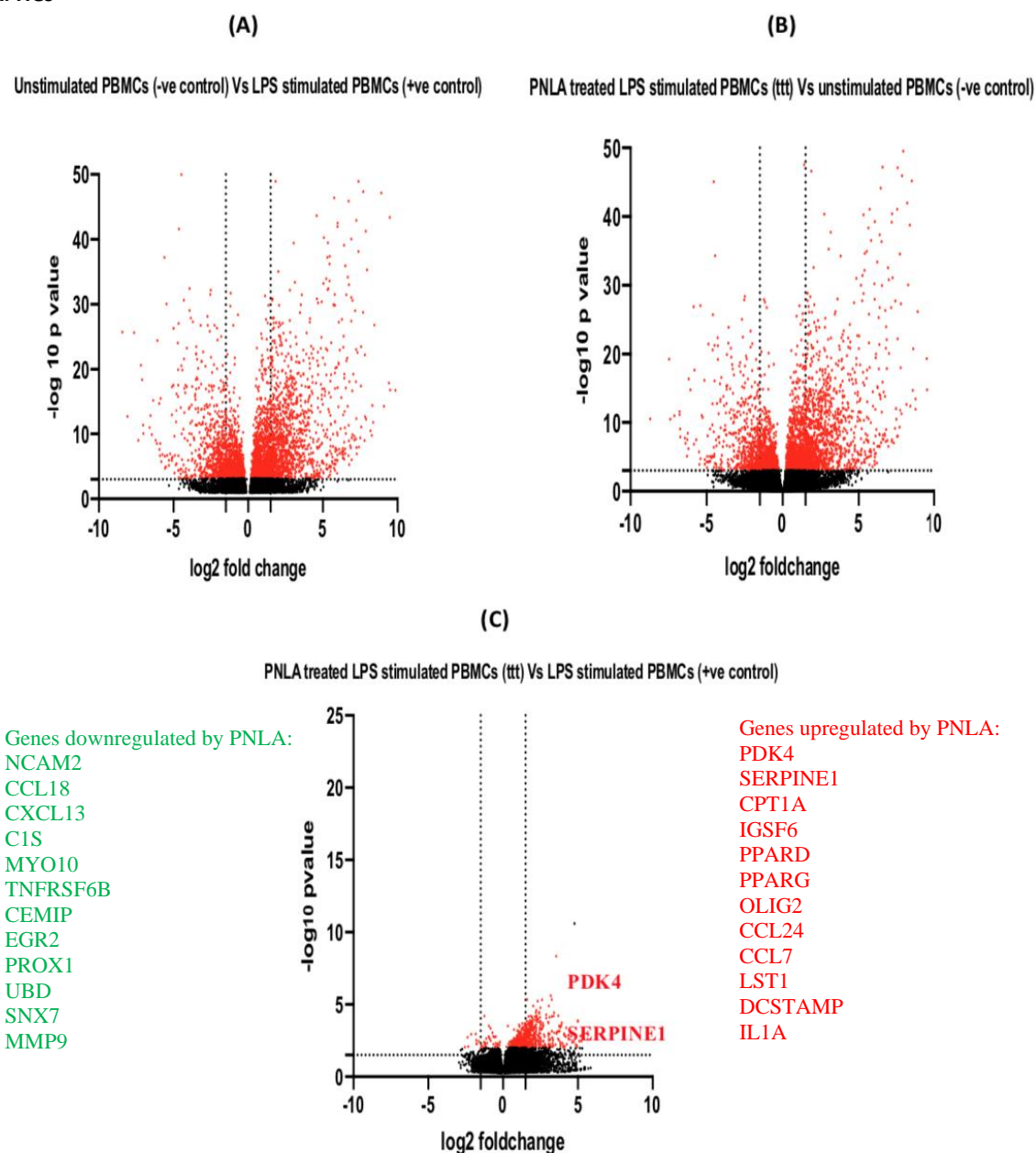


Figure 5.4. Volcano plots of the global gene expression profile of HCs.

Dotted lines identify genes whose expression was significantly regulated ($\log_2 \text{FC} < -1.5$ and > 1.5 , $p < 0.05$) after 24 hours of 25 μM PNLA or vehicle treatment and 16 hours post 100 ng/ml LPS stimulation. (A) shows unstimulated versus LPS stimulated PBMCs; (B) shows PNLA treated, LPS stimulated versus vehicle stimulated PBMCs; (C) shows PNLA treated, LPS stimulated versus vehicle treated, LPS stimulated PBMCs from HCs and RAs. Plots were performed on (GraphPad Prism version 8) with genes marked as p value < 0.05 .

(B) RA patients

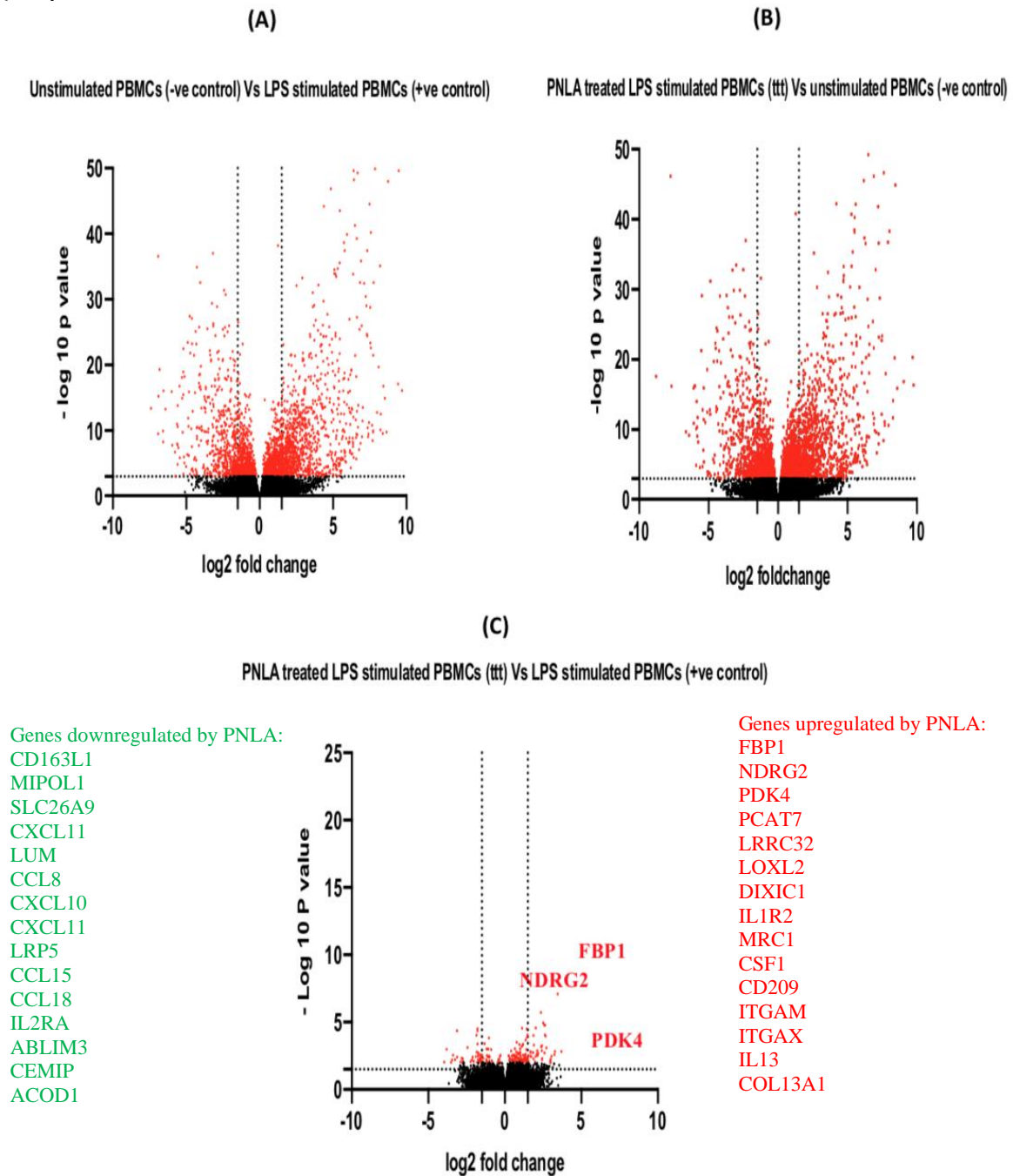


Figure 5.5. Volcano plots of the global gene expression profile of RA patients.

Dotted lines identify genes whose expression was significantly regulated (\log_2 FC < -1.5 and > 1.5 , $p < 0.05$) after 24 hours of $25 \mu\text{M}$ PNLA or vehicle treatment and 16 hours post 100 ng/ml LPS stimulation. (A) shows unstimulated versus LPS stimulated PBMCs; (B) shows PNLA treated, LPS stimulated versus vehicle stimulated PBMCs; (C) shows PNLA treated, LPS stimulated versus vehicle treated, LPS stimulated PBMCs from HCs and RAs. Plots were performed on (GraphPad Prism version 8) with genes marked as p value < 0.05 .

5.2.4. DEGs that were statistically significantly regulated by PNLA in PBMCs from RA patients or HCs.

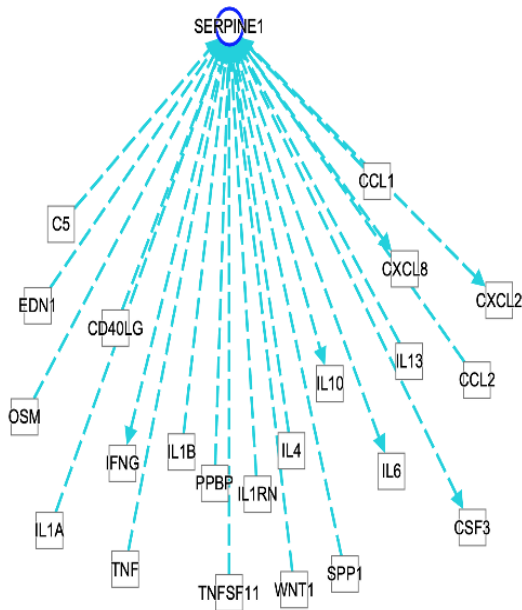
Figure 5.6 shows the genes and their ingenuity network with the important molecules affecting RA and atherosclerosis (details of each molecule and the nature of their relationship are not provided here). SERPINE1 and PDK4 were significantly upregulated in PNLA treated LPS stimulated PBMCs of HCs. While FBP1, NDRG2, and PDK4 were significantly upregulated in PNLA treated LPS stimulated PBMCs in RA patients (adjusted p-value < 0.05).

1. **Serine protease inhibitor-1 (SERPINE-1) or plasminogen activator inhibitor-1 (PAI-1).** This gene was upregulated by PNLA in HCs (adjusted p=0.002436451; log₂ FC=2.60348701). Plasminogen activators (PAs) are serine proteases that exhibit fibrinolytic activity, and their functions are regulated by plasminogen activator inhibitors (PAI). PAI-1 is a 43-kDa protein belonging to the serpin family that inhibits tissue and urokinase plasminogen activators (tPA and uPA; respectively). uPA/tPA system has been reported to be involved in the degradation of proteins and activation of proteolytic enzymes in the ECM (Rabieian *et al.* 2018) and the conversion of plasminogen to plasmin as summarised in **Figure 5.23**. Although PAI-1 regulates the levels of some cytokines and cell migration (Xu *et al.* 2009), its classical role is thought to be the suppression of fibrinolysis.
2. **Pyruvate dehydrogenase kinase-4 (PDK4).** This gene was upregulated by PNLA in both HCs and RA patients (adjusted p=9.94E-11; log₂ FC=3.784). Four PDK isoforms have been identified in humans, PDK 1, 2, 3, and 4 (Bower-Kinley *et al.* 1998). These isoforms are known to perform similar functions due to the strong conservation of their primary structure, even though they are expressed differently in different cell types (Dlamini *et al.* 2015). Diurnal variation in PDK4 expression in blood cells has been reported to be associated with plasma free FA levels, supporting an important aspect of metabolic fuel switching (Yamaguchi *et al.* 2018).
3. **Fructose biphosphatase-1(FBP-1).** This gene was upregulated by PNLA in RA patients (adjusted p=0.0001937; log₂ FC=3.47737035). FBP-1 is a gluconeogenesis regulatory enzyme that catalyses the hydrolysis of fructose 1,6-bisphosphate to fructose 6-phosphate, acting as a rate-limiting enzyme in gluconeogenesis. Gluconeogenesis is an important pathway for maintaining glucose homeostasis during fasting and low carbohydrate diet intake. In mammalian cells, there are two major pathways to maintain glucose homeostasis: the catabolic glycolysis/oxidative phosphorylation pathway and the

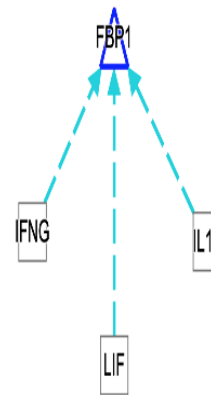
anabolic gluconeogenesis pathway. Altered energy metabolism is proving to be an important differentiating feature of immune cells (monocytes and macrophages), which has been regarded as one of the hallmarks of inflammation (Hosomi and Kunisawa 2020). Recently, it was shown that glycolysis is required for LPS activation and adhesion of human CD14⁺CD16⁻ monocytes (Lee *et al.* 2019), while IL-6 production by M2 macrophages is inhibited by inhibitors of glycolysis (Chiba *et al.* 2017). Together, this suggests that the anti-migratory and anti-inflammatory effects of PNLA may be in part mediated by its effect on glucose metabolism via FBP-1.

- 4. N-myc downregulated gene (NDRG2).** This gene was upregulated by PNLA in RA patients (adjusted $p=0.01731276$; \log_2 FC=2.36119863). It is a member of the N-myc downregulated gene family, which belongs to the alpha/beta hydrolase superfamily. NDRG2 consists of 4 members (NDRG1-4) that show a high level of homology. NDRG2 is highly expressed in the heart, skeletal muscle, cartilage, brain, kidney, and epidermis (Hu *et al.* 2006; Kim *et al.* 2016; Melotte *et al.* 2010). Overexpression of NDRG2 mRNA promotes inhibition of active IL-10 (Lee *et al.* 2010) as we can see in **Figure 5.6 (D)**. The most important functions of the NDRG2 gene are cell proliferation, differentiation, development, stress responses, negative regulation of cytokine production, negative regulation of the ERK1 and ERK2 cascades, and signal transduction. It was shown that NDRG2 expression is implicated in the regulation of the activated leukocyte cell adhesion molecule (ALCAM) in the differentiation of monocytic cells into DCs (Choi *et al.* 2008). NDRG2 promotes bone morphogenic protein-2 (BMP2)-induced osteoblastic differentiation and calcification by activating the JAK3/STAT3 signalling pathway (Chen *et al.* 2020).

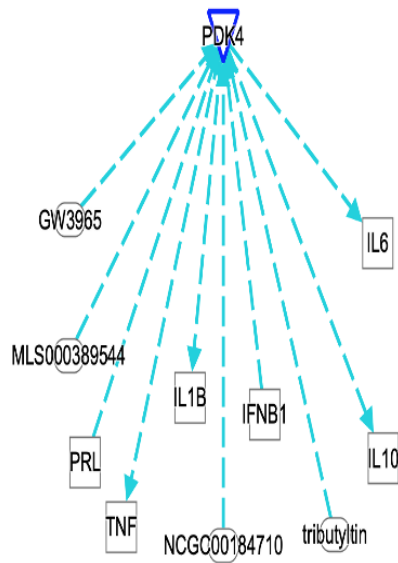
A. SERPINE1



B. FBP1



C. PDK4



D. NDRG2

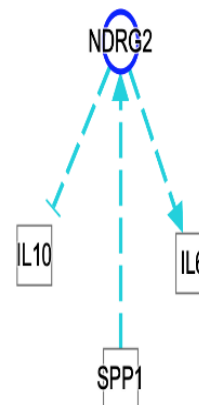


Figure 5.6. The network of the top significant affected genes by PNLA treatment.

The significantly upregulated genes by PNLA pre-treatment versus vehicle treatment of LPS stimulated PBMCs, and their effectors with inflammatory cytokines, chemokines, and molecules based on data set findings in IPA are shown. (Adjusted p value < 0.05).

5.2.5. Canonical Pathways

Using the IPA software, the canonical pathways were determined for all the comparison conditions mentioned in the volcano plots (**Figures 5.4 and 5.5**). I then compared the top canonical pathways for both HCs and RA patients: PNLA-treated and LPS-stimulated PBMCs versus vehicle treated and LPS stimulated PBMCs. **Figure 5.7** shows the interesting pathways in the pathogenesis and treatment of RA and cell metabolism.



Figure 5.7. Canonical pathways of HCs and RA patients of PNLA treatment and LPS stimulation versus vehicle treatment and LPS stimulation of PBMCs

The comparison analysis of the top canonical pathways following 24 hours of PNLA, or vehicle treated and 16 hours of post LPS stimulation of PBMCs per participant was performed in IPA (Log₂ FC>1.2, P<0.05). The pathways shown are mainly involved in the pathogenesis of RA and atherosclerosis.

Overall, the canonical pathways that were altered by PNLA treatment were leukocyte adhesion and diapedesis, IL-8, acute phase response, STAT3, dermatan, as well as chondroitin sulphate degradation in both HCs and RA patients. For the pathways related mainly to RA, altered T cell and B cell signalling, the role of osteoblasts, osteoclasts, and chondrocytes, IL-10 signalling, the role of macrophages, fibroblasts, ECs, and integrin signalling were affected. Interestingly, pathways related to atherosclerosis were more affected in HCs than RA. In HCs, metabolic pathways affecting adipogenesis, glucose metabolism, and cholecystokinin signalling were altered more than in RA, in addition to ROS and NO production.

Due to the variation within the data, there was a smaller chance of differences in gene expression emerging as significant in PNLA treated PBMCs versus LPS stimulated cells with an adjusted p-value ≤ 0.05 . Accordingly, differences with an unadjusted p-value ≤ 0.05 were included in the results section.

5.2.6. Venn diagrams for significant DEGs in HCs and RA patients

5.2.6.1. Venn diagrams of the top 500 genes among the comparison of three experimental conditions in HCs.

1. Comparison of annotated genes, unstimulated versus LPS stimulated (A), LPS stimulated versus PNLA treated (B), and PNLA treated versus unstimulated (C), from HCs.

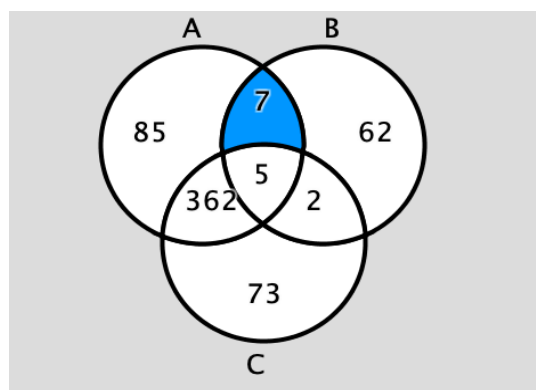


Figure 5.8. Venn diagram of HCs DEGs overlap comparisons A and B

The diagram is showing the number of novel genes in each subset corresponding to the treatment and control conditions. The overlap between (A) and (B) is 7 specific genes. **Key:** **A** (unstimulated PBMCs vs LPS stimulated PBMCs), **B** (PNLA treated and LPS stimulated PBMCs vs LPS stimulated PBMCs), and **C** (PNLA treated and LPS stimulated vs un-stimulated PBMCs).

Table 5.1. Genes that overlap between 2 comparison groups in HCs.

(A: controls vs LPS and B: PNLA vs LPS). The red arrows indicate an increase, while the green arrows indicate a decrease in the expression level.

| Table 5.1.1. Genes that are upregulated by LPS and downregulated by PNLA treatment ($p < 0.05$ / FC < -1.2) | | | | |
|---|--|--|----------|---------|
| Gene symbol | Expr p-value (A)/ Exp Log Ratio (A) | Expr p-value (B)/ Exp Log Ratio (B) | Location | Type(s) |

| | | | | |
|--------------|---------------------|---------------------|---------------------|-----------|
| C1R | ↑ (1.15E-16/ 2.802) | ↓ (0.000073/-1.267) | Extracellular Space | peptidase |
| CCL18 | ↑ (1.02E-21/ 6.048) | ↓ (0.00124/-1.894) | Extracellular Space | cytokine |
| C1S | ↑ (2.09E-14/3.625) | ↓ (0.00235/-1.4) | Extracellular Space | peptidase |
| MYO10 | ↑ (9.88E-16/4.019) | ↓ (0.00347/-1.428) | Cytoplasm | enzyme |

Table 5.1.2. Genes that are downregulated by LPS and upregulated by PNLA treatment (p<0.05/ FC>1.2)

| Gene symbol | Expr p-value (A)/ Expr Log Ratio (A) | Expr p-value (B)/ Expr Log Ratio (B) | Location | Type(s) |
|--------------------|---|---|-----------------|---------|
| PK4 | ↓ (3.58E-25/-6.08) | ↑ (9.94E-11/3.784) | Cytoplasm | kinase |
| CD209 | ↓ (7.2E-18/-3.31) | ↑ (0.00439/1.2) | Plasma Membrane | other |

Table 5.1.3. Genes that are up regulated by LPS and PNLA treatment (p < 0.05/ FC>1.2)

| | | | | |
|-------------|---------------------|--------------------|---------------------|-----------|
| FGL2 | ↑ (1.17E-14/-3.513) | ↑ (0.000804/1.499) | Extracellular Space | peptidase |
|-------------|---------------------|--------------------|---------------------|-----------|

Genes upregulated by LPS and downregulated by PNLA

The overlapping comparison in **Table 5.1.1**; genes that were significantly upregulated by LPS and downregulated by PNLA are: complement 1R, 1S (C1R, C1S), CCL18, and MYO10.

C1R, C1S. C1s gene encodes a serine protease, and C1s beta chain is a major constituent of the human complement subcomponent C1. C1s associates with two other complement components, C1r and C1q, to form C1, which is the first component of the serum complement system. The complement system acts in the innate immune response by ultimately triggering phagocytosis, inflammation, and rupturing the bacterial cell wall (Aderem and Underhill 1999). On the other hand, the high incidence of autoimmunity in patients with genetic deficiencies of the early classical complement component C1 suggests that these molecules may play roles in maintaining peripheral tolerance. Like most other complement components, C1R and C1S are produced primarily in the liver and macrophages.

CCL18 (MIP-4) is a protein coding gene primarily expressed in monocytes, macrophages, and immature DCs and plays a crucial role in immune and inflammatory responses. The biological roles of CCL18 include proliferation, chemoattraction, migration, and activation (Takayasu *et al.* 2013). In cell culture experiments, expression of CCL18 mRNA in blood PBMCs was induced by TNF- α (Auer *et al.* 2007). Some reported monocytes and macrophages were shown

to constitutively express only low levels of CCL18, but the CCL18 production could be upregulated in these cells by LPS (Pivarcsi *et al.* 2004; Schraufstatter *et al.* 2004; Song *et al.* 2000).

MYO10 is a protein coding gene that encodes a member of the myosin superfamily. The biological roles of MYO10 include cell motility and shape regulation, cytoskeleton-dependent intracellular transport, Fc γ receptor signalling pathway, phagocytosis, regulation of cell-cell adhesion, and signal transduction. This gene plays a role in integration of F-actin and microtubule cytoskeletons during meiosis and in the formation of the podosome belt in osteoclasts (Bohil *et al.* 2006).

Genes downregulated by LPS and upregulated by PNLA.

In **Table 5.1.2**, genes that were downregulated by LPS and upregulated by PNLA are PDK4, CD209, and FGL2.

PDK4 is discussed above in section 5.2.4.

CD209 this gene encodes a C-type lectin that functions in cell adhesion and pathogen recognition. It is a pathogen-recognition receptor (PRR) expressed on the surface of immature DCs and involved in the initiation of the primary innate immune response that recognises a wide range of evolutionarily divergent pathogens. CD209 is thought to mediate the endocytosis of pathogens, which are subsequently degraded in lysosomal compartments (Engering *et al.* 2002). The receptor returns to the cell membrane surface, and the pathogen-derived antigens are presented to resting T-cells via MHC class II proteins to initiate the adaptive immune response. Among its functional domains are carbohydrate binding and recognition, mannose and protein binding, endocytosis, intracellular signal transduction, leukocyte cell-cell adhesion, and peptide antigen transport.

Genes upregulated by LPS and PNLA treatments. In Table 5.1.3.

Fibrinogen-like protein 2 (FGL2). FGL2 plays a vital role in the pathogenesis of some critical inflammatory diseases by possessing immunomodulatory activity through the mediation of immune coagulation the regulation of the maturation and proliferation of immune cells. Findings from previous studies indicate that FGL2 is known for suppressing the activated immune system (Liu *et al.* 2013). The role of FGL2 in the activation of macrophages was confirmed by the detection of significantly decreased macrophage activation markers (CD11b, CD11c, and CD71) expression as well as the inhibition of cell migration and inflammatory cytokine (IL-8 and MMP-9) production in an LPS-induced FGL2 knockdown human THP-1 cell line (Liu *et al.* 2010). FGL2 is strongly upregulated in LPS stimulated PBMCs.

2. Comparison of annotated genes of unstimulated versus LPS stimulated (A), LPS stimulated versus PNLA treated and LPS stimulated (B), and unstimulated versus PNLA treated and LPS stimulated (C) PBMCs from HCs.

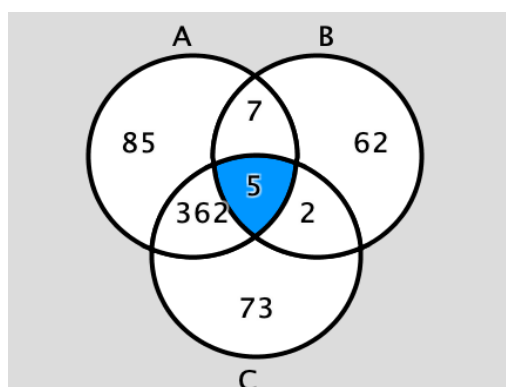


Figure 5.9. Venn diagram of HCs DEGs overlap comparisons A, B and C

The diagram shows the number of novel genes in each subset corresponding to the treatment and control conditions. The total DEGs were identified by 3 group comparisons. The overlap between (A) (B) and (C) is 5 specific genes. **Key:** A (unstimulated PBMCs Vs LPS stimulated PBMCs) B (PNLA treated LPS stimulated PBMCs vs LPS stimulated PBMCs) and C (PNLA treated LPS vs unstimulated PBMCs).

Table 5.2. Genes that overlap between 3 the comparison groups in HCs

(A: control vs LPS; B: PNLA vs LPS; and C: PNLA vs control).

| Table 5.2.1. Genes that are downregulated by LPS and PNLA treatment ($p < 0.05$ / $FC < -1.2$) | | | | | |
|--|---|---|---|-----------------|------------------------|
| Gene symbol | Expr p-value (A)/ Expr Log Ratio (A) | Expr p-value (B)/ Expr Log Ratio (B) | Expr p-value (C)/ Expr Log Ratio (C) | Location | Type(s) |
| GFRA2 | ↓ 6.99E-21/-3.348 | ↓ 4.31E-03/-1.238 | ↓ 1.8E-26/-4.586 | Plasma Membrane | transmembrane receptor |
| CTTNBP2 | ↓ (2.84E-21/-4.471) | ↓ (0.00897/-1.383) | ↓ (1.33E-27/-5.854) | Cytoplasm | other |

| Table 5.2.2. Genes that are upregulated by LPS and PNLA treatment ($p < 0.05$ / $FC > 1.2$) | | | | | |
|---|------------------|----------------|------------------|---------------------|----------|
| IL1A | ↑ 5.56E-33/5.314 | ↑ 0.0058/1.241 | ↑ 6.96E-45/6.456 | Extracellular Space | cytokine |

| Table 5.2.3 Genes that are downregulated/ upregulated by PNLA treatment ($p < 0.05$ / $FC < 1.2$) | | | | | |
|---|-------------------|----------------------|-------------------|---------------------|----------|
| CXCL13 | ↑ 1.48E-27/8.448 | ↓ 0.00495/ -2.033 | ↑ 1.05E-14/6.414 | Extracellular Space | cytokine |
| FUCA1 | ↓ 5.88E-38/-5.601 | ↑ 0.0098/1.234 | ↓ 5.33E-22/-4.467 | Cytoplasm | enzyme |

Genes downregulated by LPS and PNLA

Table 5.2.1 shows genes that are downregulated by LPS where PNLA cannot reverse the downregulation. These included GFRA2 and CTTNBP2. In **Table 5.2.2**, LPS upregulated IL1A, and PNLA could not prevent the upregulation significantly.

GFRA2 (TGF-Beta-Related Neurotrophic Factor Receptor 2). The protein encoded by this gene is a member of the glial cell line-derived neurotrophic factor (GDNF) receptor family. It is a GPI-linked cell surface receptor for both GDNF and neurturin (NTN), that play key roles in the control of neuron survival and differentiation. The biological process includes regulation of the phosphorylation of STAT proteins and of the transmembrane receptor protein tyrosine kinase signalling pathway.

CTTNBP2 (Cortactin-binding protein 2). It is a protein-coding gene; a similar gene in rats interacts with a central regulator of the actin cytoskeleton. It has actin cytoskeleton organisation and cytoskeletal regulatory protein binding functions and regulates IL-1 β signalling (Chen *et al.* 2012). No direct relation to this gene was found in the literature in relation to its implications in RA.

Genes upregulated by LPS and PNLA

IL1A. The IL-1 α /IL-1 β /IL-1RA gene cluster is located on the long arm of chromosome 2. The polymorphism of this gene, which codes for IL-1 cytokines, is associated with RA. IL-1 and its receptor are involved in the pathogenesis of various acute and chronic inflammatory diseases, including RA and atherosclerosis (Garlanda and Jaillon 2016).

Genes affected by LPS and PNLA

Table 5.2.3 showed that CXCL13 was upregulated by LPS but downregulated by PNLA, while FUCA1 was downregulated by LPS but upregulated by LPS.

CXCL13. Upregulation of human CXCL13 mRNA in PBMC and in synovial tissue is associated with RA (Manzo *et al.* 2008; Schmutz *et al.* 2005). CXCL13 has roles in monocyte migration, trafficking, adhesion, and chemoattraction.

FUCA1 (Alpha-L-fucosidase 1). It is associated with carbohydrate binding activity, fucosidase activity, hydrolase activity, and acting on glycosyl bonds. It has biological functions in regulating enzymes involved in fructose, cholesterol, glycolipid, and glycosaminoglycan catabolic processes. The protein encoded by this gene is a lysosomal enzyme involved in the degradation of fucose-containing glycoproteins and glycolipids. Among its related pathways are the metabolism of proteins and the innate immune system.

5.2.6.2 Venn diagrams of the top 500 genes in the comparison of three experimental conditions in RA patients.

1. Comparison of annotated genes: unstimulated versus LPS stimulated (A), LPS stimulated versus PNLA treated and LPS stimulated (B), and unstimulated versus PNLA treated and LPS stimulated (C) in RA patients.

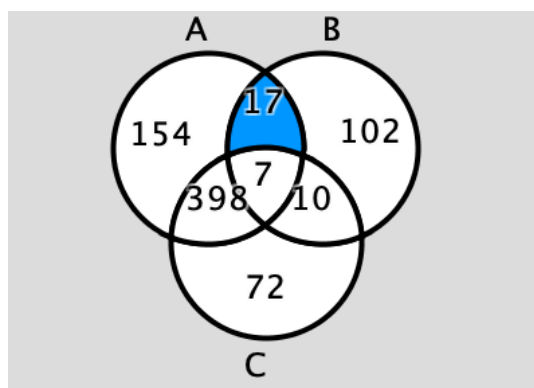


Figure 5.10. Venn diagram of RA patients DEGs: comparison A and B

The diagram shows the number of novel genes in each subset corresponding to the treatment and control conditions. The overlap between (A) and (B) is 17 specific genes. **Key:** A (unstimulated control vs LPS stimulated), B (PNLA treated LPS stimulation vs LPS stimulation control). C (PNLA treated LPS vs stimulation PBMCs).

Table 5.3. Genes that are upregulated by LPS and downregulated by PNLA in RA.

(Column A: control vs LPS; column B: PNLA vs LPS)

| 5.3. Genes downregulated by PNLA and upregulated by LPS ($p < 0.05$ / $FC < 1.2$) | | | | |
|---|---|---|---------------------|-------------------------|
| Symbol | Expr p-value (A)/ Expr Log Ratio (A) | Expr p-value (B)/ Expr Log Ratio (B) | Location | Type (s) |
| CEMIP | ↑ 5.18E-14/3.533 | ↓ 0.0000429/-1.781 | Cytoplasm | enzyme |
| ABHD17C | ↑ 1.49E-12/2.942 | ↓ 0.000392/-1.332 | Plasma Membrane | enzyme |
| SLC39A14 | ↑ 8.21E-17/2.449 | ↓ 0.00106/-0.894 | Plasma Membrane | transporter |
| ABCB5 | ↑ 2.09E-13/6.206 | ↓ 0.00251/-1.61 | Plasma Membrane | transporter |
| MUC1 | ↑ 4.46E-11/3.119 | ↓ 0.00288/-1.17 | Plasma Membrane | other |
| FERMT2 | ↑ 7.8E-11/2.853 | ↓ 0.00372/-1.101 | Cytoplasm | other |
| CCL15 | ↑ 8.86E-17/5.693 | ↓ 0.00646/-1.621 | Extracellular Space | cytokine |
| CCL15-CCL14 | ↑ 8.05E-14/4.909 | ↓ 0.00718/-1.561 | Other | other |
| KANK1 | ↑ 1.21E-13/3.659 | ↓ 0.00873/-1.198 | Nucleus | transcription regulator |
| MIR5572 | ↑ 3.56E-11/7.361 | ↓ 0.0083/-1.602 | Other | microRNA |

Genes are upregulated by LPS and downregulated by PNLA.

In RA, **Table 5.3.** show that PNLA downregulated CEMIP, ABHD17C, SLC39A14, ABCB5, MUC1, FERMT2, CCL15, CCL15-CCL14, KANK1, and miRNA 5572 (column B), which were upregulated by LPS stimulated PBMC (column A).

CEMIP binds to hyaluronic acid and hydrolyzes high molecular weight hyaluronic acid to produce an intermediate-sized product, a process that may occur through rapid vesicle endocytosis and recycling without intracytoplasmic accumulation or digestion in lysosomes. In RA, CEMIP is referred to as an angiogenic marker and participates in hyaluronic acid degradation (Deroyer *et al.* 2019).

ABHD17C hydrolyzes FAs from S-acylated cysteine residues in proteins. Decreased cell viability ratio strongly decreased nuclear factor of activated T cells (NFAT1)-GFP nuclear translocation that may potentially be of clinical importance. No direct implications for RA have been found.

SLC39A14 belongs to a subfamily of proteins that show the structural characteristics of zinc transporters (Taylor and Nicholson 2003). Zinc is an essential cofactor for many enzymes. It is involved in protein, nucleic acid, carbohydrate, and lipid metabolism, as well as in the control of gene transcription, growth, development, and differentiation. Among the biological processes that SLC39A14 is involved in are cellular zinc ion homeostasis, chondrocyte differentiation, gluconeogenesis, and positive regulation of the GPCR protein signalling pathway.

ABCB5 is a member of the p-glycoprotein family that belongs to the ATP-binding cassette (ABC) transporter superfamily of integral membrane proteins. These proteins participate in the ATP-dependent transmembrane transport of structurally diverse molecules ranging from small ions, sugars, and peptides to more complex organic molecules (Chen *et al.* 2005). ABCD5 has a role in controlling proinflammatory signalling circuits utilising TLR4, IL-1 β , IL-8, and CXCR1 signalling (Ksander *et al.* 2014). Interference of active human ABCB5 protein by blocking the Ig complex decreases the secretion of human IL-1 β protein from cancer cell lines (Wilson *et al.* 2014). Although this gene is downregulated by PNLA upon LPS stimulation in RA patients, its role in RA has not yet been defined in the literature.

MUC1 encodes a membrane-bound protein that is a member of the mucin family. These proteins play a role in intracellular signalling through phosphorylation and protein-protein interactions. MUC1-N terminal domain release induces conformational changes in MUC1-C that alter its ligand status and subsequently activates downstream cell signalling pathways such as MAPK, P13K/Akt, and wingless type (Wnt) pathways (Hollingsworth and Swanson

2004). MUC1-C also associates with and modulates various transcription factors, including STAT3, NF- κ B, p53, and β -catenin and binds the target gene promoter region to drive their expression (Ahmad *et al.* 2011; Li *et al.* 2004; Wei *et al.* 2005). TNF- α signals via NF- κ B.

FERMT2 is a scaffolding protein that binds to phosphoinositides in the cell membranes, and enhances integrin activation, integrin-mediated cell adhesion onto the ECM, and cell spreading.

CCL15 (MIP-5) is a chemotactic factor that attracts T-cells and monocytes, but not neutrophils, eosinophils, or B-cells. It acts mainly via CCR1, but also binds to CCR3.

CCL15-CCL14 the CC chemokines, are secreted proteins characterised by two adjacent cysteines. The genes chemokine (C-C motif) ligand 14 and chemokine (C-C motif) ligand 15 are adjacent loci and express read-through transcripts spanning both loci. The read-through transcripts were originally interpreted as bicistronic (loci responsible for generating a protein) transcripts, but they are represented as non-coding because they are candidates for nonsense-mediated mRNA decay.

KANK1 the functions of the KANK family include the control of cytoskeleton formation by regulating actin polymerisation together with inhibition of actin fibre formation and cell migration (Tadijan *et al.* 2021). KANK1 is a transcription factor that involves phosphorylation through PI3K/Akt signalling, protein binding, transcription regulation, and cytoskeleton organisation.

MIR5572 is a short non-coding miRNA that is involved in post-transcriptional regulation of gene expression in multicellular organisms by affecting both the stability and translation of mRNAs. miRNAs will be discussed in some detail in Chapter 7.

Table 5.4. Genes that are downregulated by LPS and upregulated by PNLA.

(Column A: control vs LPS; column B: PNLA vs LPS)

| 5.4. Genes that are upregulated by PNLA and downregulated by LPS ($p < 0.05$ /FC > -1.2) | | | | |
|---|---|--|---------------------|-------------|
| Symbol | Expr p-value (A)/Exp fold change (A) | Expr Log Ratio (B)/ Exp fold change (B) | Location | Type(s) |
| PDK4 |  4.7E-11/ -4.084 |  1.11 E-9/2.509 | Cytoplasm | kinase |
| FCN1 |  1.32E-16/-4.812 |  0.00051/1.893 | Extracellular Space | other |
| ACP5 |  9.93E-15/-3.151 |  0.000127/1.453 | Cytoplasm | phosphatase |
| OLFM1 |  1.54E-14/-5.587 |  0.00198/2.173 | Cytoplasm | other |
| C11orf45 |  1.95E-17/-4.05 |  0.00531/1.274 | Extracellular Space | other |

| | | | | |
|---------------|-------------------|-----------------|-----------------|-------|
| PTGFRN | ↓ 1.16E-19/-5.201 | ↑ 0.00648/1.475 | Plasma Membrane | other |
| CD101 | ↓ 6.24E-16/-3.756 | ↑ 0.00879/1.141 | Plasma Membrane | other |

Genes downregulated by LPS and upregulated by PNLA.

Table 5.4 shows that PDK4, FCN1, ACP5, OLFM1, C11orf45, PTGFRN, and CD101 were downregulated by LPS (column A) but upregulated by PNLA (column B).

PDK4 was upregulated in both HC and RA. Its functions have been discussed in section 5.2.4.

FCN1 (Ficolin 1) protein encoded by FCN1 is predominantly expressed in PB leukocytes (monocytes and neutrophils). It binds to the sugar moieties of PAMPs displayed on microbes and activates the lectin pathway of the complement system. Extracellular lectin functions as a pattern recognition receptor in innate immunity.

ACP5 provides instructions for making an enzyme called tartrate-resistant acid phosphatase type 5 (TRAP). The TRAP enzyme primarily regulates the activity of osteopontin, which is produced in osteoclasts and immune cells. In the immune system, osteopontin is found primarily in macrophages and DCs.

OLFM1 interacts with the non-canonical NF- κ B-inducing kinase (NIK; also known as MAP3K14) and represses the phosphorylation of its downstream substrate IKK α . Knockdown of NIK impaired the ability of OLFM1 to repress NF- κ B signalling, cell growth, or migration (Shi *et al.* 2016).

PTGFRN (prostaglandin F2 receptor negative regulator) encodes a protein that inhibits the binding of PGF2- α to its specific EP receptor (Orlicky *et al.* 1996). Elevated biosynthesis of PGF2 has been reported in patients with RA, and PGF2 α has been found in their urine (Hoxha 2018). CV risk factors, such as DM, obesity, smoking, and thickening of the intima-media ratio in the carotid artery, have been variably associated with elevations in PGF2 α .

CD101 the leukocyte surface protein CD101 is expressed on several immune cells, such as DC, monocytes, and activated T cells (Jovanovic *et al.* 2011). It prevents the nuclear translocation of nuclear factor of the activated T-cells to the nucleus.

2. **Comparison of annotated genes in unstimulated versus LPS stimulated (A), LPS stimulated versus PNLA treated and LPS stimulated (B), and unstimulated versus PNLA treated and LPS stimulated PBMCs (C) from RA patients.**

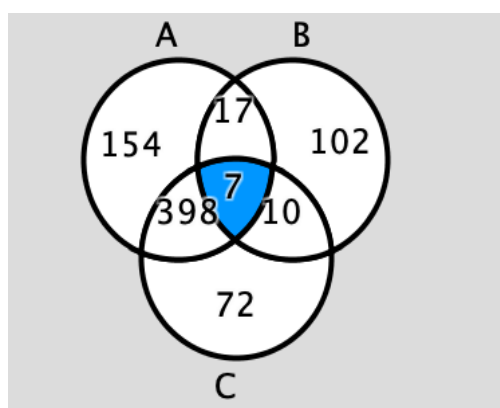


Figure 5.11. Venn diagram of RA patients DEGs overlap comparisons A, B and C

Key: A (unstimulated PBMCs vs LPS stimulated PBMCs) B (PNLA treated and LPS stimulated PBMCs vs LPS stimulated PBMCs). C (PNLA treated and LPS stimulated vs vehicle stimulated PBMCs).

Table 5.5. Genes that overlap between the 3 comparison groups in RA

(A: control vs LPS; B: PNLA vs LPS; and C: PNLA vs control)

| Table 5.5.1. Genes that are downregulated by PNLA treatment ($p < 0.05$ / $FC < -1.2$) | | | | | |
|--|---|---|---|---------------------|-------------------------|
| Symbol | Expr p-value (A)/ Expr Log Ratio (A) | Expr p-value (B)/ Expr Log Ratio (B) | Expr p-value (C)/ Expr Log Ratio (C) | Location | Type(s) |
| ACOD1 | ↑ 2.53E-50/ 9.471 | ↓ 0.00345/-1.569 | ↑ 1.8E-37/7.921 | Cytoplasm | enzyme |
| ARNT2 | ↑ 7.91E-36/ 8.21 | ↓ 0.00531/-1.642 | ↑ 6.23E-23/6.582 | Nucleus | transcription regulator |
| CCL8 | ↑ 2.13E-25/ 7.303 | ↓ 0.00364/-1.881 | ↑ 1.19E-16/5.437 | Extracellular Space | cytokine |
| CCL18 | ↑ 1.78E-19/5.787 | ↓ 0.00859/-1.466 | ↑ 4.96E-11/4.332 | Extracellular Space | cytokine |
| IL2RA | ↑ 1.05E-24/5.456 | ↓ 0.00475/-1.416 | ↑ 8.31E-14/4.056 | Plasma Membrane | transmembrane receptor |

| Table 5.5.2. Genes that are upregulated by PNLA treatment ($p < 0.05$ / $FC > 1.2$) | | | | | |
|---|---|---|---|-----------------|-------------|
| Symbol | Expr p-value (A)/ Expr Log Ratio (A) | Expr p-value (B)/ Expr Log Ratio (B) | Expr p-value (C)/ Expr Log Ratio (C) | Location | Type(s) |
| VSIG4 | ↓ 6.66E-24/-4.32 | ↑ 0.0057/1.231 | ↓ 8.8E-14 -3.178 | Plasma Membrane | other |
| SLC37A2 | ↓ 1.26E-35/-4.28 | ↑ 0.00887/1.866 | ↓ 4.24E-22/-3.402 | Cytoplasm | transporter |

Genes upregulated by LPS and downregulated by PNLA.

Table 5.5.1 shows genes that are downregulated (upper panel) and upregulated (lower panel) by PNLA. Genes that were significantly downregulated are ACOD1, ARNT2, CCL18, CCL8 and IL2RA.

ACOD1 is a protein coding gene, is upregulated by LPS and in the PBMCs of patients after acute sepsis. ACOD1-mediated itaconic acid production contributes to the antimicrobial activity of macrophages. It is involved in the inhibition of the inflammatory response and acts as a negative regulator of the TLRs-mediated inflammatory innate response. On the other hand,

mouse ACOD1 protein increases the production of ROS, IL-6, and TNF- α in RAW264.7 macrophages treated with LPS (Li *et al.* 2013).

ARNT2 is a transcription factor that encodes the beta subunit of a heterodimeric transcription factor called hypoxia-inducible factor 1 (HIF1). This protein is required for the ligand-binding subunit to translocate from the cytosol to the nucleus after ligand binding. Among its related pathways are cytochrome P450, arranged by substrate type, and regulation of lipid metabolism by PPAR α .

CCL8 is a chemotactic factor that attracts monocytes, lymphocytes, basophils, and eosinophils. Annotations in GO related to this gene include protein kinase activity and chemokine activity. Among its related pathways are ERK signalling, and the cellular response to IL-1, TNF- α , and IFN- γ .

IL2RA is a gene that encodes an IL-2 receptor subunit. IL2RA gene variations are associated with RA in humans. Besides the HLA-DRB1 SE, IL2RA is the only genetic risk factor for the development of RA, and for both radiographic progression and persistence, this underlines the relevance of IL2RA for RA (van Steenbergen *et al.* 2015). TNF- α increases the expression and activation of IL-2RA (Muñoz-Fernández *et al.* 1990; Schiller *et al.* 1991).

Genes upregulated by PNLA and downregulated by LPS

Table 5.5.2 shows that VSIG4 and SLC37A2 are significantly upregulated by PNLA.

VSIG4 is a B7 family-related protein that is expressed by resting macrophages. VSIG4 is a membrane protein belonging to the complement receptor of the immunoglobulin superfamily (CRIg) (Vgot *et al.* 2006). Macrophages lacking VSIG4 exhibit significant increases in NLRP3 and IL-1 β transcription, caspase-1 activation, apoptosis, and IL-1 β secretion in response to NLRP3 inflammasome stimuli (Huang *et al.* 2019).

SLC37A2 is a human gene that encodes for the SLC37A2 protein. SLC37A2 is an endoplasmic reticulum-anchored phosphate-linked glucose-6-phosphate transporter that is highly expressed in macrophages and neutrophils.

5.2.7. Comparison analysis

Using the IPA software (<https://www.qiagenbioinformatics.com/products/ingenuity-pathway-analysis>), the comparison analysis was performed for all the above-mentioned experimental conditions of HCs and RA patients, where the interest of this project is looking at the regulator effectors for the genes involved in the transcription of inflammatory cytokines, lipid metabolism, and some drugs used for treating RA or reducing hyperlipidaemia.

I further exported the data files for those genes and produced heatmaps using Broad Morpheus software. Heatmap visualisations using $\log_2FC > 1.2$ are shown in **Figures 5.12 and 5.13**, for HCs and RA, respectively.

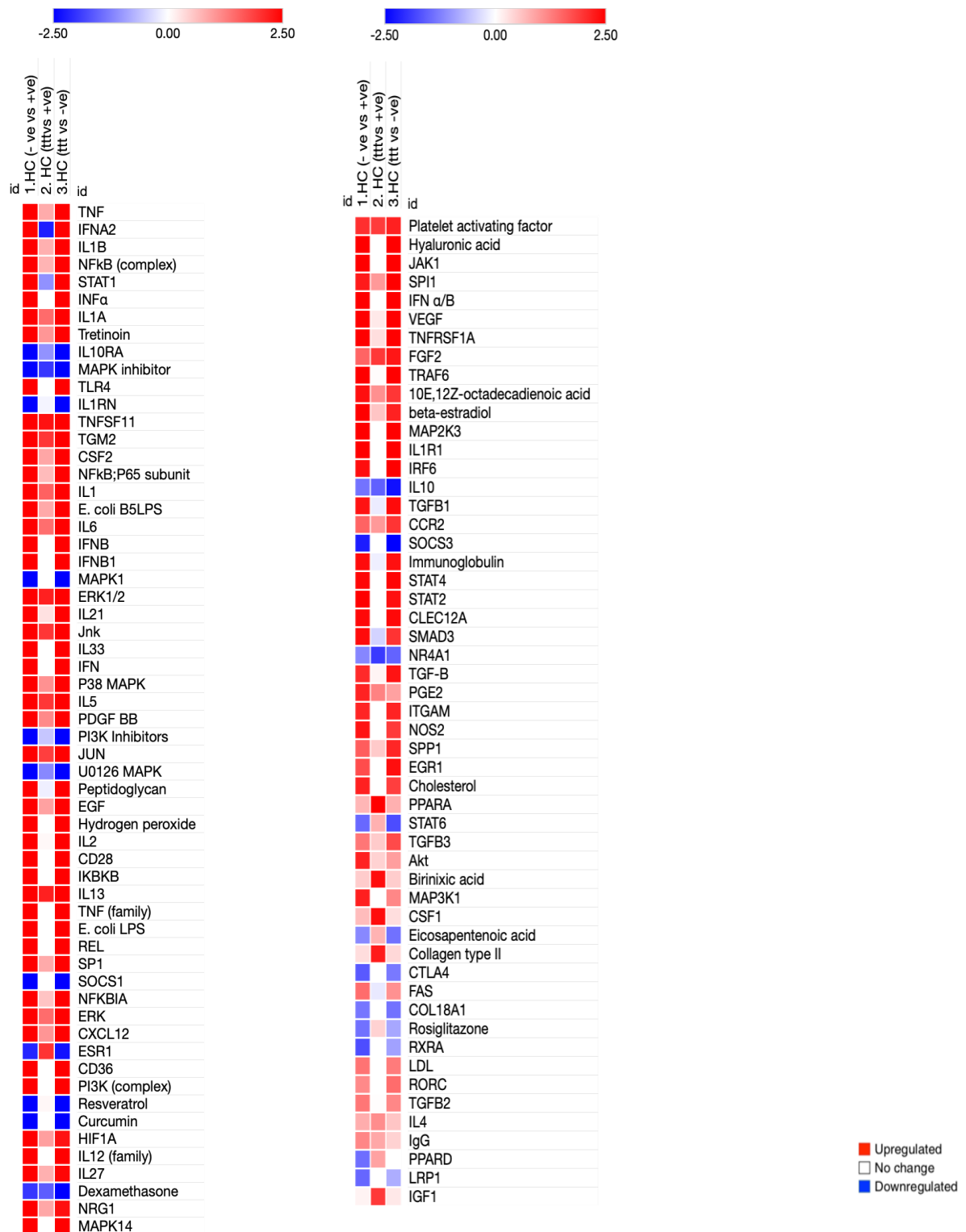


Figure 5.12. Heatmap of differentially expressed upstream regulators for the comparison analysis of HCs.

IPA analysis of genes associated with upstream regulators that predicted the activated state (red) and predicted the inhibited state (blue) is shown. Relative expression heat maps of the differentially expressed genes regulated by; 1. unstimulated (vehicle) versus LPS stimulated PBMCs 2. PNLA treated LPS stimulated versus vehicle treated LPS stimulated PBMCs 3. PNLA treated LPS stimulated versus unstimulated (vehicle) treated PBMCs ($\log_2FC > 1.2$, $P < 0.05$) are shown. The genes shown here are mainly involved in cytokine production, lipid metabolism, drugs used for treating RA or reducing the hyperlipidaemia, and transcription regulators.

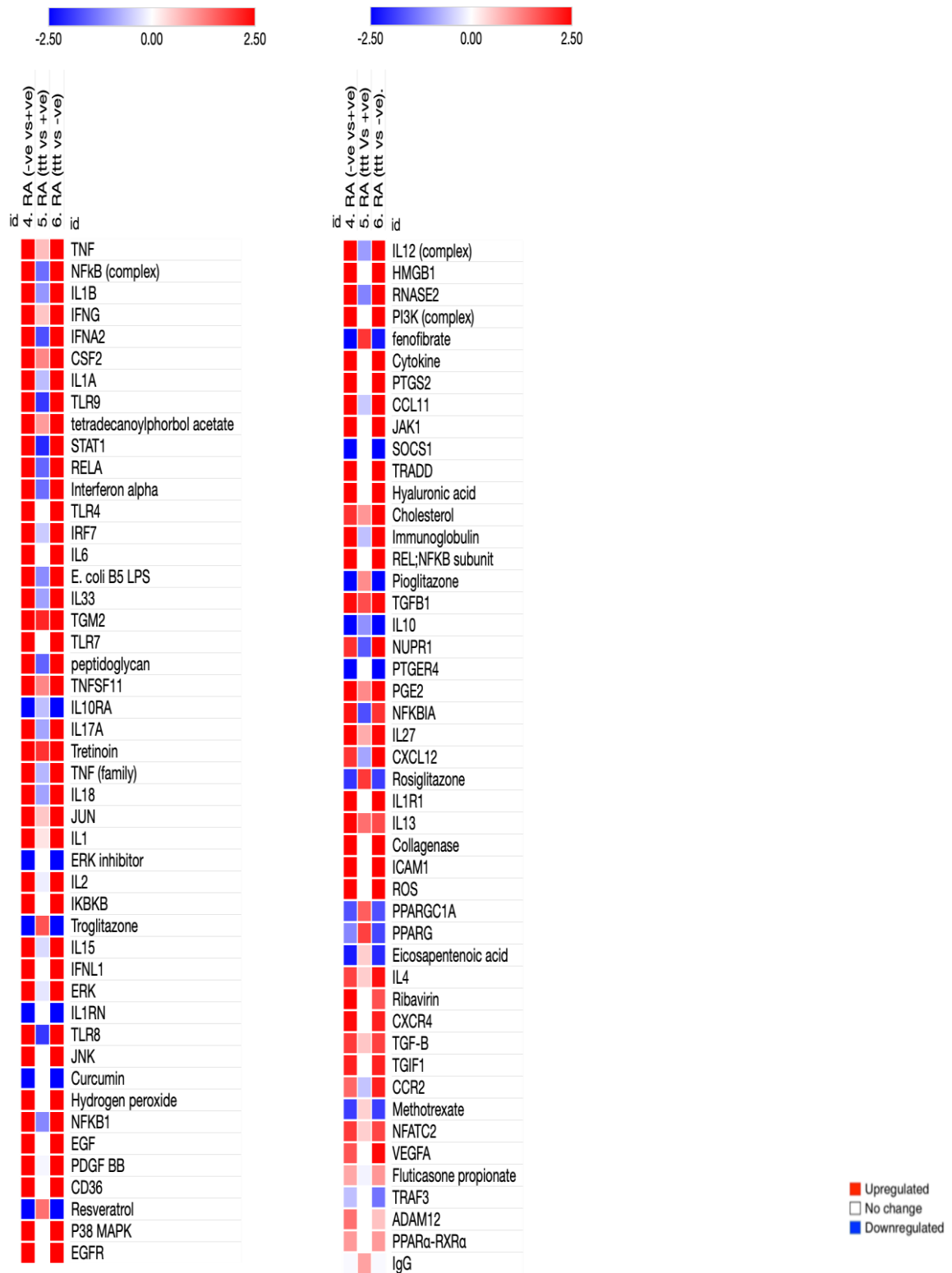


Figure 5.13. Heatmap of differentially expressed upstream regulators for the comparison analysis of RA.

IPA analysis of genes associated with upstream regulators that predicted the activated state (red) and predicted the inhibited state (blue) are shown. Relative expression heat maps of the differentially expressed genes regulated by; 1. unstimulated (vehicle) versus LPS stimulated PBMCs 2. PNLA treated LPS stimulated versus vehicle treated LPS stimulated PBMCs 3. PNLA treated LPS stimulated versus unstimulated (vehicle) treated PBMCs ($\text{Log}_2 \text{FC} > 1.2$, $P < 0.05$) are shown. The genes shown here are mainly involved in cytokine production, lipid metabolism, drugs used for treating RA or reducing the hyperlipidaemia, and transcription regulators.

5.2.8. Upstream regulator effectors

5.2.8.1. Upstream regulators for the effectors of PNLA treated LPS stimulated PBMCs vs LPS stimulated PBMCs from HCs and RA patients.

The IPA software (<https://www.qiagenbioinformatics.com/products/ingenuity-pathway-analysis>) provides a prediction of the likely upstream regulator responsible for the expression changes observed in the experimental dataset (**Figure 5.12** and **5.13**). Most of the transcripts seen are predicted to be inhibited, apart from the nuclear receptors (PPARs) which show an activation pattern. NF- κ B was found to be the first most-significant upstream regulator (p-value = 1.82e-07) (**Figure 5.14** and **Table 5.6**). Next, STAT1 was predicted to be inhibited (p-value = 1.39E-04) (**Figure 5.15** and **Table 5.7**). PPARs will be discussed next, followed by IL1 and CCR2. Pathway analysis predicted upstream inhibition of IL-1 α (p=1.02 E-02), IL-1 β (p=1.69 E-03), and CCR2 (p=3.06 E-03).

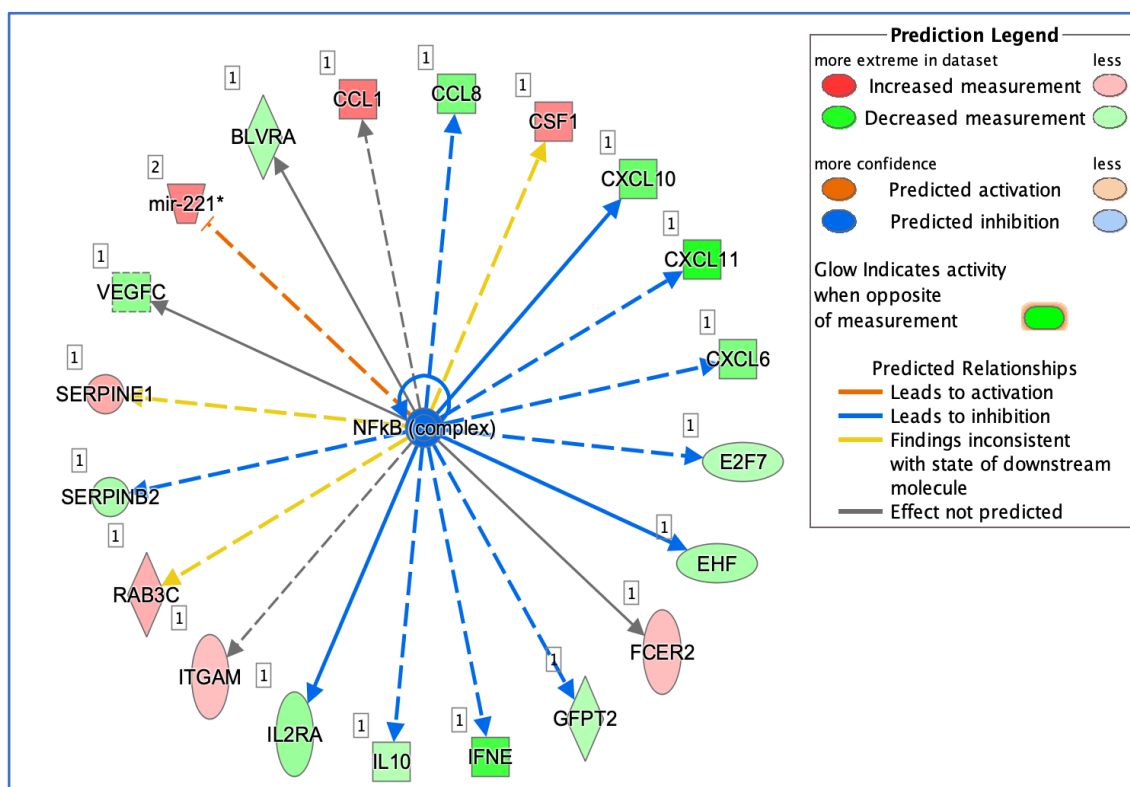


Figure 5.14. NF- κ B upstream regulator as an effector of PNLA treatment of LPS stimulated PBMCs from RA patients and HCs.

Table 5.6. NF- κ B measurement prediction is inhibited.

NF- κ B complex is predicted to be inhibited z score (-2.483), overlap p-value (1.82 E-07) 12 out of 20 genes have measurement directions consistent with inhibition of NF- κ B (complex).

| Genes in dataset | Prediction based on measurement direction | Expression Log ratio | Findings in the literature |
|------------------|---|----------------------|----------------------------|
| CCL1 | Affected | 2.177 | Regulates (2) |

| | | | |
|-----------------|-----------|--------|-------------------|
| mir-221 | Inhibited | 1.979 | Downregulates (2) |
| CSF1 | Activated | 1.875 | Upregulates (2) |
| SERPINE1 | Activated | 1.372 | Upregulates (1) |
| RAB3C | Activated | 1.28 | Upregulates (1) |
| FCER2 | Affected | 1.026 | Regulates (1) |
| ITGAM | Affected | 1.013 | Regulates (3) |
| E2F7 | Inhibited | -1.022 | Upregulates (1) |
| GFPT2 | Inhibited | -1.04 | Upregulates (1) |
| IL10 | Inhibited | -1.046 | Upregulates (7) |
| BLVRA | Affected | -1.165 | Regulates (3) |
| EHF | Inhibited | -1.19 | Upregulates (2) |
| SERPINB2 | Inhibited | -1.203 | Upregulates (2) |
| IL2RA | Inhibited | -1.416 | Upregulates (4) |
| VEGFC | Affected | -1.557 | Regulates (3) |
| CXCL6 | Inhibited | -1.822 | Upregulates (5) |
| CCL8 | Inhibited | -1.881 | Upregulates (2) |
| CXCL10 | Inhibited | -2.103 | Upregulates (34) |
| IFNE | Inhibited | -2.608 | Upregulates (1) |
| CXCL11 | Inhibited | -3.132 | Upregulates (3) |
| CCL1 | Affected | 2.177 | Regulates (2) |

NF- κ B when PBMCs are stimulated by LPS, the canonical signalling pathway is initiated and significantly activates NF- κ B while PNLA is predicted to inhibit this activation, as we can see in the heatmap of upstream regulators (**Figure 5.13**) and the upstream regulator effector network of NF- κ B (**Figure 5.14**) where 12 genes of the overall 20 genes were inhibited, as demonstrated in **Table 5.6**.

STAT1 is predicted to be inhibited upon PNLA treatment (**Figure 5.15A**), and 7 out of 9 genes implicated in the regulation of STAT1 were inhibited by PNLA (**Table 5.7**). STAT1 involvement in RA pathogenesis can be summarised in **Figure (5.15B)**. JAK inhibitors reduce the phosphorylation of STAT1 (discussed in the Introduction (Chapter 1)).

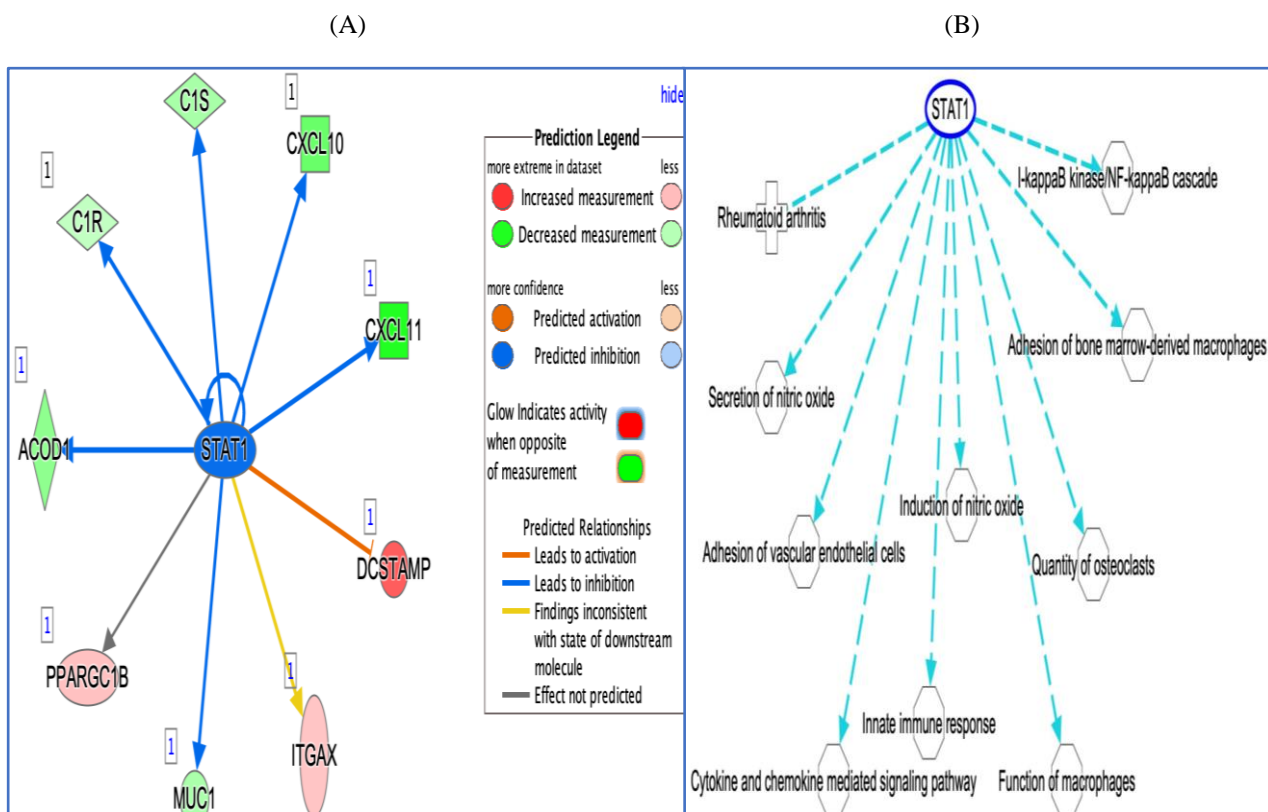


Figure 5.15. STAT1 upstream regulator as an effector and their pathologic roles in RA.

(A) STAT1 upstream regulator as an effector following PNLA treatment of LPS stimulated PBMCs from HCs and RA patients. (B) The STAT1 network and its interaction with the molecules involved in the pathogenesis of RA and atherosclerosis.

Table 5.7. STAT1 measurement prediction is inhibited.

STAT1 is predicted to be inhibited (Z- score -2.129). Overlap p-value 1.39E-04 7 of 9 genes have measurement directions consistent with inhibition of STAT1.

| Genes in data set | Prediction (based on measurement direction) | Expression Log ratio | Findings in the literature |
|-------------------|---|----------------------|----------------------------|
| DCSTAMP | Inhibited | 2.593 | Downregulates (1) |
| PPARGC1B | Affected | 0.981 | Regulates (2) |
| ITGAX | Activated | 0.921 | Upregulates (2) |
| C1R | Inhibited | 0.849 | Upregulates (1) |
| MUC1 | Inhibited | -1.170 | Upregulates (1) |
| C1S | Inhibited | -1.215 | Upregulates (1) |
| ACOD1 | Inhibited | -1.569 | Up regulates (2) |
| CXCL10 | Inhibited | -2.103 | Upregulates (35) |
| CXCL11 | Inhibited | -3.132 | Upregulates (4) |

Nuclear receptors (NRs) are a class of proteins found within the cytoplasm or nucleus of cells that are responsible for sensing the presence of certain molecules. In response, these receptors work in concert with other proteins to regulate the expression of specific genes, thereby controlling the development, homeostasis, and metabolism of the organism. NRs can directly bind to DNA and regulate the expression of adjacent genes; hence, these receptors are classified as transcription factors. Ligand binding to a NR, results in a conformational change in the receptor, which in turn activates the receptor, resulting in the up regulation of gene expression. NRs can also inhibit inflammation by antagonising the actions of transcription factors such as NF- κ B through a process called trans-repression. NR superfamily is classified into six main subfamilies: Thyroid Hormone Receptor-like: includes (thyroid receptor and retinoic acid receptor), PPARs, liver X receptor (LXR), and vitamin D receptor (VDR).

PPARs stand for peroxisome proliferator-activated receptors. Peroxisome proliferators arise because they induce an increase in the size and number of peroxisomes. Peroxisomes are subcellular organelles found in all eukaryotic cells that contain enzymes for respiration and for cholesterol and lipid metabolism. PPARs form heterodimers with retinoid X receptors (RXRs) that regulate the transcription of various genes. Three subtypes of PPARs are known: PPAR-alpha (α), PPAR-delta or beta (δ or β), and PPAR-gamma (γ). PPARs were found to be central for the effect of bioactive compounds on FA metabolism. They play a critical role in the cellular fasting response and are involved in the control of FA synthesis and oxidation. PPAR β/δ are ubiquitously expressed and are often found in higher abundance than PPAR α or γ . PPAR- γ is expressed in many tissues, including adipose tissue, muscle, vascular cells, and macrophages. NR is also activated by n3 and n6-PUFAs (Latruffe and Vamecq 1997), metabolites of FAs, including EPA, HETEs (Coward *et al.* 2002), LTB₄ (Krey *et al.* 1997), and PGD₂. PUFA affects hepatic gene transcription through at least three distinct mechanisms: (i) a PPAR-dependent pathway, (ii) a prostanoid pathway, and (iii) a PPAR and prostanoid-independent pathway. These FAs can be converted to prostanoids in nonparenchymal hepatic cells, like Kupffer or ECs. Upon appropriate activation, released prostanoids, like PGE₂, can activate GPC prostanoid receptors (e.g., EP₃) on hepatic parenchymal cells, initiating a signal transduction cascade that leads to a suppression of FAS mRNA (Jump *et al.* 1999). PPARs, once activated via a ligand, bind to promoter elements of target genes, regulate the peroxisomal beta-oxidation pathway of FAs, and function as a transcription activator for the acyl-CoA oxidase gene (ACOX).

PPAR- α is a gene that encodes the subtype PPAR- α , which is a nuclear transcription factor. PPAR- α is a key regulator of lipid metabolism and functions as a transcription activator for the

ACOX1 and P450 genes. It is activated by oleylethanolamide, a naturally occurring lipid that regulates satiety. PPAR α inhibits the expression of a variety of inflammatory genes, such as IL-6 and inducible COX-2 and reduces NO production in murine macrophages exposed to bacterial LPS (Grabacka and Reiss 2008). These events can be attributed to the antagonistic action of PPAR against the main transcription factors mediating inflammatory responses, NF- κ B, and AP-1. Diseases associated with PPAR- α include fatty liver disease, coronary artery disease, DM, and hyperlipidaemia.

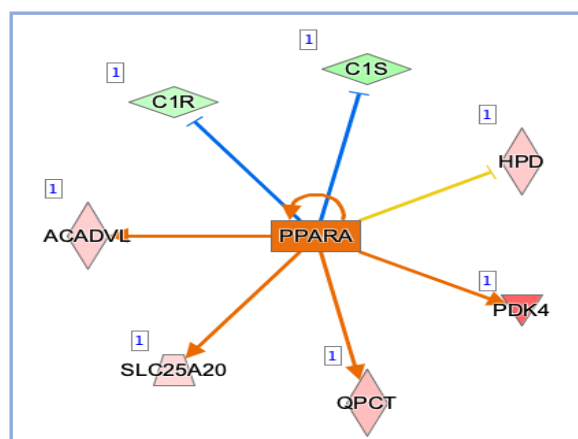


Figure 5.16. PPARA upstream regulator, as an effector following PNLA treatment of LPS stimulated PBMCs from HCs and RA patients.

Table 5.8. PPAR- α measurement prediction is activated.

PPAR- α is predicted to be *activated* (Z- score 2.543). Overlap (p-value 9.22E-05) 7 of 8 genes have measurement directions consistent with activation of PPARA.

| Genes in data set | Prediction based on measurement direction | Expression Log ratio | Findings in the literature |
|-------------------|---|----------------------|----------------------------|
| PDK4 | Activated | 3.784 | Upregulates (9) |
| MMP9 | Affected | 1.862 | Regulates (1) |
| NCF2 | Activated | 1.099 | Upregulates (1) |
| QPCT | Activated | 1.007 | Upregulates (1) |
| NCPT1A | Activated | 0.750 | Upregulates (19) |
| ACADVL | Activated | 0.609 | Upregulates (10) |
| C1R | Inhibited | -1.267 | Down regulates (1) |
| C1S | Inhibited | -1.400 | Downregulates (1) |

PPAR- δ / β also known as PPAR- δ (D)/ PPAR- β (B), is a protein coding gene. The encoded protein is thought to function as an integrator of transcriptional repression and NR signalling. It may inhibit the ligand-induced transcriptional activity of PPAR- α and PPAR- γ . In this study,

LPS significantly attenuates PPARs while PNLA is predicted to activate it as can be seen in the heatmap of the upstream regulator in the comparison analysis (**Figure 5.13**) and in the upstream regulator effector network (**Figure 5.17**) where 6 genes of overall 7 genes in PPARD were activated (**Table 5.9**).

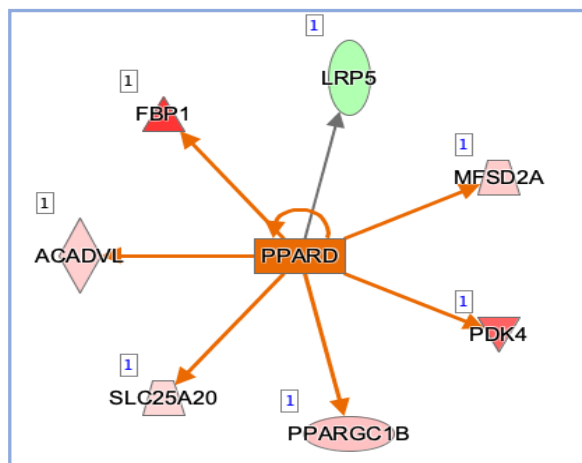


Figure 5.17. PPARD upstream regulator, as an effector following PNLA treatment of LPS stimulated PBMCs from HCs and RA patients.

Table 5.9. PPAR- δ measurement prediction is activated.

PPAR- δ is predicted to be **activated** Z-score (2.415). Overlap (P-value 3.95E-04) 6 out of 7 genes have measurement directions consistent with activation of PPARD.

| Genes in data set | Prediction based on measurement direction | Expression Log ratio | Finding in the literature |
|-------------------|---|----------------------|---------------------------|
| FBP1 | Activated | 3.477 | Upregulates (2) |
| PDK4 | Activated | 2.509 | Upregulates (19) |
| PPARGC1B | Activated | 0.981 | Upregulates (1) |
| MFSD2A | Activated | 0.808 | Upregulates (1) |
| ACADVL | Activated | 0.777 | Upregulates (2) |
| SLC25A20 | Activated | 0.641 | Upregulates (2) |
| LRP5 | Affected | -1.087 | Regulates (1) |

PPAR- γ the protein encoded by PPAR- γ gene, has been implicated in the pathology of numerous diseases, including obesity, DM, and atherosclerosis. Ligands that bind PPAR- γ include hypolipidemic drugs and FAs. PPAR- γ is a key regulator of adipocyte differentiation and glucose homeostasis and acts as a critical regulator of gut homeostasis by suppressing NF- κ B-mediated proinflammatory responses. Low PPAR- γ reduces the capacity of adipose tissue to store fat, resulting in increased storage of fat in non-adipose tissue (lipotoxicity). PPAR- γ agonists have been shown to inhibit atherosclerosis development in animal (Li *et al.* 2000) and

human studies (Ivanova *et al.* 2017; Skochko and Kaidashev 2017). PPAR- γ agonists, the glitazones, are used as therapeutic agents in several conditions associated with CV risk, including DM (Ivanova *et al.* 2017). It is possible that some of the anti-atherogenic effects of these agents are achieved via non-PPAR- γ -related mechanisms (i.e., non-genomic effects). PPAR- γ is predicted to be activated in HCs and RA patients (**Figures 5.12 and 5.13**).

PPARGC1A the protein encoded by this gene, is a transcriptional coactivator that regulates the genes involved in energy metabolism. This protein interacts with PPAR- γ and provides a direct link between external physiological stimuli and the regulation of mitochondrial biogenesis. PPARGC1A is a major factor that regulates muscle fibre type determination. This protein may also be involved in controlling blood pressure, regulating cellular cholesterol homeostasis, and the development of obesity. It plays an essential role in metabolic reprogramming in response to dietary availability through the coordination of the expression of a wide array of genes involved in glucose, FA metabolism, and metabolic genes, such as PDK4. 6 out of 8 genes have measurement directions consistent with activation of PPARGC1A in RA patients (**Figure 5.18**).

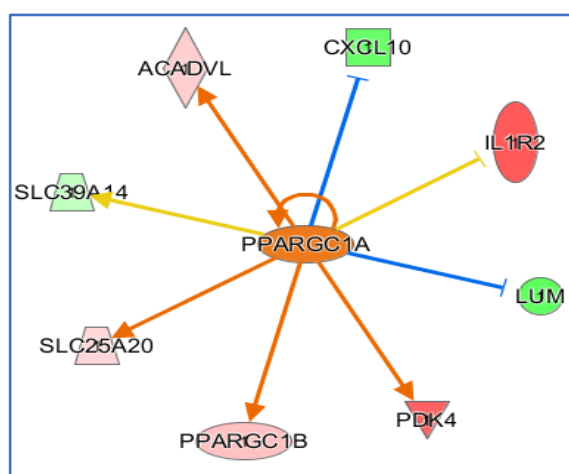


Figure 5.18. PPARGC1A upstream regulator as an effector following PNLA treated LPS stimulated PBMCs from RA patients.

PPARGC1B is a protein that may be involved in fat oxidation, non-oxidative glucose metabolism, and the regulation of energy expenditure. Among its related pathways are regulation of lipid metabolism by PPAR- α and mitochondrial gene expression. It is repressed by saturated FAs such as palmitate and stearate in skeletal muscle cells. It is induced by insulin and reduced by ageing in skeletal muscle. PPARGC1B is downregulated in type 2 DM subjects. **IL-1 α** is a protein coding gene and a member of the IL-1 cytokine family (discussed in the Introduction).

IL-1 β is a protein coding gene and a member of the IL-1 cytokine family. The cytokine is produced by activated macrophages as an important mediator of the inflammatory response (discussed in the introduction). Among the canonical pathways in which this gene is involved are TLR, SOCS, MAPK signalling, Erk, STAT3, TGF- β , and MIF.

IL-18 is encoded for the proinflammatory cytokine IL-18, which augments NK cell activity in spleen cells and stimulates IFN- γ production. Among its related pathways is ERK signalling. Upon binding to IL-18R1 and IL-18RAP, it forms a signalling ternary complex, that activates NF- κ B, triggering the synthesis of inflammatory mediators such as IL-1 cytokine.

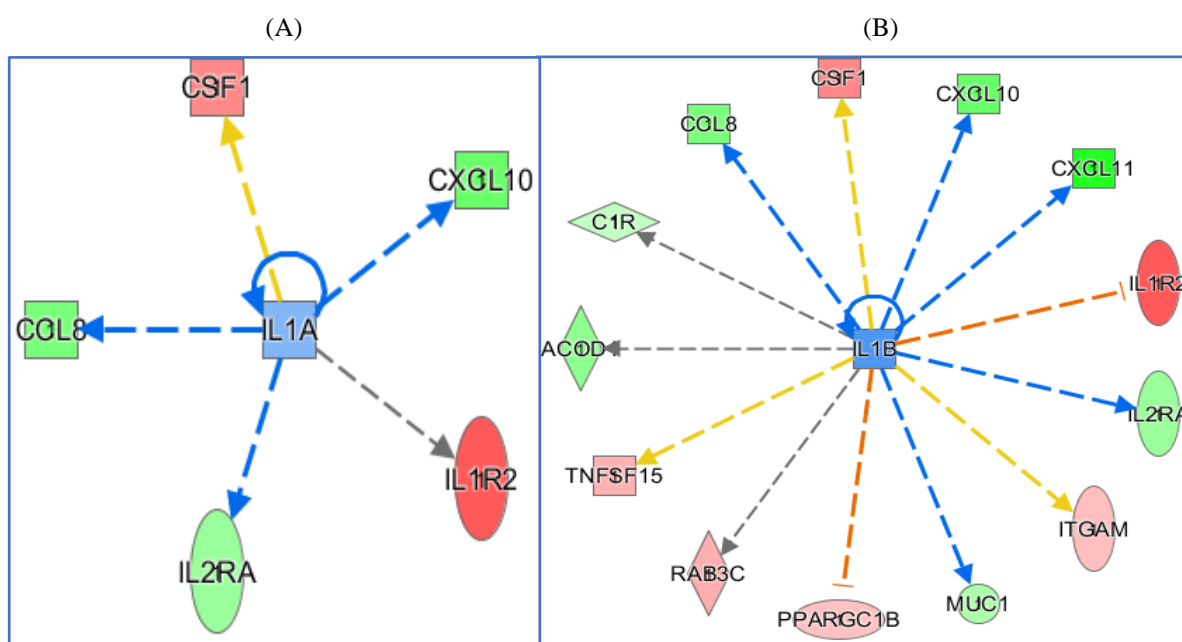


Figure 5.19. The upstream regulators for IL-1 α and IL-1 β .

The upstream regulatory networks of IL-1 of PNLA treated and LPS stimulated vs LPS stimulation PBMCs from RA patients as supported by the dataset.

CCR2 is the protein receptor for CCL2, a chemokine that specifically mediates monocyte chemotaxis. CCL2 is involved in monocyte infiltration in RA and atherosclerosis. CCR2 binding with CCL2 on monocytes and macrophages mediates chemotaxis and migration to the injury site through the activation of the PI3K cascade (Gschwandtner *et al.* 2019; Yadav *et al.* 2010).

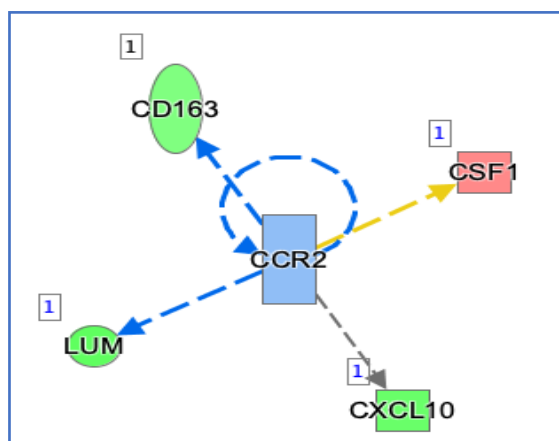


Figure 5.20. The upstream regulation networks for CCR2.

The upstream regulatory networks of CCR2 of PNLA treated and LPS stimulated vs LPS stimulation, as supported by the dataset.

PGE2 the eicosanoid encoded by this gene, is a member of the GPCR family. Regulates the level and stability of COX-2 mRNA and leads to the phosphorylation of glycogen synthase kinase-3. COX-2 converts AA to PGH₂, from which the other PGs and thromboxane are synthesised (discussed in detail in the Introduction (Chapter 1)).

IL-6 is a protein-coding gene that encodes the cytokine IL-6. The function of this gene is implicated in a wide variety of inflammation-associated diseases, including RA and atherosclerosis. The protein is primarily produced at sites of acute and chronic inflammation, where it is secreted into the serum and induces a transcriptional inflammatory response through IL-6R. It is a potent inducer of the acute phase response, plays an essential role in the final differentiation of B-cells into Ig-secreting cells, and is involved in lymphocyte and monocyte differentiation (discussed in detail in the Introduction (Chapter 1)).

TNFSF11 (Tumour Necrosis Factor Ligand Superfamily Member 11; RANKL) is a protein coding gene. Diseases associated with TNFSF11 include RA. It induces osteoclastogenesis by activating multiple signalling pathways in osteoclast precursor cells and causing long-lasting oscillations in the intracellular concentration of Ca²⁺, resulting in the activation of the nuclear factor of activated T-cells, cytoplasmic 1 (NFATC1), which translocates to the nucleus and induces osteoclast-specific gene transcription to allow differentiation of osteoclasts (Park *et al.* 2017). Annotations related to this gene include cytokine activity and TNF receptor superfamily binding.

IL-15 the protein encoded by this gene, is a proinflammatory cytokine that induces the activation of JAK as well as the phosphorylation and activation of transcription activators such as STAT3. In neutrophils, it probably stimulates phagocytosis by signalling through the IL-15 receptor.

IL-17A the protein encoded by this gene, is a proinflammatory cytokine produced by activated T cells. This cytokine regulates the activities of NF- κ B and MAPK. The IL-17 cytokine can stimulate the expression of IL-6 and PTGS2/COX-2, as well as enhance the production of NO. High levels of IL-17 are associated with IA.

IL-10RA the protein encoded by this gene, is a receptor for IL-10. It has been shown to mediate the immunosuppressive signal of IL-10, and thus inhibit the synthesis of proinflammatory cytokines. Activation of this receptor leads to tyrosine phosphorylation of JAK1 and Tyk2 kinases. These kinases then phosphorylate STAT3. Once phosphorylated, STAT3 homodimerizes, translocates to the nucleus, and activates the expression of anti-inflammatory genes.

PIK3R1 (phosphoinositide-3-kinase regulatory subunit 1). PI3-Ks (phosphatidylinositol 3-kinases) is a family of lipid kinases capable of phosphorylating the 3' OH of the inositol ring of phosphoinositides. They are responsible for coordinating a diverse range of cell functions, including proliferation and survival. They also have an important role in signalling in response to Fibroblast Growth Factor Receptor 1 (FGFR1), FGFR2, FGFR3, FGFR4, platelet-derived growth factor (PDGF)RA, PDGFRB and ITGB2. The PIK3R1 gene encodes a regulatory subunit, this regulatory subunit plays an important role in the metabolic actions of insulin, and a mutation in this gene has been associated with insulin resistance.

LUM this gene encodes a member of the small leucine-rich proteoglycan (SLRP) family that includes biglycan, fibromodulin, and osteoglycin. In this bifunctional molecule, the protein moiety binds collagen fibrils, and the highly charged hydrophilic glycosaminoglycans regulate cartilage development, ECM organization, and keratan sulphate biosynthetic process. Lumican is the major keratan sulphate proteoglycan, which regulates collagen fibril organisation, epithelial cell migration, and tissue repair.

IL-33 a protein coding gene, and among its related pathways is the metabolism of proteins. It encodes for IL-33, an important cytokine in the pathogenesis of atherosclerosis and RA. IL-33 binds to and signals through the interleukin-1 receptor-like 1 (IL1RL1), which in turn activates the NF- κ B and MAPK signalling pathways in target cells.

CXCL10 encodes a pro-inflammatory cytokine that is involved in a wide variety of processes such as chemotaxis, differentiation, activation of peripheral immune cells, regulation of cell growth, apoptosis, and modulation of angiostatic effects (Sidahmed *et al.* 2012). Mechanistically, binding of CXCL10 to the CXCR3 receptor activates G protein-mediated signalling and results in downstream activation of the phospholipase C-dependent pathway, an increase in intracellular Ca²⁺ production, and actin reorganisation (Verzija *et al.* 2008).

CXCL11 is a protein-encoding gene. Gene expression of CXCL11 is strongly induced by IFN- γ and IFN- β , and weakly induced by IFN- α . This chemokine elicits its effects on its target cells by interacting with the cell surface chemokine receptor CXCR3, with a higher affinity than the other ligands CXCL9 and CXCL10. CXCL11 is chemotactic for activated T cells.

LRP5 (low-density lipoprotein receptor-related protein 5) regulates the canonical Wnt signalling pathway. Absence of LRP5 and the canonical Wnt pathway leads to a dyslipidemic profile by promoting lipid and macrophage retention in the vessel wall and increasing leucocyte-driven systemic inflammation (Borrell-Pagès *et al.* 2015). The proteins from the Wnt pathway are upregulated in HC Wnt aortas, and this increase is lost when LRP5 is absent.

5.3. Discussion

In Chapter 4, we showed that PNLA significantly reduced TNF- α , IL-6, and PGE2 produced by LPS stimulated enriched monocytes and macrophages from patients with RA and HCs. In this Chapter, we explored the possible mechanism by which PNLA mediates these effects using next generation sequencing of RNA. Data from this Chapter suggested PNLA has significant immuno-metabolic effects, they also highlighted the interaction between metabolism and inflammation.

An *ex vivo* model system was used to examine the anti-inflammatory responses of PNLA in human PBMCs challenged with LPS. Although the model is designed to assess inflammatory responses, many of the genes regulated by PNLA are involved in cholesterol and lipid metabolism, along with the actions of NRs. This is consistent with clinical observations, where the predominant effect of n6-PUFA dietary supplementation is the lowering of circulating TG levels (Calder 2015). In fact, the lipid-lowering effect of n-3 PUFAs is often seen even in the absence of an anti-inflammatory response (Gillies *et al.* 2012). The effect of nutrients on gene expression is an area of considerable interest, so the number of genes coding for key regulatory proteins in metabolic pathways has been investigated. Some studies concluded that the transcriptional response to dietary PUFA is very rapid, occurring in less than 3 hours, which may suggest that PUFA directly modulate gene transcription rather than exerting their influence by modifying membrane lipid FA composition and altering hormone release or signalling (Calder 2015; Simopoulos 1996).

It is suggested that n-3 PUFAs act on the NF- κ B pathway to decrease the expression of adhesion molecules and the production of inflammatory cytokines and COX-2 metabolites (Calder 2013). EPA has been shown to decrease phosphorylation of I κ B in human monocytes and decrease endotoxin-induced activation of NF- κ B (Novak *et al.* 2003; Zhao *et al.* 2004). DHA has also been shown to reduce NF- κ B activation in stimulated macrophages (Lee *et al.* 2001) and DCs (Kong *et al.* 2010) via decreased I κ B phosphorylation.

IPA suggested that a batch of immunoregulatory genes and transcription regulators were affected upon PNLA treatment; these upstream regulators have been implicated in the pathophysiology of many immune and metabolic diseases. Interestingly, recent studies have emphasised a tight link between the metabolic state and the phenotype of immune inflammatory cells, or the immune-regulatory system. Reprogramming of metabolic activity in RA can result in the resolution of inflammation (McGarry *et al.* 2016). The data show close interactions between innate immunity, metabolism, and inflammation, further elucidation of

this interaction may provide new insights into new therapeutic approaches in RA. Four genes were most significantly changed and upregulated by PNLA treatment: PDK4, FBP1, PAI-1 (SERPINE1), and NDRG2. PDK4, PAI-1, and FBP-1 have important roles in the control of metabolic pathways. Studies on these genes in RA, atherosclerosis, or chronic inflammatory diseases are limited and should be assessed in the future. When DEGs were analysed by IPA, it predicted upstream activation of NRs, PPARs involved in the anti-inflammatory process, and inhibition of NF- κ B and STAT1, which are involved in signal transduction of many pro-inflammatory cytokines, including TNF- α , IL-1, IL-6 and IFN- γ . These results are consistent with the reduced production of TNF- α and IL-6 by LPS-stimulated PBMCs after PNLA treatment in Chapter 4.

Interestingly, PDK4 is implicated in both metabolic and inflammatory pathways. PDK4 shifts metabolism from glucose to FA oxidation. For instance, increased release of FFAs from adipose tissue under fasting would be expected to influence metabolism in relevant tissues partly through ligand activation of PPARs and PDK4 expression, which is mediated partly through PPAR δ/β , PPAR α and PPAR α -agonists (Jeong *et al.* 2012; Pettersen *et al.* 2019; Sugden *et al.* 2001) (**Figure 5.21**). PDK4 expression is typically induced when the blood free FA level increases, as occurs during starvation. Increased levels of PDK4, e.g., due to starvation (Pettersen *et al.* 2019), favour inactivation of the pyruvate dehydrogenase enzyme (PDH) in oxidative tissues, and thereby implement a metabolic shift from glucose to FA oxidation and regulate *de novo* FA biosynthesis (**Figure 5.21**). Therefore, increased PDK4 expression was a rather consistent sign of increased FA oxidation. The effects of such events will vary depending on tissue and cell type; RA augments the process of metabolic shift from glucose oxidation to lactate production, several studies suggest that a change in activity of the PDH complex is a major factor (Souto-Carneiro *et al.* 2020; Taylor and Sivakumar 2005). The glucose and lipid metabolisms were impaired in PDK4^{-/-} mice. PDK4 deficiency dramatically reduced the expression of genes related to FA uptake, synthesis, and gluconeogenesis. In addition to elevated phosphorylated AMPK (p-AMPK), JNK and diminished p-ERK, p-p38, and p-Akt proteins were observed (Zhang *et al.* 2010; Zhang *et al.* 2018). Future investigations of PDK4's non-canonical function and its crosstalk with cytosolic molecules would greatly expand our understanding of its regulatory roles in rheumatoid diseases.

NF- κ B is involved in cellular responses to stimuli such as stress, cytokines (including TNF- α and IL-1), free radicals, heavy metals, oxidised LDL, and bacterial/viral antigens. Recently, it has been shown that PDK4 can interact with the p65 subunit of NF- κ B via direct protein-

protein interaction by sequestering the p65 subunit in the cytoplasm and inhibiting its translocation into the nucleus (**Figure 5.22(A)**). PDK4 deficiency triggered hepatic apoptosis concomitantly with increased numbers of aberrant mitochondria, disrupted mitochondrial respiration, generated excessive ROS, sustained c-JNK activation, and reduced levels of GSH. All of these facilitate PDK4 and p65 protein dissociation and release p65 to accelerate its nuclear translocation, as shown in **Figure 5.22(B)** (Zhang *et al.* 2010). This, in turn, facilitated p65 binding to the TNF promoter to activate TNF-TNFR1 apoptotic pathway (Wu *et al.* 2018). Previous studies by Chen *et al.* (2011) showed that rats fed on a diet containing *P. koraiensis* oil had elevated activity of GSH in the serum. NF- κ B p100/p49 subunit has dual functions, such as cytoplasmic retention of attached NF- κ B proteins and generation of p50 by co-translational processing. The p100/p49 subunit and other NF- κ B subunits have been shown to use conserved amino acids to interact with each other in-order to form homo-or heterodimers (Dlamini *et al.* 2015). Also, it has been identified that death domain (DD) containing proteins, such as NF- κ B subunit p100/p49 (referred to as p100), are a potential interacting partner for PDK4. These proteins are known to be involved in apoptosis and inhibit NF- κ B by binding it and therefore retaining it in the cytoplasm (Dlamini *et al.* 2015; Ghosh *et al.* 1998).

Swiss-Pdb Viewer application was used to visualise the 3-dimensional (3D) structure of the modelled hPDK4. The positions of the amino acids that are conserved between hPDK4 and NF- κ B subunits were located and visualised within the 3D structure of hPDK4 (Dlamini *et al.* 2015). Three amino acids are known to be important in NF- κ B subunit dimerization, these are lysine 214, cysteine 215, and histidine 249 (on hPDK4). NF- κ B amino acids corresponding to hPDK4 Lysine 214 and histidine 249 are involved in the direct dimer formation of the NF- κ B subunits through side chain interactions, whereas those corresponding to cysteine 215 use the polypeptide backbone to form the NF- κ B dimer. Interestingly, aspartic acid 216 showed total conservation between hPDK4 and NF- κ B subunits. This amino acid has not previously been shown to play a role in NF- κ B subunit dimer formation, these findings indicate that hPDK4 may potentially interact with NF- κ B (Dlamini *et al.* 2015). The other amino acid of interest is histidine, which is conserved in all NF- κ B subunits but only in human and rat PDK4 and not in the other isoforms. The other amino acids that are involved in the dimerization of the NF- κ B subunits were not conserved in the other PDK isoforms of both human and rat origin.

PNLA treatment was associated with increased PDK4 mRNA expression levels. However, the expression levels of other PDK isoenzymes (PDK1-3) were not significantly affected. There is an increase in the expression of mouse PDK4 mRNA in mouse white adipose tissue that involves an n-3 enriched diet (Xie *et al.* 2021).

PDK4 expression may alter cytokine production via the pathway mentioned. Consequently, this would lead to a diminished TNF activated pathway by preventing NF- κ B nuclear translocation. We therefore used bioinformatics and IPA tools to uncover possible interacting partners for PDK4 and further explore downstream analysis and networking in PDK4 activity. The PDK4 pathway may be a new therapeutic target in RA. In recent years, some research results have indicated that lipid metabolism plays an important role in cartilage and its related tissue diseases, including OA and RA (Xie *et al.* 2021).

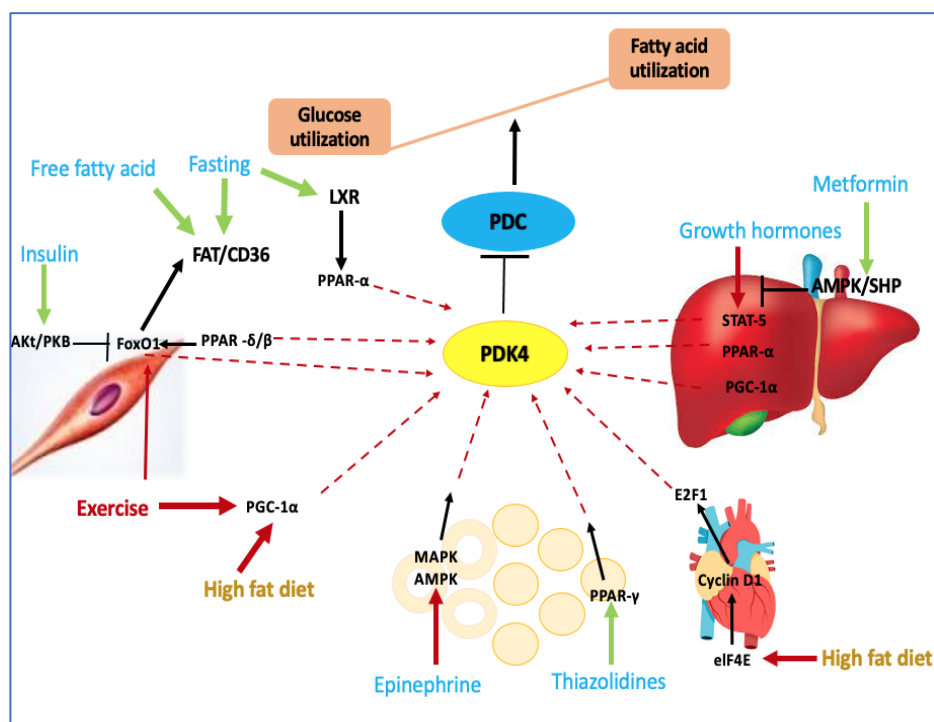


Figure 5.21. Transcriptional regulation pathways of PDK4 in different tissues under various nutritional states. Inactivation of PDC by up-regulation of PDK4 can switch glucose catabolism to fatty acid utilisation. There are different transcriptional regulation pathways in skeletal muscle, liver, white adipose tissue, and heart under various nutritional conditions (energy deprivation, HFD consumption, exercise, diseases, drugs). Abbreviation. Akt/PKB: protein kinase B; AMPK: 5'-AMP-activated protein kinase; CD36: Cluster of differentiation 36; eIF4E: Eukaryotic initiation factor 4E; FAT: Fatty acid transporter; FoxO1: Forkhead box protein O1; LXR: Liver X receptor; MAPK: p38 mitogen-activated protein kinase; PDC: Pyruvate dehydrogenase complex; PDK4: Pyruvate dehydrogenase kinase 4; PGC1 α : PPAR- γ co-activator 1 α ; PPARs: Peroxisome proliferator-activated receptors; SHP: Small heterodimer partner; STAT5: Signal transducer and activator of transcription 5. Modified from Zhang *et al.* (2014).

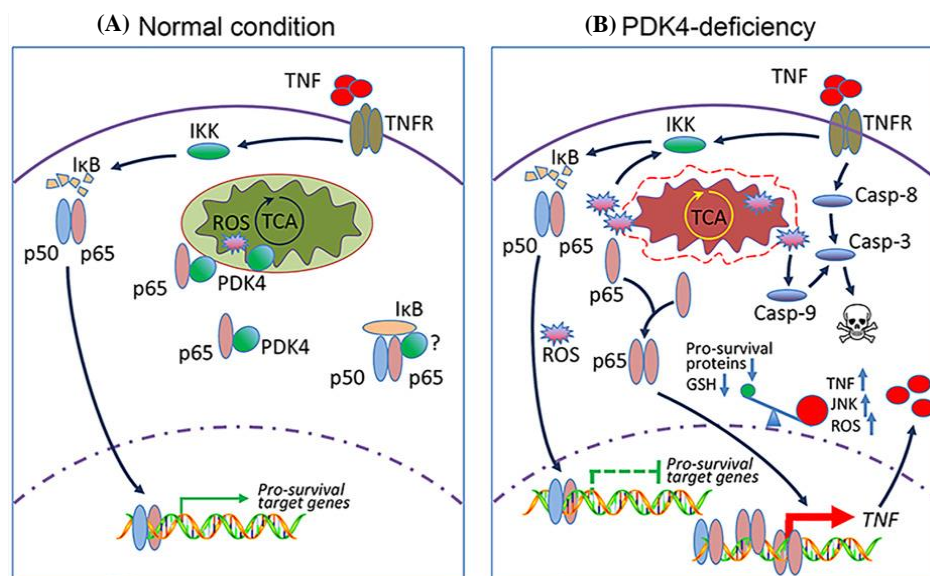


Figure 5.22. The physiological effects of PDK4 show PDK4 as a checkpoint in the NF- κ B/TNF-mediated response. (A) Under normal cellular conditions. PDK4 interacts with NF- κ B/p65 and sequesters p65 in the cytoplasm, mitochondrial respiration and ROS production remain normal. (B) Knockout of PDK4. Disrupts mitochondrial respiration and generates excessive ROS which facilitates PDK4 and p65 protein dissociation and releases p65 to accelerate its nuclear translocation. Excessive ROS may also deplete cellular GSH and activate JNK. In the nucleus of PDK4-deficient cells, pro-survival genes are less/not responsive to p65 transactivation, whereas TNF is activated, which in turn induces caspase-8 and the extrinsic apoptosis pathway. In addition, ROS leads to the activation of caspase-9 and the intrinsic apoptosis pathway. Collectively, PDK4 deficiency can lead to increased ROS, decreased GSH, and sustained JNK activation that shifts the pro-survival function NF- κ B towards facilitating TNF-mediated effect (Taken from Dlamini *et al.* 2015).

PNLA regulates SERPINE-1/PAI-1, which in turn regulates the PA system's tissue plasminogen activator/ uro plasminogen activator (t-PA /u-PA). t-PA is a glycoprotein mainly produced by the endothelium to mediate fibrin dissolution, while u-PA is produced by cells of the connective tissue, where it has specific binding sites on different kinds of cells (Rabieian *et al.* 2018) and is responsible for plasmin-dependent tissue remodelling. The balance between proteinases and proteinase inhibitors is important to achieve the optimal level of proteolytic activity required for cells invasively. High levels of plasmin generated by the u-PA or t-PA secreted by the cells may cause uncontrolled ECM degradation and interrupt the cell-matrix interactions necessary for cell migration and tissue invasion (**Figure 5.23**). Recent evidence shows that the PA system is capable of degrading the bone matrix *in vitro*, supporting the pathophysiological role of uPA and its bound receptor in the development of bone erosion (Cericin *et al.* 1998; Runday *et al.* 1997). In conclusion, overexpression of PAI-1 reduces ECM degradation via perturbing the PA system and regulates tissue remodelling (Rabieian *et al.* 2018). Thus, drugs that modulate the activity of the synovial fibrinolytic system may be of potential interest in the treatment of synovial inflammation. The interaction of PAI-1 levels

with a variety of molecules (e.g., tPA, uPA, and LRP) could potentially have an effect on cell adhesion and migration (Cao *et al.* 2006; Rabieian *et al.* 2018; Zhou *et al.* 2003). PAI-1 was suggested to be involved in tissue remodelling or fibrosis because of its potential for plasmin inhibition and MMP-mediated matrix degradation of pro-MMPs to MMPs. In addition, PAI-1 has been implicated as a mediator in other processes, including RA, atherosclerosis, and bacterial infections. It also significantly modulates cellular adhesion, wound healing, and angiogenesis (Wu *et al.* 2015). SERPINE1 regulates EC proliferation (Ploplis *et al.* 2004), apoptosis (Abderrahmani *et al.* 2012; Balsara and Ploplis 2008), and migration (Isogai *et al.* 2001), and is upregulated in the injured neonatal heart (Darehzereshki *et al.* 2015). In a study by Saxne and colleagues, the PAI-1 level in the SF was found to be elevated in 30% of RA patients with inflamed joints. PGE2 is suggested to play an important role in the regulation of plasmin activation and proteinase expression, which might further trigger the degradation of the ECM. The expression of SERPINE1/PAI-1 in human articular chondrocytes is suppressed by the effect of PGE2 via the EP4 receptor (*in vitro*). Campbell and colleagues reported that TNF- α and IL-1 downregulate, and TGF- β and basic fibroblast growth factor (bFGF) upregulate basal levels of human cartilage/chondrocyte PAI-1 (Campbell *et al.* 1994). TGF- β positively regulates PAI-1 gene expression via two main pathways, including Smad-mediated canonical and non-canonical pathways. Irrespective of the cell type or tissue, the TGF- β pathway is the major driver of the fibrotic response, and PAI-1 is a crucial downstream effector molecule of TGF- β .

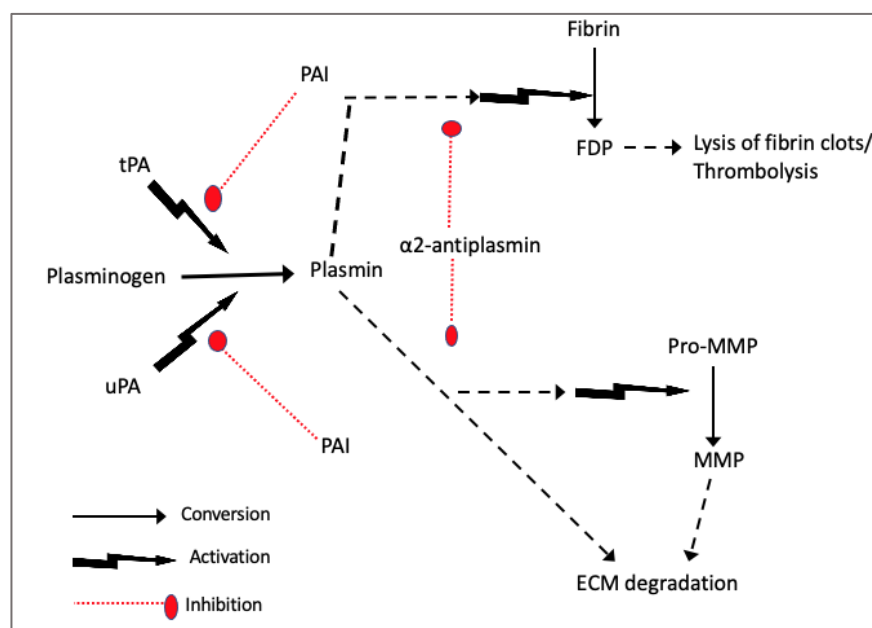


Figure 5.23. tPA and uPA activate the conversion of plasminogen into plasmin and consequently activate MMPs, leading to degradation of ECM within the inflamed joint; PAI inhibit this process. Plasmin also converts fibrin into fibrin degradation products, which lead to the lysis of fibrin clots and thrombolysis within injured tissues and blood vessels. PAI inhibits the processes converting plasminogen into plasmin by inhibiting tPA and uPA; as a result, it inhibits the degradation of the ECM and leads to fibrosis and remodelling of the injured tissues and vessels. Modified from Rabieian *et al.* (2018).

PAI-1 is produced in trace amounts under normal physiological conditions. Persistently elevated PAI-1 levels or overexpression may lead to DM, atherosclerosis, thrombosis, and multiple organ fibrosis (Crandall *et al.* 2000; Rabieian *et al.* 2018). Mutations in PAI-1 and the related genes (PLAU, PLAU, and PLAT) are associated with such conditions as impaired wound healing and chronic inflammatory conditions (Rabieian *et al.* 2018; Yamamoto *et al.* 2005). PAI-1 is an essential repressor of cardiac fibrosis in mammals. It has been defined that the novel cardiomyocyte-specific regulatory mechanism for TGF- β production is by PAI-1, and TGF- β is downstream of PAI-1, which explains the paradoxical effect of PAI-1 deficiency in promoting cardiac-selective fibrosis. Thus, PAI-1 is a molecular switch that controls the cardiac TGF- β axis and its early transcriptional effects that lead to myocardial fibrosis. In the last decades, evidence has accumulated that the fibrinolytic cascade is involved in both the generation of cartilage damage and the genesis and maintenance of synovial inflammation (Cericin *et al.* 1998). This concept seems to be supported by the presence of inflammatory synovial membrane and its production by synovial fibroblasts, as well as by the local release of plasmin and proteolytic enzymes (Cericin *et al.* 1998). The inflammatory mediator PGE₂, induced by inflammation in joint diseases, has been reported to deteriorate the metabolism of articular chondrocytes. In light of this, in OA patients, the levels of PAI-1 in cell lysates (mRNA), and culture supernatants assessed by ELISA were lowered by the presence of PGE₂, confirming the inhibitory effect of PGE₂ on PAI-1 expression/secretion by chondrocytes (Masuko 2009).

Higher NDRG2 expression was correlated with reduced inflammation and CD68⁺ macrophage recruitment in inflammatory foci, while a decrease in NDRG2 expression enhanced inflammation and CD68⁺ macrophage infiltration (Wei *et al.* 2020). Wei *et al.* showed that NDRG2 deficient mice exhibited increased serum LPS levels compared with WT mice. Thus, they examined whether NDRG2 deficiency facilitated LPS-induced inflammation. As expected, LPS induced significant inflammation was characterised by dose-dependent increases in the levels of IL-1 β , IL-6, TNF- α and CXCL1/2 expression. Additionally, NDRG2 deficient mice exhibited markedly higher LPS permeability and increased IL-1 β , IL-6, TNF- α , and CXCL1/2 expression, suggesting an enhanced inflammatory response. These data suggested that intestine-specific NDRG2 deficiency increased LPS permeability and promoted LPS-induced inflammation and inflammatory colitis (Wei *et al.* 2020).

In Chapter 4, we showed that PNLA reduced IL-6 released by LPS stimulated enriched monocytes/macrophages from RA patients, which is consistent with observations in LPS-induced murine microglial BV-2 cells (Chen *et al.* 2015). However, no significant effect of PNLA on IL-6 mRNA expression was seen in the current study, although we see a trend of inhibition, as demonstrated in the heatmap of upstream regulator effectors of HCs (**Figure 5.12**), and the heatmap of RA patients (**Figure 5.13**). These results may be because the transcription effect on IL-6 genes is less than 18 hours. However, Baker in 2021 also found that PNLA had no significant effect on the expression of the IL-6 gene in ECs (EA. hy926).

IPA identified three important pathways, NF- κ B, STAT1 and PPARs. The JAK/STAT pathway is important in RA and other chronic inflammatory diseases, as evidenced by the approval of JAK inhibitors for the treatment of RA, psoriatic arthritis, and inflammatory bowel diseases. JAKs are linked to the cytoplasmic domains of many cytokines. When ligands bind to cytokine receptors, JAKs are phosphorylated, which allows the recruitment and phosphorylation of different STAT molecules, as discussed in the introduction on page 37. Phosphorylated STATs dimerize and translocate into the nucleus, resulting in gene transcription. STAT1 is activated by IFNs and common gamma chain cytokines such as IL-2, and the IL-6 family of cytokines. The importance of the STAT1 pathway in RA has been extensively reviewed (McInnes and Schett 2017).

The role of NF- κ B has already been discussed. It is key in M1 polarisation, which accordingly can regulate the transcription of the above-mentioned cytokines (IL-1, IL-2, IL-6, IL-12, and TNF- α), chemokines (IL-8, CCL2), adhesion molecules, and inducible effector enzymes (iNOS and COX-2) (Wall *et al.* 2010). PNLA is predicted to inhibit NF- κ B, STAT1, Jun, and IRK1/2 (**Figures 5.12** and **5.13**). Chen *et al.* (2015) suggested that PNLA can inhibit the activation of NF- κ B through the downregulation of LPS-induced iNOS protein expression. These inhibitory effects could be accounted for, in part, by the inactivation of MAPK signalling. More recent studies show that PNLA tends to block the activity of NF- κ B via decreased degradation of I κ B in human monocytes and human THP-1 monocytes (Baker *et al.* 2021; Patterson *et al.* 2012).

Proteins of the NR superfamily act as intracellular transcription factors that directly regulate gene expression in response to lipophilic molecules (Sladek 2011; Schulman and Heyman 2004). Several NRs that respond to dietary lipids can be seen as upstream regulators of PNLA treatment in both HCs and RA patients (**Figures 5.16-5.18**), including the FA receptors PPAR α , β/δ , γ and PPARGC1B. Importantly, in the regulation of inflammation, PPARs are

anti-inflammatory in part by inhibiting NF- κ B (Li *et al.* 2000; Necela *et al.* 2008; Patterson *et al.* 2011). PPARs are regulated by PUFA. PPAR α is activated by fibrates, which lower TGs and increase HDL cholesterol. EPA and individual n3-PUFAs activated PPAR- α to a similar extent, with little distinction. Activated PPAR- γ induces LPL and FA transporters (CD36), adipocyte differentiation, and has anti-inflammatory effects such as inhibition of cytokine and COX-2 expression (Jiang 1998; Merez-Sadowska *et al.* 2020). PPAR γ plays an important role in M2 polarisation and modulates the phosphorylation of MAPK p38 and IL-6 production, and polarisation to the M1 phenotype (Rossi *et al.* 2000; Straus *et al.* 2000). PPAR- γ has received considerable attention as a target of anti-diabetic and anti-inflammatory drugs. Gillies *et al.* suggested that PUFAs function mainly by altering membrane lipid composition, cellular metabolism, signal transduction, and regulation of gene expression (Gillies *et al.* 2012). PPAR- γ activation in macrophages can antagonise NF- κ B, AP-1, and STAT1 signalling pathways (Li *et al.* 2000; Necela *et al.* 2008; Patterson *et al.* 2011). Among its many effects, tocilizumab affects macrophage function by increasing PPAR γ (Obeng *et al.* 2016). PPAR- γ stimulates ox-LDL efflux via the LXR pathway within the macrophages, which consequently can lead to a reduction in ox-LDL accumulation (**Figure 5.24(A)**) (Patterson *et al.* 2011).

Crosstalk between PPAR α and LXR via SREBP-1c has been reported, whereby overexpression of PPAR α inhibited LXR-induced SREBP-1c promoter activity through a reduction of LXR binding to its activator, RXR (Patterson *et al.* 2012). SREBP-1c expression in a human hepatoma cell line was reduced following PNLA treatment, a transcriptional activator required for lipid homeostasis (Lee and Han 2016). SREBP-1c regulates transcription of the LDL receptor gene as well as the FA and, to a lesser degree, the cholesterol synthesis pathway (Lee *et al.* 2016). PPAR α and its general metabolic functions are summarised in **Figure 5.24(B)**.

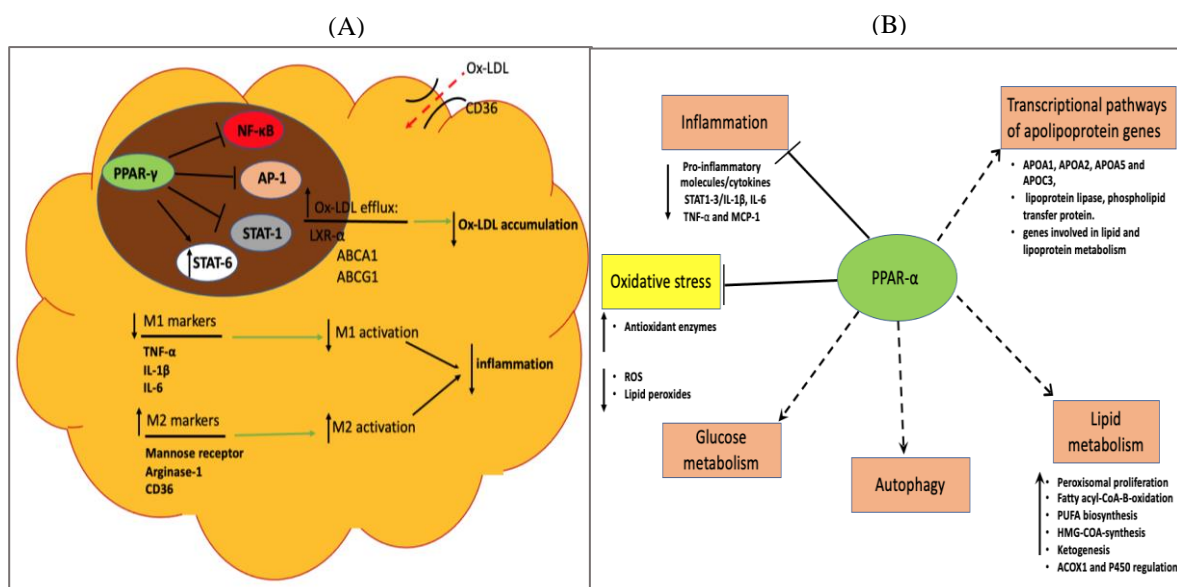


Figure 5.24. The effects of PPAR- γ activation in macrophages and general effects of PPAR- α .

(A) Most of the anti-inflammatory actions of the PPARs arise through their ability to antagonise NF- κ B, AP-1 and STAT1 signalling pathways. By inhibiting NF- κ B, AP1, and STAT1, the PPAR- γ represses the expression of several genes that are involved in the inflammatory response, including cytokines, and through inhibition of M1 activation, increases cholesterol efflux through activating ABCA1 and ABCG1, and reduces ox-lipid uptake via inhibition of CD36 activation. (B) PPAR α has also been reported to control the duration and magnitude of the inflammatory response through its ability to induce the expression of genes encoding proteins that are involved in the catabolism of pro-inflammatory lipid mediators, regulation of glucose metabolism, inhibition of oxidative stress, and expression of pro-inflammatory cytokines. Adapted from Patterson *et al.* (2011).

There are genes that fail to reach statistical significance after multiple adjustment; hence, an unadjusted p-value was used. These genes are interesting in RA and atherosclerosis and are C1S, C1R, CCL18, CCL8, CCL2, CCL15, MYO10, CXCL13, CEMIP, FERMT2, ACOD1, and LRP-5; they were upregulated by LPS and downregulated by PNLA. FGL2 is upregulated by PNLA and LPS, while FUCA1 and GFRA2 are both downregulated by PNLA and LPS.

In RA, there is strong evidence that both the classical and alternative pathways of complement are pathologically activated in human as well as animal models (Okroj *et al.* 2007). The classical pathway can be initiated by several triggers present in the inflamed joint, such as deposited autoantibodies, dying cells, and cartilage proteins such as fibromodulin. B cells producing autoantibodies, which in turn form immune complexes, contribute to RA pathogenesis partly via activation of complement (Okroj *et al.* 2007).

CCL18 mRNA is highly expressed in PBMCs from SF and PB in RA and is highly expressed in the synovium by macrophages and ECs (Auer *et al.* 2007). Levels of CCL18 in RA were higher than in OA in serum, SF, cartilage, and synovial tissue; these levels were positively correlated with disease activity and RF levels and pathologically manifested in the patients (Auer *et al.* 2007). CCL18 production by macrophages is highly upregulated in the presence of fibroblasts, partially because of the collagen produced by the fibroblasts (Prasse *et al.* 2006). CCL18 enhanced IL-6, CCL2, and MMP production in RA from FLS *in vitro*. IL-6 has a wide range of functions on lymphocytes, hepatocytes, hematopoietic progenitor cells, and fibroblasts and plays important roles in autoimmune diseases. CCL2 can cause monocyte migration into the synovium, and MMP-3 is thought to contribute to pannus invasion and cartilage degradation (all discussed in the Introduction). CCL18 could induce the migration of T cells, B cells, monocytes/macrophages, and DCs. Therefore, CCL18 influences inflammatory cell accumulation in the RA synovium. CCL18 caused significantly increased expression of chemokines (CXCL8, CCL3, and CCL22), IL-10, and PDGF (Schraufstatter *et al.* 2012).

Collectively, Takayasu *et al* suggested that CCL18 released in the RA synovium may activate FLS and is partly involved in the pathogenesis of RA (Takayasu *et al.* 2013).

The knockdown of CEMIP in ApoE^{-/-} mice protected against HFD-induced atherosclerosis, as shown by reduced aortic lesion areas, aortic sinus lesion areas, and the concentration of blood lipids compared with mice normally expressing CEMIP (Xue *et al.* 2020).

FERMT3 is upregulated in atherosclerosis, especially unstable plaques, mainly in cells of monocytic origin that correlate with M2 macrophage markers and clustered with inflammatory and macrophage markers, while FERMT2 correlates with SMC-rich plaque markers and clusters with SMC markers (Oksala *et al.* 2015).

The CXCL13 protein increases the formation of the synovium germinal centre in RA (McInnes and Schett 2007). CXCL13 protein decreases the binding of CCL18 protein and cell surface expression in human PBMCs in cell culture (Krohn *et al.* 2013). *In-vitro*, CXCL13 exerts anti-apoptotic effects in primary monocytes, THP-1 macrophages, and vascular SMC. CXCL13 increases arginase-1 (the enzyme that is involved in NO metabolism and is associated with the M2 phenotype). CXCL13 showed increased expression within atherosclerotic carotid plaques as compared with non-atherosclerotic vessels and within the atherosclerotic lesions. CXCL13 was expressed by macrophages and SMC in all stages of plaque progression (Smedbakken *et al.* 2011). Human CXCL13 protein has been suggested to be used as a biomarker for measuring the efficacy of MTX, ofatumumab, and JAKi in the treatment of RA. Recent studies assessed CXCL13 in response to this therapeutic intervention, and the majority indicated a fall in levels in response to treatment. In some cases, this reduction was only seen in treatment responders. High CXCL13 levels predicted failure to achieve disease remission with MTX (Bechman *et al.* 2020; Lee *et al.* 2020).

CCL15 (MIP) is highly expressed in ST and PB in patients with RA. MMPs activate CCL15 to increase monocyte recruitment during inflammation. CCL15 has been identified in SF from arthritic patients at concentrations of 10-100-fold higher than those of CCL3 and CCL5 (Berahovich *et al.* 2005). This chemokine was suggested to contribute to cellular recruitment that is observed in the pathogenesis of RA and atherosclerosis.

FGL2 was upregulated by LPS and PNLA; FGL2 knockdown in THP-1 cells significantly downregulated LPS-induced phosphorylation of p38-MAPK while upregulating

phosphorylation of c-Jun N-terminal kinase (JNK) (Liu *et al.* 2010). On the other hand, FGL2^{+/+} mice developed severe arthritis with clinical and histological manifestations characteristic of RA, whereas FGL2^{-/-} mice failed to develop any clinical manifestation or histological evidence of arthritis.

Among the genes that were downregulated by LPS but upregulated by PNLA were CD209, SLC37A2, ACP5, FCN1, CD101, PTGFRN, and VSIG4.

In DCs, CD209 is a high-affinity receptor for ICAM2 and ICAM3 by binding to mannose-like carbohydrates (Geijtenbeek *et al.* 2000). CD209 can act as a DC rolling receptor that mediates *trans*-endothelial migration of DC precursors from blood to tissues by binding endothelial ICAM2. It also regulates DC-induced T-cell proliferation by binding to ICAM3 on T-cells in the immunological synapse formed between DC and T cells, and CD209 works as a crosstalk between DCs and NK cells (Engering *et al.* 2002). As reported by Yang *et al.* SMs from RA patients showed lower expression of CD209, which is correlated with anti-inflammatory (M2) macrophages (Yang *et al.* 2020).

Overexpression of SLC37A2 lowers macrophage glycolysis and significantly reduces LPS-induced pro-inflammatory cytokine expression (Wang *et al.* 2019; Wang *et al.* 2020). Studies suggest that SLC37A2 dampens macrophage inflammation by down-regulating glycolytic reprogramming as a part of the macrophage negative feedback system to curtail acute innate activation (Wang *et al.* 2020). Increased glucose flux through glycolysis is a hallmark of inflammatory macrophages and is essential for inflammatory functions.

Rat ACP5 decreases production of IL-1 β protein, biosynthesis of NO, and generation of superoxide-anion (Bune *et al.* 2001). Mice lacking ACP5 have disordered macrophage inflammatory responses and reduced clearance of *Staphylococcus aureus* (Bune *et al.* 2001).

Some studies find that there is no association between FCN1 polymorphisms and RA development (Catarina *et al.* 2016). While others reported that the FCN1 gene is associated with the development of RA and that upregulation of human FCN1 mRNA in bone marrow-derived mononuclear cells is associated with RA (Nakamura *et al.* 2006). Serum levels of FCN1 were elevated in patients with RA (Michihito *et al.* 2019). Mutation of the mouse FCN β gene to the mutant mouse FCN1 gene (knockout) in the CIA model decreases joint inflammation and damage (Banda *et al.* 2017).

CD101 can be considered a differentiation marker of the monocyte/leukocyte lineage. It was found only in small percentages in T lymphocytes freshly isolated from the PB of HCs expressed CD101. In RA patients, CD8⁺ cells expression of CD101 surface expression was highly correlated with functional suppressor activity within the CD4⁺ Treg population (Jovanovic *et al.* 2011).

PTGFRN antisense DNA decreases the accumulation of lipid droplets in 3T3-L1 cells (an adipocyte cell line derived from mice) that is increased by dexamethasone and insulin protein (Orlicky *et al.* 1998). 3T3-L1 cells are sensitive to lipid-lowering drugs.

VSIG4 is upregulated by PNLA. It has been demonstrated that VSIG4 down-regulates macrophage activation and M1 polarisation in response to inflammatory stimuli *in vitro* and *in vivo*, it inhibits macrophage activation in response to LPS. Interestingly, a VSIG4-Fc fusion protein seems to protect against the development of experimental arthritis (Katschke *et al.* 2007) and immune-mediated liver injuries (Jung *et al.* 2012). VSIG4^{-/-} mice are susceptible to HFD-caused obesity in association with insulin resistance. Conversely, activating VSIG4 antagonises activation signals in macrophages via the PI3K/Akt-STAT3 pathway, leading to PDK-2 upregulation and subsequent inhibition of mitochondrial PDH activity via phosphorylation. Which results in a reduction in pyruvate/acetyl-CoA conversion, mitochondrial ROS secretion, and suppression of M1-like gene expression through inducing PDH phosphorylation and macrophage inhibition (Li *et al.* 2017). Overproduction of ROS actively participates in the pathogenesis of RA through activating the inflammatory signalling pathways, including MAPK, NF-κB, and guanylate cyclase.

Both n-3 and n-6 PUFAs are often interchangeable in regulating gene expression. However, it is well known that n-3 PUFA are more potent ligands to these NRs than n-6 PUFA (Schmitz and Ecker 2008). Both lipogenic and glycolytic enzymes, such as pyruvate kinase (PK), can be suppressed by PNLA because of the activation of PDK4. These effects of PNLA may also account in part for their hypo-triglyceridemic effects and inhibit gene transcription in adipocytes and lipid uptake, as the genes suppressed here are LRP5, SLC37A2, and ARNT2.

Limitations

This study was exploratory and the first to be done with PNLA in RA patients. One limitation of this chapter is the measurement of transcripts in whole PBMCs. Future investigations may benefit from cell specificity since signatures unique to specific cell types with low abundance may be diluted and unrecognised in whole blood. However, such a signature may have less potential for clinical application than a signature discernible from whole blood or PBMCs. That would require alternative protocols for patient sample collection and downstream RNA processing. Alternatively, one subset of cells can be selected and isolated for the WGT in the same exact conditions as PBMCs while different time points are performed to catch the exact timing whereby changes in inflammatory mediators and eicosanoids transcripts can be seen based on the relative expressions of time.

The second limitation of this study is that many of the genes identified had not previously been associated with RA, further studies are needed to validate the expression and levels of expression of these genes in synovial samples. Preclinical animal models using gene knockout may also help to assess the functions of the PNLA-modified genes and their roles in inflammation.

As with most bioinformatic network analysis studies of human disease, this study had another limitation. The study sample size was relatively small, and the sampling method was randomly selected. This did not eliminate the effects of gender, co-morbidity, and the use of certain medications that could alter gene expression, including methotrexate, biologic drugs, and DD. The genes obtained and their pathways will need to be confirmed by PCR, protein assays, and functional studies in patients with RA and controls. The final limitation that we see in WGT experiments is the very high cost, so I used 25 μ M PNLA treatment and examined a subset of genes for common transcriptional regulators. This costs £300 per sample for complete library construction and sequencing. This limits the opportunity to assess different concentrations of PNLA and compare and contrast their biological effects.

Chapter 6: Effect of PNLA on the levels of intracellular cytokines expressed by CD14⁺CD16⁺ monocyte subsets that are implicated in the pathogenesis of RA and Atherosclerosis

6.1. Introduction and aims

Multiple studies have reported an expansion of human monocytes in RA and atherosclerosis. However, the causes and the functional and pathogenic significance of this phenomenon remain poorly understood. Our observation on the impact of PUFA and diet on inflammation led us to pursue a more extensive and basic characterization of monocytes in RA upon LPS challenge and PNLA therapy. This is based on previous studies on the effect of diet changes on the behaviour of monocytes. For example, hyperglycemia is associated with increased levels of inflammatory monocytes and a reduction of serum IL-10 in prediabetic patients (Israel *et al.* 2016). It is not clear whether PNLA has a preventative effect, maintains homeostatic balance within the immune cells, or can induce the expression of IL-10 *ex vivo*. PNLA and its potential applications in this field need to be explored.

In Chapter 4, I worked on PBMCs, particularly monocytes selected by adherence and differentiated into HMDMs. The studies showed the effect of PNLA on reducing the levels of pro-inflammatory cytokines TNF- α , IL-6, and IL-1 β produced in cell culture supernatants in RA patients and HCs following LPS activation. Cytokine levels in supernatants are not necessarily an adequate parameter of total cytokine production since they may be immediately metabolised or bound by mononuclear cells. Therefore, we further assessed the impact of PNLA on intracellular cytokines at the cellular level (CD14⁺CD16⁺) to confirm the previous finding on its effect on the cytokine levels in cell-free supernatants. Furthermore, we sought to correlate monocytic cytokine levels with disease activity parameters, as previous studies have shown a positive correlation (Woo *et al.* 2018) with the effect of PNLA.

Previous research indicated that intermediate monocytes (CD14⁺⁺CD16⁺) are the major producers of pro-inflammatory cytokines, responsible for an increase in disease activity, and they expand by more than 5% in RA relative to HCs and activate Th17 cells within the joint (Rossol *et al.* 2012). Additionally, *in vitro* studies demonstrated that the most avid scavenging of modified lipoprotein particles by human monocytes occurred within the HLA-DR mid subset of intermediate monocytes. Roger *et al* also confirmed, through an *in vitro* assay for modified lipid uptake assessed by Bodipy[®] staining and flow cytometric analysis, that intermediate monocytes scavenge ox-LDL more avidly than classical or non-classical

monocytes, and this scavenging was associated with intermediate monocyte production of inflammatory cytokines TNF- α , IL-1, and IL-6 (Rogacev *et al.* 2012). The number of white blood cells within the BM can be an indication of the inflammatory status of an individual. Wild-type mice treated with n-3 PUFA were found to have a reduced proportion of white blood cells within their BM in contrast to the mice treated with vehicle control (Joe 2018). Whether PNLA influences the proportion of CD14⁺ monocytes was investigated in this Chapter. Indeed, inflammatory diseases appear to be driven by chronic stimulation of the natural protective functions of specific immune cell subtypes. For example, the uncontrolled accumulation of monocytes and T cells in atherosclerotic plaques (Hansson and Libby 2006; Weber *et al.* 2008) and in the joint with inflammatory synovitis (McInnes and Schett 2011).

The objectives of this Chapter are:

- Assess the proportion of the CD14⁺ population expressing pro-inflammatory cytokines pre-treated with PNLA or vehicle and following the LPS challenge previously studied in Chapter 4.
- Assess other important pro- and anti-inflammatory cytokines produced by CD14⁺ monocytes, such as IL-8, CCL2 (MCP-1), and IL-10.
- Determine the correlation between CD14⁺ monocytes' expression of the studied cytokines and RA disease activity and laboratory markers.

LSR Fortessa (BD Biosciences) in the Central Biotechnology Flow Cytometry Core Facility at Cardiff University School of Medicine was used for all the experiments to address these questions.

6.2. Results

6.2.1. Monocyte phenotyping (granularity) was increased upon PNLA treatment.

Flow cytometry analysis of SSC-A, LPS, and PNLA exposed CD14CD16 monocytes has increased the magnitude of SSC-A, accounts for an increase in cell granularity (**Figure 6.1**) in comparison with vehicle-treated cells.

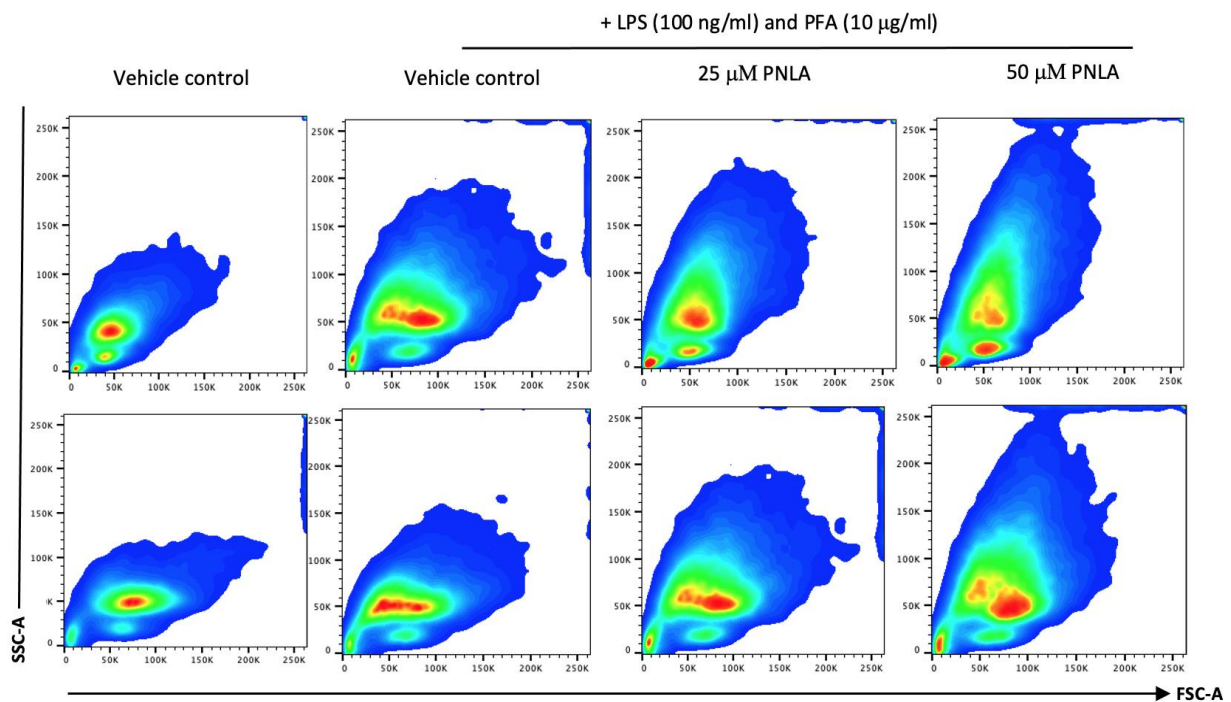


Figure 6.1. Smoothed density plots for the visualisation of unstimulated or LPS-stimulated CD14CD16 monocytes after vehicle or PNLA exposure. CD14CD16 cells without prior incubation with PNLA (vehicle control) or with 24 hours prior exposure to PNLA 25 and 50 µM followed by a 9-hour exposure to 100 ng/ml LPS and 10 µg/ml PFA. Monocytes were visualised by LSR Fortessa and analysed at Flowjo software V10 for SSC-A and FSC-A.

Looking again in more detail at the granularity of only fluorescently selected CD14⁺ monocytes, we determined that there was an increase in cell granularity based on SSC-A as measured and arbitrary assigned as K units (1000). **Figure 6.2** is a representative smoothed density (A) and contour plots (B), while **Table 6.1** represents the average data obtained from (n=21) RA patients and **Figure 6.3** shows the mean +/- SEM from 21 RA patients as performed on GraphPad Prism V8.

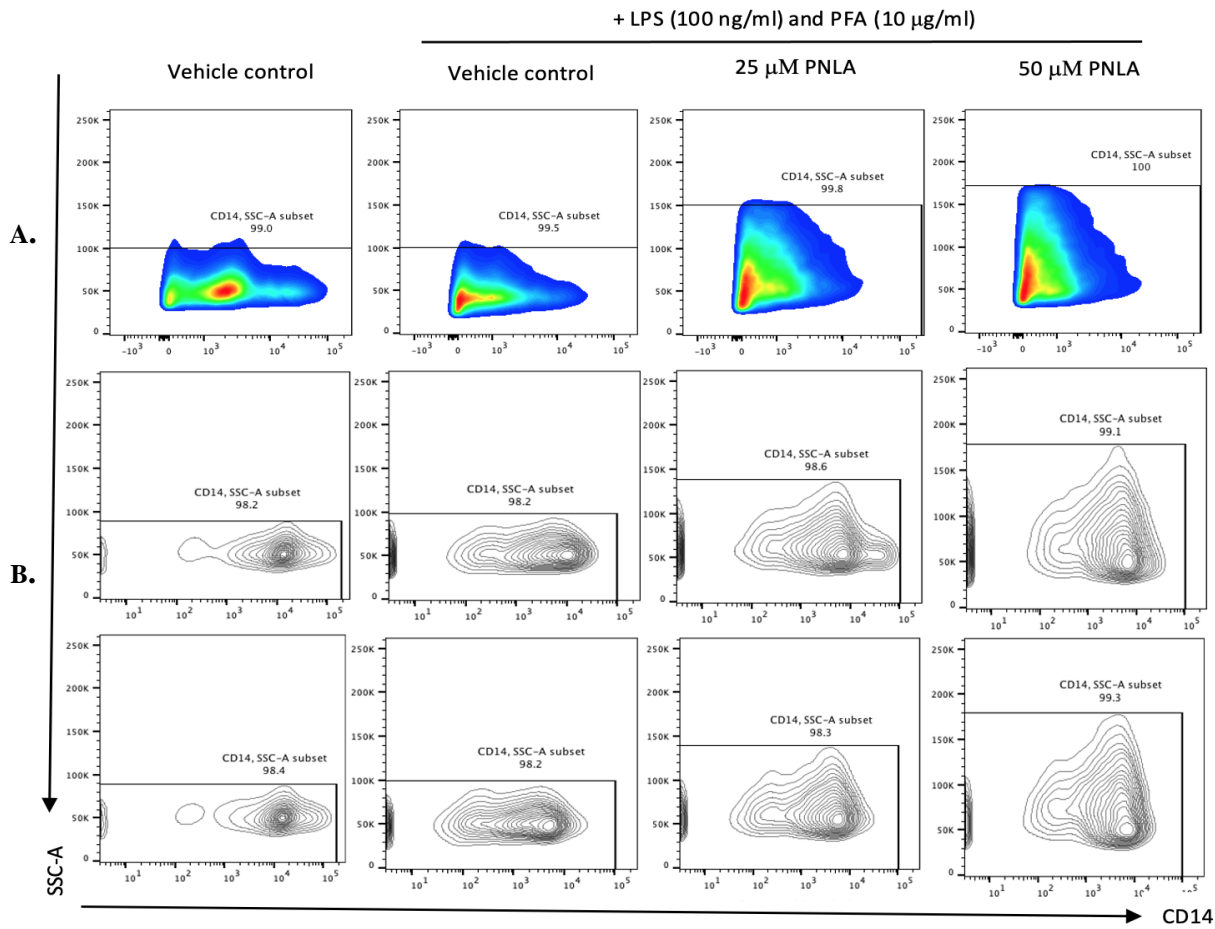


Figure 6.2. Smoothed density plots and contour plots of unstimulated or LPS stimulated CD14⁺ monocytes after vehicle or PNLA exposure.

(A) Smoothed plots (B) contour plots of CD14⁺ cells without prior incubation with PNLA (vehicle control) or with 24 prior exposures to PNLA 25 μ M and 50 μ M followed by 9-hour exposure to 100 ng/ml LPS and 10 μ g/ml PFA. CD14⁺ monocytes were visualised by LSR Fortessa and analysed at Flowjo software V10 for SSC-A and CD14-A; RA (n=21).

Table 6.1. The granularity of unstimulated or LPS stimulated CD14⁺ monocytes after vehicle or PNLA exposure.

| Subject | Vehicle treated subsets (k) | Vehicle +LPS treated subsets(k) | 25 μ M PNLA +LPS treated subsets (k) | 50 μ M PNLA +LPS treated subsets (k) |
|---------------------------|-----------------------------|---------------------------------|--|--|
| RA (1) | 100 | 100 | 120 | 120 |
| RA (2) | 80 | 80 | 80 | 90 |
| RA (3) | 110 | 120 | 130 | 150 |
| RA (4) | 110 | 110 | 150 | 190 |
| RA (5) | 80 | 90 | 150 | 170 |
| RA (6) | 150 | 150 | 210 | 230 |
| RA (7) | 130 | 130 | 170 | 210 |
| RA (8) | 170 | 150 | 210 | 230 |
| RA (19) | 150 | 150 | 170 | 180 |
| RA (10) | 110 | 140 | 150 | 180 |
| RA (11) | 140 | 140 | 150 | 150 |
| RA (12) | 50 | 50 | 70 | 110 |
| RA (13) | 60 | 70 | 80 | 90 |
| RA (14) | 150 | 170 | 180 | 180 |
| RA (15) | 140 | 170 | 170 | 180 |
| RA (16) | 150 | 160 | 230 | 250 |
| RA (17) | 170 | 190 | 230 | 250 |
| RA (18) | 70 | 70 | 110 | 150 |
| RA (19) | 170 | 190 | 260 | 270 |
| RA (20) | 100 | 120 | 160 | 180 |
| RA (21) | 100 | 110 | 150 | 170 |
| Mean | 119 (P = N.S) | 127 | 159 (P = ***) | 182 (P = ***) |
| Std. Error of Mean | 8.11 | 8.74 | 11.1 | 10.2 |

The granularity units of CD14⁺ monocytes from (n=21) RA patients were determined, and the granularity units (k) were assigned arbitrary values of 1000.

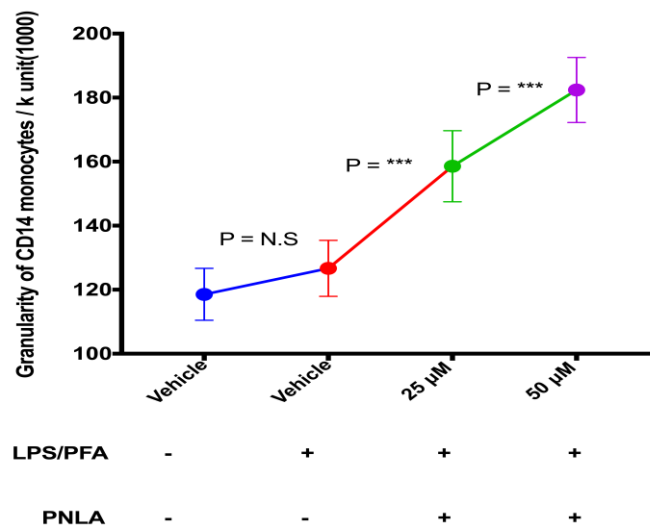


Figure 6.3. The granularity of CD14⁺ is increased following PNLA treatment.

Cells without prior incubation with PNLA (vehicle control) or with 24 hours prior exposure to PNLA 25 and 50 µM followed by (8-9 hours exposure to 100 ng/ml LPS and 10 µg/ml PFA). The granularity of CD14⁺ monocytes presented as the mean \pm SEM RA (n=21) as shown in **Table 6.1** was visualised by LSR Fortessa and analysed at Flowjo software V10 for SSC-A and CD14-A.

6.2.2. CD14CD16 monocytes' microscopic morphology was affected upon LPS stimulation and PNLA treatment.

Visualisation of the images under the brightfield microscope; the photographs were taken at the PNLA concentrations used in this Chapter (25, 50 μM) with or without exposure to LPS (at 100 ng/mL for 10 hours). **Figure 6.4** shows confluent monocytes after PNLA and LPS exposure, which are compared to control (unstimulated cells or LPS stimulated cells). Interestingly, PNLA treated cells appear to be slightly larger in diameter than stimulated cells, which appear to have shrunk or atrophied following an LPS challenge. Untreated monocyte cells (**Figure 6.4A**), LPS-activated cells (**Figure 6.4B**), or PNLA 25 and 50 μM and LPS-activated cells (**Figure 6.4(C and D)**), respectively.

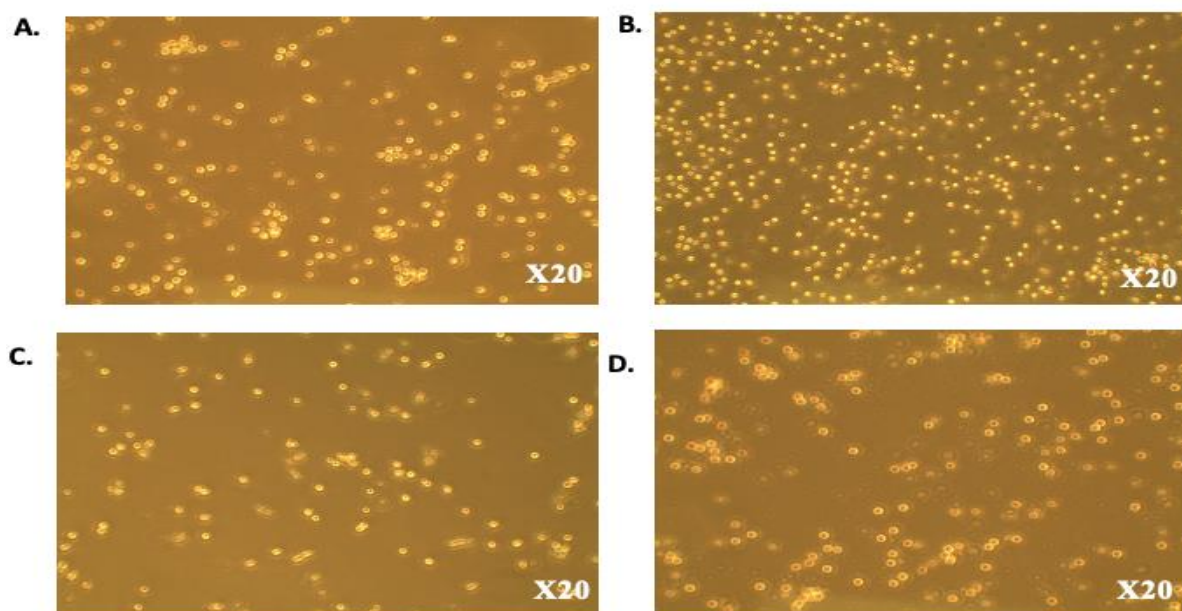


Figure 6.4. Visualisation of unstimulated or LPS stimulated CD14CD16 monocytes after vehicle or PNLA exposure.

CD14CD16 cells were incubated without prior incubation with PNLA or LPS; vehicle control (A); or with a 9-hour exposure to LPS (100 ng/ml) and PFA (10 $\mu\text{g/ml}$) (B); or with incubation with PNLA 25 μM , and 50 μM , followed by a 9-hour exposure to 100 ng/ml LPS and 10 $\mu\text{g/ml}$ PFA (C) and (D), respectively. Motoc live imaging of CD14CD16 monocytes at a magnification of 20X under transmitted light Images were taken kindly with the assistance of Dr. James Burston.

6.2.3. CD14⁺ monocytes expressing (TNF- α , IL-6, IL-1 β , CCL2) cytokines.

Figure 6.5 shows representative dot plots of CD14⁺ monocytes, stained with IgG isotype control for intracellular cytokine markers (TNF- α , IL-6, IL-1 β , and CCL2) in unstimulated, LPS stimulated with or without PNLA pre-treatment (25 and 50 μ M).

To calculate the percentage of cells expressing cytokines, the following formula was used for each participant:

$$\% \text{ CD14}^+ \text{ cells expressing cytokines} = 100 \times \frac{\text{Number of CD14}^+ \text{ expressing cytokines}}{\text{Total number of CD14}^+} + \text{LPS (100 ng/ml)/ PFA (10 } \mu\text{g/ml)}$$

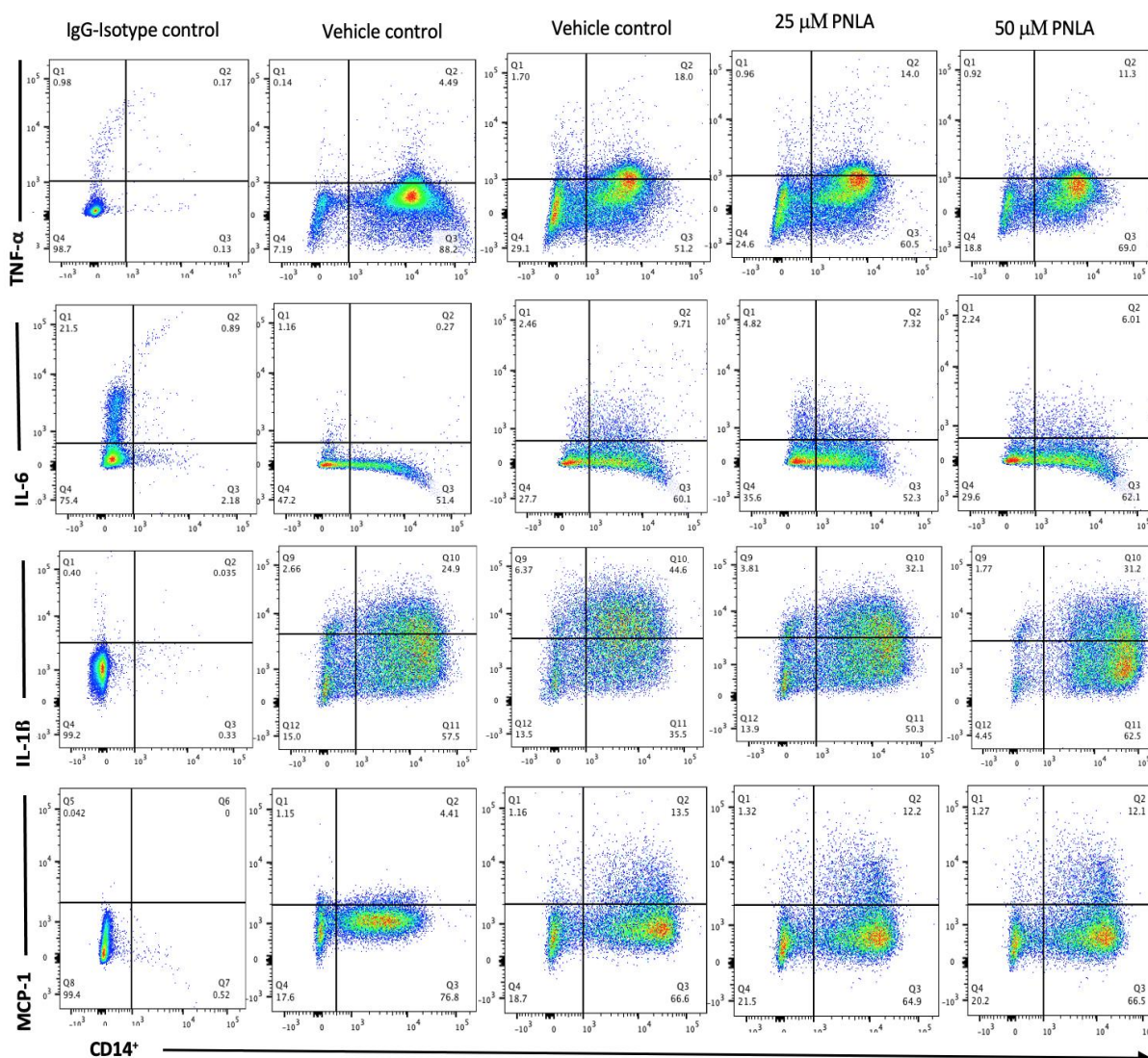


Figure 6.5. The percentage of CD14⁺ monocytes positively expressing cytokines was determined by flow cytometry analysis.

Representative dot plots of the enriched CD14⁺ monocyte population from the PB of RA patients, vehicle- or PNLA-treated activated monocytes with gating strategy, the percentage of cells in each quadrant was determined to calculate the total percentages of cytokines expressing cells. Representative analysis of the number of the IgG isotype activated cells that stained positive for isotype CD14⁺ cytokines expressing cells (the first column far left), the control (vehicle treated monocytes or vehicle treated and LPS activated monocytes) (second and third middle columns, respectively), and the last 2 columns far right represent PNLA treatment at (25 and 50 μ M) and LPS activated monocytes, respectively.

6.2.3.1. Intracellular TNF- α expression was reduced significantly upon PNLA treatment.

LPS stimulated CD14⁺ monocytes increased TNF- α producing cells ($20.2 \pm 2.96\%$; $p \leq 0.0001$) in comparison with non-stimulated monocytes ($3.69 \pm 0.83\%$). Pre-incubating monocytes with 25 or 50 μM PNLA reduced the percentages of CD14⁺ cells producing TNF- α to $16.1 \pm 2.96\%$ and $15.2 \pm 2.81\%$, both at ($p=0.048$ and 0.016), respectively (**Figure 6.6A**).

6.2.3.2. Intracellular IL-6 expression was reduced significantly upon PNLA treatment.

The percentage of CD14⁺ monocytes expressing IL-6 increased from $3.11\% \pm 0.78\%$ in non-stimulated cells to $17.6\% \pm 2.49\%$ ($p \leq 0.0001$) after LPS stimulation. Pre-incubating monocytes with 25 or 50 μM PNLA reduced the percentages of CD14⁺ cells expressing IL-6 to $14.2\% \pm 2.07\%$ and $14.2\% \pm 2.00\%$ ($p=0.011$ and 0.013), respectively (**Figure 6.6B**).

6.2.3.3. Intracellular IL-1 β expression was reduced significantly upon PNLA treatment.

LPS stimulated CD14⁺ monocytes increased IL-1 β producing cells (42.99 ± 4.94 ; $p \leq 0.0001$) in comparison with non-stimulated monocytes ($9.86 \pm 2.91\%$). Pre-incubating monocytes with 25 or 50 μM PNLA reduced the percentages of CD14⁺ cells expressing IL-1 β to ($37.5 \pm 3.62\%$ and $37.2 \pm 3.61\%$; $p \leq 0.05$), respectively (**Figure 6.6C**).

6.2.3.4. Intracellular CCL2 (MCP-1) expression was not reduced significantly upon PNLA treatment.

LPS stimulated CD14⁺CD16⁺ monocytes increased CCL2 expressing cells to (10.1 ± 1.76 ; $p \leq 0.001$) in comparison with ($2.78 \pm 0.98\%$) in non-stimulated monocytes. Pre-incubating monocytes reduced the percentages of CD14⁺ cells expressing CCL2 to ($9 \pm 1.65\%$ and $8.74 \pm 1.41\%$) ($p=0.50$ and 0.33 , respectively) with PNLA treatment (**Figure 6.6D**).

6.2.3.5. Intracellular IL-8 expression was reduced significantly upon PNLA treatment.

LPS stimulation increased the percentage of CD14⁺ monocytes expressing IL-8 to $55.1 \pm 7.91\%$ ($p \leq 0.001$) in comparison with ($4.81 \pm 3.8\%$) in non-stimulated monocytes. Pre-incubating monocytes with 25 or 50 μM PNLA slightly reduced the percentages of CD14⁺ cells expressing IL-8 to $47.2 \pm 7.97\%$ and $48.2 \pm 6.58\%$ ($p=0.066$ and 0.0318 , respectively) (**Figure 6.6E**). The differences were statistically significant only for 50 μM PNLA.

6.2.3.6. Intracellular IL-10 expression was unaffected upon PNLA treatment.

LPS stimulation did not affect IL-10 expression in CD14⁺ monocytes. The percentage of IL-10 expressing CD14⁺ monocytes was $25.5 \pm 3.51\%$; in comparison with $34.2 \pm 11.0\%$ ($p=0.35$) in non-stimulated monocytes. Pre-treatment with 25 or 50 μM PNLA had no effect on the percentages of CD14⁺ cells expressing IL-10 ($25.7 \pm 5.81\%$ and $28.4 \pm 6.18\%$) ($p=0.94$ and 0.50 , respectively) (**Figure 6.6F**).

Monocytes were analysed and assessed for intracellular cytokine levels (IL-8 and IL-10) using the same steps and gating strategy as in **Figure (6.5)** above.

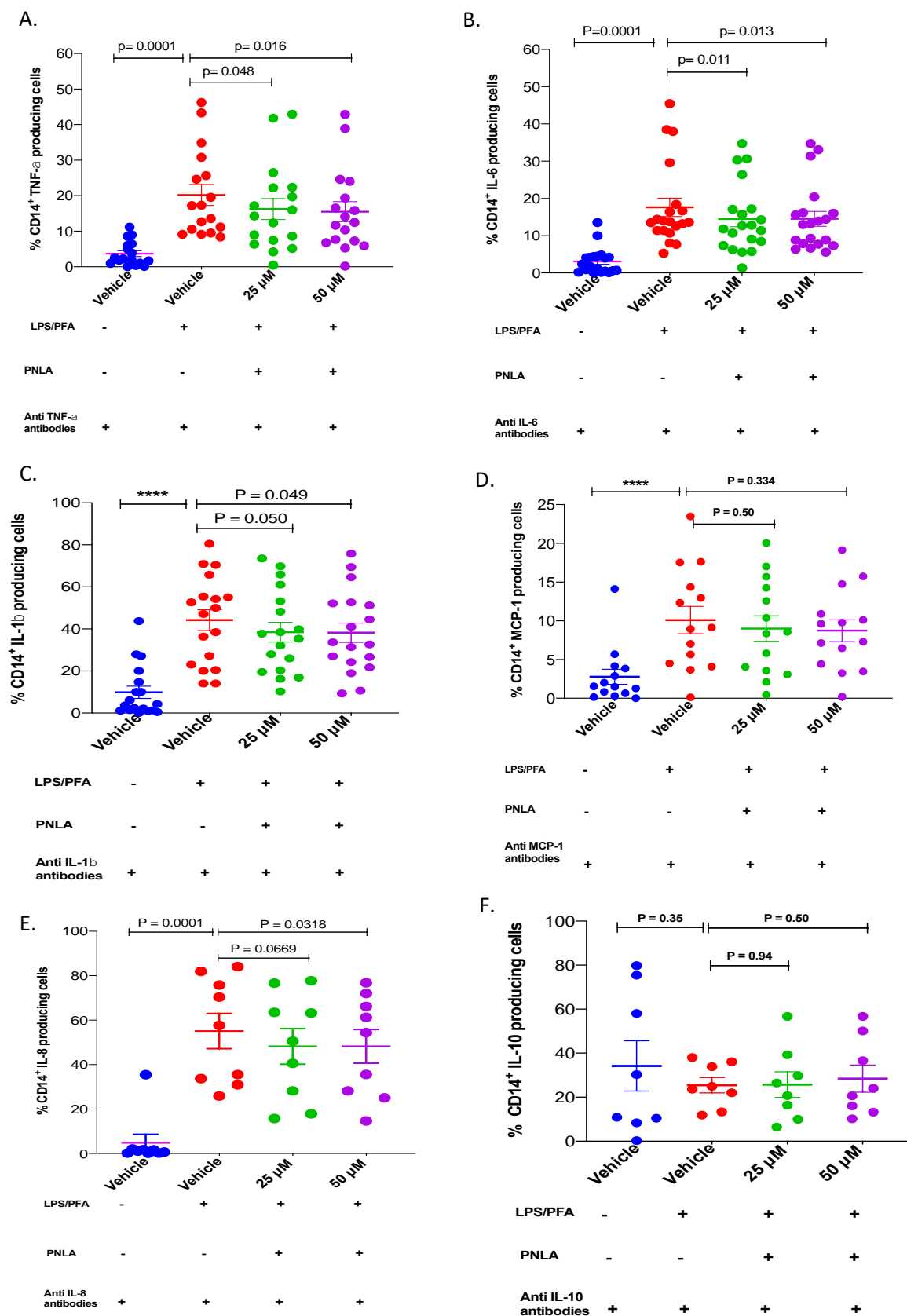


Figure 6.6. CD14⁺-expressing cytokines were significantly reduced following PNLA treatment.

TNF- α , IL-6 and IL-1 β were reduced in (A), (B), and (C) respectively. Purified monocytes were incubated with 25 and 50 μ M PNLA followed by 24-hours 100 ng/ml LPS stimulation for 8 hours from (n=20) obtained from RA patients (n=20). Then, cells were stained and analysed for the expression of TNF- α , IL-6 and IL-1 β antibodies using flow cytometry; all samples run in duplicates or triplicates. The same methodology was applied for CCL2 (MCP-1) (D), where (n=14) RA patients were recruited, and for IL-8 and IL-10 (E and F, respectively). The data are presented as the mean \pm SEM, and each dot (\bullet) represents the average of one participant. Statistical analysis was performed using a one-way ANOVA and a Tukey's post-hoc-test, where (**** $p \leq 0.0001$, * $p \leq 0.05$, and otherwise as illustrated).

6.2.4. Intracellular cytokine expression upon PNLA treatment did not significantly correlate with the patients' characteristics: gender, ACPA, RF, CRP, ESR, DD, age, and DAS28.

Next, to test whether there is an association between the PNLA effect on the percentage of intracellular cytokine levels (TNF- α , IL-6, IL-1 β , and IL-8) and the patients biological data, laboratory data, and DAS28, the following formula was used to calculate the percentage of cytokine reduction from the data obtained on the percentage of CD14⁺ cells expressing cytokines using 25 μ M PNLA.

$$\% \text{ reduction in CD14}^+ \text{ monocytes expressing cytokines by PNLA} = 100 \times \frac{(\text{LPS stimulated and vehicle treated} - \text{LPS stimulated and PNLA treated})}{\text{LPS stimulated and vehicle treated}}$$

The correlation was analysed by two-tailed Spearman rank correlation between the percentage reduction in cytokine expressing CD14⁺ monocytes and patient and disease characteristics. The results are presented in **Table 6.2**. CRP correlated significantly positively with ESR (R=0.613, p=0.004). Also, a significant positive correlation was found between IL-1 β and ESR (R=0.477, p=0.034). However, the later p-value was not adjusted for multiple comparisons. No statistically significant correlation was found between the reduction in cytokine expressing CD14⁺ monocytes by PNLA and the patients' characteristics.

Table 6.2. Correlation analysis of the reduction in CD14⁺ cells expressing cytokines against a variety of clinical indices and laboratory biomarkers.

| | % Reduction in CD14 ⁺ IL-6 expression | % Reduction in CD14 ⁺ TNF- α expression | % Reduction in CD14 ⁺ IL-1 β expression | Age | DD | ESR | CRP | DAS28 |
|--------|--|---|--|-------|-------|--------|------|-------|
| Age | -.058 | -.169 | .270 | | | | | |
| | .808 | .475 | .250 | | | | | |
| DD | .122 | -.022 | -.138 | .205 | | | | |
| | .610 | .927 | .563 | .387 | | | | |
| ESR | .090 | -.117 | .477* | -.164 | -.064 | | | |
| | .706 | .622 | .034* | .490 | .789 | | | |
| CRP | .003 | -.277 | .308 | -.245 | .054 | .613** | | |
| | .990 | .238 | .187 | .298 | .821 | .004** | | |
| DAS 28 | .038 | -.063 | .214 | -.185 | .011 | .435 | .400 | |
| | .872 | .791 | .366 | .434 | .962 | .056 | .081 | |

R-value on top, with corresponding p-values on the lighter rows below. DD; disease duration, ESR; erythrocyte sedimentation rate, CRP; C-reactive protein, and DAS28; disease activity score 28. Red shown* highlight the significant correlations.

Figure 6.7 shows the correlation between the percentage of reduction in cytokines expressed by CD14⁺ monocytes with ESR and CRP.

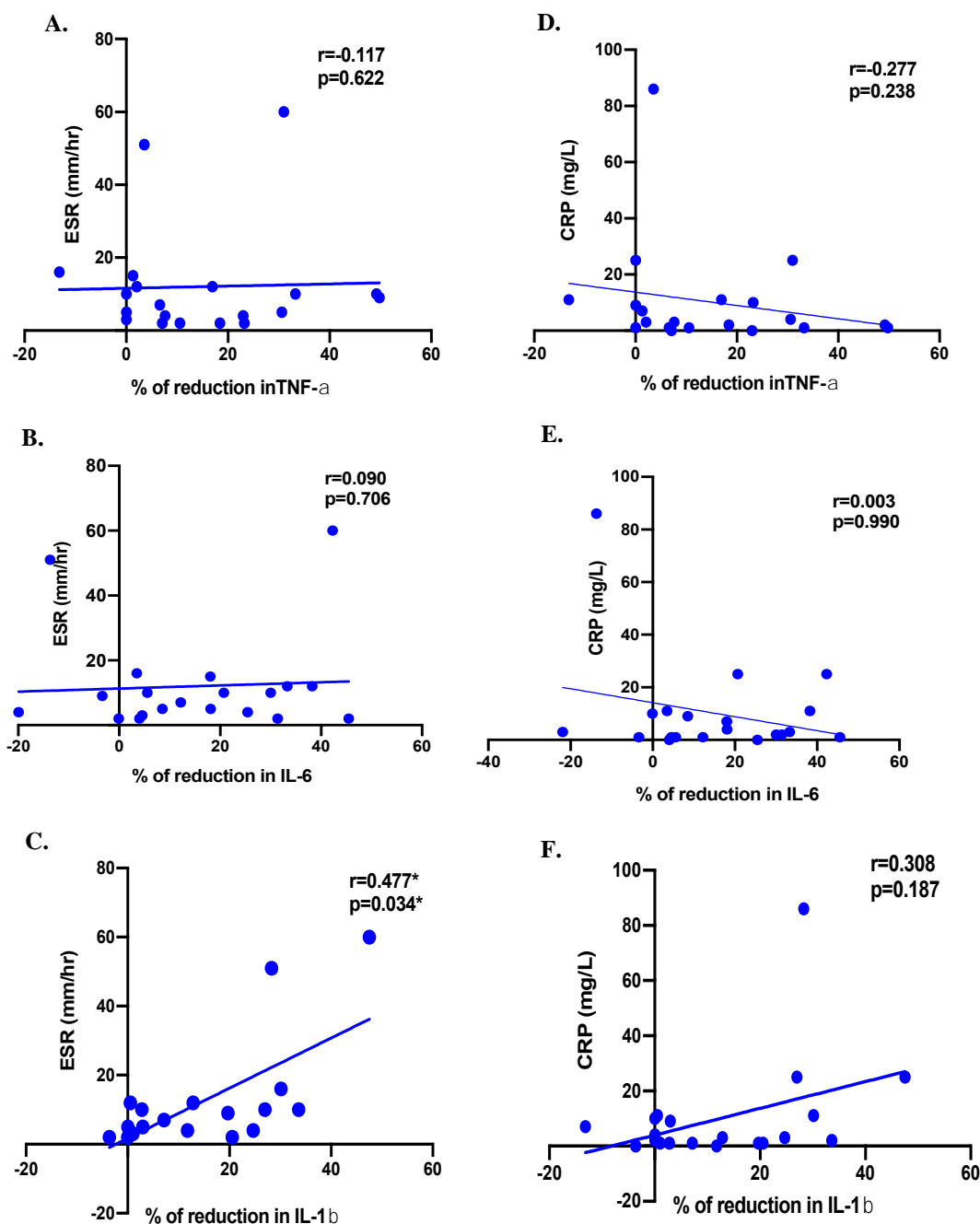


Figure 6.7. There was no correlation between the levels of reduced cytokines and ESR or CRP.

TNF, IL-6 (A and B, respectively), and ESR show no correlation, while IL-1 β (C) correlated with ESR ($r = 0.477^*$, $p = 0.034^*$), but not significantly after Bonferroni adjustment. There was no correlation between the levels of reduced cytokines TNF, IL-6, and IL-1 β , and CRP (D, E, and F), respectively, in RA patients. The correlation was determined using non-parametric Spearman's rank analysis. RA (n=20). ESR; Erythrocyte sedimentation rate, CRP; C-reactive protein.

Figure 6.8 shows the correlation between the percentage of reduction in cytokines expressed by CD14⁺ monocytes with age and DD.

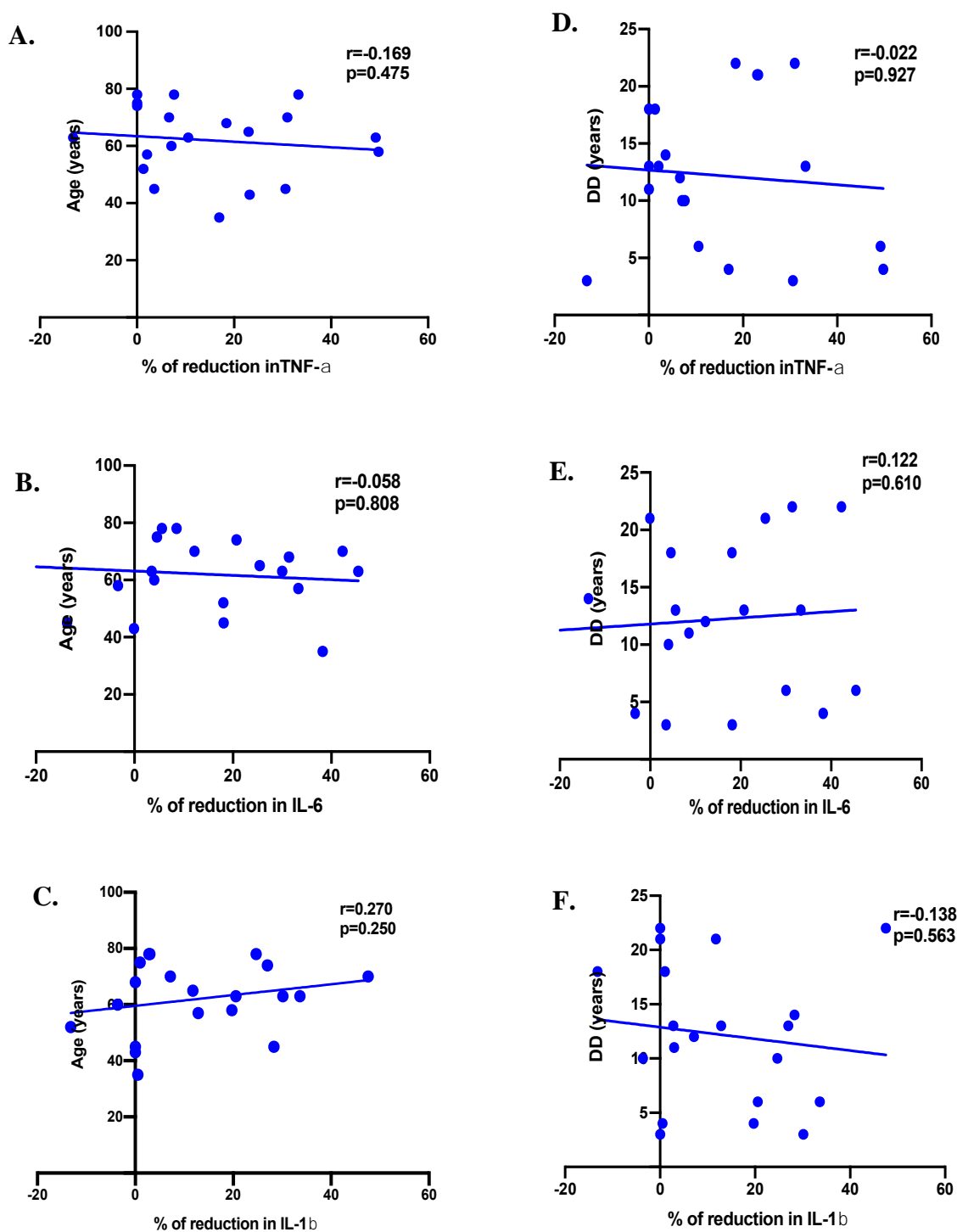


Figure 6.8. There was no correlation between the levels of reduced cytokines and the age or DD. A, B, and C show no correlation between TNF- α , IL-6 and IL-1 β and the age, while D, E, and F show no correlation between the reduced cytokines and the DD of RA patients. The correlation was determined using non-parametric Spearman's rank analysis ($n=20$). DD; disease duration.

Figure 6.9 shows the correlation between the percentage reduction in cytokines expressed by CD14⁺ monocytes with DAS28.

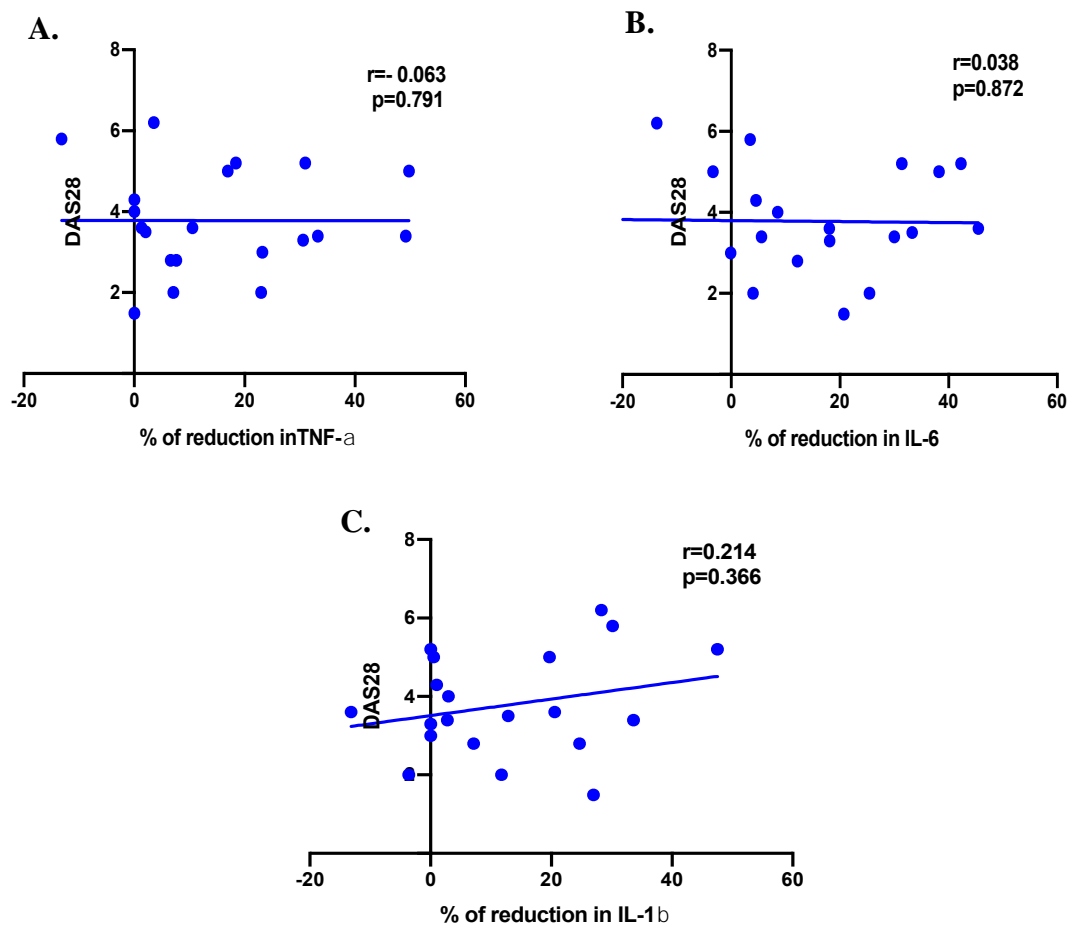


Figure 6.9. There was no correlation between the levels of reduced cytokines and DAS28.

A, B, and C show no correlation between TNF- α , IL-6, and IL-1 β , and DAS28. The correlation was determined using non-parametric Spearman's rank analysis (n=20). DAS-28; Disease activity scoring-28.

6.2.4.1. There is no correlation between the reduction in different cytokines expressed by CD14⁺ monocytes.

There was no significant correlation between the percentage reduction in different cytokine expressed by CD14⁺ monocytes. **Figure 6.10** shows (A) the correlation between IL-6 and IL-1 β ($r = 0.0557$, $p=0.816$), (B) IL-6 and TNF- α ($r = 0.159$, $p=0.501$), and (C) the correlation between TNF- α and IL-1 β is ($r = 0.159$, $p=0.50$) for all RA patients.

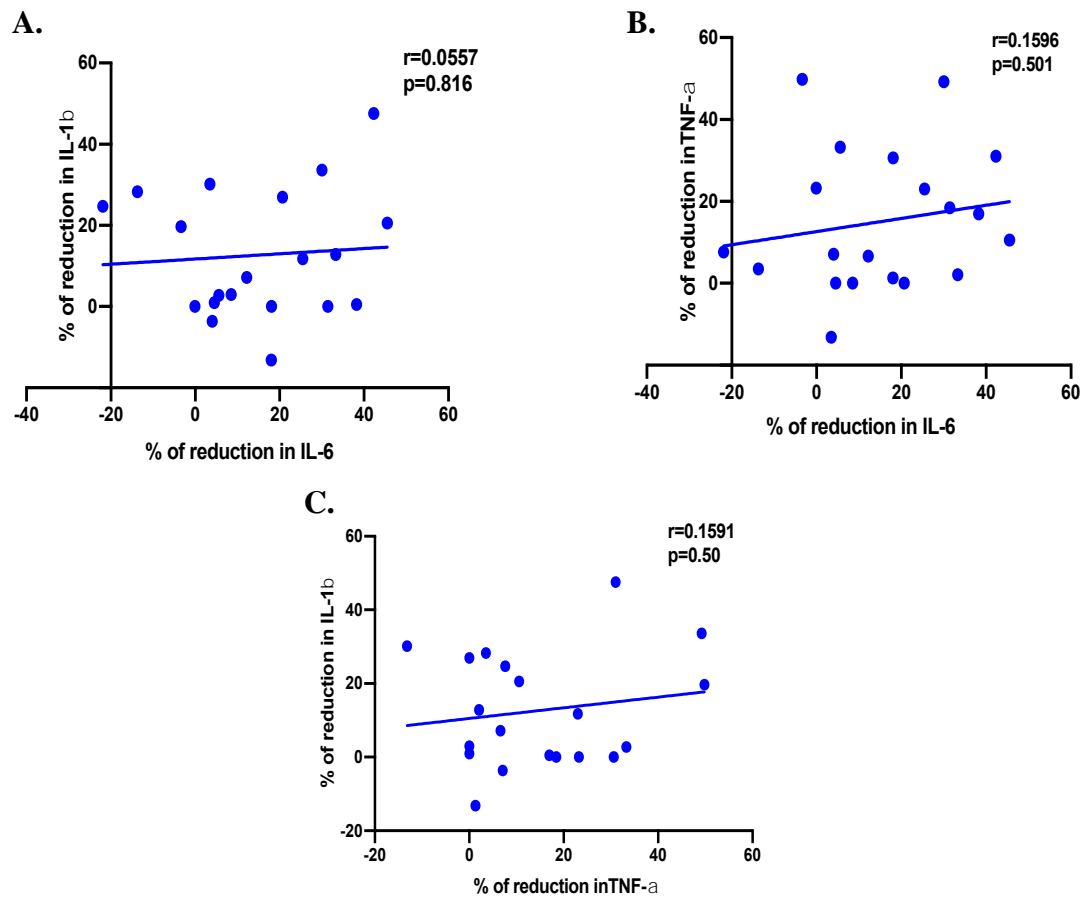


Figure 6.10. There was no correlation between the levels of all the reduced cytokines.

(TNF- α and IL-6), (IL-1 β and IL-6) and (TNF- α and IL-1 β) (A, B, and C) respectively of RA patients. Correlation was determined using non-parametric Spearman's rank analysis ($n=20$).

6.2.4.2. Gender and reduction in cytokines expressed by CD14⁺ monocytes.

There was no significant difference between gender and the reduction in cytokine expressing CD14⁺ monocytes. The change in the percentage of cytokine-expressing CD14⁺ monocytes was similar in females and males, with a higher percentage of reduction in females, but the differences were not significant (**Figure 6.11**); (A) The percentage of reduction in TNF- α expressing CD14⁺ monocytes was $15.6 \pm 4.67\%$ for females and $12.7 \pm 4.51\%$ for males; (B) The percentage reduction in IL-6 expressing CD14⁺ monocytes was $17.11 \pm 4.4\%$ for females while it was $7.12 \pm 11.04\%$ for males; (C) The percentage of reduction in IL-1 β expressing CD14⁺ monocytes in females was $14.2 \pm 3.94\%$ while in males, it was $6.30 \pm 7.39\%$.

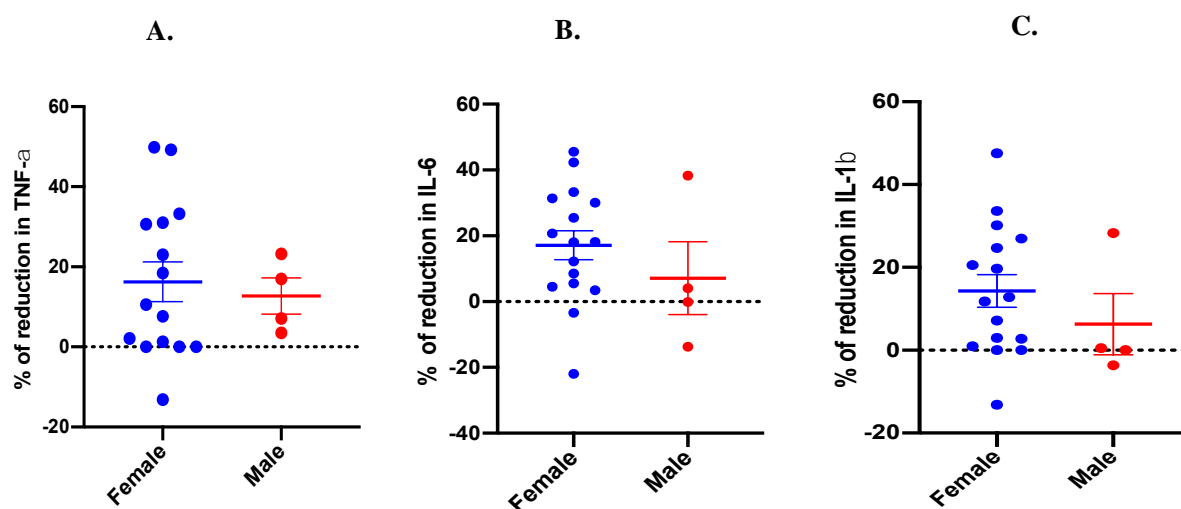


Figure 6.11. There was no correlation between the levels of reduced cytokines and the gender of RA patients.

(A) % of reduction in TNF- α (15.6 ± 4.67) for females while for males (12.7 ± 4.51), (B) % of reduction in IL-6 (17.11 ± 4.4) for females while in males (7.12 ± 11.04), and (C) % of reduction in IL-1 β in females (14.2 ± 3.94) while in males (6.30 ± 7.39). Analysis was determined using a non-parametric 2 tailed t test ($n=20$); $F=16$, $M=4$.

6.2.4.3. Serological status and level of cytokines (TNF- α , IL-6, and IL-1 β); RF and ACPA positivity

No statistical difference was observed between serological status (RF or ACPA) and changes in the percentage of cytokine-expressing CD14⁺ cells. ACPA status (**Figure 6.12**); (A) % of reduction in TNF- α expressing CD14⁺ monocytes were ($21.34 \pm 5.74\%$) in ACPA positive participants while in ACPA negative participants ($8.94 \pm 5.86\%$); (B) % of reduction in IL-6 expressing CD14⁺ monocytes were ($17.06 \pm 6.93\%$) in ACPA positive participants while in ACPA negative participants ($7.46 \pm 5.38\%$); (C) % of reduction in IL-1 β expressing CD14⁺ monocytes were ($13.97 \pm 5.87\%$) in ACPA positive participants while in ACPA negative

patients ($8.91 \pm 5.26\%$). ACPA results were not available for 3 patients, so they were excluded from the analysis.

(Figure 6.12) (D) The percentage reduction in TNF- α expressing CD14⁺ monocytes was $19.53 \pm 6.10\%$ in RF positive, while $13.10 \pm 5.64\%$ in RF negative participants; **(E)** The percentage reduction in IL-6 expressing CD14⁺ monocytes was $16.77 \pm 4.4\%$ in RF positive participants, while $7.12 \pm 11.04\%$ in RF negative participants; **(F)** The percentage reduction in IL-1 β expressing CD14⁺ monocytes was $15.11 \pm 5.54\%$ in RF positive patients, while in RF negative patients, it was $9.72 \pm 4.03\%$.

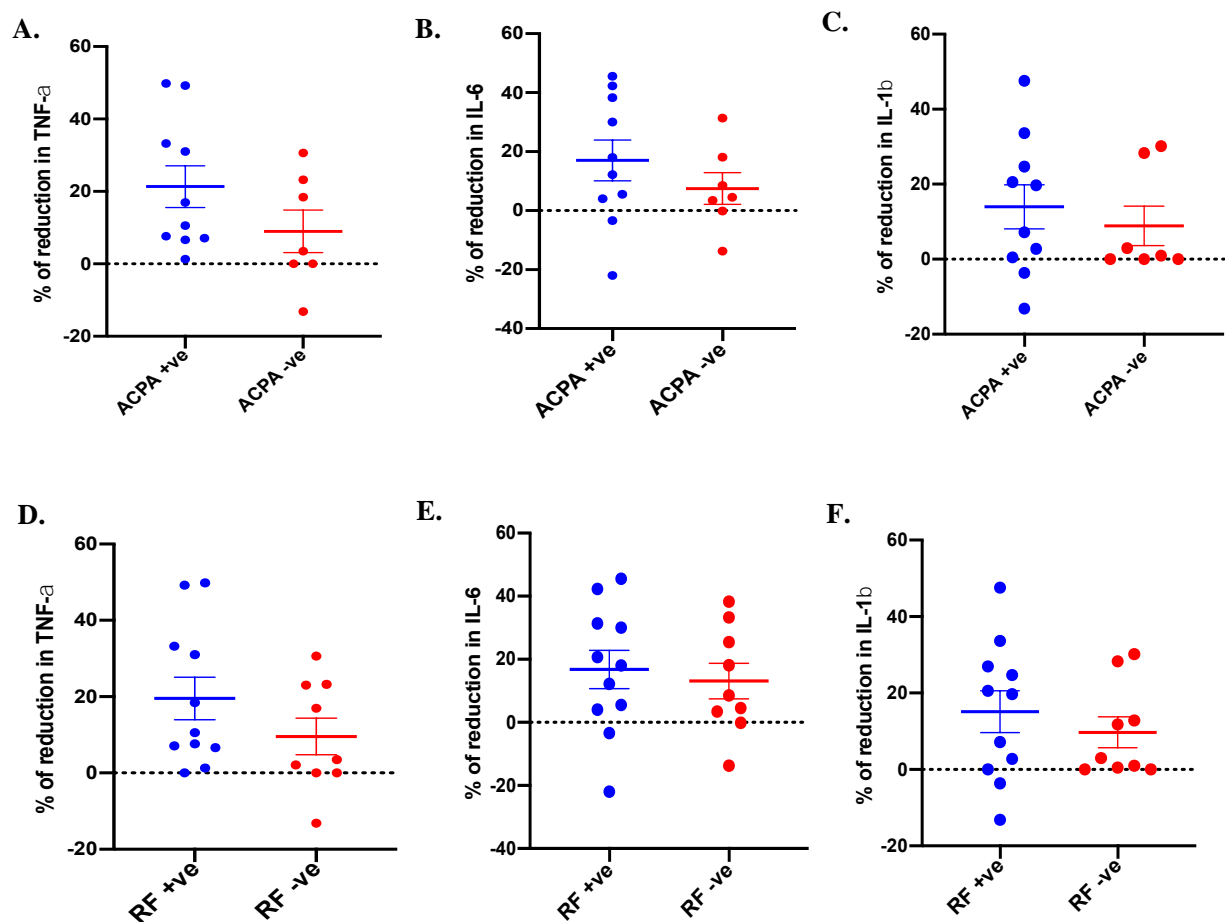


Figure 6.12. There was no correlation between the levels of reduced cytokines and RF status.

(A) % of reduction in TNF- α (21.34 ± 5.74) in ACPA positive participants, while in ACPA negative participants (8.94 ± 5.86); (B) % of reduction in IL-6 (17.06 ± 6.93) in ACPA positive, while in ACPA negative participants (7.46 ± 5.38); (C) % of reduction in IL-1 β (13.97 ± 5.87) in ACPA positive, while in ACPA negative patients (8.91 ± 5.26). For RF status: (D) % of reduction in TNF- α (19.53 ± 6.10) in RF positive participants while in RF negative participants (13.10 ± 5.64); (E) % of reduction in IL-6 (16.77 ± 4.4) in RF positive participants, while in RF negative participants (7.12 ± 11.04). (F) % of reduction in IL-1 β (15.11 ± 5.54) in RF positive, while in RF negative patients (9.72 ± 4.03). Analysis was determined using a non-parametric 2 tailed t test ($n=20$); RF +ve =11, -ve = 9; ACPA+ve = 10, -ve = 7.

6.3. Discussion

The pathologic effects of the cytokines produced by monocytes in RA and atherosclerosis have been extensively reviewed in this thesis. Studies in this Chapter investigated the effect of PNLA on the percentages of CD14⁺ monocytes expressing cytokines. We showed that PNLA significantly reduces CD14⁺ monocytes expressing (TNF- α , IL-6, IL-1 β , and IL-8) (**Figure 6.6 (A, B, C, and E)**), which supports our data in Chapter 4 where PNLA reduces TNF- α , IL-6, and IL-1 β in the supernatants of activated monocytes upon LPS challenge. With regards to IL-8, it was not measured in the supernatants of monocytes.

Looking at CD14CD16 monocytes in terms of morphological or phenotypic changes, their granularity upon PNLA treatment was increased as judged by SSC-A (**Figures 6 (1, 2)**). The exact explanation cannot be determined by flow cytometry, and to answer this, techniques such as confocal microscopy and image stream may clarify whether PNLA is trying to oppose the activation caused by LPS endotoxin in the form of autophagy (autophagocytosis) or whether this may result from the apoptotic reaction of PNLA against the endotoxins. Autophagocytosis is a regulated mechanism of the cell to remove unnecessary or dysfunctional components. Increased inside scatter has no correlation with cell death or viability, as demonstrated by Zombie aqua L/D dye. Despite the lack of direct evidence, it is possible that the cells are undergoing autophagy and the increase in granularity is due to increased autophagosome formation as a condition of “cleaning out” damaged cells to regenerate newer, healthier cells, as imaging under fluorescent microscopy (**Figure 6.4**) also shows hypertrophied (expansion) features in comparison to the shrinking (atrophic) appearances. Moreover, there were lower percentages of CD14⁺ cells in PNLA-treated cells in comparison with LPS-treated cells, and this percentage may provide an index of the cell count of an individual. Monocyte counts are routinely available in the clinic and could provide a quantitative measure to help guide therapeutic decisions. Circulating monocyte numbers are increased in patients with active RA but fall in patients who respond to TNF-blockade. A reduction in monocyte count predicts sustained remission in RA patients treated with anti-TNF therapy (Shipa *et al.* 2021). Kawanaka *et al.* also found that patients with active RA showed higher frequencies of CD14CD16 blood monocytes, with the frequency of these cells decreasing in patients that responded well to therapy (Kawanaka *et al.* 2002). Chara *et al.* (2015) showed that the increased level of total circulating monocytes; classical and intermediate monocytes, in treatment-naïve RA patients predicted a sub-optimal or no-response to MTX treatment. Further to the increase in the number of monocytes in RA mentioned earlier, in atherosclerosis, the correlation between elevated monocyte counts and a higher risk for cardiac events has been

confirmed in many reports (Zhuang *et al.* 2017). Additionally, other studies demonstrated that elevated intermediate monocyte counts play a pivotal role in the growth and stability of already existing atherosclerotic plaques or cardiac attacks (Cappellari *et al.* 2017; Imanishi *et al.* 2010; Kashiwagi *et al.* 2010; Ozaki *et al.* 2017; Rogacev *et al.* 2012).

In Chapter 3, PNLA reduced monocyte migration that was stimulated by the chemokine CCL2, while in Chapter 5, PNLA is predicted to inhibit CCR2 (ligand of CCL2) as an upstream regulator. In this Chapter, PNLA did not reduce CD14⁺ monocytes expressing CCL2 significantly (**Figure 6.6 (F)**). This contrasts with Baker *et al.* (2020) who reported that CCL2 and ICAM1 were reduced upon PNLA treatment in cell culture (EA. hy926 cells) supernatants, but anti-human CD54 (ICAM-1) surface expression in the same cell model was not significantly reduced using flow cytometry.

The effect of PNLA on reducing LPS stimulated cytokine production by purified monocytes was independent of gender, age, DD, serological status, and DAS28 RA (**Table 6.2**). No statistically significant correlation was found between these variables and the percentage reduction in cytokine expression, apart from IL-1 β and ESR. For the latter, the difference was not statistically significant after Bonferroni correction for multiple comparisons. This suggests the nutritional values of n-6 diet is not restricted by patient characteristics. This was the first study for PNLA using clinical samples, and to my knowledge, there has been no previous study that has studied the correlation between the biologic effect of PNLA and patients' characteristics.

Results of flow cytometric analysis by Chen *et al.* also showed the infiltration of different types of immune cells in mouse ear tissue, including leukocytes (CD45⁺), neutrophils (Ly6G⁺CD45⁺), and macrophages (F4/80⁺CD45⁺), was obvious after 6 hours of 12-O-tetradecanoylphorbol-13-acetate (TPA) stimulation. However, the topical injection of PNLA before the TPA administration significantly reduced the numbers of these infiltrating immune cells as compared with the TPA group (Chen *et al.* 2019). Relative to the non-stimulated control, topical administration of TPA onto the mouse dorsal skin surface promoted p-MAPK after 2 hours of stimulation. The topical treatment of PNLA before the TPA stimulation suppressed the expression of p-38 by 55% and JNK-MAPK by 32%, respectively. However, no such effect on the expression of p-ERK-MAPK was observed. My observation in Chapter 4 is that PNLA is predicted to inhibit p-ERK, p-38 MAPK and AKT in HCs and ERK, JUN in RA patients, as shown in the heatmaps (**Figures 5.12, 5.13**), respectively.

In addition, Chen *et al* reported the ability of PNLA and $\Delta 7$ -ETrA to significantly suppress TPA-induced oedema by lowering both ear thickness and biopsy weight (Chen *et al.* 2019). Based on the results of FA analysis, no detectable amounts of PNLA or $\Delta 7$ -ETrA in the ear biopsy sample were found (Chen *et al.* 2019). This is likely because only a small amount (3 μ g) of PNLA or $\Delta 7$ -ETrA was injected into the ear. Once injected PUFA was diffused or/and metabolised, fewer of them could substitute for phospholipid AA. This observation is inconsistent with the results of other studies, which documented that in cultured cells, cellular FA composition and lipid-derived pro-inflammatory mediator production could be manipulated by dietary PUFA supplementation. This means that there is a discrepancy between studies conducted in cell culture and those performed using experimental animals. To answer this, a lipidomic technique may provide information regarding the changes in FA composition within a cell. The mechanisms by which metabolites alter monocyte functions have many aspects in common with the concept of innate immune cell memory, where initial priming with a stimulus leads to sustained epigenetic reprogramming that culminates in a phenotypic change upon subsequent challenge.

Next, this work has been extended to study the gene expression levels of purified CD14CD16 monocytes from RA patients with active disease using RNA-seq.

Chapter 7: Effects of PNLA on the inflammatory gene expressions of activated CD14CD16 monocytes implicated in the pathogenesis of RA and atherosclerosis

7.1. Introduction and aims

In Chapter 5, we used RNA-seq to investigate the gene expression levels of PBMCs upon PNLA or vehicle treatment and LPS challenge in a similar incubation period to that done when using ELISA in Chapter 4.

Recent evidence showed that metabolic responses to LPS differ in human myeloid cells (Stienstra *et al.* 2017). Moreover, the different types of cells in our bodies are genetically identical but express different genes. Thus, the products of some of these genes will be proteins on the cell surface, some will be secreted, and others will be proteins within the cell; they dictate the function of the cell. Therefore, we sought to sort and purify CD14CD16 monocytes as one category of PBMCs. Monocytes are the main mononuclear phagocytes (MPS) of the innate immune system. They are divided up into 3 subsets based on the expression of CD14 and CD16: CD14⁺⁺CD16⁻, CD14⁺CD16⁺, and CD14⁻CD16⁺ (Ziegler-Heitbrock *et al.* 2010) as reviewed in the Introduction. A growing body of research, however, suggests that monocyte heterogeneity may go beyond these 3 populations (Appleby *et al.* 2013; Villani *et al.* 2017). However, currently, it is widely accepted in scientific research that human monocytes can be identified using the markers CD14 and CD16, and this has been applied in this chapter for sorting and purifying monocytes. Monocytes from RA patients have been sorted to investigate the effect of PNLA after LPS stimulation for an incubation period of 4 hours on gene expression by RNA-seq. This incubation time aims to capture cytokine gene transcription by monocytes based on published literature. The objective is to provide, for the first time, an unbiased analysis of the effect of PNLA on LPS-activated monocytes from patients with active RA. It is well known that the development of protective immunity is shaped by the interactions of the host immune system with components of bacterial cells such as *E. coli* LPS.

The extraction of high-quality RNA, fragmentation of the purified RNA, and removal of rRNA, which represent 80-90% of total RNA in eukaryotic cells (**Figure 7.1**), and the preparation of cDNA libraries were key steps that required significant effort to generate high-quality sequencing reads, followed by the bioinformatic work. The bioinformatics include mapping to a reference genome and the provisional check through differential expression and functional

analyses, including downstream application (all these steps were discussed in detail in Chapter 5) or are illustrated otherwise in this Chapter.

Exposure of human monocytes to the endotoxin LPS, which signals through TLR4, rapidly induces many types of microRNA (miRNA) expression (Furer *et al.* 2010). Interestingly, here in this Chapter, PNLA-treated and LPS-stimulated CD14/CD16 monocytes expressed a variety of miRNAs. Gene transcription and translation may need to be adjusted to meet the demands of a single eukaryotic cell, and protein expression is of great significance for overall cellular functionality. Non-coding RNAs, or miRNAs, have a strong role as post-transcriptional regulators of gene expression and are predicted to affect up to 30% of all human protein-encoding genes (Furer *et al.* 2010). Importantly, miRNAs can inhibit the expression of a certain protein by means of translation repression or even mRNA degradation, but some miRNAs even stimulate translation (Filkova' *et al.* 2012).

A growing body of literature suggests that miRNAs play important roles in cardiac (Andreou *et al.* 2015), skeletal muscle development (Furer *et al.* 2010) and immune function (Calder 2008). A large number of disease states, including inflammatory disorders and cardiovascular conditions, have been implicated in changes in miRNA expression, which contribute to the pathogenesis and production of pro-inflammatory chemokines and cytokines (Furer *et al.* 2010; Najm *et al.* 2019; Virtue *et al.* 2012). In addition, some miRNAs in peripheral monocytes strongly correlate with clinical markers of rheumatoid disease activity (Najm *et al.* 2019). During the last decade, evidence has shown that epigenetic mechanisms, the most widely investigated of which are miRNAs, contribute significantly to RA pathogenesis (Najm *et al.* 2019). Altered miRNA expression has been associated with enhanced inflammatory pathway signalling, and increased secretion of pro-inflammatory cytokines. The abnormal expression pattern of miRNAs described in various pathologies has drawn extensive attention. Suppression of overexpressed miRNAs or reconstituting the expression by restoration of silenced miRNAs may be of therapeutic profit in many fields (Filkova' *et al.* 2012). Besides, there are no investigations concerning the impact of n-6 PUFA on miRNA expression by these cells from RA patients.

The miRNAs are small, single-stranded (20–22 nucleotides), synthesised in the nucleus from non-coding genes or exons of coding genes by RNA polymerase II giving rise to a pri-miRNA. In the nucleus, this pri-miRNA is transformed into a pre-miRNA of about 70 nucleotides. The pre-miRNA is exported into the cytoplasm and, by interacting with Dicer, is cleaved into

double-stranded RNA with a 3' and 5' sequence. One of the strands binds to the RISC complex, which results in the association of the mature miRNA with its target mRNA, resulting in either its degradation or inhibition of its translation (Najm *et al.* 2019). Different miRNAs have been reported to regulate positively or negatively TNF α expression or signalling pathways in arthritis, most notably by directly targeting various components of the NF- κ B pathway (Najm *et al.* 2019). The aim of the studies in this Chapter is to explore the WGT profile of CD14CD16 monocytes purified from active RA patients following PNLA supplementation for 24 hours and LPS stimulation for 4 hours using RNA seq.

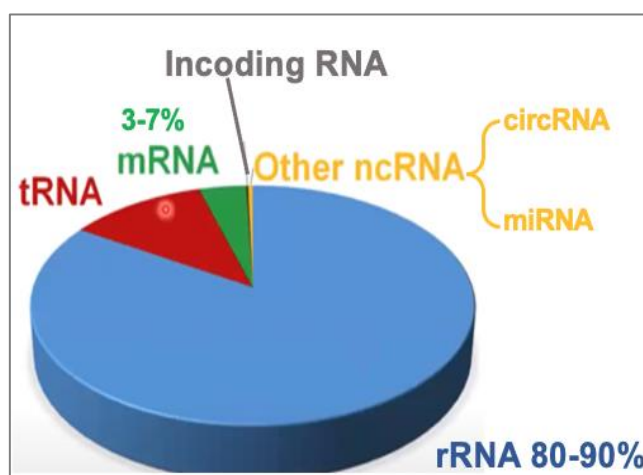


Figure 7.1. Eukaryotic RNA categories.

Total RNA mass can include ribosomal RNA (rRNA), coding or messenger RNA (mRNA), transfer RNA (tRNA), long non-coding RNA (lncRNA), and non-coding RNA, which includes circular (circ) and micro (miRNA).

7.2. Results

The datasets generated and/or analysed during the current chapter are available in the ArrayExpress repository at this link:

<https://eur03.safelinks.protection.outlook.com/?url=https%3A%2F%2Fwww.ebi.ac.uk%2Farrayexpress%2Fexperiments%2FE-MTAB-11585&data=04%7C01%7Ctakalara%40cardiff.ac.uk%7Cffa10886d9aa45f2293308da08cdc3f5%7Cbdb74b3095684856dbf06759778fcbc%7C1%7C0%7C637831977088935528%7CUnknown%7CTWFpbGZsb3d8eyJWljojMC4wLjAwMDAiLCJQIjoiV2luMzIiLCJBTiI6IklhaWwiLCJXVCI6Mn0%3D%7C3000&sd=IZkhO4Xdj9H75VbAdk%2FHaPm4RjU%2F31V4diScRPXE3rI%3D&reserved=0> Accession number to a dataset: E-MTAB-11585

7.2.1. Principle component analysis (PCA)

PCA was performed in R using normalised data from the DESeq2 analysis. The data were clustered using the top 50 most significant DEGs overall comparisons. The plot shows the results of the first 2 PC and each plot represents all the genes studied (3240 genes; **Figure 7.2**) or represents 50 genes (**Figure 7.3**). The results show samples clustering within groups, demonstrating that inter-sample variation in gene expression is all within the normal range.

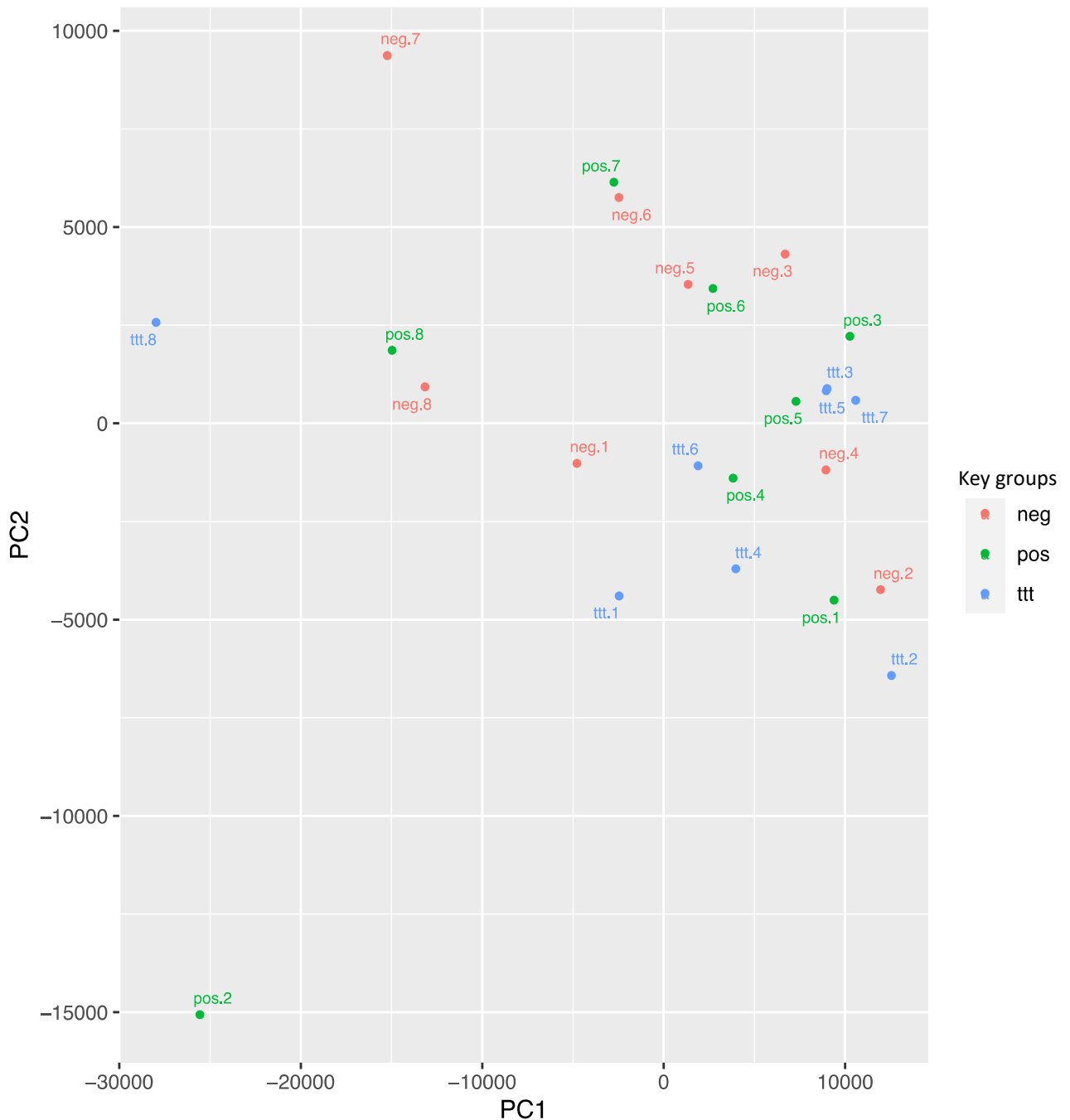


Figure 7.2. Principal component analysis (PCA) from the DESeq2 analysis of all DEGs.

Each principal component (PC) on the y-axis is plotted against the variance it contributes within the dataset on the x-axis. The horizontal line indicates an arbitrary threshold for PCs that contributes a significant proportion of the variance. PCA analysis was performed on the 24 samples to discover trends in the data, as samples in the same area of the graph are considered to be genetically similar. Each dot is an individual sample representative of all genes studied (3240), and all samples are colour coded per condition as shown. Neg: unstimulated unsupplemented, pos: LPS stimulated, and ttd: LPS stimulated and PNLA supplemented CD14CD16 monocytes. 230

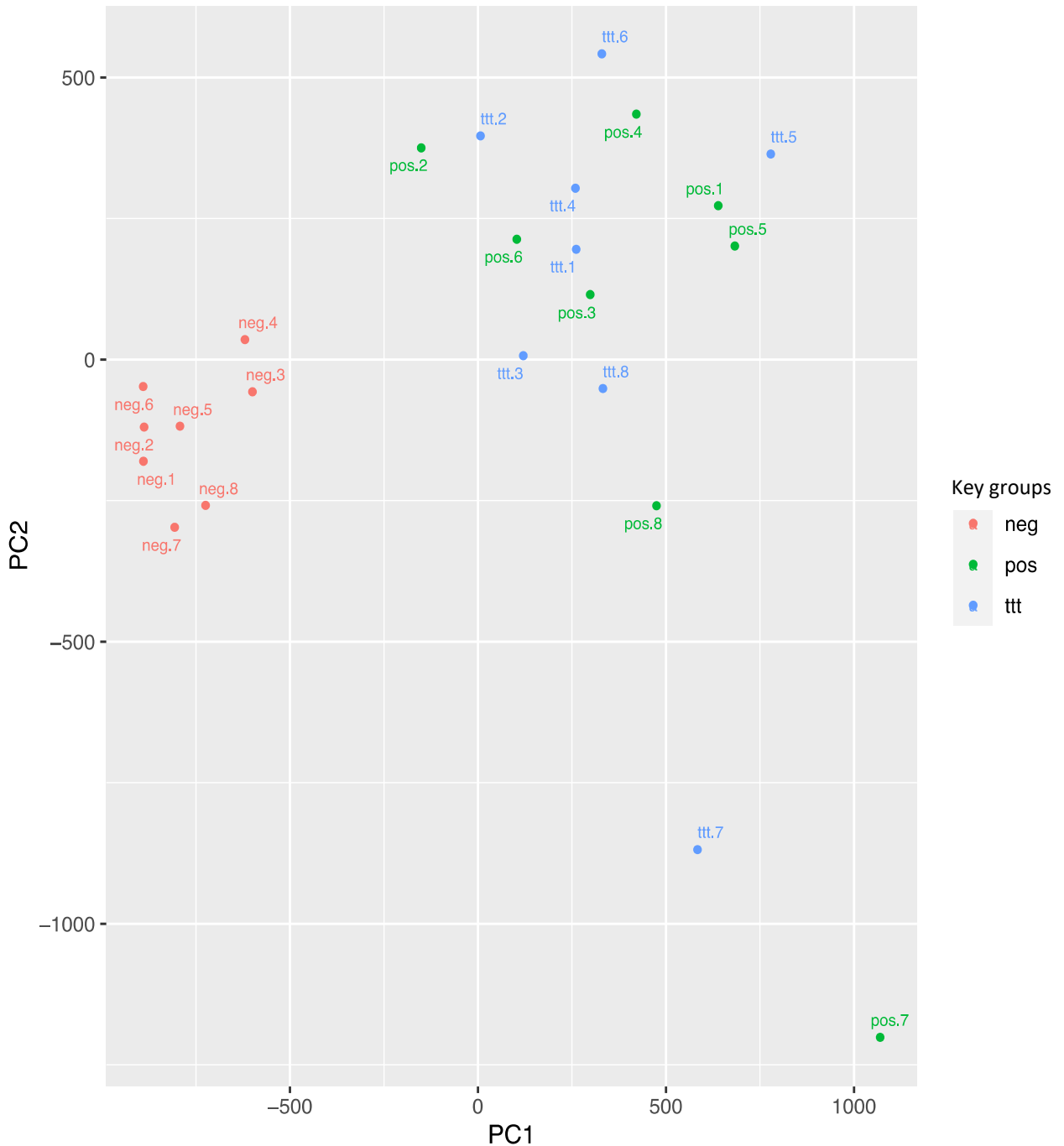


Figure 7.3. Principal component analysis (PCA) from the DESeq2 analysis of top 50 DEGs. Each principal component (PC) on the y-axis is plotted against the variance it contributes within the dataset on the x-axis. The horizontal line indicates an arbitrary threshold for PCs that contributes a significant proportion of the variance. PCA analysis was performed on the 24 samples to discover trends in the data, as samples in the same area of the graph are considered to be genetically similar. Each dot represents an individual sample representative of 50 genes, and all samples are colour coded per condition as shown. Neg: unstimulated unsupplemented, pos: LPS stimulated, and ttt: LPS stimulated and PNLA supplemented CD14CD16 monocytes.

7.2.2. Heatmap

The heatmap (**Figure 7.4**) shows main clusters of DEGs for all the treatment conditions mentioned earlier for (n=8) active RA patients generated from the Broad Morpheus Institute software (<https://software.broadinstitute.org/morpheus/>). The map shows the expression of 500 genes with a significant p value of <0.05 in CD14CD16 monocytes.

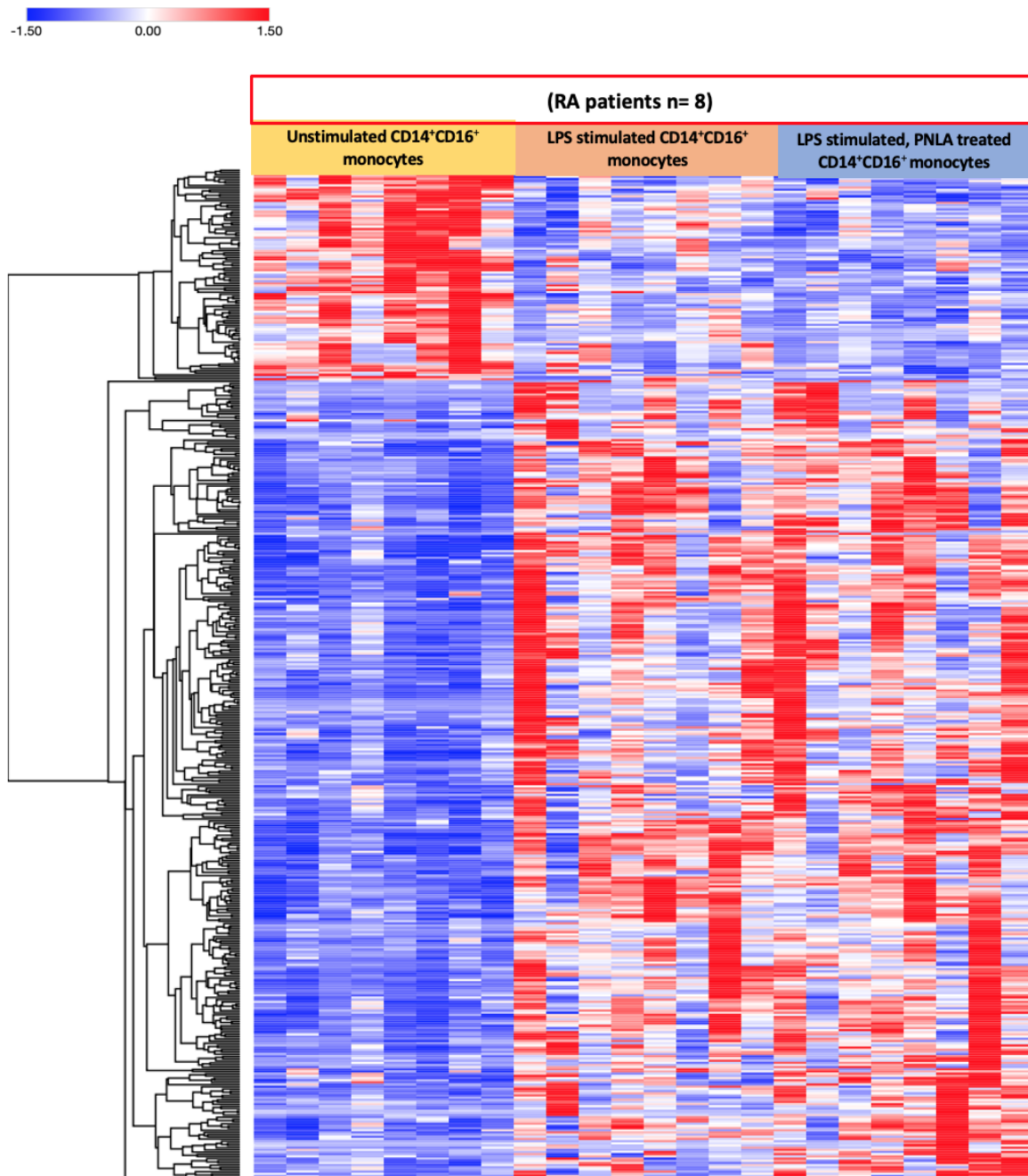


Figure 7.4. Heatmap for the whole genomic transcriptome of significantly expressed genes.

The main clusters of 24 samples from (n=8) active RA patients had 3 conditions per participant: condition 1. for the unstimulated monocytes, condition 2. LPS stimulated and vehicle treated, and condition 3. PNLA treated and LPS stimulated monocytes. The map was following an FPKM reading of 5 using broad Morpheus software. Heatmap visualisations used log₂ fold change (log₂FC). Data sets were hierarchically clustered using one minus Pearson correlation coefficient. FPKM; fragments per kilobase million.

7.2.3. Volcano plots

Using GraphPad Prism version 8, RA patients' global significant and non-significant genes of coding and non-coding genes were plotted as volcano plots, and comparisons between groups were performed as shown in **Figure 7.5** for the top 500 DEGs from all participants. The statistically significant DEGs are shown outside and above the dotted lines; with ($\log_2 \text{FC} < -1$ and >1) and p value < 0.05 .

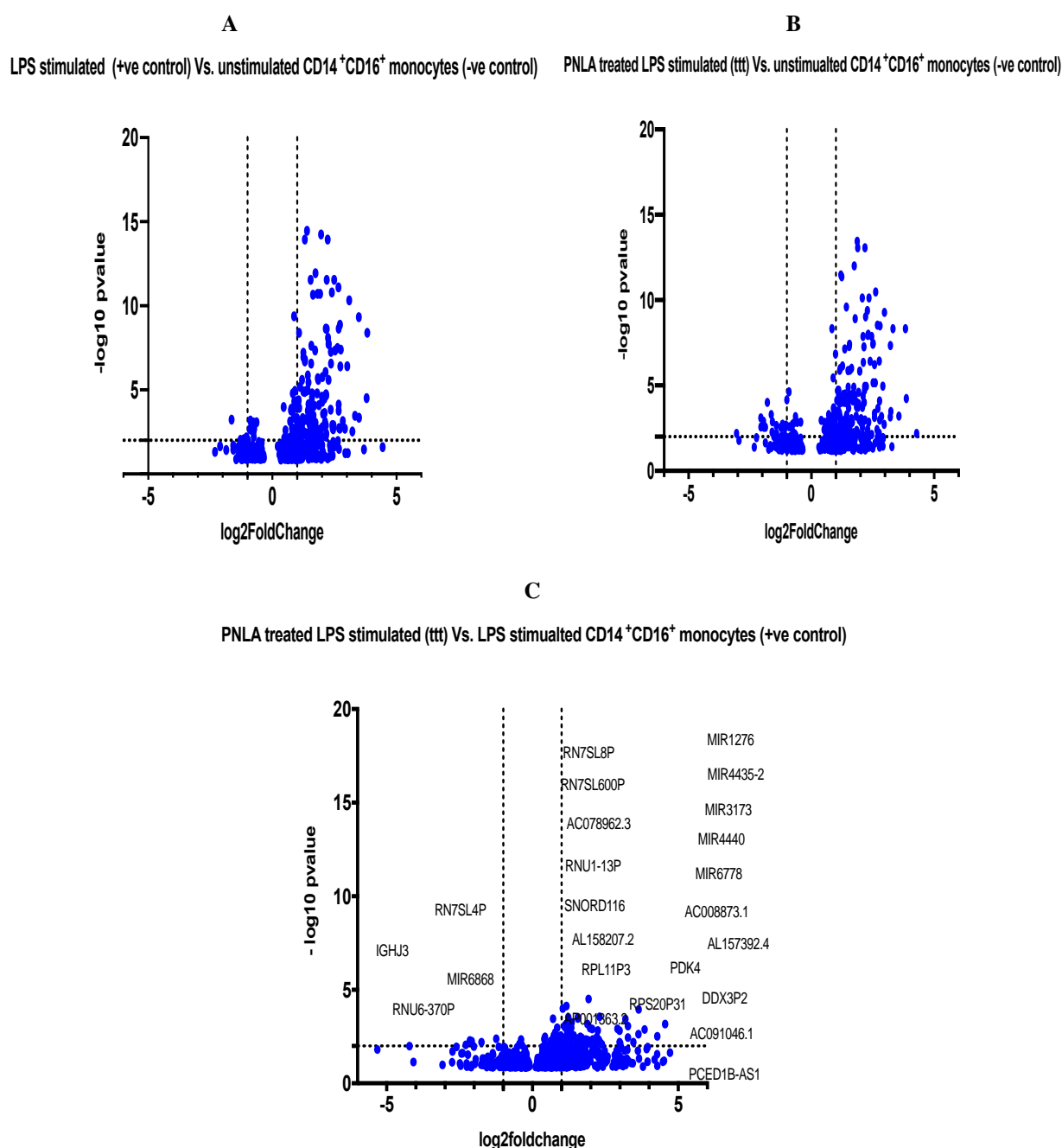


Figure 7.5. Volcano plots of the global gene expression profile of RA patients.

Dotted lines identify genes whose expression was significantly regulated ($\log_2 \text{FC} < -1$ and >1 ; $p < 0.05$) after 24 hours of 25 μM PNLA or vehicle treatment and 4 hours post 100 ng/ml LPS stimulation. **(A)** shows LPS stimulated versus unstimulated monocytes; **(B)** shows PNLA treated, LPS stimulated versus unstimulated monocytes; **(C)** shows PNLA treated, LPS stimulated versus LPS stimulated monocytes from RA. Plots were performed on (GraphPad Prism version 8); genes marked as p value < 0.05 .

7.2.4. Protein coding genes of CD14CD16 monocytes whose expression was significantly affected by PNLA treatment.

Raw data with a p-value ≤ 0.05 were filtered to select only the protein coding DEGs affected upon PNLA treatment and LPS stimulation in comparison with LPS stimulated monocytes. Of the total 87 genes, 40 were downregulated and 47 were upregulated, as shown in **Tables 7.1** and **7.2**, respectively. The genes highlighted in red have the same observation of expression in Chapter 5 as the DEGs from PBMCs of RA patients.

Table 7.1. Down-regulated protein coding genes.

| Gene symbol | P value | log2FoldChange |
|-------------|------------|----------------|
| SPCS1 | 0.00457316 | -0.3889066 |
| RHNO1 | 0.00772516 | -0.445853 |
| MRPL9 | 0.00897261 | -0.3562887 |
| MT-ND1 | 0.0111281 | -1.1519433 |
| HAUS2 | 0.01408627 | -0.2589403 |
| AC113189.9 | 0.02021096 | -0.6329407 |
| HSPA1L | 0.02261342 | -0.8068353 |
| MT-CO2 | 0.02426093 | -0.8215064 |
| CHCHD4 | 0.02494514 | -0.5253673 |
| NIT1 | 0.02578718 | -0.2936841 |
| PAIP1 | 0.02652437 | -0.2093219 |
| OTUB1 | 0.02863435 | -0.2062052 |
| MEN1 | 0.02892991 | -0.2316949 |
| OTUB1 | 0.02863435 | -0.2062052 |
| MEN1 | 0.02892991 | -0.2316949 |
| ATMIN | 0.03039483 | -0.2434687 |
| MT-ATP6 | 0.03071407 | -0.9914844 |
| ENOX2 | 0.0310368 | -0.2614889 |
| LSM1 | 0.03115697 | -0.2821932 |
| ARL2BP | 0.03163195 | -0.2534689 |
| MT-ND5 | 0.0331925 | -0.8105088 |
| FZD2 | 0.03337634 | -1.0574003 |
| EEFSEC | 0.03359343 | -0.2823531 |
| SHARPIN | 0.03434721 | -0.3720591 |
| MEA1 | 0.03439924 | -0.2134155 |
| AC007731.4 | 0.03477517 | -0.4368948 |
| PPP1R7 | 0.03567901 | -0.2324188 |
| JMJD4 | 0.03582529 | -0.3678366 |
| ZNF428 | 0.03871094 | -0.703142 |
| SLC10A3 | 0.03940111 | -0.3316 |
| NDUFA7 | 0.04031457 | -0.3793683 |
| GZF1 | 0.04091086 | -0.2745701 |
| PDCL | 0.04245787 | -0.2803202 |
| CCDC51 | 0.04318786 | -0.2952535 |
| MT-ND4 | 0.04695626 | -0.6759886 |
| DEDD | 0.04699614 | -0.2218534 |
| DSTN | 0.04760566 | -0.238492 |
| DCTN2 | 0.04838837 | -0.182193 |
| TRAPPC2L | 0.04892909 | -0.4731658 |
| EDARADD | 0.04985603 | -1.4593028 |

Table 7.2. Upregulated protein coding genes

| Gene symbol | P value | log2FoldChange |
|-----------------|------------|----------------|
| LY6G5B | 0.00034881 | 0.70755274 |
| PDK4 | 0.00036415 | 3.18958087 |
| BRF1 | 0.00325595 | 0.4337583 |
| ACAA2 | 0.00343723 | 0.91003443 |
| ZBTB34 | 0.00427356 | 0.40754133 |
| ACADVL | 0.00443301 | 0.93393128 |
| AC007375.2 | 0.00654865 | 0.84877037 |
| SPINK4 | 0.00699286 | 2.33516822 |
| CPT1A | 0.00844875 | 0.69292304 |
| AC090227.2 | 0.0102456 | 0.7761555 |
| GRIK1 | 0.01072531 | 1.04080934 |
| HSD17B8 | 0.01459802 | 0.63690587 |
| AC008481.3 | 0.01575296 | 0.67745158 |
| AP4B1 | 0.01597519 | 0.35373153 |
| PLIN2 | 0.01695979 | 1.52650127 |
| NPEPL1 | 0.0178674 | 0.34366431 |
| KDM4C | 0.01845432 | 0.4053604 |
| CCDC88B | 0.01847757 | 0.92737706 |
| IRF3 | 0.01931028 | 0.38814126 |
| HSPB9 | 0.02058611 | 1.00732108 |
| AC012651.1 | 0.02101049 | 0.40204391 |
| AL133500.1 | 0.02345169 | 0.53492741 |
| MRE11 | 0.02539087 | 0.33449725 |
| XPA | 0.02547796 | 0.40955563 |
| RNF166 | 0.02632569 | 0.60565988 |
| MTG1 | 0.02779212 | 0.41040856 |
| SOX15 | 0.02786463 | 0.51263859 |
| ZNF48 | 0.02819684 | 1.1309529 |
| ANKRD23 | 0.03246504 | 0.6371512 |
| C12orf75 | 0.03294798 | 1.55318072 |
| CCER2 | 0.03297806 | 1.2292063 |
| CCDC194 | 0.0345181 | 1.23143686 |
| SLC25A42 | 0.03850798 | 1.12134178 |
| GHRL | 0.03879516 | 0.4293575 |
| ALG13 | 0.03960082 | 0.41540235 |
| CRABP2 | 0.04073619 | 1.4878064 |
| MTRNR2L8 | 0.04206278 | 0.50185453 |
| ROM1 | 0.04371743 | 0.47498045 |
| ST14 | 0.04414583 | 0.94104069 |
| SIGIRR | 0.04453364 | 1.12389203 |
| ZBTB40 | 0.04498858 | 0.17567415 |
| AKR1B1 | 0.04687118 | 0.62649418 |
| RCN3 | 0.04840635 | 0.57764257 |
| CLDND2 | 0.048774 | 1.63566507 |
| KLHDC4 | 0.04980061 | 0.6491871 |
| ETFA | 0.04981843 | 0.24752697 |
| JMJD7-PLA2G4B | 0.05002327 | 0.48261373 |
| SLC25A20 | 0.05004554 | 0.50986113 |

7.2.5. Noncoding microRNA (miRNA) analysis of CD14CD16 monocytes

In this analysis, up- or downregulated miRNAs were identified when there was at least a two-fold change between 2 comparison groups (Log2FoldChange) (n=8 for each subgroup) and a p-value < 0.05.

Venn diagrams (**Figure 7.6**) showed that 35 miRNAs were differentially expressed in LPS stimulated versus unstimulated monocytes, (7 were downregulated and 28 were upregulated) (A). (B) PNLA-treated or LPS stimulated versus unstimulated monocytes identified 68 miRNAs that were differentially expressed, with 8 downregulated and 60 upregulated. (C) PNLA treatment or LPS stimulation versus LPS stimulation in monocytes showed 6 downregulated miRNAs and 46 upregulated miRNAs.

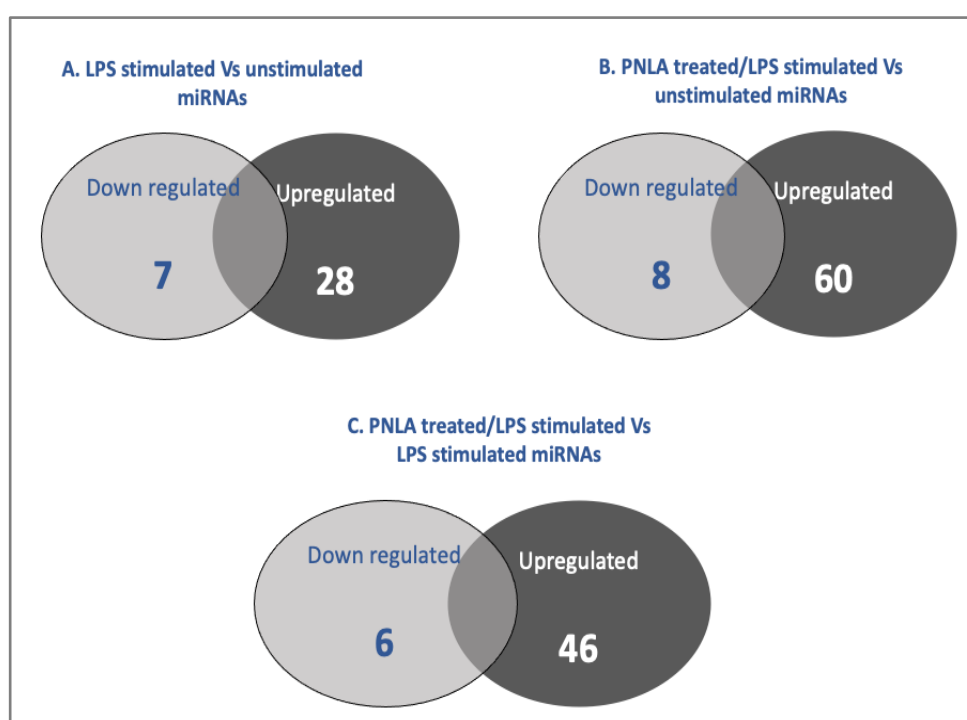


Figure 7.6. Venn diagrams showing the significantly affected miRNAs.

(A) unstimulated (vehicle) vs LPS-stimulated monocytes B) PNLA-treated LPS-stimulated vs vehicle-treated LPS-stimulated monocytes, and (C) PNLA-treated LPS-stimulated vs unstimulated (vehicle-treated) monocytes (p value < 0.05).

7.2.6. Impact of combination PNLA supplementation and LPS stimulation versus LPS stimulation

As the main interest is to determine PNLA affected miRNAs; **Table 7.3** and **Table 7.4** shows downregulated miRNAs and upregulated miRNAs based on the Venn diagram **Figure 7.6** (C).

Table 7.3. Down-regulated miRNAs

| miRNA symbol | P value | log2FoldChange |
|--------------|------------|----------------|
| MIR637 | 0.00634466 | -1.7466434 |
| MIR4326 | 0.01094654 | -1.0103594 |
| MIR6886 | 0.02544526 | -2.4344905 |

| | | |
|---------|------------|------------|
| MIR1909 | 0.03026114 | -0.5482978 |
| MIR671 | 0.03855069 | -0.3497858 |
| MIR7111 | 0.04708788 | -0.7253948 |

Table 7.4. Upregulated miRNAs

| miRNA symbol | P value | log2FoldChange |
|--------------|------------|----------------|
| MIR8066 | 0.00011357 | 3.64199116 |
| MIR1276 | 0.00068454 | 4.55094396 |
| MIR3173 | 0.00110552 | 1.97460738 |
| MIR664B | 0.00153033 | 2.99076371 |
| MIR6773 | 0.00233385 | 3.63985987 |
| MIR6778 | 0.00311499 | 4.28591091 |
| MIR374C | 0.00311767 | 1.39533476 |
| MIR374B | 0.00345498 | 1.38208333 |
| MIR3161 | 0.00427845 | 1.24687388 |
| MIR219B | 0.00459433 | 2.06906127 |
| MIR3922 | 0.00475857 | 2.27944349 |
| MIR219A2 | 0.00489499 | 1.91298973 |
| MIR1914 | 0.00518867 | 1.27590652 |
| MIR505 | 0.00605733 | 2.10537396 |
| MIR3140 | 0.00680206 | 1.7364798 |
| MIR941-3 | 0.00757542 | 1.69321925 |
| MIR324 | 0.00761552 | 1.15616334 |
| MIR4722 | 0.00929873 | 1.51670221 |
| MIR4755 | 0.00933625 | 1.27252376 |
| MIR3176 | 0.0098648 | 1.436178 |
| MIR3978 | 0.01044756 | 1.75906105 |
| MIR4435-2 | 0.01158254 | 3.95408034 |
| MIR4440 | 0.01358341 | 2.9973427 |
| MIR1470 | 0.01443236 | 3.92022505 |
| MIR570 | 0.01560925 | 0.86245152 |
| MIR6719 | 0.0184946 | 2.4778449 |
| MIR365B | 0.01973051 | 0.8725209 |
| MIR6516 | 0.01995768 | 0.95898745 |
| MIR28 | 0.01996707 | 2.18139375 |
| MIR1260B | 0.02060822 | 0.90146242 |
| MIR6744 | 0.02068237 | 2.1691624 |
| MIR4434 | 0.02440112 | 1.15863809 |
| MIR342 | 0.02533851 | 1.74143132 |
| MIR620 | 0.02730656 | 1.53792619 |
| MIR6755 | 0.02833511 | 1.46159167 |
| MIR3679 | 0.03570583 | 1.29447685 |
| MIR3188 | 0.03579885 | 1.95841277 |
| MIR7107 | 0.03760526 | 0.76246923 |
| MIR32 | 0.04072735 | 2.48790672 |
| MIR4725 | 0.04135483 | 0.96185387 |
| MIR5088 | 0.04231274 | 1.47488951 |
| MIR378H | 0.04286645 | 1.24063468 |
| MIR7150 | 0.04294533 | 1.80549093 |
| MIR6763 | 0.04328839 | 1.63076905 |
| MIR626 | 0.04458306 | 1.48601166 |

7. 2. 7. miRNAs target mRNAs

Using the miRNA target filter in IPA, 72 miRNAs were uploaded into the core analysis, and target information was available for 39 miRNAs. The associated mRNAs and pathways related to chronic inflammatory diseases and the cell metabolic pathway are shown in **Table 7.5**. Expression fold change and expression p-value were determined based on Fisher's exact test right-tailed in IPA. The filter has selected miRNAs with a high or moderate level of confidence based on the database. Several miRNAs identified in this study were previously documented, which supports the validity of the data set.

Table 7.5. Selected miRNAs target mRNA and the relevant associated pathways as per the IPA database.

| miRNA ID | Expr p-value | Expr Log Ratio | mRNA symbol | Expr p-value | Expr Log Ratio | Pathway |
|--------------------|--------------|----------------|----------------------|--------------|----------------|--|
| miR-3173 | 0.0011 | 1.975 | CRABP2 | 0.0407 | 1.488 | Acute phase response, retinoid acid mediated apoptosis signalling. |
| miR1260B | 0.0206 | 0.901 | JMJD7-PLA2G4B | 0.05 | 0.483 | ERK/MAPK signalling, glucocorticoid receptor signalling, MIF regulation of Innate Immunity, MIF-mediated glucocorticoid regulation, p38 MAPK signalling, Phospholipase C signalling, VEGF family ligand-receptor interactions. |
| miR-646 | 0.0702 | 3.95 | | | | |
| miR-1909 | 0.0303 | -0.548 | FZD2 | 0.0334 | -1.057 | Adipogenesis pathway, osteoarthritis pathway, role of macrophages, fibroblasts and Endothelial Cells in rheumatoid arthritis, role of osteoblasts, osteoclasts, and chondrocytes in rheumatoid arthritis. |
| miR-1909 | 0.0303 | -0.548 | SIGIRR | 0.0445 | 1.124 | NF- κ B signalling, TLR Signalling, TREM1 signalling. |
| miR-7150 | 0.0429 | 1.805 | | | | |
| miR-6868-5P | 0.0025 | 1.501 | | | | |
| miR-2861 | 0.0611 | -1.178 | LSM1 | 0.0312 | -0.282 | Systemic lupus erythematosus signalling. |
| miR-374B | 0.0034 | 1.382 | ETFA | 0.0498 | 0.248 | NAD signalling pathway |
| miR-4440 | 0.0136 | 2.997 | ATMIN | 0.0304 | -0.243 | Role of CHK Proteins in cell cycle checkpoint control. |
| miR-4440 | 0.0136 | 2.997 | GHRL | 0.0388 | 0.429 | Leptin signalling in obesity. |
| miR-548L | 0.0712 | 1.677 | | | | |
| miR-626 | 0.0446 | 1.486 | PDK4 | 0.000364 | 3.19 | Glucocorticoid receptor signalling, reelin signalling, senescence pathway. |
| miR-3173 | 0.0611 | 1.975 | | | | |
| miR-2861 | 0.0611 | -1.178 | | | | |
| miR-28 | 0.0200 | 2.181 | | | | |
| miR-7150 | 0.0429 | 1.805 | | | | |
| miR-3188 | 0.0358 | 1.958 | | | | |

| | | | | | | |
|-----------------|--------|--------|----------------|---------|--------|---|
| miR-3934 | 0.0470 | 1.072 | | | | |
| miR-637 | 0.0063 | -1.747 | SPCS1 | 0.00457 | -0.389 | Insulin secretion signalling pathway |
| miR-671 | 0.0386 | -0.35 | MT-ATP6 | 0.0307 | -0.991 | Glucocorticoid receptor signalling, mitochondrial dysfunction, oxidative phosphorylation, sirtuin signalling pathway, estrogen receptor signalling, |
| miR-3934 | 0.0758 | 1.072 | | | | |
| miR-3188 | 0.0358 | 1.958 | | | | |
| miR-7150 | 0.0429 | 1.805 | ACAA2 | 0.00344 | 0.91 | Fatty acid β -oxidation I, glutaryl-CoA degradation, ketogenesis, ketolysis, super pathway of cholesterol biosynthesis. |
| miR-5088 | 0.0423 | 1.475 | | | | |
| miR-4521 | 0.0542 | 2.853 | | | | |
| miR-7150 | 0.0429 | 1.805 | PAIP1 | 0.0265 | -0.209 | CSDE1 signalling pathway, EIF2 signalling, Insulin secretion signalling pathway. |

One of the targeted pathways, PDK4, was noted and discussed in Chapter 5. PDK4 is targeted by miRNAs; miR-3173, miR-2861, miR-626, miR-28, miR-7150, miR-3188, miR-879-5p, miR-393-5p, miR-708-5p, and miR-12118 (**Figure 7.5**).

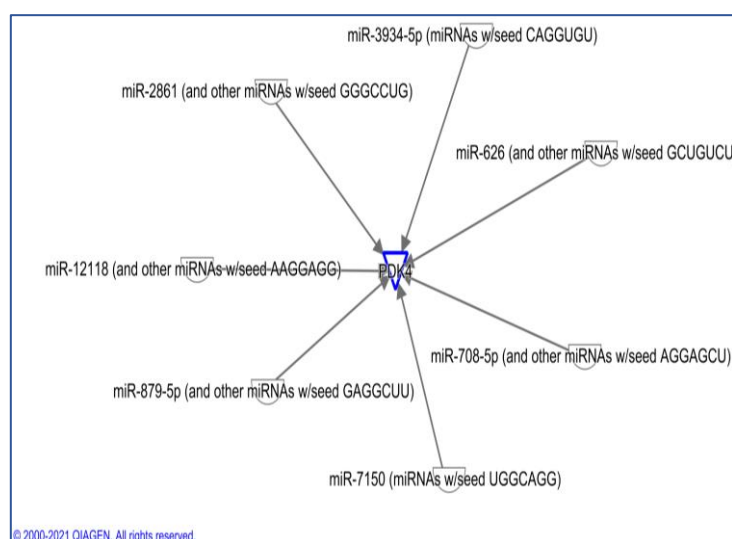


Figure 7.7. mRNA PDK4 is a target for miRNAs.

SIGIRR (single-immunoglobulin interleukin-1 receptor-related molecule, also known as Toll/interleukin-1 receptor 8 (TIR-8)), was first characterised as an inhibitor of IL-1R and TLR signalling by interaction with IRAK-1 and TRAF-6 in a 293 human cell line (Drexler *et al.* 2010). SIGIRR is one of the mRNAs that was activated by miRNAs upon PNLA treatment. It negatively modulates immune responses because of its role in the inhibition of NF- κ B signalling and TLR signalling (Drexler *et al.* 2010; Riva *et al.* 2012; Wald *et al.* 2003). SIGIRR is mostly expressed intracellularly in primary human monocytes, macrophages, and DCs (Drexler *et al.* 2010). SIGIRR in this study is targeted by 3 miRNAs, as shown in **Figure 7.8A**,

which are miR-7150, miR-1909-3p, and miR-6868-5p based on IPA high and moderate prediction confidence.

SIGIRR downstream regulatory effects are shown in **Figure 7.8B**, which include IL-1 β , and TNF- α . SIGIRR also targets NF- κ B, TLRs, and TRIM1 signalling pathways.

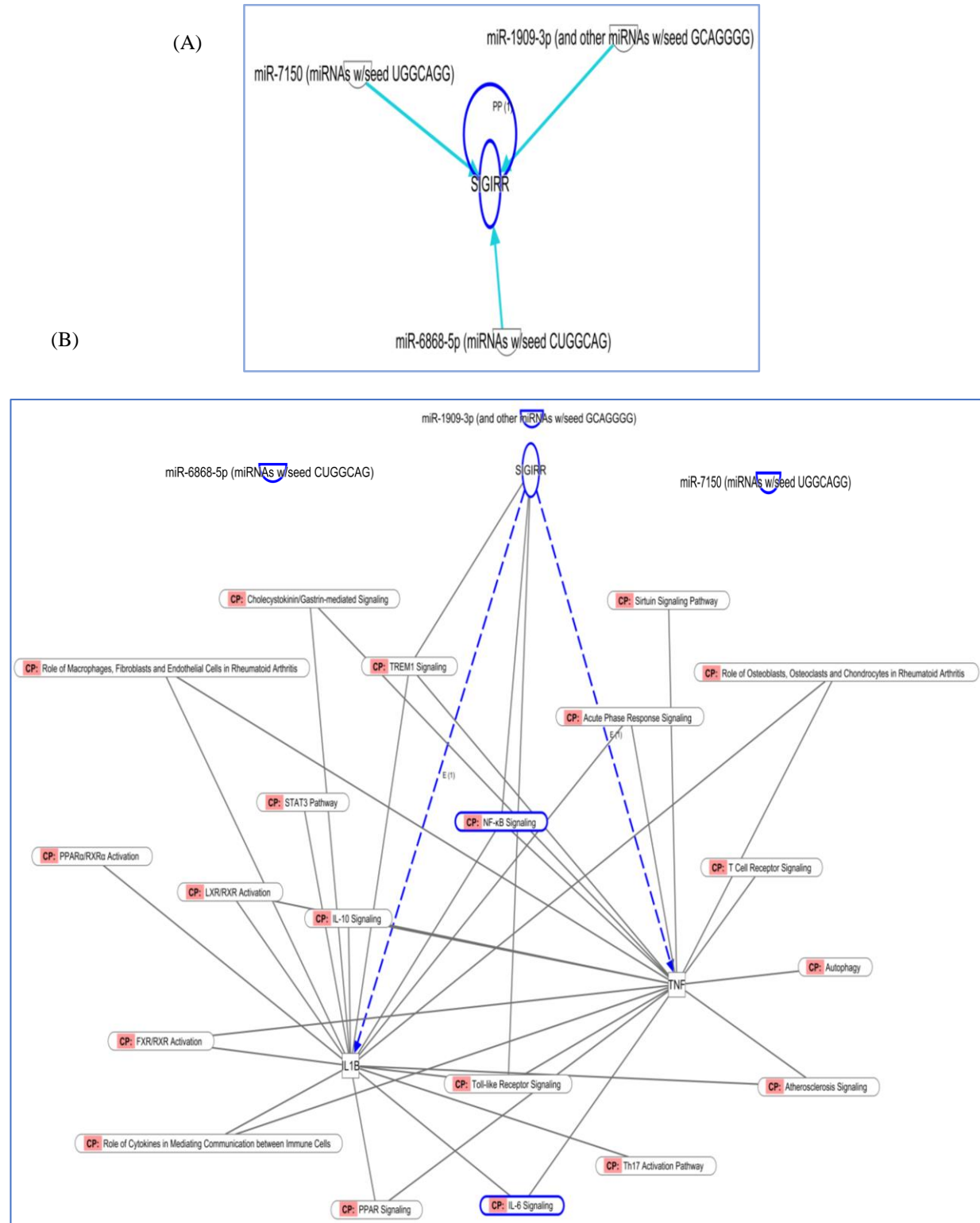


Figure 7.8. SIGIRR is downstream for miRNAs and upstream of canonical pathways.

(A) miR-1909-3P, miR-7150, miR-6868-5P, and (other miRNAs w/seed GCAGGGG) targeted SIGIRR mRNA; (B) SIGIRR upstream for many signalling pathways involved in the regulation of transcription factors, inflammatory cytokines, and metabolic molecules. CP; the Canonical Pathway.

7.2.8. Pathway analysis

Deep understanding of the entire set of results of high-throughput gene expression studies has often been challenging, caused by the complicated process of data analysis and the limited biological interpretation that could be extracted from the large datasets generated through bench experiments. As a consequence, genome-wide analyses have tended to focus on changes in expression for specific genes (Chun *et al.* 2014; Liu *et al.* 2006) or small groups of genes associated with a specific pathway (Ferreira *et al.* 2015). Hence, we determined and summarised the pathways significantly affected by PNLA using IPA to identify pathways, including the entire dataset adjusted p- and fold-change values as shown in sections (7.2.8.1-7.2.8.3).

7.2.8.1. Graphical summary of pathways analysis

Figure 7.9 provides an overview of major biological themes in IPA analysis; it selects the most significant entities in the core analysis and shows how they relate to each other. Biological processes and regulators include those with a z-score ≥ 2 . Nodes are coloured by their predicted activity in the analysis, where orange nodes are predicted to be activated with a z-score ≥ 2 . While blue coloured entities with z scores ≤ 2 are predicted to be inhibited. The analysis concerning PNLA treatment, activating KLF15, AGO2, FLCN, SIRT3, and Sirtuin signalling pathways and inhibiting STAT3, CLPP, TFE3, and DAP3.

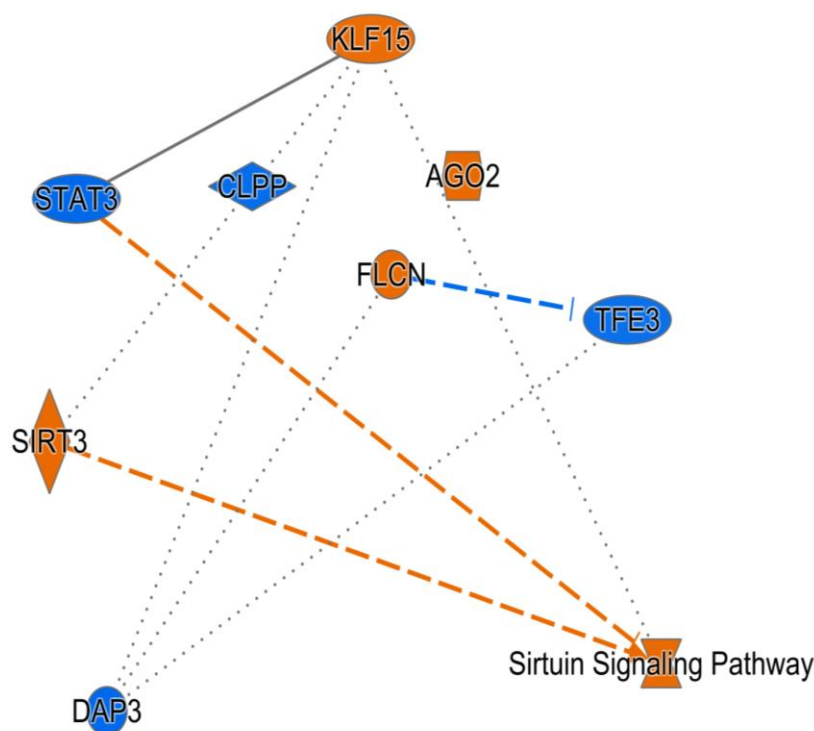


Figure 7.9. Graphical summary showing the most significant transcription factors and regulators affected by PNLA. The orange colour goes with the direction of activation while the blue is the inhibition state.

KLF15 (Kruppel-like factor 15) is an important member of the KLFs family, which are transcription factors important in regulating inflammation. KLFs are involved in numerous pathological processes associated with atherogenesis and associated with the regulation of various signal transduction pathways (Liu *et al.* 2018).

Mice with a systemic and smooth muscle-specific deficiency of KLF15 exhibited an aggressive inflammatory vasculopathy in two distinct models of vascular disease: orthotopic carotid artery transplantation and diet-induced atherosclerosis (Lu *et al.* 2013). KLF15 deficiency is seen in several CV disorders, such as heart failure and aortic aneurysm (Liu *et al.* 2018). KLF15 expression is reduced in atherosclerotic tissues from human aortic samples, with an approximately 7-fold reduction in KLF15 mRNA expression compared with nonatherosclerotic control aortae (Liu *et al.* 2018). KLF15 is an essential regulator of VSMC proinflammatory activation, which alters the acetylation status and activity of the proinflammatory factor NF- κ B (Lu *et al.* 2013).

The mammalian **SIRT (Sirtuin)** family of proteins has seven members, named SIRT1 to SIRT7. SIRTs have the potential to reduce the inflammatory component of atherosclerotic disease and may have the potential to alter the course of atherogenesis (Sosnowska *et al.* 2017).

SIRT1 a NAD⁺ dependent histone deacetylase downregulates both the innate and adaptive immune response in mice. SIRT1 can inhibit the NF- κ B pathway directly by itself or indirectly via the forkhead family of transcription factors (FoxO) (De Gregorio *et al.* 2020; Sosnowska *et al.* 2017). SIRT1 deacetylase was initially shown to deacetylate RelA/p65 at lysine 310 residue, which leads to reduced NF- κ B transcriptional activity (Kong *et al.* 2013; Qiu *et al.* 2021). Substrates of SIRT1 are particularly abundant and include the NF- κ B transcription factor RelA/p65, AP-1 family transcription factor c-Jun and c-Myc. Kong *et al.* (2013) reported that SIRT1 suppressed IL-12 production in human DCs through direct interaction with the NF- κ B transcription factor c-Rel. This may regulate NF- κ B, which regulates the expression of cytokines, chemokines, and other pro-inflammatory agents. Also, recent studies suggest that SIRT1 has functions in chondrocytes and synoviocytes during IA and modulates a variety of cell types during arthritis (Huang *et al.* 2012; Moon *et al.* 2013; Niederer *et al.* 2011). SIRT1 was found to be constitutively upregulated in synovial tissues and cells from patients with RA compared to OA (Krause *et al.* 2002).

SIRT3 regulates several mitochondrial functions and has important roles in maintaining homeostasis. SIRT3 is believed to be a positive regulator of macroautophagy in adipocytes. In mature adipocytes, overexpression of SIRT3 activated macroautophagy, mainly on lipid droplets (LDs), through activating the AMP-activated protein kinase (AMPK)-unc-51-like kinase 1 (ULK1) pathway, which in turn resulted in smaller LD sizes and reduced lipid accumulation. Moreover, SIRT3 overexpression causes the instability of LDs in adipocytes and participates in the control of FA metabolism. SIRT3 knockout mice demonstrate abnormal lipid metabolism associated with abnormal accumulations of acylcarnitines and TGs in the livers of these animals during fasting (Sosnowska *et al.* 2017).

AGO2 (Argonaute 2) encodes a member of the Argonaute family of proteins, which plays a role in RNA interference. The encoded protein is highly basic, it may interact with dicer1 and play a role in short-interfering-RNA-mediated gene silencing. The silencing of miRNA is mediated by AGO proteins that induce mRNA deadenylation, degradation, or translational inhibition. AGO2 has the molecular functions of miRNA binding, mRNA binding, nucleic acid binding, protein binding in translation initiation factor activity, RNA binding, and siRNA binding.

DAP3 (Death associated protein 3) is a mitochondrial ribosomal small subunit protein that is involved in mitochondrial physiology, apoptosis, and TNF-associated cell death pathways (Kim *et al.* 2007). Recent data indicated that DAP3 mainly localises in the matrix of mitochondria (Xiao *et al.* 2015). Overexpression of DAP3 leads to a significant increase in cell death. DAP3 appears to act downstream of pro-apoptotic stimuli such as IFN- γ , TNF- α , Fas ligand and upstream of several caspases, such as caspases 8 and 9 (Kim *et al.* 2007). Recently, it has been shown that human DAP3 binds in a ligand-dependent manner to several members of the NR family, such as the GCs receptor, thyroid hormone receptor, and PPARs receptor (Kim *et al.* 2007). Knockdown of DAP3 in mitochondria leads to defects in mitochondrial-encoded protein synthesis and abnormal mitochondrial dynamics. Furthermore, autophagy is inhibited in the DAP3-depleted cells, which sensitises cells to different types of death stimuli (Xiao *et al.* 2015).

STAT3 is a member of the STAT protein family. STATs are cytoplasmic proteins that are rapidly tyrosine-phosphorylated by JAKs, as discussed in the introduction. In RA, in response to cytokines and growth factors, including IFNs, GM-CSF, IL-6, and IL-10, members of STAT family are phosphorylated by JAKs, and then may form homo- or heterodimers with another member of the STAT family. Dimerized STAT3 translocate to the nucleus, where they can activate transcription (act as transcription activators) of seven known STAT proteins that are involved in apoptosis, survival, motility, and regulation of the expression of antiapoptotic and immune response genes. STAT3 also upregulates SOCS3 in macrophages (Wang *et al.* 2011), which in turn inhibits IL-6 signalling via binding to gp130. Consequently, IL-6 induces transient STAT3 activation, while SOCS3 does not block IL-10 activation of STAT3; therefore, IL-10 induces prolonged STAT3 activation. STAT3 activation is reduced by inhibitors of IL-6 and JAK, which are licenced treatment for RA.

TFE3 (Transcription Factor E3) is a protein that in humans is encoded by the TFE3 gene. TFEB (T-Cell Transcription Factor EB) and TFE3 collaborate with each other in activated macrophages and microglia to induce autophagy (**Figure 7.10**) (Pastore *et al.* 2016). Mice depleted of either TFEB or TFE3 showed reduced expression of cytokines and chemokines induced by LPS, including IL-1 β , TNF, CCL3, CCL4, and CCL5, in the liver, spleen, and lung (Pastore *et al.* 2016). TFE3 and TFEB knockout mice have been shown to promote lysosome biogenesis and the induction of autophagy in response to innate immune activation (Brady *et al.* 2018). Autophagosome and lysosome compartments are essential for xenophagy, and there

were reduced of percentages of subsequent destruction of intracellular pathogens. It was therefore speculated that TFE3 and TFEB might define unique transcriptional modules governing cytokines/chemokines versus autophagic/lysosomal genes depending on their respective activities together, which would allow attempts at the innate immune response to prevent runaway inflammation (Brady *et al.* 2018).

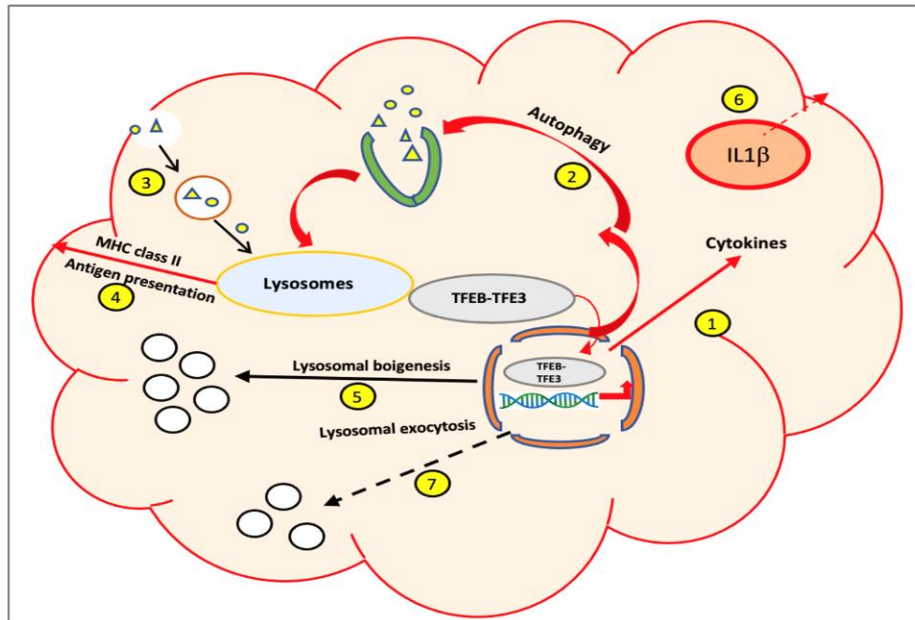


Figure 7.10. Immune-specific functions of TFEB and TFE3.

TFEB and TFE3 control a multitude of cellular processes involved in inflammation and the immune response, including: (1) cytokine and chemokine production; (2) induction of autophagy with immune specific implications; (3) endocytosis, phagosome formation, and bactericidal activity; (4) enhancement of MHC class II antigen presentation and inhibition of cross-presentation; and (5) induction of lysosomal biogenesis, further driving degradation of cargoes captured by autophagy and phagocytosis. Despite the lack of direct evidence, it is also likely that TFEB and TFE3 play a role in the unconventional secretion of the pro-inflammatory cytokines and in the secretion of immune-specific molecules through the exocytosis of secretory lysosomes or lysosome-related organelles (7). Adapted from Brady *et al.* (2018).

7.2.8.2. Canonical pathway

IPA (Qiagen) was used to identify canonical pathways associated with differentially regulated transcripts identified between genotypes affected by PNLA and relevant pathways. They were determined by their p-value (**Figure 7.11**).

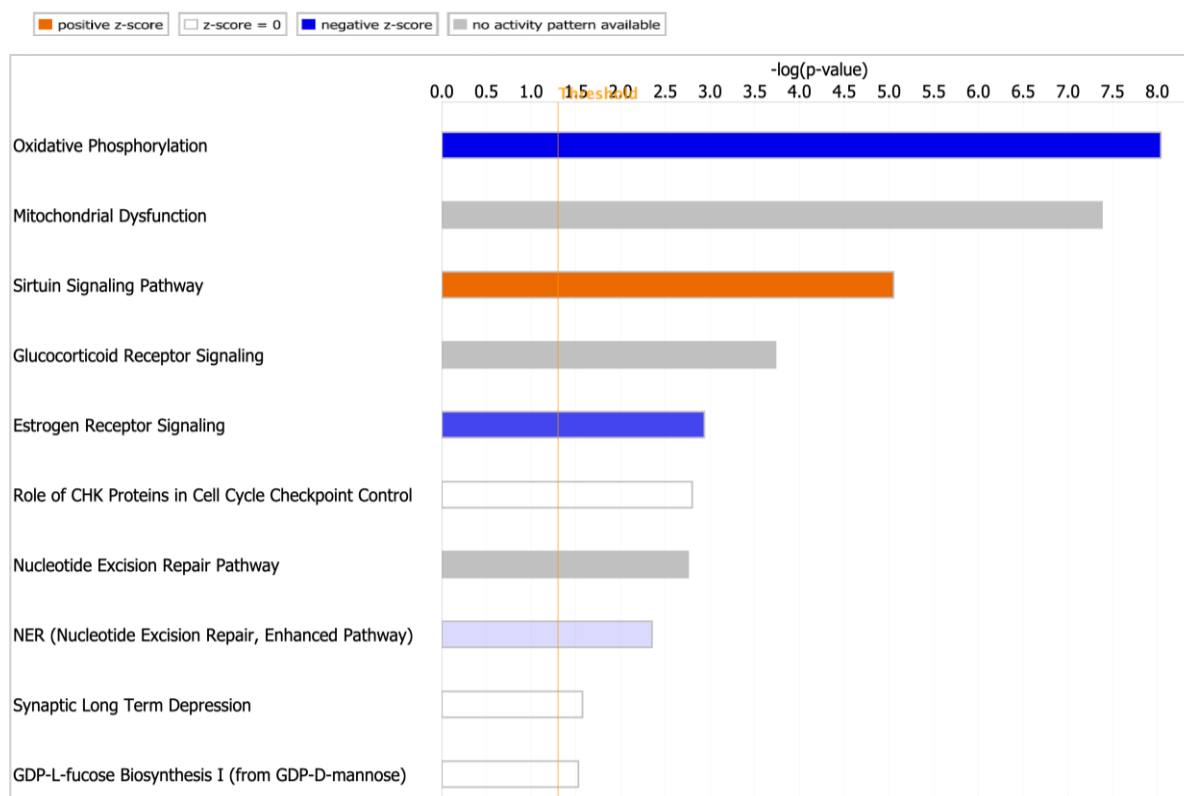


Figure 7.11. Canonical pathways bar chart for PNLN effect on activated CD14CD16 monocytes.

The top 10 most significant canonical pathways for the dataset are shown, as calculated by Fisher's exact test right tailed. The colour of the bar is a measure of the z-score, which reflects the direction of the expression change (pathway activation or inhibition). An orange bar represents an overall positive z-score (the majority of genes are upregulated), while a blue bar represents an overall negative z-score (the majority of genes are downregulated). White bars possess a z-score that is zero or close to zero. Grey bars highlight pathways for which IPA is unable to make a prediction. The orange line graph represents the ratio (the number of genes that meet cut-off criteria in the dataset divided by the total number of known genes attributed to that pathway in the IPA reference gene set).

The canonical pathway most significantly associated with the differentially expressed transcripts was 'oxidative phosphorylation' (p-value = 9.14E-09) (**Figure 7.12**). Of the 91 genes attributed to this pathway in the IPA reference dataset, 13 were differentially expressed in the experimental dataset, which are ATP5PF, COX15, COX17, MT-ATP6, MT-CO2, MT-ND1, MTND2, MTND4, MTND5, MT-ND4L, NDUFA7, NDUFA8, and NDUFB4. These proteins are all located in the cytoplasm of the inner mitochondrial membrane and function as enzymes or transporters for the mitochondria. Although oxidative phosphorylation is a vital part of metabolism, it produces ROS such as SOD_2 and H_2O_2 , which lead to the propagation of free radicals, damaging cells and contributing to immune alterations and disease.

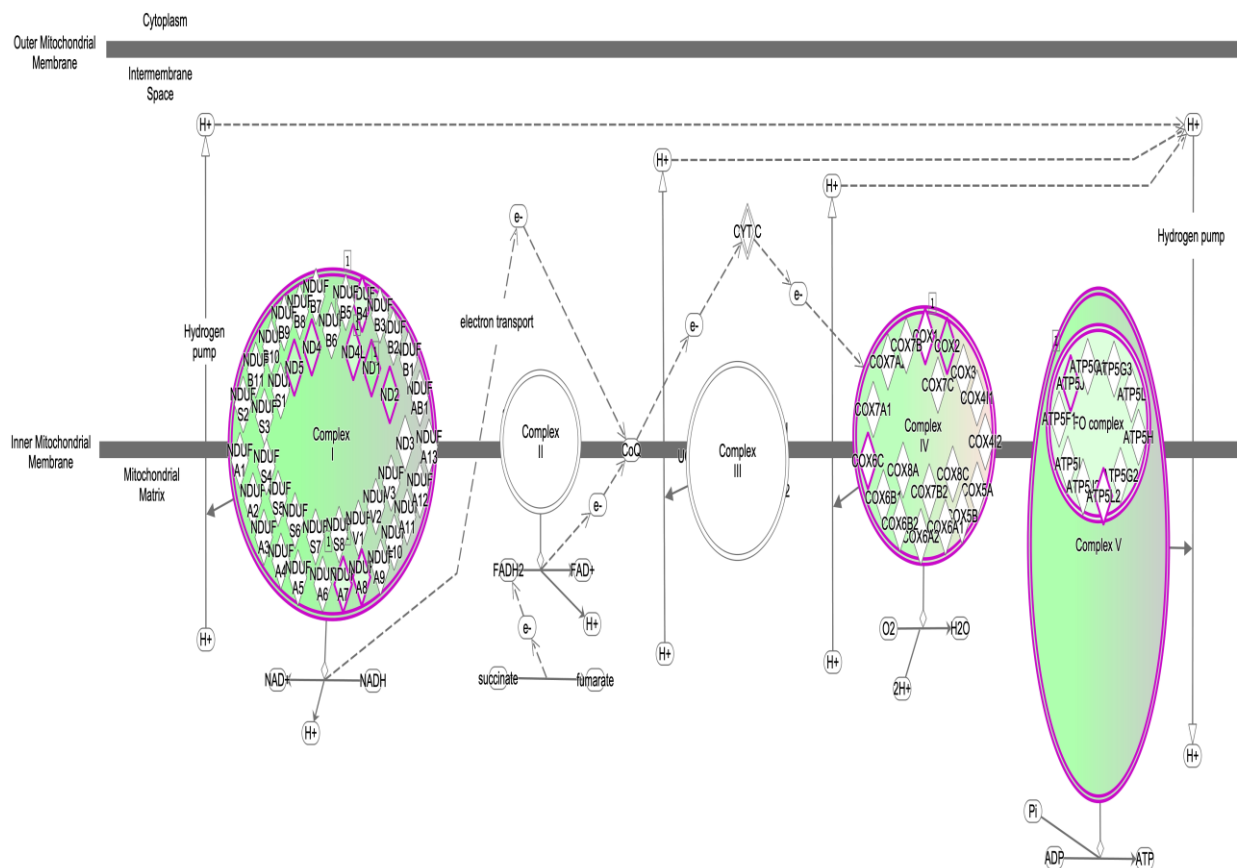


Figure 7.12. Oxidative phosphorylation downstream pathway analysis affected by PNLA.

Oxidative phosphorylation consists of five protein-lipid enzyme complexes (Complex I-V) located in the mitochondrial inner membrane that contain flavins; (flavinmononucleotide (FMN) and flavin adenine dinucleotide (FAD)), quinoid compounds (coenzyme Q10, CoQ10), and transition metal compounds (iron-sulphur clusters, hemes, and protein-bound copper). These enzymes are designated complex I (NADH: ubiquinone oxidoreductase), complex II (succinate: ubiquinone oxidoreductase), complex III (ubiquinol: ferrocyanochrome c oxidoreductase), complex IV (ferrocyanochrome c: oxygen oxidoreductase or cytochrome c oxidase), and complex V (ATP synthase). Complex I transport electrons from NADH to ubiquinone. Complex II catalyses the oxidation of succinate to fumarate and transfers electrons to the ubiquinone pool of the respiratory chain. Complex III transfers electrons from ubiquinol to cytochrome c, coupled with the transfer of electrons across the inner mitochondrial membrane. Complex IV, the final step in the electron transport chain, is the reduction of molecular oxygen by electrons derived from cytochrome c. Complex V, the final enzyme in the oxidative phosphorylation pathway, uses a proton gradient generated by the respiratory chain for ATP synthesis, where protons flow from intermembrane mitochondrial space to the matrix.

Oxidative phosphorylation (OXPHOS) is the production of ATP using energy derived from the transfer of electrons in an electron transport system and occurs by chemiosmosis (**Figure 7.12**). The process is accomplished through oxidation-reduction reactions in the mitochondria. During OXPHOS, electrons are transferred from electron donors to electron acceptors, referred to as the electron transport chain. A pool of STAT3 is localised in the mitochondria. In liver and heart cells, knockout of STAT3 significantly reduced the activities of complexes I and II of the electron transport chain (ETC) (Wegrzyn *et al.* 2009).

The second most significantly associated canonical pathway was ‘mitochondrial dysfunction’ (p-value = 4.18E-08). Of the 120 genes attributed to this pathway in the IPA reference dataset, 15 were differentially expressed in the experimental dataset. The mitochondria are the energy producing organelles in each cell of the body, as discussed above. Mitochondrial dysfunction, characterised by a loss of efficiency in the electron transport chain and reductions in the synthesis of energy molecules such as ATP, is a characteristic of all chronic diseases. As the inflammatory response progresses, ATP is consumed, resulting in the build-up of the metabolites lactate, NAD⁺ and AMP. These metabolites send a nutrient-deficit signal to switch the metabolic phenotype of the M1 macrophage and turn its activity towards the M2 via AMPK, activation of NAMPT, and SIRT activation.

The sirtuin signalling pathway is the third most significant canonical pathway that was activated in response to PNLA treatment versus LPS stimulation (p-value = 8.89E-06). Of 192 genes, 16 were affected in this pathway, followed by glucocorticoid and estrogen receptor signalling at p-values of 1.86E-04 and 1.16E-03, respectively.

7.2.8.3. Overlapping canonical pathways

Overlapping canonical pathways allows visualisation of the shared biology in pathways through the common genes participating in the pathways. Exploring pathway analysis results in a set of molecules acting across more than one pathway. The network of overlapping canonical pathways shows each pathway as a single node, coloured proportionally to the right-tailed Fisher’s Exact Test p-value, where brighter red = more significant. A line connects any two pathways when there is at least one data set molecule in common between them. The lines can show exactly how many molecules and genes are in common between each pair of pathways. The number below the node is displaying the p-values for that canonical pathway. The p-values are the same as those available in the canonical pathways bar chart. In this analysis, there are two groups of pathways: a metabolism-related set and another, larger set composed of many signalling pathways, as shown in **Figure 7.13**.

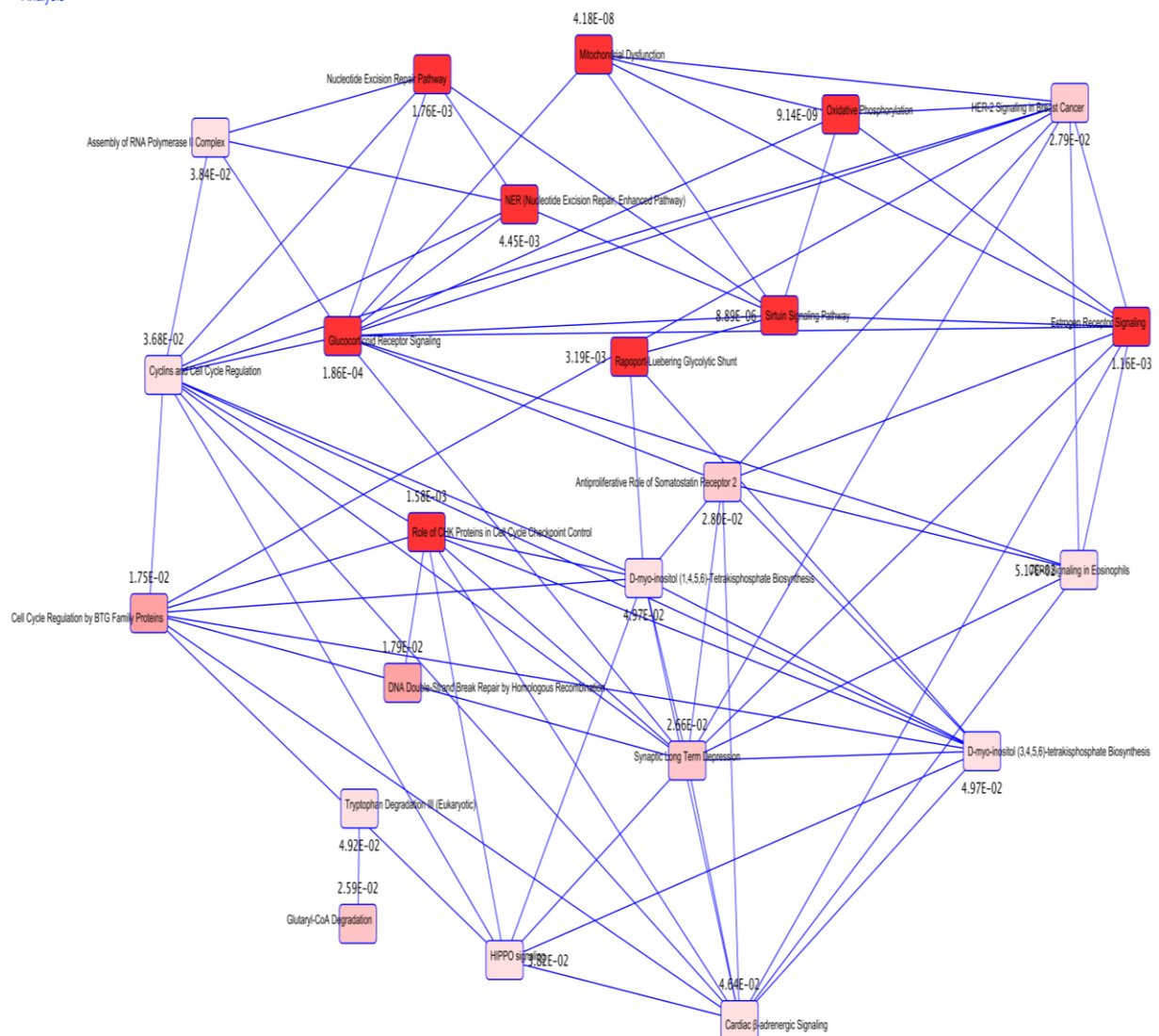


Figure 7.13. Overlapping canonical pathways.

Bright red nodes are the most significant, and the dark red is less significant. P-value is demonstrated while each line can display how many genes or molecules shared between the 2 nodes in the experimental dataset.

7.2.9. Comparison analysis

Using the IPA software, a comparison analysis was performed for all experimental conditions, which particularly sought upstream analysis for the genes involved in the transcription of inflammatory cytokines, lipid metabolism, FAs, and some drugs used for treating RA or hyperlipidaemia. I further exported the data files for those genes from IPA and reproduced heatmaps using Broad Morpheus software. Heatmap visualisations using $\log_2FC > 1.2$. (**Figure 7.14**).

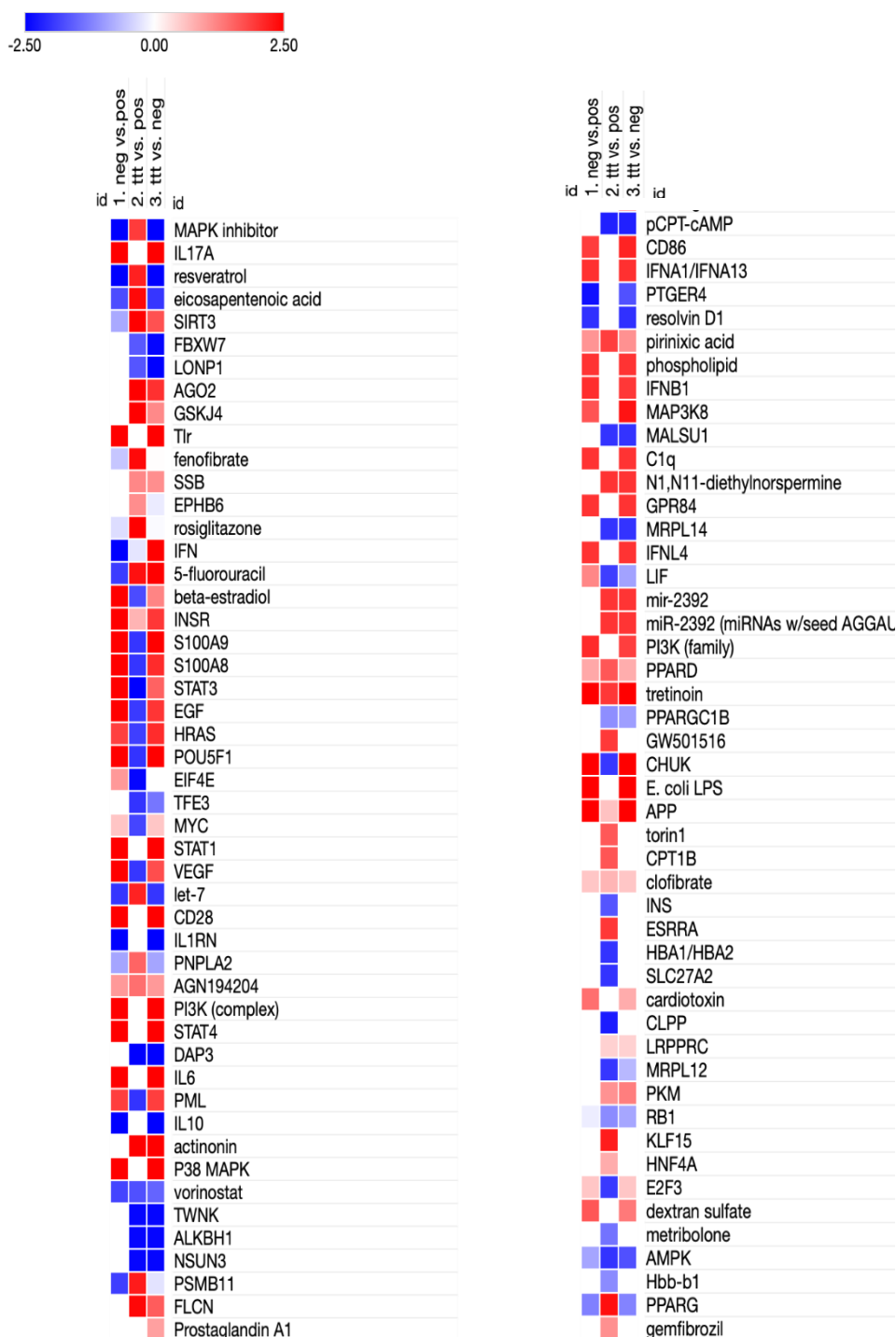


Figure 7.14. Heatmap of differentially expressed upstream regulators from the comparative analysis of RA patients.

Data were analysed using IPA (Qiagen Inc., <https://www.qiagenbioinformatics.com/products/ingenuity-pathway-analysis>). IPA analysis of DEGs associated with upstream regulators that predicted an activated state (red) and a predicted inhibited state (blue) is shown. Data files were exported for those genes from IPA and reproduced as heatmaps using Broad Morpheus software, available at (<https://software.broadinstitute.org/morpheus/>). Relative expression heat maps of the differentially expressed regulators regulated by; (1) unstimulated (vehicle) vs LPS-stimulated monocytes, (2) PNLA-treated LPS-stimulated vs vehicle-treated LPS-stimulated monocytes, and (3) PNLA-treated LPS-stimulated vs unstimulated (vehicle-treated) monocytes ($\text{Log}_2 \text{FC} > 1.2$, $p < 0.05$) are shown. The regulators shown here are mainly involved in cytokine production, lipid and FA metabolism, drugs used for treating hyperlipidaemia, miRNAs, and transcription factors. FA; fatty acid, LPS; Lipopolysaccharide, PNLA; pinolenic acid, ttt; treatment.

7.2.10. Upstream regulators

IPA also provides a prediction of the likely upstream regulators responsible for the expression changes observed in the experimental dataset (**Table 7.6** and **Figures 7.15, 16**). The activation z-score is used to indicate the likely activation state of the upstream regulator (predicted upregulated molecules have a positive z-score, predicted downregulated molecules have a negative z-score). The p-value of overlap is a measure of the significance of network-regulated gene enrichment within the dataset.

DAP3 is the topmost significant upstream regulator affected. AGO2, SIRT3, PPARs, EPA, LIF, and STAT3 were discussed previously in this thesis.

GSKJ4 is the 3rd most significantly affected regulator. GSK-J4 inhibits LPS-induced TNF- α production in human primary macrophages with an IC₅₀ (the molar concentration required to reduce production by 50%) of 9 μ M (Donas *et al.* 2016; Kruidenier *et al.* 2012). GSK-J4 induces endoplasmic reticulum stress-related apoptosis (Yapp *et al.* 2016).

Let 7 is a family of miRNAs, was predicted to be activated by PNLA as an upstream regulator. **Figure 7.17** shows let-7 networks with molecules and diseases. Let-7 miRNA was named “lethal-7” because its absence leads to uncontrolled cellular proliferation. Certain let-7 family members, such as let-7a and let-7e, are associated with early inflammatory and pre-apoptotic pathways, while others, such as let-7i and let-7f are involved in later phases of transcription and downstream elements of apoptosis. Such regulatory elements as let 7 miRNAs and the timeline of expression of these miRNAs have a subsequent impact on cytokine and chemokine release. Recent bioinformatic predictions have shown several genes, such as FOXP1, AKT2, and PPARGC1A, to be targets of different let-7s (let-7a/7d/7e/7f) (Bernstein *et al.* 2021).

Several factors control the expression of let 7 via regulatory loops. NF- κ B reduces let-7 levels. While let-7 can inhibit IL-6 expression, this can activate NF- κ B and complete a positive feedback loop (Hunter and Jones 2015; Jones 2011). In the CIA, disease severity was markedly ameliorated after treatment with let-7g-5p mimics. Interestingly, STAT3 was found to be a target of let-7a, and the JAK-STAT3 pathway is regulated by miRNA let-7 (Thammaiah and Jayaram 2016). We speculate that let-7 may regulate the activity of monocytes by targeting the JAK-STAT3 signalling pathway.

All members of the let-7 family have been linked to the regulation of vascular and EC, and SMCs, which are critical in the pathogenesis of atherosclerosis (Brennan *et al.* 2017; Chen and Juo 2012). Data reported that ox-LDL inhibited let-7g expression via a LOX-1/ROS/ERK/AP-1 pathway and, inversely, let-7g could directly target LOX-1 to comprise a negative feedback regulation that was involved in VSMC proliferation and migration (Chen and Juo 2012).

CHUK is a serine kinase that is an inhibitor of NF- κ B kinase subunit alpha (IKK- α). CHUK is predicted to be inhibited by PNLA. CHUK plays a key role in the negative feedback of NF- κ B canonical signalling to limit inflammatory gene activation.

Table 7.6. Top predicted upstream regulators based on the IPA dataset.

| Upstream regulator | Molecule Type | Activation z-score | p-value of overlap |
|---------------------------------|-------------------------|--------------------|--------------------|
| DAP3 | other | -3 | 2.31E-14 |
| Actinonine | chemical reagent | 3 | 5.04E-11 |
| GSKJ4 | chemical reagent | 3.317 | 3.01E-08 |
| AGO2 | translation regulator | 2.646 | 2.16E-08 |
| SIRT3 | enzyme | 2.818 | 3.03E-06 |
| EPA | chemical drug | 2.425 | 4.16E-03 |
| LIF | cytokine | -1.897 | 1.74E-03 |
| PPAR-γ | transcription regulator | 2.355 | 1.00E-03 |
| KLF15 | transcription regulator | 2.226 | 1.07E03 |
| PPAR-δ | transcription regulator | 1.651 | 4.78E-02 |
| STAT3 | transcription regulator | -3.203 | 3.37E-02 |
| AMPK | complex | -2 | 1.09E-02 |
| VEGF | group | -1.969 | 1.00E-02 |
| MYC | transcription regulator | -1.822 | 1.00E-02 |
| CHUK | kinase | -1.964 | 3.96E-01 |

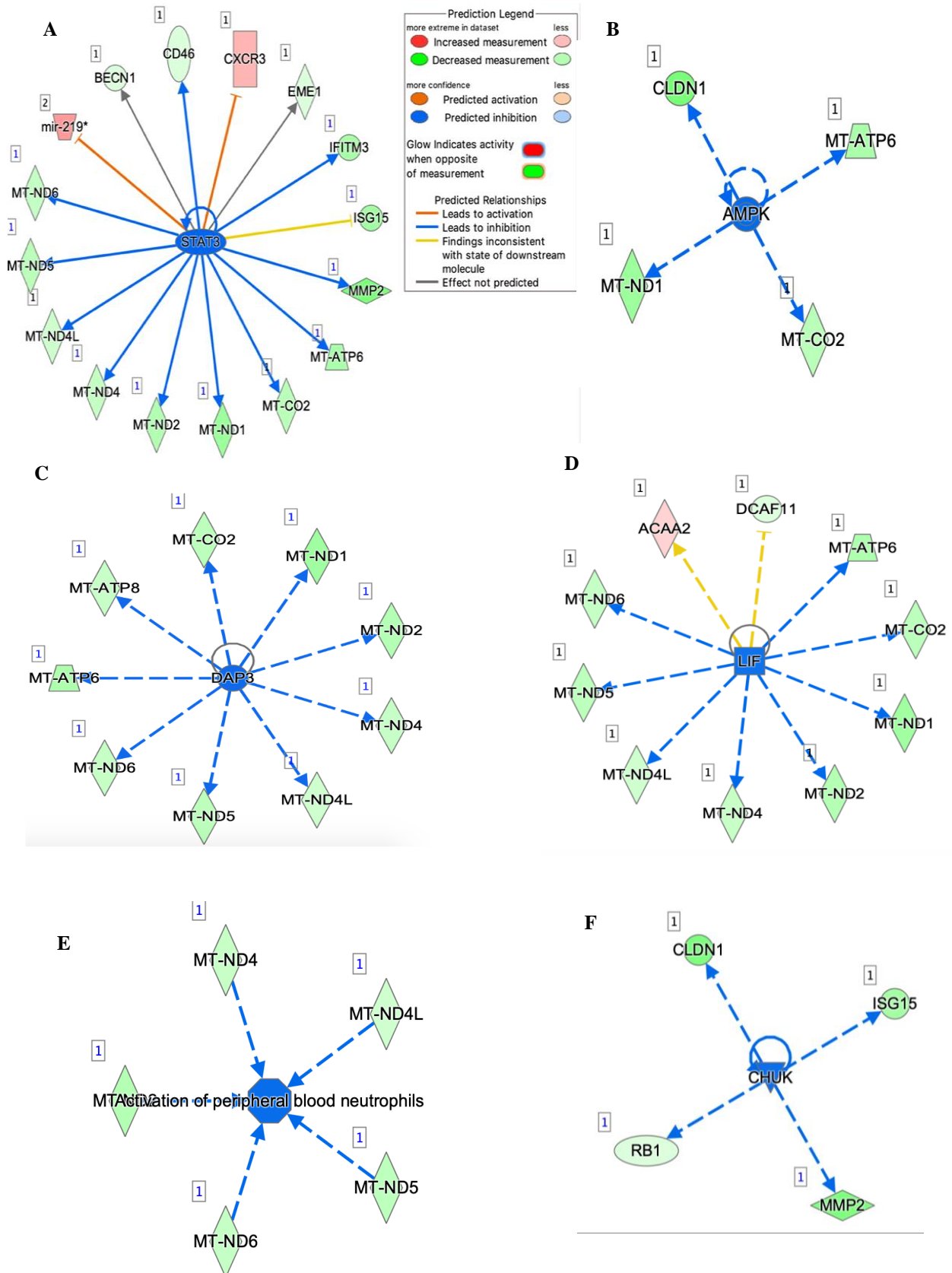


Figure 7.15. Upstream regulators as effectors of PNLA treatment on LPS stimulated monocytes. (A) STAT3 14 of 16 genes have measurement directions consistent with inhibition of STAT3 (B) AMPK 4 out of 4 genes have measurement directions consistent with the inhibition of AMPK (C) DAP3 9 out of 9 genes have measurement directions consistent with the inhibition of DAP3 (D) LIF 9 out of 10 genes have measurement directions consistent with inhibition of LIF (E) Activation of peripheral blood neutrophil 5 out of 5 molecules were predicted to be inhibited (F) CHUK 4 out of 4 molecules were inhibited.

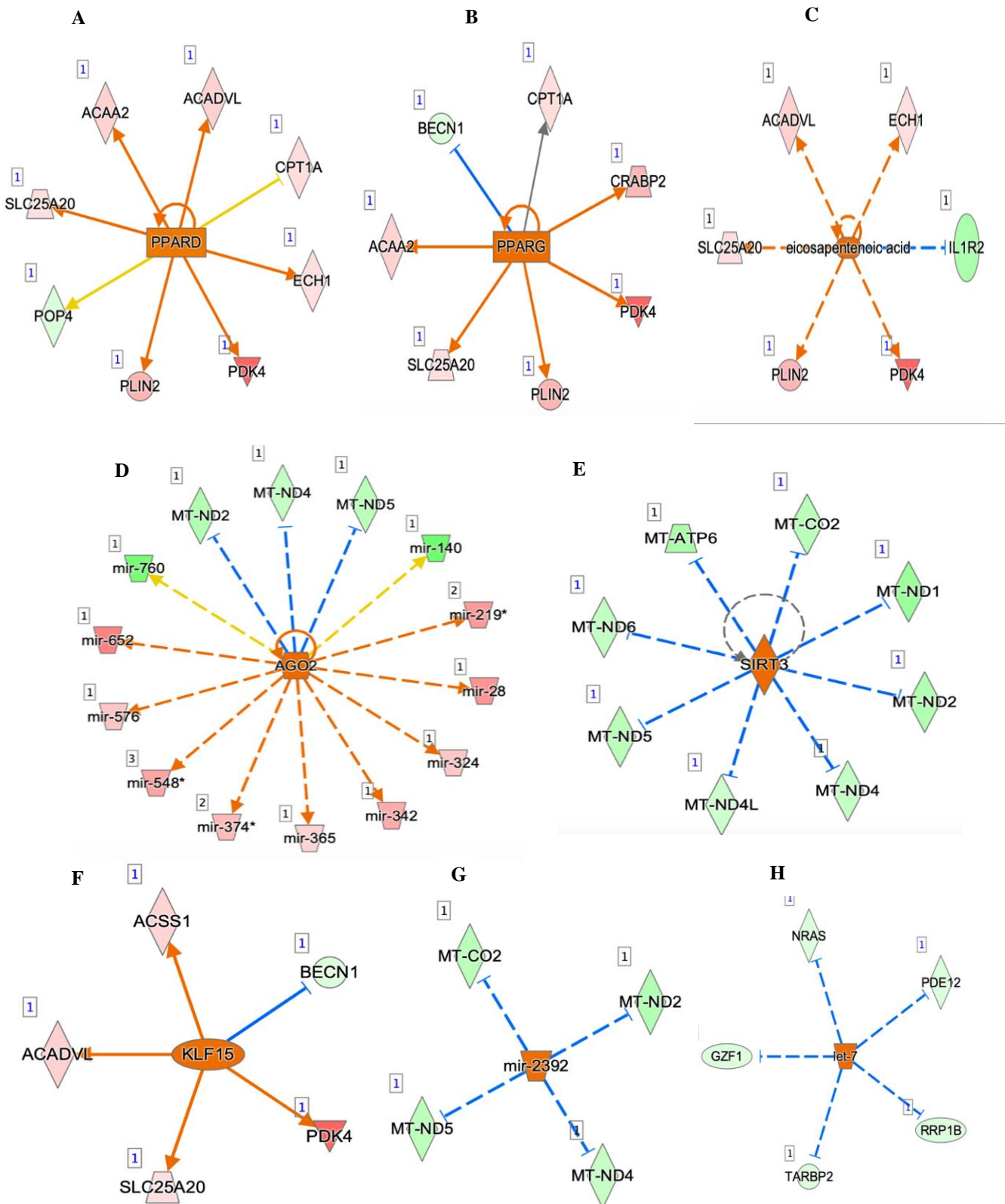
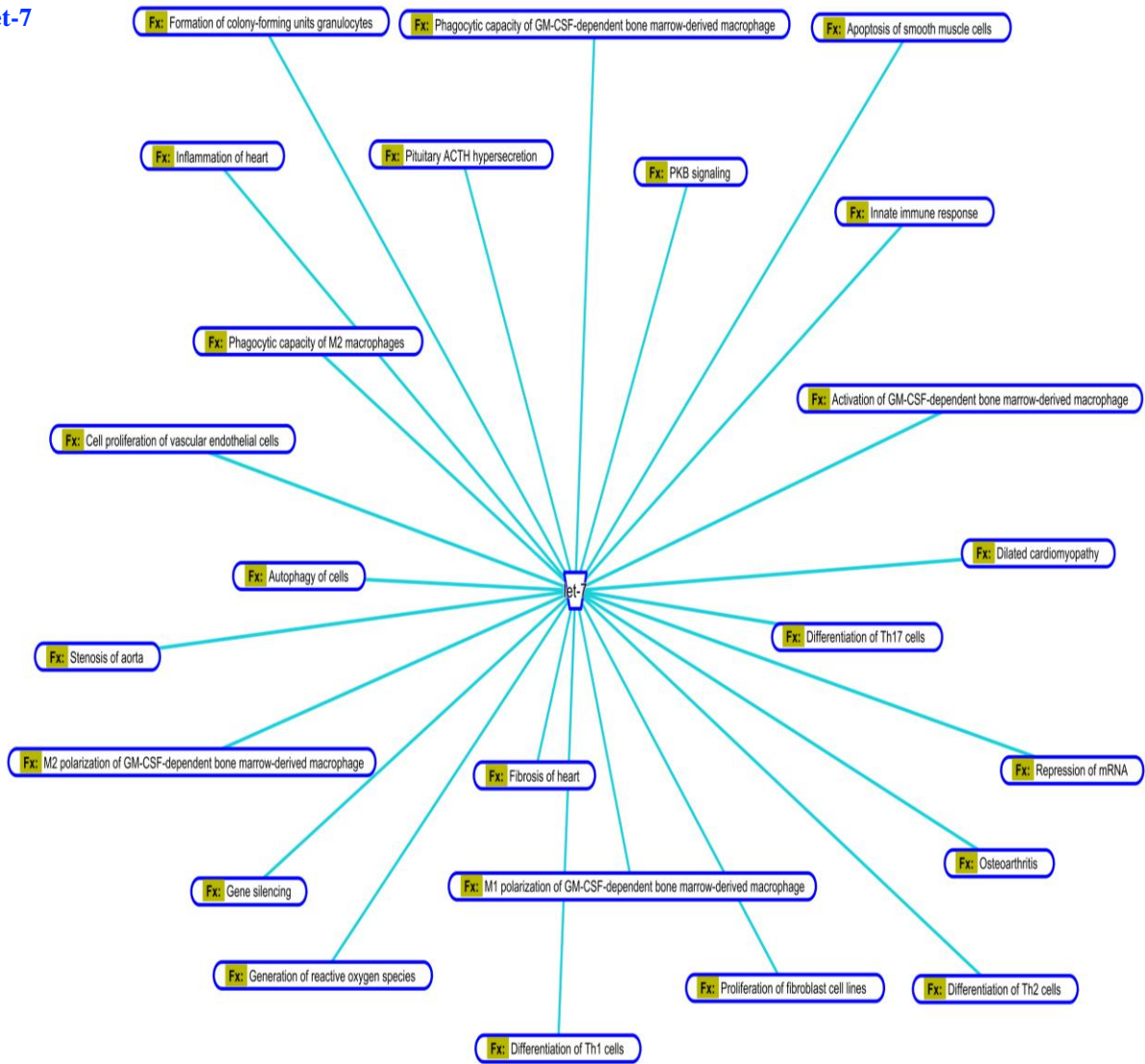


Figure 7.16. Upstream regulators as effectors of PNLN treatment on LPS stimulated monocytes.

(A) **PPARD** 7 out of 8 genes have measurement directions consistent with the activation (B) **PPARG** 6 out of 7 genes have measurement directions consistent with the activation (C) **EPA** 5 out of 6 genes have measurement directions consistent with the activation (D) **AGO2** 9 out of 14 genes have measurement directions consistent with the activation. (E) **SIRT3** 8 genes have measurement directions consistent with SIRT3 activation. (F) **KLF15** 4 out of 5 have measurement directions consistent with the activation (G) **mir2392** and (H) **Let-7**.

Let-7



© 2000-2021 QIAGEN. All rights reserved.

Figure 7.17. Let 7 associated networks as supported by the IPA database. Fx; Function

7.3. Discussion

In this Chapter, the effect of PNLA on gene expression in purified monocytes was investigated. The results suggested that PNLA has an effect on genes associated with the signal transduction pathways of TNF- α and IL-6, supporting results from previous chapters. Interestingly, it extends these observations and identifies potential effects on inflammatory, metabolic pathways, mitochondrial function, an important part of immunometabolism, as well as miRNAs.

By inhibiting OXPHOS, PNLA may decrease the ability of pathogenic cells to generate sufficient ATP to proliferate and survive, thus promoting the resolution of inflammation through metabolic reprogramming. Many researchers believe that autoimmune diseases are primarily mitochondrial diseases and recently researchers have interpreted those mitochondria are a key player in the pathogenesis and treatment of RA (Clayton *et al.* 2021). One such example is the use of alpha-lipoic acid (ALA), a co-factor for mitochondrial a-keto dehydrogenase complexes, which has been shown to attenuate the development of CIA in mice by Lee *et al.* Amelioration of joint disease by ALA was associated with a reduction in oxidative stress as well as inhibition of inflammatory cytokine activation and NF- κ B DNA binding activity. Moreover, ALA inhibited bone destruction *in vivo* and osteoclastogenesis *in vitro* (Filippin *et al.* 2008). Studies with the TNF- α inhibitors etanercept and infliximab have demonstrated a reduction of oxidative stress markers in patients with RA. It has also been demonstrated that methotrexate can suppress directly or indirectly the generation of active oxygen metabolites induced by IL-6, which in turn is produced after stimulation with TNF- α in synovial cells of RA (Cooper *et al.* 2012) as well as in polymorphonuclear cells.

The DEGs identified in this Chapter are linked to mitochondrial function and autophagy. Mitochondria can induce autophagy. Autophagy is a highly conserved process for the self-degradation of cellular components, including long-lived proteins, damaged organelles, and pathogens (Parzych and Klionsky 2014). When autophagy occurs, double membrane vesicles termed phagophores are initiated, and they expand to engulf cytosolic content to form autophagosomes. The autophagosome outer membrane docks and fuses with the lysosomal membrane, and the cargo is subsequently degraded by the lysosomal hydrolases. Not only can the organelles be removed by selective autophagy, but they can also contribute to the process of autophagy. Macrophage autophagy plays a protective role in atherosclerosis by reducing inflammation and promoting cholesterol efflux (Sosnowska *et al.* 2017).

Genes and biologic pathways identified in this Chapter include KLF15, SIRT, TFE3, DAP3, and STAT3. STAT3 is an established target in RA, as evident from the use of inhibitors of JAK and IL-6 in treatment. Amongst these SIRT signalling pathways, several have been suggested as therapeutic targets in RA and atherosclerosis (Fu *et al.* 2017; Kong *et al.* 2013).

Activation of SIRT has beneficial effects on lipid metabolism and as antioxidants, as shown in **Figure 7.18** (Sosnowska *et al.* 2017), as well as being a critical immune suppressor of both T cell and macrophage activation. In the CIA, mice injected with the adenovirus vector Ad-SIRT6 showed attenuated severity of arthritis and hind paw thickness, as well as radiographic and pathologic findings.

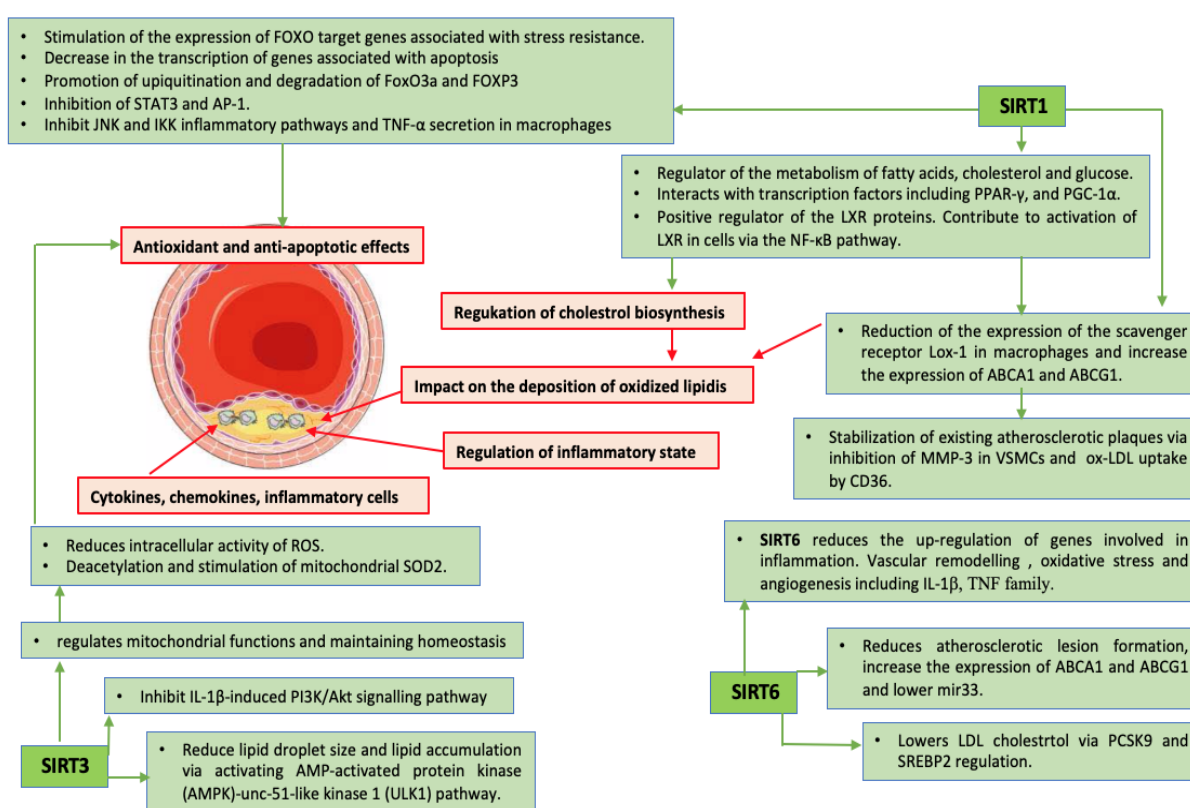


Figure 7.18. An overview of potential interactions of SIRTs with the pathophysiological process in atherosclerosis.

SIRT1: sirtuin1; LXR: liver X receptor; ROS: reactive oxygen species; SOD2: superoxide dismutase; LOX1: (lectin-like oxidized low-density lipoprotein receptor-1); FOXO: fork head Box O; FoxO3a; factor forkhead box O-3; IL-1β: interleukin-1beta, TNF: tumour necrosis factor; PCSK9: proprotein convertase subtilisin/kexin type 9; SREBP2: sterol regulatory element binding transcription factor 2. VSMC: vascular smooth muscle cells; ABCA1, G1: ATP binding cassette family A1, G1; FOXP3; fork head box P3; PI3K/Akt: PI3K: phosphatidylinositol 3-kinase/protein kinase B; ox-LDL: oxidised low-density lipoprotein; STAT3: signal transducer and activator of transcription-3; AP-1: activator protein 1. Adapted from Sosnowska *et al.* (2017).

SIRT1 stabilises existing atherosclerotic plaques by enhancing the activity of the tissue inhibitor of MMP-3 in VSMCs as well as exerting CD36-dependent and -independent activities on ox-LDL uptake (Sosnowska *et al.* 2017). SIRT1 modulates cholesterol biosynthesis in the liver (Li *et al.* 2007) resulting in a reduction of serum lipid levels (Feige *et al.* 2008). These effects are associated with the fact that SIRT1 is a positive regulator of the LXR proteins, important regulators of the metabolism of FAs, cholesterol, and glucose. LXR regulates reverse cholesterol transport, a process that removes cholesterol from macrophages and prevents foam cell formation. SIRT1 may promote deacetylation and subsequent activation of LXR and increase the expression of ABCA1 and ABCG1, which contribute to reverse cholesterol transport and the suppression of foam cell formation and cholesterol loading in macrophages (Li *et al.* 2007; Picard *et al.* 2004). Moreover, it was reported that SIRT1 interacts with transcription factors PPAR- γ and peroxisome PPAR co-activator 1-alpha (PGC-1 α) (Rodgers *et al.* 2005) and may also contribute to activation of LXR in cells via the NF- κ B pathways (Zeng *et al.* 2013), as summarised in **Figure 5.24**.

Silencing of SIRT1 promoted apoptosis in RASFs, whereas SIRT1 overexpression protected cells from apoptosis. Inhibition of SIRT1 enzymatic activity by inhibitors, siRNA, and overexpression of an enzymatically inactive form of SIRT1 reduced LPS-induced levels of TNF α in monocytes. Similarly, knockdown of SIRT1 resulted in a reduction of pro-inflammatory IL-6 and IL-8 in RASFs. SIRT1 is highly expressed in human vascular ECs (Sosnowska *et al.* 2017) and regulates many cellular processes essential for cell survival, including apoptosis, inflammation, stress resistance, cell growth, cell senescence, and metabolism. SIRT1 deficiency contributes to increased inflammation, oxidative stress, foam cell formation, impaired NO production, and autophagy, thereby promoting vascular atherosclerosis and ageing (Brunet *et al.* 2004; Chung *et al.* 2010; Zeng *et al.* 2013)

SIRT6 overexpression was associated with reduced expression of pro-atherosclerotic genes, including IL- β and TNF family members, and reduced adhesion of monocytes to ECs (Niederer *et al.* 2011). SIRT6 also protects against atherosclerosis by reducing foam cell formation through an autophagy-dependent pathway. He *et al.* indicated that SIRT6 overexpression lowers the level of miR-33, which increases autophagy flux and upregulates ABCA1 and ABCG1 expression, promoting cholesterol efflux and preventing macrophage foam cell formation at the same time (He *et al.* 2017). Recently, Xu *et al.* 2016 reported that SIRT6 reduces the formation of atherosclerotic lesions via the attenuation of endothelial dysfunction and vascular inflammation (Sosnowska *et al.* 2017). Haploinsufficiency SIRT6^{+/-} mice had

increased rates of atherogenesis associated with elevated VCAM-1 (Xu *et al.* 2016). SIRT6 expression is decreased in atherosclerotic lesions from ApoE^{-/-} mice (Liu *et al.* 2016) and human patients (Balistreri *et al.* 2015).

In lipid metabolism, SIRT6 reduces LDL-cholesterol levels through the regulation of the PCSK9 gene (Sosnowska *et al.* 2017). A deficiency of hepatic SIRT6 increased PCSK9 gene expression, which leads to hepatic LDL-receptor degradation and subsequently increases the plasma level of LDL-cholesterol. Moreover, overexpression of SIRT6 in mice fed an HFD lowers LDL-cholesterol (Tao *et al.* 2013). SIRT6 and FOXO3 have an impact on total cholesterol levels in the circulation via regulation of the SREBP2 gene, and both suppress SREBP2 gene expression, a major regulator of cholesterol biosynthesis in the liver (Tao *et al.* 2013). An activator of SIRT6, such as resveratrol, has been suggested by some researchers as showing therapeutic potential in RA and atherosclerosis (Fu *et al.* 2017; Kong *et al.* 2013).

NAD⁺ is likely induced based on oxidative phosphorylation inhibition, SIRT6 activations, and NAD signalling pathway, as indicated in **Table 7.5**, following PNLA treatment. NAD⁺ boosters from *in vitro* experiments with PBMCs from RA patients improve oxidative, apoptotic, and inflammatory status by increasing intracellular NAD⁺ levels. Also, NAD⁺ boosters promoted a deep reduction of intracellular ROS levels, the percentage of apoptotic cells, and the expression levels of key inflammatory mediators, such as IL-6, IL-8, IL1- β , TNF- α , CCL2, IL-23, and STAT3 (Perez-Sanchez *et al.* 2021). While NAD⁺ is reduced in PBMCs and plasma from RA patients compared with HCs and is directly related to disease activity (Perez-Sanchez *et al.* 2021). Anti-TNF therapy was restored and correlated with NAD⁺ levels, which were directly correlated to clinical effectiveness and the clinical response promoted by anti-TNF therapy (changes in DAS28) (Perez-Sanchez *et al.* 2021). Altogether, NAD⁺ boosters may be considered a novel therapeutic tool for RA patients.

Overexpression of KLF15 in the human EC line (Eahy926) exhibited a protective effect against TNF- α induced dysfunction (Liu *et al.* 2018). Overexpression of KLF15 markedly suppressed the rate of cellular adhesion and downregulated levels of CCL2, ICAM-1, TGF- β , and phospho-p65 (p-p65) in TNF- α induced Eahy926 cells. Overexpression of KLF15 markedly enhanced cell viability in addition to increasing the expression levels of eNOS but did not exhibit a significant difference regarding the quantity of released NO compared with the control group in the same cell model (Liu *et al.* 2018). Taken together, these studies identify KLF15 as a novel molecular regulator of vascular inflammation and diseases.

TFE3 is a transcription factor that is inhibited by PNLA treatment. Previous work revealed a novel and important role of TFE3 and TFEB in the transcriptional regulation of the immune response, which is in the innate immune system, and have been implicated in the activation of macrophages, including the promotion of their bactericidal functions, lysosome exocytosis, and the production of various cytokines and chemokines (Brady *et al.* 2018) (**Figure 7.14**).

Mice depleted of either TFEB or TFE3 showed reduced expression of most of the analysed cytokines and chemokines. TFEB controls the expression of lysosomal genes and regulates the expression of many genes involved in lysosomal-related processes, including lysosomal exocytosis, phagocytosis, endocytosis, autophagy, modulation of specialised types of autophagic processes such as mitophagy (Nezich *et al.* 2015) and lipophagy (Settembre *et al.* 2013), and promoting plasma membrane cellular clearance. Following sustained exposure to LPS, the levels of TFE3 in macrophages remained constant, whereas dramatic fluctuations in TFEB mRNA and protein levels were observed (Pastore *et al.* 2016).

LIF is an inflammatory gene that plays a key role in the terminal differentiation of myeloid leukemic cells. The expression of LIF was attenuated upstream by PNLA treatment compared to the vehicle control cells (**Figure 7.15D**). LIF binds to the specific LIF receptor, which forms a heterodimer with a specific subunit common to all members of that family of receptors, the gp130 signal transducing subunit. This leads to the activation of the JAK/STAT and MAPK cascades.

MiRNAs have been implicated in vascular inflammation and the pathobiology of RA (Filkova *et al.* 2012). Certain miRNAs linked to vascular inflammation were found to be affected by cellular PUFA enrichment (Roessler *et al.* 2017). In RA, miRNAs are being assessed as a potential therapy. Individual miRNAs can target several genes. At the same time, the same gene expression can be regulated by several miRNAs directly or indirectly in a synergistic or opposing way, as can be seen in PDK4 and SIGIRR (**Figures 7.8**), respectively. PUFAs are known to be incorporated into the cell membrane of monocytes, macrophages, or ECs, the major cellular players in inflammatory diseases, and thereby can affect cellular signal transduction.

It was found that freshly isolated monocytes from healthy donors expressed high levels of SIGIRR. The expression of SIGIRR mRNA was substantially reduced during differentiation into macrophages (Drexler *et al.* 2010). SIGIRR overexpression inhibited TLR-induced TNF-

α and IL-10 and IFN- γ -inducible protein 10 (IP-10) production in HMDMs and DCs. The role of SIGIRR as an inhibitor of inflammation was confirmed *in vivo* since SIGIRR^{-/-} mice developed a more severe disease in both CIA models (Drexler *et al.* 2010). Overexpression of SIGIRR in primary human DCs as well as in M-CSF-differentiated macrophages resulted in the inhibition of TLR-2/6, TLR-3, TLR-4, TLR-5, TLR-7/8, and IL-1R signalling (Drexler *et al.* 2010). Overexpression of SIGIRR in human RA synovial cells led to the inhibition of spontaneously produced cytokines, thereby defining its role as an inhibitor of inflammation in a human disease-relevant model (Drexler *et al.* 2010).

Current evidence suggests that TIR8/SIGIRR dampens TLRs-mediated activation and cell effector functions and inhibits signalling receptor complexes of IL-1 family members associated with Th1 (IL-18), Th2 (IL-33), and Th17 (IL-1) differentiation (Riva *et al.* 2012; Gulen *et al.* 2010). Stable overexpression of TIR8/SIGIRR diminished NF- κ B-mediated IL-8 responses to TLR ligands (Riva *et al.* 2012). Moreover, others reported that human monocytes up-regulated the TIR8/SIGIRR transcript during sepsis and sterile systemic inflammation, which was associated with reduced TNF α and enhanced IL-10 production in response to LPS (Riva *et al.* 2012). Riva *et al.* reviewed also that some studies reported that TIR8/SIGIRR inhibits NF- κ B and JNK activation dependent on ILRs or TLRs family member activation but not TNF α -dependent NF- κ B activation or IFN- γ -dependent STAT1 activation.

SIGIRR has been identified as a novel potential treatment for RA, consisting of the targeting of ILRs or TLRs signalling proteins or transcription factors by miRNAs. In particular, miR-155, miR-21, miR-146a, miR-132, miR-9, and miR-147 have all been significantly implicated in the immune response initiated by IL-1R or TLRs (Riva *et al.* 2012). For instance, the induction of transcription of miR-146a or miR-9 by LPS, TNF α and IL-1 α is dependent on NF- κ B, and in turn, miR-146a potentially targets TRAF6 and IRAK-1, whereas miR-9 targets the NF- κ B1 transcript, dampening the immune response (Riva *et al.* 2012). SIGIRR in this study was activated by target activation of miR-7150 and inhibition of miR-1909-3P and miR-6868-5P and signals through NF- κ B, TLR, and TREM1 signalling (**Table 7.5**).

One of the important observations in this Chapter was the regulation of miRNAs by PNLA. Elevated serum levels of miR38 and miR486 were associated with increased susceptibility to the development of RA. While elevated miR-22 and miR-103a were associated with susceptibility to the development of RA in individuals with positive ACPAs (Evangelatos *et al.* 2019). In SMs of RA patients, the miR-223 level was elevated, which was associated with

increased proinflammatory cytokine secretion (Evangelatos *et al.* 2019). On the other hand, it affects osteoclastogenesis *in vitro* and possibly attenuates bone erosion formation.

miR432-5p miRNAs are regarded as negative regulators of the translation of mRNA associated with the pathogenesis of RA and have higher expression in relapsed patients, who never achieved clinical remission (Fernández-Ruiz *et al.* 2018). miR-9 is upregulated in monocytes after activation with LPS. This miRNA controls NF- κ B activation by targeting its p50 subunit, preventing dimerization with the p65 subunit and the activation of pro-inflammatory cytokines (Bazzoni *et al.* 2009). There is a trend of downregulation of miR-9 by PNLA, but this inhibition does not reach statistical significance.

While miR-155 was overexpressed significantly upon LPS stimulation, PNLA was unable to reverse the overexpression. In RA PB monocytes, miR-155 correlated positively and significantly with DAS28. Overexpression of miR-155 in PB monocytes led to an increased production of chemokines (CCL3/MIP-1 α , CCL4/MIP-1 β , CCL5/RANTES, and CCL8/MCP2) while upregulating homeostatic CCR7 and downregulating CCR3 and CCR2. This deregulation of miR-155 in RA monocytes contributes to monocyte retention at sites of inflammation (Almesmari *et al.* 2016). CD14⁺ monocytes from PBMCs and SF of RA patients are known to exhibit resistance to apoptosis as miR-155 is overexpressed, and a corresponding decrease of two predicted miR-155 targets, apoptosis mediators CASP10 and APAF1, was also observed. This may explain a possible role of miR-155 overexpression in CD14⁺ monocyte's resistance to apoptosis (Najm *et al.* 2019). Overexpression of miR-155 in CD14⁺ cells from SF enhanced the expression of TNF α , IL-1 β , IL-6, and IL-8 (Filková *et al.* 2012). Interestingly, miR-155 is increased in PBMC from RA patients compared with HCs and is upregulated during the differentiation of IL-17-producing cells (Filková *et al.* 2012). miR155^{-/-} mice did not develop arthritis in the CIA model, and the genetic silence of the miR-155 gene led to resistance to arthritis development. Thus, increased miR-155 in local macrophages enhances their survival and cytokine production. On the other hand, miR-155, which is also induced in a macrophage inflammatory response, limits the overproduction of inflammatory cytokines during the late phase of LPS-mediated DC activation (Filková *et al.* 2012). By studying miR-155 levels in PBMCs of patients with active disease, Li *et al.* (2013) found that the higher the miR-155 levels, the higher the ESR and the DAS28 were, irrespective of RF or ACPA presence, and serum miR-155 levels have also been reported to correlate with disease activity.

miR-221 was further identified as playing a proinflammatory role in RA *in vitro*, and data suggest miR-221 inhibition as a potential therapeutic target (Najm *et al.* 2019). miR-146 was shown to be higher in patients with active systemic juvenile idiopathic arthritis and M2 macrophages (Najm *et al.* 2019). When miR-146a is overexpressed *in vitro*, it can promote downstream M1 macrophage polarisation. (Filkova *et al.* 2012). Pauley *et al.* (2008) found that high levels of miR-16 and miR-146a in PBMCs of RA patients were associated with active disease, whereas low levels of these miRNAs were associated with remission of RA. A few years earlier, the same team of researchers demonstrated that serum miR-16 levels were inversely proportional to DAS28. Low levels of miR-125b in PBMCs (but not in plasma) of treatment-naïve RA patients have been associated with a worse clinical picture. On the contrary, Filkova *et al.* (2014) showed no correlation between miR-16, miR-132, miR-146 and miR-155 serum levels and clinical characteristics or inflammation markers in RA patients. However, for some miRNAs studied, such as miR-125b and miR-146a in RA patients, no definitive conclusions can be drawn at present due to conflicting reported results. Still, the strongest data available are for miR-24, miR-125a, and miR-155, whose increases in the PB could be used to diagnose RA (Najm *et al.* 2019). Additional research is needed for other miRNAs to draw definite conclusions.

Many other studies reported that altered miRNA levels might reflect disease activity. Murata *et al.* (2013) showed that the more active the disease was, the higher the levels of circulating miR-24 were. Additionally, patients with active RA had statistically higher serum levels of miR-194 and miR-432 and lower miR-210 levels than those in remission. miR-221 and miR-222 levels in PBMCs have been found to be analogous to disease activity, and miR-432 was downregulated significantly by PNLA. High pre-therapy serum levels of miR-16, miR-125b, and miR-223 in patients with RA were associated with better response to therapy with non-biologic DMARDs, mainly methotrexate (Evangelatos *et al.* 2019).

miRNA expression differs depending on the stage of the disease between patients, with early RA (ERA; defined as a disease with less than 12 months of symptom duration) and patients with established disease. In ERA, serum levels of miR-16, miR-146a, miR-155, and miR-223 are lower than in established RA. Moreover, patients with ERA have significantly lower serum levels of miR-16 and miR-223 compared to HCs, so these two miRNAs could serve as biomarkers to distinguish patients with ERA from healthy individuals. Serum miR-16, miR-25, miR-214, miR-223, miR-346, miR-371b, miR-378d, miR-483, and miR-642b could

contribute to the early recognition of RA patients (Evangelatos *et al.* 2019). As for miR-223, its levels are increased in the SMs of RA patients, and miR-223 overexpression leads to increased proinflammatory cytokine secretion (Evangelatos *et al.* 2019). PNLA has reduced the expression of both miR-25 and miR-223, but this reduction did not reach statistical significance. Decreased levels of miR-30a in inflamed synovial tissues are correlated with reduced apoptosis and enhanced autophagy in RASFs and SMs (Evangelatos *et al.* 2019).

The expression levels of miRNAs in PBMCs of RA patients were found to be elevated for miR-16, miR-103a, miR-132, miR-145, miR-146a, miR-155, miR-221, miR-222, and miR-301a, while miR-21, miR-125b, and miR-548a were decreased (Evangelatos *et al.* 2019). These alterations lead mainly to enhanced cytokine secretion and disturbed innate and adaptive immune balance in PB. In one study of 1800 miRNAs in the PB of treatment-naïve Chinese RA patients with the active disease, elevated levels of miR-181d, miR-4634, and miR-4764 were found, while miR-9, miR-122, miR-219-2, miR-342, miR-3925, and miR-3926 were reduced (Evangelatos *et al.* 2019). The concentration of some miRNAs in the serum was increased in patients with RA, such as miR-221, miR-488, miR-499, miR-551b, and miR-5196 (Evangelatos *et al.* 2019). Among these, miRNA-342 was upregulated, while miR-499 and miR-5196 were downregulated by PNLA treatment.

Collectively, many miRNAs were modulated by PNLA, suggesting potential post-transcriptional regulation of metabolic and immune responses, which has not been described previously. Multiple miRNAs target PDK4, SIGIRR, MT-ATP6 (mitochondrial RNA), and Acetyl-CoA Acyltransferase2 (ACAA2) (a metabolic and mitochondrial gene). One of the key targets of miRNAs regulated by PNLA was PDK4, which was consistent with the observations in Chapter 5. Also, all the upstream effectors-PPARs, EPA, fenofibrate, and resveratrol —were activated by PNLA treatment, as was observed in Chapter 5, though replication and validation of these results are required. Data from this Chapter provides evidence that PNLA modulates cellular miRNA profiles in monocytes that are implicated in inflammation and cellular metabolism and have not been shown previously.

Chapter 8: General Discussion

8.1 Introduction

Despite advances in therapeutic strategies and though progress has been made in understanding many different aspects of RA treatment, long-term disease remission remains elusive. Although there is an increasing number of new biotherapies, a substantial number of RA patients still do not respond sufficiently to current treatment options, and this warrants the identification of new therapeutic targets and the development of novel therapies for RA.

Macrophages produce many cytokines and chemokines, which play important roles in the pathogenesis of RA. Macrophages are also important in the pathogenesis of atherosclerosis. They are the most abundant immune cells within atherosclerotic plaques and orchestrate the initiation, progression, and destabilisation of these lesions. Accelerated atherosclerosis and CV death are the major causes of mortality in RA. As discussed in the Introduction to this thesis, both inflammation and traditional CV risk factors, such as hyperlipidaemia, contribute to an increased risk of CVD in RA. Indeed, proatherogenic lipids cause inflammation, and Ox-LDL is pro-inflammatory, immunogenic, and proatherogenic (Chistiakov *et al.* 2016; Salonen *et al.* 1992). Importantly, these conditions are associated with a pro-inflammatory phenotype of circulating monocytes (Stienstra *et al.* 2017). Therefore, monocytes and macrophages are key therapeutic targets for reducing synovitis and CV mortality in RA. Indeed, interventions that reduce both inflammation and proatherogenic lipid metabolism would be beneficial.

In RA, a healthy diet is recommended by guidelines without specifying any kind of food. n-3 and n-6 PUFAs have shown their potential as immunosuppressants and anti-inflammatory agents (Calder 1996; Khanna *et al.* 2017). However, there is some uncertainty regarding this, and scientific research on nutraceuticals and diet is, generally, limited in RA. At the start of my PhD research, my interest was in nutraceuticals, particularly in CVD. This is based on the belief that CVD is driven by dysfunctional lipid metabolism, and therefore, there is a major research focus on diet in CVDs. During my research, I had the opportunity to investigate this in RA, a disease that has CVD as one of its major causes of mortality. In RA, inflammation and traditional metabolic risk factors interact to amplify cardiovascular risk.

8.2 Dietary intervention in RA

Auto-antibody response in RA may start in the gut. RA and other chronic diseases, including CVD, obesity, and diabetes, are strongly influenced by nutrition and food metabolism.

Opposite to the Western diet, the MD diet is considered one of the healthiest diets today. MD's protective properties have been attributed to its antioxidant and anti-inflammatory effects. MD has been advocated as beneficial in RA.

In recent years, several studies have investigated the role of diet and nutrition as potential tools for RA prevention and management (Gioia *et al.* 2020). Several nutrients, such as PUFAs, have been suggested as having a protective role in RA development and reducing disease symptoms and progression. Gut microbiota alterations and body composition modifications are potential mechanisms for how diet influences RA onset and progression. Rosillo *et al.* found that an olive oil diet suppressed the phosphorylation of STAT3 and thus repressed IL-17 production (Rosillo *et al.* 2016). In addition, Khanna *et al.* showed that in mice fed with olive oil, levels of phosphorylated JNK and p38 proteins were reduced (Khanna *et al.* 2017). In mouse models of RA, dietary intake of anthocyanins was shown to decrease TNF- α levels (Khanna *et al.* 2017).

Nutrients can modulate the inflammatory state. Consequently, the pro- or anti-inflammatory properties of specific foods and their components have emerged in the nutrition sciences (Gioia *et al.* 2020). Postprandial inflammation is a component of the normal stress reaction to food in cells. Among different nutrients, LA (an n-6 precursor) and ALA (an n-3 precursor) are the only essential FAs that the body cannot synthesise. Regarding fat, several studies reported pro-inflammatory effects of trans-FA, with increased levels of TNF- α , IL-1, CRP, and vascular endothelial dysfunction. In contrast, the n-3 PUFA, mainly present in fish oils, is inversely correlated with IL-6, MMP3, and CRP levels. Different studies have suggested FAs as possible protective nutrients for RA. Di Giuseppe *et al.* observed a reduction (of 35% in RA risk) in women with a dietary intake of n-3 PUFA higher than 0.21 g/day (Gioia *et al.* 2020). A Danish prospective population-based cohort study confirmed a decreased risk of RA (about 49%) for patients with a dietary intake of 30 g fatty fish (>8 g fat/100 g fish) (Gioia *et al.* 2020), while a medium consumption of fatty fish (3–7 g fat/100 g fish) was associated with a significantly higher risk of RA.

Antioxidant nutrients, variably present in different foods, such as n-6 FA, act as scavengers of free radicals and alter several important biological processes. They inhibit cell proliferation and cholesterol absorption, reduce inflammation, and modulate many redox reactions (Gioia *et al.* 2020). Among these functions, prevention and delaying atherosclerosis are two of the most relevant. Epidemiological *in vivo* and *in vitro* studies suggested different preventive effects in

atherogenesis, including the reduction of LDL oxidation, oxidative stress, chemotaxis, inflammation, the release of NO, cell adhesion, and platelet aggregation (Gioia *et al.* 2020). Overall, although some studies suggested an association between dietary habits and RA development, mainly regarding fruit, vegetable, and meat intake, the evidence is still inconclusive (Gwinnutt *et al.* 2022). In this thesis, I studied PNLA, a constituent of the pine nut, as a potential dietary therapeutic candidate in RA. Previous experimental data indicated that n-6 PUFA has anti-inflammatory and lipid-modulating effects (as discussed in the Introduction).

8.3 Key findings from the study

Overall, the results in this thesis highlighted PNLA as a potential therapeutic agent capable of exerting beneficial effects on a variety of anti-inflammatory and immune-metabolic processes both *in vitro* and *ex vivo*. The key findings are summarised below.

Chapter 3. PNLA had no detrimental effects on the viability or proliferation of THP-1 macrophages (**Figure 3.1**) or primary HMDMs (**Figure 3.7**). PNLA reduced CCL2-induced monocyte migration (**Figure 3.2**), macropinocytosis (**Figure 3.3**), and ox-LDL uptake by macrophages (**Figure 3.4**). These key findings were all confirmed in HMDMs (**Figures 3.8-3.9**). Additionally, PNLA had no effect on macrophage phagocytic activity or ROS levels in THP-1 monocytes or macrophages (**Figure 3.6**). A summary of the specific assays carried out in this Chapter is summarised in **Figure 8.1**.

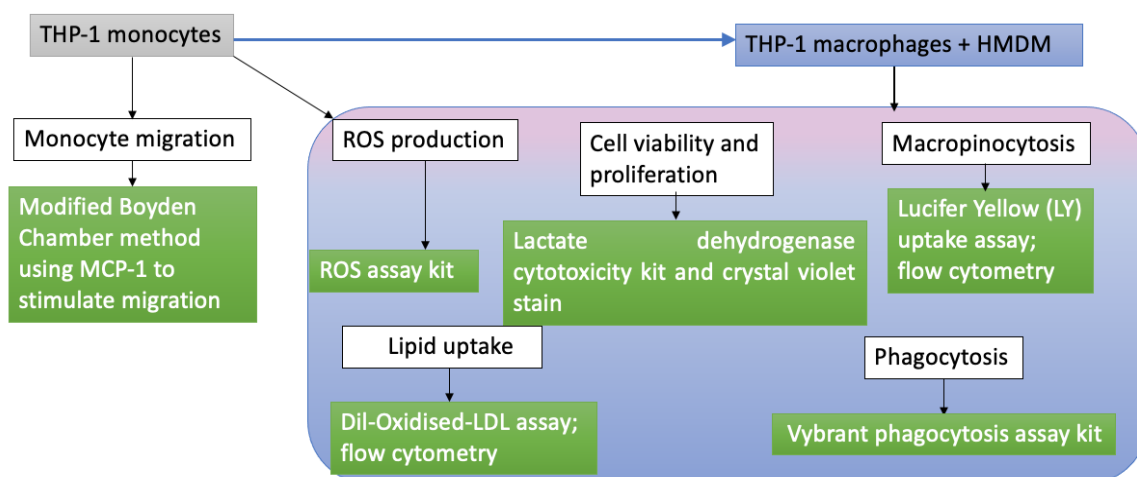


Figure 8.1. Key experimental procedures conducted in Chapter 3

Chapter 4. PNLA had no detrimental effect on the viability or proliferation of PBMCs from RA patients and HCs (**Figures 4.1-4.2**). PNLA reduced pro-inflammatory cytokines produced

by LPS-activated monocytes from RA patients and HCs, including TNF- α , IL-6, and PGE2 (**Figures 4.3, 4.5, 4.9**). These effects were confirmed in differentiated macrophages as shown in **Figures 4.4, 4.6, and 4.10**. The effect on IL-1 β was significant in HCs, but not in RA (**Figures 4.7, 4.8**), and NO was significantly reduced by 25 μ M and not 50 μ M PNLA in macrophages from both HCs and RA patients (**Figure 4.11**).

Chapter 5. RNA-seq and WGT analysis of PBMCs from patients with RA and HCs found that DEGs were upregulated by PNLA, including PDK4, PAI or SERPINE1, NDRG2, and FBP1 (**Figure 5.6**). IPA suggested inhibition of pro-inflammatory transcription factors such as NF- κ B, and STAT1 (**Figures 5.14, 5.15**) and activation of anti-inflammatory transcription factors such as PPARs (**Figure 5.16-5.18**). Venn diagrams were used to illustrate key DEGs that were up- or down-regulated by LPS and PNLA in HC and RA patients (**Figures 5.8-5.11**).

Chapter 6. Using flow cytometry, PNLA was found to reduce the intracellular production of TNF- α , IL-6, IL-1 β , and IL-8 by activated CD14⁺ monocytes (**Figure 6.6**). There was no correlation between the PNLA reduction of cytokines and RA patients' clinical and laboratory disease markers (**Table 6.2**).

Chapter 7. RNA-seq of CD14⁺ monocytes suggested PNLA inhibited oxidative phosphorylation and mitochondrial dysfunction, while it activates the SIRT signalling pathway. Many DEGs were identified, e.g., PDK4, ACADVL, CPT1A, and SLC25A20, and were also expressed in PBMCs (see Chapter 4). Most importantly, this is the first study to show that many miRNAs were modulated (upregulated or downregulated) by PNLA (**Tables 7.3-7.4**). Amongst these, the let 7 family of miRNAs has a variety of anti-inflammatory and anti-atherogenic actions (**Figures 7.16H and 7.17**). Notably, the JAK-STAT3 pathway is regulated by miRNA let-7. Of note, several miRNAs target PDK4 and SIGIRR, as shown in **Figures 7.7 and 7.8A**. SIGIRR downstream regulatory effects include IL-1 β , TNF- α , NF- κ B and TRIM1 signalling pathways (**Figure 7.8B**). On the other hand, PDK4 regulates TNF- α and NF- κ B as reported in Chapter 5.

Recently, the role of miRNA in innate and adaptive immune responses has been widely investigated. RA and atherosclerosis are examples of chronic inflammatory diseases in which miRNAs have been shown to modulate pathogenic processes in the joints and blood vessels, with the potential to serve as biomarkers for both the inflammatory processes and therapeutic

responses (Brennan *et al.* 2017; Furer *et al.* 2010). Studies over the last decade in RA have shown that dysregulations of miRNAs in PB and synovial mononuclear cells are associated with joint inflammation and destruction. To our knowledge, there is no data on the impact of PUFAs on miRNA expression in monocytes/macrophages. The data presented in Chapter 7 is novel and addresses this important knowledge gap.

Taken together, the results in this thesis suggest that PNLA may mediate its anti-inflammatory and metabolic effects by impacting mitochondrial function, gene transcription, and post-transcriptional modification through miRNAs.

8.4 The role of mitochondrial dysfunction in driving inflammation in RA

RA synovium is hypoxic, which increases ROS production through OXPHOS in mitochondria (Taylor and Sivakumar 2005). Chronic ROS exposure can result in mitochondrial damage or dysfunction and shift immunometabolism from OXPHOS to aerobic glycolysis, which induces the transformation of immune cells into pro-inflammatory phenotypes and releases DAMPs that can perpetuate inflammation (Panga *et al.* 2019). To clear the damaged mitochondria, the cell initiates mitophagy, a selective form of autophagy in macrophages. M1 macrophages treated with the autophagic inhibitor 3-methyladenine or cyclosporine A displayed an increase in mitochondrial mass and decreased secretion of TNF- α and IL-1 β , and NF- κ B may be involved in reprogramming the energy metabolism of cells to sustain them (Cai *et al.* 2020). Based on our findings, PNLA may inhibit both the autophagy and apoptosis pathways (**Figure 7.10**). However, the role of mitophagy in the RA disease process is still unclear. Restoring mitochondrial function is a potential therapeutic strategy. In previous studies, PNLA was shown to protect against pro-inflammatory cytokines and oxidative mediators in cell lines and animal models. However, investigations of its effects on macrophage metabolism and mitochondrial function in the context of RA are lacking.

8.5 Macrophages' immunometabolism during inflammation and diseases

Cellular metabolism modulates immune cell function. Macrophage activation is accompanied by metabolic changes, while altering cellular metabolism impacts the function of macrophages. Stienstra *et al.* (2017) reviewed an impressive body of evidence on the metabolic reprogramming of myeloid cells after LPS stimulation (Palsson-McDermott *et al.* 2015; Ruiz-Garcia *et al.* 2011; Rodriguez-Prados *et al.* 2010; Tan *et al.* 2015). Upon activation, immune cells drastically increase their demand for nutrients to generate ATP to survive and mount an effective immune response. ATP is preferably generated using glucose but can also be

generated via lipids or amino acids (Fox *et al.* 2005; Gleeson and Sheedy 2016). Importantly, the type and fate of nutrients used by immune cells strongly differ and appear to correspond to the functional requirements of the cell. Although it is not particularly clear why this should be important in macrophages because LPS-activated macrophages do not proliferate. One possible consequence is the production of nicotinamide adenine dinucleotide phosphate (NADPH) for NO and ROS production, or possibly nucleotides for mRNA, lncRNA, or miRNA synthesis. Interestingly, metabolic processes such as glycolysis, the Krebs cycle or tricarboxylic acid (TCA), and FA metabolism have highly specific effects on monocyte and macrophage function. Manipulation of these pathways can dramatically alter the functioning of these cells. Immunometabolism plays a key role in glycolytic reprogramming during inflammation. Glucose forms pyruvate during glycolysis and then enters the mitochondria, where it participates in the TCA cycle and OXPHOS, producing large amounts of ATP (Cai *et al.* 2020; Quiñonez-Flores *et al.* 2016). Under acute energy requirements, glycolysis is rapidly regulated; during chronic hypoxic inflammation, pyruvate is converted to lactate, which is known as glycolytic reprogramming (Cai *et al.* 2020). OXPHOS is diverted from glycolysis after the production of pyruvate, which is shuttled to the mitochondria and enters the TCA cycle. The TCA cycle converts pyruvate or lactate into acetyl-CoA, which is then condensed, thereby forming citrate, as shown in **Figure 8.2A**. Increased synthesis of acetyl-CoA from citrate meets the biosynthetic demands of inflammatory macrophages, including the synthesis of FAs, cholesterol, NO, and PGs. NO can inhibit the electron transport chain (ETC) complex, resulting in a decrease in mitochondrial respiration, which decreases the synthesis of ATP. Downstream of citrate and acetyl-CoA, fatty acid synthetase (FAS) is an integral part of the macrophage inflammatory programme and organises the plasma membrane for the inflammatory signalling (Van den Bossche *et al.* 2017). FAS deficiency has been shown to change plasma membrane composition, cholesterol retention, and Rho GTPase trafficking, thereby blunting inflammatory signalling and the adhesion and migration of macrophages (Cai *et al.* 2020; Van den Bossche *et al.* 2017). Moreover, macrophages activated by LPS increase the accumulation of succinate, resulting in the stabilisation of HIF1- α and the induction of IL-1 β and IL-6 (Van den Bossche *et al.* 2017). ARNT2 is a transcription factor that encodes the beta subunit of a heterodimeric HIF1 and is inhibited by PNLA as shown in Chapter 5 (**Table 5.22.1**). FA oxidation is the most fruitful regulator of cellular ATP. Short-chain FAs can diffuse passively into the mitochondria for oxidation, whereas medium- and long-chain FAs are imported into the mitochondria through conjugation to CPT1. FA oxidation yields several products, including acetyl-CoA, NADH, and flavin adenine dinucleotide (FADH₂), which can be used by the TCA cycle, ETC

to generate ATP. In contrast, FA synthesis utilises products derived from other metabolic pathways, including glycolysis, the TCA-derived citrate pathway, and the pentose phosphate pathway, to provide TAG and phospholipids necessary for differentiation and proliferation. Also, mitochondrial citrate shuttled from the TCA cycle to the cytosol after LPS stimulation drives FA biosynthesis, which is needed for the expansion of the endoplasmic reticulum and Golgi to support cytokine release by DCs and macrophages (Everts *et al.* 2014). Overall, various lines of evidence have now established a firm link between metabolic adaptations and macrophage function, including anti-microbial properties and cytokine production (Stienstra *et al.* 2017).

In summary, increased glycolysis has been observed in activated inflammatory cells (Kelly and O'Neill 2015). Enhanced glycolysis in inflammatory macrophages is associated with the inhibition of select steps of the TCA cycle, that assist inflammatory processes; hence, aerobic glycolysis is critical for inflammatory cell activation (Van den Bossche *et al.* 2017; Zhang *et al.* 2019). In inflammatory macrophages, this cycle is disrupted in two places: after citrate and after succinate.

In RA, glucose metabolism has been shown to play an important role in disease pathogenesis (Xu *et al.* 2019). The hypoxic synovial tissues of RA patients have increased glycolytic enzyme gene expression and glycolytic activity. The key enzymes of glycolysis, such as PK, are downstream of the glucose metabolic pathway and irreversibly catalyse the conversion of phosphoenolpyruvate (PEP) to pyruvate (Xu *et al.* 2019). Pyruvate kinase (M2) PKM2, an isoform of PK, is highly expressed in tumour cells, leading to increased glucose uptake, a transition from OXPHOS to glycolysis, and the accumulation of glucose metabolites. It provides favourable and necessary conditions for the growth and survival of tumour cells (Xu *et al.* 2019). In recent years, studies have confirmed that the expression level of PKM2 in the synovial tissue of patients with RA is significantly higher than that in patients with OA. Activated PKM2 phosphorylates STAT1 and STAT3, and then promotes the production of the pro-inflammatory cytokines IL-6, TNF- α , and IL-1 β (Cai *et al.* 2020; Weyand and Goronzy 2020). Therefore, PKM2 may participate in the pathogenesis of RA through metabolic or non-metabolic pathways (Quiñonez-Flores *et al.* 2016), thereby contributing to synovial hypertrophy in RA, which has been described as having the characteristics of tumour-like proliferation.

In atherosclerosis, a study comparing human monocytes isolated from HCs or individuals with CVD, Shirai *et al.* mechanistically explored the concept of ‘monocyte priming’ concerning cellular metabolic status. After *ex vivo* stimulation with LPS and IFN- γ monocytes isolated from the atherosclerotic patients produced more IL-6 and IL-1 β than monocytes from HCs. Notably, the enhanced glucose uptake and glycolysis of atherosclerotic monocytes drives mitochondrial ROS production and oxidative stress, resulting in PKM2 assembly and translocation to the nucleus and subsequent inflammatory signalling. Molecular-level investigation of the underlying mechanisms identified the glucose–ROS–PKM2–STAT3 pathway, through which glucose utilisation led to unbalanced ROS generation from the mitochondrial respiratory chain, which in turn induced the redox-sensitive enzyme PKM2. It then phosphorylates and activates STAT3 to promote the production of the inflammatory cytokines IL-1 β and IL-6 (Van den Bossche *et al.* 2017).

Results in this thesis found that PK was inhibited by PNLA based on activation of PDK4 (Chapters 5 and 7), downregulation of STAT1/STAT3, TNF- α /IL-1 β , and ERK. PNLA may impact macrophage immunometabolism, which could advance the management of RA as well as CVD.

8.6 Biologic effects of PNLA

The following biologic effects of PNLA were described in this thesis:

8.6.1 Regulation of inflammation and immune pathways

NF- κ B and STAT1 are upstream pathways predicted to be modulated by PNLA in PBMCs from patients with RA and/or HC (Chapter 5). NF- κ B and STAT1 pathways are important in the signal transduction of pro-inflammatory cytokines, including TNF- α and IL-6. Reductions in the production of IL-6, TNF- α , and IL-1 β were confirmed by ELISA and intracellular cytokine staining in Chapters 4 and 6.

In studies presented in Chapter 7, PNLA activated the expression of KLF15, AGO2, FLCN, and SIRT3, and inhibited STAT3, CLPP, TFE3, and DAP3 in LPS-stimulated monocytes. The sirtuin pathway was implicated as one of those significantly affected by PNLA. This pathway is particularly interesting, and further research will be of interest as it has important roles in inflammation and metabolism (Stienstra *et al.* 2017). It has been implicated in both CVDs and RA, as discussed in Chapter 7.

8.6.2 Modulation of metabolic genes/pathways

PDK4 was a DEG whose expression was significantly upregulated by PNLA in PBMCs from RA patients and HCs. Upregulation of PDK4 was confirmed in PNLA treated monocytes (Chapter 7). PDK4 is also one of the targets of miRNAs modulated by PNLA. PDK4 is an important checkpoint in NF- κ B/TNF-mediated responses (**Figure 5.22**) and regulates lipid metabolism (**Figure 5.21**), which is consistent with the known biological effects of PNLA.

FBP1 was another DEG whose expression was significantly upregulated by PNLA in PBMCs from RA patients. It is an endogenous intermediate of the glycolytic pathway that is produced through the phosphorylation of fructose 6-phosphate. FBP is a high-energy intermediate of glycolysis and has anti-inflammatory properties. It has been demonstrated that exogenous treatment with FBP markedly attenuates arthritis (Veras *et al.* 2015), reducing joint swelling, neutrophil infiltration, articular hyperalgesia, and pro-inflammatory cytokine production while boosting IL-10 production in two experimental models of arthritis. Mechanistic studies showed that FBP mRNA expression reduces joint inflammation through the generation of extracellular adenosine and subsequent activation of the adenosine receptor A2a (Veras *et al.* 2015).

PAI-1 was suggested to be involved in tissue remodelling because of its potential role in plasmin inhibition and MMP-mediated matrix degradation of pro-matrix MMPs to MMPs. Accordingly, overexpression of PAI-1 reduces ECM degradation via perturbing the PA system (t-PA and u-PA) (Rabieian *et al.* 2018), as was discussed in Chapter 5 (**Figure 5.23**). PNLA regulates SERPINE-1/ PAI-1, which in turn regulate the PA system. PAI-1 is a crucial downstream effector molecule of TGF- β .

PPARs are involved in adipocyte differentiation and glucose homeostasis (Chapter 5). They have been implicated in the pathology of obesity, diabetes, and atherosclerosis. Recently, it was shown to regulate NF- κ B, AP-1, and ox-LDL, which have various roles in immunoregulation. PPARs are involved in the catabolism of pro-inflammatory lipid mediators, the regulation of glucose metabolism, the inhibition of oxidative stress, autophagy, and the expression of pro-inflammatory cytokines (**Figure 5.24**). They are predicted to be activated by PNLA.

SIRT1 is an NAD⁺-dependent class III histone deacetylase. Activators of SIRT1, such as resveratrol, partially decrease IL-6 production. In contrast, macrophages undergoing innate

immune tolerance after exposure to LPS exhibit a metabolic switch from glycolysis to OXPHOS and an increased NAD⁺/NADH ratio, activation of SIRT1, and consequent inhibition of inflammatory gene transcription involved in IL-1 β production, oxidative stress, angiogenesis, and vascular remodelling.

TFEB and TFE3 have also been associated with an increasing number of diseases. In many cases, TFEB and TFE3 localization, levels, and activity are affected in disease states, and modulation of these parameters represents a promising therapeutic goal for a wide variety of inflammatory diseases. This is summarised graphically in **Figure 7.10**. The recent identification of TFEB and TFE3 as master regulators of macroautophagy, autophagy, and lysosome function in activated macrophages. This raises the possibility that these transcription factors may be of central importance in linking autophagy and lysosome dysfunction with inflammatory disorders and the transcription of pro-inflammatory cytokines such as TNF- α and IL1 β (**Figure 7.10**), requiring the presence of both TFEB and TFE3 (Brady *et al.* 2018; Pastore *et al.* 2016; Takala *et al.* 2023).

8.6.3 Modulation of cellular miRNA signatures.

Among FAs under inflammatory conditions, both DHA and AA downregulate numerous miRNAs in macrophages/EC lines, which are well-known for their involvement in TLR signalling and major cell players in CVDs (Roessler *et al.* 2017). However, this is the first study documenting the effect of PNLA's impact on CD14⁺ monocyte miRNA expression from patients with RA. Bioinformatic analyses showed that the targets of these miRNAs are metabolic mRNAs such as MT-ATP6, JMJD7-PLA2G4B, ACAA2, ETFA, and GHRL, which are involved in metabolic signalling pathways including adipocyte function, glucose metabolism, CCK secretion, mitochondrial ATP synthase, the NAD signalling pathway, and FA β -oxidation (**Table 7.5**). The mechanism whereby PNLA alters miRNA expression is unknown, but the incorporation of FA into the plasma membrane, including mitochondria, is a potential explanation.

8.7 Future direction and clinical implications

For a further understanding and appreciation of the metabolic complexity of PNLA during myeloid cell activation, various aspects will require further study.

1. The dose and duration of exposure to pathogens or TLR agonists influence metabolic pathways in human monocytes. This is illustrated by the observation that short-term exposure (4 hours) drives OXPHOS and mitochondrial changes in human monocytes that

were treated with PNLA. **Figure 8.2(B)** provides a summary of some of the PNLA effects based on the regulation of OXPHOS.

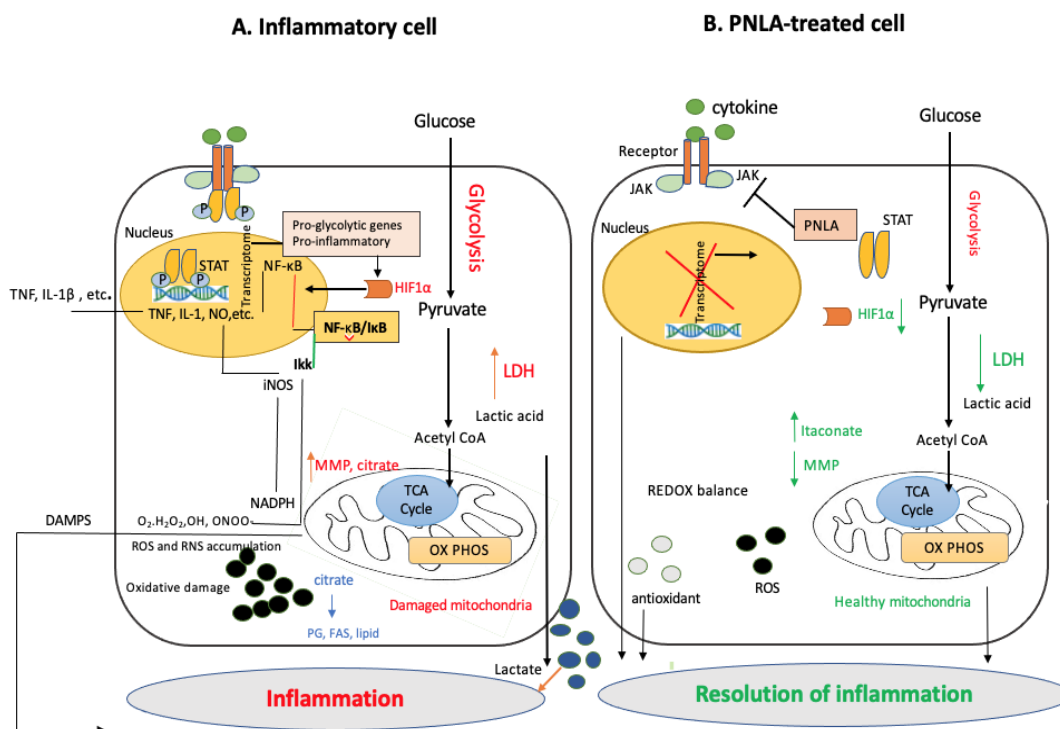


Figure 8.2. Summary on the consequences of OXPHOS in inflammatory and PNLA treated cells.

(A) Metabolic pathway in inflammatory cell models. Glucose enters the cell and is converted into pyruvate via glycolysis, which is then converted to acetyl CoA that then enters the mitochondria to undergo OXPHOS under inflammatory conditions. MMP and citrate are produced; citrate is a source of PGs (e.g., arachidonic acids) and ROS such as O₂⁻, which binds with peroxy-nitrite (ONOO⁻) to form RNS. This reactive species plays a role in the NF-κB mediated production of inflammatory mediators such as TNF, IL-1β and iNOS (Panga *et al.* 2019). The enzyme iNOS catalyses the production of NO. Also, this can lead to the activation of MMP and the depletion of GSH, all of which lead to oxidative damage. Under inflammatory conditions, HIF-1α is also produced, which activates pro-inflammatory genes such as NF-κB and STAT. JAKs phosphorylate STATs, and once STAT is phosphorylated, this leads to the transcription of pro-inflammatory cytokines.

(B) Potential actions of PNLA. Reduces LDH via activation of PDK4, which leads to less lactate and acetyl CoA and consequently results in inhibition of OXPHOS. PNLA treatment can produce less HIF1-α, and oxidative radicles; this, together with more itaconate, results in redox balance, hence the resolution of inflammation. Also, PNLA inhibits the activation of NF-κB and STAT, leading to the inactivation of the transcription of pro-inflammatory cytokines. OXPHOS; Oxidative phosphorylation, TCA cycle; tricarboxylic acid cycle, ROS; reactive oxygen species, HIF-α; hypoxia-inducible factor 1, PDK-4; pyruvate dehydrogenase kinase-4, PG; prostaglandin, LDH; lactate dehydrogenase, RNS; reactive nitrogen species, H₂O₂; hydrogen peroxide, O₂⁻; superoxide, FAS; fatty acid synthase, NO; nitric oxide. JAK; Janus-activated kinase, STAT; signal transducers and activators of transcription, iNOS; inducible nitric oxide synthetase.

- The results of mRNA and miRNA from transcriptomic studies are exploratory and need to be confirmed by qPCR and/or Western blotting at the protein level. In addition, the repressive effect of distinct miRNA species on their putative targets needs to be validated and confirmed by luciferase assays.

3. Functional studies of the proposed pathways by experimental studies and animal models will need to confirm the biological significance of the biological molecules and pathways identified in this thesis. Modern high-dimensional technologies, e.g., multi-colour flow cytometry, mass cytometry, single-cell RNA-seq, confocal microscopy, and Agilent Seahorse, could be used for assessing mitochondrial respiratory function.
4. To determine whether PNLA affects SMs, as they have been considered to change their transcriptome once they migrate from the blood into the inflamed synovial joint. It may be worth working on the transcriptome profile of SMs and assessing the PNLA effect. It is also worth comparing these profiles to those of healthy CD14⁺ monocytes.
5. In the complex immunological landscape of arthritis, the study and potential therapeutic use of one single miRNA in one single type of cell sound like a perfect approach. MiRNA sponges are miRNA inhibitors that contain multiple complementary mRNA sites for a specific miRNA. They competitively bind to miRNAs and prevent miRNAs from binding to their targets (Filková *et al.* 2012). In particular, the role of miRNA in PNLA-mediated biologic effects should be explored further in experimental and animal models.
6. Ultimately, human trials will be needed to clarify the role of PNLA in controlling inflammation in RA and atherosclerosis. RCTs of pine nuts, or PNLA, and double-blind control studies of PNLA supplements will be optimal.

8.8 Conclusion

The results in this thesis are promising, and when considered in conjunction with previously demonstrated immunomodulatory effects of PUFA, they highlight the potential benefits of PNLA supplementation as a potential anti-inflammatory intervention. PNLA is an active ingredient, and its functional products are currently attracting a lot of research interest. While several clinical studies have demonstrated the beneficial effects of n-3 PUFA in a variety of conditions, the studies in this thesis provide novel insights into the role of PNLA in RA and/or atherosclerosis.

Supplementary

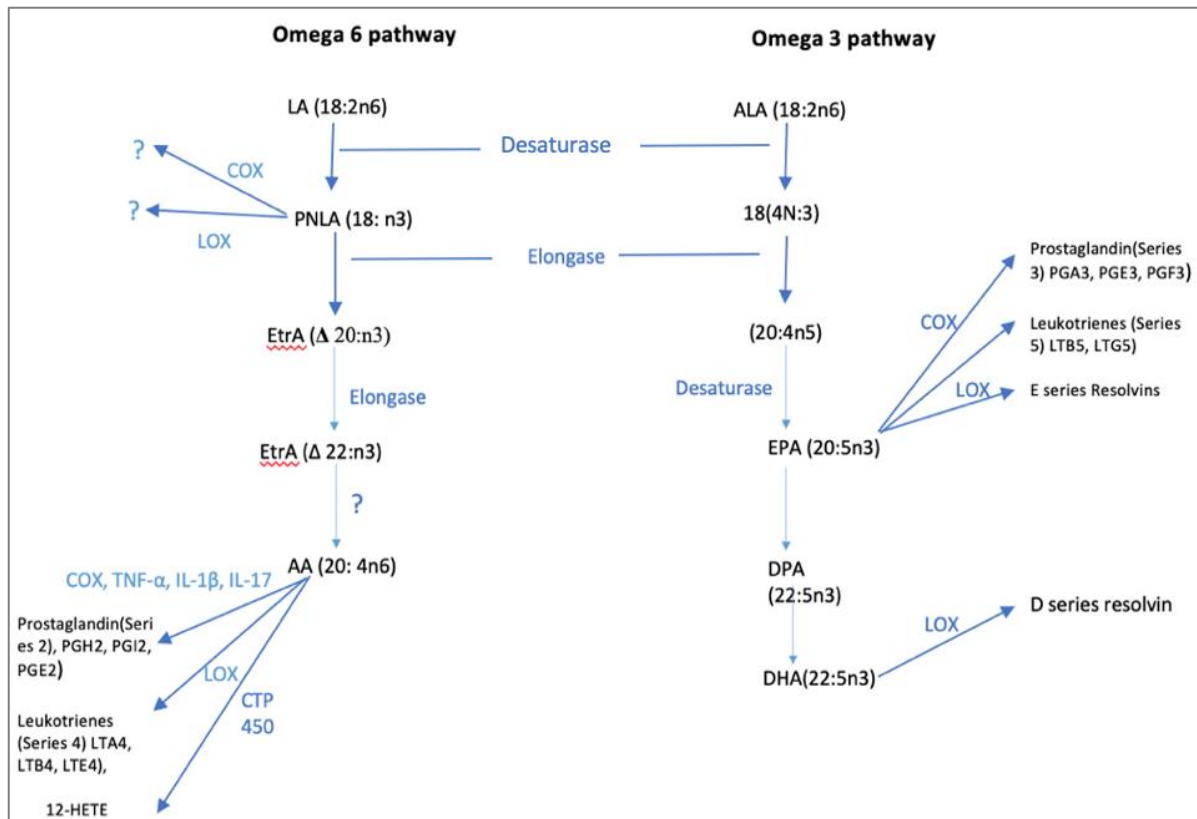


Figure 1. Overview of n-3 and n-6 PUFAs pathways and the suggested mechanism of PNLA metabolism.

LA: Linolenic acid, PNLA: Pinolenic acid, Etra: Eicosatrienoic acid, AA: Arachidonic acid, ALA: Alpha linolenic acid, EPA: Eicosapentaenoic acid, DHA: Docosahexaenoic acid, DPA: docosapentaenoic acid, COX: Cyclooxygenase, and LOX: Lipoxygenase.

Table 1. The demographic and laboratory data of RA patients that were recruited for studies in Chapter 4.

| Subject | Gender | Age (y) | DD (y) | RF | ACPA | DAS28 | ESR | CRP | Treatment |
|---------|--------|------------|-----------|----|------|-------|-----|-----|-------------|
| RA1 | F | 48 | 1 | 1 | 1 | 3.26 | 7 | 2 | MTX |
| RA2 | M | 70 | 3 | 0 | 0 | 1.13 | 5 | 1 | |
| RA3 | F | 60 | 14 | 1 | 1 | 3.17 | 10 | 2 | |
| RA4 | F | 59 | 3 | 1 | 1 | 4.99 | 7 | 6 | |
| RA5 | F | 60 | 11 | 1 | 1 | 4.65 | 11 | 5 | Rituximab |
| RA6 | F | 38 | 2 | 1 | 1 | 3.41 | 22 | 11 | MTX |
| RA7 | F | 43 | 3 | 1 | 1 | 4.7 | 11 | 3 | |
| RA8 | F | 20 | 3 | 0 | 1 | 4.4 | 22 | 6 | |
| RA9 | F | 66 | 1 | 0 | 1 | 2 | 6 | 10 | |
| RA10 | F | 62 | 3 | 0 | 0 | 2 | 8 | 3 | Rituximab |
| RA11 | F | 78 | 12 | 0 | 0 | 2.2 | 12 | 4 | |
| RA12 | M | 68 | 5 | 1 | 1 | 4.09 | 29 | 25 | |
| RA13 | F | 67 | 3 | 0 | 0 | 4.33 | 2 | 5 | |
| RA14 | F | 62 | 13 | 1 | 1 | 5.4 | 33 | 15 | Rituximab |
| RA15 | F | 62 | 14 | 0 | 0 | 5.39 | 48 | 53 | Rituximab |
| RA16 | F | 53 | 16 | 0 | 0 | 5.42 | 30 | 21 | |
| RA17 | F | 63 | 12 | 0 | 1 | 4.5 | 2 | 3 | |
| RA18 | F | 75 | 12 | 1 | 1 | 1.87 | 2 | 2 | Tocilizumab |
| RA19 | F | 42 | 4 | 1 | 1 | 4.42 | 6 | 0 | MTX |
| RA20 | F | 36 | 4 | 1 | 1 | 0.8 | 3 | 0 | |
| RA21 | F | 42 | 3 | 1 | 1 | 3.1 | 4 | 22 | MTX |
| RA22 | F | 28 | 4 | 1 | 1 | 2.1 | 4 | 0 | |
| RA23 | F | 66 | 3 | 0 | 1 | 1.25 | 6 | 2 | |
| RA24 | F | 64 | 11 | 1 | 1 | 3 | 3 | 3 | Rituximab |
| RA25 | F | 67 | 8 | 1 | 1 | 2 | 15 | 0 | Infliximab |
| RA26 | F | 46 | 13 | 0 | 0 | 3.1 | 2 | 0 | Tocilizumab |
| RA27 | M | 47 | 14 | 1 | 1 | 2.8 | 13 | 1 | Rituximab |
| RA28 | F | 63 | 13 | 0 | 1 | 2.8 | 17 | 1 | Infliximab |
| RA29 | F | 62 | 15 | 0 | 0 | 3 | 5 | 2 | Rituximab |

F; Female, M; Male, DD; disease duration, y; years, ACPA; Anti-citrullinated protein antibody, RF; rheumatoid factor, ESR; erythrocytes sedimentation rate and the normal ESR is < 20 mm/hour for female and <10 mm/hour for male CRP; C-reactive protein and the normal CRP is < 4.9 mg/l. MTX; methotrexate.

Table 2. Demographics, laboratory, and clinical data of 6 RA patients and 6 HCs that were used in Chapter 5.

| Subject | Gender | Age(Y) | DD(Y) | RF | ACPA | DAS28 | CRP | Treatment |
|------------|--------|--------|-------|------|------|-------|-----|-------------------------|
| RA1 | F | 63 | 16 | + ve | + ve | 2.8 | 6 | MTX, infliximab |
| RA2 | M | 69 | 6 | + ve | + ve | 2.06 | 30 | MTX |
| RA3 | F | 34 | 2 | - ve | + ve | 2.8 | 39 | Leflunomide |
| RA4 | F | 37 | 5 | + ve | + ve | 0.6 | 2 | MTX, hydroxychloroquine |
| RA5 | F | 60 | 14 | - ve | - ve | 2.72 | 11 | Leflunomide |
| RA6 | F | 78 | 18 | + ve | (NA) | 2 | 15 | MTX, Rituximab |
| HC1 | M | 49 | - | - | - | - | - | - |
| HC2 | F | 22 | - | - | - | - | - | - |
| HC3 | F | 46 | - | - | - | - | - | - |
| HC4 | F | 49 | - | - | - | - | - | - |
| HC5 | F | 41 | - | - | - | - | - | - |
| HC6 | F | 48 | - | - | - | - | - | - |

F; female, M; male, DD; disease duration, Y; years, ACPA; Anti-citrullinated protein antibody, RF; rheumatoid factor, ESR; erythrocytes sedimentation rates the normal ESR is < 20mm/h for female and <10 mm/h for male CRP; C-reactive protein and the normal CRP is < 4.9 mg/l. MTX; methotrexate; NA: not available.

Table 3. Demographic, clinical, and laboratory data on RA patients that was used in Chapter 6.

| Subject | Age (y) | Gender | DD (y) | RF | ACPA | ESR | CRP | DAS28 | Treatment |
|---------|---------|--------|--------|-----|------|-----|-----|-------|------------------|
| RA1 | 63 | F | 6 | +ve | +ve | 10 | 2 | 3.4 | Rituximab + MTX |
| RA2 | 52 | F | 18 | +ve | +ve | 15 | 7 | 3.6 | Infliximab |
| RA3 | 68 | F | 22 | +ve | -ve | 2 | 2 | 5.2 | Rituximab |
| RA4 | 78 | F | 10 | +ve | -ve | 4 | 3 | 2.8 | Tocilizumab |
| RA5 | 63 | F | 3 | -ve | -ve | 16 | 11 | 5.2 | Tocilizumab |
| RA6 | 70 | F | 22 | +ve | -ve | 60 | 25 | 5.2 | Infliximab |
| RA7 | 45 | F | 3 | -ve | +ve | 5 | 4 | 3.3 | Rituximab + MTX |
| RA8 | 35 | M | 4 | -ve | -ve | 12 | 11 | 5 | Rituximab + MTX |
| RA9 | 78 | F | 13 | +ve | +ve | 10 | 1 | 3.4 | Infliximab + MTX |
| RA10 | 58 | F | 4 | +ve | +ve | 9 | 1 | 5 | Rituximab + MTX |
| RA11 | 43 | M | 21 | -ve | -ve | 2 | 10 | 3 | Infliximab |
| RA12 | 75 | F | 18 | -ve | -ve | 3 | 1 | 4.3 | Infliximab + MTX |
| RA13 | 74 | F | 13 | +ve | NA | 10 | 25 | 1.49 | Rituximab + MTX |
| RA14 | 70 | F | 12 | +ve | +ve | 7 | 1 | 2.8 | Tocilizumab |
| RA15 | 45 | M | 14 | -ve | -ve | 51 | 86 | 5.2 | Rituximab+ MTX |
| RA16 | 78 | F | 11 | -ve | -ve | 5 | 9 | 4 | Rituximab |
| RA17 | 63 | F | 6 | +ve | +ve | 2 | 1 | 3.6 | Rituximab |
| RA18 | 57 | F | 13 | -ve | NA | 12 | 3 | 3.5 | Rituximab, MMF |
| RA19 | 65 | F | 21 | -ve | NA | 4 | 0 | 2 | Tocilizumab |
| RA20 | 60 | M | 10 | +ve | +ve | 2 | 0 | 2 | Rituximab |

F; female, M; male, DD; disease duration, y; years, ACPA; Anti-citrullinated protein antibody, RF; rheumatoid factor, ESR; erythrocytes sedimentation rates the normal ESR is < 20mm/hour for female and <10 mm/hour for male CRP; C-reactive protein and the normal CRP is <4.9 mg/l. MTX; methotrexate, MMF; mycophenolate mofetil, y; years, NA: not available. Patients in remission are shown in red.

Table 4. Demographic, clinical, and laboratory information on RA patients that was used in Chapter 7.

| Subject | Gender | Age (y) | DD (y) | RF | ACPA | DAS | CRP | ESR | Treatment |
|------------|--------|------------|-----------|------|------|-----|-----|-----|----------------|
| RA1 | F | 57 | 18 | - ve | + ve | 5.1 | 32 | 36 | Abatacept |
| RA2 | F | 55 | 22 | + ve | + ve | 5 | 1 | 5 | Infliximab |
| RA3 | F | 56 | 12 | +ve | + ve | 5.2 | 17 | 10 | Rituxamab |
| RA4 | F | 58 | 14 | +ve | + ve | 5 | 0 | 8 | Rituxamab |
| RA5 | M | 68 | 11 | +ve | + ve | 5 | 6 | 2 | Rituxamab, MTX |
| RA6 | F | 63 | 13 | +ve | + ve | 4.8 | 2 | 8 | Rituxamab, MTX |
| RA7 | F | 70 | 17 | +ve | + ve | 5.7 | 11 | 21 | Rituxamab |
| RA8 | M | 64 | 12 | +ve | + ve | 5.5 | 34 | 46 | Rituxamab, MTX |

F; Female, M; Male, DD; disease duration, y; years, ACPA; Anti-citrullinated protein antibody, RF; rheumatoid factor, ESR; erythrocytes sedimentation rate and the normal ESR is < 20 mm/hour for female and <10 mm/hour for male CRP; C-reactive protein and the normal CRP is < 4.9 mg/l. MTX; methotrexate.

S1. Library Preparation, including ribosomal RNA depletion, using the NEBNext Ultra II RNA Library Prep Kit for Illumina.

1. Depletion of ribosomal RNA

200 ng of total RNA with a RIN value > 8 was depleted of ribosomal RNA (rRNA) in all samples using the NEBNext® rRNA Depletion kit which enriches polyadenylated transcripts as well as non-polyadenylated RNA (such as non-coding RNAs and antisense transcripts), removes rRNA and leaves all other RNAs (e.g., mRNAs, miRNAs, lncRNAs etc.) for downstream sequencing steps. The kit employs the efficient RNase H method, as well as complete probe tiling of rRNA, thereby ensuring that even degraded rRNA is hybridised and subsequently removed. Efficient removal of rRNA was confirmed on the Agilent 4200 TapeStation using a High Sensitivity RNA ScreenTape (Agilent Technologies, UK) following the manufacturer's instructions.

2. Probe Hybridisation to RNA

200 ng of total RNA of good quality and RIN > 8 was diluted with nuclease-free water to a final volume of 12 µl in a PCR tube and the RNase H incubation step was performed at 37°C. Then, RNA/Probe hybridisation reaction was assembled on ice as in **Table 5**.

Table 5. RNA hybridisation reaction

| RNA/Probe hybridisation reaction | Volume (µl) |
|--|-------------|
| 200 ng of total RNA in Nuclease-free Water | 12 µl |
| NEBNext rRNA depletion | 1 µl |
| NEBNext probe hybridisation buffer | 2 µl |
| Total volume | 15 µl |

The samples were mixed thoroughly and centrifuged down in a microcentrifuge to collect the liquid from the side of the tube. Samples were then placed in a thermocycler and analysed using the following methodology in **Table 6** with the heated lid set to 105°C.

Table 6. Hybridisation reaction thermocycler programme

| Temperature | Time |
|-------------------|-----------|
| 95°C | 2 min |
| Ramp down to 22°C | 0.1°C/sec |
| Hold at 22°C | 5 min |

The samples were centrifuged down in a microcentrifuge, placed on ice, and proceeded immediately to RNase H Digestion.

3. RNase H Digestion

The following RNase H digestion reaction (**Table 7**) was assembled on ice:

Table 7. RNase H digestion reaction

| RNase H digestion reaction | Volume (μ l) |
|------------------------------------|-----------------------------|
| Hybridised RNA from (Step 4.3.4.1) | 15 μ l |
| RNase H reaction buffer | 2 μ l |
| NEBNext RNase H | 2 μ l |
| Nuclease-free water | 1 μ l |
| Total volume | 20 μl |

The samples were mixed thoroughly by pipetting up and down at least 10 times, and then briefly centrifuged in a microcentrifuge. The samples then incubated in a thermocycler for 30 min at 37°C with the lid set to 40°C, centrifuged in a microcentrifuge and placed on ice. Proceeded immediately to DNase I Digestion.

4. DNase I Digestion

The following DNase I digestion reaction (**Table 8**) was assembled on ice:

Table 8. DNase I digestion reaction

| DNase I master mix | Volume (μ l) |
|--|-----------------------------|
| RNase H treated RNA from (Step 4.3.4.2.) | 20 μ l |
| DNase I reaction buffer | 5 μ l |
| NEBNext DNase I (RNase-free) | 2.5 μ l |
| Nuclease-free water | 22.5 μ l |
| Total volume | 50 μl |

The samples were mixed thoroughly by pipetting up and down at least 10 times, and briefly centrifuged in a microcentrifuge. The samples then incubated in a thermocycler for 30 min at 37°C with the heated lid set to 40°C (or off). Briefly, the samples were centrifuged in a microcentrifuge placed on ice and proceeded immediately to the RNA Purification step.

5. RNA Purification using NEBNext RNA Sample Purification Beads

The NEBNext RNA Sample Purification Beads were added to each RNA sample from the previous step and mixed thoroughly by pipetting up and down at least 10 times. The mixture was incubated for 15 min on ice to bind RNA to the beads. The samples were then placed on a magnetic rack to separate the beads from the supernatant. After the solution was clear, the supernatant was removed and discarded carefully. 200 μ l of freshly prepared 80% ethanol was

added to each sample while in the magnetic rack, incubated at RT for 30 sec and then the supernatant was carefully removed and discarded. The beads were then air dried for up to 5 min to completely remove residual ethanol while the tubes were on the magnetic rack with the lid open. The RNA was eluted from the beads by adding 7 μ l of Nuclease-free water after removing it from the magnetic rack and mixed thoroughly by pipetting up and down at least 10 times. The samples were then incubated for 2 min at RT and placed on the magnetic rack until the solution was clear (~ 2 min). 5 μ l of the supernatant containing RNA was removed and transferred to a nuclease-free tube. Finally, the samples were placed on ice and proceeded to RNA Fragmentation and Priming.

6. RNA Fragmentation and Priming

The following fragmentation and priming reactions (**Table 9**) were assembled on ice. Fragment sizes of approximately 260 bp to 280 bp are recommended.

Table 9. Fragmentation and priming reaction

| Fragmentation and priming reaction | Volume (μ l) |
|--|-------------------|
| Ribosomal RNA depleted sample from the previous step | 5 μ l |
| NEBNext first strand synthesis reaction buffer | 4 μ l |
| Random primers | 1 μ l |
| Total volume | 10 μ l |

The samples were mixed thoroughly by pipetting up and down 10 times. They were then placed on a thermocycler and incubated at 94°C for 15 min (suggested fragmentation times based on the RIN value of RNA input). Immediately the samples were transferred to ice and proceeded to First Strand cDNA Synthesis.

7. First Strand cDNA Synthesis

The first strand synthesis reaction (**Table 10**) was assembled on ice by adding the following components to the 10 μ l of fragmented and primed RNA from the previous step. The reaction was mixed thoroughly by pipetting up and down 10 times. Samples were incubated in a pre-heated thermocycler with the heated lid set to \geq 80°C (**Table 11**).

Table 10. First-strand cDNA synthesis reaction

| First-strand synthesis reaction | Volume (μ l) |
|--|-------------------|
| Fragmented and primed RNA (4.3.3.2.6) | 10 μ l |
| NEBNext strand specificity reagent | 8 μ l |
| NEBNext first strand synthesise enzyme mix | 2 μ l |

| | |
|---------------------|------------|
| Total volume | 20 μ l |
|---------------------|------------|

Table 11. First-strand cDNA synthesis thermocycler programme

| Step | Temp | Time |
|------|------|--------|
| (1) | 25°C | 10 min |
| (2) | 42°C | 15 min |
| (3) | 70°C | 15 min |
| (4) | 4°C | Hold |

Proceeded directly to Second Strand cDNA Synthesis.

8. Second Strand cDNA Synthesis

The second strand cDNA synthesis reaction (**Table 12**) was assembled on ice by adding the following components to the first strand synthesis product from the previous step.

Table 12. Second strand cDNA synthesis reaction

| Second strand synthesis reaction | Volume (μ l) |
|--|-------------------|
| First-strand synthesis product (previous step) | 20 μ l |
| NEBNext second strand synthesis reaction buffer with dUTP mix (10X) | 8 μ l |
| NEBNext second strand synthesis enzyme mix | 4 μ l |
| Nuclease-free water | 48 μ l |
| Total volume | 80 μ l |

The samples were kept on ice, mixed thoroughly by pipetting up and down at least 10 times, and incubated in a thermocycler for 1 hour at 16°C with the heated lid set to \leq 40°C (or off) to synthesise the second cDNA strand.

9. Purification of double-stranded cDNA using AMPure XP Purification Beads

144 μ l (1.8X) of vortexed and resuspended AMPure XP were added to the second strand synthesis reaction (~ 80 μ l), vortexed on a vortex mixer and then incubated for 5 min at RT. The samples were centrifuged in a microfuge to collect any sample from the sides of the tube. The tube was placed on a magnet to separate beads from the supernatant. After the solution was clear, the supernatant was carefully removed and discarded. 200 μ l of prepared 80% ethanol was added to each tube while in the magnetic rack, incubated at RT for 30 sec and then the supernatant was carefully removed and discarded. The beads were then air-dried for up to 5 min while the tubes were on the magnetic rack with the lid open. Then, the tubes were removed from the magnetic rack and the cDNA was eluted from the beads by adding 53 μ l of

0.1X TE Buffer (provided) to the beads and mixed well on a vortex mixer. Then, quickly the tubes were centrifuged, incubated for 2 min at RT, and placed on the magnetic rack until the solution was clear. 50 μ l of the supernatants were transferred to clean nuclease-free PCR tubes and stored overnight at -20°C on completion of the cDNA stage.

10. End Prep of cDNA Libraries

The end prep master mix was made on ice in a clean nuclease-free tube by adding the following components to 50 μ l of the second strand synthesis product from the previous step. The mixture was then vortexed and divided between samples (**Table 13**).

Table 13. End prep mix

| End Prep Reaction | Volume (μ l) |
|---|-------------------|
| Second strand cDNA synthesis product (4.3.3.2.9.) | 50 μ l |
| NEBNext Ultra II End prep reaction buffer | 7 μ l |
| NEBNext Ultra II end prep enzyme mix | 3 μ l |
| Total volume | 60 μ l |

The samples were mixed thoroughly, and quick centrifugation was performed to collect all liquid from the sides of the tube. The mixture was incubated in a thermocycler for the end prep reaction, with a heated lid set to $\geq 75^\circ\text{C}$ (**Table 14**). Afterwards, proceeded immediately to adaptor ligation.

Table 14. End prep thermocycler programme

| Step | Temperature | Time (Mins) |
|------|-------------|-------------|
| (1) | 20°C | 30 |
| (2) | 65°C | 30 |
| (3) | 4°C | ∞ |

11. Adaptor Ligation

NEBNext Adaptor for Illumina was diluted 25-fold in adaptor dilution buffer and kept on ice before setting up the ligation reaction. Then, the ligation reaction was assembled on ice by adding the following components, in the order given to the end prep reaction product from the previous step.

Table 15. Adaptor ligation mix

| Component | Volume (μ l) |
|--------------------------------------|-------------------|
| End prepped DNA | 60 μ l |
| Diluted NEBNext® adaptor | 2.5 μ l |
| NEBNext ligation enhancer | 1 μ l |
| NEBNext Ultra II ligation master mix | 30 μ l |
| Total Volume | 93.5 μ l |

The mixture was then pipetted, quickly centrifuged to collect all liquid from the sides of the tube and incubated for 15 min at 20°C (heated lid off) in a thermocycler. 3 μ l of USER® enzyme was added to the ligation mixture resulting in a total volume of 96.5 μ l. The samples were mixed, briefly centrifuged, and then incubated for 15 min at 37°C in a thermocycler with the heated lid set to \geq 45°C. Then, proceed immediately to the purification of the ligation reaction.

12. Purification of the ligation reaction using AMPure XP beads (Beckman Coulter).

87 μ l of NEBNext sample purification beads (0.9X) was added to each ligation reaction and mixed well on a vortex mixer at least 10 times, and incubated for 10 min at RT. The mixture was centrifuged in a microcentrifuge and placed on a magnetic rack to separate beads from the supernatant; after the solution was clear, the supernatant was discarded. 200 μ l of 80% ethanol was added while in the magnetic rack, incubated at RT for 30 sec, and then the supernatants were carefully discarded. The residual ethanol was completely removed, and the beads were air dried for up to 5 min while the tubes were on the magnetic rack with the lid open, and the samples were removed then from the magnetic rack. DNA was eluted from the beads by adding 17 μ l of 0.1X TE to the beads, the samples were mixed well by vertexing, incubated for 2 min at RT then returned to the magnetic stand. Once the solution became clear, 15 μ l of the supernatants were transferred to clean PCR tubes and proceeded to PCR enrichment.

13. PCR Library Enrichment

A master mix was prepared for the PCR enrichment of each library (**Table 16**). Following the addition of the PCR enrichment master mix, a unique index primer was added to each sample. The components were mixed well and centrifuged in a microcentrifuge.

Table 16. PCR library enrichment mix

| Component | Volume/library (μ l) |
|---------------------------------|---------------------------|
| Adaptor Ligated DNA | 15 μ l |
| NEBNext Ultra II Q5® Master Mix | 25 μ l |
| Index (X)/Universal PCR Primer | 10 μ l |

| | |
|---------------------|------------|
| Total Volume | 50 μ l |
|---------------------|------------|

The samples were then placed on the thermocycler for PCR library enrichment (**Table 17**). This was also used to add a unique identified index to each library to allow multiplexing during RNA-seq. The number of PCR cycles for steps 2 and 3 can be variable and depends on the amount of input RNA. The number of cycles is important since too many cycles can result in the over-amplification of PCR products. Over amplification can be identified in subsequent quality control on the TapeStation by evidence of large molecular weight products (>500 bp) on the trace. Conversely, too few cycles will result in low library yields. Here 11 cycles have been applied.

Table 17. PCR library enrichment cycling conditions.

| Cycle step | Temp | Time | Cycles |
|-----------------------------|------|----------|--------|
| Initial Denaturation | 98°C | 30 sec | 1 |
| Denaturation | 98°C | 10 sec | 11 |
| Annealing/Extension | 65°C | 75 sec | |
| Final Extension | 65°C | 5 min | 1 |
| Hold | 4°C | ∞ | - |

14. Purification of the PCR reaction using AMPure XP beads (Beckman Coulter).

For each PCR reaction, 45 μ l (1X) of resuspended AMPure XP beads was added and the mixture vortexed. The samples were then incubated at RT for 5 min, briefly centrifuged, and then placed on the magnetic rack to separate beads from the solution. After aspirating and discarding the supernatants, the beads were washed for 30 sec with 80% ethanol. Following the removal of the second wash, the beads were air-dried for 5 min before removing samples from the rack. To elute the DNA, 23 μ l of 0.1 X TE was added to each sample, the samples were returned to the magnetic rack and upon the solution turning clear, 20 μ l of the solution, containing the eluted purified cDNA, was transferred to new strip tubes. Samples were then stored at -20°C.

15. Library Quantification

The libraries were quantified using the Agilent 4200 TapeStation and D1000 ScreenTape (Agilent Technologies). Briefly, the D1000 reagent was equilibrated at RT and Agilent 4200 TapeStation software was launched, ScreenTape device was loaded into the Agilent 4200 TapeStation system and loading tips were placed into the TapeStation. For running the ladder, 15 μ L D1000 sample buffer was prepared and mixed with 5 μ L D1000 Ladder; samples were prepared by mixing 15 μ L D1000 sample buffer with 5 μ L DNA sample. The samples and

ladder were centrifuged briefly to a position at the bottom of the tubes, which were then positioned into the 4200 TapeStation instruments and analysed by the Agilent TapeStation software. To ascertain the insert size, distribution, and the Qubit® (Life Technologies) was used to perform the fluorometric quantitation of the concentrations of the libraries (as described in the previous section). D1000 ScreenTape Electropherograms of completed libraries were checked for all the samples and they passed the QC as shown in the Methods Chapter (**Figure 2.17**).

S2. Optimisation of RNA-seq of PBMCs

An initial step in RNA-seq is fragmenting RNA into suitable sizes for sequencing. For the HiSeq 4000 platform, fragment sizes of approximately 280 bp to 300 bp are recommended. Thus, the fragmentation of RNA into suitable sizes was optimised by incubating the recovered RNA for period between 2 and 8 min at 94°C (**Figure 2**). Bioanalyzer confirmed that an optimal peak size was obtained when fragmenting peripheral RNA for 6 min.

Libraries were then prepared as outlined in section 3. Initially, rRNA was removed using magnetically labelled beads specific to rRNA sequences. When placed in a magnetic field, this removes rRNA and leaves all other RNAs (e.g., mRNAs, miRNAs, lncRNAs etc.) for downstream sequencing steps. The NEBNext® Ultra™ II Directional RNA Library Prep Kit for Illumina® was used to generate cDNA libraries of optimal size. Reads were mapped to the reference genome as outlined in the Methods Chapter (**Figure 2.18**).

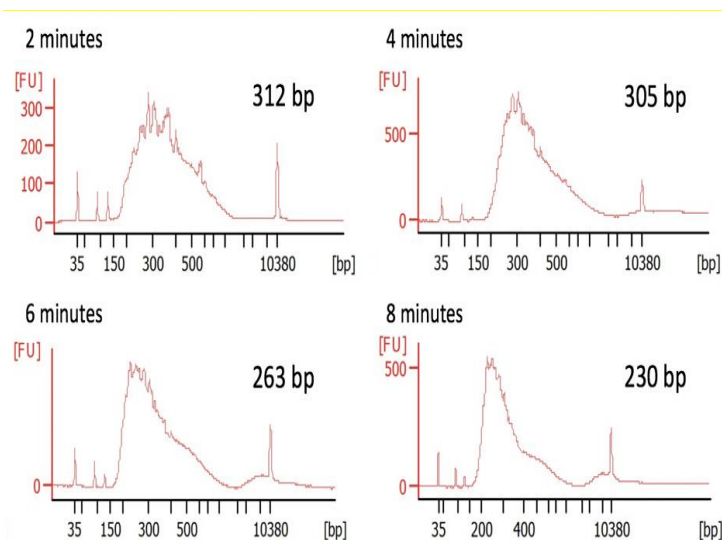


Figure 2. Fragmentation time for peripheral blood RNA.

Total RNA was fragmented for the indicated amount of time. Libraries were made with the resulting fragmented RNA and the peak size was determined by running on a Bioanalyzer. The peak size for each product is indicated in base pairs. The optimal peak size for library preparation for the Illumina platform is approximately 280 - 300 bp. Fragmentation time is based on the RIN values.

S3. Sequencing on HiSeq 4000 flow cells in Chapter 5

Following DNA validation, the libraries were diluted and normalised to 10 nM with 10 mM Tris-Cl with 0.1% Tween, pooled together, and clustered on the cBot 2 (Illumina) following the manufacturer's recommendations. Each cluster of dsDNA bridges was denatured, and the reverse strand was removed by specific base cleavage, leaving the forward DNA strand. The 3' ends of the DNA strands and flow cell-bound oligonucleotides were blocked to prevent interference with the sequencing reaction. The sequencing primer was hybridised to the complementary sequence on the Illumina adapter on the unbound ends of the templates in the clusters. The flow cell now contains >300 million (M) clusters with ~1,000 molecules/cluster and is ready for sequencing. Each whole flow cell has a capacity for 2.5 billion (B) reads (technically, this is pairs of reads: a read is the number of times each cluster is sequenced for the number of bases). The pool was then sequenced across multiple lanes, using a 75-base paired-end (2x75bp PE) dual index read format on the Illumina® HiSeq4000 according to the manufacturer's instructions. The HiSeq4000 flow cells have 8 lanes. Therefore, we calculated the number of reads/lanes as $2.5 \text{ B}/8 = \sim 310 \text{ M}$. So, as we calculated earlier for 36 samples at 40 M reads per sample i.e., $36 \times 40 \text{ M} = 1440 \text{ M}$. Accordingly, the number of lanes needed to give the required number of reads was $1440/310 = \sim 4.5$ lanes.

To conform to ENCODE guidelines, libraries were sequenced to have greater than 40 M mapped reads.

(encodeproject.org/documents/cede0cbe-d324-4ce7-ace4-f0c3eddf5972).

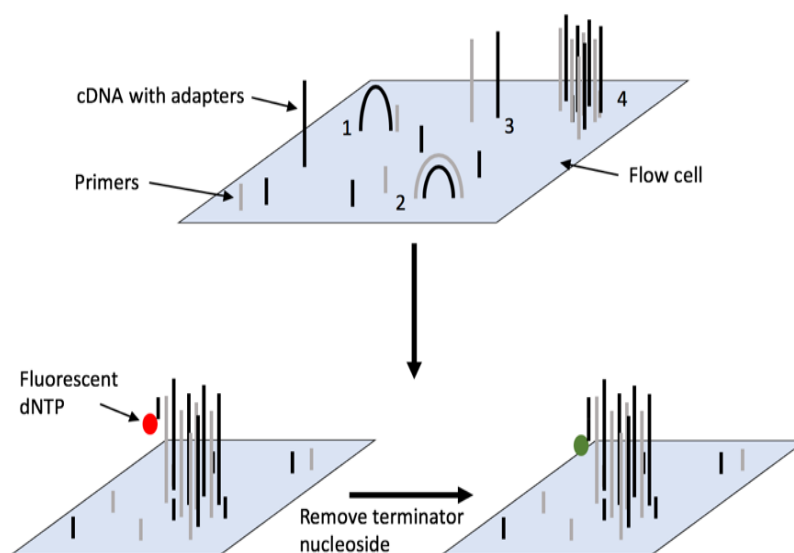


Figure 3. Illumina HiSeq 4000 sequencing chemistry.

The cDNA sequence is determined by a strategy termed 'reversible terminator sequencing'. The flow cell contains primers that are complementary to the adapters ligated to the cDNA library (1). Each fragment is then copied by bridge amplification (2). Clusters formed of thousands of copies of each fragment are made by rounds of amplification (4). Fluorescently labeled 'terminator' dNTPs are added to determine the sequence. The 3' end of the dNTPs is blocked to prevent extension and to allow imaging of the fluorescence. The sequencing proceeds by removing the blocked 3' end and fluorescent label. The next dNTP can then be incorporated, and the cycle continues to obtain the full sequence.

S4. Sequencing on HiSeq 6000 flow cells in Chapter 7

The library pool was sequenced on one lane of an S1 (200 cycles) flow cell using XP workflow for a 2x100bp PE dual index format on the NovaSeq6000 sequencing system (illumina®) according to the manufacturer's instructions. Each sample was generated and barcoded before sequencing.

XP Kit Reagents include: DPX1, DPX2, and DPX3 are Ex Amplifier (Amp) reagents provided in individual tubes for the NovaSeq Xp workflow as provided in (NovaSeq 6000 S1 Reagent Kit). Combining these reagents creates the ExAmp master mix that is mixed with library pools before loading onto the flow cell. The S1 flow cell generates up to 1.6 billion single reads that pass through the filter with an output of up to 333 gigabases (Gb) (according to NovaSeq specifications web page) at 2 x 100 bp. The S1 NovaSeq 6000 flow cells have 2 lanes. 24 samples have gained approximately 50 million reads per sample. The flow cell is a glass-based substrate containing billions of nano-wells in an ordered arrangement, which increases the number of outputs reads and sequencing data. Clusters are generated in the nano-wells, from which sequencing is then performed according to the manufacturer's instructions.

To generate fastq files for each sample, the run data undergoes a step of demultiplexing. Following a successful basic QC check of reads and subsets mapping to a reference genome, packaging of fastq data and QC outputs into web pages was then passed for bioinformatic analysis.

Table 18. The top 53 significant DEG of PNLA treated/LPS-stimulated PBMCs Vs LPS stimulated PBMCs of HCs.

| Ensemble/Gene ID | geneName | geneBiotype | log2FoldChang | pvalue | padj |
|------------------|------------|----------------|---------------|-------------|------------|
| ENSG00000004799 | PDK4 | protein_coding | 3.553538697 | 4.56E-09 | 0.00011829 |
| ENSG00000165685 | TMEM52B | protein_coding | 3.179882889 | 2.49E-06 | 0.02436451 |
| ENSG00000187185 | AC092118.1 | lncRNA | 3.249576637 | 4.51E-06 | 0.02436451 |
| ENSG00000110090 | CPT1A | protein_coding | 1.601688728 | 4.64E-06 | 0.02436451 |
| ENSG00000106366 | SERPINE1 | protein_coding | 2.603487012 | 4.69E-06 | 0.02436451 |
| ENSG00000267615 | AC087289.4 | lncRNA | 2.314995165 | 5.77E-06 | 0.02496533 |
| ENSG00000140749 | IGSF6 | protein_coding | 2.022034543 | 1.25E-05 | 0.04114094 |
| ENSG00000187134 | AKR1C1 | protein_coding | 3.055892836 | 1.26827E-05 | 0.04114094 |
| ENSG00000265743 | AC138207.5 | lncRNA | 2.494511804 | 1.71378E-05 | 0.04941588 |
| ENSG00000182612 | TSPAN10 | protein_coding | 2.229570032 | 2.57E-05 | 0.06675355 |
| ENSG00000232118 | BACH1-AS1 | lncRNA | 2.412601378 | 3.42E-05 | 0.07375349 |
| ENSG00000279339 | AC100788.2 | TEC | 2.19266831 | 3.49E-05 | 0.07375349 |
| ENSG00000287040 | AL590560.5 | lncRNA | 3.402074439 | 3.74E-05 | 0.07375349 |
| ENSG00000270760 | AD001527.1 | lncRNA | 2.421463404 | 4.09E-05 | 0.07375349 |
| ENSG00000212232 | SNORD17 | snoRNA | 2.884309097 | 5.02E-05 | 0.07375349 |
| ENSG00000279757 | AC132068.1 | TEC | 3.691415032 | 5.97E-05 | 0.07375349 |

| | | | | | |
|-----------------|------------|----------------|--------------|-------------|------------|
| ENSG00000187904 | AC097382.1 | lncRNA | 2.250806366 | 6.00E-05 | 0.07375349 |
| ENSG00000159403 | C1R | protein_coding | -1.252011503 | 6.23E-05 | 0.07375349 |
| ENSG00000266710 | RN7SL48P | misc_RNA | 3.367638389 | 6.29E-05 | 0.07375349 |
| ENSG00000287496 | AC093227.3 | lncRNA | 1.838895112 | 6.35E-05 | 0.07375349 |
| ENSG00000270072 | AC090559.2 | lncRNA | 2.186813396 | 6.52E-05 | 0.07375349 |
| ENSG00000203437 | AC022080.1 | pseudogene | 3.258111504 | 6.73E-05 | 0.07375349 |
| ENSG00000276672 | AL161891.1 | lncRNA | 1.70990702 | 6.79E-05 | 0.07375349 |
| ENSG00000185432 | METTL7A | protein_coding | 2.140616723 | 7.00E-05 | 0.07375349 |
| ENSG00000258323 | AC073575.1 | lncRNA | 1.937209125 | 7.26E-05 | 0.07375349 |
| ENSG00000259402 | AC090515.5 | lncRNA | 2.471416504 | 7.65E-05 | 0.07375349 |
| ENSG00000281162 | LINC01127 | lncRNA | 3.101372917 | 7.67E-05 | 0.07375349 |
| ENSG00000280474 | AL356481.2 | lncRNA | 2.283038451 | 8.67E-05 | 0.07765848 |
| ENSG00000251656 | PRELID3BP5 | pseudogene | 2.88041747 | 8.68E-05 | 0.07765848 |
| ENSG00000259735 | AC092868.2 | lncRNA | 1.975346703 | 9.69E-05 | 0.08383187 |
| ENSG00000240015 | AC084024.1 | lncRNA | 2.251250734 | 0.000104351 | 0.08735495 |
| ENSG00000211459 | MT-RNR1 | Mt_rRNA | 2.356832745 | 0.000107717 | 0.08735495 |
| ENSG00000284642 | AL139424.2 | lncRNA | 2.252434637 | 0.000114171 | 0.08978335 |
| ENSG00000271717 | AC022146.2 | lncRNA | 2.104051183 | 0.000117975 | 0.09004633 |
| ENSG00000223799 | IL10RB-DT | lncRNA | 1.80981124 | 0.000128382 | 0.09518999 |
| ENSG00000275975 | MetazoaSrp | misc_RNA | 5.007476022 | 0.000128521 | NA |
| ENSG00000258904 | AL157871.5 | lncRNA | 1.592904709 | 0.000142835 | 0.09850421 |
| ENSG00000266651 | AC093484.4 | lncRNA | 1.936761154 | 0.000143217 | 0.09850421 |
| ENSG00000267231 | AC005786.2 | lncRNA | 4.992512571 | 0.000147799 | NA |
| ENSG00000254649 | AP003086.2 | lncRNA | 2.502715514 | 0.000150234 | 0.09850421 |
| ENSG00000279357 | AC007224.2 | TEC | 2.232004958 | 0.00015469 | 0.09850421 |
| ENSG00000285653 | AC006238.2 | lncRNA | 2.356308009 | 0.000160371 | 0.09850421 |
| ENSG00000279549 | AP000437.1 | TEC | 1.984067706 | 0.000160635 | 0.09850421 |
| ENSG00000251194 | AL133330.1 | lncRNA | 1.898807262 | 0.00016183 | 0.09850421 |
| ENSG00000272582 | AL031587.3 | lncRNA | 3.012402676 | 0.000164297 | 0.09850421 |
| ENSG00000143409 | MINDY1 | protein_coding | 1.806990456 | 0.000175421 | 0.09850421 |
| ENSG00000228686 | AL590723.1 | lncRNA | 1.708951711 | 0.000177973 | 0.09850421 |
| ENSG00000204176 | SYT15 | protein_coding | 1.862401522 | 0.000178047 | 0.09850421 |
| ENSG00000274607 | RNU6-866P | snRNA | 2.472050153 | 0.000178625 | 0.09850421 |
| ENSG00000254263 | AC022973.4 | lncRNA | 1.855255495 | 0.000182197 | 0.09850421 |
| ENSG00000236352 | AC005220.1 | lncRNA | 3.928522017 | 0.000185119 | NA |
| ENSG00000172000 | ZNF556 | protein_coding | 3.041444608 | 0.000192763 | 0.10059032 |
| ENSG00000267412 | AC092068.2 | lncRNA | 2.657297847 | 0.000193808 | 0.10059032 |

Table 19. The top 57 significant DEG of PNLA treated/ LPS stimulated PBMCs Vs LPS stimulated PBMCs of RA patients.

| Ensembl/GeneID | geneName | geneBiotype | log2FoldChange | pvalue | padj |
|-----------------|------------|----------------|----------------|----------|----------|
| ENSG00000165140 | FBP1 | protein_coding | 3.47737035 | 7.19E-09 | 0.000194 |
| ENSG00000231806 | PCAT7 | lncRNA | 3.44806052 | 8.06E-08 | 0.001086 |
| ENSG00000165795 | NDRG2 | protein_coding | 2.36119863 | 1.93E-06 | 0.017313 |
| ENSG00000004799 | PDK4 | protein_coding | 2.50859968 | 1.11E-05 | 0.074687 |
| ENSG00000259760 | AC015660.2 | lncRNA | 2.62256257 | 1.66E-05 | 0.07503 |
| ENSG00000259590 | LINC02244 | lncRNA | 2.57390279 | 1.67E-05 | 0.07503 |
| ENSG00000137507 | LRRC32 | protein_coding | 2.02082328 | 2.73E-05 | 0.086568 |
| ENSG00000134013 | LOXL2 | protein_coding | 1.12609515 | 2.75E-05 | 0.086568 |
| ENSG00000177675 | CD163L1 | protein_coding | -1.77973489 | 3.09E-05 | 0.086568 |
| ENSG00000150764 | DIXDC1 | protein_coding | 1.42658761 | 3.21E-05 | 0.086568 |
| ENSG00000103888 | CEMIP | protein_coding | -1.78059377 | 4.29E-05 | 0.098593 |
| ENSG00000169248 | CXCL11 | protein_coding | -3.13227681 | 4.39E-05 | 0.098593 |

Supplementary

| | | | | | |
|-----------------|------------|----------------|-------------|----------|----------|
| ENSG00000260314 | MRC1 | protein_coding | 2.61252454 | 8.73E-05 | 0.162608 |
| ENSG00000090659 | CD209 | protein_coding | 1.47798017 | 8.75E-05 | 0.162608 |
| ENSG00000145555 | MYO10 | protein_coding | -1.84537386 | 9.52E-05 | 0.162608 |
| ENSG00000184371 | CSF1 | protein_coding | 1.87487851 | 9.66E-05 | 0.162608 |
| ENSG00000115590 | IL1R2 | protein_coding | 2.65594184 | 0.000108 | 0.170549 |
| ENSG00000102575 | ACP5 | protein_coding | 1.45257106 | 0.000127 | 0.190727 |
| ENSG00000246214 | AC024588.1 | lncRNA | -1.03942441 | 0.000151 | 0.213982 |
| ENSG00000173698 | ADGRG2 | protein_coding | 1.36045784 | 0.00021 | 0.282519 |
| ENSG00000072778 | ACADVL | protein_coding | 0.77703044 | 0.000304 | 0.390278 |
| ENSG00000136379 | ABHD17C | protein_coding | -1.33233985 | 0.000392 | 0.479752 |
| ENSG00000177575 | CD163 | protein_coding | -1.77942583 | 0.00041 | 0.480402 |
| ENSG00000099377 | HSD3B7 | protein_coding | 1.18540251 | 0.000429 | 0.481199 |
| ENSG00000135902 | CHRND | protein_coding | 0.9496019 | 0.000456 | 0.491474 |
| ENSG00000085265 | FCN1 | protein_coding | 1.89328474 | 0.00051 | 0.521097 |
| ENSG00000224596 | ZMIZ1-AS1 | lncRNA | 1.15903636 | 0.000522 | 0.521097 |
| ENSG00000131435 | PDLIM4 | protein_coding | 2.42266995 | 0.000579 | 0.556449 |
| ENSG00000279196 | AC135048.4 | TEC | 1.1046554 | 0.000628 | 0.583494 |
| ENSG00000179636 | TPPP2 | protein_coding | 2.37472391 | 0.000674 | 0.60519 |
| ENSG00000174502 | SLC26A9 | protein_coding | -2.43602337 | 0.000755 | 0.655618 |
| ENSG00000284122 | MIR6717 | miRNA | 2.71141062 | 0.000803 | 0.675838 |
| ENSG00000277744 | AC011462.4 | lncRNA | 0.9984548 | 0.000912 | 0.723852 |
| ENSG00000131370 | SH3BP5 | protein_coding | 0.65699818 | 0.000914 | 0.723852 |
| ENSG00000259546 | AC027808.1 | lncRNA | -1.19308531 | 0.000976 | 0.741587 |
| ENSG00000162337 | LRP5 | protein_coding | -1.08687639 | 0.000991 | 0.741587 |
| ENSG00000240993 | RN7SL459P | misc_RNA | -3.80053008 | 0.001024 | NA |
| ENSG00000104635 | SLC39A14 | protein_coding | -0.89364012 | 0.00106 | 0.754821 |
| ENSG00000166145 | SPINT1 | protein_coding | 1.4012234 | 0.001065 | 0.754821 |
| ENSG00000258604 | AL161668.4 | lncRNA | 2.41708776 | 0.001273 | 0.857721 |
| ENSG00000231170 | AC002451.1 | lncRNA | 2.12125909 | 0.001274 | 0.857721 |
| ENSG00000121057 | AKAP1 | protein_coding | 0.40701494 | 0.00137 | 0.899685 |
| ENSG00000270813 | NANOGNBP3 | pseudogene | 3.2680832 | 0.001504 | NA |
| ENSG00000235637 | AC069023.1 | lncRNA | 3.69376568 | 0.001534 | NA |
| ENSG00000270069 | MIR222HG | lncRNA | 0.75274445 | 0.001541 | 0.980489 |
| ENSG00000236304 | AP001189.1 | lncRNA | 1.68935656 | 0.001565 | 0.980489 |
| ENSG00000155846 | PPARGC1B | protein_coding | 0.98101589 | 0.001666 | 0.995084 |
| ENSG00000239856 | RN7SL225P | misc_RNA | -1.83725414 | 0.001686 | 0.995084 |
| ENSG00000183019 | MCEMP1 | protein_coding | 1.68058224 | 0.0017 | 0.995084 |
| ENSG00000111452 | ADGRD1 | protein_coding | 1.84799484 | 0.001795 | 0.999957 |
| ENSG00000120162 | MOB3B | protein_coding | 1.00016384 | 0.001858 | 0.999957 |
| ENSG00000164935 | DCSTAMP | protein_coding | 2.59267864 | 0.001876 | 0.999957 |
| ENSG00000283419 | MIR6874 | miRNA | -1.74120509 | 0.00193 | 0.999957 |
| ENSG00000130558 | OLFM1 | protein_coding | 2.17314158 | 0.001985 | 0.999957 |
| ENSG00000283920 | MIR6743 | miRNA | 0.86673416 | 0.001998 | 0.999957 |

CD14⁺ monocyte percentages were reduced following PNLA treatment.

The level of activated monocytic cells can be used as an indirect marker of an individual's inflammatory status. LPS significantly downregulated CD16 expression such that the monocyte subset could not be identified. Hence, analyses focused on CD14⁺ monocytes.

PNLA reduced percentages of activated CD14⁺ monocytes. Representative **Figure 4** NovoExpress flow cytometry software was used to determine the gates and the gating strategy, showing the percentage of CD14⁺ monocytes, which was significantly reduced following PNLA treatment. Vehicle versus LPS stimulated monocytes was 76.37 ± 3.45 ($p=0.04$), while PNLA treated versus LPS stimulation were $61.37 \pm 5.92\%$ and $58.59 \pm 8.70\%$ for 25 and 50 μM PNLA respectively ($p=0.001$) (**Figure 5**) and (**Table 20**).

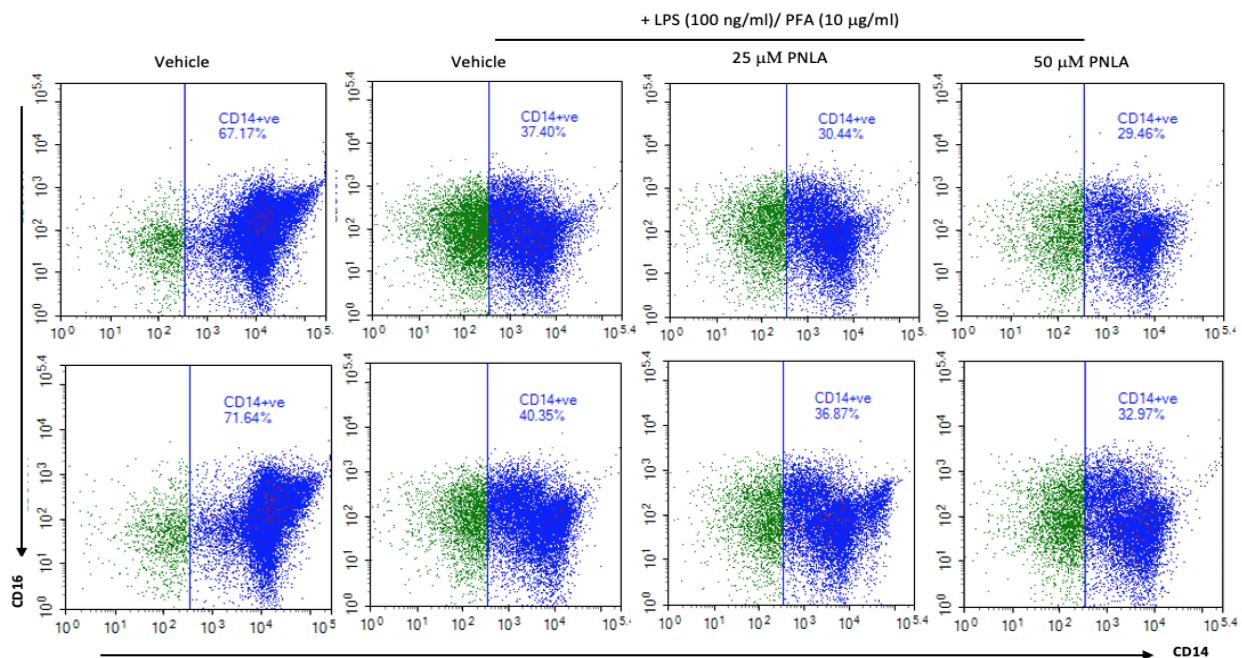


Figure 4. Percentages of CD14⁺ monocytes were determined following PNLA treatment by flow cytometry analysis. Representative dot plots of enriched CD14⁺ pan-monocyte populations from PB of RA patients without prior incubation with PNLA; vehicle control; or with 24 hours prior exposure to vehicle or PNLA 25 μM or 50 μM (followed by 9-hour 100 ng/ml LPS and 10 $\mu\text{g/ml}$ PFA). This gating strategy and the represented sample analysis were kindly done by Dr. Graham Bottley in the NoVo Express software. RA (n=19). The analysis gate was set using appropriate control samples.

Table 20. Percentages of CD14+ monocytes in (n=19) RA patients.

| Subject | Vehicle treated subsets (%) | Vehicle +LPS treated subsets (%) | 25 μ M PNLA +LPS treated subsets (%) | 50 μ M PNLA +LPS treated subsets (%) |
|--------------------|-----------------------------|----------------------------------|--|--|
| RA (1) | 61 | 67.5 | 54.1 | 44.55 |
| RA (2) | 90 | 91 | 77 | 69.86 |
| RA (3) | 88 | 76.3 | 66.5 | 70 |
| RA (4) | 91.5 | 80.1 | 75.5 | 70.9 |
| RA (5) | 91.5 | 66.9 | 58 | 55 |
| RA (6) | 85 | 86.1 | 72.5 | 69.8 |
| RA (7) | 76.9 | 70.8 | 76 | 65.3 |
| RA (8) | 56.5 | 70.8 | 72 | 69 |
| RA (19) | 56.5 | 65.1 | 57 | 55 |
| RA (10) | 50.55 | 22.4 | 29 | 27 |
| RA (11) | 62.9 | 65.25 | 57 | 55 |
| RA (12) | 51.35 | 44.95 | 47.3 | 44.75 |
| RA (13) | 92 | 50.48 | 45.6 | 45.6 |
| RA (14) | 62.4 | 29 | 29.7 | 21.95 |
| RA (15) | 78.9 | 46.15 | 34.5 | 38.2 |
| RA (16) | 93 | 75.8 | 69 | 65 |
| RA (17) | 38.35 | 48.9 | 34 | 30 |
| RA (18) | 96.4 | 97 | 97 | 96 |
| RA (19) | 84.1 | 79.1 | 75 | 77.2 |
| Mean | 74.0 (P = N.S) | 66.8 | 58.4 (P = *) | 56.3 (P = ***) |
| Std. Error of Mean | 4.15 | 4.60 | 4.34 | 4.38 |

Each value represents the mean of an experimental duplicate.

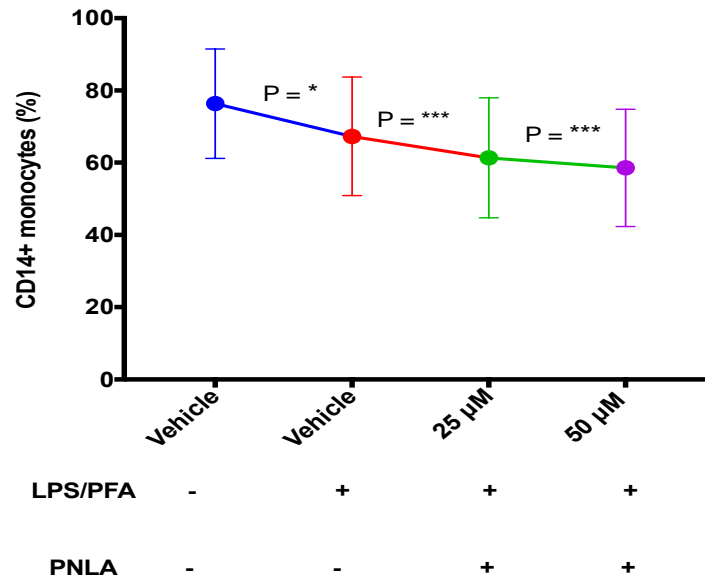


Figure 5. Proportion of CD14⁺ monocytes is reduced following PNLA treatment. Purified monocytes were incubated with 25 or 50 µM PNLA for 24-hours followed by (100 ng/ ml LPS stimulation and 10 µg/ml PFA for 9 hours). Data shown as (the mean +/- SEM) from (n=19) RA patients' samples were done in duplicates. Statistical analysis was performed using one-way ANOVA and Dunn's post-hoc-test in GraphPad Prism V8, where (p-values as illustrated). Monocytes were visualised by LSR Fortessa and analysed at Flowjo software V10.

References

- Abdulrazaq, M., Innes, J.K. and Calder, P.C. (2017). Effect of ω -3 polyunsaturated fatty acids on arthritic pain: A systematic review. *Nutrition* **39** (40):57–66.
- Abhishek, A., Doherty, M., Kuo, C.-F., Mallen, C.D., Zhang, W. and Grainge, M.J. (2017). Rheumatoid arthritis is getting less frequent—results of a nationwide population-based cohort study. *Rheumatology* **56**(5):736–744.
- Abou-Zeid, A., Saad, M. and Soliman, E. (2011). MicroRNA 146a Expression in Rheumatoid Arthritis: Association with Tumor Necrosis Factor-Alpha and Disease Activity. *Genetic Testing and Molecular Biomarkers* **15**(11), 807–812.
- Acosta-Rodriguez, E.V., Napolitani, G., Lanzavecchia, A., and Saluusto, F. (2007). Interleukins 1beta and 6 but not transforming growth factor-beta are essential for the differentiation of interleukin 17- producing human T helper cells. *Nature Immunology*. **8**(9):942–9.
- Adams, O.J., Stanczak, M.A., von Gunten, S. and Läubli, H., (2018). Targeting sialic acid-Siglec interactions to reverse immune suppression in cancer. *Glycobiology*, **28**(9): 640-647
- Addobbati, C., de Azevêdo Silva, J., Tavares, N.A., Monticeli, O., Xavier, R.M., Brenol, J.C.T., Crovella, S., Chies, J.A.B. and Sandrin-Garcia, P., (2016). Ficolin gene polymorphisms in systemic lupus erythematosus and rheumatoid arthritis. *Annals of human genetics*, **80**(1):1–6.
- Aderem, A. and Underhill, D.M., (1999). Mechanisms of phagocytosis in macrophages. *Annual review of immunology*, **17**(1):593-623.
- Agca, R., Heslinga, S.C., Rollefstad, S., Heslinga, M., McInnes, I.B., Peters, M.J.L., Kvien, T.K., Dougados, M., Radner, H., Atzeni, F. and Primdahl, J., (2017). EULAR recommendations for cardiovascular disease risk management in patients with rheumatoid arthritis and other forms of inflammatory joint disorders: 2015/2016 update. *Annals of the rheumatic diseases*, **76**(1):17-28.
- Aiello, R. J., Bourassa, P. A. K., Lindsey, S., Weng, W. F., Natoli, E., Rollins, B. J. and Milos, P. M. (1999). Monocyte chemoattractant protein-1 accelerates atherosclerosis in apolipoprotein E-deficient mice. *Arteriosclerosis Thrombosis and Vascular Biology* **(19)**:1518-1525.
- Alahmadi, A., & Ramji, D. P. (2022). Monitoring modified lipoprotein uptake and macropinocytosis associated with macrophage foam cell formation. In *Atherosclerosis Methods in Molecular Biology*, **2419**: 247-255.
- Alamanos, Y., Voulgari, P.V. and Drosos, A.A. (2006). Incidence and Prevalence of Rheumatoid Arthritis, Based on the 1987 American College of Rheumatology Criteria: A Systematic Review. *Seminars in Arthritis and Rheumatism* **36**(3):182–188.
- Albina JE, Abate JA, Henry WL (1991): Nitric oxide production is required for murine resident peritoneal macrophages to suppress mitogen-stimulated T cell proliferation: role of IFN- γ in the induction of the nitric oxide synthesizing pathway. *Journal Immunology*, **1** (147):140-148.
- Aletaha, D., Neogi, T., Silman, A. J., Funovits, J., Felson, D. T., Bingham III, C. O., ... & Hawker, G. (2010). 2010 rheumatoid arthritis classification criteria: an American College of Rheumatology/European League Against Rheumatism collaborative initiative. *Arthritis and rheumatism*, **62**(9): 2569–2581.
- Alexander Dobin Carrie A. Davis Felix Schlesinger Jorg DrenkowChris Zaleski Sonali Jha Philippe Batut Mark ChaissonThomas R. Gingeras (2013) STAR: ultrafast universal RNA-seq aligner, *Bioinformatics* **29** (1):15–21.
- Alfaddagh, A., Elajami, T.K., Saleh, M., Mohebali, D., Bistran, B.R. and Welty, F.K., (2019). An omega-3 fatty acid plasma index \geq 4% prevents the progression of coronary artery plaque in patients with coronary artery disease on statin treatment. *Atherosclerosis*, **285**:153–162.

References

- Alivernini, S., Peluso, G., Fedele, A.L., Toluoso, B., Gremese, E. and Ferraccioli, G. (2016). Tapering and discontinuation of TNF- α blockers without disease relapse using ultrasonography as a tool to identify patients with rheumatoid arthritis in clinical and histological remission. *Arthritis research and therapy*, **18**(1):39.
- Alonso, M.N., Wong, M.T., Zhang, A.L., Winer, D., Suhoski, M.M., Tolentino, L.L., ... Galel, D.M. (2011). TH1, TH2, and TH17 cells instruct monocytes to differentiate into specialized dendritic cell subsets. *Blood* **118**(12):3311–3320.
- Al-Saeed A. (2011). Gastrointestinal and Cardiovascular Risk of Nonsteroidal Anti-inflammatory Drugs. *Oman medical journal*, **26**(6):385–391.
- Amr, A.R. and Abeer, E.E.K., (2011). Hypolipideimic and hypocholestermic effect of pinenuts in rats fed a high fat, cholesterol-diet. *World Applied Sciences Journal*, **15**(12):1677.
- Ananth, L., Prete, P.E. and Kashyap, M.L. (1993). Apolipoproteins A-I and B and cholesterol in synovial fluid of patients with rheumatoid arthritis. *Metabolism* **42**(7):803–806.
- Andreaskos E, Sacre S, Foxwell BM, Feldmann M. (2005). The toll-like receptor-nuclear factor kappaB pathway in rheumatoid arthritis. *Front Biosci* **10**:2478–88.
- Andres V, Pello OM, Silvestre-Roig C (2012). Macrophage proliferation and apoptosis in atherosclerosis. *Current Opinion. Lipidol.* **23**(5):429–438.
- Andreou, I., Sun, X., Stone, P.H., Edelman, E.R. and Feinberg, M.W., (2015). miRNAs in atherosclerotic plaque initiation, progression, and rupture. *Trends in molecular medicine*, **21**(5):307–318.
- Angata, T., Brinkman-Van der Linden, E.C., (2002). I-type lectins. *Biochimica et Biophysica Acta (BBA) - General Subjects* **1572**(2-3):294–316.
- Angelotti, Francesca, Alice Parma, Giacomo Cafaro, Riccardo Capecchi, Alessia Alunno, and Ilaria Puxeddu. "One year in review (2017): *pathogenesis of rheumatoid arthritis*." *Clin Exp Rheumatol* **35**(3):368–78.
- Anzinger, J. J., Chang, J., Xu, Q., Buono, C., Li, Y., Leyva, F. J., Park, B.-C. *et al.* (2010). Native Low-Density Lipoprotein Uptake by Macrophage Colony-Stimulating Factor-Differentiated Human Macrophages Is Mediated by Macropinocytosis and Micropinocytosis. *Arteriosclerosis Thrombosis and Vascular Biology* **30**:2022–2318.
- Appleby, L.J., Nausch, N., Midzi, N., Mdlulaza, T., Allen, J.E. and Mutapi, F. 2013. Sources of heterogeneity in human monocyte subsets. *Immunology letters* **152**(1):32–41.
- Arend, W.P. and Dayer, J.M., 1990. Cytokines and cytokine inhibitors or antagonists in rheumatoid arthritis. *Arthritis and rheumatism*, **33**(3):305–315.
- Ariza-Ariza, R., Mestanza-Peralta, M. and Cardiel, M.H. (1998). Omega-3 fatty acids in rheumatoid arthritis: an overview. *Seminars in Arthritis and Rheumatism* **27**(6):366–370.
- Arora, S., Rafiq, A. and Jolly, M. (2016). Management of rheumatoid arthritis: Review of current guidelines. *Journal of Arthroscopy and Joint Surgery* **3**(2):45–50.
- Asset, G., Leroy, A., Bauge, E., Wolff, R.L., Fruchart, J.C. and Dallongeville, J., (2000). Effects of dietary maritime pine (*Pinus pinaster*)-seed oil on high-density lipoprotein levels and in vitro cholesterol efflux in mice expressing human apolipoprotein AI. *British Journal of Nutrition*, **84**(3):353–360
- Athanasou N. A. (1995). Synovial macrophages. *Annals of the rheumatic diseases*, **54**(5), 392–394.

References

- Auer J, Bläss M, Schulze-Koops H, Russwurm S, Nagel T, Kalden JR, Röllinghoff M, Beuscher HU. (2007). Expression and regulation of CCL18 in synovial fluid neutrophils of patients with rheumatoid arthritis. *Arthritis Research Therapy* ;**9**(5):R94.
- Auwerx, J. (1991). The human leukemia cell line, thp-1: a multifaceted model for the study of monocyte-macrophage differentiation. *Eperientia* **47**:22–31.
- Avina-Zubieta, J.A., Thomas, J., Sadatsafavi, M., Lehman, A.J. and Lacaille, D. (2012). Risk of incident cardiovascular events in patients with rheumatoid arthritis: a meta-analysis of observational studies. *Annals of the rheumatic diseases* **71**(9):1524–1529.
- Aviña-Zubieta, J.A., Choi, H.K., Sadatsafavi, M., Etminan, M., Esdaile, J.M. and Lacaille, D. (2008). Risk of cardiovascular mortality in patients with rheumatoid arthritis: a meta-analysis of observational studies. *Arthritis Care and Research* **59**(12):1690–1697.
- Baeten, D., Boots, A.M., Steenbakkers, P.G., Elewaut, D., Bos, E., Verheijden, G.F., Verbruggen, G., Miltenburg, A.M., Rijnders, A.W., Veys, E.M. and De Keyser, F., (2000). Human cartilage gp-39+, CD16+ monocytes in peripheral blood and synovium: correlation with joint destruction in rheumatoid arthritis. *Arthritis and Rheumatism: Official Journal of the American College of Rheumatology*, **43**(6):1233–1243.
- Baker EJ, Yusof MH, Yaqoob P, Miles EA, Calder PC. (2018). Omega-3 fatty acids and leukocyte-endothelium adhesion: Novel anti-atherosclerotic actions. *Molecular Aspects of Medicine*.**64**:169–81.
- Baker, E.J., Valenzuela, C.A., De Souza, C.O., Yaqoob, P., Miles, E.A. and Calder, P.C., (2020). Comparative anti-inflammatory effects of plant-and marine-derived omega-3 fatty acids explored in an endothelial cell line. *Biochimica et Biophysica Acta (BBA)-Molecular and Cell Biology of Lipids*, **1865**(6):158662.
- Baker, E.J., Miles, E.A. and Calder, P.C., (2021). A review of the functional effects of pine nut oil, pinolenic acid and its derivative eicosatrienoic acid and their potential health benefits. *Progress in Lipid Research*, **82**- 101097.
- Balestrieri, M.L., Rizzo, M.R., Barbieri, M., Paolisso, P., D’Onofrio, N., Giovane, A., Siniscalchi, M., Minicucci, F., Sardu, C., D’Andrea, D. and Mauro, C., 2015. Sirtuin 6 expression and inflammatory activity in diabetic atherosclerotic plaques: effects of incretin treatment. *Diabetes*, **64**(4):1395–1406.
- Basu, A., Schell, J. and Scofield, R.H. (2018). Dietary fruits and arthritis. *Food & Function* **9**(1):70–77.
- Bax, M., van Heemst, J., Huizinga, T.W. and Toes, R.E. (2011). Genetics of rheumatoid arthritis: what have we learned?. *Immunogenetics*, **63**(8):459–466.
- Bazan J.F., Bacon K.B., Hardiman G., Wang W., Soo K., Rossi D., Greaves D.R., Zlotnik A. and Schall T.J. (1997). A new class of membrane bound chemokine with a CX3C motif. *Nature* 385:640.
- Bazzoni, F., Rossato, M., Fabbri, M., Gaudiosi, D., Mirolo, M., Mori, L., and Locati, M. (2009). Induction and regulatory function of miR-9 in human monocytes and neutrophils exposed to proinflammatory signals. *Proceedings of the National Academy of Sciences*, **106**(13): 5282-5287.
- Bechman, K., Dalrymple, A., Southey-Bassols, C., Cope, A.P. and Galloway, J.B. (2020). A systematic review of CXCL13 as a biomarker of disease and treatment response in rheumatoid arthritis. *BMC rheumatology* **4**(1): 70–70.
- Belge, K.-U., Dayyani, F., Horelt, A., Siedlar, M., Frankenberger, M., Frankenberger, B., ... Ziegler-Heitbrock, L. (2002). The Proinflammatory CD14⁺ CD16⁺ DR⁺⁺ Monocytes Are a Major Source of TNF. *The Journal of Immunology* **168**(7):3536–3542.

References

- Bellinati-Pires R, Waitzberg DL, Salgado MM & Carneiro-Sampaio MM. (1993). Functional alterations of human neutrophils by medium-chain triglyceride emulsions: evaluation of phagocytosis, bacterial killing, and oxidative activity. *Journal of Leukocyte Biology*, **53**:404–410
- Berahovich, R.D., Miao, Z., Wang, Y., Premack, B., Howard, M.C. and Schall, T.J., (2005). Proteolytic activation of alternative CCR1 ligands in inflammation. *The Journal of Immunology*, **174**(11):7341–7351.
- Bernstein, D.L., Jiang, X. and Rom, S. 2021. let-7 microRNAs: Their Role in Cerebral and Cardiovascular Diseases, Inflammation, Cancer, and Their Regulation. *Biomedicines* **9**(6):606.
- Bleier, J.I., Pillarisetty, V.G., Shah, A.B. and DeMatteo, R.P. (2004). Increased and long-term generation of dendritic cells with reduced function from IL-6-deficient bone marrow. *Journal of Immunology*. **172**:7408–7416.
- Bobryshev, Y. V (2006). Monocyte recruitment and foam cell formation in atherosclerosis. *Micron* **37**:208–222.
- Boers M (2007). Studying the benefit/risk ratio of glucocorticoids in rheumatoid arthritis. *The Journal of Rheumatol*; **34**(4): 661-663
- Boers M, Nurmohamed MT, Doelman CJA, Lard LR, Verhoeven AC, Voskuyl, A. E., ... and van der Linden, S. (2003). Influence of glucocorticoids and disease activity on total and high-density lipoprotein cholesterol in patients with rheumatoid arthritis. *Annals of Rheumatic Diseases*; **62**:842–845.
- Boers M, Verhoeven AC, Markusse HM, van de Laar MA, Westhovens R, van Denderen, J. C., ... and van der Linden, S (1997). Randomised comparison of combined step-down prednisolone, methotrexate and sulphasalazine with sulphasalazine alone in early rheumatoid arthritis. *Lancet*; **350** (9074):309–318.
- Bohil AB, Robertson BW, Cheney RE. (2006). Myosin-X is a molecular motor that functions in filopodia formation. *Proceedings of the National Academy of Sciences*, **103**(33):12411–12416.
- Borrell-Pagès, M., Romero, J.C. and Badimon, L., (2015). LRP 5 deficiency down-regulates Wnt signalling and promotes aortic lipid infiltration in hypercholesterolaemic mice. *Journal of cellular and molecular medicine*, **19**(4):70–777.
- Book, C., Saxne, T. and Jacobsson, L.T., (2005). Prediction of mortality in rheumatoid arthritis based on disease activity markers. *The Journal of rheumatology*, **32**(3):430–434.
- Bosshart, H. and Heinzemann, M. (2016). THP-1 cells as a model for human monocytes. *Annals of Translational Medicine* **4** (21):438.
- Bottini, N., Peterson, E. J. Tyrosine phosphatase PTPN22 (2014). Multifunctional regulator of immune signalling, development, and disease. *Annual review of immunology* **32**: 83–119.
- Boyette, L.B., Macedo, C., Hadi, K., Elinoff, B.D., Walters, J.T., Ramaswami, B., ... Metes, D.M. (2017). Phenotype, function, and differentiation potential of human monocyte subsets. *PloS one* **12**(4)e0176460.
- Bowen, K.J., Harris, W.S. and Kris-Etherton, P.M., (2016). Omega-3 fatty acids and cardiovascular disease: are there benefits?. *Current treatment options in cardiovascular medicine*, **18**(11):69.
- Boyle, W.J., Simonet, W.S. and Lacey, D.L. (2003). Osteoclast differentiation and activation. *Nature* **423**(6937):337–342.
- Bradley JR, Johnson DR, Pober JS. (1993). Endothelial activation by hydrogen peroxide. Selective increases of intercellular adhesion molecule-1 and major histocompatibility complex class I. *Am J Pathol* **142**(5):1598–1609.
- Bradley, J.R. (2008). TNF-mediated inflammatory disease. *The Journal of Pathology* **214**(2):149–160.
- Brady, O.A., Martina, J.A. and Puertollano, R. (2018). Emerging roles for TFEB in the immune response and

References

inflammation. *Autophagy* **14**(2):181–189.

Bredt, D.S. and Snyder, S.H. (1994). Nitric oxide: A physiologic messenger molecule. *Annual Review of Biochemistry*. **63**:175–95.

Brennan, E. et al. (2017). Protective Effect of let-7 miRNA Family in Regulating Inflammation in Diabetes-Associated Atherosclerosis. *Diabetes* **66**(8):2266.

Breyer, R.M., Bagdassarian, C.K., Myers, S.A. and Breyer, M.D. (2001). Prostanoid receptors: subtypes and signalling. *Annual review of pharmacology and toxicology* **41**(1):661–690.

Briggs TA, Rice GI, Daly S, et al (2011). Tartrate-resistant acid phosphatase deficiency causes a bone dysplasia with autoimmunity and a type I interferon expression signature. *Nature Genetics*, **43**(2):127–131.

Brunet, A., Sweeney, L.B., Sturgill, J.F., Chua, K.F., Greer, P.L., Lin, Y., Tran, H., Ross, S.E., Mostoslavsky, R., Cohen, H.Y. and Hu, L.S., (2004). Stress-dependent regulation of FOXO transcription factors by the SIRT1 deacetylase. *Science*, **303**(5666):2011–2015.

Brzustewicz, E. and Bryl, E. (2015). The role of cytokines in the pathogenesis of rheumatoid arthritis – Practical and potential application of cytokines as biomarkers and targets of personalized therapy. *Cytokine* **76**(2):527–536.

Buckley, M.L. and Ramji, D.P. (2015). The influence of dysfunctional signalling and lipid homeostasis in mediating the inflammatory responses during atherosclerosis. *Biochim. Biophys. Acta - Molecular of Basis Disease*. **1852**:1498–1510.

Bugatti, S., Vitolo, B., Caporali, R., Montecucco, C. and Manzo, A. (2014). B cells in rheumatoid arthritis: from pathogenic players to disease biomarkers. *BioMed research international* :**2014** (681678–681678).

Bune AJ, Hayman AR, Evans MJ, Cox TM (2001). Mice lacking tartrate-resistant acid phosphatase (Acp 5) have disordered macrophage inflammatory responses and reduced clearance of the pathogen, *Staphylococcus aureus*. *Immunology*, **102**(1):103–113.

Burmester, G.R., Bijlsma, J.W.J., Cutolo, M. and McInnes, I.B. (2017). Managing rheumatic and musculoskeletal diseases past, present and future. *Nature Reviews Rheumatology* **13**:443.

Cai, W., Yu, Y., Zong, S. and Wei, F. (2020). Metabolic reprogramming as a key regulator in the pathogenesis of rheumatoid arthritis. *Inflammation Research*: **69**(11): 1087-1101

Calabresi, E., Petrelli, F., Bonifacio, A., Puxeddu, I. and Alunno, A. (2018). One year in review 2018: pathogenesis of rheumatoid arthritis. *Clinical Experimental Rheumatology* **36**(2):175–184.

Calder, P.C. (1998). Immunoregulatory and anti-inflammatory effects of n-3 polyunsaturated fatty acids. *Brazilian Journal of Medical and Biological Research*, **31**:467– 490.

Calder, P.C. (2015a). Functional Roles of Fatty Acids and Their Effects on Human Health. *Journal of Parenteral and Enteral Nutrition*; **39**(1):18S–32S.

Calder, P.C., (2015b). Marine omega-3 fatty acids and inflammatory processes: effects, mechanisms and clinical relevance. *Biochimica et Biophysica Acta (BBA)-Molecular and Cell Biology of Lipids*, **1851**(4):469-484.

Calder, P.C. and Zurier, R.B. (2001). Polyunsaturated fatty acids and rheumatoid arthritis. *Current Opinion in Clinical Nutrition and Metabolic Care* **4**(2):115-121.

Calder, P.C. (2018). 90th Anniversary Commentary: ω -3 Fatty Acids, Cytokines, and Lymphocyte Proliferation in Young and Older Women. *The Journal of Nutrition* **148**(10):1663–1666.

References

- Cambridge, G., Acharya, J., Cooper, J.A., Edwards, J.C. and Humphries, S.E. (2013). Antibodies to citrullinated peptides and risk of coronary heart disease. *Atherosclerosis* **228**(1):243–246.
- Campbell IK, Wojta J, Novak U, Hamilton JA (1994). Cytokine modulation of plasminogen activator inhibitor-1 (PAI-1) production by human articular cartilage and chondrocytes. Down-regulation by tumor necrosis factor alpha and up-regulation by transforming growth factor-B basic fibroblast growth factor. *Biochim Biophys Acta*, **1226**(3):277–285.
- Campbell, I.K., van Nieuwenhuijze, A., Segura, E., O'Donnell, K., Coghill, E., Hommel, M., ... Wicks, I.P. (2011). Differentiation of inflammatory dendritic cells is mediated by NF- κ B1-dependent GM-CSF production in CD4 T cells. *The Journal of Immunology* **186**(9):5468–5477.
- Cao, C., Lawrence, D.A., Li, Y., Von Arnim, C.A., Herz, J., Su, E.J., Makarova, A., Hyman, B.T., Strickland, D.K. and Zhang, L., (2006). Endocytic receptor LRP together with tPA and PAI-1 coordinates Mac-1-dependent macrophage migration. *The EMBO journal*, **25**(9):1860-1870.
- Cappellari, R., D'Anna, M., Bonora, B.M., Rigato, M., Cignarella, A., Avogaro, A. and Fadini, G.P., 2017. Shift of monocyte subsets along their continuum predicts cardiovascular outcomes. *Atherosclerosis*, **266**:95–102.
- Caputo, M., Zirpoli, H., Torino, G. and Tecce, M.F. (2011) Selective regulation of UGT1A1 and SREBP-1c mRNA expression by docosahex- aenoic, eicosapentaenoic, and arachidonic acids. *Journal of Cell Physiology*, **226**:187–193
- Carbone, F., Bonaventura, A., Liberale, L., Paolino, S., Torre, F., Dallegri, F. Cutolo, M. (2018). Atherosclerosis in Rheumatoid Arthritis: Promoters and Opponents. *Clinical Reviews in Allergy and Immunology*, **58**(1): 1-14
- Carette S. (2007) All patients with rheumatoid arthritis should receive corticosteroids as part of their management. *Journal of Rheumatology*, **34**:656–60.
- Carlin, L.M., Stamatiades, E.G., Auffray, C., Hanna, R.N., Glover, L., Vizcay-Barrena, G., Hedrick, C.C., Cook, H.T., Diebold, S. and Geissmann, F., (2013). Nr4a1-dependent Ly6Clow monocytes monitor endothelial cells and orchestrate their disposal. *Cell*, **153**(2):362–375.
- Carman, C.V. (2009), Mechanisms for transcellular diapedesis: probing and pathfinding by 'invadosome-like protrusions'. *Journal of cell sciences*. **122**(17):3025–35.
- Carrillo-Galvez, A.B., Cobo, M., Cuevas-Ocaña, S., Gutiérrez-Guerrero, A., Sánchez-Gilabert, A., Bongarzone, P., García-Pérez, A., Muñoz, P., Benabdellah, K., Toscano, M.G. and Martín, F., (2015). Mesenchymal Stromal Cells Express GARP/LRRC 32 on Their Surface: Effects on Their Biology and Immunomodulatory Capacity. *Stem cells*, **33**(1):183–195.
- Carswell, E.A., Old, L.J., Kassel, R., Green, S., Fiore, N. and Williamson, B. (1975). An endotoxin-induced serum factor that causes necrosis of tumors. *Proceedings of the National Academy of Sciences*, **72**(9):3666–3670.
- Catrina, A.I., Joshua, V., Klareskog, L. and Malmström, V. (2016). Mechanisms involved in triggering rheumatoid arthritis. *Immunological Reviews* **269**(1):162–174.
- Causey, J.L. Korean pine nut fatty acids induce satiety-producing hormone release in overweight human volunteers. *The 231st American Chemical Society National Meeting and Exposition*, **26**(30)
- Cerinic, M.M., Generini, S., Partsch, G., Pignone, A., Dini, G., Konttinen, Y.T. and Del Rosso, M. (1998). Synoviocytes from osteoarthritis and rheumatoid arthritis produce plasminogen activators and plasminogen activator inhibitor-1 and display u-PA receptors on their surface. *Life Sciences*, **63**(6):441–453.
- Cesari, M., Penninx, B.W., Newman, A.B., Kritchevsky, S.B., Nicklas, B.J., Sutton-Tyrrell, K., Tracy, R.P., Rubin, S.M., Harris, T.B. and Pahor, M., (2003). Inflammatory markers and cardiovascular disease (the health, aging and body composition [health ABC] study). *The American journal of cardiology*, **92**(5):522-528.

References

- Chan, F.K.-M., Moriwaki, K. and De Rosa, M.J. (2013). Detection of necrosis by release of lactate dehydrogenase activity. *Methods in Molecular biology*, **979**:65–70.
- Chara, L., Sánchez-Atrio, A., Pérez, A., Cuende, E., Albarrán, F., Turrión, A., ... Monserrat, J. (2015). The number of circulating monocytes as biomarkers of the clinical response to methotrexate in untreated patients with rheumatoid arthritis. *Journal of translational medicine* **13**(1):2.
- Chattopadhyaya R., D. Pathak and D.P. Jindal, Antihyperlipidemic agents. (1996). *A review. Indian Drugs*, **33**:85-98.
- Chen KG, Szakács G, Annereau JP, Rouzaud, F, Liang, X. J, Valencia, J. C, ... and Gottesman, M. M (2005). Principal expression of two mRNA isoforms (ABCB 5alpha and ABCB 5beta) of the ATP-binding cassette transporter gene ABCB 5 in melanoma cells and melanocytes. *Pigment Cell Res*, **18**(2):102–112.
- Chen S-J, Chuang L-T, Liao J-S, Huang W-C, Lin H-H (2015). Phospholipid incorporation of non-methylene-interrupted fatty acids (NMIFA) in murine microglial BV-2 cells reduces pro-inflammatory mediator production. *Inflammation*, **38** (6):2133–45.
- Chen, C.J., Kono, H., Golenbock, D., Reed, G., Akira, S. and Rock, K.L., (2007). Identification of a key pathway required for the sterile inflammatory response triggered by dying cells. *Nature medicine*, **13**(7):851-856.
- Chen, J., Cao, J., Fang, L., Liu, B., Zhou, Q., Sun, Y., Wang, Y., *et al.* (2014). Berberine derivatives reduce atherosclerotic plaque size and vulnerability in apoe^{-/-} mice. *Journal of Translational Medicine*. **12**:326.
- Chen, K.-C. and Juo, S.-H.H. (2012). MicroRNAs in atherosclerosis. *The Kaohsiung Journal of Medical Sciences*, **28**(12):631–640.
- Chen, Q., Wang, Q., Zhu, J., Xiao, Q. and Zhang, L. (2017c). Reactive oxygen species: key regulators in vascular health and diseases, *Journal of Pharmacology*. **175**(8), 1279-1292.
- Chen, S. J., Hsu, C.-P., Li, C.-W., Lu, J.-H. and Chuang, L.-T. (2011). Pinolenic acid inhibits human breast cancer MDA-MB-231 cell metastasis in vitro. *Food chemistry* **126**(4):1708–1715.
- Chen, S., Wang, J., Cai, C. and Xie, X. (2020). N-myc Downstream-Regulated Gene 2 (NDRG2) Promotes Bone Morphogenetic Protein 2 (BMP2)-Induced Osteoblastic Differentiation and Calcification by Janus Kinase 3 (JAK3)/Signal Transducer and Activator of Transcription 3 (STAT3) Signalling Pathway. *Medical Science Monitor* **26**. e918541-1.
- Chen, S.J., Huang, W.C., Shen, H.J., Chen, R.Y., Chang, H., Ho, Y.S., Tsai, P.J. and Chuang, L.T., (2020). Investigation of Modulatory Effect of Pinolenic Acid (PNA) on Inflammatory Responses in Human THP-1 Macrophage-Like Cell and Mouse Models. *Inflammation*, **43**(2):518–531.
- Chen, S.J., Kao, Y.H., Jing, L., Chuang, Y.P., Wu, W.L., Liu, S.T., Huang, S.M., Lai, J.H., Ho, L.J., Tsai, M.C. and Lin, C.S., (2017). Epigallocatechin-3-gallate reduces scavenger receptor A expression and foam cell formation in human macrophages. *Journal of agricultural and food chemistry*, **65**(15):3141–3150
- Chen, Y. K., Chen, C. Y., Hu, H. T., & Hsueh, Y. P. (2012). CTTNBP2, but not CTTNBP2NL, regulates dendritic spinogenesis and synaptic distribution of the striatin-PP2A complex. *Molecular biology of the cell*, **23**(22):4383–4392.
- Chistiakov, D.A., Bobryshev, Y.V. and Orekhov, A.N. (2016). Macrophage-mediated cholesterol handling in atherosclerosis. *Journal of cellular and molecular medicine* **20**(1):17–28

References

- Chehade, L., Jaafar, Z.A., El Masri, D., Zmerly, H., Kreidieh, D., Tannir, H., Itani, L. and El Ghoch, M., (2019). Lifestyle Modification in Rheumatoid Arthritis: Dietary and Physical Activity Recommendations Based on Evidence. *Current rheumatology reviews*, **15**(3):209–214.
- Chiba S, Hisamatsu T, Suzuki H, Mori K, Kitazume MT, Shimamura K, Mizuno S, Nakamoto N, Matsuoka K, Naganuma M, Kanai T (2017). Glycolysis regulates LPS-induced cytokine production in M2 polarized human macrophages. *Immunology Letters*, **183**:17–23.
- Cho, S.-M., Lee, E.-O., Kim, S.-H. and Lee, H.-J. (2014). Essential oil of *Pinus koraiensis* inhibits cell proliferation and migration via inhibition of p21-activated kinase 1 pathway in HCT116 colorectal cancer cells. *BMC Complementary and Alternative Medicine* **14**(1): 1-9
- Choi, E.Y., Jin, J.Y., Choi, J.I., Choi, I.S. and Kim, S.J., (2014). DHA suppresses Prevotella intermedia lipopolysaccharide-induced production of proinflammatory mediators in murine macrophages. *British Journal of Nutrition*, **111**(7):1221–1230.
- Chomarat, P., Banchereau, J., Davoust, J. and Palucka, A.K. (2000). IL-6 switches the differentiation of monocytes from dendritic cells to macrophages. *Nature Immunology*. **1**:510–514.
- Choy, E (2012). Understanding the dynamics: pathways involved in the pathogenesis of rheumatoid arthritis, *Rheumatology*, **51** (5):3–11,
- Choy, E. and Dayer, J.-M. (2009). Therapeutic targets in rheumatoid arthritis: the interleukin-6 receptor. *Rheumatology* **49**(1):15–24.
- Choy, E., Ganeshalingam, K., Semb, A.G., Szekanecz, Z. and Nurmohamed, M. (2014). Cardiovascular risk in rheumatoid arthritis: recent advances in the understanding of the pivotal role of inflammation, risk predictors and the impact of treatment. *Rheumatology (Oxford)* **53**(12):2143–2154.
- Christensen, I. E., Lillegraven, S., Mielnik, P., Bakland, G., Loli, L., Sexton, J., Uhlig, T., Kvien, T. K., and Provan, S. A. (2022). Serious infections in patients with rheumatoid arthritis and psoriatic arthritis treated with tumour necrosis factor inhibitors: data from register linkage of the NOR-DMARD study. *Annals of the rheumatic diseases*, **81**(3):398–401.
- Chuang, L.-T., Tsai, P.-J., Lee, C.-L. and Huang, Y.-S. (2009). Uptake and Incorporation of Pinolenic Acid Reduces n-6 Polyunsaturated Fatty Acid and Downstream Prostaglandin Formation in Murine Macrophage. *Lipids* **44**(3):217–224.
- Chung HT, Pae HO, Choi BM, Billiar TR, Kim YM (2001): Nitric oxide as a bioregulator of apoptosis. *Biochemical Biophysical Research Communications*, **282**:1075–1079.
- Chung, E.J. (2016). Targeting and therapeutic peptides in nanomedicine for atherosclerosis. *Experimental Biology and Medicine*. **241**:891–898.
- Chung, M., Kim, J., Choi, Hyo-Kyoung, Choi, Hee-Don, Noh, S.K. and Kim, B.H. (2019). A Structured Pine Nut Oil Has Hypocholesterolemic Activity by Increasing LDLR Gene Expression in the Livers of Obese Mice. *European Journal of Lipid Science and Technology* **121**(6):1900049.
- Clarke, S.D. and Jump, D.B., (1994). Dietary polyunsaturated fatty acid regulation of gene transcription. *Annual review of nutrition*, **14**(1):83-98.
- Cleland, L.G., James, M.J. and Proudman, S.M., (2005). Fish oil: what the prescriber needs to know. *Arthritis research and therapy*, **8**(1):1-9.
- Cohen, S.B., Emery, P., Greenwald, M.W., Dougados, M., Furie, R.A., Genovese, M.C., ... Totoritis, M.C. (2006). Rituximab for rheumatoid arthritis refractory to anti-tumor necrosis factor therapy: Results of a multicentre,

References

randomized, double-blind, placebo-controlled, phase III trial evaluating primary efficacy and safety at twenty-four weeks. *Arthritis and Rheumatism* **54**(9):2793–2806.

Cohen, Stanley, Mark C. Genovese, Ernest Choy, Fernando Perez-Ruiz, Alan Matsumoto, Karel Pavelka, Jose L. Pablos et al (2017). "Efficacy and safety of the biosimilar ABP 501 compared with adalimumab in patients with moderate to severe rheumatoid arthritis: a randomised, double-blind, phase III equivalence study." *Annals of the rheumatic diseases* **76**(10):1679–1687.

Coleman, R.A., Smith, W.L. and Narumiya, S. (1994). International Union of Pharmacology classification of prostanoid receptors: properties, distribution, and structure of the receptors and their subtypes. *Pharmacological reviews* **46**(2):205–229.

Collison, J. (2019). Origins of synovial macrophages revealed. *Nature Reviews Rheumatology* **15**(8):451–451

Conesa, A., Madrigal, P., Tarazona, S., Gomez-Cabrero, D., Cervera, A., McPherson, A., Szczesniak, M.W., Gaffney, D.J., Elo, L.L., Zhang, X. and Mortazavi, A., (2016). A survey of best practices for RNA-seq data analysis. *Genome biology*, **17**(1):1-19.

Connolly, D., Fitzpatrick, C., O'Toole, L., Doran, M. and O'Shea, F. (2015). Impact of Fatigue in Rheumatic Diseases in the Work Environment: A Qualitative Study. *International journal of environmental research and public health* **12**(11):13807–13822.

Cooper, D.L., Martin, S.G., Robinson, J.I., Mackie, S.L., Charles, C.J., Nam, J., ... Morgan, A.W. (2012). FcγRIIIa Expression on Monocytes in Rheumatoid Arthritis: Role in Immune-Complex Stimulated TNF-α Production and Non-Response to Methotrexate Therapy. *PLOS ONE* **7**(1):e28918.

Costa-Rosa LFBP., Curi R, Bond JA., Newsholme P., Newsholme EA. (1995). Propionate modifies lipid biosynthesis in rat peritoneal macrophages. *General Pharmacology*, **26**:411-416.

Cowart, L.A., Wei, S., Hsu, M.H., Johnson, E.F., Krishna, M.U., Falck, J.R. and Capdevila, J.H., (2002). The CYP4A isoforms hydroxylate epoxyeicosatrienoic acids to form high affinity peroxisome proliferator-activated receptor ligands. *Journal of Biological Chemistry*, **277**(38):35105–35112.

Crandall, D.L., Groeling, T.M., Busler, D.E. and Antrilli, T.M., (2000). Release of PAI-1 by human preadipocytes and adipocytes independent of insulin and IGF-1. *Biochemical and biophysical research communications*, **279**(3):984-988.

Cros, J., Cagnard, N., Woollard, K., Patey, N., Zhang, S.-Y., Senechal, B., ... Geissmann, F. (2010). Human CD14^{dim} Monocytes Patrol and Sense Nucleic Acids and Viruses via TLR7 and TLR8 Receptors. *Immunity* **33**(3):375–386.

Cross, M., Smith, E., Hoy, D., Carmona, L., Wolfe, F., Vos, T. March, L. (2014). The global burden of rheumatoid arthritis estimates from the Global Burden of Disease 2010 study. *Annals of the Rheumatic Diseases* **73**(7):1316.

Curtis CL, Hughes CE, Flannery CR, et al (2000). n-3 Fatty acids specifically modulate catabolic factors involved in articular cartilage degradation. *Journal of Biological Chemistry*; **275**:721-724.

Cutolo, M. and Nikiphorou, E. (2018). Don't neglect nutrition in rheumatoid arthritis! *RMD open* **4**(1):e000591.

Cuzzocrea, S., Chatterjee, P. K., Mazzon, E., McDonald, M. C., Dugo, L., Di Paola, R., ... Thiemermann, C. (2002). Beneficial effects of GW274150, a novel, potent and selective inhibitor of iNOS activity, in a rodent model of collagen-induced arthritis. *European Journal of Pharmacology*, **453**:119–129.

Curi R, Bond JA, Calder PC and Newsholme EA (1993). Propionate regulates lymphocyte proliferation and metabolism. *General Pharmacology*, **24**:591-597.

References

- Crilly, A., Burns, E., Nickdel, M.B., Lockhart, J.C., Perry, M.E., Ferrell, P.W., Baxter, D., Dale, J., Dunning, L., Wilson, H. and Nijjar, J.S., (2012). PAR2 expression in peripheral blood monocytes of patients with rheumatoid arthritis. *Annals of the rheumatic diseases*, **71**(6):1049-1054
- Combes, T.W., Orsenigo, F., Stewart, A., Mendis, A.J.R., Dunn-Walters, D., Gordon, S. and Martinez, F.O., (2021). CSF1R defines the mononuclear phagocyte system lineage in human blood in health and COVID-19. *Immunotherapy Advances*, **1**(1):003.
- Chung, S., Yao, H., Caito, S., Hwang, J.W., Arunachalam, G. and Rahman, I. (2010). Regulation of SIRT1 in cellular functions: role of polyphenols. *Archives of biochemistry and biophysics*, **501**(1):79-90.
- Clayton SA, MacDonald L, Kurowska-Stolarska M, Clark AR. (2021) Mitochondria as Key Players in the Pathogenesis and Treatment of Rheumatoid Arthritis. *Frontier Immunology*. **29**(12):673916.
- Darlington, L.G. and Stone, T.W. (2001). Antioxidants and fatty acids in the amelioration of rheumatoid arthritis and related disorders. *British Journal of Nutrition* **85**(3):251–269.
- Dlamini, Z., Ntlabati, P., Mbita, Z. and Shoba-Zikhali, L. (2015). Pyruvate dehydrogenase kinase 4 (PDK4) could be involved in a regulatory role in apoptosis and a link between apoptosis and insulin resistance. *Experimental and Molecular Pathology* **98**(3):574–584.
- Davignon, J.-L., Hayder, M., Baron, M., Boyer, J.-F., Constantin, A., Apparailly, F., ... Cantagrel, A. (2012). Targeting monocytes/macrophages in the treatment of rheumatoid arthritis. *Rheumatology* **52**(4):590–598.
- Dayer, J.-M., Oliviero, F. and Punzi, L. (2017). A Brief History of IL-1 and IL-1 Ra in Rheumatology. *Frontiers in pharmacology* **8**:293–293.
- Dawczynski, C., Schubert, R., Hein, G., Müller, A., Eidner, T., Vogelsang, H., Basu, S. and Jahreis, G., (2009). Long-term moderate intervention with n-3 long-chain PUFA-supplemented dairy products: effects on pathophysiological biomarkers in patients with rheumatoid arthritis. *British journal of nutrition*, **101**(10):1517-1526.
- De Caterina R, Cybulsky MI, Clinton SK, Gimbrone MA, Jr., Libby P (1994). The omega-3 fatty acid docosahexaenoate reduces cytokine-induced expression of proatherogenic and proinflammatory proteins in human endothelial cells. *Arteriosclerosis and Thrombosis*; **14** (11):1829–36.
- Deane, K.D., Demoruelle, M.K., Kelmenson, L.B., Kuhn, K.A., Norris, J.M. and Holers, V.M. (2017). Genetic and environmental risk factors for rheumatoid arthritis. *Best practice and research. Clinical rheumatology* **31**(1):3–18.
- de Gregorio, E., Colell, A., Morales, A. and Mari, M., (2020). Relevance of SIRT1-NF- κ B axis as therapeutic target to ameliorate inflammation in liver disease. *International Journal of Molecular Sciences*, **21**(11):3858.
- Degen, L., Matzinger, D., Drewe, J. and Beglinger, C., (2001). The effect of cholecystokinin in controlling appetite and food intake in humans. *Peptides*, **22**(8):1265–1269.
- DeLuca P, Rossetti RG, Alavian C, *et al* (1999). Effects of gammalinolenic acid on interleukin-1 beta and tumor necrosis factor-alpha secretion by stimulated human peripheral blood monocytes: *studies in vitro and in vivo*. *Journal of Medical Investigation*; **47**:246–250.
- Devaraj S, Singh U, Jialal I (2009). The evolving role of C-reactive protein in atherothrombosis. *Clinical Chemistry*. **55**(2):229–38.
- de Pablo P, Romaguera D, Fisk HL, Calder PC, Quirke AM, Cartwright AJ, Panico S, Mattiello A, Gavrila D, Navarro C, Sacerdote C, Vineis P, Tumino R, Ollier WE, Michaud DS, Riboli E, Venables PJ, Fisher BA (2018). High erythrocyte levels of the n-6 polyunsaturated fatty acid linoleic acid are associated with lower risk of subsequent

References

- rheumatoid arthritis in a southern European nested case-control study. *Annals of Rheumatic Diseases*. **77**(7):981–987.
- de Roos, B., Mavrommatis, Y., and Brouwer, I. A. (2009). Long-chain n-3 polyunsaturated fatty acids: new insights into mechanisms relating to inflammation and coronary heart disease. *British journal of pharmacology*, **158**(2), 413–428.
- Deng, Y., Huang, X., Wu, H., Zhao, M., Lu, Q., Israeli, E., Dahan, S., Blank, M. and Shoenfeld, Y., (2016). Some like it hot: the emerging role of spicy food (capsaicin) in autoimmune diseases. *Autoimmunity reviews*, **15**(5):451–456.
- Deroyer, C., Charlier, E., Neuville, S., Malaise, O., Gillet, P., Kurth, W., Chariot, A., Malaise, M. and de Seny, D., (2019). CEMIP (KIAA1199) induces a fibrosis-like process in osteoarthritic chondrocytes. *Cell death and disease*, **10**(2):1–17.
- Drexler, S.K., Kong, P., Inglis, J., Williams, R.O., Garlanda, C., Mantovani, A., ... Foxwell, B.M.J. (2010). SIGIRR/TIR-8 is an inhibitor of toll-like receptor signalling in primary human cells and regulates inflammation in models of rheumatoid arthritis. *Arthritis and Rheumatism* **62**(8):2249–2261.
- del Rincon I, O'Leary DH, Haas RW, Escalante A (2005). Effect of glucocorticoids on the arteries in rheumatoid arthritis. *Erratum appears in arthritis and rheumatism*. **52**(2):678.
- Dieguez-Gonzalez, R., Akar, S., Calaza, M., Gonzalez-Alvaro, I., Fernandez-Gutierrez, B., Lamas, J.R., de la SERNA, A.R., Caliz, R., Blanco, F.J., Pascual-Salcedo, D. and Velloso, M.L., 2009. Lack of association with rheumatoid arthritis of selected polymorphisms in 4 candidate genes: CFH, CD209, eotaxin-3, and MHC2TA. *The Journal of Rheumatology*, **36**(8):1590–1595.
- DiGiovine E.S., Nuki G. and Duff G.W. (1988). Tumor necrosis factor in synovial exudates. *Annals of Rheumatic Diseases*. **47**(9):768-772
- Dinarello, C.A., (2011). Interleukin-1 in the pathogenesis and treatment of inflammatory diseases. *Blood, The Journal of the American Society of Hematology*, **117**(14): 3720–3732.
- Dooper, M.M.B.W., Riel, B.V., Graus, Y.M.F. and M'Rabet, L. (2003). Dihomo- γ -linolenic acid inhibits tumour necrosis factor- α production by human leucocytes independently of cyclooxygenase activity. *Immunology* **110**(3):348–357.
- Doherty, T.M., Seder, R.A. and Sher, A. (1996). Induction and regulation of IL-15 expression in murine macrophages. *The Journal of Immunology* **156**(2):735–741.
- Donas C, et al. (2016) The histone demethylase inhibitor GSK-J4 limits inflammation through the induction of a tolerogenic phenotype on DCs. *J Autoimmun*; **75**:105–117.
- Dugas, B., M. Djavad Mossalayi, C. Damais, and J.P. Kolb. (1995): Nitric oxide production by human monocytes: evidence for a role of CD23. *Immunology Today*. **16**:574–580.
- Duffy, D. and Rader, D.J. (2006). Emerging Therapies Targeting High-Density Lipoprotein Metabolism and Reverse Cholesterol Transport. *Circulation* **113**(8):1140–1150.
- Duthie, P., Hill, A.B. and Osmond-Clarke, M.H., (1960). A comparison of prednisolone with aspirin or other analgesics in the treatment of rheumatoid arthritis. *Annals of rheumatic Disease*, **19**:331.
- Edwards, C. J., Syddall, H., Goswami, R., Goswami, P., Dennison, E. M., Arden, N. K., (2007). Hertfordshire Cohort Study Group. The autoantibody rheumatoid factor may be an independent risk factor for ischaemic heart disease in men. *Heart (British Cardiac Society)*, **93**(10):1263–1267.

References

- Edwards, C.J. (2005). Immunological therapies for rheumatoid arthritis. *British medical bulletin*, **73**(1):71–82
- Elliott, M. J., Maini, R. N., Feldmann, M., Long-Fox, A., Charles, P., Katsikis, P., ... and Woody, J. N. (1993). Treatment of rheumatoid arthritis with chimeric monoclonal antibodies to tumor necrosis factor α . *Arthritis & Rheumatism*, **36**(12):1681–1690.
- Eriksson, J.K., Neovius, M., Ernestam, S., Lindblad, S., Simard, J.F. and Askling, J. (2013). Incidence of Rheumatoid Arthritis in Sweden: A Nationwide Population-Based Assessment of Incidence, Its Determinants, and Treatment Penetration. *Arthritis Care and Research* **65**(6):870–878.
- Engering A, Geijtenbeek TB, van Vliet SJ, Wijers, M, van Liempt, E, Demaurex, N., ... and van Kooyk, Y. (2002). The dendritic cell-specific adhesion receptor DC-SIGN internalizes antigen for presentation to T cells. *Journal of Immunology*. **168**(5):2118–2126.
- Estrada-Capetillo, L., Hernández-Castro, B., Monsiváis-Urenda, A., Alvarez-Quiroga, C., Layseca-Espinosa, E., Abud-Mendoza, C., ... González-Amaro, R. (2013). Induction of Th17 lymphocytes and Treg cells by monocyte-derived dendritic cells in patients with rheumatoid arthritis and systemic lupus erythematosus. *Clinical and Developmental Immunology*.2013:584303.
- Estevão-Silva, C.F., Ames, F.Q., de Souza Silva-Comar, F.M., Kummer, R., Tronco, R.P., Cuman, R.K.N. and Bersani-Amado, C.A., (2016). Fish oil and adjuvant-induced arthritis: inhibitory effect on leukocyte recruitment. *Inflammation*, **39**(1):320–326.
- FAO, 2015. FAOSTAT. *Food and Agriculture Organization of the United Nations*, Rome, Italy.
- Fadok V.A., Bratton D.L., Konowal A., Freed, P.W. Westcott J.Y. and Henson P.M. (1998). Macrophages that have ingested apoptotic cells in vitro inhibit proinflammatory cytokine production through autocrine/paracrine mechanisms involving TGF- β , PGE2, and PAF. *Journal of Clinical Investigation*. **101**:890–898.
- Fahmi, H., Di Battista, J.A., Pelletier, J., Mineau, F., Ranger, P. and Martel-Pelletier, J. (2001). Peroxisome proliferator-activated receptor γ activators inhibit interleukin-1 β -induced nitric oxide and matrix metalloproteinase 13 production in human chondrocytes. *Arthritis and Rheumatism* **44**(3):595–607.
- Farrelt AJ, Blake DR, Palmer RMJ, Moncada S (1992). Increased concentration of nitrite in synovial fluid and serum samples suggest increased nitric oxide synthesis in rheumatic diseases. *Annals of Rheumatic Disease* **51**:1219–1222.
- Farragher, T.M., Goodson, N.J., Naseem, H., Silman, A.J., Thomson, W., Symmons, D. and Barton, A. (2008). Association of the HLA-DRB1 gene with premature death, particularly from cardiovascular disease, in patients with rheumatoid arthritis and inflammatory polyarthritis. *Arthritis and Rheumatism: Official Journal of the American College of Rheumatology* **58**(2):359–369.
- Fattahi, M.J. and Mirshafiey, A. (2012). Prostaglandins and Rheumatoid Arthritis. *Arthritis* 2012-239310:1–7.
- Feldmann, M. and Maini, R.N. (2001). Anti-TNF- α therapy of rheumatoid arthritis: What Have We Learned? *Annual Review of Immunology* **19**(1):163–196.
- Feige, J.N., Lagouge, M., Canto, C., Strehle, A., Houten, S.M., Milne, J.C., Lambert, P.D., Matakis, C., Elliott, P.J. and Auwerx, J., (2008). Specific SIRT1 activation mimics low energy levels and protects against diet-induced metabolic disorders by enhancing fat oxidation. *Cell metabolism*, **8**(5):347–358.
- Ferramosca A, Savy V, Einerh and A W. C., and Zara, V. (2008). Pinus koraiensis seed oil (PinnoThin™) supplementation reduces body weight gain and lipid concentration in liver and plasma of mice. *Journal of Animal and Feed Sciences*. **17**:621-30.
- Fernandez-Ruiz, J.C., Ramos-Remus, C., Sánchez-Corona, J., Castillo-Ortiz, J.D., Castañeda-Sánchez, J.J., Bastian, Y., Romo-García, M.F., Ochoa-González, F., Monsivais-Urenda, A.E., González-Amaro, R. and Enciso-Moreno, J.A.,

References

- (2018). Analysis of miRNA expression in patients with rheumatoid arthritis during remission and relapse after a 5-year trial of tofacitinib treatment. *International immunopharmacology*, **63**:35–42.
- Ferreira, G.B., Vanherwegen, A.S., Eelen, G., Gutiérrez, A.C.F., Van Lommel, L., Marchal, K., Verlinden, L., Verstuyf, A., Nogueira, T., Georgiadou, M. and Schuit, F., (2015). Vitamin D3 induces tolerance in human dendritic cells by activation of intracellular metabolic pathways. *Cell reports*, **10**(5):711–725.
- Filippin, L.I., Vercelino, R., Marroni, N.P. and Xavier, R.M. (2008). Redox signalling and the inflammatory response in rheumatoid arthritis. *Clinical and Experimental Immunology* **152**(3):415–422.
- Filková, M., Jüngel, A., Gay, R.E. and Gay, S., (2012). MicroRNAs in rheumatoid arthritis. *BioDrugs*, **26**(3):131–141.
- Firestein GS., Boyle DL., Yu C Paine., M. M., Whisenand, T. D., Zvaifler, N. J., Arend, W. P. (1994). Synovial interleukin-1 receptor antagonist and interleukin-1 balance in rheumatoid arthritis. *Arthritis and Rheumatism*.**37**:644–52
- Firestein, G.S., Budd, R.C., Gabriel, S.E., McInnes, I.B. and O'Dell, J.R., (2016). Kelley and Firestein's textbook of rheumatology e-book. *Elsevier Health Sciences*.
- Firestein, G.S. and McInnes, I.B. (2017). Immunopathogenesis of rheumatoid arthritis. *Immunity* **46**(2):183–196.
- Fonseca, J., Edwards, J., Blades, S. and Goulding, N. (2002). Macrophage subpopulations in rheumatoid synovium: Reduced CD163 expression in CD4+ T lymphocyte-rich microenvironments. *Arthritis and Rheumatism* **46**(5):1210–1216.
- Fox, C.J., Hammerman, P.S. and Thompson, C.B., (2005). Fuel feeds function: energy metabolism and the T-cell response. *Nature Reviews Immunology*, **5**(11):844–852.
- Frommer, K.W., Zimmermann, B., Meier, F.M., Schröder, D., Heil, M., Schäffler, A., Gay, S. (2010). Adiponectin-mediated changes in effector cells involved in the pathophysiology of rheumatoid arthritis. *Arthritis and Rheumatism* **62**(10):2886–2899.
- Furer, V., Greenberg, J.D., Attur, M., Abramson, S.B. and Pillinger, M.H. (2010). The role of microRNA in rheumatoid arthritis and other autoimmune diseases. *Clinical Immunology* **136**(1):1–15.
- Fukui, S., Iwamoto, N., Takatani, A., Igawa, T., Shimizu, T., Umeda, M., ... Kawakami, A. (2018). M1 and M2 Monocytes in Rheumatoid Arthritis: A Contribution of Imbalance of M1/M2 Monocytes to Osteoclastogenesis. *Frontiers in Immunology* **8**:1958.
- Fujino, T., Asaba, H., Kang, M.J., Ikeda, Y., Sone, H., Takada, S., Kim, D.H., Ioka, R.X., Ono, M., Tomoyori, H. and Okubo, M., (2003). Low-density lipoprotein receptor-related protein 5 (LRP5) is essential for normal cholesterol metabolism and glucose-induced insulin secretion. *Proceedings of the National Academy of Sciences*, **100**(1):229–234.
- Fu, W., Wojtkiewicz, G., Weissleder, R., Benoist, C. and Mathis, D., (2012). Early window of diabetes determinism in NOD mice, dependent on the complement receptor CR1g, identified by noninvasive imaging. *Nature immunology*, **13**(4):361–368.
- Gabriel SE (2008). Cardiovascular morbidity and mortality in rheumatoid arthritis. *Am J Med*; 121(10 Suppl 1):S9–14.
- Gallagher, H., Williams, J.O., Ferekidis, N., Ismail, A., Chan, Y.-H., Michael, D.R., ... Ramji, D.P. (2019). Dihomo- γ -linolenic acid inhibits several key cellular processes associated with atherosclerosis. *Biochimica et Biophysica Acta (BBA) - Molecular Basis of Disease* **1865**(9):2538–2550.

References

- Gan, R.W., Bemis, E.A., Demoruelle, M.K., Striebich, C.C., Brake, S., Feser, M.L., ... Norris, J.M. (2017). The association between omega-3 fatty acid biomarkers and inflammatory arthritis in an anti-citrullinated protein antibody positive population. *Rheumatology* **56**(12):2229–2236.
- Garcia, S., Hartkamp, L.M., Malvar-Fernandez, B. van Es, I. E., Lin, H., Wong, J., ... and Reedquist, K. A (2016). Colony-stimulating factor (CSF) 1 receptor blockade reduces inflammation in human and murine models of rheumatoid arthritis. *Arthritis Research Therapy* **18**(1):1-14.
- Geijtenbeek, T. B., Kwon, D. S., Torensma, R., Van Vliet, S. J., Van Duijnhoven, G. C., Middel, J., van Kooyk, Y. (2000). DC-SIGN, a dendritic cell-specific HIV-1-binding protein that enhances trans-infection of T cells. *Cell*, **100**(5), 587-597.
- Geusens E Wouters C, Nijs J, Jiang, Y, and Dequeker, J. (1994). Long-term effect of omega-3 fatty acid supplementation in active rheumatoid arthritis: a 12-months, double-blind, controlled study. *Arthritis and Rheumatism*; **37**:824–9.
- Gioxari, A., Kaliora, A.C., Marantidou, F. and Panagiotakos, D.P. (2018). Intake of ω -3 polyunsaturated fatty acids in patients with rheumatoid arthritis: A systematic review and meta-analysis. *Nutrition* **45**:114–124.e4.
- Gillies, P. J., Bhatia, S. K., Belcher, L. A., Hannon, D. B., Thompson, J. T., and Vanden Heuvel, J. P. (2012). Regulation of inflammatory and lipid metabolism genes by eicosapentaenoic acid-rich oil. *Journal of lipid research*, **53**(8), 1679–1689.
- Gomez, Paul F., Michael H. Pillinger, Mukundan Attur, Nada Marjanovic, Mander Dave, Jean Park, Clifton O. Bingham, Hayf Al-Mussawir, and Steven B. Abramson (2005). Resolution of inflammation: prostaglandin E2 dissociates nuclear trafficking of individual NF- κ B subunits (p65, p50) in stimulated rheumatoid synovial fibroblasts. *The Journal of Immunology* **175** (10):6924–6930.
- González, R.M., Gil, J.F., Cortes, J.I., Olmos, C.F., Ortiz-Sanjuan, F., Garcia, E.G., ... Ivorra, J.R. (2017). AB0356 Association between cardiovascular risk factors and carotid intima-media thickness in patients with rheumatoid arthritis. *Abstracts Accepted for Publication. BMJ Publishing Group Ltd and European League Against Rheumatism*, **1173**:1–1173.
- Gonzalo-Gil, E. and Galindo-Izquierdo, M. (2014). Role of Transforming Growth Factor-Beta (TGF) Beta in the Physiopathology of Rheumatoid Arthritis. *Reumatología Clínica* **10**(3):174–179.
- Gonzalez-Gay, M.A., Llorca, J., Sanchez, E., Lopez-Nevot, M.A., Amoli, M.M., Garcia-Porrua, C., Ollier, W.E.R. and Martin, J., (2004). Inducible but not endothelial nitric oxide synthase polymorphism is associated with susceptibility to rheumatoid arthritis in northwest Spain. *Rheumatology*, **43**(9):1182-1185.
- Gong, Y., Slee, R.B., Fukai, N., Rawadi, G., Roman-Roman, S., Reginato, A.M., Wang, H., Cundy, T., Glorieux, F.H., Lev, D. and Zacharin, M., (2001). LDL receptor-related protein 5 (LRP5) affects bone accrual and eye development. *Cell*, **107**(4):513–523.
- Goodson, N.J., Wiles, N.J., Lunt, M., Barrett, E.M., Silman, A.J. and Symmons, D.P.M. (2002). Mortality in early inflammatory polyarthritis: Cardiovascular mortality is increased in seropositive patients. *Arthritis and Rheumatism* **46**(8):2010–2019.
- Goodson, N. J., Symmons, D.P, Scott D.G, Bunn. D, Lunt, M., and Silman, A.J (2005). Baseline levels of C-reactive protein and prediction of death from cardiovascular disease in patients with inflammatory polyarthritis: a ten-year followup study of a primary carebased inception cohort. *Arthritis and Rheumatism*, **52**:2293–2299.
- Gordon, S. and Taylor, P.R. (2005). Monocyte and macrophage heterogeneity. *Nature reviews immunology* **5**(12):953.

References

- Gordon, S. and F.O. Martinez, Alternative activation of macrophages: mechanism and functions. *Immunity*, 2010. **32**(5):593–604.
- Gordon, S., Alternative activation of macrophages. *Nature Review Immunology*, 2003. **3**(1):23–35.
- Granström, E., Hamberg, M., Hansson, G. and Kindahl, H., (1980). Chemical instability of 15-keto-13, 14-dihydro-PGE₂: the reason for low assay reliability. *Prostaglandins*, **19**(6):933–957.
- Grabacka, M. and Reiss, K. (2008). Anticancer Properties of PPAR α -effects on cellular metabolism and inflammation. *PPAR research*, **2008**:930705.
- Gracie, J.A., Forsey, R.J., Chan, W.L., Gilmour, A., Leung, B.P., Greer, M.R., ... Xu, D. (1999). A proinflammatory role for IL-18 in rheumatoid arthritis. *The Journal of clinical investigation* **104**(10):1393–1401.
- Griess, P. (1879) Bemerkungen zu der abhandlung der H.H. Weselsky und Benedikt "Ueber einige azoverbindungen." *Berichte der deutschen chemischen Gesellschaft*, **12**(1):426–8.
- Griffith, M., Walker, J. R., Spies, N. C., Ainscough, B. J., and Griffith, O. L. (2015). Informatics for RNA Sequencing: A Web Resource for Analysis on the Cloud. *PLoS Comput Biol*, **11**(8):e1004393.
- Gschwandtner, M., Derler, R. and Midwood, K.S., (2019). More than just attractive: how CCL2 influences myeloid cell behavior beyond chemotaxis. *Frontiers in immunology*, **10**:2759.
- Guo, Q., Wang, Y., Xu, D., Nossent, J., Pavlos, N.J. and Xu, J. (2018). Rheumatoid arthritis: pathological mechanisms and modern pharmacologic therapies. *Bone Research* **6**(1):15.
- Guo, Y., Walsh, A.M., Fearon, U., Smith, M.D., Wechalekar, M.D., Yin, X., Cole, S., Orr, C., McGarry, T., Canavan, M. and Kelly, S., (2017). CD40L-dependent pathway is active at various stages of rheumatoid arthritis disease progression. *The Journal of Immunology*, **198**(11):4490–4501.
- Gulen, M.F., Kang, Z., Bulek, K., Youzhong, W., Kim, T.W., Chen, Y., Altuntas, C.Z., Bak-Jensen, K.S., McGeachy, M.J., Do, J.S. and Xiao, H., (2010). The receptor SIGIRR suppresses Th17 cell proliferation via inhibition of the interleukin-1 receptor pathway and mTOR kinase activation. *Immunity*, **32**(1):54–66.
- Gutkind JS. (1998). Cell growth control by G protein-coupled receptors: from signal transduction to signal integration. *Oncogene*, **17**(11):1331–42.
- Gutzwiller, J.P., Degen, L., Matzinger, D., Prestin, S. and Beglinger, C., (2004). Interaction between GLP-1 and CCK-33 in inhibiting food intake and appetite in men. *American Journal of Physiology-Regulatory, Integrative and Comparative Physiology*, **287**(3):562-567.
- Guerne, P.A., Desgeorges, A., Jaspar, J.M., Relic, B., Peter, R., Hoffmeyer, P. and Dayer, J.M., 1999. Effects of IL-6 and its soluble receptor on proteoglycan synthesis and NO release by human articular chondrocytes: comparison with IL-1. Modulation by dexamethasone. *Matrix biology*, **18**(3):253–260.
- Gwinnutt, J. M., Wiczorek, M., Balanescu, A., Bischoff-Ferrari, H. A., Boonen, A., Cavalli, G., ... and Verstappen, S. M. (2022). 2021 EULAR recommendations regarding lifestyle behaviours and work participation to prevent progression of rheumatic and musculoskeletal diseases. *Annals of the rheumatic diseases*.
- Hagen, K.B., Dagfinrud, H., Moe, R.H., Osterås, N., Kjekshus, I., Grotle, M. and Smedslund, G. (2012). Exercise therapy for bone and muscle health: an overview of systematic reviews. *Biomedical Central medicine* **10**:167–167.
- Hagen, K.B., Byfuglien, M.G., Falzon, L., Olsen, S.U. and Smedslund, G. (2009). Dietary interventions for rheumatoid arthritis. *Cochrane Database of Systematic Reviews*. (1): CD006400.

References

- Hamilton, J.A. (2008) Colony-stimulating factors in inflammation and autoimmunity. *Nature Review Immunology*. **8**(7): 533-44.
- Hamers, A.A., Dinh, H.Q., Thomas, G.D., Marcovecchio, P., Blatchley, A., Nakao, C.S., Kim, C., McSkimming, C., Taylor, A.M., Nguyen, A.T. and McNamara, C.A., (2019). Human monocyte heterogeneity as revealed by high-dimensional mass cytometry. *Arteriosclerosis, thrombosis, and vascular biology*, **39**(1):25–36.
- Hansson, G.K. and Libby, P. (2006). The immune response in atherosclerosis: a double-edged sword. *Nature Review of Immunology*. **6**:508–519.
- Harris, E.D. (1983). Glucocorticoid Use in Rheumatoid Arthritis. *Hospital Practice* **18**(9):137–146.
- Harre, U. and Schett, G. (2017). Cellular and molecular pathways of structural damage in rheumatoid arthritis. *Seminars in Immunopathology* **39**(4):355–363.
- Harris, J.E., Emkey, R., Nichols, J. and Newberg, A. (1983). Low dose prednisone therapy in rheumatoid arthritis: a double-blind study. *The Journal of rheumatology* **10**(5):713–721.
- Haringman JJ, Gerlag DM, Smeets TJ, Baeten D, van den Bosch F, Bresnihan B, Breedveld FC, Dinant HJ, Legay F, Gram H, Loetscher P, Schmouder R, Woodworth T, Tak PP (2006). A randomized controlled trial with an anti-CCL2 (anti-monocyte chemotactic protein 1) monoclonal antibody in patients with rheumatoid arthritis. *Arthritis and Rheumatism*.**54**(8):2387-92.
- Hayman AR (2008). Tartrate-resistant acid phosphatase (TRAP) and the osteoclast/immune cell dichotomy. *Autoimmunity*.**41**(3):218–23.
- Heinrich, P.C., Castell, J.V. and Andus, T (1990). Interleukin-6 and the acute phase response. *Biochemical Journal*, **265**(3):621–36.
- Hepburn, A.L., J.C. Mason, and K.A. Davies (2004) Expression of Fcγ and complement receptors on peripheral blood monocytes in systemic lupus erythematosus and rheumatoid arthritis. *Rheumatology (Oxford)*. **43**(5):547–54.
- Hirose, S., Lin, Q., Ohtsuji, M., Nishimura, H. and Verbeek, J.S. (2019). Monocyte subsets involved in the development of systemic lupus erythematosus and rheumatoid arthritis. *International Immunology*. **31**(11):687-696.
- Hjorth, E., Zhu, M., Toro, V.C., Vedin, I., Palmblad, J., Cederholm, T., Freund-Levi, Y., Faxen-Irving, G., Wahlgund, L.O., Basun, H. and Eriksdotter, M., (2013). Omega-3 fatty acids enhance phagocytosis of alzheimer's disease-related amyloid-β 42 by human microglia and decrease inflammatory markers. *Journal of Alzheimer's Disease*, **35**(4):697–713.
- Hosomi, K. and Kunisawa, J., (2020). Diversity of energy metabolism in immune responses regulated by microorganisms and dietary nutrition. *International immunology*, **32**(7):447–454.
- Hoxha, M. (2018). A systematic review on the role of eicosanoid pathways in rheumatoid arthritis. *Advances in Medical Sciences* **63**(1):22–29.
- Hoffman RA, Langrehr JM, Billiar TR, Curran RD, Simmons RL (1990): Atloantigen-induced activation of rat splenocytes is regulated by the oxidative metabolism of L-arginine. *Journal of Immunology* **145**:222-2226.
- https://www.bioinformatics.babraham.ac.uk/projects/trim_galore/1 September (2021), date last accessed.
- <https://www.bioinformatics.babraham.ac.uk/projects/fastqc/>1 September (2021), date last accessed.

References

https://www.encodeproject.org/documents/cede0cbe-d324-4ce7-ace4-f0c3eddf5972/@download/attachment/ENCODE%20Best%20Practices%20for%20RNA_v2.pdf.

Huang, Y.-S., Pereira, S.L. and Leonard, A.E. (2004). Enzymes for transgenic biosynthesis of long-chain polyunsaturated fatty acids. *Biochimie* **86**(11):793–798.

Huebner, S.M., Olson, J.M., Campbell, J.P., Bishop, J.W., Crump, P.M. and Cook, M.E., (2013). Dietary trans-10, cis-12 CLA reduces murine collagen-induced arthritis in a dose-dependent manner. *The Journal of nutrition*, **144**(2):177-184.

Hu, Y., Sparks, J.A., Malspeis, S., Costenbader, K.H., Hu, F.B., Karlson, E.W. and Lu, B., (2017). Long-term dietary quality and risk of developing rheumatoid arthritis in women. *Annals of the rheumatic diseases*, **76**(8):1357-1364.

Hunter, C. and Jones, S. (2015). IL-6 as a Keystone Cytokine in Health and Disease. *Nature Immunology*.**16**:448–57

Huang, X., Feng, Z., Jiang, Y., Li, J., Xiang, Q., Guo, S., Yang, C., Fei, L., Guo, G., Zheng, L. and Wu, Y., (2019). VSIG4 mediates transcriptional inhibition of Nlrp3 and Il-1 β in macrophages. *Science advances*, **5**(1):7426.

Huang W, Shang W, Wang H, Wu W, Hou S (2012). Sirt1 overexpression protects murine osteoblasts against TNF- α -induced injury in vitro by suppressing the NF- κ B signalling pathway. *Acta Pharmacologica Sinica*,**33**(5):668–74.

IL6R Genetics Consortium Emerging Risk Factors Collaboration (2012). Interleukin-6 receptor pathways in coronary heart disease: a collaborative meta-analysis of 82 studies. *The Lancet*, **379**(9822):1205–1213.

Ikeda T, Sasaki K, Ikeda K, Yamaoka G, Kawanishi K, Kawachi Y, Uchida T, Takahara J, Irino S. (1998) A new cytokine-dependent monoblastic cell line with differentiates to macrophages with macrophage colony-stimulating factor (M-CSF) and to osteoclast-like cells with M-CSF and interleukin-4. *Blood*, **91**(12):4543–53.

Ingersoll, M.A., Spanbroek, R., Lottaz, C., Gautier, E.L., Frankenberger, M., Hoffmann, R., ... Tacke, F. (2010a). Comparison of gene expression profiles between human and mouse monocyte subsets. *Blood* **115**(3):e10–e19.

Irvine, K.M., Andrews, M.R., Fernandez-Rojo, M.A., Schroder, K., Burns, C.J., Su, S., Wilks, A.F., Parton, R.G., Hume, D.A. and Sweet, M.J., (2009). Colony-stimulating factor-1 (CSF-1) delivers a proatherogenic signal to human macrophages. *Journal of leukocyte biology*, **85**(2):278–288.

Ishida N, Hayashi K, Hoshijima M, Ogawa T, Koga S, Miyatake Y, Kumegawa M, Kimura T, Takeya T (2002). Large scale gene expression analysis of osteoclastogenesis in vitro and elucidation of NFAT2 as a key regulator. *Journal of Biological Chemistry*. **277**(43):41147–56.

Imanishi, T., Ikejima, H., Tsujioka, H., Kuroi, A., Ishibashi, K., Komukai, K., Tanimoto, T., Ino, Y., Takeshita, T. and Akasaka, T., (2010). Association of monocyte subset counts with coronary fibrous cap thickness in patients with unstable angina pectoris. *Atherosclerosis*, **212**(2):628–635.

Innala, L., Möller, B., Ljung, L., Magnusson, S., Smedby, T., Södergren, A., Öhman, M.L., Rantapää-Dahlqvist, S. and Wållberg-Jonsson, S., (2011). Cardiovascular events in early RA are a result of inflammatory burden and traditional risk factors: a five year prospective study. *Arthritis research and therapy*, **13**(4):131.

Iwahashi, M., Yamamura, M., Aita, T., Okamoto, A., Ueno, A., Ogawa, N., ... Makino, H. (2004). Expression of toll-like receptor 2 on CD16+ blood monocytes and synovial tissue macrophages in rheumatoid arthritis. *Arthritis and Rheumatism*, **50**(5):1457–1467.

Jacob, A., Hensley, L., Safratowich, B. et al. (2007). The role of the complement cascade in endotoxin-induced septic encephalopathy. *Laboratory Investigation* **87**:1186–1194.

References

- Jha MK, Song GJ, Lee MG, Jeoung NH, Go Y, Harris RA, Park DH, Kook H, Lee IK, Suk K. (2015). Metabolic Connection of Inflammatory Pain: Pivotal Role of a Pyruvate Dehydrogenase Kinase-Pyruvate Dehydrogenase-Lactic Acid Axis. *Journal of Neuroscience*, **35**(42):14353–69.
- Jiang, Y. Genant, H. K., Watt, I., Cobby, M., Bresnihan, B., Aitchison, R., and McCabe, D. (2000). A multicentre, double-blind, dose- ranging, randomized, placebo-controlled study of recombinant human interleukin-1 receptor antagonist in patients with rheumatoid arthritis: radiologic progression and correlation of Genant and Larsen scores. *Arthritis and Rheumatism*, **43**:1001–1009
- jamei, M. and C.V. Carman (2010). New observations on the trafficking and diapedesis of monocytes. *Current Opinion Haematology*, **17**(1):43–52.
- James, E.A., Rieck, M., Pieper, J., Gebe, J.A., Yue, B.B., Tatum, M., ... Buckner, J.H. (2014). Citrulline-Specific Th1 Cells Are Increased in Rheumatoid Arthritis and Their Frequency Is Influenced by Disease Duration and Therapy. *Arthritis & Rheumatology*, **66**(7):1712–1722.
- Joe, M. (2018). Anti-inflammatory actions of nutraceuticals: Novel emerging therapies for atherosclerosis? *PhD thesis Cardiff University*.
- Jones, S.A., Takeuchi, T., Aletaha, D., Smolen, J., Choy, E.H. and McInnes, I. (2018). Interleukin 6: The biology behind the therapy. *Considerations in Medicine* **2**(1):2.
- Jovanovic, D.V., Boumsell, L., Bensussan, A., Chevalier, X., Mancini, A. and Di Battista, J.A., (2011). CD101 expression and function in normal and rheumatoid arthritis-affected human T cells and monocytes/macrophages. *The Journal of rheumatology*, **38**(3):419–428.
- Jung, D.Y. et al. (2013). KLF15 Is a Molecular Link between Endoplasmic Reticulum Stress and Insulin Resistance. *PLOS ONE* **8**(10):e77851.
- Jüni, P., Nartey, L., Reichenbach, S., Sterchi, R., Dieppe, P.A. and Egger, M., (2004). Risk of cardiovascular events and rofecoxib: cumulative meta-analysis. *The lancet*, **364**(9450):2021–2029.
- Jump, D.B., Thelen, A., Ren, B. and Mater, M., (1999). Multiple mechanisms for polyunsaturated fatty acid regulation of hepatic gene transcription. *Prostaglandins, leukotrienes and essential fatty acids*, **60**(5-6):345–349.
- Kamari, Y., Shaish, A., Shemesh, S., Vax, E., Grosskopf, I., Dotan, S., White, M., Voronov, E., Dinarello, C.A., Apte, R.N. and Harats, D., (2011). Reduced atherosclerosis and inflammatory cytokines in apolipoprotein-E-deficient mice lacking bone marrow-derived interleukin-1 α . *Biochemical and biophysical research communications*, **405**(2):197–203.
- Kampstra, A.S.B. and Toes, R.E.M. (2017). HLA class II and rheumatoid arthritis: the bumpy road of revelation. *Immunogenetics* **69**(8):597–603.
- Kang, S., Tanaka, T., Narazaki, M. and Kishimoto, T. (2019). Targeting Interleukin-6 Signalling in Clinic. *Immunity* **50**(4):1007–1023.
- Kang, Y.H., Kim, K.K., Kim, T.W. and Choe, M. (2015). Anti-atherosclerosis effect of pine nut oil in high-cholesterol and high-fat diet fed rats and its mechanism studies in human umbilical vein endothelial cells. *Food Science and Biotechnology*, **24**(1):323–332.
- Kaptoge, S., Di Angelantonio, E., Lowe, G., Pepys, M.B., Thompson, S.G., Collins, R. and Danesh, J., (2010). Emerging Risk Factors Collaboration C-reactive protein concentration and risk of coronary heart disease, stroke, and mortality: an individual participant meta-analysis. *Lancet*, **375**(9709):132–140.
- Karpouzias, G.A., Malpeso, J., Choi, T.-Y., Li, D., Munoz, S. and Budoff, M.J. (2014). Prevalence, extent and composition of coronary plaque in patients with rheumatoid arthritis without symptoms or prior diagnosis of coronary artery disease. *Annals of the Rheumatic Diseases*, **73**(10):1797–1804.

References

- Karpouzas, G., Ormseth, S., Hernandez, E. and Budoff, M. (2021). Differences in low density lipoprotein(LDL) particle composition and oxidation may underlie the paradoxical association of low LDL with higher coronary atherosclerosis burden in rheumatoid arthritis.. *Annals of the Rheumatic Diseases*, **80**(1):58.
- Karnovsky, M.L. Metchnikoff in Messina (1981). A century of studies on phagocytosis. *New England Journal of Medicine*. **304**(19):1178–80.
- Kashiwagi, M., Imanishi, T., Tsujioka, H., Ikejima, H., Kuroi, A., Ozaki, Y., Ishibashi, K., Komukai, K., Tanimoto, T., Ino, Y. and Kitabata, H., (2010). Association of monocyte subsets with vulnerability characteristics of coronary plaques as assessed by 64-slice multidetector computed tomography in patients with stable angina pectoris. *Atherosclerosis*, **212**(1):171–176.
- Kats, A., Norgård, M., Wondimu, Z., Koro, C., Quezada, H.C., Andersson, G. and Yucel-Lindberg, T. (2016). Aminothiazoles inhibit RANKL- and LPS-mediated osteoclastogenesis and PGE2 production in RAW 264.7 cells. *Journal of Cellular and Molecular Medicine* **20**(6):1128–1138.
- Kaur, J., Syngle, A., Krishan, P., Vohra, K., Garg, N., Kaur, L. and Chhabra, M. (2014). IL-6 inhibition improves nitric oxide in rheumatoid arthritis. *Internet Journal of Rheumatology and Clinical Immunology* **2**(1).
- Kay, J. and Calabrese, L. (2004). The role of interleukin-1 in the pathogenesis of rheumatoid arthritis. *Rheumatology* **43**(3):2–9.
- Khan, A.H., Carson, R.J. and Nelson, S.M.,(2008). Prostaglandins in labor-a translational approach. *Front Biosci*, **13**:5794–5809.
- Khanna, S., Jaiswal, K.S. and Gupta, B. (2017). Managing rheumatoid arthritis with dietary interventions. *Frontiers in nutrition* **4**:52.
- Khandpur, R., Carmona-Rivera, C., Vivekanandan-Giri, A., Gizinski, A., Yalavarthi, S., Knight, J.S., Friday, S., Li, S., Patel, R.M., Subramanian, V. and Thompson, P., (2013). NETs are a source of citrullinated autoantigens and stimulate inflammatory responses in rheumatoid arthritis. *Science Translational Medicine*, **5**(178):178ra40-178ra40.
- Khovidhunkit, W., A. H. Moser, J. K. Shigenaga, C. Grunfeld, and K. R. Feingold. (2001). Regulation of scavenger receptor class B type I in master liver and Hep3B cells by endotoxin and cytokines. *Journal of Lipid Research*. **42**:1636–1644.
- Kawanaka, N., Yamamura, M., Aita, T., Morita, Y., Okamoto, A., Kawashima, M., Iwahashi, M., Ueno, A., Ohmoto, Y. and Makino, H., (2002). CD14+, CD16+ blood monocytes and joint inflammation in rheumatoid arthritis. *Arthritis & Rheumatism*, **46**(10):2578–2586.
- Kapoor R, Huang YS. Gamma linolenic acid (2006): an antiinflammatory omega-6 fatty acid. *Current Pharmacology and Biotechnology* **7**(6):531–4.
- Keffer, J., Probert, L., Cazlaris, H., Georgopoulos, S., Kaslaris, E., Kioussis, D., & Kollias, G. (1991). Transgenic mice expressing human tumour necrosis factor: a predictive genetic model of arthritis. *The EMBO journal*, **10**(13): 4025–4031.
- Kennedy, A., Fearon, U., Veale, D.J. and Godson, C. (2011). Macrophages in synovial inflammation. *Frontiers in immunology* **2**:52–52.
- Kim, H. R., Chae, H. J., Thomas, M., Miyazaki, T., Monosov, A., Monosov, E., ... and Reed, J. C. . (2007). Mammalian dap3 is an essential gene required for mitochondrial homeostasis in vivo and contributing to the extrinsic pathway for apoptosis. *The FASEB Journal* **21**(1):188–196.
- Kim, K.-W., Kim, B.-M., Won, J.-Y., Lee, K.-A., Kim, H.-R. and Lee, S.-H. (2019). Toll-like receptor 7 regulates osteoclastogenesis in rheumatoid arthritis. *The Journal of Biochemistry*, **166**(3):259–270.

References

- Kim, B., Nam, S., Lim, J.H. and Lim, J.-S. (2016). NDRG2 Expression Decreases Tumor-Induced Osteoclast Differentiation by Down-regulating ICAM1 in Breast Cancer Cells. *Biomolecules and therapeutics* **24**(1):9–18.
- Kim, M.-J., Kim, H.-S., Lee, S.-H., Yang, Y., Lee, M.-S. and Lim, J.-S. (2014). NDRG2 controls COX-2/PGE₂-mediated breast cancer cell migration and invasion. *Molecules and cells* **37**(10):759–765.
- Kinne, R.W., Stuhlmüller, B. and Burmester, G.-R. (2007). Cells of the synovium in rheumatoid arthritis. Macrophages. *Arthritis Research and Therapy* **9**(6):224.
- Kinne R.W., Stuhlmüller B., Palombo-Kinne E. and Burmester G.R. (2000). The role of macrophages in the pathogenesis of rheumatoid arthritis. In: Rheumatoid arthritis: *The New frontiers in pathogenesis and treatment*. **2**(189):69–87.
- Klareskog, L., Forsum, U., Kabelitz, D., Plöen, L., Sundström, C., Nilsson, K., Wigren, A. and Wigzell, H., (1982). Immune functions of human synovial cells. phenotypic and t cell regulatory properties of macrophage-like cells that express hla-dr. *Arthritis and Rheumatism: Official Journal of the American College of Rheumatology*, **25**(5):488–501.
- Klingenberg, R. and Hansson, G.K. (2009). Treating inflammation in atherosclerotic cardiovascular disease: emerging therapies. *European Heart Journal* **30**(23):2838–2844.
- Koch, A.E., Burrows, J.C., Skoutelis, A., Marder, R., Domer, P.H., Anderson, B. and Leibovich, S.J., (1991). Monoclonal antibodies detect monocyte/macrophage activation and differentiation antigens and identify functionally distinct subpopulations of human rheumatoid synovial tissue macrophages. *The American journal of pathology*, **138**(1):165.
- Koch, A.E., (2005). Chemokines and their receptors in rheumatoid arthritis: future targets?. *Arthritis and Rheumatism*, **52**(3):710-721.
- Komai-Koma, M., Gracie, J.A., Wei, X., Xu, D., Thomson, N., McInnes, I.B. and Liew, F.Y. (2003). Chemoattraction of human T cells by IL-18. *The Journal of Immunology* **170**(2):1084–1090.
- Kobayashi, Y., Take, I., Yamashita, T., Mizoguchi, T., Ninomiya, T., Hattori, T., ... Takahashi, N. (2005). Prostaglandin E2 Receptors EP2 and EP4 Are Down-regulated during Differentiation of Mouse Osteoclasts from Their Precursors. *Journal of Biological Chemistry* **280**(25):24035–24042.
- Köller, M., Wachtler, P., David, A., Muhr, G. and König, W., (1997). Arachidonic acid induces DNA-fragmentation in human polymorphonuclear neutrophil granulocytes. *Inflammation*, **21**(5):463-474.
- Kong W, Yen JH, Vassiliou E, Adhikary S, Toscano MG, Ganea D. (2010) Docosahexaenoic acid prevents dendritic cell maturation and in vitro and in vivo expression of the IL-12 cytokine family. *Lipids Health Disease*, **9**:12.
- Kong S, Yeung P, Fang D. (2013) The Class III Histone Deacetylase Sirtuin 1 in Immune Suppression and Its Therapeutic Potential in Rheumatoid Arthritis. *Journal of Genetics and Genomics*.**40**(7):347-354.
- Komai-Koma, M., Gracie, J.A., Wei, X.Q., Xu, D., Thomson, N., McInnes, I.B. and Liew, F.Y., (2003). Chemoattraction of human T cells by IL-18. *The Journal of Immunology*, **170**(2):1084–1090.
- Krohn SC, Bonvin P, Proudfoot AE. (2013). CCL18 exhibits a regulatory role through inhibition of receptor and glycosaminoglycan binding. *PLoS One*.**8**(8):e72321.
- Krause, A., Scaletta, N., Ji, J.-D. and Ivashkiv, L.B. (2002). Rheumatoid Arthritis Synoviocyte Survival Is Dependent on Stat3. *The Journal of Immunology* **169**(11):6610-6616.

References

- Kremer, J.M., Bigauoette, J., Michalek, A.V., Timchalk, A., Linger, L. and Rynes, R.I., (1985). Huyak, C., Ziemianski, J., and Bartholamew. LE Effects of manipulation of dietary fatty acids on clinical manifestations of rheumatoid arthritis. *The Lancet*, **325**(8422):184-187.
- Kruidenier L, et al. (2012). A selective jumonji H3K27 demethylase inhibitor modulates the proinflammatory macrophage response. *Nature*; **488**(7411):404–408.
- Ksander BR, Kolovou PE, Wilson BJ, Saab KR, Guo Q, Ma J, McGuire SP, Gregory MS, Vincent WJ, Perez VL, Cruz-Guilloty F, Kao WW, Call MK, Tucker BA, Zhan Q, Murphy GF, Lathrop KL, Alt C, Mortensen LJ, Lin CP, Zieske JD, Frank MH, Frank NY (2014). "ABC5 is a limbal stem cell gene required for corneal development and repair". *Nature*. **511** (7509): 353–357.
- Kumar A, Takada Y, Boriek AM, Aggarwal BB. Nuclear factor-kappaB (2004): its role in health and disease. *Journal of Molecular Medicine*, **82**(7):434-448.
- Kurowska-Stolarska, M. and Alivernini, S. (2017). Synovial tissue macrophages: friend or foe? *RMD Open* **3**(2):e000527.
- Lau CS, Morley KD, Belch JJ. (1993). Effects of fish oil supplementation on non-steroidal anti-inflammatory drug requirement in patients with mild rheumatoid arthritis: a double-blind placebo-controlled study. *British Journal of Rheumatology* **32**(11):982-989.
- Läubli, H., Alisson-Silva, F., Stanczak, M.A., Siddiqui, S.S., Deng, L., Verhagen, A., Varki, N. and Varki, A., (2014). Lectin galactoside-binding soluble 3 binding protein (LGALS3BP) is a tumor-associated immunomodulatory ligand for CD33-related Siglecs. *Journal of Biological Chemistry*, **289**(48):33481–33491.
- Latruffe, N. and Vamecq, J., (1997). Peroxisome proliferators and peroxisome proliferator activated receptors (PPARs) as regulators of lipid metabolism. *Biochimie*, **79**(2-3):81–94.
- Lech, M. and Anders, H.-J. (2013). Macrophages and fibrosis: How resident and infiltrating mononuclear phagocytes orchestrate all phases of tissue injury and repair. *Biochimica et Biophysica Acta (BBA) - Molecular Basis of Disease* **1832**(7):989–997.
- Leclerc, D., Pham, D.N.T., Levesque, N., Truongcao, M., Foulkes, W.D., Sapienza, C. and Rozen, R., (2017). Oncogenic role of PDK4 in human colon cancer cells. *British journal of cancer*, **116**(7):930–936.
- Lee, A.R. and Han, S.N. (2016). Pinolenic Acid Downregulates Lipid Anabolic Pathway in HepG2 Cells. *Lipids*. **51**(7):847–855.
- Lee MKS, Al-Sharea A, Shihata WA, Bertuzzo Veiga C, Cooney OD, Fleetwood AJ, Flynn MC, Claeson E, Palmer CS, Lancaster GI, Henstridge DC, Hamilton JA, Murphy AJ. (2019) Glycolysis Is Required for LPS-Induced Activation and Adhesion of Human CD14+CD16- Monocytes. *Frontiers Immunology*, **6**(10):2054.
- Lee, Y.K., Choi, K.H., Kwak, H.S. and Chang, Y.H., (2018). The preventive effects of nanopowdered red ginseng on collagen-induced arthritic mice. *International journal of food sciences and nutrition*, **69**(3):308–317
- Lee JY, Sohn KH, Rhee SH, Hwang D (2001). Saturated fatty acids, but not unsaturated fatty acids, induce the expression of cyclooxygenase-2 mediated through Toll-like receptor 4. *Journal of Biological Chemistry*, **276**(20):16683–9.
- Lee, A.R. and Han, S.N. (2016). Pinolenic Acid Downregulates Lipid Anabolic Pathway in HepG2 Cells. *Lipids*, **51**(7):847–855.
- Lee, M.M. and Wong, Y.H., (2009). CCR1-mediated activation of nuclear factor- κ B in THP-1 monocytic cells involves pertussis toxin-insensitive G α 14 and G α 16 signalling cascades. *Journal of leukocyte biology*, **86**(6), 1319–1329.

References

- Lee MM, Chui RK, Tam IY, Lau AH, Wong YH. (2012) CCR1-mediated STAT3 tyrosine phosphorylation and CXCL8 expression in THP-1 macrophage-like cells involve pertussis toxin-insensitive G α (14/16) signalling and IL-6 release. *Journal of Immunology*; **189**(11):5266–76.
- Lee EB, Kim A, Kang K, Kim H, Lim JS. (2010). NDRG2-mediated Modulation of SOCS3 and STAT3 Activity Inhibits IL-10 Production. *Immune Network*. **10**(6):219–29.
- Lee, E.J., Lilja, S., Li, X., Schäfer, S., Zhang, H. and Benson, M. (2020). Bulk and single cell transcriptomic data indicate that a dichotomy between inflammatory pathways in peripheral blood and arthritic joints complicates biomarker discovery. *Cytokine* **127**:154960.
- Leeb, B.F., Sautner, J., Andel, I. and Rintelen, B., (2006). Intravenous application of omega-3 fatty acids in patients with active rheumatoid arthritis. The ORA-1 trial. An open pilot study. *Lipids*, **41**(1):29-34.
- Leibovich SJ, Polverini PJ, Jong TW et al. (1994). Production of angiogenic activity by human monocytes requires an L-arginine/nitric oxide-synthase-dependent effector mechanism. *Proceedings of the National Sciences* **91**(10): 4190-4194.
- Lenz, P., Gessner, J.E., Sautes, C. and Schmidt, R.E., (1996). Fey-Receptor III (CD16) is Involved in NK-8 Cell Interaction. *Immunobiology*, **196**(4)387-398.
- Leung, B.P., Culshaw, S., Gracie, J.A., Hunter, D., Canetti, C.A., Campbell, C., Cunha, F., Liew, F.Y. and McInnes, I.B., (2001). A role for IL-18 in neutrophil activation. *The Journal of Immunology*, **167**(5)2879-2886.
- Lewis, M.J., Barnes, M.R., Blighe, K., Goldmann, K., Rana, S., Hackney, J.A., ... Pitzalis, C. (2019). Molecular Portraits of Early Rheumatoid Arthritis Identify Clinical and Treatment Response Phenotypes. *Cell Reports* **28**(9):2455-2470.e5.
- Liao Y, Smyth GK and Shi W (2014). featureCounts: an efficient general purpose program for assigning sequence reads to genomic features. *Bioinformatics*, **30**(7):923-30.
- Li Y, Zhang P, Wang C, Han C, Meng J, Liu X, Xu S, Li N, Wang Q, Shi X, Cao X. (2013). Immune responsive gene 1 (IRG1) promotes endotoxin tolerance by increasing A20 expression in macrophages through reactive oxygen species. *J Biol Chem*. **288**(23):16225-34.
- Li, H., Zhang, D., Yu, J., Liu, H., Chen, Z., Zhong, H. and Wan, Y., (2018). CCL18-dependent translocation of AMAP1 is critical for epithelial to mesenchymal transition in breast cancer. *Journal of cellular physiology*, **233**(4):3207-3217.
- Li, J., Diao, B., Guo, S., Huang, X., Yang, C., Feng, Z., Yan, W., Ning, Q., Zheng, L., Chen, Y. and Wu, Y., (2017). VSIG4 inhibits proinflammatory macrophage activation by reprogramming mitochondrial pyruvate metabolism. *Nature communications*, **8**(1) 1-14.
- Li, Y., Zhao, M. and Xiao, W. (2018). KLF15 Regulates the Expression of MMP-3 in Human Chondrocytes. *Journal of Interferon & Cytokine Research* **38**(8) 356–362.
- Li, X., Zhang, S., Blander, G., Jeanette, G.T., Krieger, M. and Guarente, L., (2007). SIRT1 deacetylates and positively regulates the nuclear receptor LXR. *Molecular cell*, **28**(1):91-106.
- Lin, S., Liu, X., Liu, B. and Yu, Y., (2017). Optimization of pine nut (*Pinus koraiensis*) meal protein peptides on immunocompetence in innate and adaptive immunity response aspects. *Food and Agricultural Immunology*, **28**(1):109-120.
- Lin, C.-Y., Wang, W.-H., Chen, S.-H., Chang, Y.-W., Hung, L.-C., Chen, C.-Y. and Chen, Y.-H. (2017). Lipopolysaccharide-Induced Nitric Oxide, Prostaglandin E2, and Cytokine Production of Mouse and Human Macrophages Are Suppressed by Pheophytin-b. *International journal of molecular sciences* **18**(12):2637.

References

- Linsel-Nitschke, P. and Tall, A.R., (2005). HDL as a target in the treatment of atherosclerotic cardiovascular disease. *Nature reviews Drug discovery*, **4**(3): 193-205.
- Lioté, F., Boval-Boizard, B., Weill, D., Kuntz, D. and Wautier, J.-L. (1996). Blood Monocyte Activation in Rheumatoid Arthritis: Increased Monocyte Adhesiveness, Integrin Expression, and Cytokine Release. *Clinical & Experimental Immunology*. **106**(1):13-19.
- Liu, Z., Wang, J., Huang, X., Li, Z. and Liu, P., (2016). Deletion of sirtuin 6 accelerates endothelial dysfunction and atherosclerosis in apolipoprotein E-deficient mice. *Translational Research*, **172**:18–29.
- Liu, B., Xu, L., Yu, X., Li, W., Sun, X., Xiao, S., and Wang, H. . (2018). Protective effect of KLF15 on vascular endothelial dysfunction induced by TNF- α . *Molecular Medicine Reports* **18**(2):1987–1994.
- Liu PT, Stenger S, Li H, Wenzel L, Tan BH, Krutzik SR, Ochoa MT, Schaubert J, Wu K & Meinken C et al. (2006)Toll-like receptor triggering of a vitamin D-mediated human antimicrobial response. *Science* **311**: 1770–1773.
- López-Mejías, R., Genre, F., Remuzgo-Martínez, S., Robustillo-Villarino, M., García-Bermúdez, M., Llorca, J., ... Miranda-Filloo, J.A. (2015). Protective role of the interleukin 33 rs3939286 gene polymorphism in the development of subclinical atherosclerosis in rheumatoid arthritis patients. *PLoS One* **10**(11):e0143153.
- Lopetuso, L. R., Scaldaferrri, F., Petito, V., and Gasbarrini, A. (2013). Commensal Clostridia: leading players in the maintenance of gut homeostasis. *Gut pathogens*, **5**(1):23.
- Love MI, Huber W, Anders S (2014). Moderated estimation of fold change and dispersion for RNA-seq data with DESeq2. *Genome Biology*, **15**(12):1-21.
- Lourdudoss, C., Wolk, A., Nise, L., Alfredsson, L. and Vollenhoven, R. van (2017). Are dietary vitamin D, omega-3 fatty acids and folate associated with treatment results in patients with early rheumatoid arthritis? Data from a Swedish population-based prospective study. *BMJ open* **7**(6): e016154.
- Lubberts E, van den Berg WB (2013). Cytokines in the Pathogenesis of Rheumatoid Arthritis and Collagen-Induced Arthritis. In: Madame Curie Bioscience Database. Austin (TX): *Landes Bioscience*; 2000–2013.
- Lu, Y., Zhang, L., Liao, X., Sangwung, P., Prosdocimo, D. A., Zhou, G., Jain, M. K. (2013). Kruppel-like factor 15 is critical for vascular inflammation. *The Journal of clinical investigation*, **123**(10), 4232-4241.
- Lundy, S.K., et al. (2007), *Cells of the synovium in rheumatoid arthritis. T lymphocytes*. *Arthritis Research and Therapy*. **9**(1): 202.
- Lusis, A. J. (2000). Atherosclerosis. *Nature* **407**(6801):233–241.
- Ma, Y. and Pope, R.M., (2005). The role of macrophages in rheumatoid arthritis. *Current pharmaceutical design*, **11**(5):569-580.
- MacIntyre I, Zaidi M, Alam ASMT, Dalta HK, Moonga BS, Lidbury PS, Hecker M, Vane JR (1991): Osteoclastic inhibition: an action of nitric oxide not mediated by cyclic GMP. *Proceedings of the National Academy of Sciences*, **88**(7):2930-2940
- MacGregor AJ, Dhillon VB, Binder A, Forte CA, Knight BC, et al (1992). Fasting lipids and anticardiolipin antibodies as risk factors for vascular disease in systemic lupus erythematosus. *Annals of the Rheumatic Diseases*; **51**:152–5.
- Madge LA, Sierra-Honigmann MR, Pober JS (1999). Apoptosis-inducing agents cause rapid shedding of tumor necrosis factor receptor 1 (TNFR1). A nonpharmacological explanation for inhibition of TNF-mediated activation. *J Biol Chem*; **274**(19):13643–13649.

References

- Madhok, R., et al. (1993). *Serum interleukin 6 levels in rheumatoid arthritis: correlations with clinical and laboratory indices of disease activity. Annals of the Rheumatic Diseases*, **52**(3): 232–4.
- Magaro, M., Zoli, A., Altomonte, L., Mirone, L., De Sole, P., Di Mario, G. and De Leo, E., (1992). Effect of fish oil on neutrophil chemiluminescence induced by different stimuli in patients with rheumatoid arthritis. *Annals of the rheumatic diseases*, **51**(7):877–880.
- Mantegazza AR, Magalhaes JG, Amigorena S, Marks MS (2013). Presentation of phagocytosed antigens by MHC class I and II. *Traffic*. **14**(2):135-52.
- Martinez, F.O. and Gordon, S. (2014). The M1 and M2 paradigm of macrophage activation: *time for reassessment*. *F1000prime reports* **2014**(6).
- Maradit-Kremers, H., Nicola, P.J., Crowson, C.S., Ballman, K.V., Jacobsen, S.J., Roger, V.L. and Gabriel, S.E. (2007). Raised erythrocyte sedimentation rate signals heart failure in patients with rheumatoid arthritis. *Annals of the Rheumatic Diseases* **66**(1):76–80.
- Martel-Pelletier, J., Pelletier, J.P. and Fahmi, H., (2003). Cyclooxygenase-2 and prostaglandins in articular tissues. In *Seminars in arthritis and rheumatism*. **33**(3):155–167.
- Masuko, K. (2018). A Potential Benefit of “Balanced Diet” for Rheumatoid Arthritis. *Frontiers in Medicine* **5**:141.
- Mateen, S., Zafar, A., Moin, S., Khan, A.Q. and Zubair, S. (2016). Understanding the role of cytokines in the pathogenesis of rheumatoid arthritis. *Clinical Chemical Acta*. **455**:161–171.
- Masuko, K. (2009). A suppressive effect of prostaglandin E2 on the expression of SERPINE1/plasminogen activator inhibitor-1 in human articular chondrocytes: An in vitro pilot study. *Open Access Rheumatology: Research and Reviews*, 1:9-15.
- Mason, R.P., (2019). New insights into mechanisms of action for omega-3 fatty acids in atherothrombotic cardiovascular disease. *Current atherosclerosis reports*, **21**(1):2.
- Matsuno, Y., Umeno, J., Esaki, M., Hirakawa, Y., Fuyuno, Y., Okamoto, Y., Hirano, A., Yasukawa, S., Hirai, F., Matsui, T., Hosomi, S., Watanabe, K., Hosoe, N., Ogata, H., Hisamatsu, T., Yanai, S., Kochi, S., Kurahara, K., Yao, T., Torisu, T., ... Matsumoto, T. (2019). Measurement of prostaglandin metabolites is useful in diagnosis of small bowel ulcerations. *World journal of gastroenterology*, **25**(14):1753–1763.
- Matheson, L., Harcourt, D. and Hewlett, S. (2010). ‘Your whole life, your whole world, it changes’: partners’ experiences of living with rheumatoid arthritis. *Musculoskeletal Care* **8**(1):46–54.
- Marszalek, J.R. and Lodish, H.F., (2005). Docosahexaenoic acid, fatty acid–interacting proteins, and neuronal function: breastmilk and fish are good for you. *Annual review cell developmental biology*, **21**:633–657.
- Manzo A, Vitolo B, Humby F, Caporali R, Jarrossay D, Dell'accio F, Ciardelli L, Ugucioni M, Montecucco C, Pitzalis C. (2008) Mature antigen-experienced T helper cells synthesize and secrete the B cell chemoattractant CXCL13 in the inflammatory environment of the rheumatoid joint. *Arthritis and rheumatism*. **58**(11):3377–87.
- Maruotti, N., Cantatore, F.P., Crivellato, E., Vacca, A. and Ribatti, D. (2007). Macrophages in rheumatoid arthritis. *Histology and histopathology*
- McLaren, J.E., Calder, C.J., McSharry, B.P., Sexton, K., Salter, R.C., Singh, N.N., Wilkinson, G.W.G., et al. (2010). The tnf-like protein 1a-death receptor 3 pathway promotes macrophage foam cell formation in vitro. *Journal of Immunology* **184**:5827–34.
- McLaren, J.E., Michael, D.R., Ashlin, T.G. and Ramji, D.P. (2011a). Cytokines, macrophage lipid metabolism and foam cells: implications for cardiovascular disease therapy. *Progress in Lipid Research* **50**:331– 347.

References

- McLaren, J.E., Michael, D.R., Guschina, I.A., Harwood, J.L. and Ramji, D.P. (2011b). Eicosapentaenoic acid and docosahexaenoic acid regulate modified ldl uptake and macropinocytosis in human macrophages. *Lipids*, **46**:1053–1061.
- McInnes, I.B., Buckley, C.D. and Isaacs, J.D. (2015). Cytokines in rheumatoid arthritis shaping the immunological landscape. *Nature Reviews Rheumatology* **12**:63.
- McInnes, I.B. and Schett, G. (2007). Cytokines in the pathogenesis of rheumatoid arthritis. *Nature Reviews Immunology*, **7**(6):429.
- McInnes, I.B. and Schett, G. (2011). The Pathogenesis of Rheumatoid Arthritis. *New England Journal of Medicine* **365**(23):2205–2219.
- McInnes, I.B. and Schett, G. (2017). Pathogenetic insights from the treatment of rheumatoid arthritis. *The Lancet* **389**(10086):2328–2337.
- McInnes, I.B., Al-Mughales, J., Field, M., Leung, B.P., Huang, F., Dixon, R., ... Liew, F.Y. (1996). The role of interleukin-15 in T-cell migration and activation in rheumatoid arthritis. *Nature medicine* **2**(2):175.
- McInnes, I.B., Buckley, C.D. and Isaacs, J.D. (2016). Cytokines in rheumatoid arthritis—shaping the immunological landscape. *Nature Reviews Rheumatology* **12**(1):63.
- McCartney-Francis, N., Allen, J.B., Mizel, D.E., Albina, J.E., Xie, Q.W., Nathan, C.F. and Wahl, S.M., (1993). Suppression of arthritis by an inhibitor of nitric oxide synthase. *The Journal of experimental medicine*, **178**(2):749-754.
- McGarry, T., Biniiecka, M., Gao, W., Veale, D. and Fearon, U. (2016). A1.07 Reprogramming of metabolic pathways inhibits TLR2-induced inflammation in ra. *Annals of the Rheumatic Diseases* **75**(1):3.
- McGarry, T. T., Orr, C., Wade, S., Biniiecka, M., Wade, S., Gallagher, L., and Fearon, U. (2018). JAK/STAT Blockade Alters Synovial Bioenergetics, Mitochondrial Function, and Proinflammatory Mediators in Rheumatoid Arthritis. *Arthritis and rheumatology* **70**(12):1959–1970.
- Mellado, M., Martínez-Muñoz, L., Cascio, G., Lucas, P., Pablos, J.L. and Rodríguez-Frade, J.M. (2015). T cell migration in rheumatoid arthritis. *Frontiers in immunology* **6**:384.
- Mills CD (1991): Molecular basis of “suppressor” macrophages: arginine metabolism via the nitric oxide synthase pathway. *Journal of Immunology* **146**:2719-2723.
- Miller, J.L., Koc, H. and Koc, E.C. 2008. Identification of phosphorylation sites in mammalian mitochondrial ribosomal protein DAP3. *Protein Science* **17**(2):251–260.
- Moura, R.A., Cascão, R., Perpétuo, I., Canhão, H., Vieira-Sousa, E., Mourão, A.F., Rodrigues, A.M., Polido-Pereira, J., Queiroz, M.V., Rosário, H.S. and Souto-Carneiro, M.M., (2011). Cytokine pattern in very early rheumatoid arthritis favours B-cell activation and survival. *Rheumatology*, **50**(2):278–282.
- Midwood, K., et al. (2009). Tenascin-C is an endogenous activator of Toll-like receptor 4 that is essential for maintaining inflammation in arthritic joint disease. *Nature Medicine*, **15**(7):774–80.
- Mikołajczyk, T., Osmenda, G., Batko, B., Wilk, G., Krezelok, M., Skiba, D., ... Guzik, T. (2016). Heterogeneity of peripheral blood monocytes, endothelial dysfunction and subclinical atherosclerosis in patients with systemic lupus erythematosus. *Lupus* **25**(1):18–27.
- Miyasaka, N. (1997). Nitric oxide production in rheumatoid arthritis. *Japanese Journal of Rheumatology* **7**(3):165–172.

References

- Mizukami, Y., Matsui, T., Tohma, S. and Masuko, K., (2017). Distinct patterns of dietary intake in different functional classes of patients with rheumatoid arthritis. *Topics in Clinical Nutrition*, **32**(2):141-151.
- Moss, J.W., Davies, T.S., Garaiova, I., Plummer, S.F., Michael, D.R. and Ramji, D.P. (2016). A unique combination of nutritionally active ingredients can prevent several key processes associated with atherosclerosis in vitro. *PLoS one* **11**(3), e0151057.
- Moss, J.W.E. and Ramji, D.P. (2016b). Nutraceutical therapies for atherosclerosis. *Nature Review Cardiology*. **13**:513–532.
- Moss, J. W., Williams, J. O., Al-Ahmadi, W., O'Morain, V., Chan, Y. H., Hughes, T. R., and Ramji, D. P. (2021). Protective effects of a unique combination of nutritionally active ingredients on risk factors and gene expression associated with atherosclerosis in C57BL/6J mice fed a high fat diet. *Food and function*, **12**(8):3657-3671.
- Moore, K.J., Sheedy, F.J. and Fisher, E.A. (2013). Macrophages in atherosclerosis: a dynamic balance. *Nature Review Immunology*, **13**:709–721
- Moore, K. J. and Freeman, M. W. (2006). Scavenger receptors in atherosclerosis: Beyond lipid uptake. *Arteriosclerosis Thrombosis and Vascular Biology* **26**:1702–1711.
- Moore, K. J. and Tabas, I. (2011). Macrophages in the Pathogenesis of Atherosclerosis. *Cell* **145**:341–355.
- Moelants, E.A., Mortier, A., Damme, J.V. and Proost, P. (2013). Regulation of TNF- α with a focus on rheumatoid arthritis. *Immunology and Cell Biology* **91**(6):393–401.
- Mohan, A.K., Coté, T.R., Siegel, J.N. and Braun, M.M., (2003). Infectious complications of biologic treatments of rheumatoid arthritis. *Current opinion in rheumatology*, **15**(3):179–184.
- Mueller, I., Schnberger, T., Schneider, M., Borst, O., Ziegler, M., Seizer, P., Leder, C. *et al.* (2013). Gremlin-1 Is an Inhibitor of Macrophage Migration Inhibitory Factor and Attenuates Atherosclerotic Plaque Growth in ApoE(-/-) Mice. *Journal of Biological Chemistry* **288**:31635–31645.
- Mukherjee T, Chatterjee B, Dhar A, Bais SS, Chawla M, Roy P, George A, Bal V, Rath S, Basak S. (2017). A TNFp100 pathway subverts noncanonical NF- κ B signalling in inflamed secondary lymphoid organs. *EMBO Journal*.**36**(23):3501–3516.
- Murata, K., Furu, M., Yoshitomi, H., Ishikawa, M., Shibuya, H., Hashimoto, M., Imura, Y., Fujii, T., Ito, H., Mimori, T. and Matsuda, S., (2013). Comprehensive microRNA analysis identifies miR-24 and miR-125a-5p as plasma biomarkers for rheumatoid arthritis. *PLoS one*, **8**(7):69118.
- Mulherin, D., Fitzgerald, O. and Bresnihan, B. (1996). Synovial tissue macrophage populations and articular damage in rheumatoid arthritis. *Arthritis and Rheumatism* **39**(1):115–124.
- Munford RS. Statins and the acute-phase response. *New England Journal of Medicine* 2001; 344:2016–8.
- Müller-Ladner, U., Ospelt, C., Gay, S., Distler, O. and Pap, T., (2007). Cells of the synovium in rheumatoid arthritis. Synovial fibroblasts. *Arthritis research & therapy*, **9**(6): 1–10.
- Myasoedova, E., Crowson, C.S., Kremers, H.M., Roger, V.L., Fitz-Gibbon, P.D., Therneau, T.M. and Gabriel, S.E., (2011). Lipid paradox in rheumatoid arthritis: the impact of serum lipid measures and systemic inflammation on the risk of cardiovascular disease. *Annals of the rheumatic diseases*, **70**(3):482–487.
- Najm, A., Blanchard, F. and Le Goff, B., 2019. Micro-RNAs in inflammatory arthritis: From physiopathology to diagnosis, prognosis and therapeutic opportunities. *Biochemical pharmacology*, **165**:134–144.

References

- Nezich, C.L., Wang, C., Fogel, A.I. and Youle, R.J., 2015. MiT/TFE transcription factors are activated during mitophagy downstream of Parkin and Atg5. *Journal of Cell Biology*, **210**(3):435–450.
- Nahrendorf, M., Swirski, F.K., Aikawa, E., Stangenberg, L., Wurdinger, T., Figueiredo, J.-L., ... Pittet, M.J. (2007). The healing myocardium sequentially mobilizes two monocyte subsets with divergent and complementary functions. *The Journal of Experimental Medicine* **204**(12):3037.
- Naz, S.M., Farragher T.M., Bunn D.K., Symmons D.P, and I.N. Bruce (2008). The influence of age at symptom onset and length of followup on mortality in patients with recent-onset inflammatory polyarthritis. *Arthritis and Rheumatism*. **58**:985–989.
- Nakamura N, Shimaoka Y, Tougan T, Onda H, Okuzaki D, Zhao H, Fujimori A, Yabuta N, Nagamori I, Tanigawa A, Sato J, Oda T, Hayashida K, Suzuki R, Yukioka M, Nojima H, Ochi T. (2006). Isolation and expression profiling of genes upregulated in bone marrow-derived mononuclear cells of rheumatoid arthritis patients. *DNA Research*.**13**(4):169–83.
- Nath, S., and Mukherjee, P. (2014). MUC1: a multifaceted oncoprotein with a key role in cancer progression. *Trends in molecular medicine*, **20**(6), 332–342.
- Nathan, C., *Mechanisms and modulation of macrophage activation*. Behring Inst Mitt, **1991**(88):200–7.
- Na, Y.R., Jung, D., Song, J., Park, J.W., Hong, J.J. and Seok, S.H., 2020. Pyruvate dehydrogenase kinase is a negative regulator of interleukin-10 production in macrophages. *Journal of molecular cell biology*, **12**(7):543–555.
- Navarini, L., Afeltra, A., Gallo Afflitto, G. and Margiotta, D.P.E. (2017). Polyunsaturated fatty acids: any role in rheumatoid arthritis? *Lipids in health and disease* **16**(1):197–197.
- Nagy, G., Clark, J.M., Buzás, E.I., Gorman, C.L. and Cope, A.P. (2007). Nitric oxide, chronic inflammation and autoimmunity. *Immunology letters* **111**(1):1–5.
- Nagy, G., Koncz, A., Telarico, T., Fernandez, D., Ersek, B., Buzás, E. and Perl, A. (2010). Central role of nitric oxide in the pathogenesis of rheumatoid arthritis and systemic lupus erythematosus. *Arthritis research and therapy* **12**(3):210–210.
- Nathan C, Xie Q-W (1994): Regulation of biosynthesis of nitric oxide. *Journal of Biological Chemistry*, **269**(19): 13725-13728
- Nishitoh H, Saitoh M, Mochida Y, Takeda K, Nakano H, Rothe M, and Ichijo, H. (1999). ASK1 is essential for JNK/SAPK activation by TRAF2. *Molecular Cell*; **2**(3):389–395.
- Nagabhushanam, V., Solache, A., Ting, L. M., Escaron, C. J., Zhang, J. Y., and Ernst, J. D. (2003). Innate inhibition of adaptive immunity: Mycobacterium tuberculosis-induced IL-6 inhibits macrophage responses to IFN- γ . *Journal of Immunology*. **171**(9):4750–7.
- Narasimhan, P.B., Marcovecchio, P., Hamers, A.A. and Hedrick, C.C., (2019). Nonclassical monocytes in health and disease. *Annual review of immunology*, **37**, 439–456.
- Negi, V.S., Mariaselvam, C.M., Misra, D.P., Muralidharan, N., Fortier, C., Charron, D., Krishnamoorthy, R. and Tamouza, R., 2017. Polymorphisms in the promoter region of iNOS predispose to rheumatoid arthritis in south Indian Tamils. *International journal of immunogenetics*, **44**(3).114–121.
- Nevius, E., Gomes, A.C. and Pereira, J.P. (2016). Inflammatory cell migration in rheumatoid arthritis: A Comprehensive Review. *Clinical reviews in allergy and immunology* **51**(1):59–78.
- Nikitin PA, Rose EL, Byun TS, Parry GC, Panicker S. (2019) C1s Inhibition by BIVV009 (Sutimlimab) prevents complement-enhanced activation of autoimmune human B cells In vitro. *Journal Immunology*. **202**(4):1200–1209.

References

- Nishi, K., Itabe, H., Uno, M., Kitazato, K. T., Horiguchi, H., Shinno, K. and Nagahiro, S. (2002). Oxidized LDL in carotid plaques and plasma associates with plaque instability. *Arteriosclerosis Thrombosis and Vascular Biology* **22**:1649–1654.
- NodeK, HuoY, RuanX, YangB, SpieckerM, LeyK, ZeldinDC, LiaoJK (1999). Anti-inflammatory properties of cytochrome P450 epoxygenase-derived eicosanoids. *Science* **285**:1276–1279
- No, D.S. and Kim, I.-H. (2013). Pinolenic acid as a new source of phyto-polyunsaturated fatty acid. *Lipid Technology* **25**(6):135–138.
- Noursadeghi M, Tsang J, Miller RF, Straschewski S, Kellam P, Chain BM, Katz DR. (2009). Genome-wide innate immune responses in HIV-1-infected macrophages are preserved despite attenuation of the NF-kappa B activation pathway. *Journal of Immunology*. **182**(1):319–28.
- Novak TE, Babcock TA, Jho DH, Helton WS, Espat NJ (2003). NF-kappa B inhibition by omega -3 fatty acids modulates LPS-stimulated macrophage TNF-alpha transcription. *American Journal of Physiology-Lung Cellular and Molecular Physiology*; **284**(1): 84-89.
- Obeng, J. A., Amoruso, A., Camaschella, G. L. E., Sola, D., Brunelleschi, S., and Fresu, L. G. (2016). Modulation of human monocyte/macrophage activity by tocilizumab, abatacept and etanercept: An in vitro study. *European Journal of Pharmacology*, **780**:33–37.
- Ohashi, R., Mu, H., Wang, X., Yao, Q. and Chen, C. (2005). Reverse cholesterol transport and cholesterol efflux in atherosclerosis. *QJM: An International Journal of Medicine* **98**(12):845–856.
- Öhman, M.K., Wright, A.P., Wickenheiser, K.J., Luo, W., Russo, H.M. and Eitzman, D.T. (2010). Monocyte chemoattractant protein-1 deficiency protects against visceral fat-induced atherosclerosis. *Arteriosclerosis Thrombosis Vascular Biology*, **30**:1151–1158.
- Ohta, H., Wada, H., Niwa, T., Kirii, H., Iwamoto, N., Fujii, H., Saito, K., Sekikawa, K. and Seishima, M., (2005). Disruption of tumor necrosis factor- α gene diminishes the development of atherosclerosis in ApoE-deficient mice. *Atherosclerosis*, **180** (1).11–17.
- Olliver, M., Hiew, J., Mellroth, P., Henriques-Normark, B. and Bergman, P., (2011). Human monocytes promote Th1 and Th17 responses to *Streptococcus pneumoniae*. *Infection and immunity*, **79**(10):4210-421.
- Oltman CL, Weintraub NL, VanRollins M, Dellsperger KC (1998). Epoxyeicosatrienoic acids and dihydroxyeicosatrienoic acids are potent vasodilators in the canine coronary microcirculation. *Circulation research*, **83**(9):932-939.
- Oike, T., Sato, Y., Kobayashi, T., Miyamoto, K., Nakamura, S., Kaneko, Y., Kobayashi, S., Harato, K., Saya, H., Matsumoto, M. and Nakamura, M., (2017). Stat3 as a potential therapeutic target for rheumatoid arthritis. *Scientific reports*, **7**(1): 1-9.
- Okamoto, H., Yamamura, M., Morita, Y., Harada, S., Makino, H. and Ota, Z. (1997). The synovial expression and serum levels of interleukin-6, interleukin-11, leukemia inhibitory factor, and oncostatin M in rheumatoid arthritis. *Arthritis & Rheumatism: Official Journal of the American College of Rheumatology* **40**(6):1096–1105.
- Okroj M, Heinegård D, Holmdahl R, Blom AM (2007). Rheumatoid arthritis and the complement system. *Annals of Medicine*, **39**(7):517–530.
- Oksala, N., Pärssinen, J., Seppälä, I., Klopp, N., Illig, T., Laaksonen, R., Levula, M., Raitoharju, E., Kholova, I., Sioris, T. and Kähönen, M., (2015). Kindlin 3 (FERMT3) is associated with unstable atherosclerotic plaques, anti-inflammatory type II macrophages and upregulation of beta-2 integrins in all major arterial beds. *Atherosclerosis*, **242**(1):145–154.

References

- Orlicky DJ, Lieber JG, Morin CL, Evans RM. (1998). Synthesis and accumulation of a receptor regulatory protein associated with lipid droplet accumulation in 3T3-L1 cells. *Journal of Lipid Research*. **39**(6):1152–61.
- Orlicky DJ, Berry R, Sikela JM (1996). "Human chromosome 1 localization of the gene for a prostaglandin F2alpha receptor negative regulatory protein". *Human Genetics*. **97**(5): 655–8.
- Ospelt, C., Brentano, F., Rengel, Y., Stanczyk, J., Kolling, C., Tak, P.P., ... Kyburz, D. (2008). Overexpression of toll-like receptors 3 and 4 in synovial tissue from patients with early rheumatoid arthritis: Toll-like receptor expression in early and longstanding arthritis. *Arthritis and Rheumatism* **58**(12):3684–3692.
- O'Morain, V. L., Chan, Y. H., Williams, J. O., Alotibi, R., Alahmadi, A., Rodrigues, N. P., ... and Ramji, D. P. (2021). The Lab4P Consortium of Probiotics Attenuates Atherosclerosis in LDL Receptor Deficient Mice Fed a High Fat Diet and Causes Plaque Stabilization by Inhibiting Inflammation and Several Pro-Atherogenic Processes. *Molecular Nutrition and Food Research*, **65**(17): 2100214.
- O'Neill, L.A. and Pearce, E.J. (2016). Immunometabolism governs dendritic cell and macrophage function. *Journal of Experimental Medicine* **213**(1):15–23.
- Ozdemir, O., Gundogdu, F., Karakelleoglu, S., Sevimli, S., Pirim, I., Acikel, M., Arslan, S. and Serdar, S., (2008). Comparison of serum levels of inflammatory markers and allelic variant of interleukin-6 in patients with acute coronary syndrome and stable angina pectoris. *Coronary artery disease*, **19**(1):15-19.
- Ozaki, Y., Imanishi, T., Hosokawa, S., Nishiguchi, T., Taruya, A., Tanimoto, T., Kuroi, A., Yamano, T., Matsuo, Y., Ino, Y. and Kitabata, H., (2017). Association of toll-like receptor 4 on human monocyte subsets and vulnerability characteristics of coronary plaque as assessed by 64-slice multidetector computed tomography. *Circulation Journal*, **81**(6):837-845
- Palsson-McDermott, E.M., Curtis, A.M., Goel, G., Lauterbach, M.A., Sheedy, F.J., Gleeson, L.E., van den Bosch, M.W., Quinn, S.R., Domingo-Fernandez, R., Johnston, D.G. and Jiang, J.K., (2015). Pyruvate kinase M2 regulates Hif-1 α activity and IL-1 β induction and is a critical determinant of the warburg effect in LPS-activated macrophages. *Cell metabolism*, **21**(1):65–80
- Panga, V., Kallor, A.A., Nair, A., Harshan, S. and Raghunathan, S. (2019). Mitochondrial dysfunction in rheumatoid arthritis: a comprehensive analysis by integrating gene expression, protein-protein interactions and gene ontology data. *PLoS one* **14**(11) e0224632.
- Parekh, S., Ziegenhain, C., Vieth, B., Enard, W. and Hellmann, I., (2016). The impact of amplification on differential expression analyses by RNA-seq. *Scientific reports*, **6**(1):1–11.
- Park, E.K., Jung, H.S., Yang, H.I., Yoo, M.C., Kim, C. and Kim, K.S. (2007). Optimized thp-1 differentiation is required for the detection of responses to weak stimuli. *Inflammation Research*. **56**(1):45–50.
- Park, S., Lim, Y., Shin, S. and Han, S.N. (2013). Impact of Korean pine nut oil on weight gain and immune responses in high-fat diet-induced obese mice. *Nutraceutical Research Practice* **7**(5):352–358.
- Park, H. J., Baek, K., Baek, J. H., & Kim, H. R. (2017). TNF α Increases RANKL Expression via PGE $_2$ -Induced Activation of NFATc1. *International journal of molecular sciences*, **18**(3):495.
- Park, Y.B., Ahn, C.W., Choi, H.K., Lee, S.H., In, B.H., Lee, H.C., Nam, C.M. and Lee, S.K., (2002). Atherosclerosis in rheumatoid arthritis: morphologic evidence obtained by carotid ultrasound. *Vascular Biology*, **18** (7):1714–1719.
- Park, Y. M., Febbraio, M. and Silverstein, R. L. (2009). CD36 modulates migration of mouse and human macrophages in response to oxidized LDL and may contribute to macrophage trapping in the arterial intima. *Journal of Clinical Investigation* **119**(1):136–145.

References

- Park KH, Lee TH, Kim CW, Kim J(2013). Enhancement of CCL15 expression and monocyte adhesion to endothelial cells (ECs) after hypoxia/reoxygenation and induction of ICAM-1 expression by CCL15 via the JAK2/STAT3 pathway in ECs. *Journal Immunology*,**190**(12):6550-8.
- Park Y, Shon SK, Kim A, Kim KI, Yang Y, Cho DH, Lee MS, Lim JS. (2007) SOCS1 induced by NDRG2 expression negatively regulates STAT3 activation in breast cancer cells. *Biochem Biophys Research Communication*,**363**:361–367.
- Parzych KR, Klionsky DJ. (2014). An overview of autophagy: morphology, mechanism, and regulation. *Antioxid Redox Signal*;**20**(3):460–73.
- Pastore, N., Brady, O.A., Diab, H.I., Martina, J.A., Sun, L., Huynh, T., Lim, J.A., Zare, H., Raben, N., Ballabio, A. and Puertollano, R., (2016). TFEB and TFE3 cooperate in the regulation of the innate immune response in activated macrophages. *Autophagy*, **12**(8):1240–1258.
- Pasman, W.J., Heimerikx, J., Rubingh, C.M., van den Berg, R., O'Shea, M., Gambelli, L., Hendriks, H.F., Einerhand, A.W., Scott, C., Keizer, H.G. and Mennen, L.I., (2008). The effect of Korean pine nut oil on in vitro CCK release, on appetite sensations and on gut hormones in post-menopausal overweight women. *Lipids in Health and Disease*, **7**(1):1–10.
- Perez-Sanchez, C., L. M. Sánchez-Mendoza, M. D. C. Abalos-Aguilera, N. Barbarroja Puerto, M. Luque-Tévar, A. M. Patiño-Trives, I. Arias de la Rosa et al. "POS0394 NAD+ BOOSTERS REESTABLISH THE ALTERED NAD+ METABOLISM OF LEUKOCYTES FROM RHEUMATOID ARTHRITIS PATIENTS IMPROVING THEIR OXIDATIVE, APOPTOTIC AND INFLAMMATORY STATUS." (2021): 426–426.
- Palomino-Morales, R., Gonzalez-Juanatey, C., Vazquez-Rodriguez, T.R., Rodriguez, L., Miranda-Fillooy, J.A., Fernandez-Gutierrez, B., Gonzalez-Gay, M.A. (2010). A1298C polymorphism in the MTHFR gene predisposes to cardiovascular risk in rheumatoid arthritis. *Arthritis research and therapy* **12**(2):R71.
- Pasceri, V. and Yeh, E.T.H. (1999). A Tale of Two Diseases: Atherosclerosis and Rheumatoid Arthritis. *Circulation* **100**(21):2124–2126.
- Patterson, E., Wall, R., Fitzgerald, G.F., Ross, R.P. and Stanton, C., (2012). Health implications of high dietary omega-6 polyunsaturated fatty acids. *Journal of nutrition and metabolism*, **2012**.
- Pettersen, I.K.N., Tusubira, D., Ashrafi, H., Dyrstad, S.E., Hansen, L., Liu, X.-Z., ... Tronstad, K.J. (2019). Upregulated PDK4 expression is a sensitive marker of increased fatty acid oxidation. *Mitochondrion* **49**:97–110.
- Perdiguero, E.G., Klapproth, K., Schulz, C., Busch, K., Azzoni, E., Crozet, L., ... Geissmann, F. (2015). Tissue-resident macrophages originate from yolk-sac-derived erythro-myeloid progenitors. *Nature* **518**(7540):547.
- Petri M, Perez-Gutthann S, Spence D, Hochberg MC (1992). Risk factors for coronary artery disease in patients with systemic lupus erythematosus. *American Journal of Medicine* **93**:513–9.
- Peters, M.J.L., Symmons, D.P.M., McCarey, D., Dijkmans, B.A.C., Nicola, P., Kvien, T.K., McInnes, I.B., Haentzschel, H., Gonzalez-Gay, M.A., Provan, S. and Semb, A.,(2010). EULAR evidence-based recommendations for cardiovascular risk management in patients with rheumatoid arthritis and other forms of inflammatory arthritis. *Annals of the rheumatic diseases*, **69**(2):325–331.
- Picchio MC, Scala E, Pomponi D, Caprini E, Frontani M, Angelucci I, Mangoni A, Lazzeri C, Perez M, Remotti D, Bonoldi E, Benucci R, Baliva G, Lombardo GA, Napolitano M, Russo G, Narducci MG. (2008). CXCL13 is highly produced by Sézary cells and enhances their migratory ability via a synergistic mechanism involving CCL19 and CCL21 chemokines. *Cancer Research*. **68**(17):7137–46.
- Picard, F., Kurtev, M., Chung, N., Topark-Ngarm, A., Senawong, T., De Oliveira, R.M., Leid, M., McBurney, M.W. and Guarente, L., (2004). Sirt1 promotes fat mobilization in white adipocytes by repressing PPAR- γ . *Nature*, **429**(6993):771–776.

References

- Pierer, M., Rethage, J., Seibl, R., Lauener, R., Brentano, F., Wagner, U., Kyburz, D (2004), Chemokine secretion of rheumatoid arthritis synovial fibroblasts stimulated by Toll-like receptor 2 ligands. *Journal of Immunology*, **172**(2):1256–65
- Pisani, L.F., Lecchi, C., Invernizzi, G., Sartorelli, P., Savoini, G. and Ceciliani, F. (2009). In vitro modulatory effect of omega-3 polyunsaturated fatty acid (EPA and DHA) on phagocytosis and ROS production of goat neutrophils. *Veterinary immunology and immunopathology* **131**(1–2):79–85.
- Pompéia, C., Lopes, L.R., Miyasaka, C.K., Procópio, J., Sannomiya, P., and Curi, R.. (2000). Effect of fatty acids on leukocyte function. *Brazilian Journal of Medical and Biological Research*, **33**(11):1255–1268.
- Pompéia, C., Procópio, J. and Curi, R., (1999). Fatty acids and the immune system. *brazilian journal pharmaceutical sciences*, **35**(2):165–94.
- Popa, C., Netea, M.G., Riel, P.L.C.M. van, Meer, J.W.M. van der and Stalenhoef, A.F.H. (2007). The role of TNF- α in chronic inflammatory conditions, intermediary metabolism, and cardiovascular risk. *Journal of Lipid Research* **48**(4):751–762.
- Powell, L.D. and Varki, A., 1995. I-type lectins. *Journal of Biological Chemistry*, **270**(24): 14243–14246.
- Protheroe, A., Edwards, J.C.W., Simmons, A., Maclennan, K. and Selby, P. (1999). Remission of inflammatory arthropathy in association with anti-CD20 therapy for non-Hodgkin's lymphoma. *Rheumatology* **38**(11):1150–1152.
- Pruijn, G.J. (2015). Citrullination and carbamylation in the pathophysiology of rheumatoid arthritis. *Frontiers in immunology* **6**:192.
- Pujades-Rodriguez, M., Duyx, B., Thomas, S.L., Stogiannis, D., Rahman, A., Smeeth, L. and Hemingway, H. (2016). Rheumatoid arthritis and incidence of twelve initial presentations of cardiovascular disease: a population record-linkage cohort study in England. *PLoS one* **11**(3):e0151245.
- Puel, A., Picard, C., Lorrot, M., Pons, C., Chrabieh, M., Lorenzo, L., Mamani-Matsuda, M., Jouanguy, E., Gendrel, D. and Casanova, J.L., (2008). Recurrent staphylococcal cellulitis and subcutaneous abscesses in a child with autoantibodies against IL-6. *The Journal of Immunology*, **180**(1):647–654.
- Qin, Z. (2012). The use of thp-1 cells as a model for mimicking the function and regulation of monocytes and macrophages in the vasculature. *Atherosclerosis* **221**:2–11.
- Qiu, Y., Zhou, X., Liu, Y., Tan, S. and Li, Y., (2021). The Role of Sirtuin-1 in Immune Response and Systemic Lupus Erythematosus. *Frontiers in immunology*, **12**:632383.
- Quiñonez-Flores, C.M., González-Chávez, S.A., Del Rio Najera, D. and Pacheco-Tena, C. (2016). Oxidative stress relevance in the pathogenesis of the rheumatoid arthritis: a systematic review. *BioMed research international* 2016.
- Rabieian, R., Boshtam, M., Zareei, M., Kouhpayeh, S., Masoudifar, A. and Mirzaei, H., (2018). Plasminogen activator inhibitor type-1 as a regulator of fibrosis. *Journal of cellular biochemistry*, **119**(1):17–27.
- Rodríguez-Prados, J.C., Través, P.G., Cuenca, J., Rico, D., Aragonés, J., Martín-Sanz, P., Cascante, M. and Boscá, L., (2010). Substrate fate in activated macrophages: a comparison between innate, classic, and alternative activation. *The Journal of Immunology*, **185**(1):605–614.
- Rosillo MA, Sánchez-Hidalgo M, Sánchez-Fidalgo S, Aparicio-Soto M, Villegas I, Alarcón-de-la-Lastra C (2016). Dietary extra-virgin olive oil prevents inflammatory response and cartilage matrix degradation in murine collagen-induced arthritis. *European Journal Nutrition* **55**(1):315–25.

References

- Rahman, M.M., Bhattacharya, A. and Fernandes, G., (2008). Docosahexaenoic acid is more potent inhibitor of osteoclast differentiation in RAW 264.7 cells than eicosapentaenoic acid. *Journal of cellular physiology*, **214**(1):201–209.
- Ramiro, S., Gaujoux-Viala, C., Nam, J.L., Smolen, J.S., Buch, M., Gossec, L., ... Landewé, R. (2014). Safety of synthetic and biological DMARDs: a systematic literature review informing the 2013 update of the EULAR recommendations for management of rheumatoid arthritis. *Annals of the rheumatic diseases* **73**(3):529–535.
- Ramiro-Puig, E. and Castell, M., (2009). Cocoa: antioxidant and immunomodulator. *British Journal of Nutrition*, **101**(7):931–940.
- Ramji, D.P. and Davies, T.S. (2015). Cytokines in atherosclerosis: Key players in all stages of disease and promising therapeutic targets. *Cytokine and growth factor reviews*, **26**(6):673–685.
- Rana, A.K., Li, Y., Dang, Q. and Yang, F. (2018). Monocytes in rheumatoid arthritis: Circulating precursors of macrophages and osteoclasts and, their heterogeneity and plasticity role in RA pathogenesis. *International Immunopharmacology* **65**:348–359.
- Randolph, G.J., Sanchez-Schmitz, G., Liebman, R.M. and Schäkel, K. (2002). The CD16+ (FcγRIII+) subset of human monocytes preferentially becomes migratory dendritic cells in a model tissue setting. *Journal of Experimental Medicine*, **196**(4), pp.517-527.
- Ranganathan, V., Ciccia, F., Zeng, F., Sari, I., Guggino, G., Muralitharan, J., ... Haroon, N. (2017). Macrophage Migration Inhibitory Factor Induces Inflammation and Predicts Spinal Progression in Ankylosing Spondylitis. *Arthritis and Rheumatology* **69**(9):1796–1806.
- Rau, R. (2014). Glucocorticoid treatment in rheumatoid arthritis. *Expert opinion on pharmacotherapy* **15**(11):1575–1583.
- Rau, R., Sander, O. Wassenberg, S. (2003). Erosion healing in rheumatoid arthritis after anakinra treatment. *Annals of Rheumatic Disease*. **62**, 671–673.
- Rauch, A., Seitz, S., Baschant, U., Schilling, A.F., Illing, A., Stride, B., Kirilov, M., Takacz, A., Schmidt-Ullrich, R., Ostermay, S. and Schinke, T., (2010). Glucocorticoids suppress bone formation by attenuating osteoblast differentiation via the monomeric glucocorticoid receptor. *Cell metabolism*, **11**(6):517–531.
- Rediske, J.J., Koehne, C.F., Zhang, B. and Lotz, M., (1994). The inducible production of nitric oxide by articular cell types. *Osteoarthritis and Cartilage*, **2**(3)199–206.
- Reed, J.C. (2001). Apoptosis-regulating proteins as targets for drug discovery. *Trends in Molecular Medicine* **7**(7), 314–319.
- Reyes, A., Anders, S., Weatheritt, R.J., Gibson, T.J., Steinmetz, L.M. and Huber, W., (2013). Drift and conservation of differential exon usage across tissues in primate species. *Proceedings of the National Academy of Sciences*, **110**(38):15377–15382.
- Ricciotti Emanuela and FitzGerald Garret A. (2011). Prostaglandins and Inflammation. *Arteriosclerosis, Thrombosis, and Vascular Biology* **31**(5):986–1000.
- Ridker, P.M., Everett, B.M., Thuren, T., MacFadyen, J.G., Chang, W.H., Ballantyne, C., Fonseca, F., Nicolau, J., Koenig, W., Anker, S.D. and Kastelein, J.J., (2017). Anti-inflammatory therapy with canakinumab for atherosclerotic disease. *New England journal of medicine*, **377**(12): 1119–1131.
- Ridker, P.M., MacFadyen, J.G., Everett, B.M., Libby, P., Thuren, T., Glynn, R.J., Kastelein, J., Koenig, W., Genest, J., Lorenzatti, A. and Varigos, J., (2018). Relationship of C-reactive protein reduction to cardiovascular event

References

- reduction following treatment with canakinumab: a secondary analysis from the CANTOS randomised controlled trial. *The Lancet*, **391**(10118):319–328.
- Rigamonti Elena, Chinetti-Gbaguidi Giulia, and Staels Bart (2008). Regulation of Macrophage Functions by PPAR- α , PPAR- γ , and LXRs in Mice and Men. *Arteriosclerosis, Thrombosis, and Vascular Biology* **28**(6):1050–1059.
- Riva, F., Bonavita, E., Barbati, E., Muzio, M., Mantovani, A. and Garlanda, C. (2012). TIR8/SIGIRR is an Interleukin-1 Receptor/Toll Like Receptor Family Member with Regulatory Functions in Inflammation and Immunity. *Frontiers in Immunology* **3**:322.
- Roessler, C., Kuhlmann, K., Hellwing, C., Leimert, A. and Schumann, J., (2017). Impact of polyunsaturated fatty acids on miRNA profiles of monocytes/macrophages and endothelial cells—a pilot study. *International journal of molecular sciences*, **18**(2):284.
- Roberts, C.A., Dickinson, A.K. and Taams, L.S. (2015). The Interplay Between Monocytes/Macrophages and CD4(+) T Cell Subsets in Rheumatoid Arthritis. *Frontiers in immunology* **6**:571–571.
- Rodgers, J.T., Lerin, C., Haas, W., Gygi, S.P., Spiegelman, B.M. and Puigserver, P., (2005). Nutrient control of glucose homeostasis through a complex of PGC-1 α and SIRT1. *Nature*, **434**(7029):113-118.
- Rogacev, K.S., Cremers, B., Zawada, A.M., Seiler, S., Binder, N., Ege, P., Große-Dunker, G., Heisel, I., Hornof, F., Jeken, J. and Rebling, N.M., (2012). CD14⁺⁺ CD16⁺ monocytes independently predict cardiovascular events: a cohort study of 951 patients referred for elective coronary angiography. *Journal of the American College of Cardiology*, **60**(16):1512–1520.
- Rollins BJ, Yoshimura T, Leonard EJ, Pober JS. (1990). Cytokineactivated human endothelial cells synthesize and secrete a monocyte chemoattractant, MCP-1/JE. *American Journal of Pathology*; **136**:1229–1233
- Romero, I.G., Pai, A.A., Tung, J. and Gilad, Y. (2014). RNA-seq: impact of RNA degradation on transcript quantification. *BMC biology* **12**(1):1–13.
- Ronday, H.K., Smits, H.H., Quax, P.H., Van Der Pluijm, G., Löwik, C.W., Breedveld, F.C. and Verheijen, J.H., (1997). Bone matrix degradation by the plasminogen activation system. Possible mechanism of bone destruction in arthritis. *British journal of rheumatology*, **36**(1):9–15.
- Rosales C, Uribe-Querol E (2017). Phagocytosis: A Fundamental Process in Immunity. *Biomedical Research International*. **2017**:9042851.
- Rossi, A., Kapahi, P., Natoli, G., Takahashi, T., Chen, Y., Karin, M. and Santoro, M.G., (2000). Anti-inflammatory cyclopentenone prostaglandins are direct inhibitors of I κ B kinase. *Nature*, **403**(6765):103–108.
- Rossol, M., Meusch, U., Pierer, M., Kaltenhäuser, S., Häntzschel, H., Hauschildt, S. and Wagner, U. (2007). Interaction between transmembrane TNF- α and TNFR1/2 mediates the activation of monocytes by contact with T cells. *The Journal of Immunology* **179**(6):4239–4248.
- Rossol, M., Kraus, S., Pierer, M., Baerwald, C. and Wagner, U., (2012). The CD14^{bright}CD16⁺ monocyte subset is expanded in rheumatoid arthritis and promotes expansion of the Th17 cell population. *Arthritis and Rheumatism*, **64**(3):671–677.
- Rooney, T., Murphy, E., Benito, M., Roux-Lombard, P., FitzGerald, O., Dayer, J.M. and Bresnihan, B., (2004). Synovial tissue interleukin-18 expression and the response to treatment in patients with inflammatory arthritis. *Annals of the rheumatic diseases*, **63**(11):1393–1398.
- Roubille C, Richer V, Starnino T, et al (2015). The effects of tumour necrosis factor inhibitors, methotrexate, non-steroidal anti-inflammatory drugs and corticosteroids on cardiovascular events in rheumatoid arthritis, psoriasis and psoriatic arthritis: a systematic review and meta-analysis. *Annals Rheumatology Disease*; **74**(3):480–9.

References

- Rontoyanni, V., P Sfikakis, P., D Kitas, G. and D Protogerou, A., (2012). Marine n-3 fatty acids for cardiovascular risk reduction and disease control in rheumatoid arthritis: "Kill two Birds with one Stone"? *Current pharmaceutical design*, **18**(11):1531–1542.
- Rückert, R., Brandt, K., Ernst, M., Marienfeld, K., Csernok, E., Metzler, C., ... Bulfone-Paus, S. (2009). Interleukin-15 stimulates macrophages to activate CD4⁺ T cells: a role in the pathogenesis of rheumatoid arthritis? *Immunology* **126**(1):63–73.
- Ruiz-García, A., Monsalve, E., Novellasdemunt, L., Navarro-Sabaté, À., Manzano, A., Rivero, S., Castrillo, A., Casado, M., Laborda, J., Bartrons, R. and Díaz-Guerra, M.J.M., (2011). Cooperation of adenosine with macrophage Toll-4 receptor agonists leads to increased glycolytic flux through the enhanced expression of PFKFB3 gene. *Journal of Biological Chemistry*, **286**(22):19247–19258.
- Ruston, A. and Drevon, C. (2001). *Fatty Acids: Structure and Properties*. eLS.
- Ruth, J.H., Park, C.C., Amin, M.A., Lesch, C., Marotte, H., Shahrara, S. and Koch, A.E. (2010). Interleukin-18 as an in vivo mediator of monocyte recruitment in rodent models of rheumatoid arthritis. *Arthritis research and therapy* **12**(3):R118.
- Ruth, J.H., Volin, M.V., Haines III, G.K., Woodruff, D.C., Katschke Jr, K.J., Woods, J.M., Park, C.C., Morel, J.C. and Koch, A.E., (2001). Fractalkine, a novel chemokine in rheumatoid arthritis and in rat adjuvant-induced arthritis. *Arthritis & Rheumatism: Official Journal of the American College of Rheumatology*, **44**(7):1568–1581.
- Salonen, J.T. et al. (1992). Autoantibody against oxidised LDL and progression of carotid atherosclerosis. *Originally published as Volume 1* (339):883–887.
- Sakurai, H., H. Kohsaka, M-F. Liu, H. Higashiyama, Y. Hirata, K. Kanno, I. Saito, and N. Miyasaki. (1995). Nitric oxide production and inducible nitric oxide synthase expression in inflammatory arthritides. *Journal of Clinical Investigation*. **96**:2357-2363.
- Sattar N, McCarey DW, Capell H, McInnes IB (2003). Explaining How "High-Grade" Systemic Inflammation Accelerates Vascular Risk in Rheumatoid Arthritis. *Circulation*. **108**(24):2957–63.
- Sattar, N. and McInnes, I.B. (2005). Vascular comorbidity in rheumatoid arthritis: potential mechanisms and solutions. *Current opinion in rheumatology* **17**(3):286–292.
- Shapiro, J.A., Koepsell, T.D., Voigt, L.F., Dugowson, C.E., Kestin, M. and Nelson, J.L., (1996). Diet and rheumatoid arthritis in women: a possible protective effect of fish consumption. *Epidemiology*, **7**:(256-263).
- Sharif, K., Watad, A., Bragazzi, N.L., Adawi, M., Amital, H. and Shoenfeld, Y., (2017). Coffee and autoimmunity: more than a mere hot beverage!. *Autoimmunity reviews*, **16**(7):712–721.
- Sharif, K., Amital, H. and Shoenfeld, Y., (2018). The role of dietary sodium in autoimmune diseases: The salty truth. *Autoimmunity reviews*, **17**(11):1069–1073.
- Schaiff, W.T., Carlson, M.G., Smith, S.D., Levy, R., Nelson, D.M. and Sadovsky, Y. (2000). Peroxisome Proliferator-Activated Receptor- γ Modulates Differentiation of Human Trophoblast in a Ligand-Specific Manner. *The Journal of Clinical Endocrinology & Metabolism* **85**(10):3874–3881.
- Schett, G., K.G. Saag, and J.W. Bijlsma (2010). From bone biology to clinical outcome: state of the art and future perspectives. *Ann Rheum Dis*, **69**(8):1415–9.
- Schneemann, M., G. Schoedon, S. Hoefler, N. Blau, L. Guerrero, and A. Schaffner. (1993). Nitric oxide synthase is not a constituent of the antimicrobial armature of human mononuclear phagocytes. *Journal of Infectious Disease*. **167** (6): 358-1363.

References

- Schett, G., Elewaut, D., McInnes, I.B., Dayer, J.-M. and Neurath, M.F. (2013). How cytokine networks fuel inflammation: toward a cytokine-based disease taxonomy. *Nature medicine* **19**(7):822.
- Schett, G., Kiechl, S., Weger, S., Pederiva, A., Mayr, A., Petrangeli, M., Oberhollenzer, F., Lorenzini, R., Redlich, K., Axmann, R. and Zwerina, J., (2006). High-sensitivity C-reactive protein and risk of nontraumatic fractures in the Bruneck study. *Archives of internal medicine*. **166**(22):2495–2501.
- Schett, G. (2009), Osteoimmunology in rheumatic diseases. *Arthritis Research Therapy*. **11**(1):210.
- Schett, G. (2017). Autoimmunity as a trigger for structural bone damage in rheumatoid arthritis. *Modern Rheumatology* **27**(2):193–197.
- Schett, G., Dayer, J.-M. and Manger, B. (2016). Interleukin-1 function and role in rheumatic disease. *Nature Reviews Rheumatology* **12**(1):14–24.
- Schiff, M. H. (2000). Role of interleukin 1 and interleukin 1 receptor antagonist in the mediation of rheumatoid arthritis. *Annals of the Rheumatic Diseases* **59**(90001):1031–1108.
- Schett G, Gravalles E (2012). Bone erosion in rheumatoid arthritis: mechanisms, diagnosis and treatment. *Nature Review of Rheumatology* **8**(11): 656–664.
- Schoeniger, A., Adolph, S., Fuhrmann, H. and Schumann, J., (2011). The impact of membrane lipid composition on macrophage activation in the immune defense against *Rhodococcus equi* and *Pseudomonas aeruginosa*. *International Journal of Molecular Sciences*, **12**(11): 7510-7528.
- Schoonjans K, Watanabe M, Suzuki H, Mahfoudi A, Krey G, Wahli W, Grimaldi P, Staels B, Yamamoto T and Auwerx J (1995). Induction of the acyl-coenzyme A synthetase gene by fibrates and fatty acids is mediated by a peroxisome proliferator response element in the C promoter. *Journal of Biological Chemistry*, **270**: 19269-19276.
- Shouda, T., Yoshida, T., Hanada, T., Wakioka, T., Oishi, M., Miyoshi, K., Komiya, S., Kosai, K.I., Hanakawa, Y., Hashimoto, K. and Nagata, K., (2001). Induction of the cytokine signal regulator SOCS3/CIS3 as a therapeutic strategy for treating inflammatory arthritis. *The Journal of clinical investigation*, **108**(12):1781–1788.
- Schraufstatter, I. U., Zhao, M., Khaldoyanidi, S. K., and Discipio, R. G. (2012). The chemokine CCL18 causes maturation of cultured monocytes to macrophages in the M2 spectrum. *Immunology*, **135**(4):287–298.
- Schroder, K., Zhou, R. and Tschopp, J (2010). The NLRP3 inflammasome: a sensor for metabolic danger? *Science* **327**: 296–300
- Schuerwegh, A., Stevens, W., Bridts, C. and De Clerck, L. (2001). Evaluation of monensin and brefeldin A for flow cytometric determination of interleukin-1 beta, interleukin-6, and tumor necrosis factor-alpha in monocytes. *Cytometry*, **46** (3): 172–176.
- Schulman, I.G. and Heyman, R.A., (2004). The flip side: Identifying small molecule regulators of nuclear receptors. *Chemistry & biology*, **11**(5):639–646.
- Sharma R, Sharma PR, Kim YC, Leitinger N, Lee JK, Fu SM, Ju ST. (2011). IL-2-controlled expression of multiple T cell trafficking genes and Th2 cytokines in the regulatory T cell-deficient scurfy mice: implication to multiorgan inflammation and control of skin and lung inflammation. *Journal Immunology*. **186**(2):1268-78.
- Shand, B., C. Strey, R. Scott, Z. Morrison and S. Gieseg, (2003). Pilot study on the clinical effects of dietary supplementation with Enzogenol, a flavonoid extract of pine bark and vitamin C. *Physiotherapy Research*, **17**(5):490-494.
- Schmitz, G. and Ecker, J., (2008). The opposing effects of n-3 and n-6 fatty acids. *Progress in lipid research*, **47**(2):147-155.

References

- Shipa, M.R.A., Amarnani, R., Yeoh, S.-A., Mainuddin, M.D. and Ehrenstein, M.R. (2021). Early reduction in circulating monocyte count predicts maintenance of remission in patients with rheumatoid arthritis treated with anti-TNF therapy. *Annals of the Rheumatic Diseases*, p-220642.
- Shashkin, P., Dragulev, B. and Ley, K. (2005). Macrophage differentiation to foam cells. *Current Pharmaceutical Design* **11**:3061–3072.
- Shi, C., Jia, T., Mendez-Ferrer, S., Hohl, T.M., Serbina, N.V., Lipuma, L., ... Pamer, E.G. (2011). Bone marrow mesenchymal stem and progenitor cells induce monocyte emigration in response to circulating toll-like receptor ligands. *Immunity* **34**(4):590–601.
- Shi, C. and Pamer, E.G. (2011). Monocyte recruitment during infection and inflammation. *Nature reviews immunology* **11**(11):762.
- Settembre, C., De Cegli, R., Mansueto, G., Saha, P.K., Vetrini, F., Visvikis, O., Huynh, T., Carissimo, A., Palmer, D., Klisch, T.J. and Wollenberg, A.C., (2013). TFEB controls cellular lipid metabolism through a starvation-induced autoregulatory loop. *Nature cell biology*, **15**(6):647–658.
- Sidahmed, A.M., León, A.J., Bosinger, S.E., Banner, D., Danesh, A., Cameron, M.J. and Kelvin, D.J., (2012). CXCL10 contributes to p38-mediated apoptosis in primary T lymphocytes in vitro. *Cytokine*, **59**(2):433–441.
- Singh, U. and Jialal, I. (2006). Oxidative stress and atherosclerosis. *Pathophysiology: the official journal of the International Society for Pathophysiology / ISP* **13**:129–142.
- Sigal LH (2006). Basic science for the clinician 39: NF-kappaB-function, activation, control, and consequences. *J Clinical Rheumatology* **12**(4):207–11.
- Silver, J.S., et al. (2011). IL-6 mediates the susceptibility of glycoprotein 130 hypermorphs to *Toxoplasma gondii*. *Journal of Immunology*. **187**(1): 350–60.
- Simopoulos, A.P., (1996). The role of fatty acids in gene expression: health implications. *Annals of nutrition and metabolism*, **40**(6):303–311.
- Singh, U., Dasu, M.R., Yancey, P.G., Afify, A., Devaraj, S. and Jialal, I., (2008). Human C-reactive protein promotes oxidized low density lipoprotein uptake and matrix metalloproteinase-9 release in Wistar rats. *Journal of lipid research*, **49**(5):1015–1023.
- Sladek, F.M., (2011). What are nuclear receptor ligands?. *Molecular and cellular endocrinology*, **334**(1-2): 3–13.
- Smolen, J.S., Landewé, R., Bijlsma, J., Burmester, G., Chatzidionysiou, K., Dougados, M., van der Heijde, D. (2017). EULAR recommendations for the management of rheumatoid arthritis with synthetic and biological disease-modifying antirheumatic drugs: 2016 update. *Annals of the Rheumatic Diseases* **76**(6):960–977.
- Smolen, J.S., Landewé, R.B., Bijlsma, J.W., Burmester, G.R., Dougados, M., Kerschbaumer, A., McInnes, I.B., Sepriano, A., Van Vollenhoven, R.F., De Wit, M. and Aletaha, D., (2020). EULAR recommendations for the management of rheumatoid arthritis with synthetic and biological disease-modifying antirheumatic drugs: 2019 update. *Annals of the rheumatic diseases*, **79**(6): 685–699.
- Smolen, J.S., Han, C., Bala, M., Maini, R.N., Kalden, J.R., Van der Heijde, D., Breedveld, F.C., Furst, D.E., Lipsky, P.E. and ATTRACT Study Group, (2005). Evidence of radiographic benefit of treatment with infliximab plus methotrexate in rheumatoid arthritis patients who had no clinical improvement: a detailed subanalysis of data from the Anti-Tumor Necrosis Factor Trial in Rheumatoid Arthritis with Concomitant Therapy study. *Arthritis and Rheumatism*, **52**(4):1020–1030.

References

- Stadler J, Harbrecht BG, DiSilvio M, Curran RD, Jordan ML, Simmons RL, Billiar TR (1993): Endogenous nitric oxide inhibits the synthesis of cyclooxygenase products and interleukin-6 by rat kupffer cells. *Journal Leukocyte Biology* **53**:165–172.
- Stichtenoth DO, Fauler J, Zeidler H et al (1995): Urinary nitrate excretion is increased in patients with rheumatoid arthritis and reduced by prednisolone. *Annals of Rheumatic Disease* **54**: 820–824.
- St Clair EW, Wilkinson WE, Lang T et al (1996): Increased expression of blood mononuclear cell nitric oxide synthase type 2 in rheumatoid arthritis patients. *Journal Experimental Medicine* **184**:1173–1178.
- Stephens, N. G., Parsons, A., Schofield, P. M., Mitchinson, M. and Brown, M. J. (1996). A randomised controlled trial of vitamin E in patients with coronary disease: The Cambridge Heart Antioxidant Study (CHAOS). *Heart* **75**:176–176.
- Stefanovic-Racic, M., Stadler, J. and Evans, C.H. (1993). Nitric oxide and arthritis. *Arthritis and Rheumatism* **36**(8):1036–1044.
- Steinz, M.M., Santos-Alves, E. and Lanner, J.T. (2020). Skeletal muscle redox signalling in rheumatoid arthritis. *Clinical Science* **134**(21), pp. 2835–2850.
- Stienstra, R., Netea-Maier, R.T., Riksen, N.P., Joosten, L.A. and Netea, M.G.(2017). Specific and complex reprogramming of cellular metabolism in myeloid cells during innate immune responses. *Cell metabolism* **26**(1), pp. 142–156.
- Stock, J.L., Shinjo, K., Burkhardt, J., Roach, M., Taniguchi, K., Ishikawa, T., ... McNeish, J.D. (2001). The prostaglandin E 2 EP1 receptor mediates pain perception and regulates blood pressure. *The Journal of clinical investigation* **107**(3):325–331.
- Stroes, E.S., Thopson, P.D., Corsini, A.,Vladutiu, G,D.,Raal,F.J.,Ray,K.K, Roden, M.,et al. (2015).Statin-associated muscle symptoms:impact on statin therapy-European Atherosclerosis Society Consensus Panel Statement on Assessment, Etiology and management. *European Heart Journal* **36**(17), pp.1012–22.
- Strehl, C., Bijlsma, J.W., de Wit, M., Boers, M., Caeyers, N., Cutolo, M., ... Huizinga, T.W. (2016). Defining conditions where long-term glucocorticoid treatment has an acceptably low level of harm to facilitate implementation of existing recommendations: viewpoints from an EULAR task force. *Annals of the rheumatic diseases* **75**(6):952–957.
- Suresh, Y. and Das, U. N. (2003a). Long-chain polyunsaturated fatty acids and chemically induced diabetes mellitus: Effect of omega-3 fatty acids. *Nutrition* **19**:213–228.
- Suresh, Y. and Das, U. N. (2003b). Long-chain polyunsaturated fatty acids and chemically induced diabetes mellitus: Effect of omega-6 fatty acids. *Nutrition* **19**:93–114.
- Swanson, J. A. (1989). Phorbol esters stimulate macropinocytosis and solute flow through macrophages. *Journal of Cell Science* **94**:135–142.
- Swanson, J. A. and Watts, C. (1995). Macropinocytosis. *Trends in Cell Biology* **5**:424–428.
- Sweet, R.A., Ols, M.L., Cullen, J.L., Milam, A.V., Yagita, H. and Shlomchik, M.J. (2011). Facultative role for T cells in extrafollicular Toll-like receptor-dependent autoreactive B-cell responses in vivo. *Proceedings of the National Academy of Sciences* **108**(19):7932–7937.
- Szekanecz, Z., Kerekes, G., Der, H., Sandor, Z., Szabo, Z., Vegvari, A., ... and Soltesz, P. (2007). Accelerated atherosclerosis in rheumatoid arthritis. *Annals of the New York Academy of Sciences*, **1108**(1): 349–358.

References

- Stroes, E.S., Thopson, P.D., Corsini, A., Vladutiu, G.D., Raal, F.J., Ray, K.K., Roden, M., (2015). Statin-associated muscle symptoms: impact on statin therapy-European Atherosclerosis Society Consensus Panel Statement on Assessment, Etiology and management. *European Heart Journal* **36**(17): 1012–22.
- Strehl, C., Bijlsma, J.W., de Wit, M., Boers, M., Caeyers, N., Cutolo, M., ... Huizinga, T.W. (2016). Defining conditions where long-term glucocorticoid treatment has an acceptably low level of harm to facilitate implementation of existing recommendations: viewpoints from an EULAR task force. *Annals of the rheumatic diseases* **75**(6): 952–957.
- Sugano, M., Ikeda, I., Wakamatsu, K. and Oka, T. (1994). Influence of Korean pine (*Pinus koraiensis*)-seed oil containing cis-5, cis-9, cis-12-octadecatrienoic acid on polyunsaturated fatty acid metabolism, eicosanoid production and blood pressure of rats. *The British journal of nutrition* **72**(5):775–783.
- Szekanecz Z., Strieter R.M., Kunkel S.L. and Koch A.E. (1998). Chemokines in rheumatoid arthritis. Springer Semin. *Immunopathology* **20**, 115–140.
- Szekanecz Z. and Koch A.E. (2001). Chemokines and angiogenesis. *Current Opinion of Rheumatology*. **13**, 202–208.
- Shin, J.H., Song, J.E., Park, J.S., Shon, S.H., Lee, E.Y., Lee, E.B. and Song, Y.W. (2016). AB0071 Alpha-Enolase Expression on The Cell Surface of Osteoclast Precursors Plays A Positive Role in Osteoclastogenesis of Monocyte/macrophage in Rheumatoid Arthritis. *Annals of the Rheumatic Diseases* **75**(2):921.
- Shoelson, S.E., (2006). Lee j, Goldfine AB. *Inflammation and insulin resistance*. *Journal of Clinical Investigation*, **116**(7):1793–1801.
- Sica, A. and Mantovani, A. (2012). Macrophage plasticity and polarization: in vivo veritas. *The Journal of Clinical Investigation* **122**(3):787–795.
- Sierra-Filardi, E., Nieto, C., Domínguez-Soto, Á., Barroso, R., Sánchez-Mateos, P., Puig-Kroger, A., ... Rodríguez-Fernández, J.L. (2014). CCL2 shapes macrophage polarization by GM-CSF and M-CSF: identification of CCL2/CCR2-dependent gene expression profile. *The Journal of Immunology* **192**(8):3858–3867.
- Siouti, E. and Andreakos, E. (2019). The many facets of macrophages in rheumatoid arthritis. *Therapeutic Advances in Arthritis Diseases* **165**:152–169.
- Skurkovich, S.V., Klinova, E.G., Eremkina, E.I. and Levina, N.V., (1974). Immunosuppressive effect of an anti-interferon serum. *Nature*, **247** (5442):551
- St Clair, E.W., (1999). Interleukin 10 treatment for rheumatoid arthritis. *Annals of the rheumatic diseases*, **58**(1), 199–1102.
- Senftleber, N. K., Nielsen, S. M., Andersen, J. R., Bliddal, H., Tarp, S., Lauritzen, L., ... and Christensen, R. (2017). Marine oil supplements for arthritis pain: a systematic review and meta-analysis of randomized trials. *Nutrients*, **9**(1), 42.
- Sokolove, J., Bromberg, R., Deane, K.D., Lahey, L.J., Derber, L.A., Chandra, P.E., ... Norris, J.M. (2012). Autoantibody epitope spreading in the pre-clinical phase predicts progression to rheumatoid arthritis. *PloS one* **7**(5):e35296.
- Szafarska, A., Baj-Krzyworzeka, M., Siedlar, M., Węglarczyk, K., Ruggiero, I., Hajto, B. and Zembala, M. (2004). Antitumor response of CD14+/CD16+ monocyte subpopulation. *Experimental Hematology* **32**(8):748–755.
- Semb, A.G., Rollefstad, S., Provan, S.A., Kvien, T.K., Strandén, E., Olsen, I.C. and Hisdal, J. (2013). Carotid plaque characteristics and disease activity in rheumatoid arthritis. *The Journal of rheumatology* **40**(4):359–368.

References

- Skeoch, S. and Bruce, I.N. (2015). Atherosclerosis in rheumatoid arthritis: is it all about inflammation? *Nature Reviews Rheumatology* **11**(7):390.
- Solomon, A., Tsang, L., Woodiwiss, A.J., Millen, A.M., Norton, G.R. and Dessein, P.H. (2014). Cardiovascular disease risk amongst African black patients with rheumatoid arthritis: the need for population specific stratification. *BioMed research international* **2014**.
- Sosnowska, B., Mazidi, M., Penson, P., Gluba-Brzózka, A., Rysz, J. and Banach, M. (2017). The sirtuin family members SIRT1, SIRT3 and SIRT6: Their role in vascular biology and atherogenesis. *Atherosclerosis* **265**: 275–282.
- Souto-Carneiro, M.M., Klika, K.D., Abreu, M.T., Meyer, A.P., Saffrich, R., Sandhoff, R., Jennemann, R., Kraus, F.V., Tykocinski, L., Eckstein, V. and Carvalho, L., (2020). Effect of increased lactate dehydrogenase A activity and aerobic glycolysis on the proinflammatory profile of autoimmune CD8+ T cells in rheumatoid arthritis. *Arthritis and Rheumatology*, **72**(12):2050–2064.
- Straus, D.S., Pascual, G., Li, M., Welch, J.S., Ricote, M., Hsiang, C.H., Sengchanthalangsy, L.L., Ghosh, G. and Glass, C.K., (2000). 15-Deoxy- Δ 12, 14-prostaglandin J2 inhibits multiple steps in the NF- κ B signalling pathway. *Proceedings of the National Academy of Sciences*, **97**(9):4844–4849.
- Smedbakken LM, Halvorsen B, Daissormont I, Ranheim T, Michelsen AE, Skjelland M, Sagen EL, Folkersen L, Krohg-Sorensen K, Russell D, Holm S, Ueland T, Fevang B, Hedin U, Yndestad A, Gullestad L, Hansson GK, Biessen EA, Aukrust P (2012). Increased levels of the homeostatic chemokine CXCL13 in human atherosclerosis - Potential role in plaque stabilization. *Atherosclerosis*. **224**(1):266–73.
- Starr, A.E., Dufour, A., Maier, J. and Overall, C.M., (2012). Biochemical analysis of matrix metalloproteinase activation of chemokines CCL15 and CCL23 and increased glycosaminoglycan binding of CCL16. *Journal of Biological Chemistry*, **287**(8):5848–5860.
- Steiner, G. and Urowitz, M.B., (2009). Lipid profiles in patients with rheumatoid arthritis: mechanisms and the impact of treatment. In *Seminars in arthritis and rheumatism* **38**(5):372–381.
- Tadijan, A., Samaržija, I., Humphries, J.D., Humphries, M.J. and Ambriović-Ristov, A., (2021). KANK family proteins in cancer. *The International Journal of Biochemistry & Cell Biology*, **131**, p.105903
- Tamotsu, T., Tatsunori, T., Morishige, J., Kikuta, Y., Sugiura, T. and Satouchi, K. (1999). Non-methylene-interrupted polyunsaturated fatty acids: Effective substitute for arachidonate of phosphatidylinositol. *Biochemical and Biophysical Research Communications* **264**, 683–688.
- Tak PP., Smeets TJM., Daha MR., Kluin PM., Meijers KAE., Brand R., and Breedveld FC. (1997). Analysis of the synovial cell infiltrate in early rheumatoid synovial tissue in relation to local disease activity. *Arthritis and Rheumatism*; **40**(2):217–25.
- Takala, R., Ramji, D. P., Andrews, R., Zhou, Y., Farhat, M., Elmajee, M., Choy, E. (2022). Pinolenic acid exhibits anti-inflammatory and anti-atherogenic effects in peripheral blood-derived monocytes from patients with rheumatoid arthritis. *Scientific reports*, **12**(1): 8807.
- Takala, R., Ramji, D. P., Choy, E. (2023). The beneficial effects of pine nuts and its major fatty acid, pinolenic acid, on inflammation and metabolic perturbations in inflammatory disorders. *International Journal of Molecular Sciences*, **24**(2): 1171.
- Takeuchi, Y. Yahagi, N., Aita, Y., Murayama, Y., Sawada, Y., Piao, X., ... and Shimano, H. (2016). KLF15 Enables Rapid Switching between Lipogenesis and Gluconeogenesis during Fasting. *Cell Reports* **16**(9):2373–2386.
- Takayanagi, H. (2012). New developments in osteoimmunology. *Nature Reviews Rheumatology* **8**(11):684–689.

References

- Tarazona, S., García-Alcalde, F., Dopazo, J., Ferrer, A., Conesa, A., Differential expression in RNA-seq: a matter of depth. *Genome Research*, (2011). **21**(12): 2213–23.
- Tan, Z., Xie, N., Banerjee, S., Cui, H., Fu, M., Thannickal, V.J. and Liu, G., (2015). The monocarboxylate transporter 4 is required for glycolytic reprogramming and inflammatory response in macrophages. *Journal of Biological Chemistry*, **290**(1):46–55.
- Tao, R., Xiong, X., DePinho, R.A., Deng, C.X. and Dong, X.C., (2013). FoxO3 transcription factor and Sirt6 deacetylase regulate low density lipoprotein (LDL)-cholesterol homeostasis via control of the proprotein convertase subtilisin/kexin type 9 (Pcsk9) gene expression. *Journal of Biological Chemistry*, **288**(41):29252–29259.
- Taylor, P.C., (2020). Update on the diagnosis and management of early rheumatoid arthritis. *Clinical Medicine*, **20**(6):561.
- Taylor, K.M., Morgan, H.E., Johnson, A. and Nicholson, R.I., (2005). Structure–function analysis of a novel member of the LIV-1 subfamily of zinc transporters, ZIP14. *FEBS letters*, **579**(2):427–432.
- Taylor, P.C. and Sivakumar, B., (2005). Hypoxia and angiogenesis in rheumatoid arthritis. *Current opinion in rheumatology*, **17**(3)293–298.
- Taylor, P. C., Peters, A. M., Paleolog, E., Chapman, P. T., Elliott, M. J., McCloskey, R., ... & Maini, R. N. (2000). Reduction of chemokine levels and leukocyte traffic to joints by tumor necrosis factor α blockade in patients with rheumatoid arthritis. *Arthritis and Rheumatism: Official Journal of the American College of Rheumatology*, **43**(1):38–47
- Tedgui, A. and Mallat, Z. (2006). Cytokines in atherosclerosis: Pathogenic and regulatory pathways. *Physiological Reviews* **86**:515–581
- Torres-Castro, I., Arroyo-Camarena, Ú.D., Martínez-Reyes, C.P., Gómez-Arauz, A.Y., Dueñas-Andrade, Y., Hernández-Ruiz, J., Béjar, Y.L., Zaga-Clavellina, V., Morales-Montor, J., Terrazas, L.I. and Kzhyshkowska, J., (2016). Human monocytes and macrophages undergo M1-type inflammatory polarization in response to high levels of glucose. *Immunology letters*, **176**:81–89.
- Tsuboi, K., Sugimoto, Y. and Ichikawa, A. (2002). Prostanoid receptor subtypes. *Prostaglandins and Other Lipid Mediators* **68**:535–556.
- Tsujisawa, T., Inoue, H. and Nishihara, T. (2004). SC-19220, Antagonist of Prostaglandin E2 Receptor EP1, Inhibits Osteoclastogenesis by RANKL. *Journal of Bone and Mineral Research* **20**(1):15–22.
- Trelle, S., Reichenbach, S., Wandel, S., Hildebrand, P., Tschannen, B., Villiger, P.M., Egger, M. and Jüni, P., (2011). Cardiovascular safety of non-steroidal anti-inflammatory drugs: Network meta-analysis. *BMJ*, **342**:7086.
- Tojo, N., Asakura, E., Koyama, M., Tanabe, T. and Nakamura, N., (1999). Effects of macrophage colony-stimulating factor (M-CSF) on protease production from monocyte, macrophage and foam cell in vitro: a possible mechanism for anti-atherosclerotic effect of M-CSF. *Biochimica et Biophysica Acta (BBA)-Molecular Cell Research*, **1452**(3):275–284.
- Thomas Graham, Tacke Robert, Hedrick Catherine C. and Hanna Richard N. (2015). Nonclassical Patrolling Monocyte Function in the Vasculature. *Arteriosclerosis, Thrombosis, and Vascular Biology* **35**(6):1306–1316.
- Thomas, K.E., Galligan, C.L., Newman, R.D., Fish, E.N. and Vogel, S.N., (2006). Contribution of interferon- β to the murine macrophage response to the Toll-like receptor 4 agonist, lipopolysaccharide. *Journal of Biological Chemistry*, **281**(41):31119–31130.
- Thammaiah, C.K. and Jayaram, S. (2016). Role of let-7 family microRNA in breast cancer. *Non-coding RNA Research* **1**(1), pp. 77–82.

References

- Tran, D.Q., Andersson, J., Wang, R., Ramsey, H., Unutmaz, D. and Shevach, E.M., (2009). GARP (LRRC32) is essential for the surface expression of latent TGF- β on platelets and activated FOXP3+ regulatory T cells. *Proceedings of the National Academy of Sciences*, **106**(32):13445-13450.
- Turesson, C., O'Fallon, W.M., Crowson, C.S., Gabriel, S.E. and Matteson, E.L. (2003). Extra-articular disease manifestations in rheumatoid arthritis: incidence trends and risk factors over 46 years. *Annals of the Rheumatic Diseases* **62**(8):722
- Thalayasingam, N. and Isaacs, J.D., (2011). Anti-TNF- α therapy. *Best practice and research Clinical rheumatology*, **25**(4):549-567.
- Tsuboi, K., Sugimoto, Y. and Ichikawa, A. (2002). Prostanoid receptor subtypes. *Prostaglandins and Other Lipid Mediators* **68–69**:535–556.
- Tsujisawa, T., Inoue, H. and Nishihara, T. (2004). SC-19220, Antagonist of Prostaglandin E2 Receptor EP1, Inhibits Osteoclastogenesis by RANKL. *Journal of Bone and Mineral Research* **20**(1):15–22.
- Tsukamoto, M., Seta, N., Yoshimoto, K., Suzuki, K., Yamaoka, K. and Takeuchi, T. (2017). CD14 bright CD16+ intermediate monocytes are induced by interleukin-10 and positively correlate with disease activity in rheumatoid arthritis. *Arthritis research and therapy* **19**(1):28.
- Tu, J., Guo, Y., Hong, W., Zhang, P., Wang, X., Chen, X., Lu, S. and Wei, W., (2019). The ontogeny of synovial macrophages and the roles of synovial macrophages from different origins in arthritis. *Frontiers in immunology*, **10**:1146
- Ueki, Y., Miyake, S., Tominaga, Y. and Eguchi, K., (1996). Increased nitric oxide levels in patients with rheumatoid arthritis. *The Journal of rheumatology*, **23**(2):230–236.
- Urschel, K. and Cicha, I., (2015). TNF- α in the cardiovascular system: from physiology to therapy. *Internat J Interferon Cytokine and Mediator Research*, **7**:9–25.
- Urman, A., Taklalsingh, N., Sorrento, C. and McFarlane, I.M. (2018). Inflammation beyond the Joints: rheumatoid arthritis and cardiovascular disease. *Journal of cardiology* **2**(3):1000019.
- Van Everdingen AA, Jacobs JWG, Siewertsz Van Reesema DR, Bijlsma JWJ (2002). Low-dose prednisone therapy for patients with early active rheumatoid arthritis: Clinical efficacy, disease-modifying properties, and side effects: A randomized, double-blind, placebo-controlled clinical trial. *Annals Internal Medicine*; **136**(1):1–12.
- Van Steenberghe, H.W., Van Nies, J.A.B., Ruyssen-Witrand, A., Huizinga, T.W.J., Cantagrel, A., Berenbaum, F. and Van Der Helm-Van Mil, A.H.M., (2015). IL2RA is associated with persistence of rheumatoid arthritis. *Arthritis research & therapy*, **17**(1): 1–9.
- Van den Bossche, J., O'Neill, L.A. and Menon, D. (2017). Macrophage immunometabolism: where are we (going)? *Trends in immunology* **38**(6): 395–406.
- Van den Oever, I., Sattar, N. and Nurmohamed, M. (2014). Thromboembolic and cardiovascular risk in rheumatoid arthritis: role of the haemostatic system. *Annals of the rheumatic diseases* **73**(6): 954–957.
- van Schouwenburg, P.A., van de Stadt, L.A., de Jong, R.N., van Buren, E.E., Kruithof, S., de Groot, E., Hart, M., van Ham, S.M., Rispen, T., Aarden, L. and Wolbink, G.J., (2013). Adalimumab elicits a restricted anti-idiotypic antibody response in autoimmune patients resulting in functional neutralisation. *Annals of the rheumatic diseases*, **72**(1): 104–109.
- van Lieshout AW, van der Voort R, le Blanc LM, et al. (2006). Novel insights in the regulation of CCL18 secretion by monocytes and dendritic cells via cytokines, toll-like receptors and rheumatoid synovial fluid. *BMC Immunology*. **7**: 23.

References

- van de Laar, L., Saelens, W., De Prijck, S., Martens, L., Scott, C.L., Van Isterdael, G., Hoffmann, E., Beyaert, R., Saeys, Y., Lambrecht, B.N. and Guillems, M., (2016). Yolk sac macrophages, fetal liver, and adult monocytes can colonize an empty niche and develop into functional tissue-resident macrophages. *Immunity*, **44**(4): 755–768.
- Veras, F.P. et al. (2015). Fructose 1, 6-bisphosphate, a high-energy intermediate of glycolysis, attenuates experimental arthritis by activating anti-inflammatory adenosinergic pathway. *Scientific reports* **5**(1): 1–11.
- Verzija, D., Storelli, S., Scholten, D. J., Bosch, L., Reinhart, T. A., Streblow, D. N., ... Leurs, R. (2008). Noncompetitive Antagonism and Inverse Agonism as Mechanism of Action of Nonpeptidergic Antagonists at Primate and Rodent CXCR3 Chemokine Receptors. *Journal of Pharmacology and Experimental Therapeutics*, **325**(2): 544–555.
- Viatte, S., Plant, D. and Raychaudhuri, S. (2013). Genetics and epigenetics of rheumatoid arthritis. *Nature reviews. Rheumatology* **9**(3):141–153
- Villar-Vesga, J., Grajalas, C., Burbano, C., Vanegas–García, A., Muñoz–Vahos, C.H., Vásquez, G., ... Castaño, D. (2019). Platelet-derived microparticles generated in vitro resemble circulating vesicles of patients with rheumatoid arthritis and activate monocytes. *Cellular Immunology* **336**: 1–11.
- Virtue, A., Wang, H. and Yang, X.F., (2012). MicroRNAs and toll-like receptor/interleukin-1 receptor signalling. *Journal of haematology and oncology*, **5**(1): 1–17.
- Vojinovic, J., Tincani, A., Sulli, A., Soldano, S., Andreoli, L., Dall'Ara, F., Ionescu, R., Pasalic, K.S., Balcune, I., Ferraz-Amaro, I. and Tlustochowicz, M., (2017). European multicentre pilot survey to assess vitamin D status in rheumatoid arthritis patients and early development of a new Patient Reported Outcome questionnaire (D-PRO). *Autoimmunity reviews*, **16**(5): 548–554.
- Vogt LM, Kwasniewicz E, Talens S, et al. (2020). Apolipoprotein E Triggers Complement Activation in Joint Synovial Fluid of Rheumatoid Arthritis Patients by Binding C1q. *Journal of Immunology*.**204**(10): 2779–2790.
- Volker, D.H., FitzGerald, P.E. and Garg, M.L., (2000). The eicosapentaenoic to docosahexaenoic acid ratio of diets affects the pathogenesis of arthritis in Lew/SSN rats. *The Journal of nutrition*, **130**(3): 559–565.
- Volpato S, Guralnik JM, Ferrucci L, Balfour J, Chaves P, Fried LP, Harris TB. (2001). Cardiovascular disease, interleukin-6, and risk of mortality in older women: the women's health and aging study. *Circulation*. **103**(7): 947–53
- Volin M.V., Woods J.M., Amin M.A., Connors M.A., Harlow L.A. and Koch A.E. (2001). Fractalkine: a novel angiogenic chemokine in rheumatoid arthritis. *The American journal of pathology*, **159**(4):1521-1530.
- Wahl, S.M., Allen, J.B., Welch, G.R. and Wong, H.L., (1992). Transforming growth factor-beta in synovial fluids modulates Fc gamma RII (CD16) expression on mononuclear phagocytes. *The Journal of Immunology*, **148**(2):485–490.
- Wall, R., Ross, R.P., Fitzgerald, G.F. and Stanton, C. (2010). Fatty acids from fish: the anti-inflammatory potential of long-chain omega-3 fatty acids. *Nutrition Reviews* **68**:280–289.
- Wang, Z., Zhao, Q., Nie, Y., Yu, Y., Misra, B.B., Zabalawi, M., Chou, J.W., Key, C.C.C., Molina, A.J., Quinn, M.A. and Fessler, M.B., (2020). Solute Carrier Family 37 Member 2 (SLC37A2) Negatively Regulates Murine Macrophage Inflammation by Controlling Glycolysis. *Iscience*, **23**(5):101125.
- Wang, X., Liu, D., Ning, Y., Liu, J., Wang, X., Tu, R., ... Xiong, Y. (2017). Siglec-9 is upregulated in rheumatoid arthritis and suppresses collagen-induced arthritis through reciprocal regulation of Th17-/Treg-cell differentiation. *Scandinavian Journal of Immunology* **85**(6):433–440.
- Wang, T., Wang, G., Zhang, Y., Zhang, J., Cao, W. and Chen, X. (2019). Effect of lentivirus-mediated overexpression or silencing of MnSOD on apoptosis of resveratrol-treated fibroblast-like synoviocytes in rheumatoid arthritis. *European Journal of Pharmacology*, **844**:65–72.

References

- Wanten, G.J. and Calder, P.C., (2007). Immune modulation by parenteral lipid emulsions. *The American journal of clinical nutrition*, **85**(5):1171–1184.
- Wang, H., Lafdil, F., Kong, X. and Gao, B., (2011). Signal transducer and activator of transcription 3 in liver diseases: a novel therapeutic target. *International journal of biological sciences*, **7**(5):536.
- Wæhre, T., Yndestad, A., Smith, C., Haug, T., Tunheim, S.H., Gullestad, L., Froland, S.S., Semb, A.G., Aukrust, P. and Damås, J.K., (2004). Increased expression of interleukin-1 in coronary artery disease with downregulatory effects of HMG-CoA reductase inhibitors. *Circulation*, **109**(16):1966–1972.
- Wang, F., Sengupta, T.K., Zhong, Z. and Ivashkiv, L.B., (1995). Regulation of the balance of cytokine production and the signal transducer and activator of transcription (STAT) transcription factor activity by cytokines and inflammatory synovial fluids. *The Journal of experimental medicine*, **182**(6):1825–1831.
- Wald, D., Qin, J., Zhao, Z., Qian, Y., Naramura, M., Tian, L., Towne, J., Sims, J.E., Stark, G.R. and Li, X., (2003). SIGIRR, a negative regulator of Toll-like receptor–interleukin 1 receptor signalling. *Nature immunology*, **4**(9): 920-927.
- Wei L, MacDonald TM, Walker BR (2004). Taking glucocorticoids by prescription is associated with subsequent cardiovascular disease. *Annals of Internal Medicine*; **141**:764-70.
- Weinblatt, M.E., Keystone, E.C., Furst, D.E., Moreland, L.W., Weisman, M.H., Birbara, C.A., Teoh, L.A., Fischkoff, S.A. and Chartash, E.K., (2003). Adalimumab, a fully human anti–tumor necrosis factor α monoclonal antibody, for the treatment of rheumatoid arthritis in patients taking concomitant methotrexate: the ARMADA trial. *Arthritis and Rheumatism*, **48**(1):35-45.
- Williams, A.G., Thomas, S., Wyman, S.K. and Holloway, A.K., (2014). RNA-seq data: challenges in and recommendations for experimental design and analysis. *Current protocols in human genetics*, **83**(1), pp.11-13.
- Winchester, R., Giles, J.T., Nativ, S., Downer, K., Zhang, H., Bag-Ozbek, A., ... Bathon, J.M. (2016). Association of elevations of specific T cell and monocyte subpopulations in rheumatoid arthritis with subclinical coronary artery atherosclerosis. *Arthritis and Rheumatology* **68**(1):92–102.
- Wei, M., Ma, Y., Shen, L., Xu, Y., Liu, L., Bu, X., Guo, Z., Qin, H., Li, Z., Wang, Z. and Wu, K., (2020). NDRG2 regulates adherens junction integrity to restrict colitis and tumourigenesis. *EBioMedicine*, **61**:103068.
- Wilson BJ, Saab KR, Ma J, Schatton T, Pütz P, Zhan Q, Murphy GF, Gasser M, Waaga-Gasser AM, Frank NY, Frank MH. (2014). ABCB5 maintains melanoma-initiating cells through a proinflammatory cytokine signalling circuit. *Cancer Research*. **74**(15):4196–207.
- Weyand, C.M. and Goronzy, J.J. (2020). Immunometabolism in the development of rheumatoid arthritis. *Immunological reviews* **294**(1):177–187.
- Woo, S.J., Lim, K., Park, S.Y., Jung, M.Y., Lim, H.S., Jeon, M.G., Lee, S.I. and Park, B.H., (2015). Endogenous conversion of n-6 to n-3 polyunsaturated fatty acids attenuates K/BxN serum-transfer arthritis in fat-1 mice. *The Journal of nutritional biochemistry*, **26**(7):713–720.
- Wolf, H., Damme, M., Stroobants, S., D'Hooge, R., Beck, H. C., Hermans-Borgmeyer, I., Lüllmann-Rauch, R., Dierks, T., and Lübke, T. (2016). A mouse model for fucosidosis recapitulates storage pathology and neurological features of the milder form of the human disease. *Disease models and mechanisms*, **9**(9), 1015–1028.
- Woo, S. J., Noh, H. S., Lee, N. Y., Cheon, Y. H., Yi, S. M., Jeon, H. M., Bae, E. J., Lee, S. I., and Park, B. H. (2018). Myeloid sirtuin 6 deficiency accelerates experimental rheumatoid arthritis by enhancing macrophage activation and infiltration into synovium. *Experimental Biology and Medicine*, **38**, 228–237.

References

- Wu J, Strawn TL, Luo M, Wang L, Li R, Ren M, Xia J, Zhang Z, Ma W, Luo T, Lawrence DA, Fay WP. (2015) Plasminogen activator inhibitor-1 inhibits angiogenic signalling by uncoupling vascular endothelial growth factor receptor-2- α V β 3 integrin cross talk. *Arteriosclerosis Thrombosis and Vascular Biology*. **35**(1):111–20.
- Wu D, Meydani M, Leka LS (1999). Effect of dietary supplementation with black currant seed oil on the immune response of healthy elderly subjects. *The American journal of clinical nutrition*, **70**(4):536-543.
- Wegrzyn, J. et al. (2009). Function of mitochondrial Stat3 in cellular respiration. *Science* 323(5915): 793–797.
- Xie.K, Miles.E. A, Calder.P.C (2016). A review of the potential health benefits of pine nut oil and its characteristic fatty acid pinolenic acid. *Journal of Functional Food* **23**(1):464–473.
- Xiong, Y.-S., Cheng, Y., Lin, Q.-S., Wu, A.-L., Yu, J., Li, C., ... Wu, L.-J. (2013). Increased expression of Siglec-1 on peripheral blood monocytes and its role in mononuclear cell reactivity to autoantigen in rheumatoid arthritis. *Rheumatology* **53**(2):250–259.
- Xiao, L. et al. (2015). Death-associated Protein 3 Regulates Mitochondrial-encoded Protein Synthesis and Mitochondrial Dynamics. *Journal of Biological Chemistry* **290**(41):24961–24974.
- Xue Q, Wang X, Deng X, Huang Y, Tian W. (2020). CEMIP regulates the proliferation and migration of vascular smooth muscle cells in atherosclerosis through the WNT-beta-catenin signalling pathway. *Biochem Cell Biol*. **98**(2):249–257.
- Xu, D., Liang, J., Lin, J. and Yu, C. (2019). PKM2: A Potential Regulator of Rheumatoid Arthritis via Glycolytic and Non-Glycolytic Pathways. *Frontiers in Immunology* **10**: 2919.
- Xu, S., Bai, P. and Jin, Z.G., (2016). Sirtuins in cardiovascular health and diseases. *Trends in endocrinology and metabolism*. **27**(10):677.
- Xu, K., He, Y., Moqbel, S.A.A., Zhou, X., Wu, L. and Bao, J. (2021). SIRT3 ameliorates osteoarthritis via regulating chondrocyte autophagy and apoptosis through the PI3K/Akt/mTOR pathway. *International Journal of Biological Macromolecules* **175**: 351–360.
- Xu, Y., Zhang, Y. and Ye, J., (2018). IL-6: A potential role in cardiac metabolic homeostasis. *International journal of molecular sciences*, **19**(9)2474.
- Xu, S., Yin, M., Koroleva, M., Mastrangelo, M.A., Zhang, W., Bai, P., Little, P.J. and Jin, Z.G., (2016). SIRT6 protects against endothelial dysfunction and atherosclerosis in mice. *Aging (Albany NY)*, **8**(5):1064.
- Yang, Y.J., Zhu, Z., Wang, D.T., Liu, Y.Y., Lai, W.X., Mo, Y.L., Li, J., Liang, Y.L., Hu, Z.Q., Yu, Y.J. and Cui, L., (2018). Tanshinol alleviates impaired bone formation by inhibiting adipogenesis via KLF15/PPAR γ 2 signalling in GIO rats. *Acta Pharmacologica Sinica*, **39**(4):633–641.
- Yang, J., Zhang, L., Yu, C., Yang, X.-F. and Wang, H. (2014). Monocyte and macrophage differentiation: circulation inflammatory monocyte as biomarker for inflammatory diseases. *Biomarker research* **2**(1):1.
- Yao, C. and Narumiya, S. (2019). Prostaglandin-cytokine crosstalk in chronic inflammation. *British journal of pharmacology* **176**(3):337–354.
- Yapp, C., Carr, A.J., Price, A., Oppermann, U. and Snelling, S.J., (2016). H3K27me3 demethylases regulate in vitro chondrogenesis and chondrocyte activity in osteoarthritis. *Arthritis research and therapy*, **18**(1):1–10.
- Yaqoob P, Pala HS, Cortina-Borja M, et al. (2000); Encapsulated fish oil enriched in [alpha]-tocopherol alters plasma phospholipid and mononuclear cell fatty acid compositions but not mononuclear cell functions. *European Journal of Clinical Investigation* **30**(3):260–274.

References

- Yamamoto, T., Sawada, Y., Katayama, I. and Nishioka, K., (1998). Increased production of nitric oxide stimulated by interleukin-1beta in peripheral blood mononuclear cells in patients with systemic sclerosis. *British journal of rheumatology*, **37**(10):1123–1125.
- Yamamoto, K., Takeshita, K., Kojima, T., Takamatsu, J. and Saito, H., (2005). Aging and plasminogen activator inhibitor-1 (PAI-1) regulation: implication in the pathogenesis of thrombotic disorders in the elderly. *Cardiovascular research*, **66**(2):276–285.
- Yadav, A., Saini, V. and Arora, S., (2010). MCP-1: chemoattractant with a role beyond immunity: a review. *Clinica chimica acta*, **411**(21-22):1570–1579.
- Yao, W., Li, K. and Liao, K. (2009). Macropinocytosis contributes to the macrophage foam cell formation in RAW264.7 cells. *Acta Biochimica Et Biophysica Sinica* **41**(9):773–780.
- Yamaguchi, S., Moseley, A.C., Almeda-Valdes, P., Stromsdorfer, K.L., Franczyk, M.P., Okunade, A.L., Patterson, B.W., Klein, S. and Yoshino, J., (2018). Diurnal variation in PDK4 expression is associated with plasma free fatty acid availability in people. *The Journal of Clinical Endocrinology and Metabolism*, **103**(3):1068–1076.
- Yeo, J., Lee, Y.M., Lee, J., Park, D., Kim, K., Kim, J., ... Kim, W.J. (2019). Nitric Oxide-scavenging nanogel for treating rheumatoid arthritis. *Nano Letters* **19**(10):6716–6724.
- Yoon, B.R., Yoo, S.-J., ho Choi, Y., Chung, Y.-H., Kim, J., Yoo, I.S., ... Lee, W.-W. (2014). Functional phenotype of synovial monocytes modulating inflammatory T-cell responses in rheumatoid arthritis (RA). *PloS one* **9**(10):e109775.
- Young, J.M., B.I. Shand, P.M. McGregor, R.S. Scott and C.M. Frampton, (2006). Comparative effects of and vitamin C supplementation versus vitamin C alone on endothelial function and biochemical markers of oxidative stress and inflammation in chronic smokers. *Free Radical research*. **40**(1):85–94.
- Yusuf, S., Dagenais, G., Pogue, J., Bosch, J., Sleight, P. and Heart Outcomes Prevent Evaluat, S. (2000). Vitamin E supplementation and cardiovascular events in high-risk patients. *New England Journal of Medicine*. **342**(3):154–160.
- Yamaoka, K. (2016). Janus kinase inhibitors for rheumatoid arthritis. *Current opinion in chemical biology* **32**(1):29–33.
- Yuan Xiong, Bo-bin Mi, Meng-fei Liu, Hang Xue, Qi-peng Wu and Guo-hui Liu (2019). Bioinformatics Analysis and Identification of Genes and Molecular Pathways Involved in Synovial Inflammation in Rheumatoid Arthritis. *Medical Science Monitor* **25**:2246–2256.
- Yuan, J., Akiyama, M., Nakahama, K., Sato, T., Uematsu, H. and Morita, I. (2010). The effects of polyunsaturated fatty acids and their metabolites on osteoclastogenesis in vitro. *Prostaglandins and Other Lipid Mediators* **92**(1–4):85–90.
- Yki-Jarkiven H, Bergholm R, Leirisalo-Repo M. (2003). Increased inflammatory activity parallels increased basal nitric oxide production and blunted response to nitric oxide in vivo in rheumatoid arthritis. *Annals Rheumatic Diseases* **62**(7):630–34
- Yoshimura, A., Naka, T. and Kubo, M., (2007). SOCS proteins, cytokine signalling and immune regulation. *Nature Reviews Immunology*, **7**(6):454–465.
- Zamani, F., Zare Shahneh, F., Aghebati-Maleki, L. and Baradaran, B. (2013). Induction of CD14 Expression and Differentiation to Monocytes or Mature Macrophages in Promyelocytic Cell Lines: New Approach. *Advanced Pharmaceutical Bulletin* **3**(2):329–332.

References

- Zeng H, Fu Y, Yu W, Lin J, Zhou L, Liu L, et al. (2013). SIRT1 prevents atherosclerosis via liver-X-receptor and NF- κ B signalling in a U937 cell model. *Molecular Medicine Reports*, **8**(1):23–8.
- Zer C, Sachs G, Shin JM (2007). Identification of genomic targets downstream of p38 mitogen-activated protein kinase pathway mediating tumor necrosis factor- α signalling. *Physiological Genomics*, **22**(2):343-5.
- Zhang, M., Zhao, Y., Li, Z. and Wang, C., (2018). Pyruvate dehydrogenase kinase 4 mediates lipogenesis and contributes to the pathogenesis of nonalcoholic steatohepatitis. *Biochemical and biophysical research communications*, **495**(1) 582–586.
- Zhao, B., Li, Y. F., Buono, C., Waldo, S. W., Jones, N. L., Mori, M. and Kruth, H. S. (2006). Constitutive receptor-independent low density lipoprotein uptake and cholesterol accumulation by macrophages differentiated from human monocytes with macrophage- colony-stimulating factor (M-CSF). *Journal of Biological Chemistry*, **281**:15757–15762.
- Zhong, J., Wang, H., Chen, W., Sun, Z., Chen, J., Xu, Y., Miao, C. (2017). Ubiquitylation of MFHAS1 by the ubiquitin ligase praja2 promotes M1 macrophage polarization by activating JNK and p38 pathways. *Cell death and disease*, **8**(5): 2763-2763.
- Zhu, F., Wang, P., Kontogianni-Konstantopoulos, A. and Konstantopoulos, K. (2010). Prostaglandin (PG) D 2 and 15-deoxy- Δ 12, 14-PGJ 2, but not PGE 2, mediate shear-induced chondrocyte apoptosis via protein kinase A-dependent regulation of polo-like kinases. *Cell death and differentiation* **17**(8):1325.
- Zhuang, J., Han, Y., Xu, D., Zhu, G., Singh, S., Chen, L., Zhu, M., Chen, W., Xu, Y. and Li, X., (2017). Comparison of circulating dendritic cell and monocyte subsets at different stages of atherosclerosis: insights from optical coherence tomography. *BMC cardiovascular disorders*, **17**(1):1-10.
- Zhu, S., Park, S., Lim, Y., Shin, S. and Han, S.N. (2016). Korean pine nut oil replacement decreases intestinal lipid uptake while improves hepatic lipid metabolism in mice. *Nutrition Research and Practice*, **10**(5):477–486.
- Ziegler-Heitbrock L, Ancuta P, Crowe S, Dalod M, Grau V, Hart DN, Leenen PJ, Liu YJ, MacPherson G, Randolph GJ, Scherberich J (2010). Nomenclature of monocytes and dendritic cells in the blood. *Blood, The Journal of the American Society of Hematology*, **116**(16):74–80.